NASA CONTRACTOR REPORT

NASA CR-2642

TURBULENT BOUNDARY LAYER ON A FULL-COVERAGE FILM-COOLED SURFACE - AN EXPERIMENTAL HEAT TRANSFER STUDY WITH NORMAL INJECTION

H. Choe, W. M. Kays, and R. J. Moffat

Prepared by
STANFORD UNIVERSITY
Stanford, Calif. 94305
for Lewis Research Center

NATIONAL AERONAUTICS AND SPACE ADMINISTRATION • WASHINGTON, D. C. • JANUARY 1976

1. Report No. NASA CR-2642	2. Government Accession No.	3. Recipient's Catalog No.
4. Title and Subtitle TURBULENT BOUNDARY LAYER ON A FULL-COVERAGE FILM-COOLED SURFACE - AN EXPERIMENTAL HEAT TRANSFER STUDY WITH NORMAL INJECTION		5. Report Date January 1976
		6. Performing Organization Code
7. Author(s) H. Choe, W. M. Kays, and R. J. Moffat		8. Performing Organization Report No. HMT-22
9. Performing Organization Name and Address Stanford University Stanford, California 94305		10. Work Unit No.
		11. Contract or Grant No. NAS 3-14336
12. Sponsoring Agency Name and Address National Aeronautics and Space Administration Washington, D.C. 20546		13. Type of Report and Period Covered Contractor Report
		14. Sponsoring Agency Code
15. Supplementary Notes Final Report. Project Manager, Raymond S. Colladay, Airbreathing Engines Division, NASA Lewis Research Center, Cleveland, Ohio		

16. Abstract

Heat transfer behavior was studied in a turbulent boundary layer with full-coverage film cooling through an array of discrete holes and with injection normal to the wall surface. Stanton numbers were measured for a staggered hole pattern with pitch-to-diameter ratios of 5 and 10, an injection mass flux ratio range of 0.1 to 1.0, and a range of Reynolds number Re_x of 1.7×10^5 to 5×10^6. Air was used as the working fluid with the mainstream velocity varied from 9.14 to 33.5 m/sec (30 to 110 ft/sec). The data were taken for secondary injection temperatures equal to the wall temperature and also equal to the mainstream temperature. By use of linear superposition theory, the data may be used to obtain Stanton number as a continuous function of the injectant temperature. The heat transfer coefficient is defined on the basis of a mainstream-to-wall temperature difference. This definition permits direct comparison of performance between film cooling and transpiration cooling.

17. Key Words (Suggested by Author(s)) Film cooling; Heat transfer; Gas turbine; Boundary layer; Turbulent		18. Distribution Statement Unclassified - unlimited STAR category 34 (rev.)	
19. Security Classif. (of this report) Unclassified	20. Security Classif. (of this page) Unclassified	21. No. of Pages 296	22. Price* $8.75

* For sale by the National Technical Information Service, Springfield, Virginia 22161

TABLE OF CONTENTS

Page

NOMENCLATURE

A	Area for local averaging in Figure 4.1, or total plate heat transfer area
A^+	Van Driest damping function
AKO	Constant that determines maximum of ℓ_a
B	Blowing parameter, F/St
B_c	B at $\theta = 0.0$
B_h	B at $\theta = 1.0$
C_2	Damping constant used in the calculation of $V^+_{o,e}$
C_f	Skin friction defined as $\tau_o = C_f/2\ \rho_\infty U_\infty^2$
c_p	Specific heat at constant pressure
CL1	Constant used for the adjustment of $V^+_{o,e}$ at positive step
CL2	Constant used for the adjustment of $V^+_{o,e}$ at negative step
CPR	Ratio of thermal penetration distance over the momentum penetration distance
D	Diameter of injection tube
DPL	Jet penetration distance for momentum
F	Blowing fraction, $\rho_o V_o/\rho_\infty U_\infty$ averaged over area A
f	Distribution function for effective source, S_h , within boundary layer
g	(1) Distribution function for effective body force, S_m , within the boundary layer (2) General mass transfer coefficient
g_c	Proportionality constant in Newton's Second Law
h	(1) Heat transfer coefficient (2) Enthalpy in Appendix H
H	Shape factor, δ_1/δ_2

h_o	Unblown heat transfer coefficient
h^+	$(h-h_\infty)\sqrt{c_f/2}/\{(h_o-h_\infty)St\}$
h^*	Heat transfer coefficient used in adiabatic wall scheme
Δh	$h(\theta = 0) - h(\theta = 1)$
k	Thermal conductivity
K	(1) Acceleration constant, $\frac{\nu}{U_\infty^2}\frac{dU_\infty}{dx}$
	(2) Heat flux meter calibration constant without temperature correction
	(3) Wattmeter power correction factor
	(4) Pressure drop coefficient
K_o	Constant that determines maximum in ℓ_a
L	Flow direction pitch in injection hole geometry defined in Figure 1.1
ℓ	Mixing length
ℓ_a	Augmented mixing length
ℓ_f	Mixing length for flat plate
L_e	Lewis number
M	Blowing parameter, $\rho_2 V_2/\rho_\infty U_\infty$ averaged over the injection hole area, A_h
$\dot{m}''$	Mass flux
$\dot{m}$	Mass flow rate
Ntu	Net transfer unit, $\int UdA/\dot{m}c_p$
P	(1) Lateral pitch in injection tube array
	(2) Locally averaged pressure
	(3) General property
	(4) Power supplied to the plate
Pr	Prandtl number, ν/α

Pr_t	Turbulent Prandtl number, $\varepsilon_M/\varepsilon_H$
$\dot{q}$	Heat flow rate
$\dot{q}''$	Heat flux
$\dot{q}_o''$	Heat flux at wall
Re	Reynolds number
Re_x	$U_\infty x/\nu_\infty$
$Re_{\overline{\delta}_2}$	$U_\infty\overline{\delta}_2/\nu_\infty$
$Re_{\overline{\Delta}_2}$	$U_\infty\overline{\Delta}_2/\nu_\infty$
$Re_{\infty,D}$	$U_\infty D/\nu_\infty$
SCFM	Cubic feet per minute at standard condition
S_h	Effective heat source
S_m	Effective body force
St	Stanton number, $h/\rho_\infty U_\infty c_p$
St_o	Unblown Stanton number
St^*	Stanton number defined as $h^*/\rho_\infty U_\infty c_p$
ΔSt	$St(\theta = 0) - St(\theta = 1)$
T	Local average temperature
t	Temperature
T_{cav}	Effective casting temperature
T_g	Measured gas temperature
U	Total conductance of heat transfer
U,V,W	Local average velocities in x-, y-, and z-coordinates
u,v,w	Velocities in x-, y-, and z-coordinates
U_x	x-component of injection velocity averaged over A_h

U_τ	Friction velocity $\sqrt{\tau_o/\rho}$
U^+	U/U_τ
V_o	y-component injection velocity averaged over A
V_o^+	V_o/U_τ
$V_{o,e}^+$	Effective V_o^+ necessary to calculate the transport properties
x	Distance in the main free-stream direction; also coordinate
X_{vo}	Virtual origin of turbulent boundary layer
X^+	$U_\tau x/\nu$
y	Distance from the wall, perpendicular to the wall; also co-ordinate
y^+	$U_\tau y/\nu$
y_o	Source distance in Reference 45
z	Distance perpendicular to free-stream direction and y-direction; also coordinate

Greek Symbols

α	Thermal diffusivity
δ	Boundary layer thickness
$\delta(\ )$	Uncertainty of ( )
$\Delta(\ )$	Difference of ( )
δ_1	Displacement thickness $\int_o^\infty (1 - \rho u/\rho_\infty U_\infty)dy$
δ_2	Momentum deficit thickness $\int_o^\infty \frac{\rho u}{\rho_\infty U_\infty}(1 - \frac{U}{U_\infty})dy$
Δ_2	Enthalpy thickness $\int_o^\infty \frac{\rho u}{\rho_\infty U_\infty}\left[\frac{h - h_\infty}{h_o - h_\infty}\right]dy$

	(1) Emissivity of plate
	(2) Heat exchanger effectiveness
	(3) Arbitrary small number
ε_H	Turbulent diffusivity for heat
ε_M	Turbulent diffusivity for momentum
η	Adiabatic effectiveness, $(T_{a.w.}-T_\infty)/(T_2-T_\infty)$
θ	Non-dimensional secondary injection temperature, $(T_2-T_\infty)/(T_o-T_\infty)$
κ	Von Karman constant, 0.41
λ	General property diffusivity
λ_o	λ without discrete hole blowing
μ	Dynamic viscosity
ν	Kinematic viscosity
ρ	Density
τ	(1) Shear stress
	(2) Time coordinate
τ_o	Wall shear stress
ϕ_1	$\dfrac{St/St_o}{\dfrac{\ell n(1 + B_h)}{B_h}}$ for $\theta = 1.0$
ϕ_2	$St/St_o\Big\vert_{Re_{\overline{\Delta}_2}}$ for $\theta = 0.0$

<u>Subscript</u>

2	Secondary gas stream
a.w.	Adiabatic wall

o	Wall
d.a.	Dry air
hom.	With the homogeneous boundary conditions
non-hom.	With the non-homogeneous boundary conditions
st	Standard condition
T	(1) T-state
	(2) Total
t	Turbulent flow
∞	Free-stream (free-stream recovery if temperature)

<u>Superscript</u>

$(\ )'$	Turbulent fluctuation
$\tilde{(\ )}$	Local variation of the property
$\bar{(\ )}$	Local average of the property

TURBULENT BOUNDARY LAYER ON A FULL-COVERAGE FILM-COOLED SURFACE - AN EXPERIMENTAL HEAT TRANSFER STUDY WITH NORMAL INJECTION*

by H. Choe, W. M. Kays, and R. J. Moffat

CHAPTER I

INTRODUCTION AND BACKGROUND

It is of practical interest to study the heat transfer behavior of a turbulent boundary layer on a full-coverage, film-cooled surface. The term "full-coverage film cooling" refers to a surface containing an array of small holes through which a coolant is injected to protect the surface from a hot fluid flowing parallel to the surface. Other methods to accomplish the same effect include transpiration cooling using a porous surface, film cooling by injection through slots in the surface, and porous-strip film cooling. In many situations film cooling through three-dimensional discrete hole arrays, such as shown in Figure 1.1, is a more practical method. This is especially true for the blade-cooling problems encountered in a high performance gas turbine. Such an engine requires the highest attainable thermodynamic cycle temperature and high pressure. In the critical temperature range, a reduction of about 20°F in the blade temperature can double the life of the blade [1].

In the study of a boundary layer problem of this type there are a great many variables, both thermodynamic and geometric, which might affect the operation of the real system. This program has been restricted to uniform free-stream velocity and temperature, low velocity and low temperature difference to approximate constant property flows, and also restricted to obtaining local average heat transfer coefficients. In a practical situation, other effects may also play a significant role -- effects of variable fluid properties, high Mach number, varying free-stream velocity, etc. Investigators of turbulent boundary layers have

---

*Part of the material presented in this report was submitted by Mr. Choe to Stanford University in 1975 as a thesis in partial fulfillment of the requirements for the degree doctor of philosophy.

generally studied relatively uncomplicated basic cases where only a single unknown effect is present. When applied to actual conditions, the above-mentioned effects are then superposed on the known fundamental case.

In discrete hole, full-coverage film cooling there are many possibilities for geometry changes. In this particular program, a circular hole array with normal hole injection into the turbulent boundary layer is considered, with two different pitch-to-diameter ratios, which happen to be of particular interest to the gas turbine blade cooling problem. There are two regions of interest: the discrete hole, or full coverage, blowing region, and the recovery region downstream. Both regions are considered in this program.

A. Review of Previous Work

Full coverage film-cooling through discrete hole arrays can be approximated as transpiration cooling in the limiting case where the discrete holes are very close together and small relative to the sublayer of the boundary layer. Transpiration cooling through a uniform porous plate has been thoroughly investigated [2-9], and there already exist several two-dimensional boundary layer computing schemes which have the capability of handling very general boundary conditions, including wall mass transfer [10].

Since a row of holes can also be approximated as an equivalent slot, full-coverage film cooling has many similarities to conventional slot-film cooling. The following section will concentrate on a review of film cooling in general, including both slot and multiple holes.

A.1 Film Cooling in General

Wieghardt [11] investigated the de-icing problem on an airplane wing using a two-dimensional slot with nearly tangential injection, i.e., injection parallel to the surface. He correlated his experimental results in terms of an adiabatic wall effectiveness, η , and a parameter $x/(S \cdot M)$, where η is defined as

$$\eta \triangleq \frac{T_{a.w.} - T_\infty}{T_2 - T_\infty} \tag{1.1}$$

Here x is the distance downstream from the slot, S is the width of the slot, and M is the ratio of the mass flux through the slot to the mass flux in the free-stream. T_∞ is the free-stream temperature, T_2 is the coolant temperature, and $T_{a.w.}$ is the temperature assumed by an adiabatic wall downstream from the slot.

Seban [12], Seban and Back [13], and Hartnett et al. [14] investigated adiabatic wall effectiveness, and a heat transfer coefficient defined by:

$$\dot{q}_o'' \triangleq h^*(T_o - T_{a.w.}) \tag{1.2}$$

In this equation T_o is the actual surface temperature at some point downstream from the slot, and $T_{a.w.}$ is evaluated from the adiabatic wall effectiveness, η , for the same conditions. In other words, two different experiments are carried out to evaluate h^* , one with an insulated surface to establish η , and a second with an active heat transmitting surface. These experiments were conducted using a two-dimensional slot with tangential or near-tangential injection. The main conclusion of their investigations was that h^* had nearly the same value as the heat transfer coefficient for the case of no film cooling, except for the region very close to the slot exit. Most investigators in the field have concentrated on the acquisition of adiabatic wall effectiveness for various geometries: the injection angle was included by E. Papell [15], Haji-Sheikh [16], Artt et al. [17], Repukhov et al. [18], and Metzger et al. [19]. The thickness of the injection slot lip was varied by Kacker and Whitelaw [20]. Variable free-stream velocity was considered by Pai and Whitelaw [21] and Seban and Back [13], the turbulence level in the slot by Kacker and Whitelaw [20], and the free-stream turbulence level by Carson and Talmor [22]. Instead of a slot, a porous strip was used by Goldstein et al. [23], Escudier and Whitelaw [24], and Nishiwaki et al. [25]. Also, continued investigations on the tangential injection geometry were done by Pappel and Trout [26] and Samuel and Joubert [27]. Multiple slots and multiple rows of louvers were studied by Chin et al. [28], and a multiple row of holes by Pappel [15]. The holes studied by Pappel were very closely spaced to approximate slots.

The practice of evaluating only η was justified on the basis that the critical region for the application of film-cooling is generally some distance downstream from the location of injection.

A.2 Discrete Hole Film Cooling

Goldstein et al. [29] studied the variation of η around and downstream from a single circular hole, and Goldstein et al. [30] studied a row of holes with normal hole injection, and 35° inclined injection, and 15° and 35° skewed injection. Metzger and Fletcher [31] investigated heat transfer and adiabatic wall effectiveness for discrete hole injection. Eriksen [32] studied heat transfer with the same geometry used by Goldstein et al. [29,30], and also obtained laterally averaged heat transfer coefficients and η. LeBrocq et al. [33] investigated the behavior of η with a plate which was totally covered with a discrete hole array of $P/D = 8$, with an inline and a staggered pattern. They also investigated the effect of density, and they provided detailed velocity profiles around the holes. Launder and York [34] studied the effect of slant angle and acceleration on the same geometry as LeBrocq et al. [33]. Heat transfer data were not taken in the above two studies. Burggraf and Huffmeire [35] studied η and h^* with two rows of holes. Nina and Whitelaw [35] studied η for a discrete hole tangential slot which consists of a row of circular holes.

Ramsey and Goldstein [37] investigated temperature profiles, velocity profiles, and turbulence intensity profiles after a single hole injection. The turbulence data and the velocity profiles were taken by a hot-film probe. Metzger et al. [38] investigated heat transfer behavior on a full-coverage, film-cooled surface using a method outlined in Metzger and Fletcher [31].

A.3 Analytical Methods

For two-dimensional, slot-film cooling, several simple analyses have been proposed. One is from Stollery and El-Ehwany [39] and is basically an integral analysis with mass and energy addition into the turbulent boundary layer as a result of slot injection. This model predicts

η to be infinity at the location of injection. The model was modified by Libbrizzi and Cresci [40], and Kutateladze and Leont'ev [41], to give $\eta = 1.0$ at the location of injection. These analyses use assumed profiles for temperature and velocity.

A more thorough integral equation analysis was performed by Nicoll and Whitelaw [42], and by Haji-Sheikh [16]. Both used empirical correlations for shape factor and shear stress. Pai and Whitelaw [43] used a two-dimensional boundary layer finite difference procedure for prediction of η . For discrete hole tangential slot cooling, Patankar et al. [44] used a three-dimensional parabolic finite difference procedure for prediction of η .

For film cooling using a single hole, Eriksen et al. [45] suggested the following simple three-dimensional model. Neglecting all velocity components except U_∞ , and assuming that eddy diffusivity, ε_H , is constant throughout the field, one can obtain the governing equation,

$$U_\infty \frac{\partial T}{\partial x} = \varepsilon_H\left(\frac{\partial^2 T}{\partial x^2} + \frac{\partial^2 T}{\partial y^2} + \frac{\partial^2 T}{\partial z^2}\right) \tag{1.3}$$

Then approximating the injection fluid with a different temperature than the main flow as a point source, or line source, some distance, y_o , above the wall, they determined ε_H from experimental data on η , and y_o from temperature profiles. For a row of holes, or multiple rows of holes, superposition of this solution was suggested.

Comparison with their experiments showed that the method gave a good prediction far downstream of an injection hole, but is not good near the injection hole. Herring [46] formulated a two-dimensional boundary layer procedure by averaging the three-dimensional governing equations in the lateral direction. He used the turbulence energy equation to provide the eddy viscosity. He predicted several velocity profiles but did not predict heat transfer data. Also his velocity profile predictions did not give a good detailed comparison near the wall, which is important for heat transfer studies and for shear stress evaluation at the wall.

There have apparently been no further developments in the prediction of film cooling with a single hole or an array of holes. The analysis of Eriksen et al. did not view the problem as a boundary layer phenomenon. The actual situation is, however, more boundary-layer-like, except for a small area behind the jet where flow separation is possible. Herring was the first to use the two-dimensional boundary layer equations for the three-dimensional, angled-injection problem.

The main difficulty with all of the analytical attempts has been that there is not yet a way to handle the three-dimensional problem properly, and the experimental results have not been successfully correlated, either.

A.4 Experimental Methods

There are various methods for the acquisition of data for film cooling. In most cases, investigators have used film "heating" instead of film cooling, since for small temperature differences the non-dimensional parameter, η , must be the same for both cases.

A.4.1 Methods for the Acquisition of η

1. Use of an Adiabatic Wall

This is the most common method of obtaining adiabatic wall effectiveness. Investigators have normally used a relatively thin sheet of insulating material which is instrumented with imbedded thermocouples, with the space underneath stuffed with soft insulating materials such as fiberglass. With this method a two-dimensional map of η can be readily obtained. To obtain laterally-averaged values of η , signals from the several thermocouples at the same x-location are laterally averaged. Using infrared radiometers, Mayle and Camarata [47] and Blair and Lander [48], used urethane blocks to form the test section, and then used black paint to obtain a final finish on the top surface. With this method, they could obtain a detailed η-map, as well as η averaged across the channel at particular x-locations.

2. Use of a Mass-Transfer Analogy

This method relies on the fact that the turbulent Lewis number, $Le_t \simeq 1.0$ (Nicoll and Whitelaw [42]). The method eliminates any suspicion as to whether the adiabatic wall used is truly adiabatic or not. LeBrocq et al. [33], Launder and York [34], Kacker and

Whitelaw [20], and Pederson [49] used this scheme. To get the wall mass concentration, they used a Klathomagraph or a similar mass concentration analyzer.

3. Use of a Constant-Temperature Wall

Metzger et al. [19] used this method to obtain data on η. They used a transient technique to get heat transfer coefficients, then plotted the results as h vs. θ, where h denotes the heat transfer coefficient, based on surface to free-stream temperature difference, and θ, a non-dimensional injection gas temperature defined as:

$$\theta = \frac{T_2 - T_\infty}{T_o - T_\infty} \tag{1.4}$$

From these results it is possible to deduce η (and also h^*).

A.4.2 Methods for the Acquisition of h^*

1. Use of a Constant Heat Flux Wall

Most investigators have used this condition for the wall. Nichrome heaters are placed underneath a high-conductivity metal plate (Seban and Back [13]), or thin stainless sheets are used for heaters as well as the wall (Eriksen [32]). In this method, the power supplied to the heater is measured, as well as the wall temperature, and $T_{a.w.}$ can be evaluated from separately obtained data on η. Then h^* can be calculated from Equation (1.2).

2. Use of Constant Wall Temperature

a. Transient Tests

This technique uses a rather small and thick metal block for a test plate. Metzger et al. [19,31,38] used an aluminum block and recorded the temperature of the block while it was cooled; from that they could determine how much heat transfer occurred.

b. Steady State Tests

In this method, test plates are heated to some desired temperature, where wall temperature as well as the plate power are measured. Mayle and Camarata [47], and Blair and Lander [48], used this technique.

B. Approach to the Present Experimental Study

B.1 Presentation of the Basic Approach

Figure 1.2 shows η and St^*/St_o data from Wilson et al. [50]. Here St_o is the Stanton number based on the heat transfer coefficient, h_o, which would be obtained under the same free-stream and temperature conditions, but in the absence of film cooling. St^* is based on the heat transfer coefficient, h^*, defined by Equation (1.2). This is an example of the basic information needed to calculate surface heat flux, $\dot{q}''_o$, on a film-cooled surface using the conventional formulation of the problem employing the concept of effectiveness and adiabatic wall temperature.

There are two distinctly different regimes of interest in discrete hole cooling: the full coverage region and the recovery region. For simple film cooling with a slot, or a row of injection holes, the entire region of interest is the recovery region downstream of the injection point. When multiple rows of holes are employed (full-coverage film cooling), the recovery region downstream may still be of interest, but the main attention focuses on the wall surface between the holes. The conventional formulation of the film-cooling problem has been employed within the full coverage region, but was primarily developed to cope with the recovery region.

In this work we start with the observation that full-coverage film cooling has more of the characteristics of transpiration cooling than of the recovery region following a slot. In fact, the principal differences between full-coverage discrete hole injection and transpiration cooling are that the holes through which the coolant is injected are now large relative to the thickness of the boundary layer, and thus the coolant can be at a temperature different from the surrounding wall surface. In transpiration cooling it is generally assumed that the coolant is at the same temperature as the surrounding solid material, and that the holes are very small.

It is suggested that full coverage film cooling be treated as a special case of transpiration cooling (or, equivalently that transpiration cooling is a limiting case of full coverage discrete hole film cooling). This approach to the problem means simply that the concepts of adiabatic wall effectiveness, η , and h^* will be abandoned, and that heat transfer coefficients will be based on wall surface-to-free stream temperature difference. Behavior with a strong similarity to the simple transpired boundary layer should be anticipated. The problem of non-equilibrium between the injected fluid temperature and the wall surface can be handled by a separate set of experiments on the same apparatus. Since the applicable thermal energy differential equation of the boundary layer is linear in temperature, superposition can be used to predict performance for any injection temperature, if two fundamental data sets are available. The theory for this will be discussed later.

One advantage of this approach can be seen immediately by reference to Wilson's data in Figure 1.2. To determine whether a given system performs well or not, or how well it performs, there is no other way than calculating $\dot{q}''_o$ itself and comparing this with the value of $\dot{q}''_o$ without film cooling in a comparable condition. In transpiration cooling, however, St/St_o data directly give quantitative information on how well the system acts to reduce the heat flux. This is possible because in the heat flux evaluation the temperature difference of (T_o-T_∞) is used which is the same as for the non-film cooled surface. It seems obvious that if we follow the formulation of transpiration cooling, the interpretation of film-cooling data could be much simplified.

The flow in the boundary layer of a discrete hole, full-coverage situation is strongly three-dimensional. To resolve this problem (which is not attackable at this time), we shall need some type of averaging. An ensemble average would yield a periodic steady three-dimensional turbulent flow. To have some hope of analytic success it is necessary to make the problem two-dimensional. There are several methods of averaging which would achieve this goal. It was also desired that the averaging method be consistent with the experimental approach. This led to <u>local averaging</u>, which will be defined later.

Making room for an analytical approach is very important, because there should be a systematic way to handle the variety of geometry changes and boundary condition changes, otherwise the acquisition of all the data required will take too much money and too much effort.

B.2 Determination of Operating Domain

Review of the previous investigations lead to the following choice of parameters:

(A) $M \simeq 0.1 \sim 1.0$

Most investigators have agreed that for $M \geq 1.0$ there is almost no cooling effect with normal injection, due to jet penetration outside the boundary layer (e.g., Launder et al. [33,34] and Goldstein et al. [29,30]). With $P/D = 5$ and 10, $M = 1.0$ corresponds to F of 0.032 and 0.008 .

(B) $P/D = 5$ and 10

Most investigators have been interested in the range of $P/D = 5 \sim 10$. Metzger and Fletcher [31] used $P/D \cong 1.5$, Goldstein [30] $P/D = 3$, and Metzger et al. [38] $P/D = 4.8$, but the practical gas turbine blade-cooling designers are not interested in such a small P/D value, because it is more prone to structural failure.

Also, a staggered pattern was chosen, because LeBrocq et al. [33] showed that a staggered pattern performs better than an in-line pattern.

(C) $Re_{\bar{\delta}_2} \simeq 500 - 5000$ at the Beginning of Injection

Most investigators had a very thin boundary layer at the point of injection. Our purpose was to include the effect of $Re_{\bar{\delta}_2}$ on the heat transfer. LeBrocq et al. [33] had test plates which had discrete holes from the beginning of the plates. Metzger et al. [38] probably had a very small $Re_{\bar{\delta}_2}$ at the beginning of injection. This gives the range of Re_x from 1.7×10^5 to 5×10^6 , including the recovery region.

(D) $Re_{\bar{\Delta}_2}$ at the Beginning of Injection

Other investigators did not report this parameter explicitly. However, for the flat plate, this is the primary variable which correlates

St . The present program investigates the $Re_{\overline{\Delta}_2}$ in equilibrium with $Re_{\overline{\delta}_2}$, or with an unheated starting length before injection.

(E) $Re_{\infty,D} \simeq (0.6 \sim 2.2) \times 10^4$ $(Re_{\infty,D} \triangleq U_\infty D/\nu_\infty)$

This is a rather strange combination for Reynolds number. The ratio $Re_{\overline{\delta}_2}/Re_{\infty,D}$ is exactly $\overline{\delta}_2/D$, and once $Re_{\overline{\delta}_2}$ is considered, it is rather the choice of the investigator whether $Re_{\infty,D}$ is preferred over $\overline{\delta}_2/D$. However, in this case $Re_{\infty,D}$ is a non-dimensional number more commonly used in film cooling. The choice of this range of $Re_{\infty,D}$ gives $\overline{\delta}_2/D$ of 0.064 to 0.24 at the starting point of injection.

(F) $\theta = 0.0 , 1.0$

θ is a non-dimensional secondary injection temperature. Only two values of θ are needed since we can evaluate St at other values of θ by superposition (see Chapter III).

(G) Injection Angle - Normal to Wall

There have been experimental studies which employed non-normal injection angles. In this program, however, only normal injection is considered. This will be the basic case to which slant or compound angle injection can be compared.

(H) The Shape of Hole Geometry: Circle

There has been one experimental study by Goldstein et al. [51] for non-circular geometry. In the present study, however, straight, circular cylindrical holes are considered. For a general study of the effect of variations in shape, the three-dimensional, full N-S equations and energy equation have to be solved. This is not possible at present.

(I) Test Conditions

$Pr = 0.715 \sim 0.718$, for the working fluid of air

$U_\infty = 30 \sim 110$ ft/sec (10 m/sec - 36 m/sec)

Test plate = 10 ft. (3.05 m) total, 2 feet (60.1 cm) blowing section plus one 4 foot (1.25 m) length of test section before and one after the blown section.

$T_2 = T_\infty$ and T_o .

Secondary air flow rate = 1 cfm - 50 cfm for each row

(473 cc/sec - 23,600 cc/sec)

$T_o - T_\infty$ = 20 - 30°F (11°C - 16.7°C)

T_∞ = Ambient

D = 0.406 inch (1.03 cm)

Test section height = 8 inches (20.43 cm)

Test section width = 20 inches (50.8 cm)

Figure 1.1 shows the test plate geometry.

C. The Objectives of the Present Research

In the broadest terms, the objectives of the program are summarized as follows:

(1) Development of a test apparatus capable of accurate evaluation of the heat transfer behavior of a turbulent boundary layer with the injection of fluid through a discrete hole array.

(2) Determine the utility of a new formulation for the film cooling problem, unifying the theory of transpiration cooling and film cooling.

(3) Experimental investigation of a basic heat transfer problem with uniform free stream velocity and temperature, uniform blowing with uniform temperature, and with low speed and small temperature difference between wall and free stream.

(4) Predictions of the locally-averaged heat transfer data.

For the construction of the test apparatus, the following goals were set up:

(a) The free-stream velocity must be able to be maintained uniform in the presence of strong blowing at approximately 30, 50, 80, 100 ft/sec (10 m/sec, 16.7 m/sec, 26.7 m/sec, 33 m/sec).

(b) The apparatus must have a low turbulence level, with uniform two-dimensional free-stream.

(c) The instrumentation system and operating control must be such that the validity of the results can be verified by energy balance tests over the full range of proposed test conditions.

(d) The apparatus must produce the generally-accepted Stanton numbers and velocity profiles for the unblown condition.

(e) Secondary air temperature should be able to be set at any temperature between ambient to about 45°F (25°C) above the ambient.

(f) Each row of holes must have independent control of the flow rate and in each row, the flow rate in each hole should be uniform within 1 1/2%.

(g) The apparatus must be able to change the momentum thickness at the beginning of injection.

(h) The test plate must be segmented with good insulation, to obtain the local average of heat flux.

(i) The apparatus must have a low level of noise.

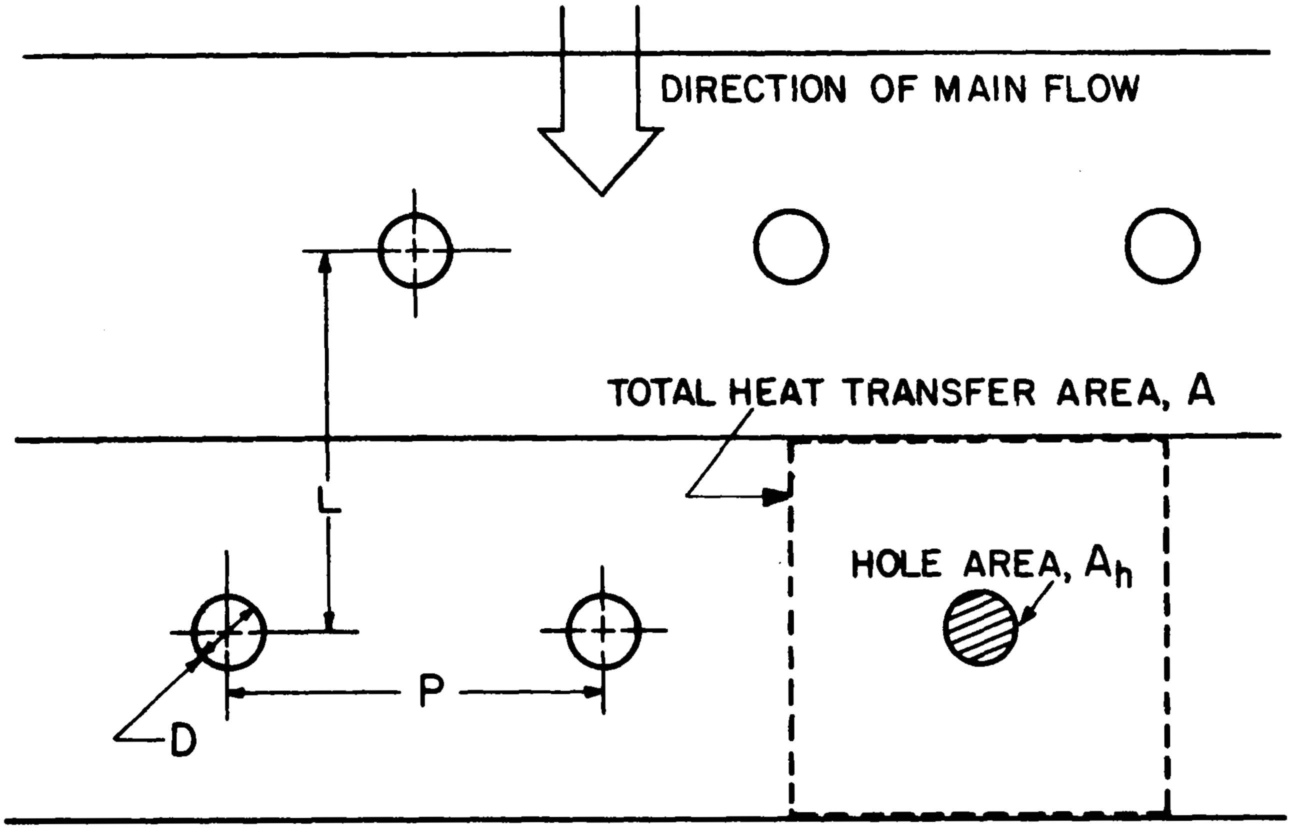

Figure 1.1 Test plate geometry for the present program.

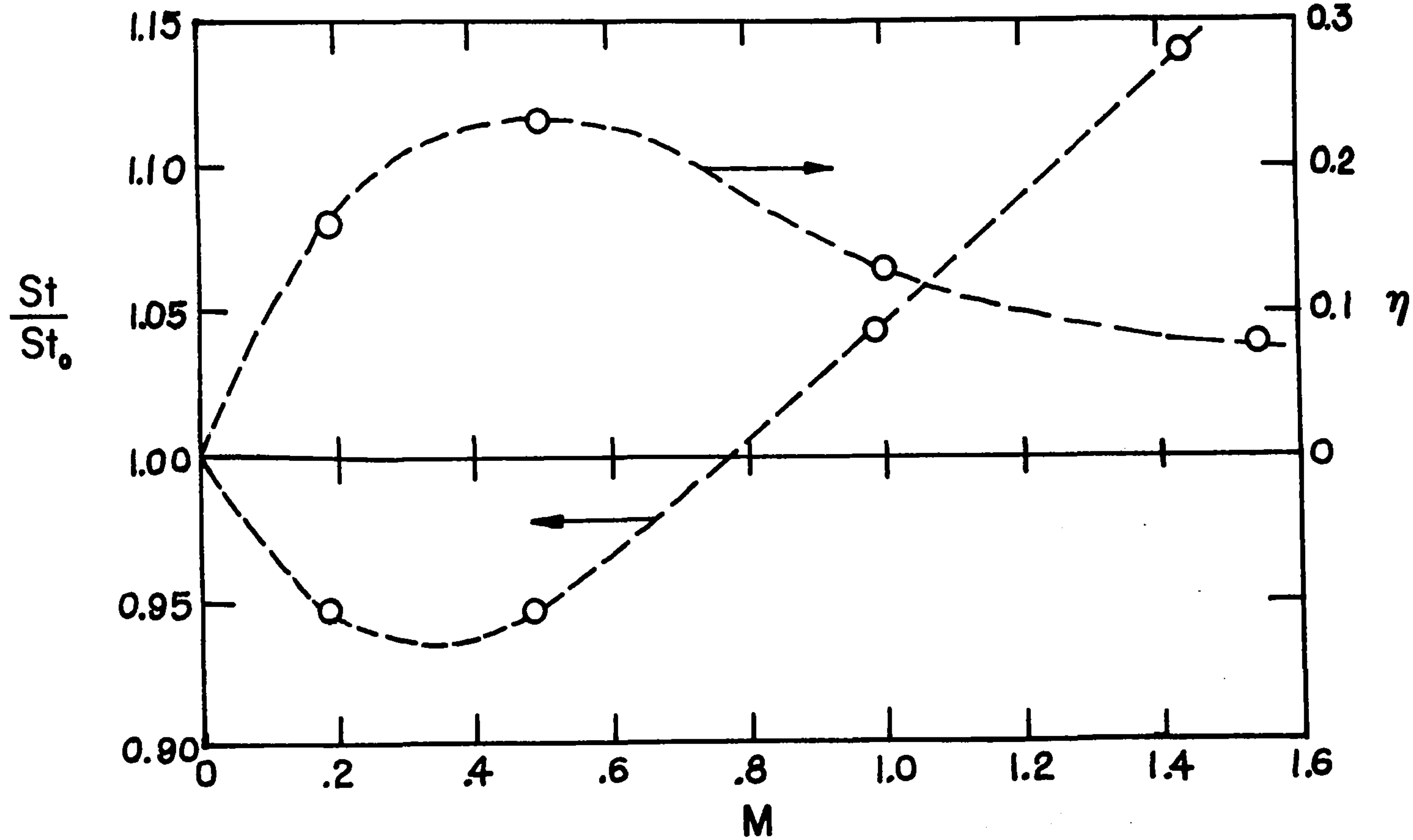

Figure 1.2 Example of heat transfer and effectiveness data from Wilson et al. [50].

CHAPTER II

THE EXPERIMENTAL APPARATUS

The apparatus used in these experiments has a basic arrangement similar to the existing transpiration rig described by Moffat [2]. This apparatus will be called the Discrete Hole Rig. Figure 2.1 shows the overall view of the Discrete Hole Rig.

A. Brief Description

The Discrete Hole Rig is a low speed, subsonic, closed-loop wind tunnel about 10 ft (3.05 m) high, 4 ft (1.22 m) wide, and 23 ft (7.02 m) long. The tunnel's structure is shown in the block diagram (Figure 2.2). There are four loops:

(1) The main air loop, which starts from the primary blower of 7100 cfm (201 m^3/min) capacity and then passes through the return ducting, oblique header, heat exchanger, and screen pack and contraction nozzle combination to produce a uniform velocity across the plane and low turbulence level, then into the test section, plenum box and then back to the blower.

(2) The secondary air loop which takes air out of the plenum box using a secondary blower and passes it through a heat exchanger/heater box combination and through the control valves to the delivery tubes (where flowrate is measured) and manifolds for distribution to each hole.

(3) The cooling water loop, which supplies the two heat exchangers, consisting of an 80 gal. (302.8ℓ) capacity water tank and supply and discharge lines to and from the tank.

(4) The hot water loop, which heats the plates upstream and downstream of the blowing section, and has two temperature-controlled water heaters.

The test section is 8 in. high (20.32 cm), 20 in. wide (50.8 cm), and 10.0 ft long (3.05 m). There are 3 main sections in the test plate.

The first 4-foot (1.22 m) test section and the last 4-foot test section were previously used for McCuen's [52] and Morretti's [53] theses work. Each of these consists of 48 individual copper plates one inch (2.54 cm) wide, insulated by 1/32 in. (0.794 mm) thick Kel-F insulation. The first 24 plates do not have the capability of being heated. The last 24 plates can be heated by hot water through copper wave guides underneath the plates. All 48 plates are instrumented to measure temperature and each of the last 24 plates has a heat flux meter. The heat flux meter is a silver-constantan thermopile which measures the temperature difference across a 1/64 in. (0.397 mm) thick bakelite plate underneath the copper plate.

A 2 ft. (60.1 cm) blowing section is located between the above two sections. This consists of 12 copper plates, each 1/4 in. thick (6.35 mm), 2 in. wide (50.8 mm), and 18 in. long (45.7 cm). The first plate acts only as a guard heater for the second plate, and has no holes. From the second plate to the 12th plate, each has either 8 or 9 holes for secondary gas injection. Each plate has 4 iron-constantan thermocouples to measure the plate temperature and one electrical heater to heat the plate. For each row of holes, the temperature of the secondary gas is measured 4 in. (10.16 cm) underneath the test plate surface, and the total flow rate to each row is measured by a hot wire type flow meter. The secondary gas temperature is controlled to the desired level by adjusting the electric power to the secondary air heater system.

The tunnel side walls and top wall are made with 1/2 in. thick (1.27 cm) plexiglass. One side wall has static pressure taps used to measure free stream velocity. The static pressure taps are 4 in. (10.16 cm) above the test plate to eliminate the effect of discrete hole blowing. The top wall has three flexible strips: two were needed for adjustment of the top wall to maintain uniform free stream velocity through the blowing section, and one allows introduction of an acceleration in the foreplate to provide small momentum thickness at the beginning of blowing.

In the following sections, detailed descriptions of the test apparatus, instrumentation, and qualification of the rig appear.

B. General Physical Arrangement

B.1 Primary Air System

The main air velocity in the test section is varied by changing the pulleys and belts on the blower and motor drive. This gives nominal test section velocities of 30 ft/sec (10 m/sec), 55 ft/sec (16.7 m/sec), 80 ft/sec (26.7 m/sec), and 110 ft/sec (33 m/sec). Air enters the main test section through an oblique inlet header to the heat exchanger; a design based on recommendations by London et al. [54]. Its shape was specified for uniform flow distribution and minimum pressure loss.

A screen pack follows the heat exchanger to reduce the non-uniformity of the main stream velocity and to reduce the turbulence level. It contains four stainless steel, #40 mesh, 0.0065 in. (0.165 mm) dia. wire screens. Based on the work of Schubauer et al. [55], this screen pack should reduce mean velocity maldistribution by a factor of 1200 and turbulent fluctuations by a factor of 10.

The screens are followed by a three-dimensional nozzle to provide a uniform inlet velocity field to the test section. The nozzle accelerates the flow from the screen pack to the test section inlet with 11.1 to 1.0 area contraction. The nozzle wall design started with the shape recommended by Rouse & Hassan [56]. The wall shape has been chosen such that the first three derivatives of flow area are zero at the nozzle exit. There is a slight acceleration in the inlet section of the nozzle to avoid separation in this region. This was accomplished by designing the nozzle length for 40 in. (101.6 cm) and cutting off the first inch when the nozzle was actually built. A Teledeltos model of each of the nozzle walls was used to check that the nozzle smoothly accelerated the flow with no tendency for separation at inlet or exit. The 8 in. (20.32 cm) height was selected to ensure that the top wall would not interfere with the injected gas at the highest blowing rate. The downstream edge of a boundary layer trip, a sharp edged square strip 1/32 in. x 1/4 in. x 20 in. (0.794 mm x 6.35 mm x 50.8 cm), is located four in. (10.16 cm) downstream of the nozzle to produce a high momentum thickness at the blowing section. To get low momentum thickness at the blowing section, the downstream edge of a trip 1/16 in. x 1/4 in. x 20 in. (1.588 mm x 6.35 mm x 50.8 cm) is located 2 in. (5.08 cm) upstream of the blowing section (see Figure 2.3).

The test section cross section consists of four sides: the bottom (the test plates), the top (the top wall), and the two sides (the side walls). Two side walls are fastened to the test plate structure and sealed with RTV cement. The movable top wall can be pivoted about its upstream end to provide for either an increasing or decreasing flow area in the flow direction. One side wall has static pressure taps 12 in. (30.5 cm) apart in the upstream and downstream plate regions and 8 in. (20.3 cm) apart in the blowing region. In the beginning of the blowing section, pressure taps are located 6 in. (15.24 cm) apart to sense the steep change of pressure. These taps are four in. (10.16 cm) above the wall so that they are not much affected by strong discrete hole blowing.

All tests described here were conducted with uniform free stream velocity. To obtain this condition, the top wall was set for each run by adjusting its elevation until there was no measurable change in the static pressure along the test section. In practice, local deviations of 0.002 in. (0.05 mm) of water have been accepted in static pressure. A probe sled, which spanned the test section, was locked onto the side walls in fixed positions over the center of the test plate at each measuring station. The probes, supported from this sled, extended down through access holes on the top wall. These access holes have plexiglass plugs which smoothly close the holes inside the tunnel when not in use. The access ports have two shapes: 3/4 in. (1.9 cm) circular holes and 1 7/8 in. x 2 1/2 in. (4.76 cm x 6.35 cm) rectangular holes. There are two rectangular holes in the blowing region, one between and above the seventh and eighth plates, and the other between and above the tenth and eleventh plates. These rectangular holes are for detailed investigation of velocity and temperature profiles around the injection holes. The probe sled at these stations can move in the flow direction with 1/4 in. (0.63 cm) intervals up to 1 in. (2.54 cm). This was accomplished by having locking holes on the top edge of the side walls at 1/4 in. (0.63 cm) intervals. The traversing mechanism itself can move on the sled in the lateral (z-) direction with intervals of 0.2 in. (0.51 cm), covering two in. (5.08 cm). This combination provides 55 measuring stations. The circular access holes are located along the centerline. In addition to these, at the exit of the contraction nozzle, at the starting point of blowing, and right after the blowing section, full sets of circular access holes are provided, extending across the width of the test section. These are primarily to check the uniformity of the boundary layer growth in the lateral direction (two-dimensionality check).

B.2 Secondary Air Supply System

The secondary blower can deliver 2200 cfm (62.2 m^3/min) of air flow rate and develops a head of 28 in. (71.1 cm) of water at 3300 rpm. For the low flow rate of secondary injection, it delivers about 500 cfm (14.15 m^3/min) with a head of 2 in. (5.08 cm) of water.

The secondary air from the blower is delivered to a wooden box, which contains a 5-row, 18 in. x 24 in. (45.72 cm x 60.96 cm) heat exchanger, and to a heater box which consists of twelve 220 volt 1 kw air heater elements. Seven sheets of copper screen are provided to make the temperature uniform, and a distribution header with eleven 2 in. (5.08 cm) pipes and 2 in. (5.08 cm) brass ball valves for the control of secondary air flow rate.

Flexible tubing connects each valve outlet to one of eleven PVC pipes, each 7 ft. long (2.14 m), and used to meter the secondary air flow rate in each row of holes. In each pipe there is a hot wire type flowmeter (see Appendix D) developed for this apparatus to handle the wide range of flow rate (1 cfm (0.472 ℓ/sec) to 50 cfm (23.6 ℓ/sec)) required for the secondary air system. For such a requirement orifice meters or rotameters would have been bulky, and expensive. Flexible tubing delivers the secondary air stream from the flowmeters to the 11 flow manifolds (Figure 2.4) located underneath the blowing test section. Delivery tubes connected with rubber tubes allow a small dislocation of PVC pipes on the manifold from the test section blowing holes. Ball valves were adjusted to achieve uniform flow in each hole in one row within 1.5% (see Manifold Valve Adjustment, Appendix E). Then the valve handles were removed to protect the calibration.

The secondary air system is enclosed to reduce heat transfer with the ambient.

B.3 Blowing Section

This two foot section provides the particular geometry for blowing. In this experiment, a staggered circular hole pattern normal to the wall is employed with $P/D = 5$ and $D = 0.406$ in. (1.03 cm) (Figure 2.5). The aluminum casting which supports the copper plate is 22 in. (55.88 cm) wide, 24 in. (61 cm) long, and 3 1/2 in. (8.89 cm) high. The assembly has twelve 2 in. (5.08 cm) wide, 18 in. (45.72 cm) long, and 1/4 in. (6.35 mm) thick copper plates yielding a heat transfer area 18 in. wide and 24 in. long. A photograph of a machined casting is shown in Figure 2.6. A cross section through one of the plates and the compartment in the aluminum casting are shown in Figure 2.7. The casting used in this experiment was modified from the one used in the smooth transpiration rig.

Since copper is such a good conductor, two heater wires for each plate were sufficient to keep the temperature of the copper within 0.03°F (0.017°C) in the flow direction on a single copper plate. To have symmetric heating, two 18 in. (45.72 cm) of AWG #28 chromel wires were imbedded into parallel heater grooves and epoxy-bonded to the copper plate. One end of the wires was jumpered with copper wire, and the other end was connected to the output terminal of a variable transformer. The heater resistance is about $8\ \Omega$.

To have well-stabilized power to the plates, the building power is passed through a servo-driven voltage stabilizer, then through a saturable-core type voltage stabilizer. The power source is used for the flow meter heaters as well as test plate heaters (Figure 2.8). After the voltage stabilizer, it goes to the step-down powerstat. This reduces the voltage to $25 \sim 40$ volts AC. Finally it goes to the individual powerstats to control the test plate power. This arrangement makes it possible to control the power over a wide range with accuracy. All electrical power cables are enclosed inside the conduit to minimize interference with the thermocouple readings. A switching arrangement permits the insertion of a precision wattmeter into each channel, as desired for data-taking purposes. The finished surface of the test plate assembly felt smooth to the touch, but during the operation, very small cracks in the plastic material in the joints appeared. These did not show any change in the hydrodynamic character of the tunnel.

Each plate has four thermocouples measuring surface temperature, about equally spaced across the span. For eight hole rows, they are 4.05 in. (10.3 cm) apart, twice the pitch distance, symmetric about the center. For nine hole rows, two inside thermocouples were 6.09 in. (15.45 cm) apart and two others 4.06 in. (10.3 cm) from the inside thermocouples, symmetric about the center. The 18 in. (45.72 cm) whole span of copper plate is used as a measuring area.

The thermocouples for measuring the plate temperature are set into the copper plate through 0.050 in. (1.27 mm) dia. holes, with their junction approximately 0.030 in. (0.762 mm) beneath the surface.

Five water passages through the aluminum casting webs are used to control the temperature of the casting. When conducting energy balance tests, either hot or cold water, as needed, was used to maintain the casting temperature within 5-10°F (3-6°C) from the test plate temperature.

B.4 The Surface Condition of the Test Plates

The test plates are made of copper and to minimize the radiation heat transfer from the surface, they were well polished with commercial copper polish. Right after polishing, the surface shone like a mirror, and the details of the surroundings could be well examined through the test surface. This mirror-like shine lessened as the experiments were continued, but it never disappeared. With these conditions, the surface emissivity was estimated from 0.05 to 0.15.

B.5 Thermal Boundary Conditions

To give the proper thermal boundary layer to match the thin momentum layer, 24 cells of the upstream plate were heated using the hot water system. This provided momentum thickness and enthalpy thickness, at the starting point of blowing, comparable to the flat plate, constant wall temperature boundary layer. For the thick boundary layer condition, the same situation could not be achieved, because the upstream plate cannot be heated on the entire length but only on the downstream half of the plate. So, as a better defined boundary condition, a step wall temperature was used in the blowing section. To achieve this, all the polyflo lines were simply disconnected from the test plate, and in the last cell, a cold water line was connected to adjust the thermal boundary layer growth to the minimum.

C. Instrumentation

C.1 Temperature Instrumentation

All temperature measurements on the Discrete Hole Rig are made with iron-constantan thermocouples, except for the boundary layer traversing thermocouple, which is made with Chromel-constantan. Samples of the iron-constantan thermocouples and the Chromel-constantan thermocouple were calibrated against a Hewlett Packard Quartz Thermometer, which is accurate within 0.02°F (0.01°C). All four samples of iron-constantan showed the same calibration curve within the accuracy of calibration, ± 0.07°F , or ± 2 μV of the thermocouple signal. The calibration curves for iron-constantan thermocouples and those for Chromel-constantan were incorporated into the data reduction program.

All the thermocouple wires are brought together into the constant temperature zone box at the back of the console panel, where they are connected to rotary thermocouple switches leading to the display of the signal through a Hewlett-Packard Integrating Digital Voltmeter, Model 2401C. The boundary layer traversing thermocouple probe has its own ice bath and has an isolated circuit of its own. The thermocouple circuit is shown in Figure 2.9, along with the heat flux meter and flowmeter circuits. The thermocouple wires were made long enough to reach the constant temperature zone box. To avoid temperature gradients along the thermocouple wires, 1/8 in. polyflo tubing guided and covered all the thermocouple wires between the thermocouple junction and the constant temperature zone box. The constant temperature zone box is lined inside with 1/32 in. thick copper plate and insulated outside with aluminum foilbacked, rock wool insulation. One diagnostic thermocouple is provided to measure the temperature difference across the diagonal of the zone box. If this diagnostic probe showed larger than 7 μV, data were not taken. All iron-constantan thermocouples shared a single ice bath reference junction.

For the thermocouples measuring the test plate temperature, enough immersion depth is given following Moffat [57] to reduce the conduction error. Thermocouples for measuring the casting web temperatures were also given enough immersion depth. For the free stream and the secondary air, there were no accountable errors in temperature measurement.

The four thermocouples from each plate were wired in parallel to one switch terminal in the constant temperature zone box. This scheme gives a good average temperature of the plate, since the signals and the wire resistances have almost the same magnitudes. Three thermocouples from each row of holes for measuring the secondary air temperature were also ganged together to give an average secondary air temperature.

For the temperature traverse in the boundary layer, Chromel-constantan thermocouples with 0.003 in. (0.08 mm) diameter were used. Enough conduction length was given to ensure negligible conduction error, following Blackwell [58]. Two thermocouple probes were made -- one to measure the temperature on the centerline of the traversing mechanism and the other to measure the temperature 1 in. upstream.

C.2 Pressure

All the static pressure and free stream dynamic pressure measurements were made with inclined manometers. The dynamic pressure for boundary layer velocity profile was measured with pressure transducers which were used by Healzer [59].

The static pressure taps were made in conformity with the existing HMT rig (see Simpson [3]). For the pitot tubes, a 0.020 in. (0.508 mm) OD hypodermic needle was used without being flattened, following Andersen [9].

C.3 Electric Power

Power delivered to each plate of the blowing section was measured by a precision AC wattmeter, which has been used in the measurement of electric power for the smooth transpiration rig. As shown in Figure 2.8, the power can be measured for each plate with a single wattmeter. The wattmeter calibration which had been used for the smooth transpiration rig was adopted, since the same instrument was used. Circuit analysis was done to account for the insertion loss (see Appendix F).

C.4 Heat Flux Meter - the Calibration of

The heat flux meter calibration was made with specially made calibration heaters. Power to the heater was measured with a Weston precision voltmeter and ammeter, both with accuracy of 1/2%. This gives a calibration accuracy of about 1%. In the process of heat flux meter calibration, the conductances between adjacent plates including the two end plates in the blowing section were measured (see Appendix G).

The initial calibration of several heat flux meters from the upstream and downstream plates showed constants 5-10% higher than Morretti's [53] recorded values.

A careful review of McCuen's [52] and Morretti's theses revealed that the calibration heater they used had a different design than the present one. They used a single nichrome heater wire, which spanned the whole width of the test plate. However, in the present case, the tunnel width is 20 in., with a more-or-less adiabatic condition for one inch on each side. To simulate this in the calibration process, the calibration heater length was made to 20 in., and instead of using a single wire, fifteen closely and uniformly laid parallel wires were used to give uniform heat flux. The difference between Morretti's and the present calibration represents a heat leak from the center to the side of the channel, if the plate is heated by electrical heaters and cooled by the cooling water. The opposite trend in heat loss will occur when in operation, because the test surface has less area than the heating area in the copper wave guide.

D. Rig Qualification

All experiments include some degree of uncertainty. In this section, to qualify the rig means to specify clearly the uncertainty bounds and to reduce them if they are unacceptably large. To reduce the uncertainty bounds, one has to propose an approximation to the heat transfer behavior of the complicated geometry of the real system or else to modify this apparatus. Then one has to devise an auxilliary experiment to confirm his approximation and to compare his model with the results of the real system. The system model is the Data Reduction Program - at least, that part which corrects for losses. By its nature, this operation is iterative, requiring simultaneous development of an analytical model and the apparatus.

In this program, the behavior of the boundary layer, the free stream, and the energy balance capability of the rig were demonstrated. In establishing the free-stream and boundary layer behavior, the spanwise uniformity of the free-stream velocity and temperature, the momentum thickness, and free-stream turbulence were checked. These investigations were to prove that the test tunnel provided a two-dimensional boundary layer with low free-stream turbulence. The energy balance results show the uncertainty bounds for the measurements of convective energy.

The final qualification tests were comparisons of the measured heat transfer behavior (under conditions of zero pressure gradient and no blowing) with the expected behavior of the flat, impermeable, smooth plate. These results showed that the agreement is within the expected uncertainty bounds.

D.1 Energy Balance Test

In the beginning of the experiment, four main heat transfer modes were considered for the heat losses. The four modes are:

1) Radiation heat transfer from the top of the copper plate to the plexiglass channel wall;

2) Conduction loss between the copper plate and the aluminum casting--the main loss was through the casting web, but the losses through the side rail and through the fiberglass insulation have a comparable magnitude; these were all lumped together to be treated as one loss because the effective potential for these losses is the same: $T_o - T_{cav}$, where T_{cav} is the effective casting average temperature;

3) Conduction loss between the adjacent plates -- these have very little contribution except the two end plates in the blowing section; except for the two at the end, theoretically estimated conductance was used; and

4) Energy lost by the secondary air stream before being injected into the main stream -- accounting for these losses also corrected for the true mean air temperature at the point of injection because the secondary gas temperature was measured four inches upstream of the point of injection. This mode of loss does not introduce any error in the enthalpy thickness measurement, but does yield an error in the Stanton number.

In the following subsections, the methods which identify each loss mechanism will be discussed.

(a) Conduction Test

In this test, conduction is the only loss mechanism. The side walls and top wall were taken off the test plate, and a 3 1/2-in. (8.9 cm) thick styrofoam block was placed on top of the test plates. No secondary air stream was present; all the test plates were heated to the essentially same temperature, and the casting was cooled by cold supply water. In this mode, the only heat transfer is by the conduction to the aluminum casting, and the electrical power supplied to the plate can be attributed to the conduction losses. The plate temperature and the casting temperature were measured. For the two plates at the ends, the conduction to the adjacent plates must be known because the upstream and the downstream plates normally have quite different temperature, as only the blowing section plates were heated. The conductances in the flow direction for the two end plates were measured in the process of heat flux calibration. From the five measured casting temperatures, twelve effective casting temperatures were calculated by linear interpolation of the five measured temperature. Then,

$$q_{COND,i} = KCOND_i(T_{o,i} - T_{CAV,i}) \tag{2.1}$$

where $\dot{q}_{COND,i}$ represents heat lost by conduction in i^{th} plate, $KOND_i$ the conduction loss constant for i^{th} plate. In reality, the styrofoam block has only 5 ∿ 6 times the thermal resistance of the insulation between the plate and the casting. To account for the heat lost through the styrofoam block, $KCOND_i$ was reduced by 15%.

This test was done twice, and the average of the two test results was used for the actual data reduction program.

(b) T2,EFF Test

With this test, the average temperature of the secondary air was measured at the injection point. This test also evaluated the total conductance between the secondary gas stream and the test plate. Nine pieces of styrofoam block, each of which had a matching hole with the plate's discrete hole, were placed on the plate with the holes aligned with the holes in the plate. The blocks served as a insulation to the secondary stream and also as mixers for achieving the mixed mean temperature at the exit. The following measurements were made: plate temperature, temperature of the gas leaving the styrofoam block (effective secondary temperature), gas temperature four inches upstream, and the secondary flowrate. Then, considering the system as a heat exchanger, we can get the following effectiveness equation:

$$\varepsilon \triangleq \frac{T_{2,eff} - T_g}{T_o - T_g} = 1 - e^{-Ntu} \tag{2.2}$$

where $T_{2,eff}$ is the effective secondary mean stream temperature, T_g the gas temperature measured four inches upstream, and

$$Ntu \triangleq \frac{UA}{\dot{m}c_p} = \frac{KCONV}{SCFM} \tag{2.3}$$

Here U is the total conductance of the system, A the contact area, $\dot{m}$ the mass flowrate, c_p the specific heat, SCFM the volume flowrate at standard conditions, and KCONV a constant proportional to the conductance UA which is a function of the flowrate.

From the measured temperature, the values of ε was evaluated and then from the effectiveness - Ntu expression, we can get KCONV as a function of SCFM*. The following correlation from data was obtained:

$$\text{KCONV} = 0.24 * \text{SCFM}^{0.35} \tag{2.4}$$

This expression is valid for the nine hole rows. If the row has n holes, SCFM was corrected by 9/n to get the proper flowrate in the individual holes; then KCONV was calculated. However, this is for the surface area of the pipe of the nine holes, so that n/9 was multiplied to get the effect from n holes. P/D = 5 geometry has n = 8 and 9 , and P/D = 10 has n = 4 and 5 .

After KCONV was obtained, $T_{2,eff}$ was calculated by measuring T_o,T_g and SCFM and by using Equation (2.2). Also the total convected energy in each row of holes, $\dot{E}_{CONV}$ was calculated as

$$\dot{E}_{CONV} = \dot{m}c_p\ (T_{2,eff} - T_g) \cong UA(T_o - T_{2,eff}) \tag{2.5}$$

where the last approximation is from the fact that $T_g \approx T_{2,eff}$, and that $T_o - T_{2,eff}$ is less liable to the measurement uncertainty.

One must know what portion of KCONV is directly from the copper plate to get the energy closure. There was no simple way of getting this information at the time of the energy balance test. Thus analytical estimations of the total conductance, and the conductance directly from the copper plate were made and the ratio was obtained as a function of SCFM. For the direct conductance from the copper plate, all the PVC pipe length which has direct contact with the copper plate, and the copper lip which has direct contact with the secondary air was considered, along with about 0.3 in. (0.762 cm) of Fiberglas insulation beneath the copper plate to account for the heat flux lines bending toward the PVC pipe.

The ratio of direct conductance to the total conductance, KFL, was obtained and expressed as

---

*Previously the average value of the KCONV = 0.32 was used. After a discussion with Mr. M. E. Crawford for this thesis work, KCONV was recast as a function of SCFM.

$$\text{KFL} = 0.21 + 0.0344 \log_{10} \text{SCFM} ,$$

$$\text{If} \quad \text{SCFM} \leq 5.0 \tag{2.6a}$$

$$\text{KFL} = 0.0762 + 0.226 \log_{10} \text{SCFM} ,$$

$$\text{If} \quad \text{SCFM} > 5.0 \tag{2.6b}$$

This result is for the nine hole rows. The rows which have n holes will have KFL calculated by SCFM multiplied by $9/n$ to get the proper flowrate in individual holes. After KCONV and KFL were obtained, the energy loss from the plate to the secondary gas stream was calculated as

$$\dot{q}_{FLOW} = \text{KFL} \cdot \dot{E}_{CONV} \tag{2.7}$$

In the above expressions, the casting was not assumed to be heated or cooled by external means. In reality, the casting temperature was controlled independent of T_o and T_g to minimize the heat loss. The correction to the external heating or cooling of the casting was simply made in the definition of ε of Equation (2.2). The denominator $(T_o - T_g)$ was expressed as

$$(T_o - T_g) = \text{KFL}(T_o - T_g) + (1 - \text{KFL})(T_o - T_g)$$

If there is no external heating or cooling to the casting, then $(T_{cav} - T_g)$ would be equal to $(1 - \text{KFL}) \cdot (T_o - T_g)$, because T_{cav} would have the temperature determined by the conductance ratio, KFL , between T_o and T_g . Thus $T_{2,eff}$ was expressed as

$$T_{2,eff} = T_g + \varepsilon \cdot \left[\text{KFL}(T_o - T_g) + (T_{cav} - T_g) \right] \tag{2.8}$$

The value of $T_{2,eff}$, then, was used for the calculation of $\dot{E}_{conv}$ and $\dot{q}_{flow}$.

(c) Flow Direction Conductance

The flow direction conduction loss, $\dot{q}_{FDCOND}$, was theoretically calculated and uniformly the conductance, S_i, was set as $S_i = 0.8$ in the expression

$$\dot{q}_{FDCOND} = S_i(T_{o,i}-T_{o,i+1}) + S_{i-1}(T_{o,i}-T_{o,i-1}) \tag{2.9}$$

(d) Radiation Loss

The effect of the channel geometry has negligible effect, and the radiating material in the air (vapor and CO_2) absorbs less than 3% of the radiated energy from the plate. Thus it is effectively calculated as

$$\dot{q}_{rad} = A_i \varepsilon_i \sigma (T_{o,i}^4 - T_\infty^4) \tag{2.10}$$

The emissivity of the surface, ε_i, was estimated from the suggested values which appear in the radiation property of copper surface and σ is the Stefan-Boltzman constant. Nominally, $\varepsilon_i = 0.12$ was used, and the hole area was considered black, which increases ε_i by 0.03 .

(e) Energy Balance Run

After all these loss mechanisms were studied and tested separately, they were put together in the Stanton number data reduction program. The total heat loss, $\dot{q}_{loss}$, was calculated as

$$\dot{q}_{loss} = \dot{q}_{cond} + \dot{q}_{flow} + \dot{q}_{FDCOND} + \dot{q}_{rad} \tag{2.11}$$

then the convected heat transfer on the surface of the copper plate was calculated as

$$\dot{q}_{conv} = \text{total power supplied} - \dot{q}_{loss} \tag{2.12}$$

and the plate Stanton number was calculated

$$St = \frac{\dot{q}_{conv}}{\rho_\infty U_\infty c_p (T_o - T_\infty) A} \tag{2.13}$$

where A is the total heat transfer area including the area of holes. The variable property correction was made to get the constant property

Stanton numbers. In the energy balance runs, the following conditions were maintained. The primary blower was run without cooling the primary heat exchanger. Then the main stream reached an equilibrium temperature, about 15°F (8.3°C) above the ambient temperature. The aluminum casting was cooled by cold water and the copper plate was heated to the same temperature as the main stream temperature. In this case, $T_o - T_\infty$ was maintained within $\pm$0.5°F ($\pm$0.3°C). This mode of operation eliminated the convective energy transfer and radiative loss from the plate. The main loss mechanisms were conduction loss and the flow loss due to the secondary air stream. The flow loss is not large unless the secondary gas stream temperature is distinctively different from the plate temperature. In the present runs, the secondary air temperature was about 1°F (0.55°C) different from the plate temperature. The runs were made at $M = 0.0$, $M = 0.45$, and $M = 0.7$, with $U_\infty = 55$ ft/sec (16.7 m/sec). These energy balance runs showed how much energy imbalance exists which indicated the accuracy of the energy measurement system. The results are shown in Figure 2.10. The accuracy of the power measurement is about $\pm$0.3 watt. This can be converted into the error in the Stanton number following Moffat [2], using the expression

$$\delta St = \frac{\delta E}{\rho_\infty U_\infty c_p \Delta T A} \tag{2.14}$$

Here $\Delta T = 23$°F (12.8°C), and U_∞ of 55 ft/sec (16.7 m/sec) were used. This Stanton number error, δSt, represents the Stanton number uncertainty caused by the uncertainty in the measurement of power. The uncertainty in St of $\delta St = 0.00005$ was found. The main reason for this high accuracy is believed to be the fiberglass insulation used underneath the copper plate.

The above result applies mainly to the $\theta = 1.0$ case, where the secondary gas temperature is the same as the plate temperature. For the $\theta = 0$ case, where the secondary gas temperature is much different from the plate temperature, the flow loss term, $\dot{q}_{flow}$, will be large. In this case, the convection coefficient in the PVC pipe was measured as KCONV, but KFL was not measured. The confidence level in the estimation of KFL in the worst case is about $\pm 20\%$. This much of the KFL change adds ± 0.6 watt to the power measurement uncertainty. This leads to the power measurement uncertainty in the $\theta = 0.0$ case of ± 1.0 watt. The Stanton numbers at $\theta = 0$ are generally high, so the percentagewise error for $\theta = 0.0$ is not much greater than that for $\theta = 1.0$. For the better accuracy for $\theta = 0.0$, an additional test would be necessary to measure KFL.

D.2 Hydrodynamic Qualification of the Tunnel

This part of the qualification was to prove that the flow in the channel was acceptably two-dimensional and that the velocity profiles were the accepted turbulent ones. Free-stream turbulence intensity was measured to show that the level in the free-stream was low enough. The stability of the hydrodynamic boundary layer was also proved by the experience of running the test rig under the various conditions.

Free-stream velocity was measured at five points over the plate upstream of the first row of holes with a Kiel probe. The velocity variation was within the measurement uncertainty.

The two-dimensionality of the boundary layer was demonstrated by taking the momentum thickness and the enthalpy thickness variation across the channel. Momentum thicknesses at the first plate on the blowing section were measured at the free-stream velocity of 55 ft/sec (16.7 m/sec). This showed very uniform boundary layer growths over the center span of the channel. At both ends of the channel width, momentum thickness was higher, which was also observed in Anderson [9] and which is believed to be due to the corner flow (Figure 2.11). For runs with a low momentum thickness, the main stream was accelerated in the region of the foreplate to produce a small boundary layer. Then the free-stream velocity was maintained at 40 ft/sec (12.2 m/sec) and the momentum thickness and the enthalpy thickness were measured across the channel, and it confirmed the above result again.

The data showed that the momentum thickness upstream of the first row of holes increases as M increases. This trend was consistent with every measurement of momentum thickness. Since the measurement station was only two in. upstream of the first row of blowing holes, this was obviously due to the flow blockage effect from the injected secondary air stream. Thus in the evaluation of virtual origin, the velocity profiles taken at $M = 0$ were used, and the increase of momentum thickness was considered as part of the discrete hole blowing effect on the hydrodynamics of the tunnel.

Figure 2.11 also shows the free-stream turbulence variation at $M = 0.6$, and one value at $M = 0$. With $M = 0$, free-stream turbulence level is about 0.4% and with $M = 0.6$ about 0.57%. The free-stream turbulence was remarkably uniform across the channel.

Figure 2.12 shows the velocity profiles for the flat plate conditions. One of the profiles was taken on the plate without holes, and the other on the plate where the holes are plugged up to produce $P/D = 10$. The comparison of these two profiles showed that the cork plug is so smooth that its effect is not felt in the velocity profile measurements. These two profiles showed good logarithmic regions and the proper wake strength. The region near the sublayer is slightly higher than expected perhaps because of pitot probe error near the wall. The skin friction coefficient in this case was found by fitting the $u - y$ to the logarithmic law of the wall in the range of $y^+ = 75$ to $y^+ = 125$ (Clauser plot). This represents the average shear stress obtained from three to five points. The two-dimensionality of the potential core and the boundary layer was confirmed; the stability of the tunnel was confirmed by several repeated measurements of the velocity profiles. Then it was decided to go ahead and take the flat plate, impermeable heat transfer data to give a final qualification of the rig.

D.3 Heat Transfer Qualification

The final qualification runs consisted of several cases of unblown heat transfer tests. The free-stream velocity was maintained at approximately 54 ft/sec (16.5 m/sec) and with the plate temperature about 25°F (13.9°C) above the free-stream temperature. The effect of changing the wall temperature level was not investigated because it was well investigated previously by Reynolds et al. [60] and Moffat [2]. After the foreplate was accelerated to produce the small momentum thickness, similar tests were made with P/D = 10 and P/D = 5 , and with free-stream velocity at approximately 40 ft/sec (12.2 m/s).

Figure 2.13 shows the results with free-stream velocity of 54 ft (16.5 m/s) and P/D = 5 . The prediction for this case was made by STAN5 [61]. The agreement is generally good. The prediction lies about 3-5% lower than the experiment. This is believed to be due to the roughness effect from open holes. In the recovery region, the heat transfer data have more scatter than in the blowing region. Since the heat flux meters are calibrated within 1% accuracy, this scatter is attributed to the incapability of the hot water system to produce a uniform test plate temperature. In a later experiment, it was found out that the 1/8 in. copper tubing, which accepts polyflo lines, can be easily clogged and that each polyflo tube had slightly different heat losses, which changed the effective water temperature to the plate. As our primary interest did not lie in the recovery region, control of the flowrate or heat loss behavior was not attempted. In this case, however, the unheated starting length effect is also present, which prevents the comparison to the simple correlation.

In the next case (Figure 2.13), with U_∞ = 40 ft/sec (12.2 m/s), the unheated length is eliminated and a comparison with the established flat plate heat transfer correlation is made possible. The first data point shows the effect of acceleration on the foreplate and gives a slightly lower value than expected. With P/D = 5 , the Stanton numbers are about 5% higher than the accepted correlation, shown as a straight line in Figure 2.13a. Interestingly enough, with P/D = 10, the Stanton numbers oscillate, and whenever the hole is plugged the Stanton number is right on the line: for the unplugged holes the Stanton numbers are slightly higher than the line. In the recovery region, the data followed the accepted correlation, with more scatter in data. This is also due to the lack of uniform plate temperature, as explained before. These two cases gave confidence that our energy measurement is quite accurate and the rig itself could perform as required for the proposed experiment. These flat plate data confirm the flat plate correlation,

$$St = 0.0295\ Pr^{-0.4}\ Re_x^{-0.2} \qquad (2.15)$$

within its experimental uncertainty. The value of Pr of 0.715 was used.

E. Uncertainty Interval

It is difficult to assess the overall uncertainty, including the possible physical changes in particular geometry. In this program, various levels of uncertainty were counted, and appear in the following table.

The propagation of uncertainties was accounted for by the procedure of Kline and McClintock [62].

Variables	Uncertainty
Static pressure	0.005 in. (0.127 mm) of water
Stagnation pressure	0.002 in. (0.0508 mm) of water
Temperature, except probe	0.25°F (0.14°C)
Temperature probe	0.15°F (0.08°C)
Secondary air flow rate	3%
Heat flux meter	1%
Distance normal to wall	0.001 in. (0.025 mm)
Flow direction conductance measured	5%
Power	0.3 watt @ $\theta = 1.0$ and 1.0 watt @ $\theta = 0.0$
Virtual origin	1 in. (2.54 cm)

For the free-stream velocity of 55 ft/sec (16.7 m/s), the Stanton number uncertainty for all the runs with $\theta = 1.0$ or with no blowing is $\pm 0.5 \times 10^{-4}$ with the given power measurement uncertainty of ± 0.3 watt. For $\theta = 0.0$ cases, KFL was not confirmed experimentally and the power measurement uncertainty increases to about 1 watt so that the Stanton number uncertainty becomes $\pm 1.5 \times 10^{-4}$. For higher velocities than 55 ft/sec (16.7 m/s), the uncertainty in the Stanton number decreases, and for the lower velocities, it increases.

The reason that the stagnation pressure could be measured more accurately than the static pressure was that the stagnation pressure was measured by the pressure transducer, which is calibrated to a precision micromanometer, and the static pressure was measured by the inclined manometer which was not calibrated. The thermocouple was calibrated with the quartz thermometer. Secondary flowrate measurement errors included the uncertainties due to ASME orifice meter accuracy, zero drift, and interpolation errors.

F. Data Reduction Program

In the processes of data reduction and instrument calibrations, various programs were written. Small programs made for the instrument calibration will not be discussed here.

Two major data reduction programs were used: one for velocity and temperature profiles and the other for heat transfer.

Program PROF converts the boundary layer velocity and temperature readings to the proper engineering unit. The trapezoidal rule for numerical integration is used to obtain the integral parameters. In the case of the flat plate, it computes the skin friction and calculates u^+ and y^+. To get skin friction, it uses the Clauser plot for y^+ of 75 to 125. And in the other option, it averages the velocity and temperature profiles to obtain the laterally averaged profiles.

The program STNO is used to reduce the heat transfer data. It contains all the calibration constants for heat flux meters and flow meters, and also contains the heat loss calibration test results and analytical models. It first accepts the raw data and then converts them into standard engineering units. The raw data and converted data are printed out separately. Then it calculates the proper non-dimensional numbers like Re_x, St and others. If the case is not a blown one, the program goes to the next case. If it has blowing, it compares the two cases, one nearly $\theta = 0$ and the other nearly $\theta = 1.0$, and then calculates the heat transfer parameters at $\theta = 0.0$ and $\theta = 1.0$ precisely. It distinguishes $P/D = 5$ from $P/D = 10$. It also performs the uncertainty analysis.

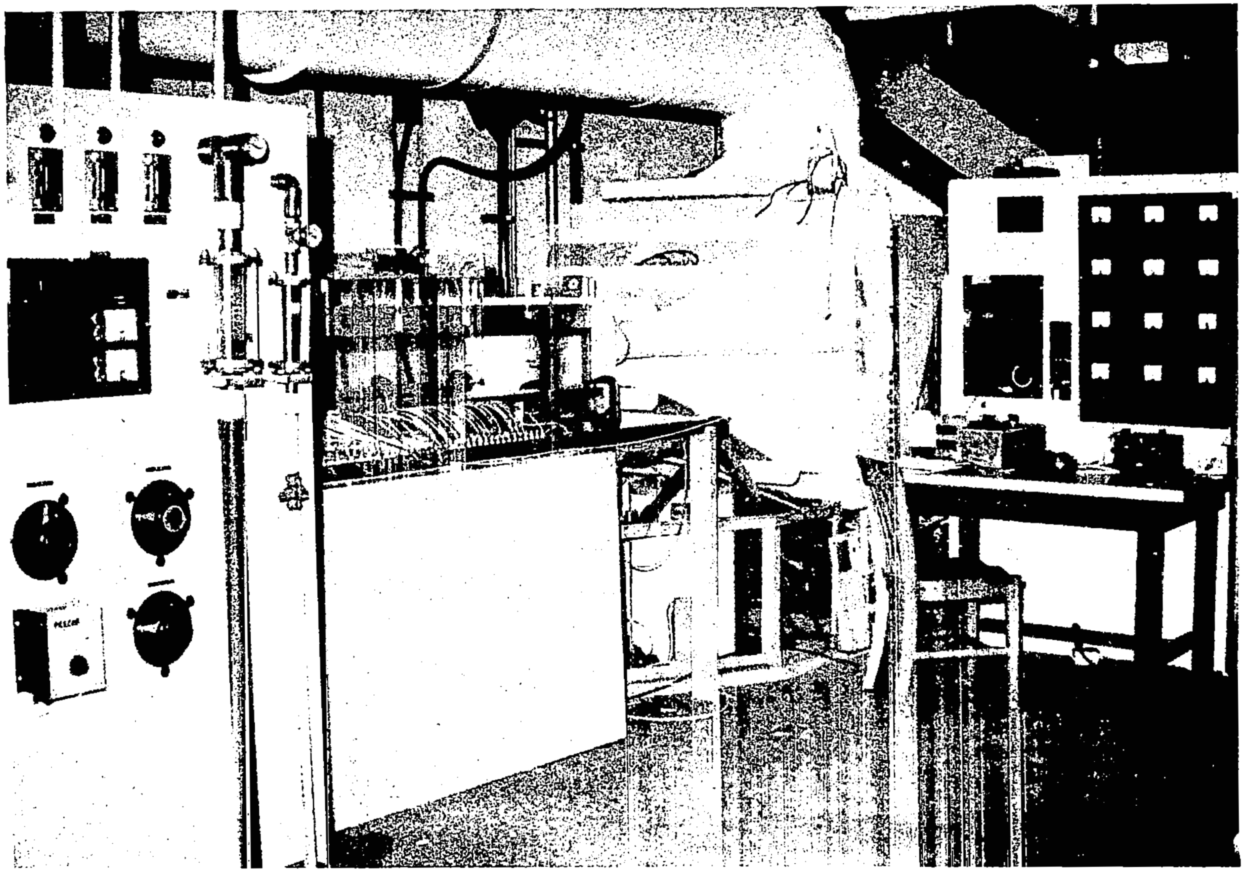

Figure 2.1 Overall view of the wind tunnel.

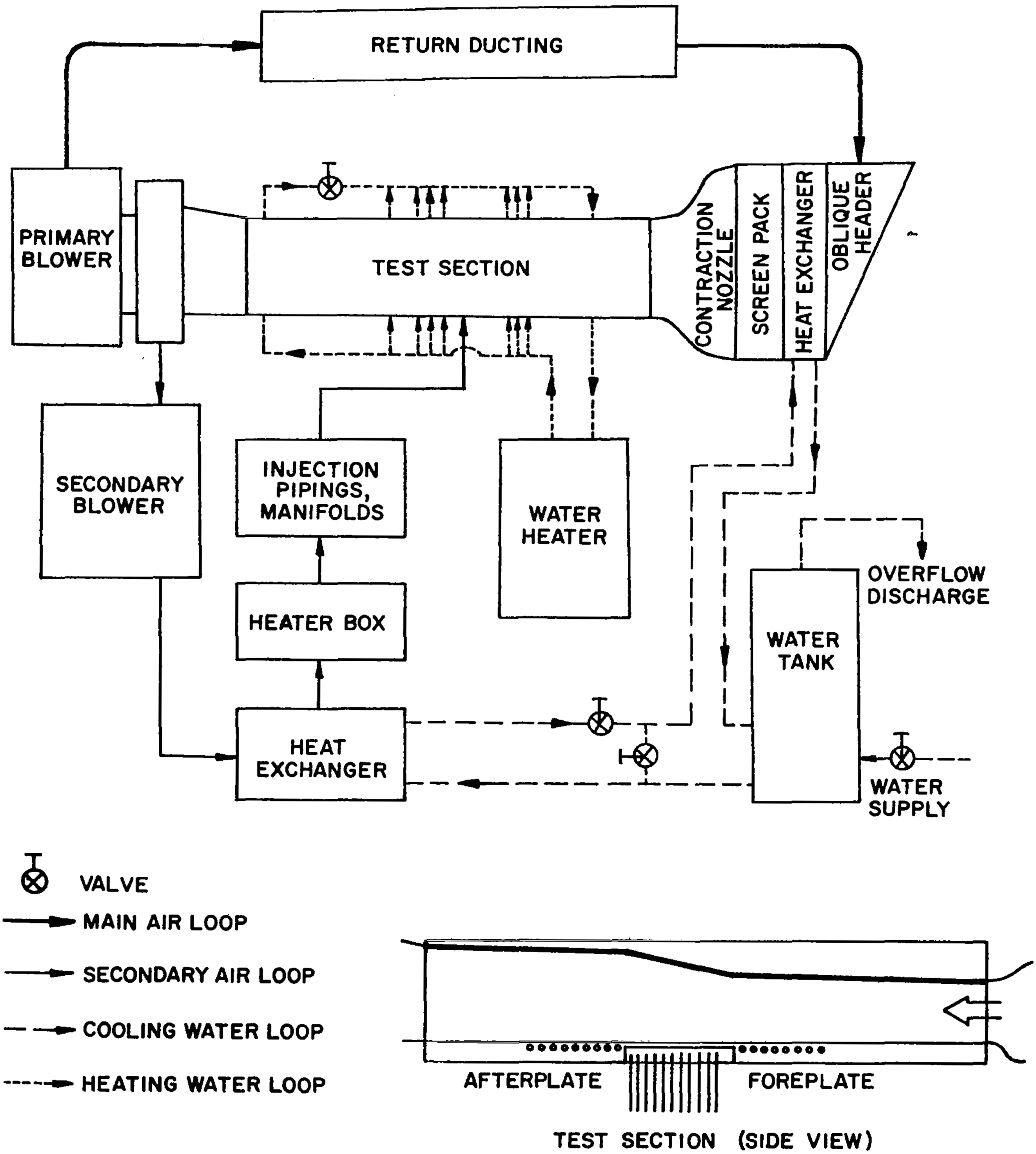

Figure 2.2 Block diagram of the wind tunnel.

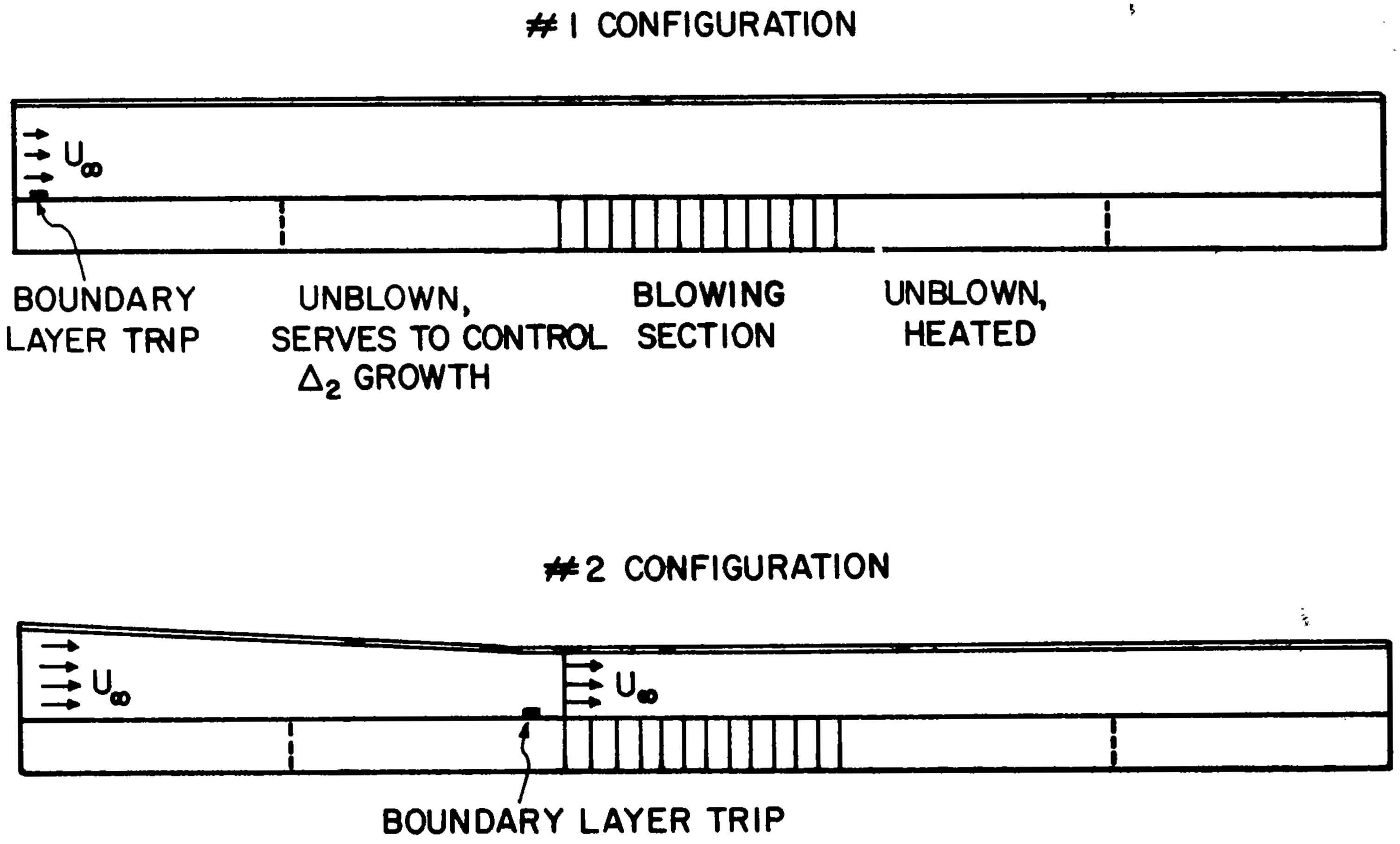

Figure 2.3 Management of top wall to produce a thin boundary layer at the starting point of blowing.

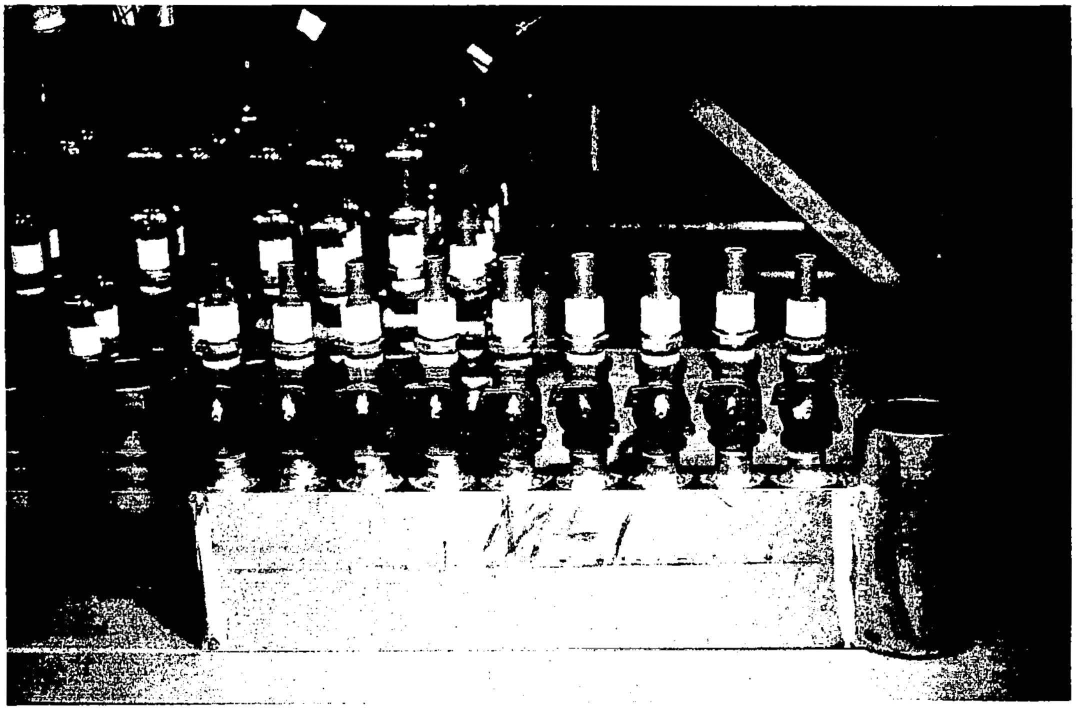

Figure 2.4 Photograph of manifolds and delivery tubes.

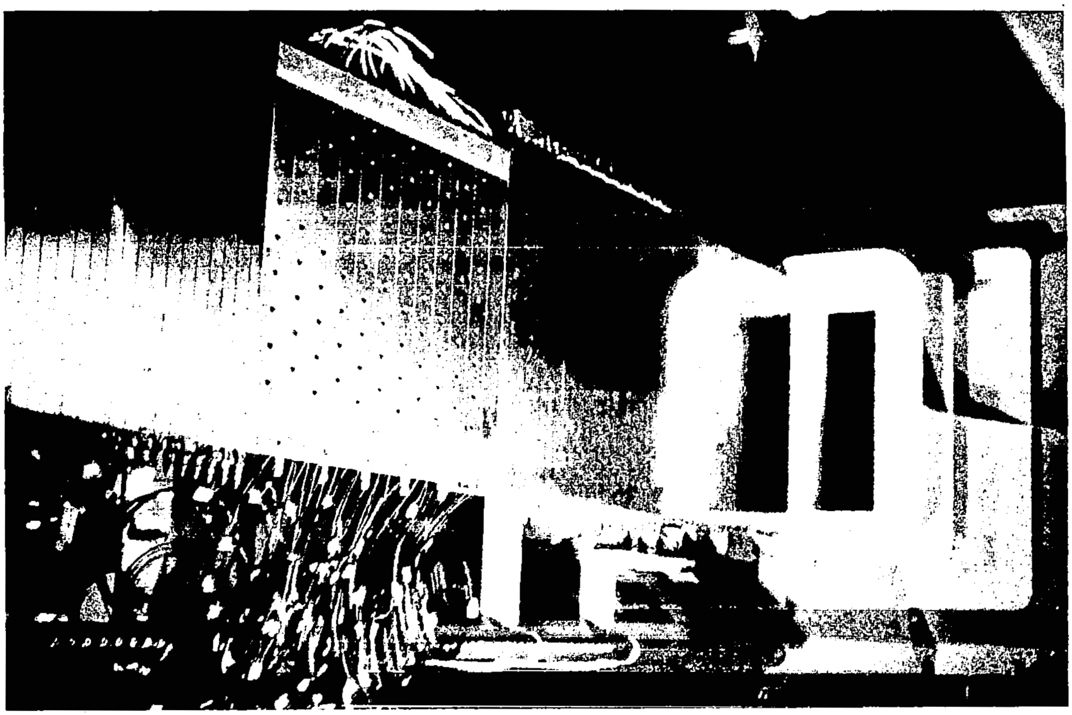

Figure 2.5 Photograph of the test surface.

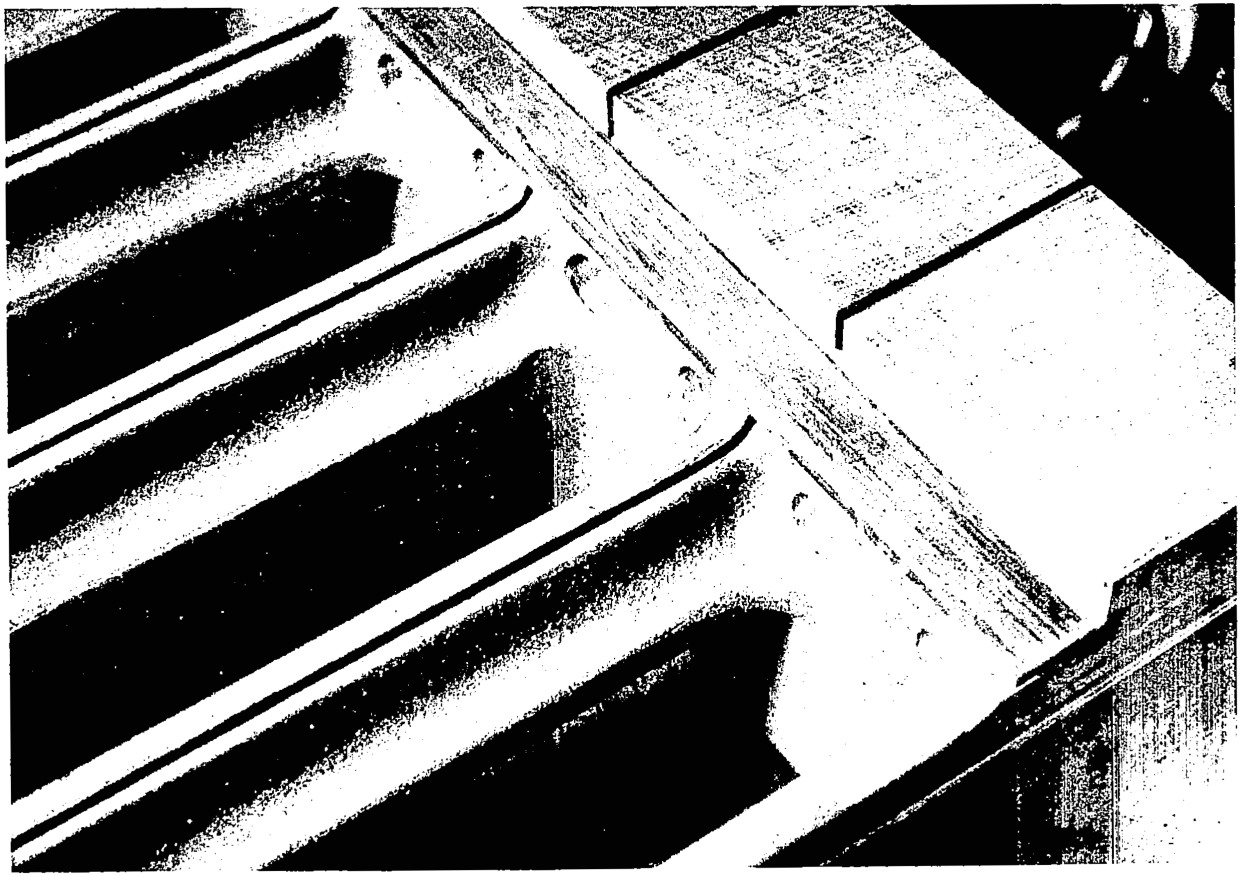

Figure 2.6 Photograph of a machined aluminum casting.

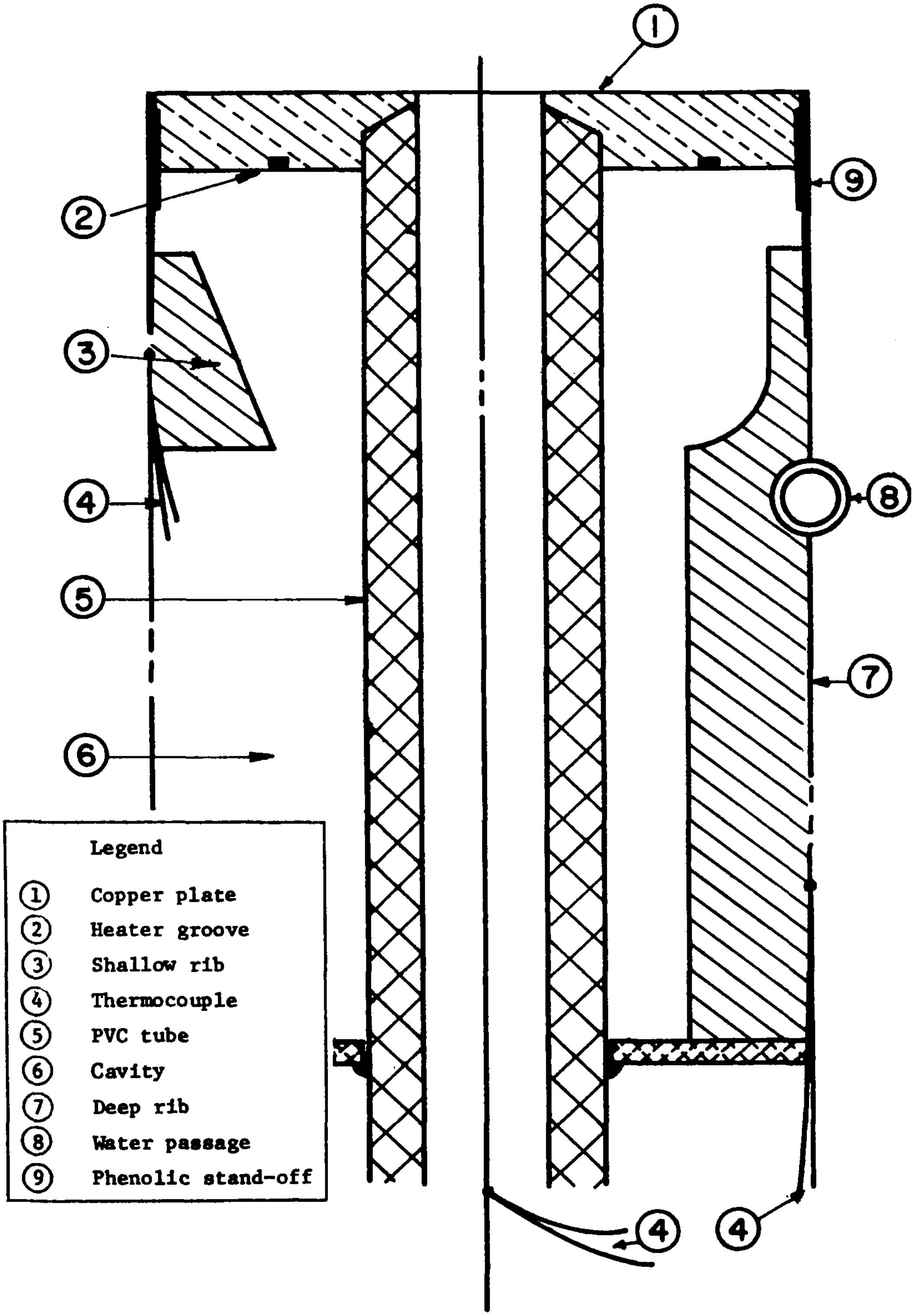

Figure 2.7 Cross section of the test plate blowing section.

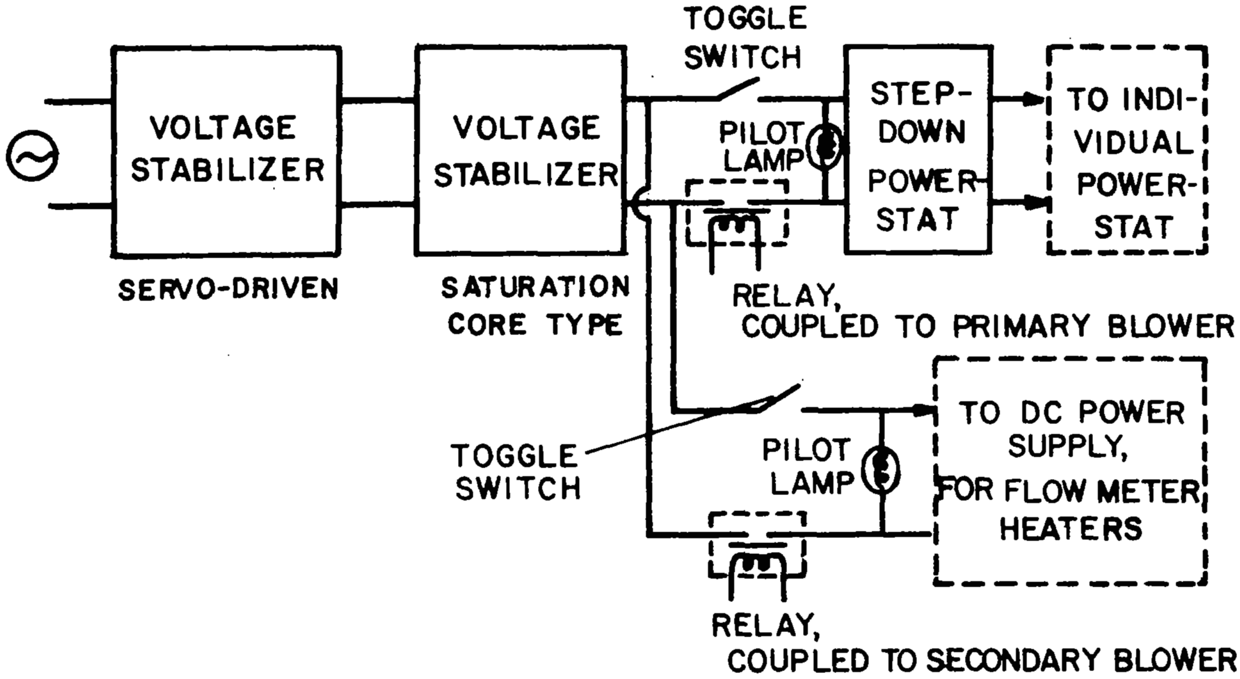

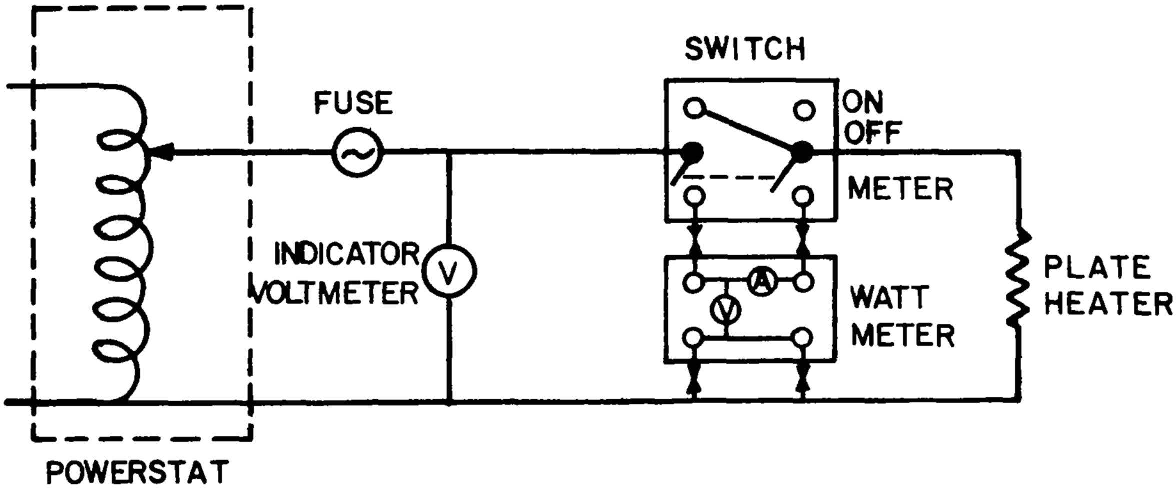

Figure 2.8 Power line diagram.

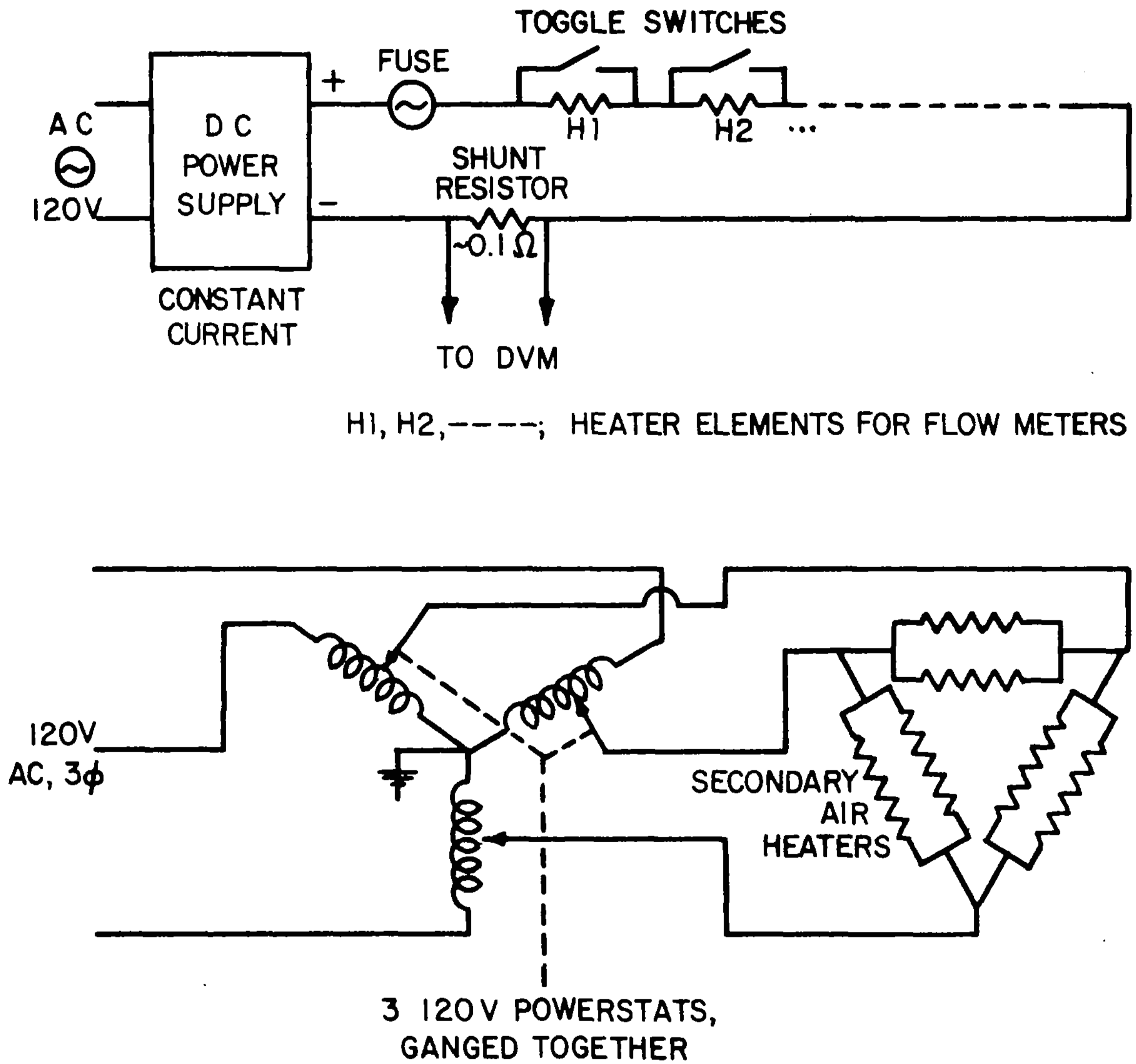

Figure 2.8 Power line diagram (contd.)

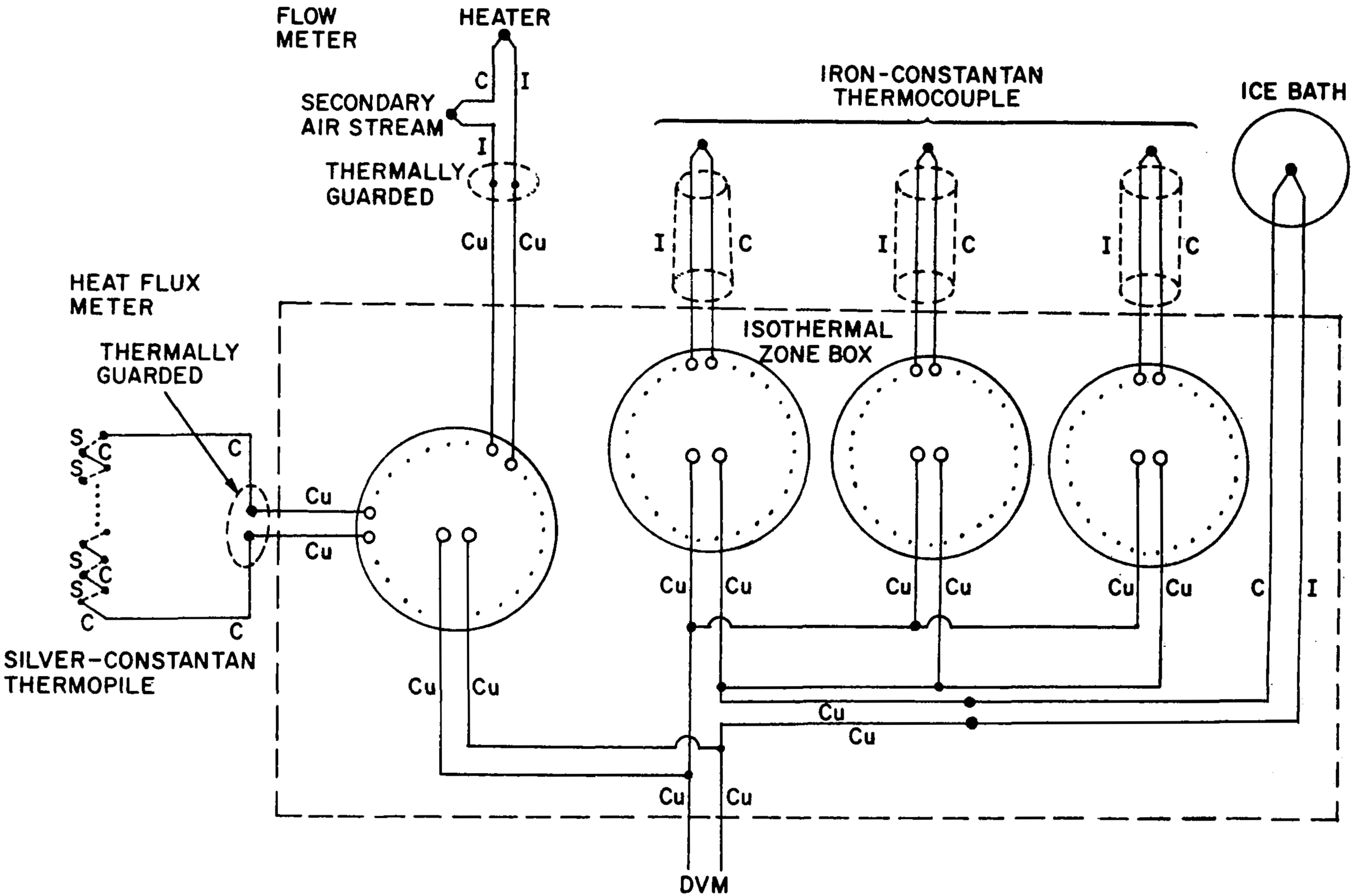

Figure 2.9 Thermocouple circuit with heat flux meter circuit.

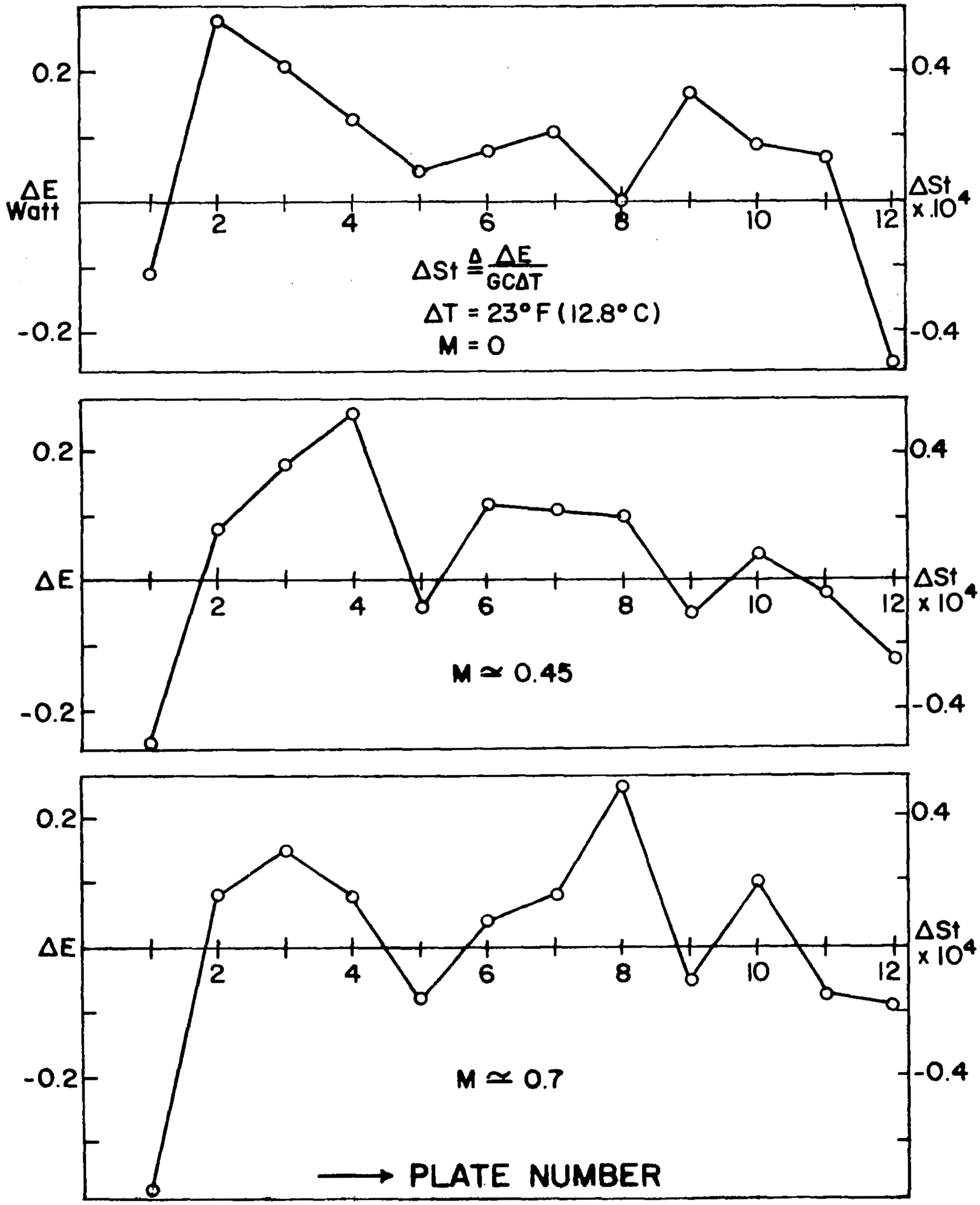

Figure 2.10 The results of energy balance tests.

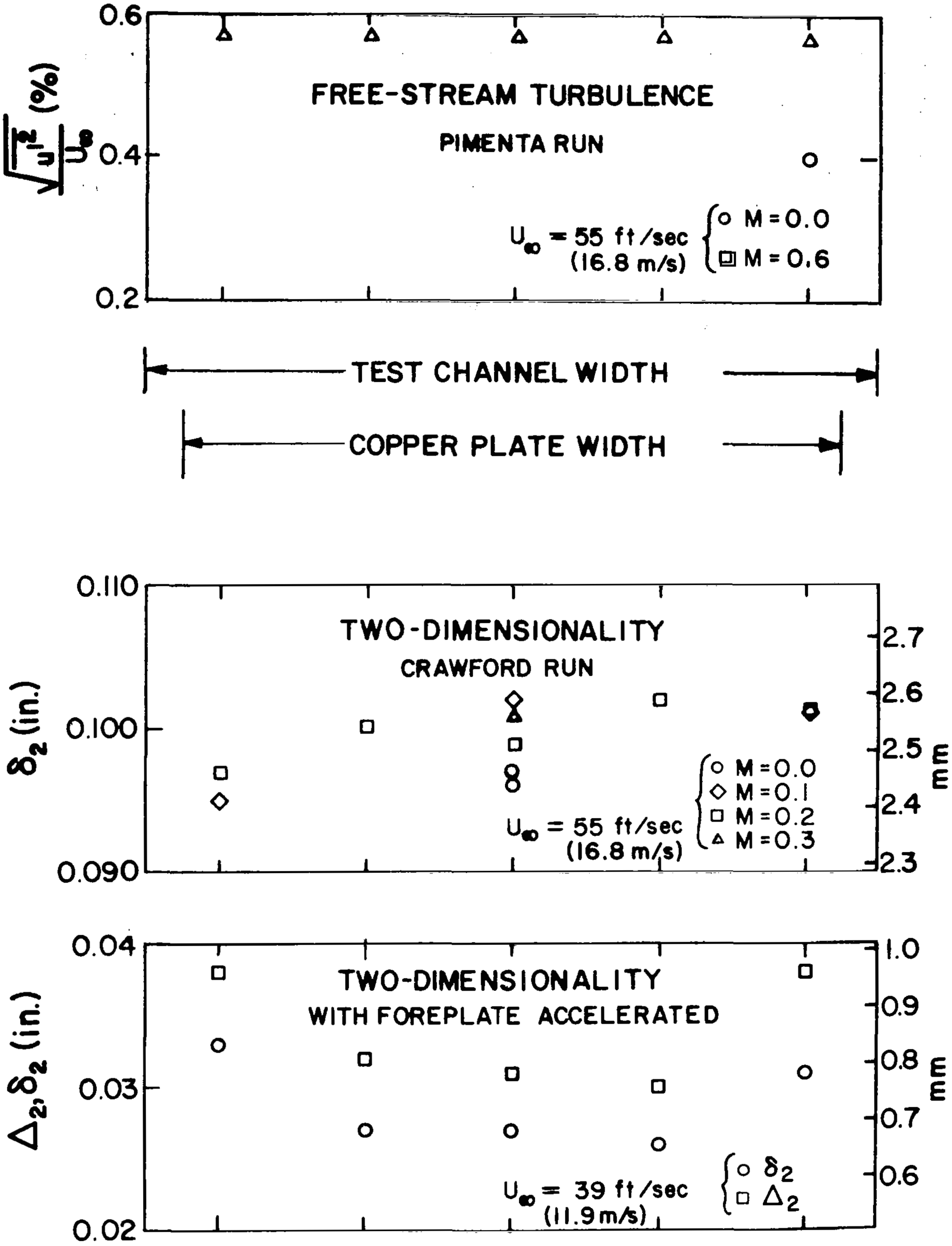

Figure 2.11 Variations of free-stream turbulence level, momentum and enthalpy thicknesses across the channel.

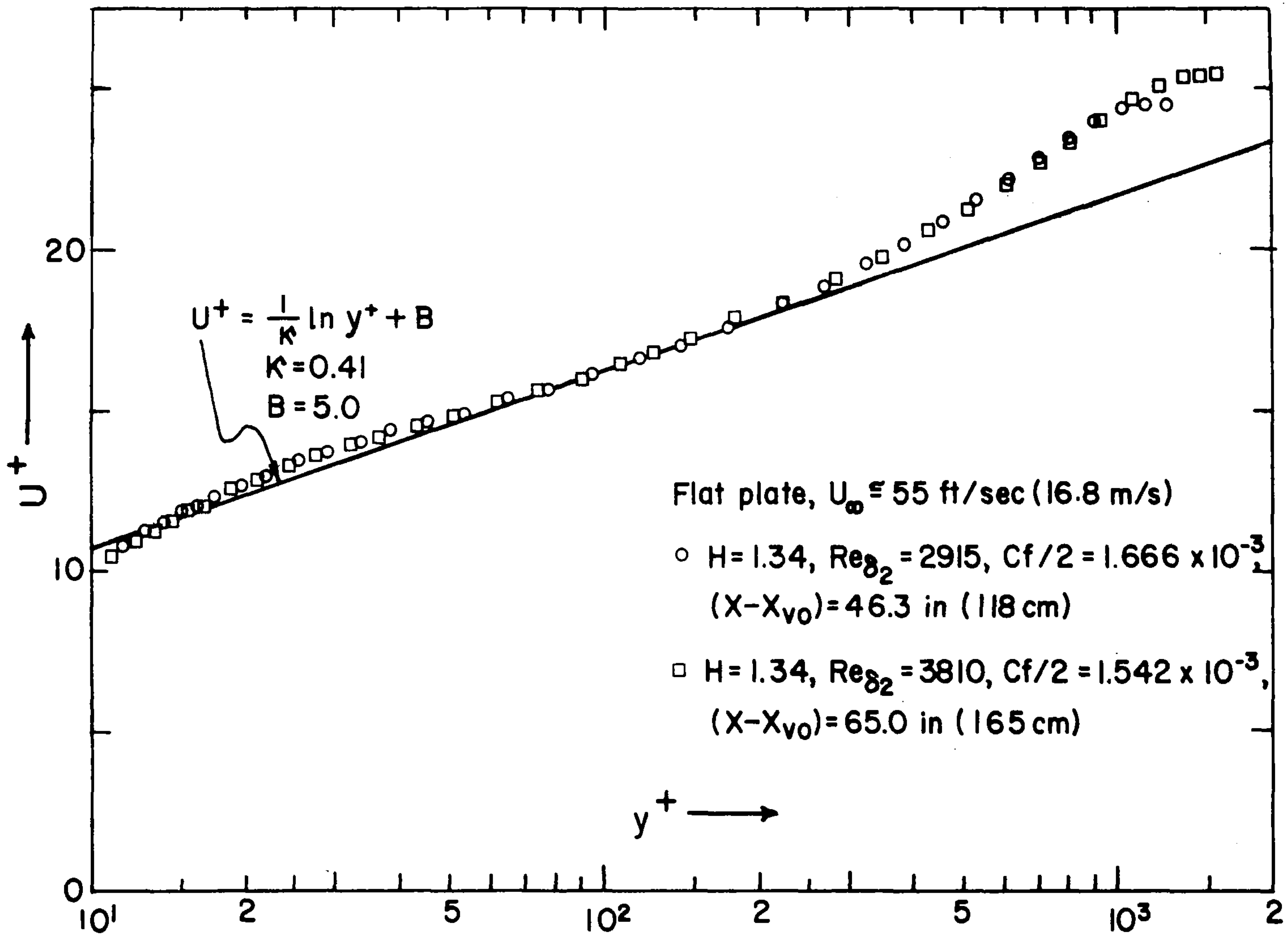

Figure 2.12 Velocity profiles without blowing.

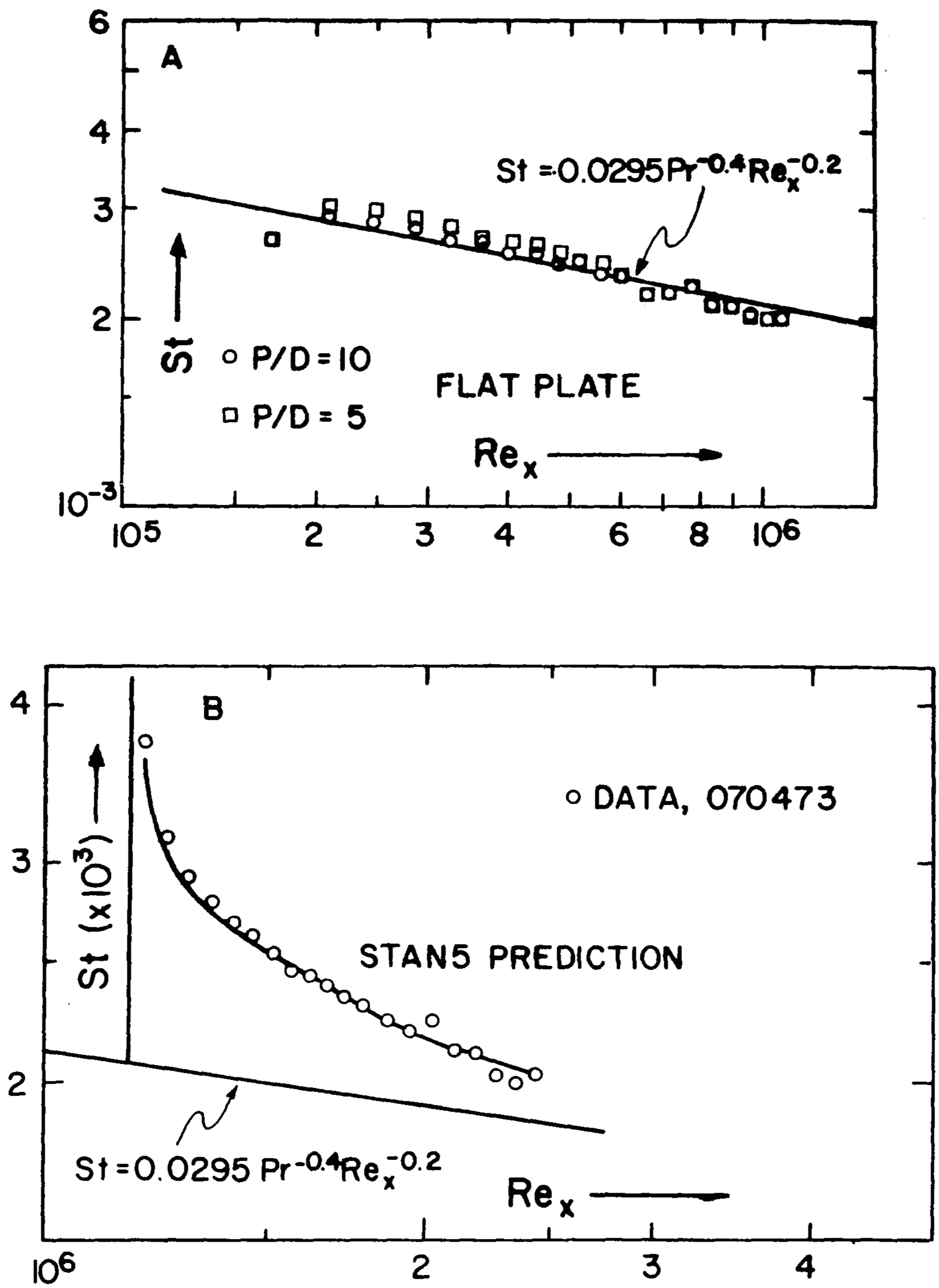

Figure 2.13 Heat transfer results for flat plate conditions.

CHAPTER III

SUPERPOSITION APPROACH FOR FILM COOLING

In this chapter, an investigation for a possible new scheme for organizing heat transfer data in full coverage film cooling is made. In particular, this proposed scheme gives a common basis for transpiration cooling and film cooling. Several advantages of the proposed scheme over the conventional one are discussed.

A. Introduction

The relationship conventionally used in film cooling theory is an adiabatic wall temperature rate equation of the form

$$\dot{q}''_o = h^*(T_o - T_{a.w.}) \tag{3.1}$$

where $T_{a.w.}$ is obtained from the adiabatic wall effectiveness, η ,

$$\eta = \frac{T_{a.w.} - T_\infty}{T_2 - T_\infty} \tag{3.2}$$

In film cooling [11-27], η has been extensively investigated for the various geometries of injection. The symbol η and the name adiabatic wall effectiveness probably originated in the pioneering work in this field by Wieghardt [11]. In the case of tangential or near-tangential slot-film cooling, the value of h_o is frequently used in place of h^* in Equation (3.1). This is justified in the far downstream region, but not near the slot [12,14]. The same situation holds for the case where a porous strip is used for fluid injection [23]. Early studies examined only the variation of adiabatic wall effectiveness, relying on the use of h_o . This approach was successful in applications like slot-film cooling of gas turbine combustion chambers, but failed when called upon to predict heat transfer rates near the injection source. In such cases, h^* cannot be approximated by h_o . Two sets of data are then required: η and h^* , each as a function of position and blowing strength.

On the other hand, in the study of heat transfer in boundary layers with blowing and suction at the wall, it is conventional to use a rate equation of the form

$$\dot{q}''_o = h(T_o - T_\infty) \tag{3.3}$$

(Moffat [2]), in which case, unlike Equation (3.1), the heat transfer is based on the wall temperature and free-stream temperature, which are known a priori. Metzger [19] proposed this scheme in film cooling and presented h/h_o as a function of the secondary injection temperature normalized by the temperature difference between free-stream and wall, θ, but later presented his data in terms of η and h^* obtained from his heat transfer data [38], following Eckert's suggestion (discussion to [19]).

In this chapter, a variation based on Equation (3.3) is proposed, developed, and compared to the conventional adiabatic wall-effectiveness scheme.

B. Film Cooling and Transpiration Cooling

In transpiration cooling with a thick porous plate, the temperature of the porous surface is always the same as that of the blown gas. The path length of the transpiration gas is so long compared to the pore size that the porous plate acts as a heat exchanger with an effectiveness of practically unity. In the case of film cooling, however, the injection geometries are such that the secondary gas temperature can be considerably different from that of the wall. In the cases using a porous strip to inject fluid the blowing is hard enough so that the boundary layer is blown off, and again the secondary injection temperature is essentially independent of the surrounding wall temperature, as in slot-film cooling.

In short, in engineering terminology, transpiration cooling implies $\theta = 1.0$ necessarily, while with film cooling, θ is a variable parameter. The independence of θ may well be a better identifier of "transpiration" vis-à-vis "film cooling" than is the physical geometry.

C. Linearity of the Governing Energy Equation

The governing energy equation for low-speed, constant-property flow is linear in temperature, and the boundary conditions prescribed in the study of film cooling or transpiration cooling are also linear. It is frequently useful to take advantage of linearity to construct solutions to complex problems by superposing solutions to simple problems.

Let us discuss a situation in which the solid plate is uniformly at t_o and fluid at a temperature t_2 is injected through holes in the plate. Let the solution to the energy equation be denoted as $T(0)$ when $\theta = 0$ and $T(1)$ when $\theta = 1$. As a consequence of the linearity of the energy equation we can write:

$$T(\theta)^{*} = T(0) + \theta \times \Delta T , \tag{3.4}$$

with

$$\Delta T = T(1) - T(0) . \tag{3.5}$$

The heat transfer coefficient h is defined as

$$- k \left.\frac{\partial T}{\partial y}\right|_o = h(T_o - T_\infty) .$$

Multiplying Equation (3.4) with the operator

$$- k \left.\frac{\partial(\ )}{\partial y}\right|_o$$

and then using the definition of h, we have

$$h(\theta) = h(0) + \theta \times (h(1) - h(0)) . \tag{3.6}$$

By forming the non-dimensional Stanton number,

$$St(\theta) = St(0) + \theta \times (St(1) - St(0))$$

---

* $T(\theta)$ means $T(\theta,x,y,z)$

Experimental results show that $St(0) > St(1)$, so it is more straightforward to write

$$St(\theta) = St(0) - \theta\{St(0) - St(1)\} \quad . \tag{3.7}$$

This result is plotted in Figure 3.1 along with experimental data in support. Metzger et al. [19] also verified the linear property of heat transfer coefficient h, with respect to θ.

D. Experimental Confirmation

To show that the above result is true, experiments were run with three different values of θ at a fixed value of M (Figure 3.2). The exact values of θ and M varied within about 6% from plate to plate, but the agreement between experiment and prediction is excellent.

The above experiments confirm the theoretical result, as shown in Figure 3.1 in the coordinates of St and θ with all other parameters fixed. Values of St at any two values of θ serve to define the straight line in Figure 3.1. This is the essential property of the proposed scheme.

For all the values of θ other than 1.0 and 0.0, a simple linear interpolation or extrapolation will give the necessary St or heat transfer coefficient. If the St obtained for a particular value of M and θ falls below the $M = 0.0$ case, there is a cooling effect; otherwise an adverse effect.

E. Relationship between the Effectiveness/Adiabatic Wall Scheme and the Constant Wall Temperature Superposition Scheme

The purpose of the following text is to demonstrate the one-to-one correspondence between the two schemes and to derive several useful formulae.

Suppose one increases the value of θ until $q_o'' = 0$ in the constant wall temperature scheme. We obtain

$$\theta_{a.w.} = \theta(\dot{q}_o'' = 0) = \frac{T_2 - T_\infty}{T_{a.w.} - T_\infty} = \frac{1}{\eta} \quad . \tag{3.8}$$

The last identity is from the definition of η . Metzger et al. [38] evaluates η based on Equation (3.8). Equation (3.8) can be realized in the full coverage film-cooled region in an averaged sense around each row of injection holes. Also in the slot film-cooling case, this relationship must be realized in an averaged sense over the entire plate as in Metzger et al. [31]. In addition, θ and η can be functions of x . Thus Equation (3.8) is an approximation which is valid when Couette flow assumption is true as will be discussed in the next section.

Also, for the general wall heat flux equation,

$$\dot{q}''_o = h(\theta,M)(T_o - T_\infty) \quad .$$

$h(\theta,F)$ is, from Figure 3.1 and from the fact that h and St are proportional,

$$h(\theta,M) = h(0,M) - \theta \times \Delta h \quad .$$

$$\dot{q}''_o = h(0,M)\left\{1 - \theta \times \frac{\Delta St}{St(0,M)}\right\}(T_o - T_\infty) \quad .$$

Also, from Figure 3.1, we have

$$\frac{\Delta St}{St(0,F)} = \frac{1}{\theta_{a.w.}} = \eta \quad . \tag{3.9}$$

$$\dot{q}''_o = h(0,F)\{1 - \theta \times \eta\}(T_o - T_\infty) \quad .$$

Eckert derived a similar expression for $h^*/h(\theta,F)$ in discussion to [19]. From the definitions of θ and η , we have

$$1 - \theta \times \eta = 1 - \frac{T_2 - T_\infty}{T_o - T_\infty}\frac{T_{a.w.} - T_\infty}{T_2 - T_\infty} = 1 - \frac{T_{a.w.} - T_\infty}{T_o - T_\infty}$$

$$1 - \theta \times \eta = \frac{T_o - T_{a.w.}}{T_o - T_\infty} \tag{3.10}$$

Thus we have

$$\dot{q}''_o = h(0,M)(T_o - T_{a.w.}) \tag{3.11}$$

However, Equation (3.11) is precisely the form of the adiabatic wall scheme. We have thus shown that h^* can be equated to $h(0,M)$:

$$h^* = h(0,M) \tag{3.12}$$

Note that Equation (3.8) was essential in this derivation and the formulae derived are valid with the Couette flow approximation which is sometimes a very good approximation in the turbulent boundary layer. From this analysis we obtained several interesting relationships.

$$h^* = h(0,M) \tag{3.12}$$

$$\eta = \frac{1}{\theta_{a.w.}} = \frac{St(0,M) - St(1,M)}{St(0,M)} \tag{3.9}$$

$$1 - \eta \times \theta = \frac{T_o - T_{a.w.}}{T_o - T_\infty} \tag{3.10}$$

From plane geometry and Figure 3.1,

$$\frac{St(1,M)}{St(0,M)} = \frac{\frac{1}{\eta} - 1}{\frac{1}{\eta}} = \frac{T_2 - T_{a.w.}}{T_2 - T_\infty}$$

$$\frac{St(\theta,M)}{St(0,M)} = \frac{\frac{1}{\eta} - \theta}{\frac{1}{\eta}} = \frac{T_o - T_{a.w.}}{T_o - T_\infty}$$

Note that the last identity says

$$h(\theta,M)(T_o - T_\infty) = h(0,M)(T_o - T_{a.w.}) = \dot{q}''_o$$

which is obvious from Equations (3.1) and (3.3). Also note that in deriving this relationship it was not necessary to use the fact that the wall heat flux calculated either by Equation (3.1) or by Equation (3.3) is the same. This means our derivations are self-consistent with all other definitions and concepts.

In the case of the constant wall temperature superposition scheme, one may encounter singular points as in the pipe flow heat transfer problems. The following examples may be of interest.

(1) Case 1: $T_o = T_\infty$, $T_2 > T_o$

<u>Constant wall temperature superposition scheme</u>

Assume $T_o = \varepsilon + T_\infty$. Then

$$\theta = \frac{T_2 - T_\infty}{T_o - T_\infty} = \frac{T_2 - T_\infty}{\varepsilon}$$

$$St(\theta,F) = St(0,M) - \theta \times \Delta St$$

$$= St(0,M) - \frac{\Delta St}{\varepsilon}(T_2 - T_\infty)$$

Now

$$\dot{q}''_o = h(\theta,M)(T_o - T_\infty)$$

$$\dot{q}''_o = \left\{ h(0,M) - \frac{\Delta h}{\varepsilon}(T_2 - T_\infty)\right\} \varepsilon$$

$$\lim_{\varepsilon \to o} \dot{q}''_o = - \Delta h \times (T_2 - T_\infty)$$

$$\dot{q}''_o = - \Delta h \times (T_2 - T_o)$$

<u>Adiabatic wall scheme</u>

$$\dot{q}''_o = h^*(T_o - T_{a.w.})$$

$$= h(0,M)(T_\infty - T_{a.w.})$$

$$\dot{q}_o'' = -h(0,M)\,\frac{T_{a.w.} - T_\infty}{T_2 - T_\infty}\,(T_2 - T_\infty)$$

$$= -h(0,M) \times \eta \times (T_2 - T_\infty)$$

Now, from Equation (3.9),

$$h(0,M) \times \eta = \Delta h = h(0,M) - h(1,M)$$

$$\dot{q}_o'' = -\Delta h(T_2 - T_\infty)$$

$$\dot{q}_o'' = -\Delta h(T_2 - T_o)$$

This is the same result as before.

This problem is a special case which can be solved by the application of the superposition principle. Also, note that the heat flux at the wall has a negative sign and that temperature potential $(T_2 - T_o)$ appears.

(2) Case 2: $T_o = T_{a.w.}$

<u>Adiabatic wall scheme</u>

$$\dot{q}_o'' = h(0,M)(T_o - T_{a.w.})$$

$$\dot{q}_o'' = 0$$

<u>Constant wall temperature superposition scheme</u>

$$\dot{q}_o'' = h(\theta_{a.w.}, M)(T_o - T_\infty)$$

$$h(\theta_{a.w.}, M) = 0 \text{ by definition}$$

$$\dot{q}_o'' = 0$$

This is the same result as before.

F. Presentation of Full-Coverage Film Cooling Data

Three methods are available for the presentation of locally averaged film-cooling heat transfer data in the full coverage film-cooling geomtries. The three methods are:

Method 1: Use an adiabatic wall test module (or use the mass transfer analogy [42,49]) to obtain local and/or average η, then use a constant wall temperature (or heat flux) test module to obtain St^* based on Equation (3.1)

Method 2: Use a constant wall temperature test module and obtain $St(\theta,F)$ as a function of θ [19] or from these data obtain St^* and η [38].

Method 3: Use a constant wall temperature test module to obtain $St(0,F)$ and $St(1,F)$ and use linear superposition to compute values of St for θ other than zero and unity. This is the method used in this thesis.

The value of η obtained by Method 1 may not be the same as that obtained by Methods 2 and 3, because in Method 1 T_2 is fixed and T_o is a variable, while in Methods 2 and 3 T_o is kept constant and T_2 is changed. The following example shows that the two procedures would not give the same results for η even though the values of θ in both cases are exactly the same.

Consider two hypothetical cases with the same flow field in the two-dimensional boundary layer situation: Case I has T_2 fixed at 1.0, and the wall is adiabatic yielding $T_o = \eta(x)$ as the solution. Case II has T_o constant at 1.0 and T_2 varies as $\theta_{a.w.}(x)$ to give the adiabatic wall. This is depicted in Figure 3.3. The governing equation for both cases is

$$U\frac{\partial T}{\partial x} + V\frac{\partial T}{\partial y} = \frac{\partial}{\partial y}\left(\alpha_T\frac{\partial T}{\partial y}\right) \qquad (3.13)$$

where α_T is the total diffusivity for heat.

If the Couette flow assumption is made, then $U\frac{\partial T}{\partial x}$ will vanish and eliminate the x dependence, and Case II can be converted to Case I by dividing all the boundary conditions by $\theta_{a.w.}(x)$ and by using Equation (3.8). Without the Couettte flow assumption, the conversion is not possible. This example indicates that η in Method 2 should not be interpreted the same as in Method 1.

Also, as was discussed by Mayle et al. [47], in Method 1 the average value of $\{h(0,F) \times \eta\}$ must be approximated as the {average of $h(0,F)$} $\times$ {average of η}, to obtain the average heat flux. This approximation is not true if $h(0,F)$ or η is not constant in the z-direction. Again, in Method 3 there is no such ambiguity, since averaging h has the same effects as averaging $\dot{q}''_o$ with the locally constant $(T_o - T_\infty)$.

G. Discussion

Even though the words "adiabatic wall effectiveness" seem to denote the overall performance of cooling, it is only a partial effect of film cooling on the rate Equation (3.1). To be valid all over the protected region, both η and $St(0,F)$ must be measured.

The same information can be obtained by a superposition method, with all the effects of film cooling lumped into the function $St(\theta,F)$. This is a sufficient overall performance parameter.

For the case of constant wall temperature, the superposition scheme will require less algebraic manipulation, because it directly calculates $St(\theta,F)$ or $h(\theta,F)$ appropriate for use with the known temperature difference $(T_o - T_\infty)$.

Even more cogent arguments are related to the use of existing numerical prediction techniques for locally averaged heat transfer rates when the injectant temperature differs from the wall temperature. In the case of a constant wall temperature, the program can be executed with the actual boundary conditions (T_o, T_2 and $\dot{m}''_o$), as in any other two-dimensional boundary layer problem.

If this problem were attempted using the effectiveness/adiabatic wall temperature scheme, either an internal correlation for η would be required or the program would have to be run twice: once for the adiabatic wall temperature and the other for $h(0,F)$, for the locally averaged quasi-two-dimensional field.

From the research standpoint, to investigate the effect of one parameter on film cooling, if one follows the adiabatic wall scheme, one must have two test plate modules: one for the adiabatic wall tests and the other for the constant wall temperature tests.

If one uses the constant wall temperature superposition scheme, $St(0,F)$ and $St(1,F)$ can be obtained with equal accuracy with one constant wall temperature test plate module.

A last, but also important, point is that one can make an analogy between x-momentum and heat by making use of the similarity in the equations and the boundary conditions for heat and momentum transfer, yielding good estimates of the skin friction coefficients. In the case of a three-dimensional, full coverage discrete hole, film-cooling problem, the acquisition of skin friction data is, at best, an extremely time-consuming process.

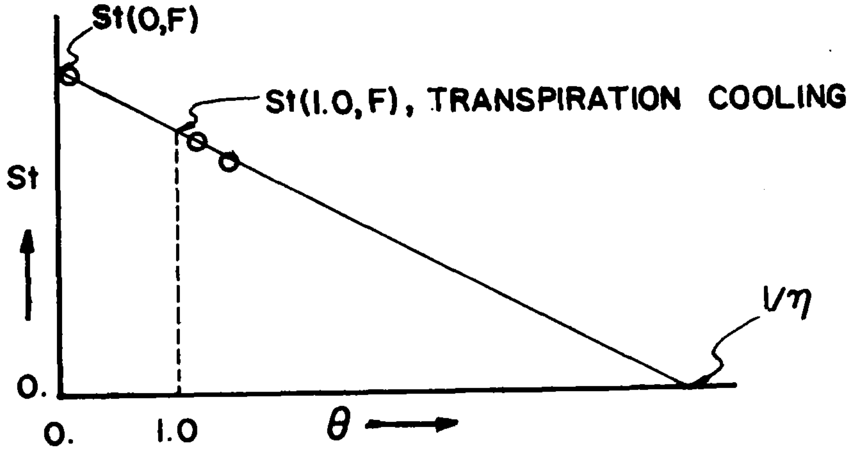

Figure 3.1 Diagram explaining transpiration cooling and film cooling in terms of heat transfer coefficients.

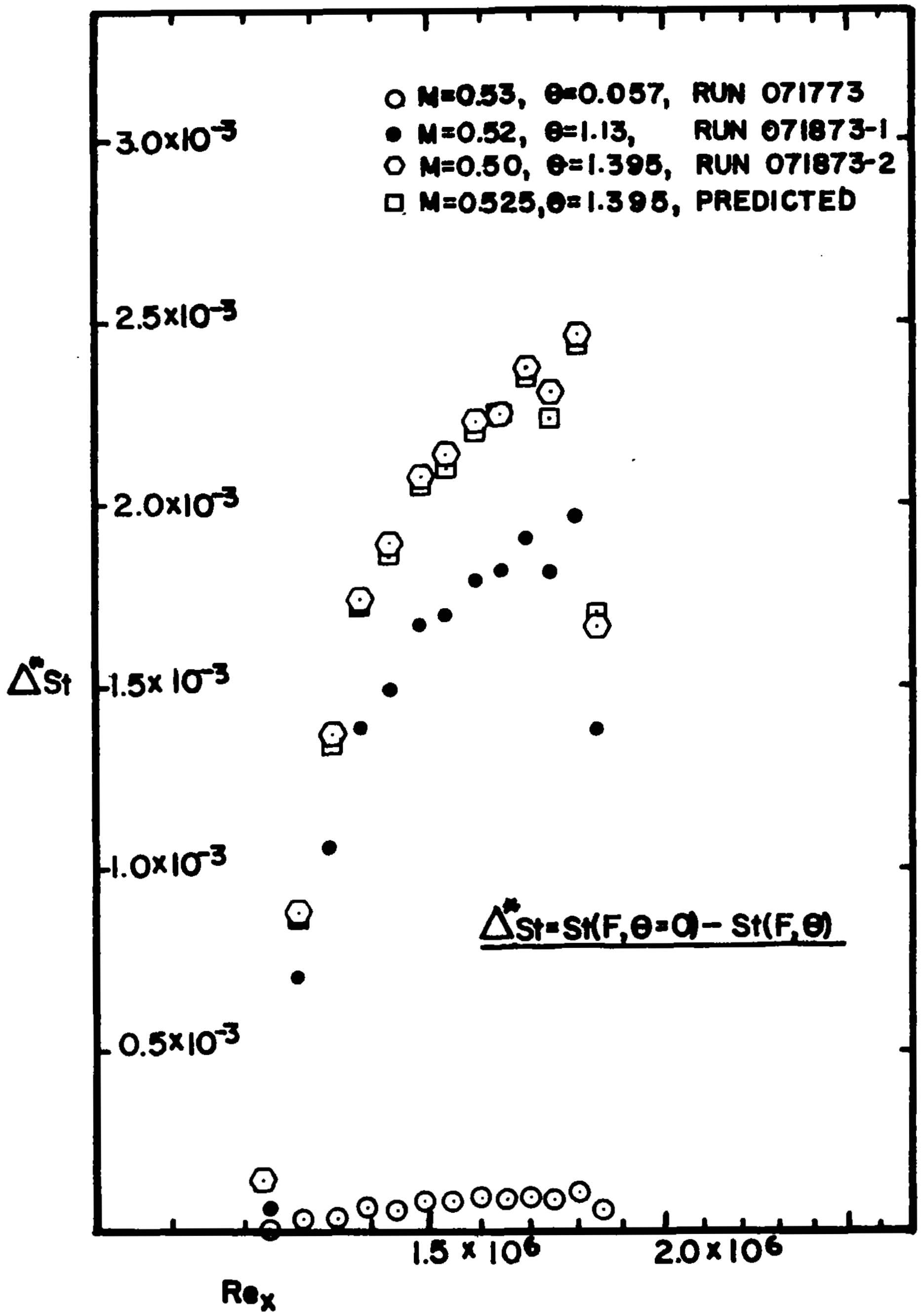

Figure 3.2 Experimental confirmation of linearity.

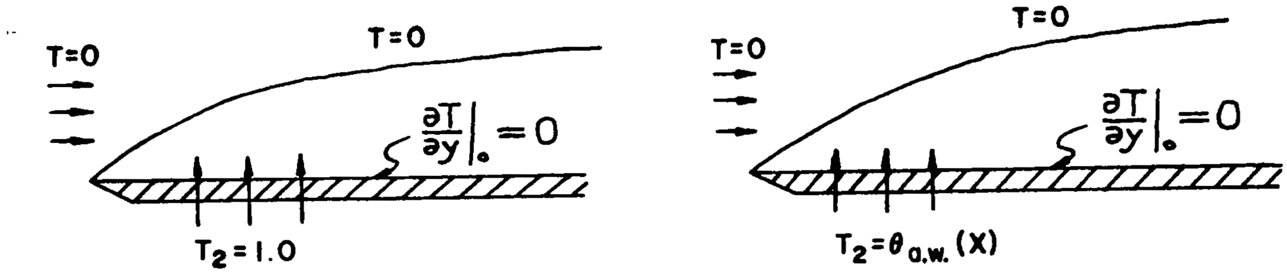

Figure 3.3 Idealized experimental conditions.

CHAPTER IV

DERIVATION OF BASIC EQUATIONS FOR LOCALLY AVERAGED PROPERTIES

A. How to Average

A complete analytical description of full coverage film-cooling through discrete hole arrays requires a full three-dimensional, Navier-Stokes equation and a full three-dimensional energy equation. The literature describing the cross flow jet field for $M > 2.0$ [63,67] contains evidence that there exists a horseshoe vortex around each jet with a complicated turbulence field. The pressure also varies around each jet. All these facts suggest that no simple approximation will capture all the physics in this case. Ramsey et al. [37] confirmed the complexity of the flow field around the jet for $M \sim 1.0$ reporting a slightly different flow field than Abramovich [67]. It was not clear whether there was a horseshoe vortex at $M = 1.0$ but flow separation was indicated. Since our interest is in the range of $M = 0.1$ to $M = 1.0$, we would expect flow separation after each jet near $M = 1.0$, accompanied by a complicated turbulence field.

This leaves us in a difficult situation. Two problems are confronted, each of which is presently beyond the state of the art. One is three-dimensional flow separation, and the other the turbulence modeling in such flow. A full, three-dimensional, Navier-Stokes equation cannot be solved successfully within a reasonable computation time for high Reynolds numbers with the present day computer capability. Also, a proper modeling for turbulence field requires an experimental input which can be only obtained through the tedious three-dimensional probing. This will be a very time-consuming task.

At this moment it is fruitful to look back at the approaches used to handle "two-dimensional" turbulent flows. Various ideas have been brought up, but basically all models and ideas use one common operation: the governing equation was averaged (ensemble-average in this case). Our primary interest is in the mean motions and mean shear stresses. Averaging brings in the well known Reynolds stress terms, due to the nonlinearity in the convective terms.

With an analogy to two-dimensional turbulent flow studies, a simpler equation can be obtained through averaging in the present case. This is related to what we really want to know in full-coverage film cooling through discrete hole arrays. Esgar et al. [1] described two problems in the gas turbine cooling situation as was mentioned in the beginning of Chapter I. Our major interest is in obtaining the overall temperature level, not the detailed temperature variation between holes. This vaguely suggests that proper averaging must be done around each hole. This is one requirement for a problem of how to average the governing equation to reduce the three-dimensional problem to a two-dimensional one. This type of analysis is only valid for a periodic array of holes, which is the most important type used for the gas turbine blade cooling application.

Another requirement for simplification is to reduce the governing equation to the boundary layer type equation. The full two-dimensional problem can be solved, but it takes considerably longer computation time than the boundary layer problem. To see whether the boundary layer approximation is valid, the boundary layer thickness was measured approximately for various values of M by using a pitot probe at the end of a stethoscope and listening to the turbulence noise intensity by ear. This rough measurement indicated that the boundary layer thickness was between one inch (2.54 cm) and four inches (10.16 cm) over the 24-inch (61 cm) distance with $M \simeq 1.0$. Thus a "boundary layer" analysis is reasonably valid.

However, the use of the boundary layer equation requires that the wall mass transfer should not be very large, because the boundary layer equation solves the x-momentum equation, not y-momentum equation. Lateral averaging as proposed by Herring [46] is a good way to reduce the three-dimensional problem to the two-dimensional problem, but does not solve the mass transfer problem. The wall mass transfer is not small. For example, for $M = 1.0$ and $P/D = 5$, wall mass transfer after lateral averaging is about $F = 0.2$, which is still very large and is not negligible. This leaves only one possibility, local average.

In our geometry, it is clear what size and shape of area we should take for local averaging: the area associated with one hole, as described in Figure 4.1. With this procedure, the wall mass transfer becomes about $F = 0.03$ with $M = 1.0$ and $P/D = 5$. For this amount of wall mass transfer, the y-momentum equation can be neglected and the boundary-layer equation can be used. The area for local average can move continuously in the x- and y-directions, so that the resulting averaged properties are still continuous functions of x and y.

With all the above approximations, the full-coverage film cooling problem becomes similar to one with the uniform, porous plate transpiration.

The decomposition of p can be made as follows:

$$p(x,y,z,t) = P(x,y) + \tilde{p}(x,y,z) + p'(x,y,z,t) \tag{4.1}$$

where P is the locally averaged property and $\tilde{p}$ is the local variation of property p which represents the difference between the ensemble average and local average, and p' represents the turbulent fluctuation term. The ensemble average of p will give $P + \tilde{p}$, but the local average of p will give P. Also, $\overline{\tilde{p}} = 0$.

B. Derivation of PDE

For the low speed, constant property flow with no body force and no energy dissipation or no energy source, the following governing equation is realized. For the sake of simplicity of notation, tensorial notation is used.

Continuity:
$$\frac{\partial u_i}{\partial x_j}\delta_{ij} = 0 \tag{4.2a}$$

Momentum:
$$\frac{\partial u_i}{\partial \tau} + u_j \frac{\partial u_i}{\partial x_j} = -\frac{1}{\rho}\frac{\partial P}{\partial x_j}\delta_{ij} + \nu\frac{\partial^2 u_i}{\partial x_j^2} \tag{4.2b}$$

Energy:
$$\frac{\partial t}{\partial \tau} + u_j \frac{\partial t}{\partial x_j} = \alpha \frac{\partial^2 t}{\partial x_j^2} \tag{4.2c}$$

where i and j run from 1 to 3. We now introduce the local averaging, and simple algebraic manipulation gives

Continuity: $\frac{\partial U_i}{\partial x_j} \delta_{ij} = 0$ (4.3a)

Momentum: $$U_j \frac{\partial U_i}{\partial x_j} = - \frac{1}{\rho} \frac{\partial P}{\partial x_j} \delta_{ij} + \nu \frac{\partial^2 U_i}{\partial x_j^2} + \frac{\partial}{\partial x_j} (-\overline{u_i' u_j'}) + \frac{\partial}{\partial x_j} (-\overline{\tilde{u}_i \tilde{u}_j}) \tag{4.3b}$$

Energy: $$U_j \frac{\partial T}{\partial x_j} = \alpha \frac{\partial^2 T}{\partial x_j^2} + \frac{\partial}{\partial x_j} (-\overline{t' u_j'}) + \frac{\partial}{\partial x_j} (-\overline{\tilde{t} \tilde{u}_j}) \tag{4.3c}$$

where i and j run through 2 , and steady state is assumed.

Now the following additional assumptions are introduced:

1. Boundary layer assumption, and
2. No abrupt change in wall mass transfer for locally averaged field.

With the introduction of the boundary layer assumption, Equations (4.3) become, using the x- and y-coordinate,

$$\frac{\partial U}{\partial x} + \frac{\partial V}{\partial y} = 0 \tag{4.4a}$$

$$U \frac{\partial U}{\partial x} + V \frac{\partial U}{\partial y} = - \frac{1}{\rho} \frac{\partial P}{\partial x} + \frac{\partial^2 U}{\partial y^2} + \frac{\partial}{\partial y} (-\overline{u' v'}) + \frac{\partial}{\partial y} (-\overline{\tilde{u} \tilde{v}}) \tag{4.4b}$$

$$0 = - \frac{1}{\rho} \frac{\partial P}{\partial y} + \frac{\partial}{\partial y} (-\overline{v'^2}) + \frac{\partial}{\partial y} (-\overline{\tilde{v}^2}) \quad \text{and} \tag{4.4c}$$

$$U \frac{\partial T}{\partial x} + V \frac{\partial T}{\partial y} = \alpha \frac{\partial^2 T}{\partial y^2} + \frac{\partial}{\partial y} (-\overline{t' v'}) + \frac{\partial}{\partial y} (-\overline{\tilde{t} \tilde{v}}) \tag{4.4d}$$

Now the y-momentum equation can be integrated as

$$\frac{P}{\rho} + \overline{\tilde{v}^2} + \overline{v'^2} = \frac{P_\infty}{\rho}$$

With the second approximation, that there is no abrupt change in wall mass transfer, we have

$$\frac{\partial}{\partial x}\,(\overline{\tilde{v}^2}) \;\sim\; O(\delta)$$

Also, $\overline{v'^2}$ is small compared to the pressure.

$$\frac{\partial P}{\partial x} = \frac{dP_\infty}{dx} \tag{4.5}$$

Then, using the Bernoulli equation in the free stream, we obtain the following governing equations:

$$\frac{\partial U}{\partial x} + \frac{\partial V}{\partial y} = 0 \tag{4.6a}$$

$$U\,\frac{\partial U}{\partial x} + V\,\frac{\partial U}{\partial y} = U_\infty\,\frac{dU_\infty}{dx} + \nu\,\frac{\partial^2 U}{\partial y^2} + \frac{\partial}{\partial y}\,(-\overline{u'v'} - \overline{\tilde{u}\tilde{v}}) \tag{4.6b}$$

$$U\,\frac{\partial T}{\partial x} + V\,\frac{\partial T}{\partial y} = \alpha\,\frac{\partial^2 T}{\partial y^2} + \frac{\partial}{\partial y}\,(-\overline{t'v'} - \overline{\tilde{t}\tilde{v}}) \tag{4.6c}$$

This is the required PDE. Note that $(-\overline{\tilde{u}\tilde{v}})$ and $(-\overline{\tilde{t}\tilde{v}})$ terms appear in addition to the turbulent correlation terms.

C. Derivation of Integral Equations

Two different approaches were taken to derive the integral equations: one from the PDE (4-6), and the other from the global conservation on the boundary layer. The comparison of these two derivations gives the wall value of $-\overline{\tilde{u}\tilde{v}}$ and $-\overline{\tilde{t}\tilde{v}}$, which is an important step in the construction of the model in solving PDE.

C.1 Derivation from PDE

By integrating Equation (4.6b) from 0 to h, where h is outside the boundary layer, we obtain

$$\int_0^h \left(U \frac{\partial U}{\partial x} + V \frac{\partial U}{\partial y}\right) dy = \int_0^h U_\infty \frac{dU_\infty}{\partial x} dy + \int_0^h \frac{\partial}{\partial y}\left(\nu \frac{\partial U}{\partial y} - \overline{u'v'} - \overline{\tilde{u}\tilde{v}}\right) dy$$

At $y = h$, $\nu \frac{\partial U}{\partial y} = 0$, $-\overline{u'v'} = 0$, and $-\overline{\tilde{u}\tilde{v}} = 0$. At $y = 0$, $\nu \frac{\partial U}{\partial y}\Big|_0 =$ $g_c \tau_o / \rho$, $-\overline{u'v'} = 0$, and $(-\overline{\tilde{u}\tilde{v}}) \neq 0$. Thus,

$$\int_0^h \left(U \frac{\partial U}{\partial x} + V \frac{\partial U}{\partial y} - U_\infty \frac{dU_\infty}{dx}\right) dy = -\frac{g_c \tau_o}{\rho_o} + (\overline{\tilde{u}\tilde{v}})_o \tag{4.7}$$

From Equation (4.6a),

$$V = V_o - \int_0^y \frac{\partial U}{\partial x} dy \tag{4.8}$$

Thus, using Equation (4.8), the left hand side of Equation (4.7) becomes:

$$\int_0^h \left(U \frac{\partial U}{\partial x} + V \frac{\partial U}{\partial y} - U_\infty \frac{dU_\infty}{dx}\right) dy = \int_0^h \left\{U \frac{\partial U}{\partial x} + \left(V_o - \int_0^y \frac{\partial U}{\partial x} dy\right) \frac{\partial U}{\partial y} - U_\infty \frac{dU_\infty}{dx}\right\} dy$$

Now, integrating by parts, we obtain

$$\int_0^h \left(\int_0^y \frac{\partial U}{\partial x} dy\right) \frac{\partial U}{\partial y} dy = \left[U \int_0^y \frac{\partial U}{\partial x} dy\right]_0^h - \int_0^h \frac{\partial U}{\partial x} U \, dy$$

$$= U_\infty \int_0^h \frac{\partial U}{\partial x} dy - \int_0^h U \frac{\partial U}{\partial x} dy$$

Using this result, Equation (4.7) becomes

$$\int_0^h \left(2U \frac{\partial U}{\partial x} - U_\infty \frac{\partial U}{\partial x} - U_\infty \frac{dU_\infty}{dx} + V_o \frac{\partial U}{\partial y}\right) dy = -\frac{g_c \tau_o}{\rho} + (\overline{\tilde{u}\tilde{v}})_o$$

By rearranging the terms and using the boundary condition for $U = 0$ at $y = 0$, we obtain

$$\frac{d}{dx}\int_0^h U(U_\infty - U)dy + \frac{dU_\infty}{dx}\int_0^h (U_\infty - U)dy = \frac{g_c \tau_o}{\rho} + V_o U_\infty - (\overline{\tilde{u}\tilde{v}})_o$$

Using the definitions of momentum-deficit thickness and displacement thickness, we have

$$\frac{d}{dx}(U_\infty^2 \delta_2) = \frac{g_c \tau_o}{\rho} + V_o U_\infty - (\overline{\tilde{u}\tilde{v}})_o - U_\infty \frac{dU_\infty}{dx}\delta_1 \tag{4.9}$$

where momentum deficit thickness, δ_2, is defined as

$$U_\infty^2 \delta_2 = \int_0^\infty U(U_\infty - U)dy$$

and displacement thickness, δ_1, is defined as

$$U_\infty \delta_1 = \int_0^\infty (U_\infty - U)dy$$

Similarly, for the energy Equation (4.6c), we can derive the energy integral equation.

$$\frac{d}{dx}\{U_\infty(T_o - T_\infty)\Delta_2\} = \frac{\dot{q}''_o}{\rho C_p} + V_o(T_o - T_\infty) + (\overline{\tilde{t}\tilde{v}})_o \tag{4.10}$$

In Equations (4.9) and (4.10), there appear $(-\overline{\tilde{u}\tilde{v}})_o$ and $(-\overline{\tilde{t}\tilde{v}})_o$, which are due to the non-equilibrium situation in the film cooling; the injection angle of the jet is not necessarily normal to the wall, and the injection gas temperature does not have to be the same as the wall temperature. These two terms are always zero in the uniform transpiration problem. Also, note that the derivation of Equations (4.9) and (4.10) used the boundary conditions $U = 0$ and $T = T_o$ at $y = 0$. These boundary conditions are true at the wall but not at $y = 0$ from local averaging, but, from the practical applications, what is important is the solid wall temperature, not the true average of the solid and the injected gas temperature. The slip boundary appears $(U \neq 0$ at $y = 0)$ if the true average velocity at $y = 0$ is used.

The above treatment provides convenience in application.

For the evaluation of $(-\overline{\tilde{u}\tilde{v}})_o$ and $(-\overline{\tilde{t}\tilde{v}})_o$, the derivation of integral equations from global conservation is necessary.

C.2 Derivation from the Global Conservation on the Boundary Layer

The control volume for mass, momentum, and energy is shown in Figure 4.2. The local average is made in area A with sides $\ell \times s$. Then all the properties are integrated within this area at x and $x + \Delta x$; then the normal bookkeeping for conservation of property is pursued. Conservation of mass within the control volume gives

$$\dot{m}_\infty \Delta x + \{\rho_\infty U_\infty (h-\overline{\delta}_1) + \frac{d}{dx} (\rho_\infty U_\infty (h-\overline{\delta}_1))\Delta x\}A = \dot{m}_o \Delta x + \rho_\infty U_\infty (h-\overline{\delta}_1)A$$

for steady state.

By integrating over the area A , we have $\dot{m}_o$ and $\dot{m}_\infty$, not $\dot{m}''_o$ and $\dot{m}''_\infty$. Also, the following identity was used.

$$\int_o^h \rho u dy = \rho_\infty U_\infty (h-\overline{\delta}_1)$$

Thus

$$\dot{m}_\infty = \dot{m}_o - \frac{d}{dx} (\rho_\infty U_\infty (h-\overline{\delta}_1))A \qquad (4.11)$$

Then collecting the forces and momentum fluxes in Figure 4.2 in the form

$$\{mom\}_{out} - \{mom\}_{in} = \Sigma \text{ forces}$$

$$\{\rho_\infty U_\infty^2(h-\overline{\delta}_1-\overline{\delta}_2) + \frac{d}{dx}(\rho_\infty U_\infty^2(h-\overline{\delta}_1-\overline{\delta}_2)\Delta x\}A + \dot{m}_\infty U_\infty + \frac{\partial U_\infty}{\partial x}\frac{\Delta x}{2} \quad \Delta x$$

$$- \dot{m}_o U_x \Delta x - \rho_\infty U_\infty^2(h-\overline{\delta}_1-\overline{\delta}_2)A$$

$$= g_c PhL - (g_c P + g_c \frac{dP}{dx}\Delta x)hL - g_c \tau_o A$$

In this expression the following identity was used:

$$\int_o^h \rho u^2 dy = \rho_\infty U_\infty^2(h-\delta_1-\delta_2)$$

Rearrangement of the momentum conservation equation gives

$$\frac{d}{dx}(\rho_\infty U_\infty^2(h-\overline{\delta}_1-\overline{\delta}_2)) + \frac{\dot{m}_o}{A}(U_\infty - U_x) = - g_c \tau_o - g_c h \frac{dP}{dx}$$

Now $g_c \frac{dP}{dx}$ can be substituted by

$$- g_c \frac{dP}{dx} = \rho_\infty U_\infty \frac{dU_\infty}{dx}$$

Then finally we obtain the following momentum integral equation:

$$\frac{d}{dx}(\rho_\infty U_\infty^2 \overline{\delta}_2) = g_c \tau_o + \frac{\dot{m}_o}{A}(U_\infty - U_x) - \rho_\infty U_\infty \overline{\delta}_1 \frac{dU_\infty}{dx}$$

In this case, fluid is considered incompressible and $\rho_\infty = \rho = \text{const.}$

$$\frac{d}{dx}(U_\infty^2 \overline{\delta}_2) = \frac{g_c \tau_o}{\rho} + \frac{\dot{m}_o}{A\rho}(U_\infty - U_x) - U_\infty \frac{dU_\infty}{dx}\overline{\delta}_1$$

Now

$$\frac{\dot{m}_o}{A\rho} = V_o$$

$$\frac{d}{dx}(U_\infty^2 \bar{\delta}_2) = \frac{g_c \tau_o}{\rho} + V_o(U_\infty - U_x) - U_\infty \frac{dU_\infty}{dx} \bar{\delta}_1 \tag{4.12}$$

Comparing Equations (4.9) and (4.12), we obtain

$$\overline{(\tilde{u}\tilde{v})}_o = V_o U_x \tag{4.13}$$

For the energy integral equation, we can obtain the following result:

$$\frac{d}{dx}\{U_\infty (T_o - T_\infty)\bar{\Delta}_2\} = \frac{\dot{q}''_o}{\rho C_p} + V_o(T_2 - T_\infty) \tag{4.14}$$

Comparing Equations (4.10) and (4.14), we obtain

$$\overline{(\tilde{t}\tilde{v})}_o = V_o(T_2 - T_o) \tag{4.15}$$

By proper non-dimensionalization, (4.12) and (4.14) can be recast in the form

$$\frac{d\, Re_{\bar{\delta}_2}}{d\, Re_x} = \frac{C_f}{2} - (1 + H)K\, Re_{\bar{\delta}_2} + F\left\{1 - \frac{U_x}{U_\infty}\right\} \tag{4.16}$$

and

$$\frac{d\, Re_{\bar{\Delta}_2}}{d\, Re_x} = St + F \cdot \theta \tag{4.17}$$

where

$$Re_{\bar{\delta}_2} = \frac{U_\infty \bar{\delta}_2}{\nu}, \quad Re_{\bar{\Delta}_2} = \frac{U_\infty \bar{\Delta}_2}{\nu}, \quad \text{and} \quad d\, Re_x = \frac{U_\infty}{\nu}\, dx$$

Comparing Equations (4.16) and (4.17) to the corresponding integral equations in the transpiration problem, we can conclude that transpiration cooling is the special case of film cooling where

$$\frac{U_x}{U_\infty} = 0 \quad \text{and} \quad \theta = 1.0 \quad \text{always}$$

$C_f/2$ and St are not necessarily the same as those in the transpiration cooling.

In this program, we are interested in U_∞ = const., (T_o-T_∞) = const. with normal injection ($U_x = 0$). Thus Equations (4.16) and (4.17) become

$$\frac{d\overline{\delta}_2}{dx} = \frac{C_f}{2} + F \tag{4.18}$$

and

$$\frac{d\overline{\Delta}_2}{dx} = St + F \cdot \theta \tag{4.19}$$

With normal injection, the only difference from the uniform transpiration problem is the appearance of θ. The effect of discrete hole injection in film cooling is contained in θ, $C_f/2$, and St through equations (4.18) and (4.19). On the other hand, with PDE Equation (4.6) explicitly shows the effect of discrete holes in terms of $(-\overline{\tilde{u}\tilde{v}})$ and $(-\overline{\tilde{t}\tilde{v}})$.

The following decomposition for $(\overline{\tilde{u}\tilde{v}})$ and $(\overline{\tilde{t}\tilde{v}})$ will be very helpful in the later development of the analytical model. We may set

$$-\overline{\tilde{u}\tilde{v}} = (-\overline{\tilde{u}\tilde{v}})_{hom} + (-\overline{\tilde{u}\tilde{v}})_{non-hom} \tag{4.20a}$$

and

$$-\overline{\tilde{t}\tilde{v}} = (-\overline{\tilde{t}\tilde{v}})_{hom} + (-\overline{\tilde{t}\tilde{v}})_{non-hom} \tag{4.20b}$$

The terms $(-\overline{\tilde{u}\tilde{v}})_{hom}$ and $(-\overline{\tilde{t}\tilde{v}})_{hom}$ are the solutions for $(-\overline{\tilde{u}\tilde{v}})_o = 0$, and $(-\overline{\tilde{t}\tilde{v}})_o = 0$. The term, $(-\overline{\tilde{u}\tilde{v}})_{non-hom}$, has V_oU_x at $y = 0$, and the term, $(-\overline{\tilde{t}\tilde{v}})_{hon-hom}$, has $V_o(T_2-T_o)$ at $y = 0$. Since $(-\overline{\tilde{u}\tilde{v}})_{hom}$ and $(-\overline{\tilde{t}\tilde{v}})_{hom}$ have zero value at the wall and at free stream, they have similar character as $(-\overline{u'v'})$ and $(-\overline{t'v'})$. Also they have similar governing equations, because they are both perturbations to the Navier-Stokes and the energy equations. Physically, it is not easy to distinguish between the turbulence correlation terms and the three-dimensional correlation terms ($-\overline{\tilde{u}\tilde{v}}$ and $-\overline{\tilde{t}\tilde{v}}$). In evaluating τ_o and $\dot{q}''_o$, we can still use the traditional definitions, as shown below.

With this decomposition, we can define the total shear stress and heat flux as

$$\frac{g_c \tau}{\rho} = \nu \frac{\partial U}{\partial y} - \overline{u'v'} - (\overline{\tilde{u}\tilde{v}})_{hom} \tag{4.21a}$$

and

$$\frac{\dot{q}''}{\rho C_p} = - \alpha \frac{\partial T}{\partial y} - \overline{t'v'} - (\overline{\tilde{t}\tilde{v}})_{hom} \tag{4.21b}$$

and

$$\frac{\partial}{\partial y} (-(\overline{\tilde{u}\tilde{v}})_{non-hom}) = S_m$$

and

$$\frac{\partial}{\partial y} (-(\overline{\tilde{t}\tilde{v}})_{non-hom}) = S_h$$

where S_m and S_h are an effective body force and an effective source. The definitions in Equations (4.21) do not change the wall shear stress and the wall heat flux,

$$\tau_o = \mu \left. \frac{\partial U}{\partial y} \right|_o$$

and

$$\dot{q}''_o = - k \left. \frac{\partial T}{\partial y} \right|_o$$

Also, using the values at the wall, we may put

$$(\overline{\tilde{u}\tilde{v}})_{non-hom} = V_o U_x g(y,x) \tag{4.22a}$$

and

$$(\overline{\tilde{t}\tilde{v}})_{non-hom} = V_o (T_2 - T_o) f(y,x) \tag{4.22b}$$

where $g(y,x)$ and $f(y,x)$ represent the distributions of the effective body force and the effective source in the boundary layer. They both have a value of 1.0 at the wall and 0 at the free-stream. The argument y was put before x to show that g and f are mainly functions of y.

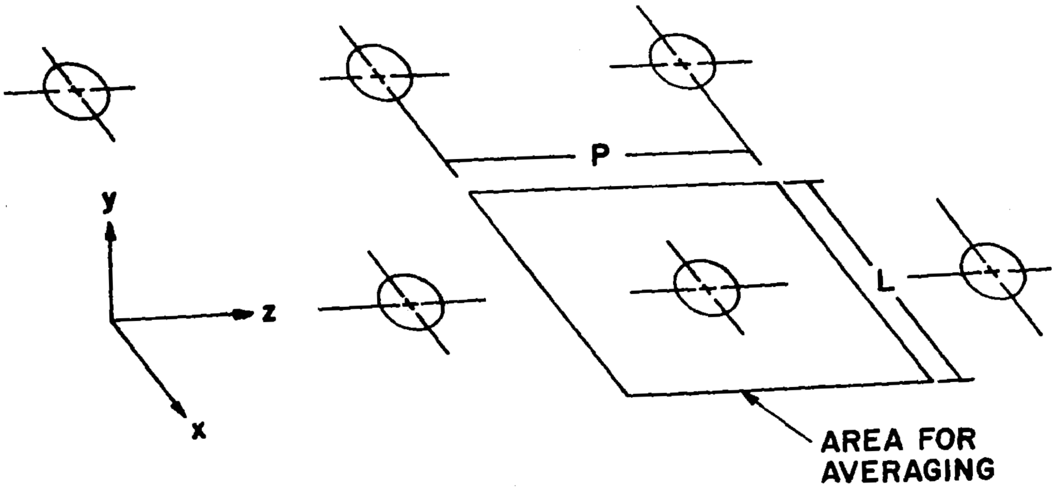

Figure 4.1 Area for local averaging.

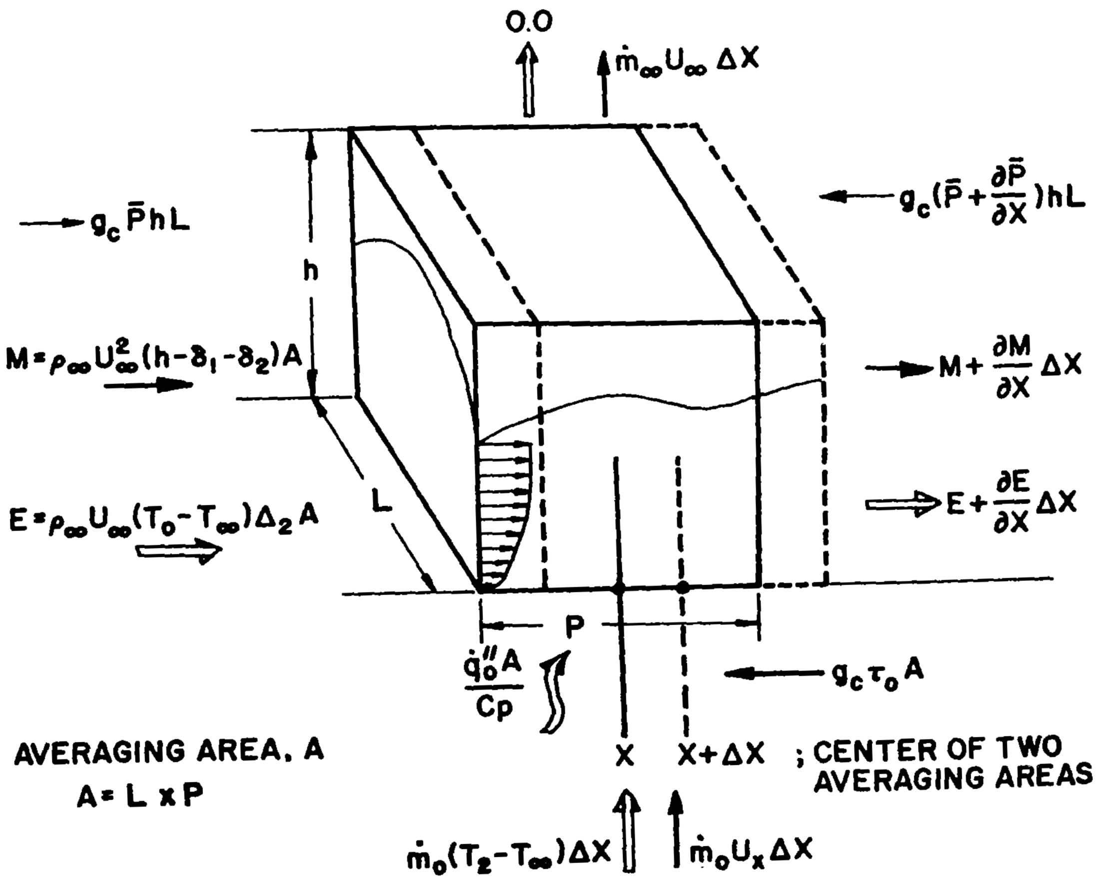

Figure 4.2 Control volume for the derivation of integral equations.

CHAPTER V

EXPERIMENTAL RESULTS

This chapter provides two types of data taken in these experiments: Stanton number data and the mean velocity and mean temperature profiles, which were used to obtain the mixing length profile.

In these experiments, there were eleven rows of holes for discrete hole blowing, with one solid plate used as a guard heater on the upstream end. In all the data presented, the second to twelfth data points represent the blowing region. The first data point plus the recovery region following the twelfth point were not blown.

All the data were taken at either $0.0 \leq \theta \leq 0.1$ or $0.9 \leq \theta \leq 1.1$, and the superposition principle (see Chapter III) was used to get the values of Stanton number for $\theta = 1.0$ and $\theta = 0.0$ precisely. For the recovery region, the average value of θ in the blowing region was used to apply the superposition principle.

The primary investigation was done at $U_\infty = 54$ ft/sec (16.5 m/sec) to determine the effect of blowing with this geometry. In these tests, the effect of the unheated starting length was certainly present. To investigate this effect, plus other secondary variables, U_∞ was varied, the unheated starting length was varied, and the momentum thickness at the first plate, δ_2 , was varied. Also, the case of $P/D = 10$ was run to investigate the effect of P/D . In addition, some untripped cases were run to show the effect of discrete hole blowing on transition. These runs are summarized in Table 5.1.

The number of data sets was kept as small as possible by changing one parameter at a time with other variables fixed. To cover the possible combination of variables appearing in Table 5.1, more than 200 data sets would be necessary. In this experiment 49 data sets were taken.

A. Stanton Number Data

A.1 Effect of M on Stanton Number (Figures 5.1 to 5.4)

Figure 5.1 shows the hydrodynamic condition at the first plate which was the guard plate, and had no holes. The flow shows a typical

Table 5-1

STANTON NUMBER RUNS

	FORE PLATE											
	UNHEATED						PARTLY HEATED		*(1) HEATED			
									TRIPPED		NOT TRIPPED	
U_∞, ft/sec (m/sec)	32 (9.75)		54 (16.5)		110 (33.6)		54 (16.5)		38 (11.6)		38 (11.6)	
*(2) $Re_{\overline{\delta}2}$	1730		2810		5320		2790		540		516	
*(2) $Re_{\overline{\Delta}2}$	70		100		170		1820		590		555	
P/D	5	10	5	10	5	10	5	10	5	10	5	10
M=0.0	X		X	X	X		X		X	X		X
M=0.1			X									
M=0.2	X		X	X	X		*(3) X		X	X	X	
M=0.3			X									
M=0.4			X									
M=0.5			*(4) X	X					X	X		
M=0.65			X									
M=0.8	X											
M=1.0	X			X								
M=variable									X			

NOTE: (1) The top wall was adjusted in the plate upstream of blowing to produce a low Reynolds number turbulent boundary layer in the blowing section.

(2) The values of $Re_{\overline{\delta}2}$ and $Re_{\overline{\Delta}2}$ listed here are taken at the starting point of blowing.

(3) For this run, the adiabatic wall effectiveness data, velocity and temperature profiles across the span between the two rows of holes were taken.

(4) For this run, three values of θ were tried.

(5) Except M=0.0, all the experiments were run at θ=0.0 and θ=1.0.

turbulent boundary layer profile with a momentum thickness Reynolds number of about 2800, and an enthalpy thickness Reynolds number about 100. The reason for the long unheated starting length is to give a better defined thermal boundary condition at the wall. The test plates were not built to produce the equilibrium ratios of boundary layer growth, thermal and momentum, for this region.

Figure 5.2 shows the heat transfer results in St vs. Re_x coordinates. The open symbols represent the $\theta = 0.0$ (i.e., $T_2 = T_\infty$) case, and the solid symbols represent $\theta = 1.0$ (i.e., $T_2 = T_o$) case. The open circles represent the case of $M = 0.0$; i.e., no blowing, used as a reference in both parts of Figure 5.2. Blowing was started at the second plate so that the second plate would not have the full effect of discrete hole blowing. At most, half of the plate feels the effect. The case $\theta = 1.0$ (Figure 5.2a) shows a decrease of Stanton number for all values of M below the no-blowing case, except in the initial region. For $M = 0.1$, Stanton number decreases below the no-blowing case even in the initial region, but then as M increases, Stanton number increases, until at $M = 0.4$, Stanton number is about the same as that of the no-blowing case. For values of $M = 0.52$ and $M = 0.63$ Stanton number increases progressively in the initial region. This behavior is confined to the initial blowing region: after about the 8th plate, the Stanton number always decreases further and further below the no-blowing case as M increases. The most pronounced reduction of Stanton number is seen in the recovery region. The decrease is, however, far less than we would expect from a transpiration cooling case with the comparable blowing. For example, for $M = 0.63$ $(F = 0.02)$, a comparable uniform transpiration would completely blow off the boundary layer and give a zero Stanton number. The heat transfer behavior in discrete hole blowing can be explained by the augmentation of turbulent mixing, caused by the discrete injection, dominant over the thermal effect of the injection. In the initial region, the augmentation of turbulence is quite sudden while the mixing of jet flow or thermal energy with the boundary layer flow is a rather gradual process. This explains the high values of Stanton number in the initial region. In the downstream the augmentation of turbulence and the thermal boundary layer growth is more or less balanced and the Stanton number gets comparatively small. Again, in the recovery region, the absence of the discrete hole injection drops the turbulence level rather suddenly but the thermal energy remains the same. This causes a drastic decrease in Stanton number in the recovery region.

The $\theta = 0.0$ case is shown in Figure 5.2b. In this case, the higher the value of M the larger the Stanton numbers, except in the recovery region where the ordering reverses. The increase of Stanton number is caused by the injected gas, whose temperature is the same as the free-stream temperature, causing an effective sink. The decrease of Stanton number in the recovery region below the no-blowing case is attributed to the thick boundary layer developed by large blowing. The effect of the thick boundary layer may be partly overcome by the fact that the injected fluid, whose temperature is the same as the free-stream temperature, creates an effective sink whose strength is proportional to the blowing rate. The decreasing effect of M at high M may be explained by the fact that the injected jet penetrates farther into the boundary layer due to its higher momentum, thus moving the "sink" further from the wall.

In Figure 5.3, results for $\theta = 1.0$ are plotted in $Re_{\overline{\Delta}_2}$ coordinate. This coordinate shows Stanton number behavior per unit of enthalpy delivered to the boundary layer. The small arrow shows the end of the blowing region. $M = 0.1$ is the only case which falls below the no-blowing case. At $M = 0.2$, Stanton number is about the same as the no-blowing case. As M increases, Stanton number increases in the first portion of the test plate but then tends to decrease faster in the downstream. This is probably due to the fact that thermal mixing becomes more important in the downstream region. Figure 5.4 shows the $\theta = 0.0$ case plotted in $Re_{\overline{\Delta}_2}$ coordinate. The regularity of the increasing pattern in the blown region is pronounced. The small arrow shows the end of the blowing region.

For applications in gas turbine blade cooling, it may not be desirable to have a strong blowing in the initial region, particularly not with a normal angle injection hole. Leading edge values of θ have been proposed to be in the range of 1.0 to 1.5; strong blowing might increase, rather than decrease, the heat load on the leading edge.

A.2 Effect of U_∞ (Figures 5.5 to 5.10)

Figure 5.5 shows the velocity profile on the first plate for U_∞ reduced to 31.5 fps (9.6 m/s). This still shows the expected flat plate turbulent boundary layer profile, as did the run at $U_\infty = 54.9$ fps (16.7 m/s) shown in Figure 5.1

Figure 5.6 shows the heat transfer results for $U_\infty \sim 32$ ft/sec (9.76 m/s). The $M = 0.2$ case was chosen for cross-comparison, and $M = 0.74$ and $M = 0.91 \sim 0.94$ were chosen for additional data. Note that for these latter values of M, Stanton numbers at $\theta = 1.0$ fall below 10^{-3} in the recovery region. In Figure 5.6b, at $M = 0.2$, and $\theta = 0.0$, the Stanton number ratio, St/St_o seems to be higher than that at U_∞ = 54 ft/sec (16.5 m/s). Otherwise, it shows similar behavior as in the previous case, and the general behavior can be explained by the augmentation of mixing, boundary layer growth and the effective sink.

The same trend is observed in Figure 5.7 as in Figure 5.3. Especially note that at $M = 0.17$, the very same behavior as at $U_\infty = 54$ ft/sec (16.5 m/s) is observed; the value of Stanton number at $M \cong 0.2$ is about that of the no-blowing Stanton number. In Figure 5.8, St/St_o is slightly higher than that at $U_\infty = 54$ ft/sec (16.5 m/s). St/St_o for fixed $Re_{\overline{\Delta}_2}$ is the usual correlation for the case of uniform transpiration. Physically this ratio represents a comparison of the non-dimensional heat transfer performance (Stanton number) of the two situations, evaluated at the same energy level of the boundary layer.

Figure 5.9 shows the velocity profile on the first plate at U_∞ = 115 ft/sec (35 m/s). This also shows the fully developed turbulent boundary layer. Figure 5.10 shows the heat transfer results at $M = 0.2$. Figure 5.10a shows Stanton number vs. Re_x for both $\theta = 1.0$ and $\theta = 0.0$. The behavior is very much similar to the $U_\infty = 54$ ft/sec (16.5 m/s) and 32 ft/sec (9.76 m/s) cases. The St/St_o ratio at fixed $Re_{\overline{\Delta}_2}$ for $\theta = 0.0$ seems to be slightly smaller than that at $U_\infty = 54$ ft/sec (16.5 m/s). At $\theta = 1.0$, the Stanton number is about the same value as that of the no-blowing case in $Re_{\overline{\Delta}_2}$ coordinate, the same behavior.

The results of this series of experiments show that St/St_o is not affected by U_∞, if properly presented. For the case $\theta = 1.0$

(resembling transpiration):

$$\frac{\left.\dfrac{St}{St_o}\right|_{Re_x}}{\dfrac{\ln(1 + B_h)}{B_h}} \neq f(U_\infty)$$

where

$$B_h = F/St$$

This will be shown in Section B along with Figure 5.20. For $\theta = 0.0$, St/St_o , evaluated at fixed $Re_{\bar{\Delta}_2}$, drops slightly as U_∞ is increased.

A.3 Effect of $\bar{\Delta}_2$ Change (Figure 5.11 to 5.13)

For this test, only half of the foreplate was heated to increase the enthalpy thickness at the beginning of blowing. The value of U_∞ was kept constant at 55 ft/sec (16.7 m/s). Figure 5.11 shows the velocity profile, and Figure 5.12 shows the temperature profile on the first plate. These two profiles show that the momentum and the thermal boundary layer are nearly in equilibrium. Figure 5.13 shows that there is no difference in behavior from Figure 5.2 to 5.4 if the same criteria as in the Subsection A.2 is used. That is, St/St_o divided by $\ln(1 + B_h)/B_h$ at fixed Re_x for $\theta = 1.0$ and St/St_o at fixed $Re_{\bar{\Delta}_2}$ for $\theta = 0.0$ are used for comparison.

A.4 Effect of P/D Change (Figure 5.14)

To see the effect of P/D change, alternate rows of holes were plugged, as well as alternate holes in the remaining rows, using fitted corks. This made it possible to produce $P/D = 10$. Figure 2.13 (see Chapter II) shows that the effect of having cork plugs is negligible on the velocity profile.

Figure 5.14 shows the heat transfer results at $P/D = 10$. The general trends of St for $\theta = 1.0$ and $\theta = 0.0$ are similar to $P/D = 5$ case, but with much-diminished effect. At $M = 1.0$ with $\theta = 1.0$, Stanton numbers are higher than those of the no-blowing case all through the blowing region, a trend not observed for $P/D = 5.0$. For the same value of M , the cooling effect from $P/D = 10$ geometry is much inferior to $P/D = 5$ geometry in Re_x coordinate. Even at the same value of F , the $P/D = 10$ case will be inferior to the $P/D = 5$ case, because higher velocity jets are formed and they will penetrate farther into the boundary layer, which eventually will decrease the effect of the protecting sink near the wall, and because the higher velocity jets tend to create a higher turbulence level.

At $M = 0.17$ with $\theta = 1.0$, St/St_o at fixed $Re_{\overline{\Delta}_2}$ seems to be about 1.0 . It is surprising that the behavior of St/St_o at $M \cong 0.2$ with $\theta = 1.0$ does not change very much from the $P/D = 5$ to the $P/D = 10$ case if compared in $Re_{\overline{\Delta}_2}$ coordinate. The small fluctuations in Stanton number are due to the fact that the alternate rows of holes are plugged up to produce $P/D = 10$.

A.5 Effect of $\overline{\delta}_2$ Change (Figure 5.15 to 5.18)

Figure 5.15 shows the velocity profile on the first plate, with the foreplate accelerated to produce the low momentum thickness. A boundary layer trip was used to obtain a quick transition to a turbulent boundary layer. In this profile, a logarithmic region appears at very small values of y^+ , $y^+ = 20 \sim 50$. This is partly due to the small value of momentum thickness and partly due to the acceleration effect which was not relaxed completely. Figure 5.16 shows the temperature profile, which is similar to the velocity profile.

Figure 5.17 shows the Stanton number at $P/D = 5$ with low $\overline{\delta}_2$. The $M = 0.0$ case is above the known correlation for the flat plate by 4-7%. This is probably due to the disturbance from open holes which is more important at low $\overline{\delta}_2$. Both in Re_x and $Re_{\overline{\Delta}_2}$ coordinates, the heat transfer behavior is essentially the same if the same correlation parameters are used. The first point has the effect of acceleration and falls below the flat plate correlation.

Figure 5.18 shows the result with $P/D = 10$ and small $\overline{\delta}_2$. Both in Re_x and $Re_{\overline{\Delta}_2}$, Stanton number behavior is very similar to that shown in Figure 5.14.

A.6 Effect of Discrete Hole Blowing on Laminar-to-Turbulent Transition (Figure 5.19)

Figure 5.19 shows the Stanton number behavior with a natural transition from a laminar to turbulent boundary layer. It shows that with $M = 0.2$, transition occurs within about 5 in. (12.7 cm). These data indicated that at the center of the channel the flow remains laminar about 30 inches downstream of the point where acceleration is stopped. Also, a pitot probe at the end of the stethoscope confirmed that the turbulent boundary layer develops from the side walls towards the center of the channel. Even after 50 inches downstream of acceleration, flow does not seem to have fully-developed turbulent flow. This is probably due to a low turbulence level ($\sim 0.4\%$) and to the acceleration. For $M = 0.0$, there appears a long transition to turbulent flow. The abrupt change in Stanton number appears between the blowing region and the recovery region because of the different methods of obtaining heat transfer coefficients between the two sections. In the blowing section, the plate energy balance is made over the whole plate area and Stanton number represents the true average value. In the recovery region, heat flux meter senses only the center two inches.

Discrete hole blowing makes a very quick transition, and it probably is not recommended to have discrete hole blowing in the laminar boundary layer region as a means of cooling the surface.

B. Construction of a Simple Theory

B.1 Couette Flow Analysis

From examination of the above Stanton number results, it is clear that heat transfer behavior has a distinctive pattern. Since we have developed the proper integral equations for momentum and energy, what we need in terms of prediction is C_f/C_{f_o} and St/St_o as functions of the variables of the integral equations. In this case, this program concerns itself with heat transfer behavior, and we need only the experimental information concerning St/St_o.

Now, invoking the Couette flow approximation on Equations (4.6a) and (4.6c), we obtain

$$\frac{dV}{dy} = 0 \tag{5.1}$$

$$V\frac{dT}{dy} = \frac{d}{dy}\left(\alpha\frac{dT}{dy} - \overline{t'v'} - \overline{\tilde{t}\tilde{v}}\right) \tag{5.2}$$

From Equation (5.1), $V = V_o$. Thus Equation (5.2) becomes

$$V_o\frac{dT}{dy} = \frac{d}{dy}\left(\alpha\frac{dT}{dy} - \overline{t'v'} - \overline{\tilde{t}\tilde{v}}\right)$$

Using Equation (4.21b), we obtain

$$V_o\frac{dT}{dy} = \frac{d}{dy}\left(-\frac{\dot{q}''}{\rho c_p}\right) + S \tag{5.3}$$

Now

$$S = -\frac{d}{dy}\left(V_o(T_2-T_o)f(y)\right)$$

To be more general, following the formulations done in Kays [68], we have

$$\dot{m}''_o\frac{dP}{dy} = \frac{d}{dy}\left(\lambda\frac{dP}{dy}\right) - \dot{m}''_o(P_2-P_o)\frac{df}{dy} \tag{5.4}$$

where P represents property in general, and $-\lambda\frac{dP}{dy}$ represents property flux. The boundary conditions for Equation (5.4) are

$$\begin{aligned} P &= P_o \quad \text{at} \quad y = 0 \\ P &= P_\infty \quad \text{at} \quad y = Y \end{aligned} \tag{5.5}$$

where Y is outside the boundary layer. Also, the property conservation in the control volume shown gives the following mass transfer relationship at the wall,

$$\dot{m}''_o = \frac{\lambda\left.\frac{dP}{dy}\right|_o}{P_2 - P_T} = g\,\frac{P_\infty - P_o}{P_2 - P_T} \tag{5.6}$$

where g represents the general mass transfer coefficient and the driving function for the film cooling situation is

$$B = \frac{P_\infty - P_o}{P_2 - P_T} = \frac{\dot{m}''_o}{g} \tag{5.7}$$

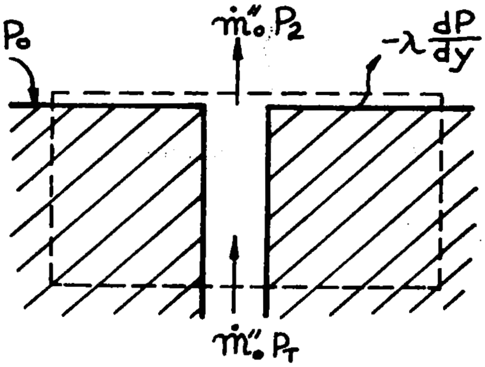

(No radiation, no lateral conduction, no chemical reaction, no source within the control volume)

Equation (5.4) can be integrated, and we obtain

$$\dot{m}''_o P - \lambda \frac{dP}{dy} + \dot{m}''_o (P_2 - P_o) f(y) = C_1$$

At $y = 0$, $\lambda \left.\frac{dP}{dy}\right|_o = \dot{m}''_o (P_2 - P_T)$

$$C_1 = \dot{m}''_o P_T$$

$$\dot{m}''_o (P - P_T) - \lambda \frac{dP}{dy} + \dot{m}''_o (P_2 - P_o) f(y) = 0$$

or

$$\dot{m}''_o (P - P_T) - \lambda \frac{d(P - P_T)}{dy} + \dot{m}''_o (P_2 - P_o) f(y) = 0 \tag{5.8}$$

(1) <u>$\theta = 1.0$ Case ($P_2 = P_o$ Case)</u>

In this case, Equation (5.8) can be integrated and we can obtain the following result, as in Kays [68]:

$$g = \frac{\ell n (1 + B_h)}{B_h} \frac{1.0}{\int_o^Y \frac{dy}{\lambda}} \tag{5.9}$$

where

$$B_h = \frac{\dot{m}''_o}{g} = \frac{P_\infty - P_o}{P_o - P_T}$$

Now, as $\dot{m}''_o \to 0$, we have

$$g_o = \lim_{\dot{m}''_o \to 0} g = \frac{1.0}{\int_o^Y \frac{dy}{\lambda_o}} \qquad (5.10)$$

Then we can form the ratio

$$\frac{g}{g_o} = \frac{\ln(1 + B_h)}{B_h} \left\{ \frac{\int_o^Y \frac{dy}{\lambda_o}}{\int_o^Y \frac{dy}{\lambda}} \right\} \qquad (5.11)$$

In the case of transpiration cooling, the quantity inside { } is unity (overall transport property does not change very much), but in the case of film cooling through discrete holes, we have

$$\phi_1 = \frac{\int_o^Y \frac{dy}{\lambda_o}}{\int_o^Y \frac{dy}{\lambda}} = \phi_1(F, P/D) \qquad (5.12)$$

(2) $\theta = 0.0$ Case ($P_2 = P_\infty$ Case)

In this case, there is no closed solution found for g/g_o , but we could guess that

$$\frac{g}{g_o} = \phi_2(B_c, F, P/D, Re_{\infty,D}) \qquad (5.13)$$

where

$$B_c = \frac{P_\infty - P_o}{P_\infty - P_T} \quad , \quad \text{and} \quad Re_{\infty,D} = \frac{U_\infty D}{\nu}$$

The $Re_{\infty,D}$ appears here because the effective source is a function of hole diameter, and the proper non-dimensional number is $Re_{\infty,D}$. Note that δ_2 or Δ_2 does not appear in this analysis. In this case a viscous length scale, ν/U_∞, is a proper length scale. ϕ_2 was found not to be a strong function of B_c.

B.2 Recommended Correlations for Integral Prediction

From Equation (4.19), we will obtain two integral equations,

$$\frac{d\bar{\Delta}_2(0)}{dx} = St(0) \tag{5.14}$$

$$\frac{d\bar{\Delta}_2(1)}{dx} = St(1) + F \tag{5.15}$$

$$\left.\frac{St(1)}{St_o}\right|_{Re_{\bar{\Delta}_2}} = \left[\frac{\ell n(1 + B_h)}{B_h}\right]^{1.25} (1 + B_h)^{0.25} \phi_1^{\,1.25} \tag{5.16}$$

$$\left.\frac{St(0)}{St_o}\right|_{Re_{\bar{\Delta}_2}} = \phi_2 \tag{5.17}$$

The factor, ϕ_1, is presented in Figure 5.20 for fixed Re_x. $St(1)/St_o\big|_{Re_x}$ is transformed into $St(1)/St_o\big|_{Re_{\bar{\Delta}_2}}$ following Whitten [3]. The factor, ϕ_2, is presented in Figure 5.21 for fixed $Re_{\bar{\Delta}_2}$. This functional variation was obtained after several trials. ϕ_1 and ϕ_2 are summarized as follows:

$$\begin{aligned} \phi_1 &= 1 + 140F \qquad \text{for} \quad P/D = 5 \\ &= 1 + 180F \qquad \text{for} \quad P/D = 10 \end{aligned}$$

$$\phi_2 = 1 + 55\ Re_{\infty,D}^{-0.29}\ F^{0.43} \quad \text{for} \quad P/D = 5$$

$$= 1 + 48\ Re_{\infty,D}^{-0.29}\ F^{0.43} \quad \text{for} \quad P/D = 10$$

The value of ϕ_1 is greater for $P/D = 10$ than for $P/D = 5$ and the value of ϕ_2 is smaller for $P/D = 10$ than for $P/D = 5$. This means that there is less spread between St(0) and St(1) for $P/D = 10$, and thus its cooling effect will be less at the comparable condition.

For the detailed procedure of solving Equations (5.14) to (5.17) for $\Delta_2(0)$, $\Delta_2(1)$, St(0) and St(1), see Whitten [3]. Once St(0) and St(1) are obtained, we can readily calculate St(θ) as

$$St(\theta) = St(0) - \theta\ \{St(0) - St(1)\} \tag{3.7}$$

using a linear superposition.

C. Profile Data

To get the local average profiles, we must average all the profiles around a hole. This, however, requires a very large number of profiles to be taken. To avoid this, velocity and temperature profiles were taken in a lateral span between the 10th and 11th row of holes. Velocity profiles were also taken between the 7th and 8th row of holes. At this point, the flow field is believed to be reasonably uniform in the x-direction so that the lateral average may not be very different from the local average.

As the M value gets larger, flow separation may be possible. Thus $M = 0.2$ was chosen for the profile study. A pitot probe was used for the velocity profile and at $M = 0.2$, and at the midpoint between two rows of holes the pitot probe error caused by a jet at the wall will be minimum (see Equation (4.4c)).

Figure 5.22 shows velocity profiles between two holes in the lateral direction. At both ends you can clearly see the velocity defect from the jet attached to the wall; and in the middle, only a small defect of the profile still remains which indicates that a jet will spread fairly well after about seven diameters downstream.

Figure 5.23 shows the temperature profiles across a span in the lateral direction, with the hole from the preceding row located in the middle. The profile shows a high plateau in the middle, due to the hot jet attached near the wall, and some small effect remains at each end, similar to the velocity profile.

These profiles were next averaged spanwise. Figures 5.24 and 5.25 show the laterally averaged velocity and temperature profiles in a semi-logarithmic scale. These two profiles indicate that there is a clearly-defined logarithmic region. Following Milikan [69], this means that there exists an inner region similarity and an outer region similarity even with the discrete hole blowing. Also, this was clear in the velocity profiles taken by LeBrocq et al. [33].

The mixing length distribution corresponding to the spanwise averaged profiles is shown in Figure 5.26. The method used for the shear stress calculation is outlined in Simpson [3]. For the momentum thickness Reynolds number, the arithmetic average of each profile is used, and the skin friction coefficient, $C_f/2$, was estimated by using the analogy between momentum and heat.

The mixing length distribution in Figure 5.26 shows a pronounced peak near $y/\delta = 0.1$. Probably at this point, the jet main boundary layer interaction is most active. Pai et al. [43] considered an augmented mixing in their film cooling predictions. From Figure 5.26, it becomes clear that the mixing length, ℓ, can be considered to be augmented by discrete hole blowing. Empirically, the following expression was obtained in the outer region where the damping effect is negligible:

$$\ell_{outer} = \kappa y + \kappa_o \left(\frac{y}{\delta}\right)^2 e^{-\left(\frac{y/\delta}{DPL}\right)^2} \tag{5.18}$$

where κy is the flat plate mixing length, DPL represents the point of maximum augmentation of mixing length, and κ_o the magnitude of maximum augmentation.

Figure 5.27 shows the shear stress distribution, which shows a constant shear stress, due to the jet-boundary layer interaction. The shear stress distribution from Simpson [3] does not show a constant shear stress region in uniform transpiration.

Figure 5.28 shows that for the inner region, a Van Driest damping function with $A^+ = 24$ will give a good representation of the augmented mixing length. The Van Driest damping function was applied to the flat plate mixing length and the augmented mixing length, as

$$\ell_{inner} = \ell_{outer}\left(1 - e^{-y^+/A^+}\right) \quad . \tag{5.19}$$

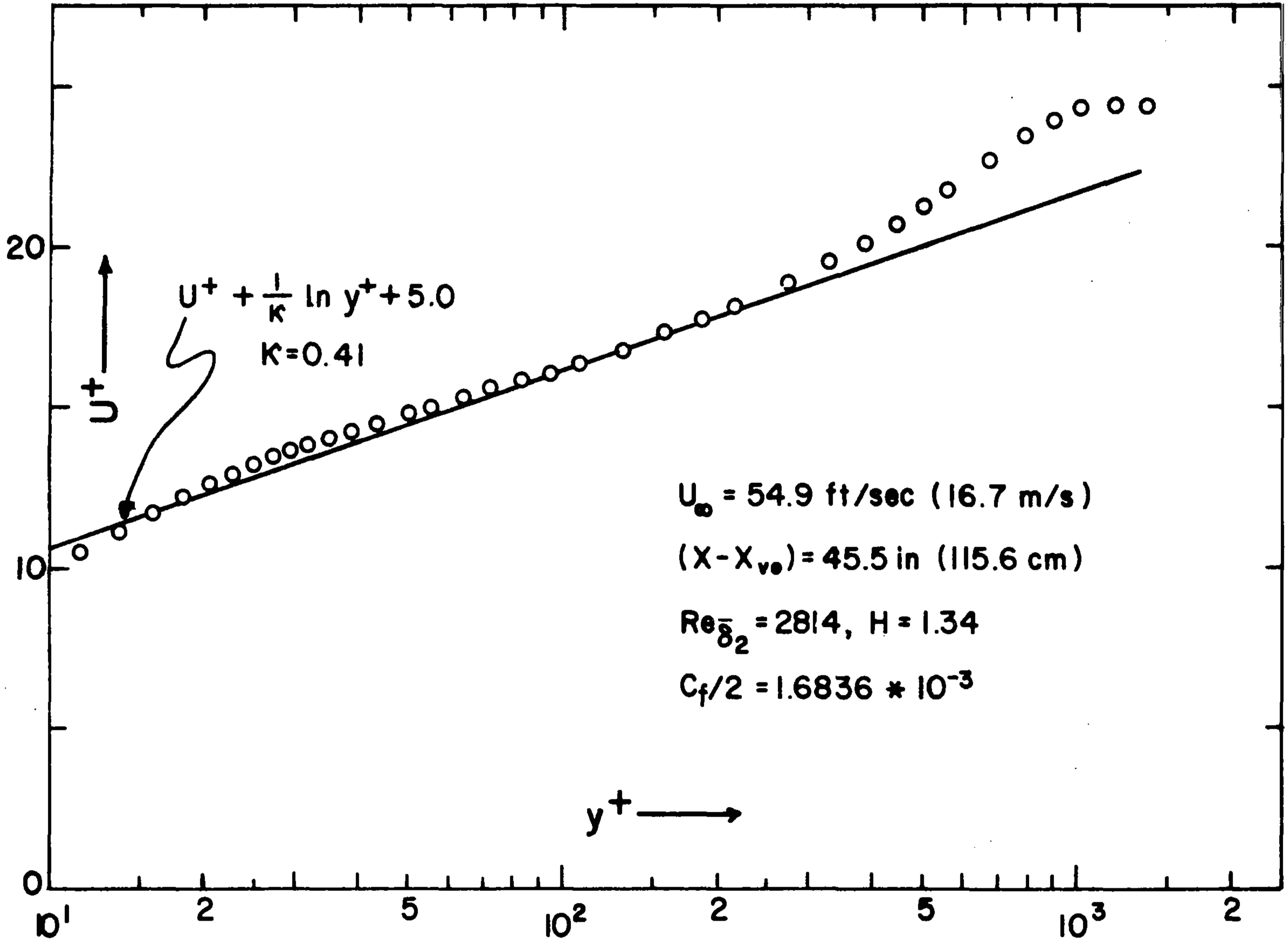

Figure 5.1 Velocity profile at U_∞ = 54 ft/sec (16.5 m/sec) on the first plate, for Figures 5.2 to 5.4 .

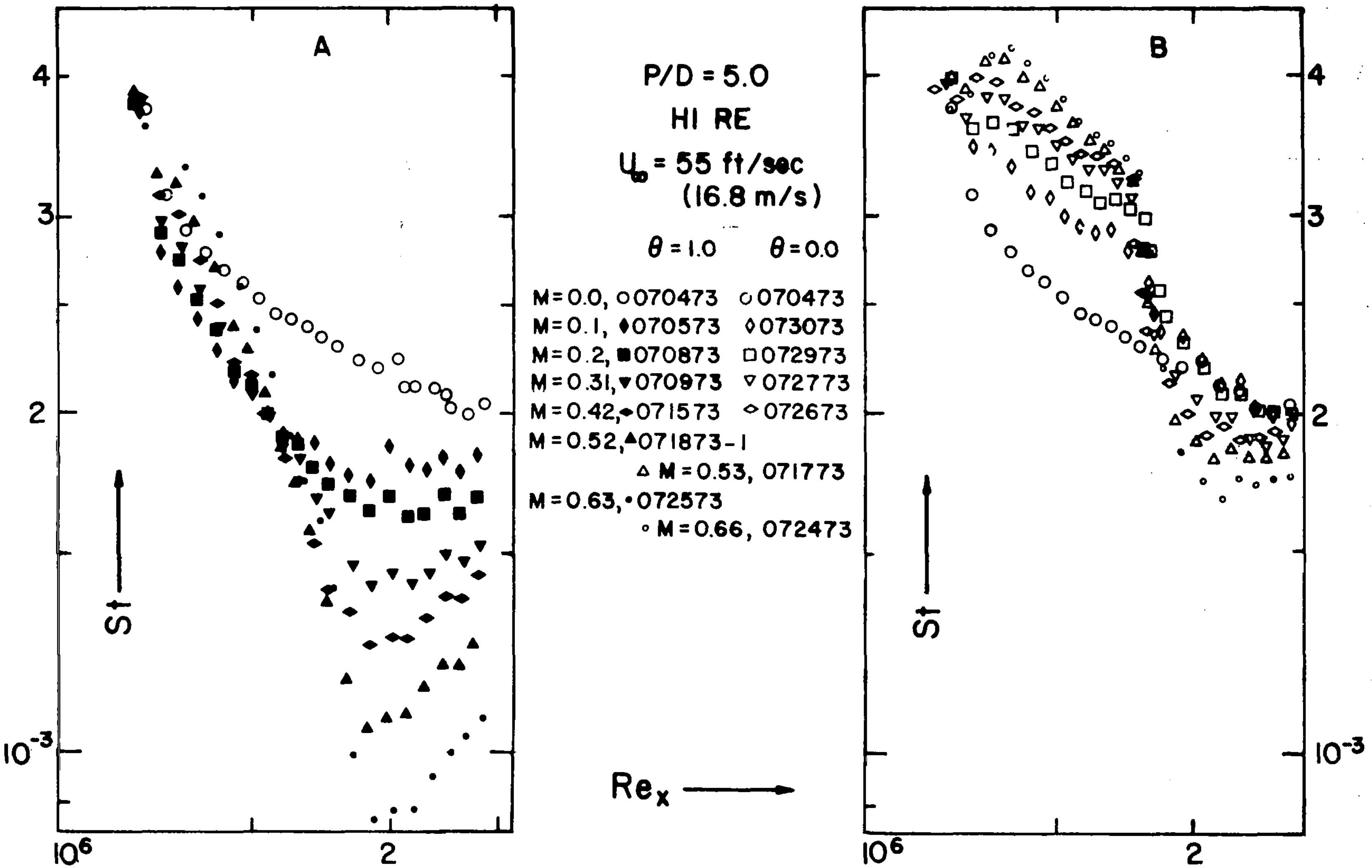

Figure 5.2 St vs. Re_x for θ = 1.0 and θ = 0.0 with P/D = 5 , with unheated starting length.

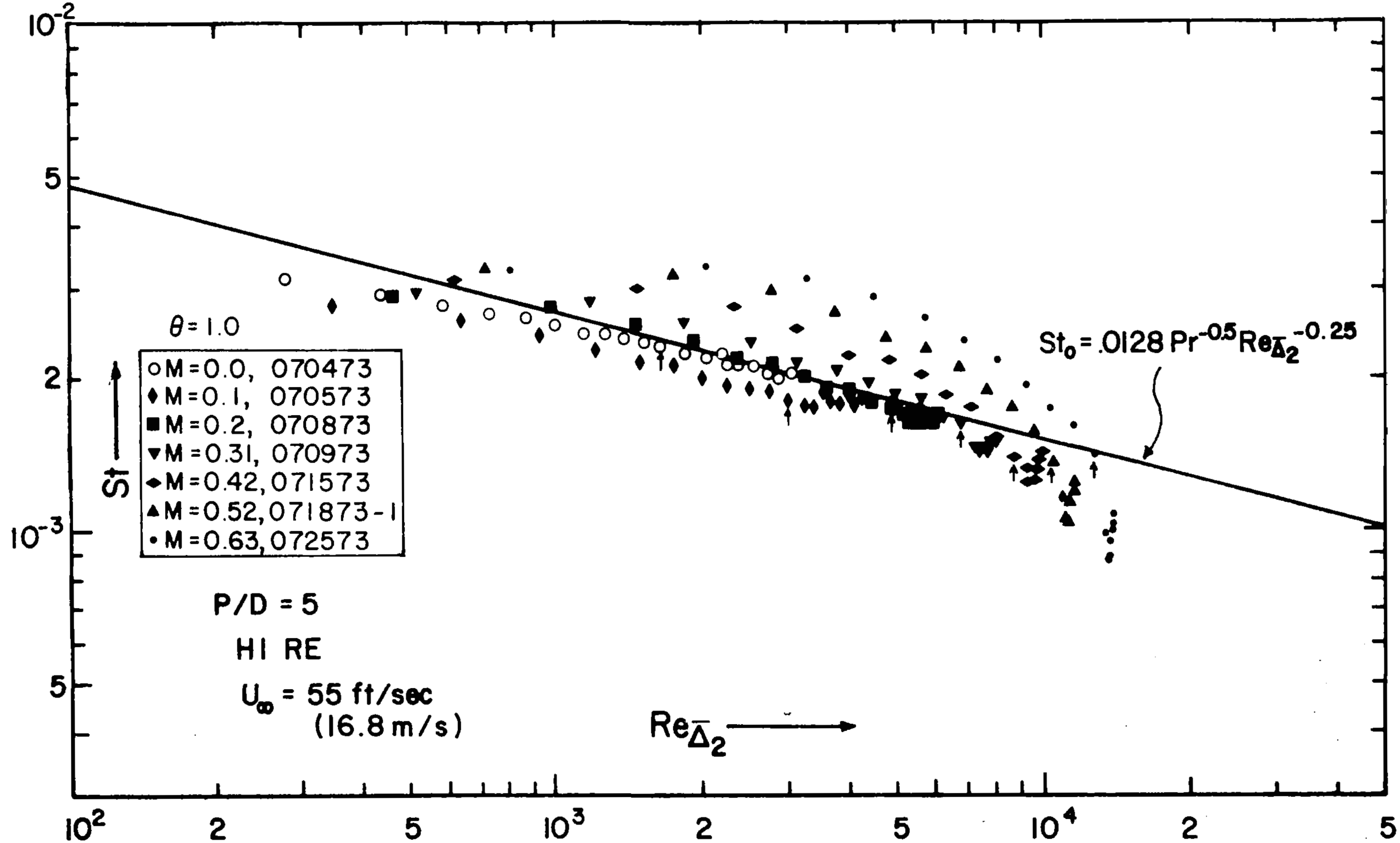

Figure 5.3 St vs. Re_{Δ_2} for θ = 1.0 (same data as Figure 5.2).

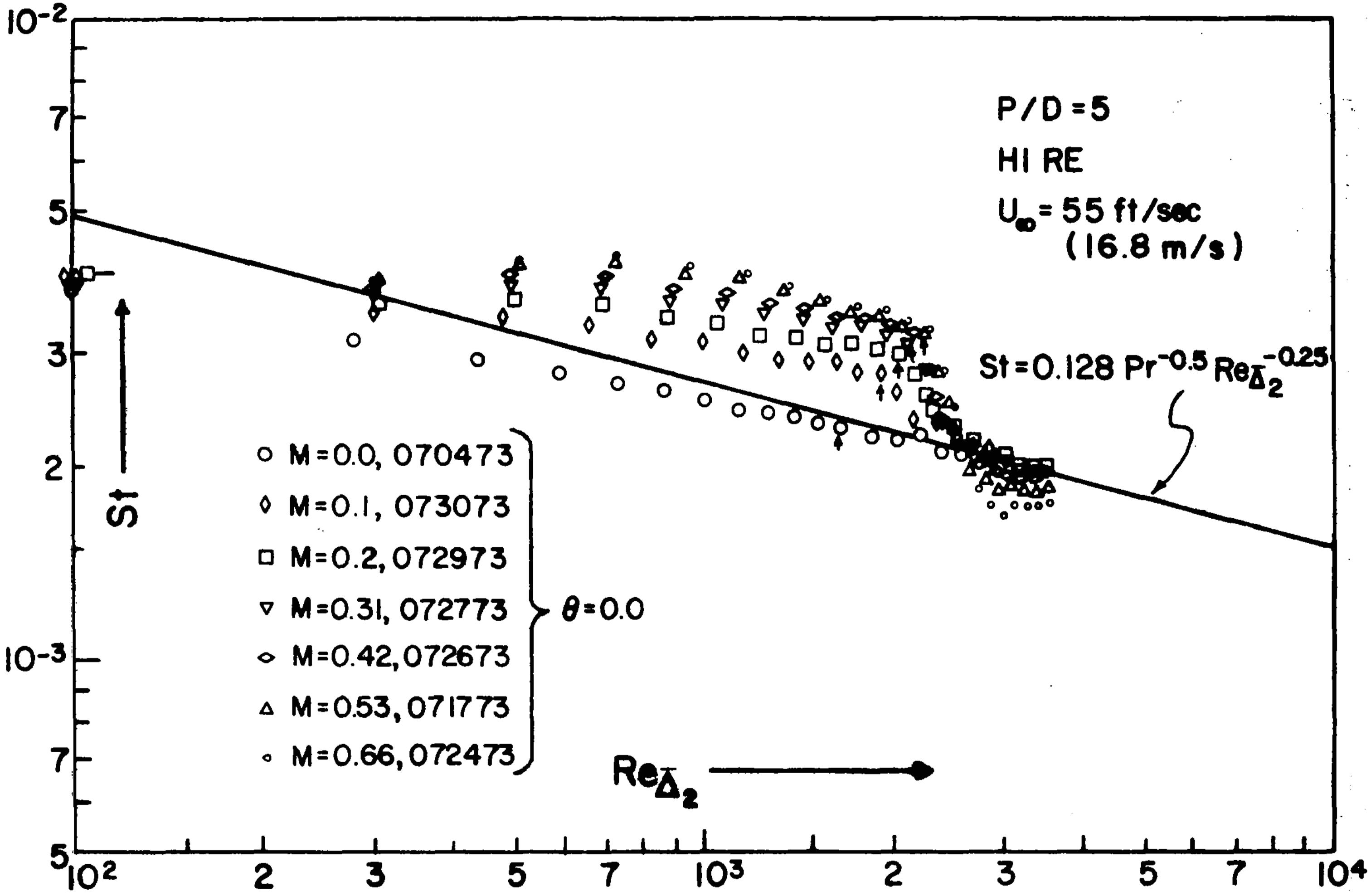

Figure 5.4 St vs. Re_{Δ_2} for $\theta = 0.0$ (same data as Figure 5.2).

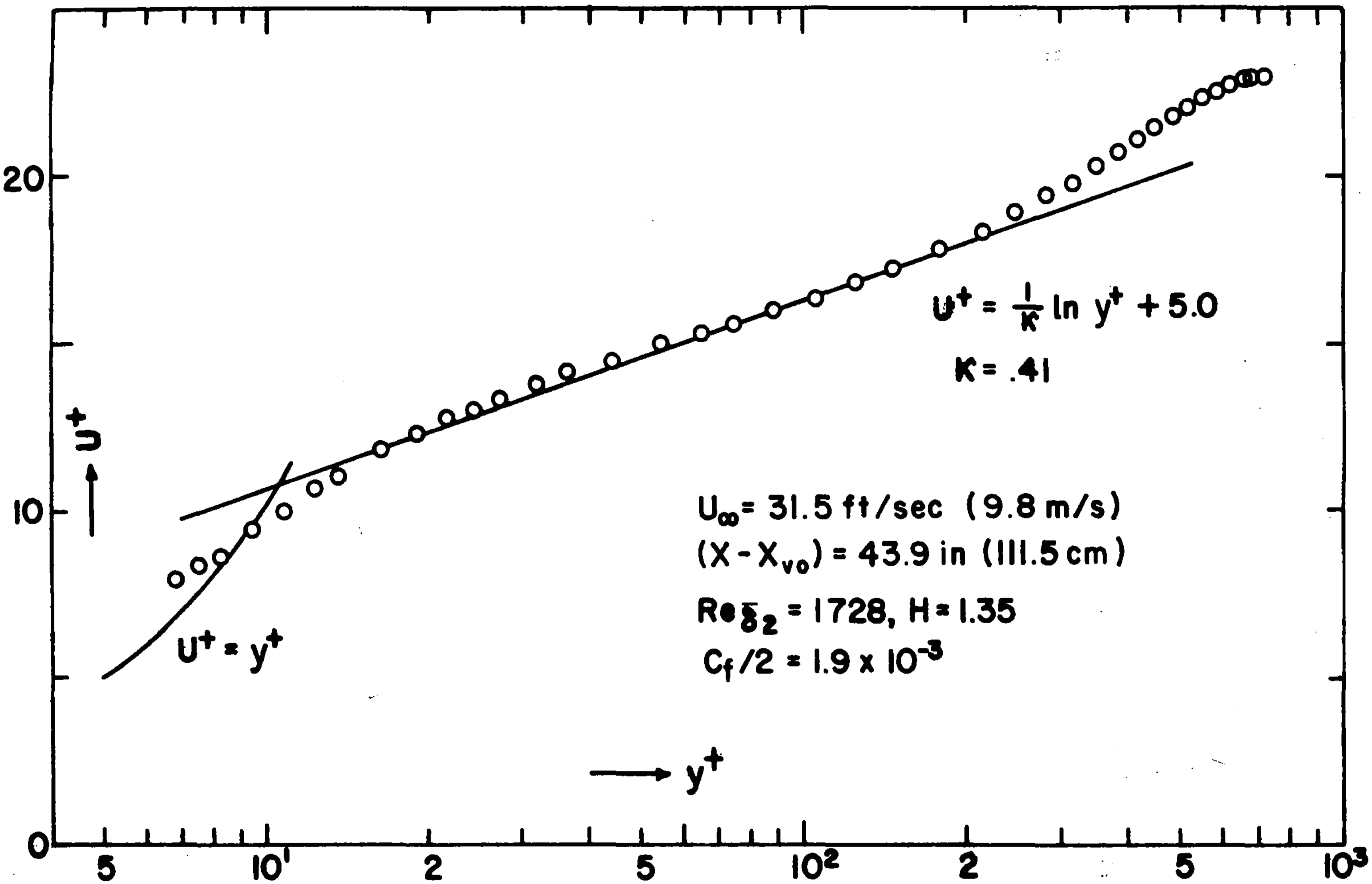

Figure 5.5 Velocity profile at U_∞ = 32 ft/sec (9.76 m/sec) on the first plate, for Figures 5.6 to 5.8.

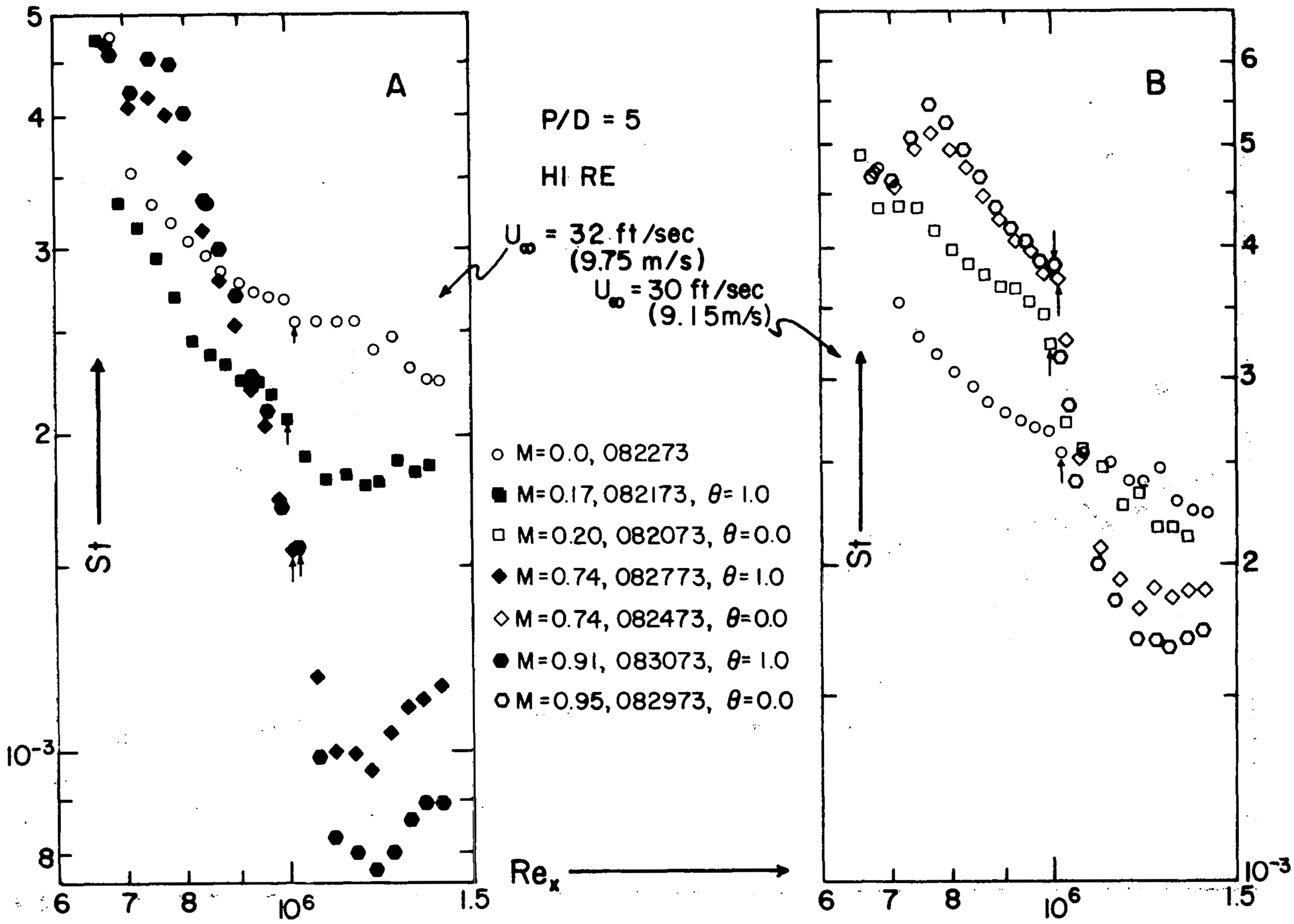

Figure 5.6 St vs. Re_x for θ = 1.0 and θ = 0.0 with P/D = 5 , with unheated starting length.

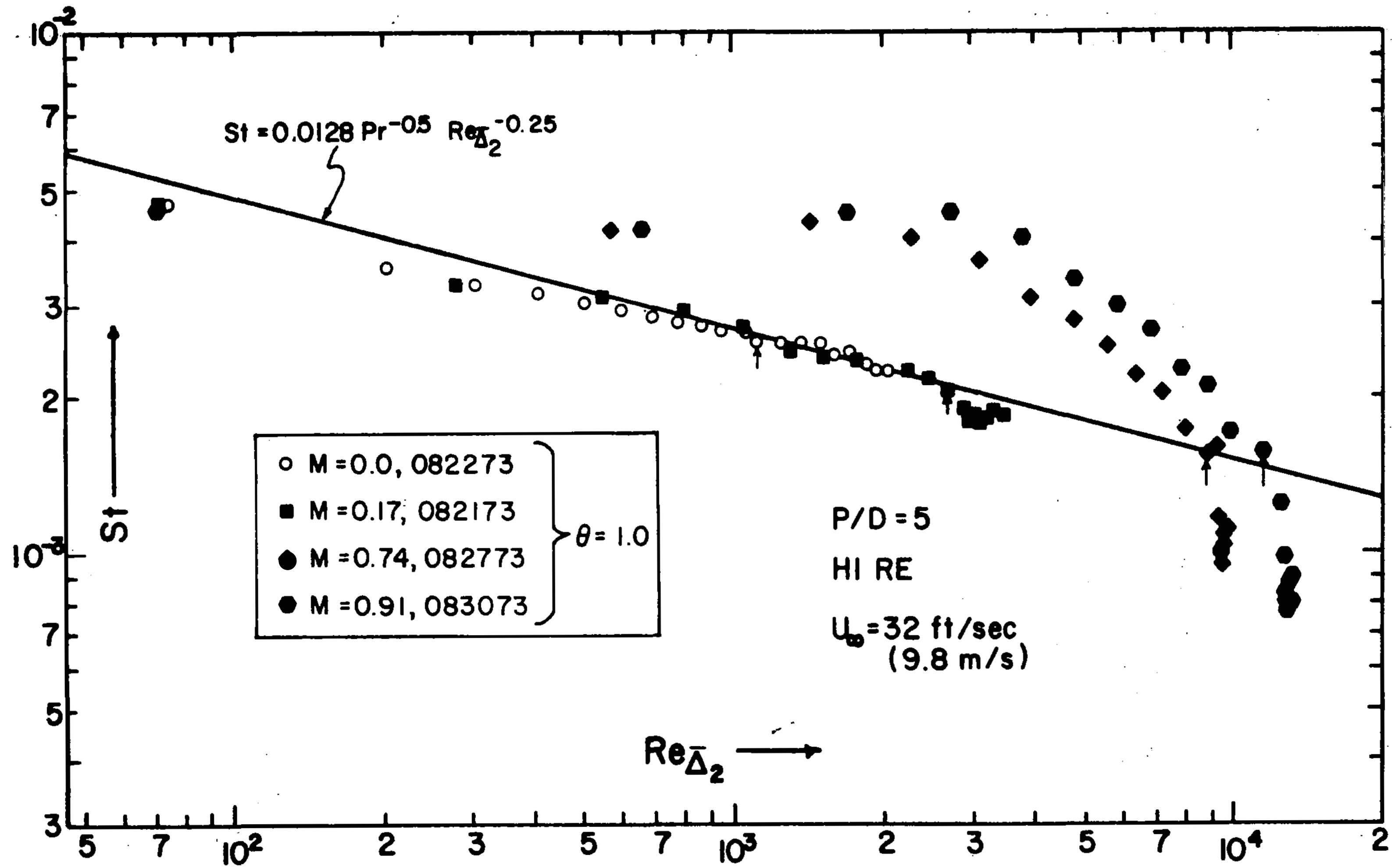

Figure 5.7 St vs. Re_{Δ_2} for θ = 1.0 (same data as Figure 5.6).

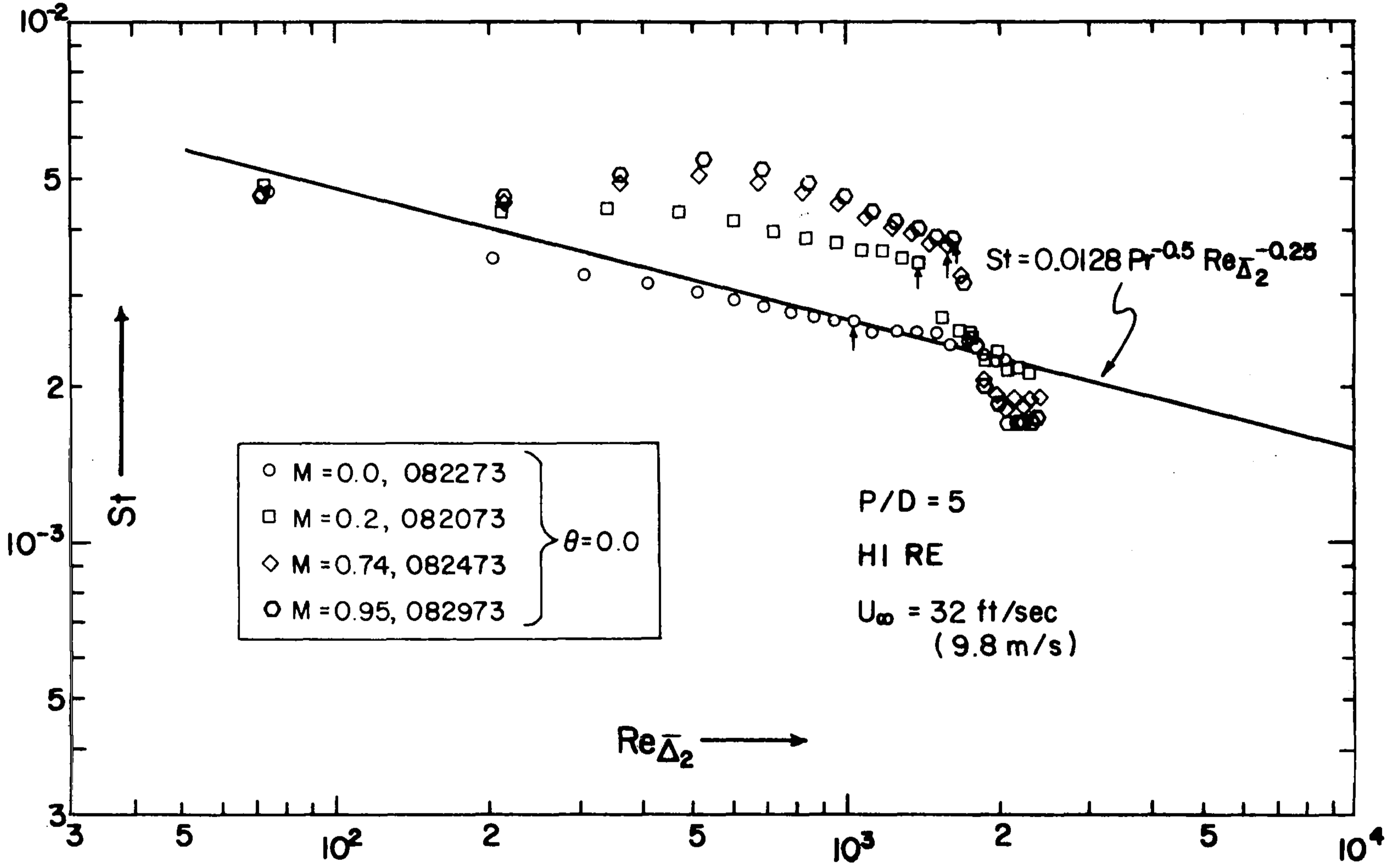

Figure 5.8 St vs. Re_{Δ_2} for $\theta = 0.0$ (same data as Figure 5.6).

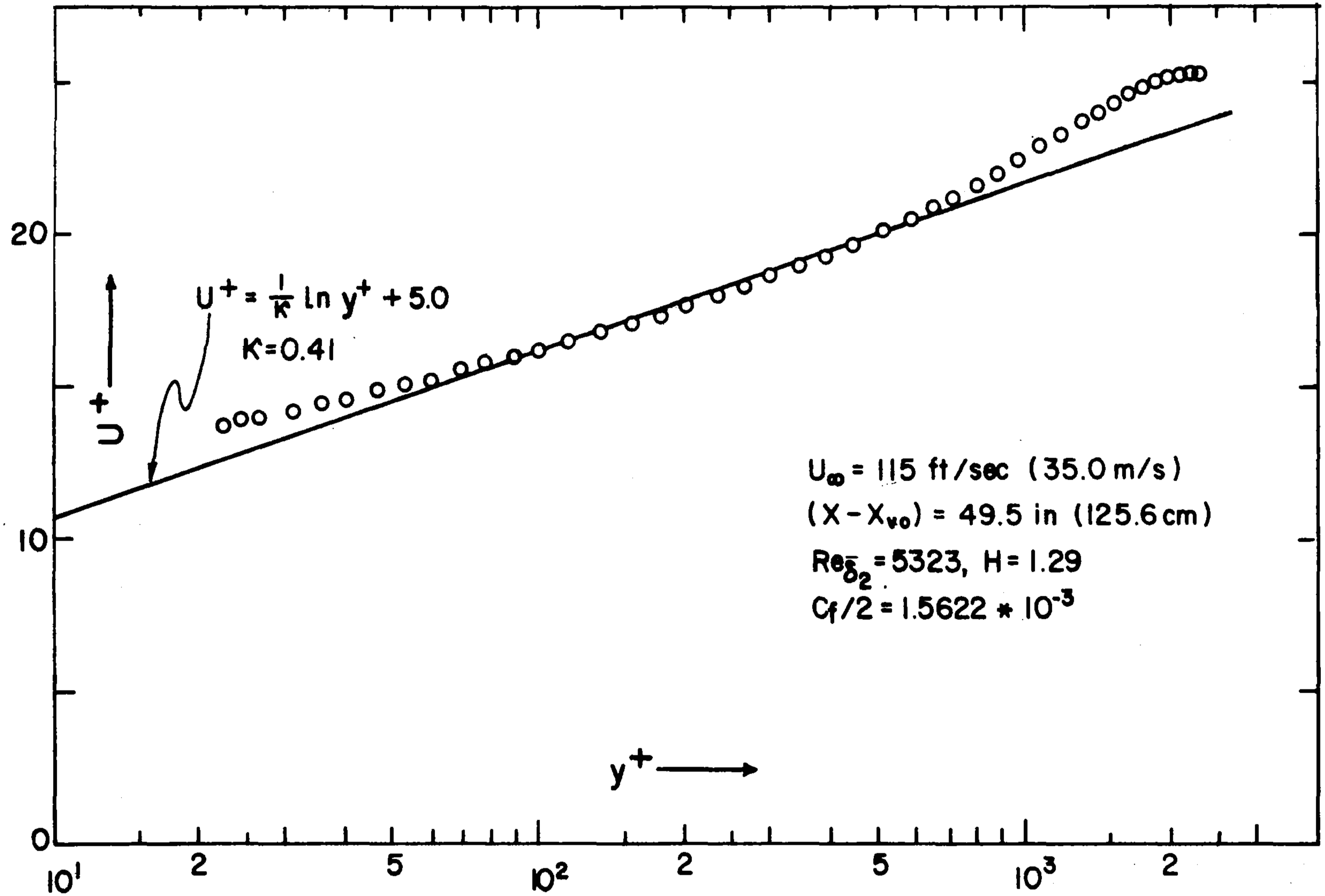

Figure 5.9 Velocity profile at U_∞ = 115 ft/sec (35.7 m/sec), on the first plate, for Figure 5.10 .

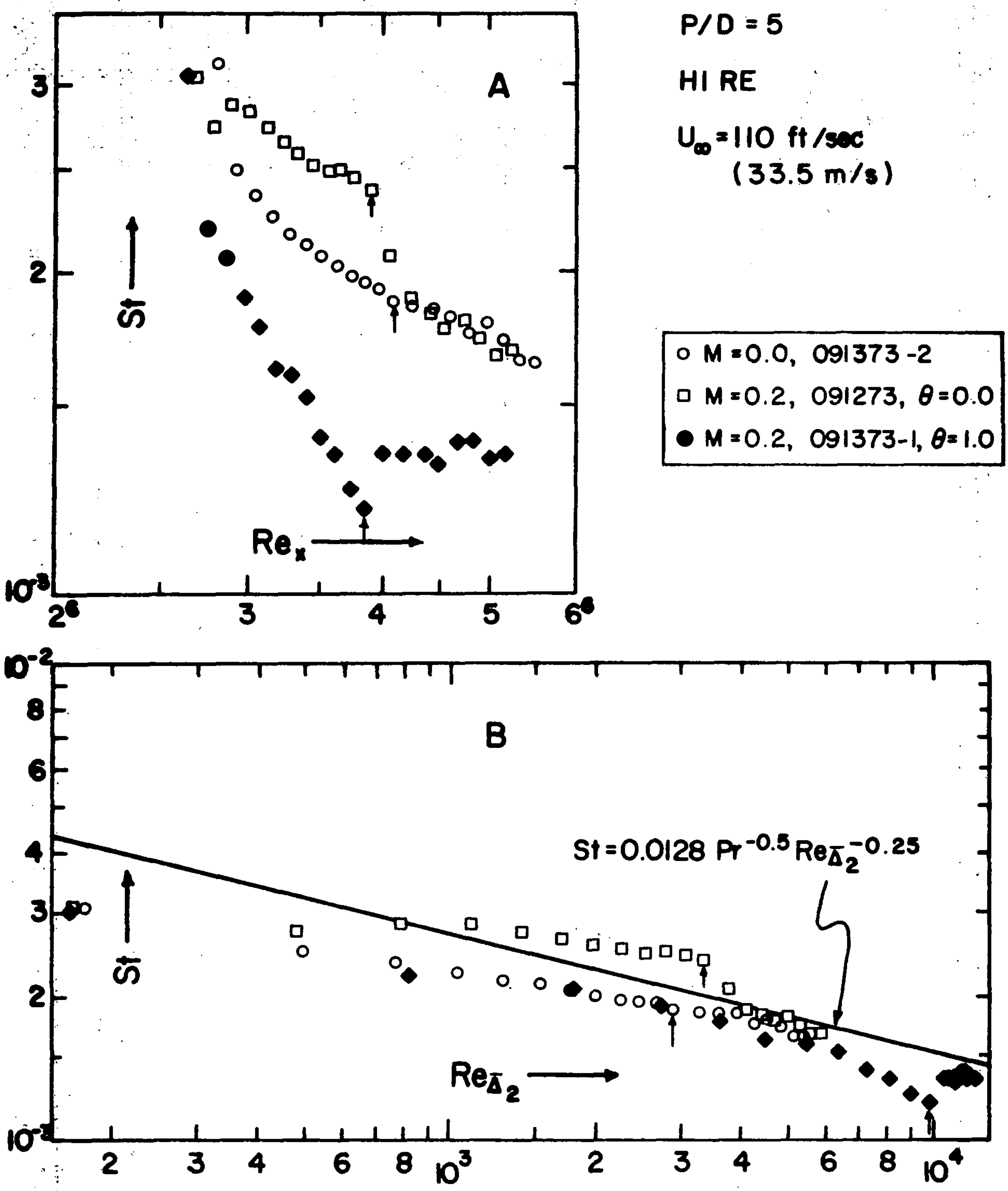

Figure 5.10 St vs. Re_x and St vs. Re_{Δ_2} for $\theta = 1.0$ and $\theta = 0.0$ at $M = 0.2$, $P/D = 5$ with unheated starting length.

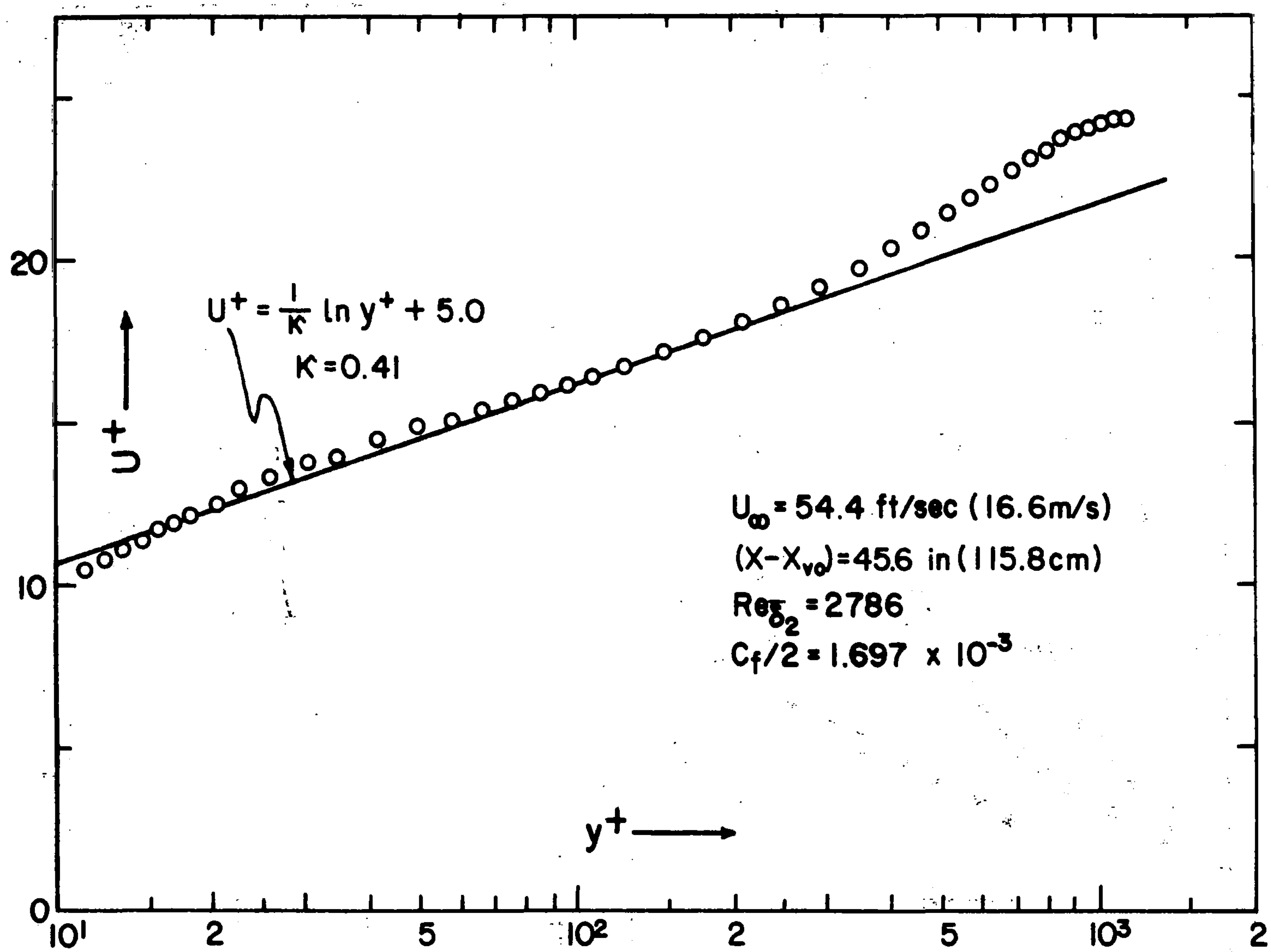

Figure 5.11 Velocity profile at U_∞ = 55 ft/sec (16.7 m/sec) on the first plate for Figure 5.13 .

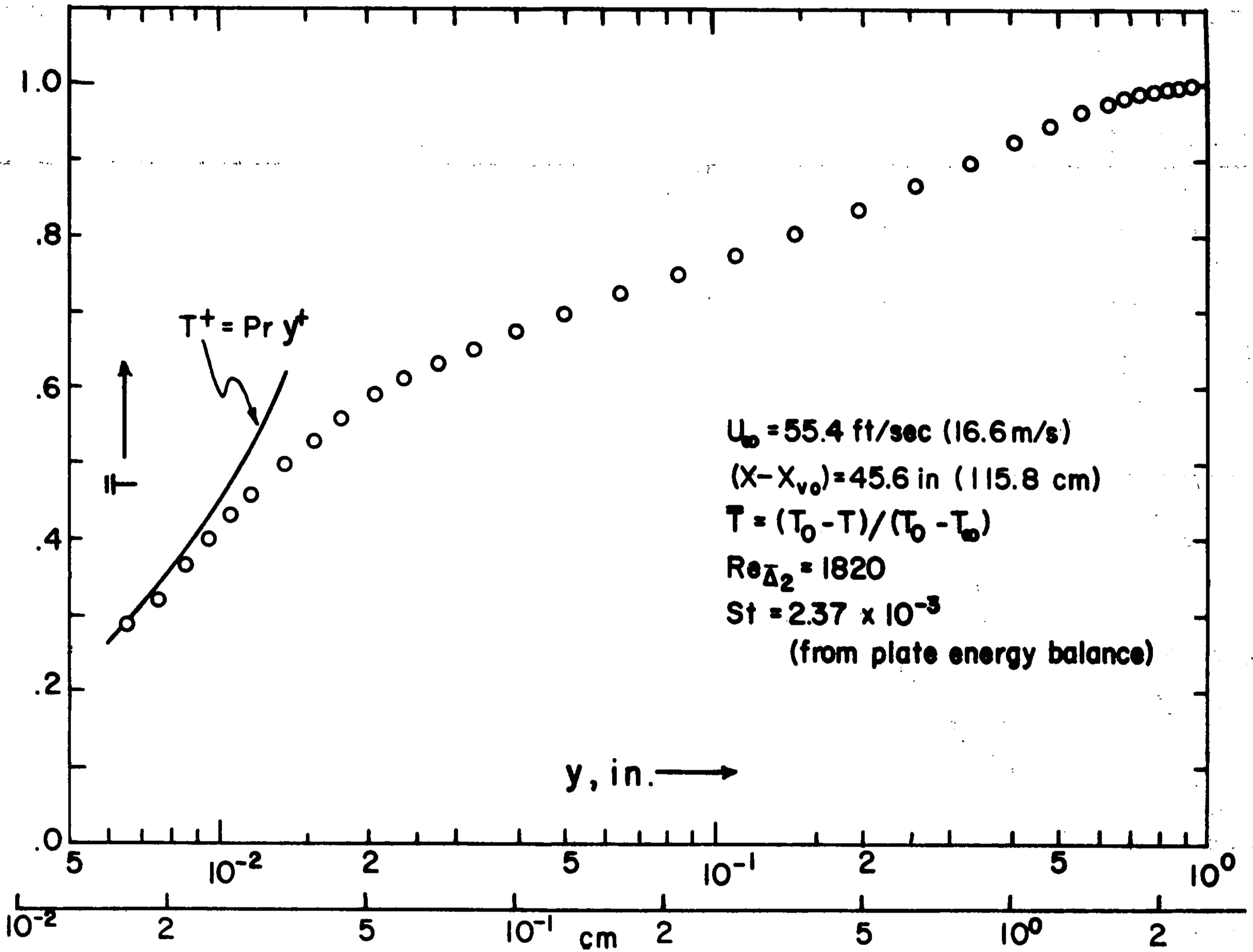

Figure 5.12 Temperature profile at U_∞ = 55 ft/sec (16.7 m/sec) on the first plate, with 24 in. (61 cm) heated on the foreplate for Figure 5.13.

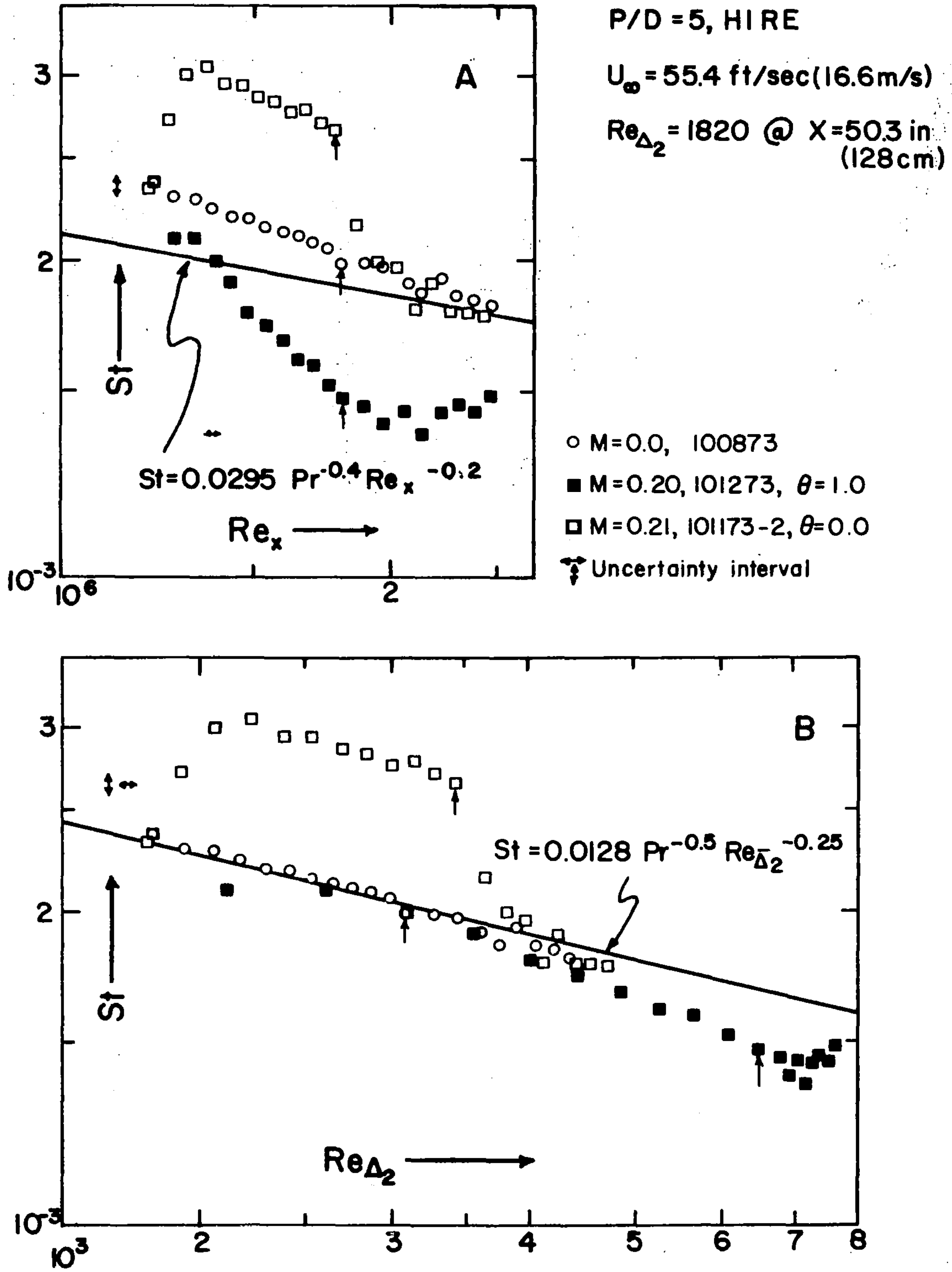

Figure 5.13 St vs. Re_x and St vs. $Re\Delta_2$ for θ = 1.0 and θ = 0.0 at M = 0.2, P/D = 5 with 24 in. (61 cm) heated on the foreplate.

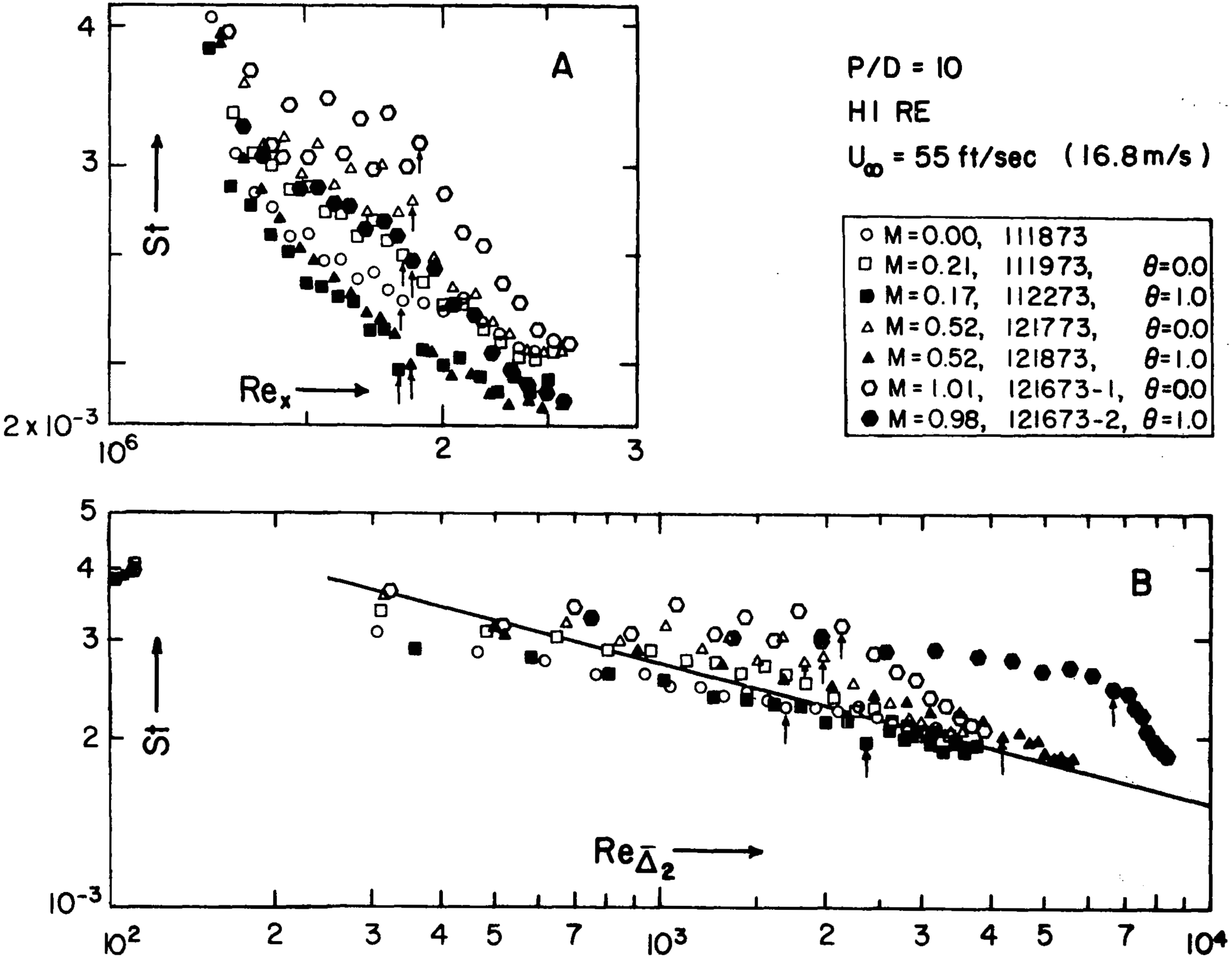

Figure 5.14 St vs. Re_x and St vs. Re_{Δ_2} for $\theta = 1.0$ and $\theta = 0.0$ at $M = 0.2$, 0.5 and 1.0 with $P/D = 10$ and an unheated starting length.

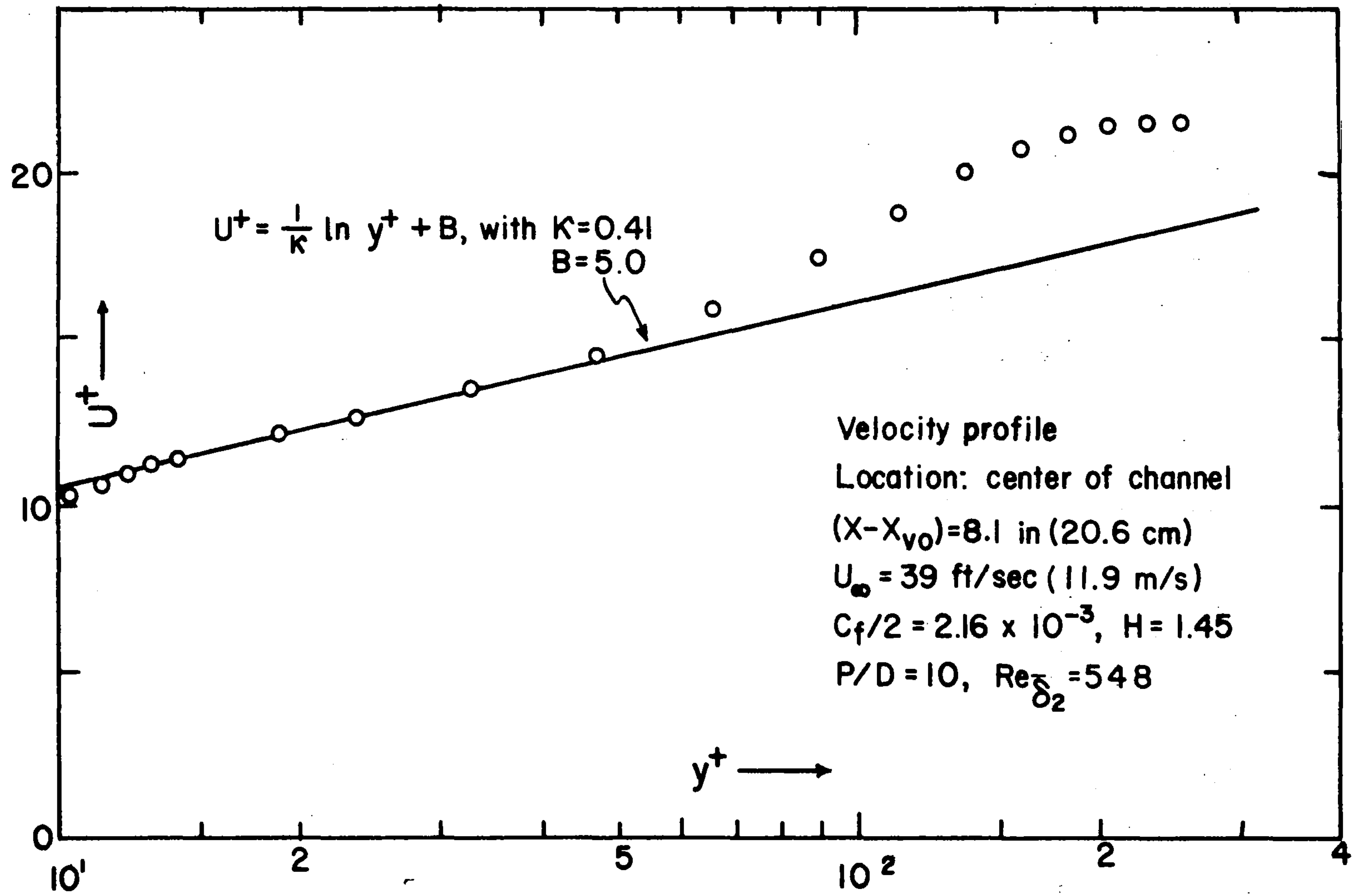

Figure 5.15 Velocity profile on the first plate, with foreplate accelerated to produce a low momentum thickness layer.

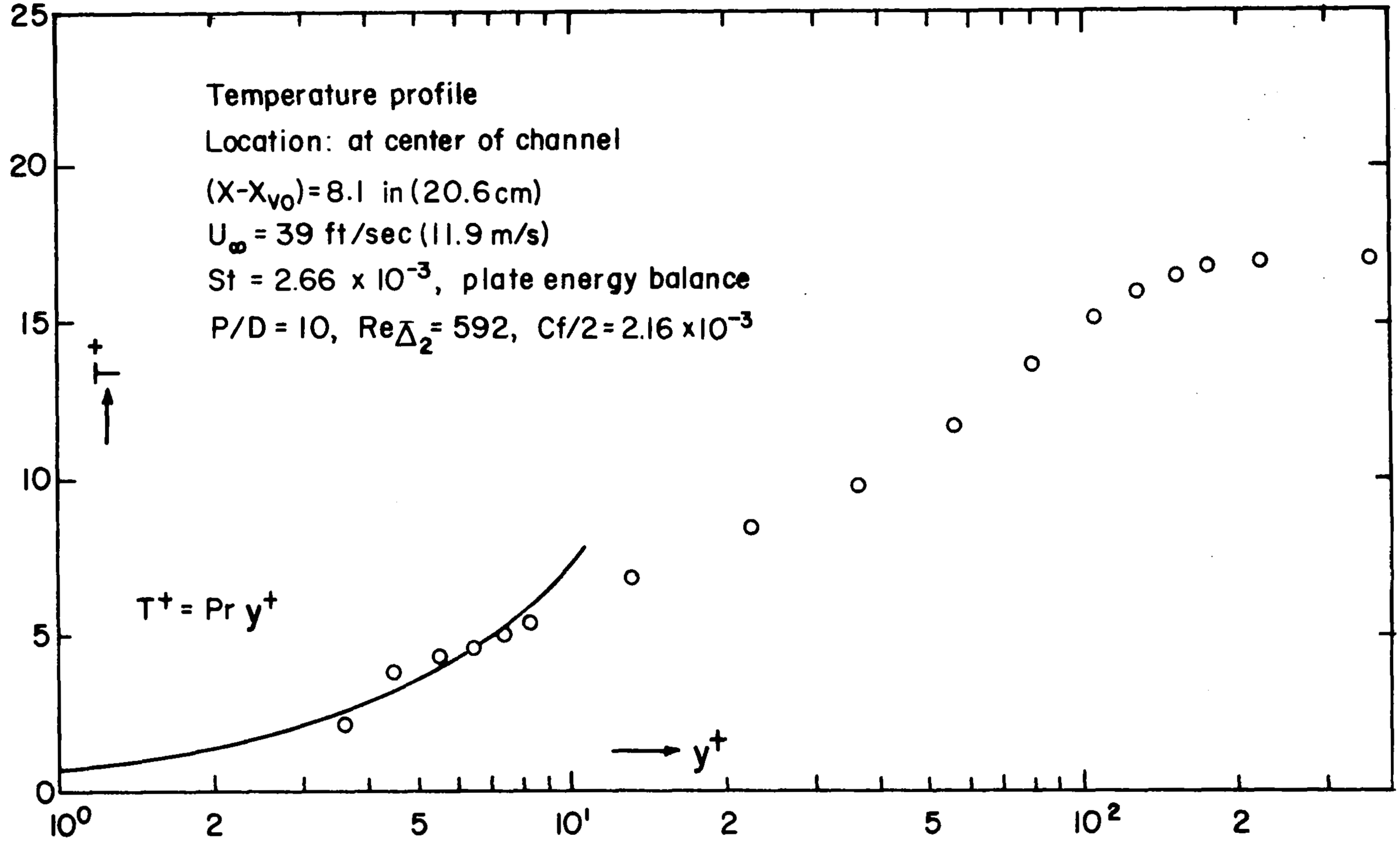

Figure 5.16 Temperature profile on the first plate, with foreplate accelerated to produce low momentum thickness.

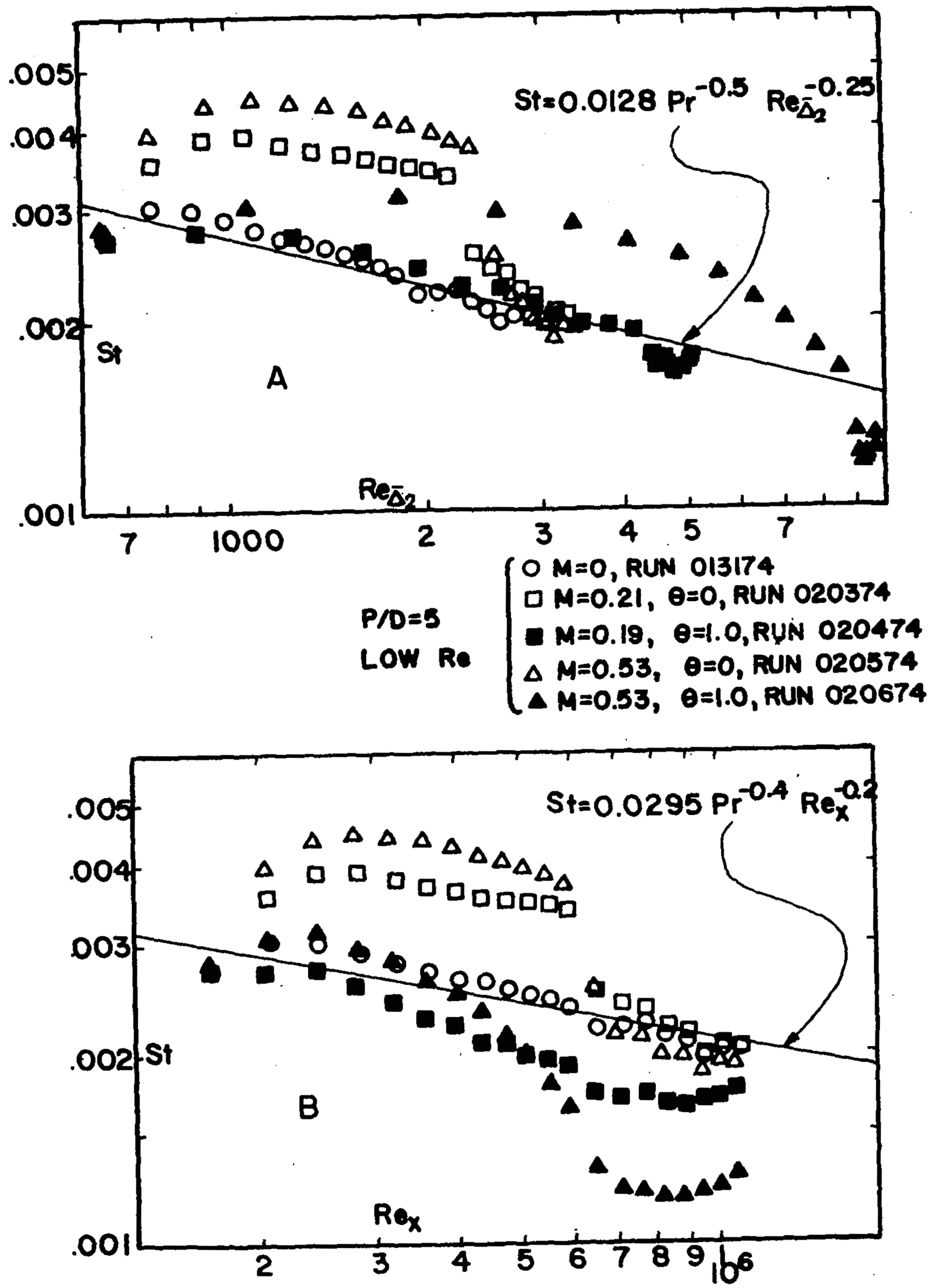

Figure 5.17 St vs. Re_x and St vs. Re_{Δ_2} for P/D = 5 with small δ_2.

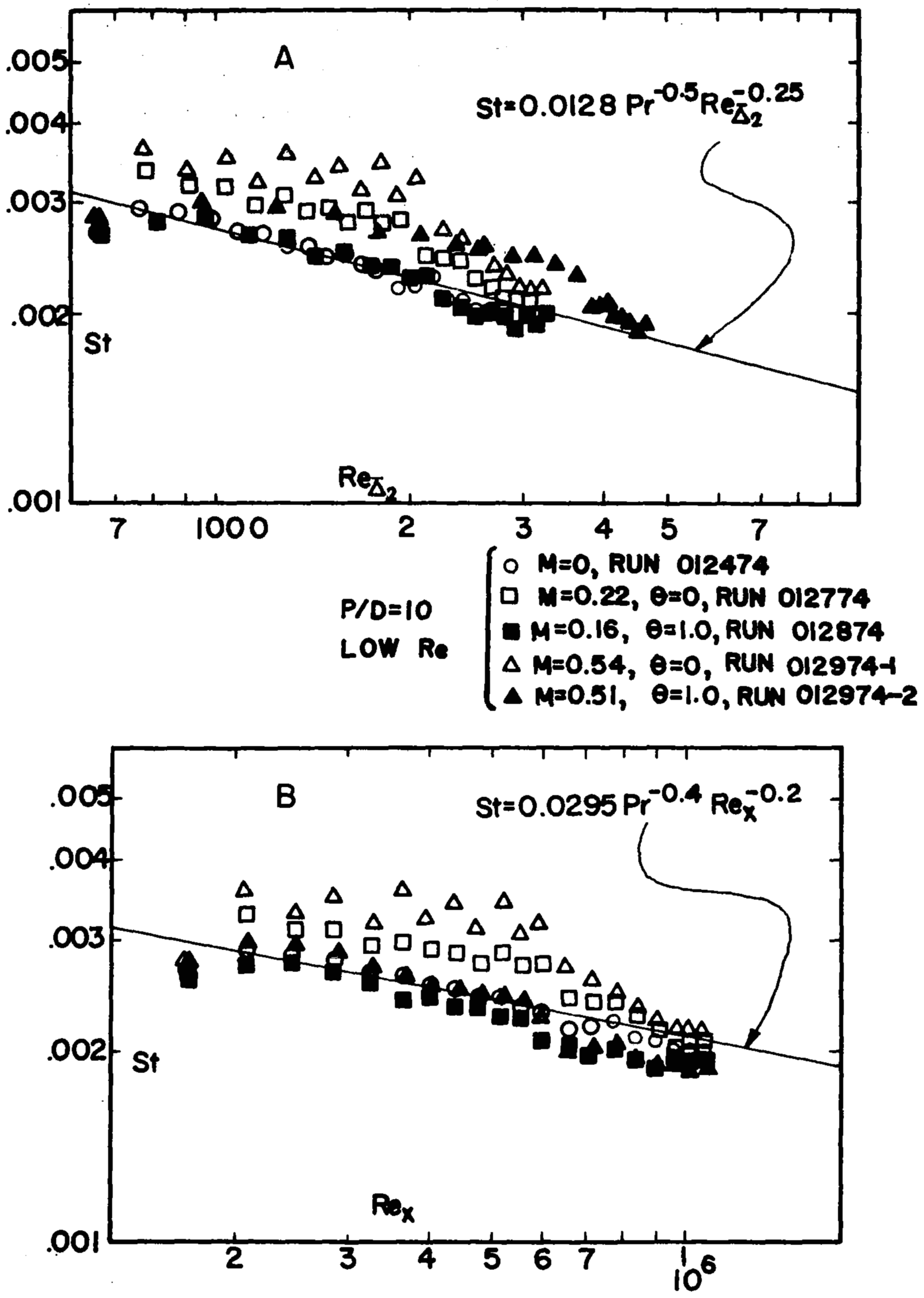

Figure 5.18 St vs. Re_x and St vs. Re_{Δ_2} for P/D = 10 with small δ_2 .

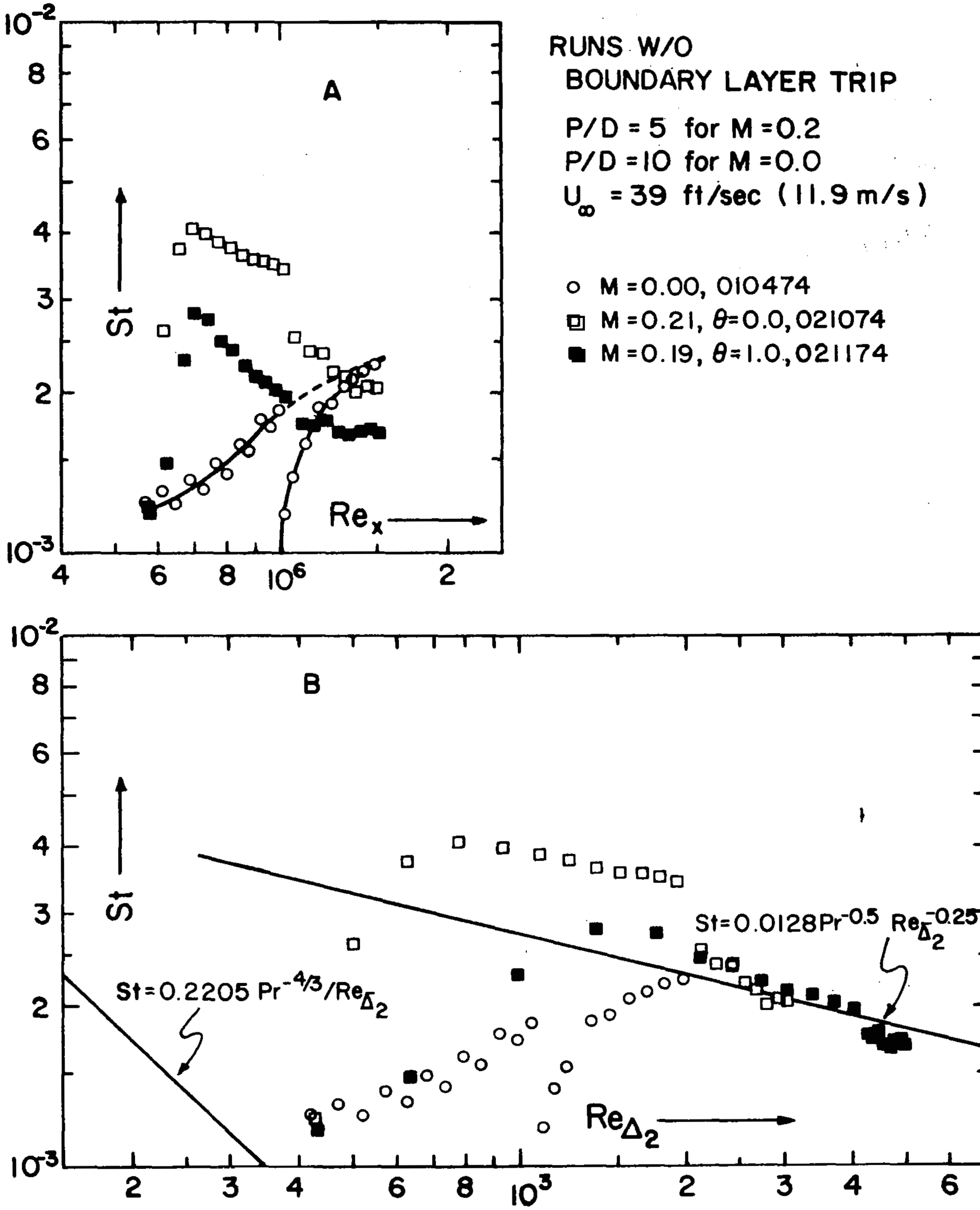

Figure 5.19 St vs. Re_x and St vs. Re_{Δ_2} for P/D = 5 with the natural transition to turbulent boundary layer.

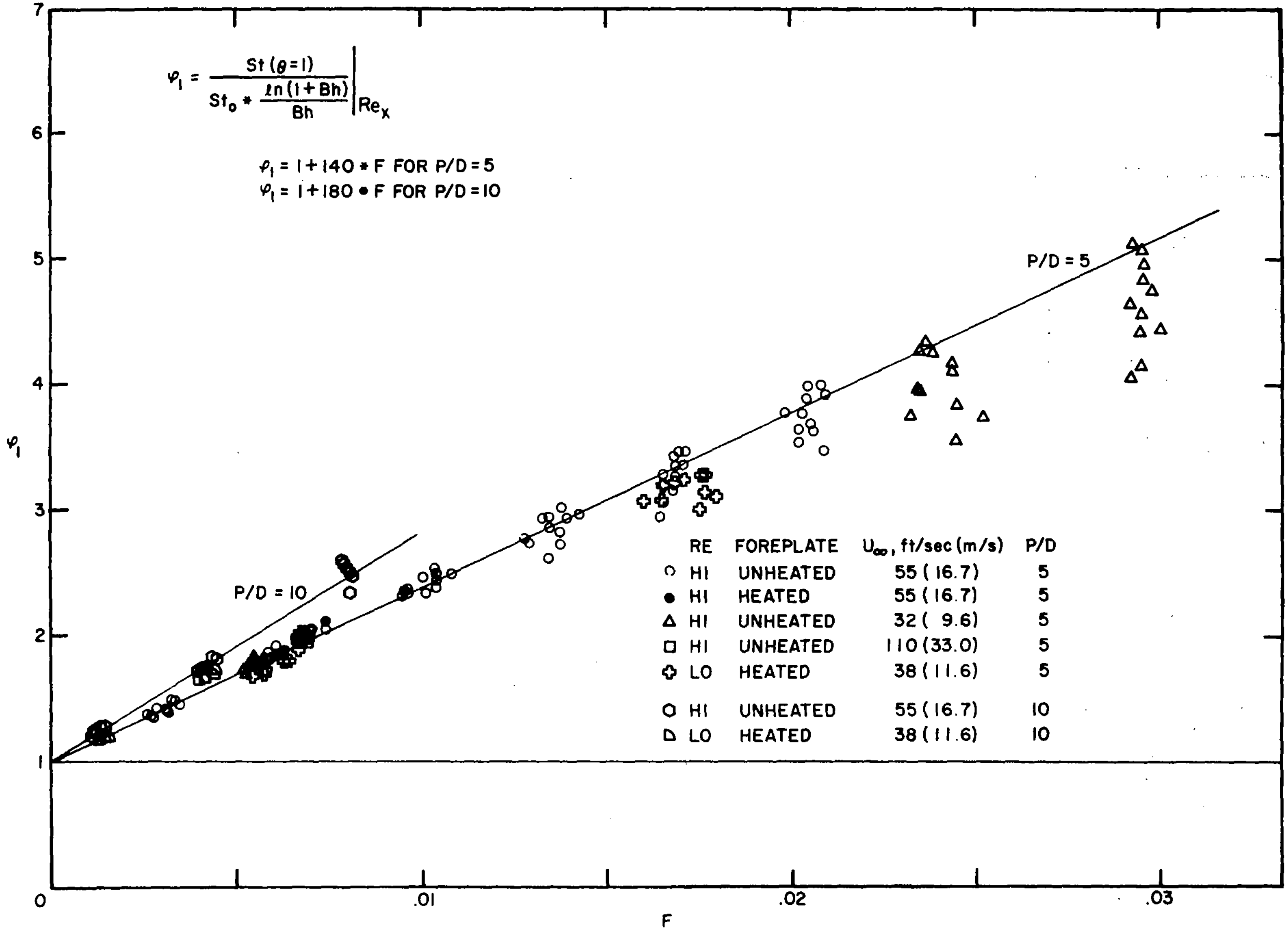

Figure 5.20 Stanton number correction factor, ϕ_1, vs. F for $\theta = 1.0$.

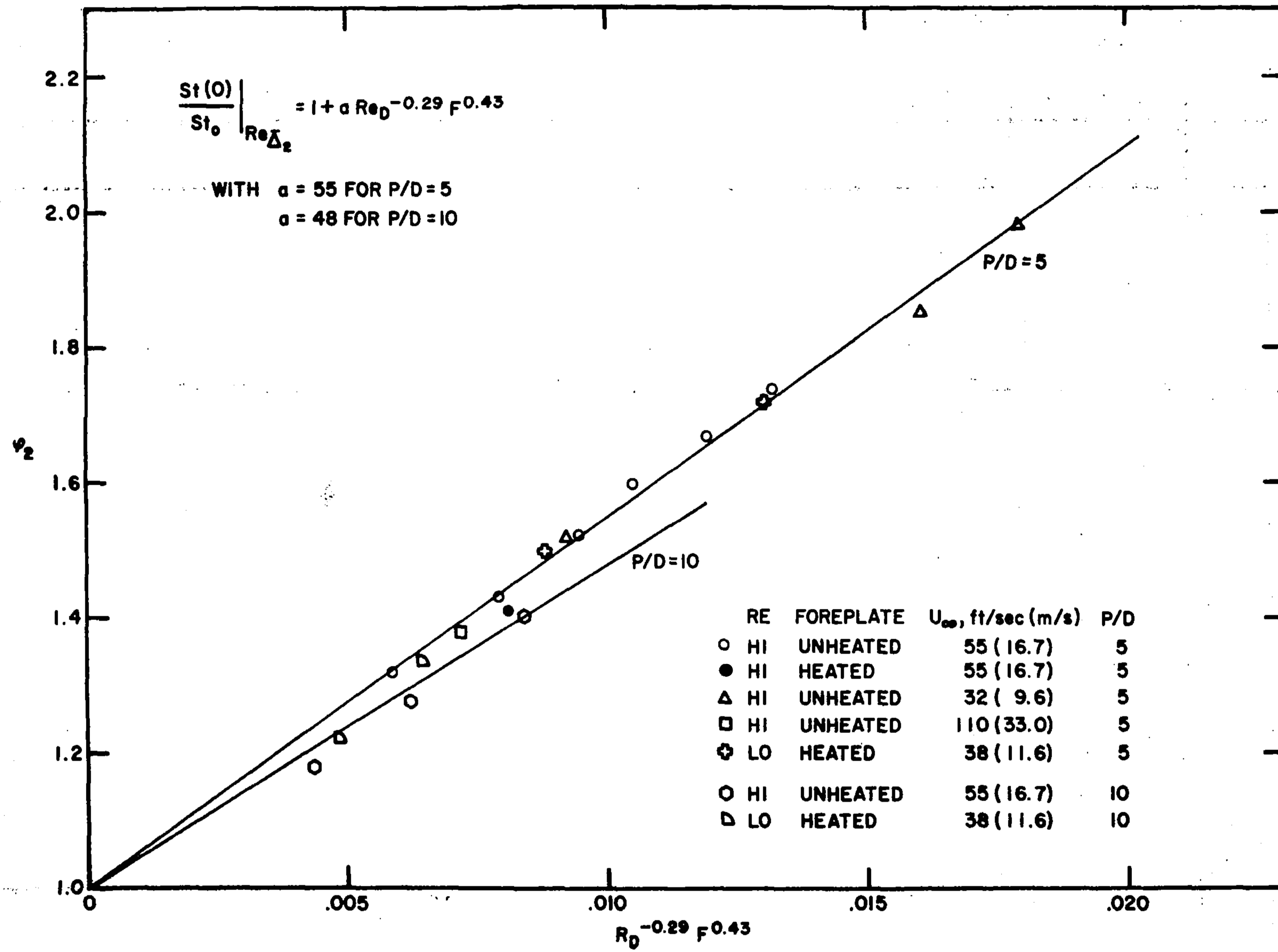

Figure 5.21 St/St_o for fixed $Re_{\bar{\Delta}_2}$ with $\theta = 0.0$.

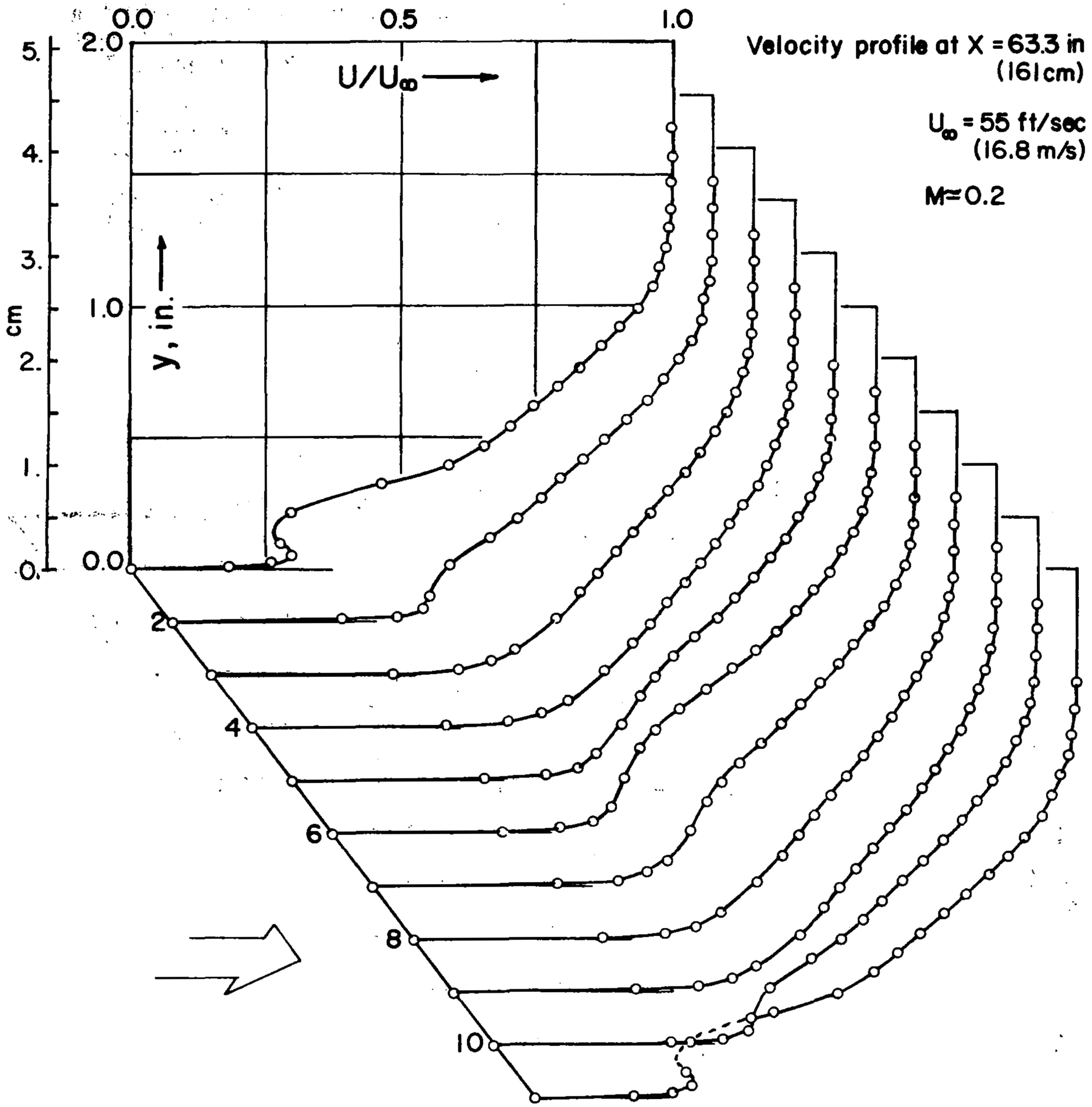

Figure 5.22 Velocity profiles between two holes in lateral direction.

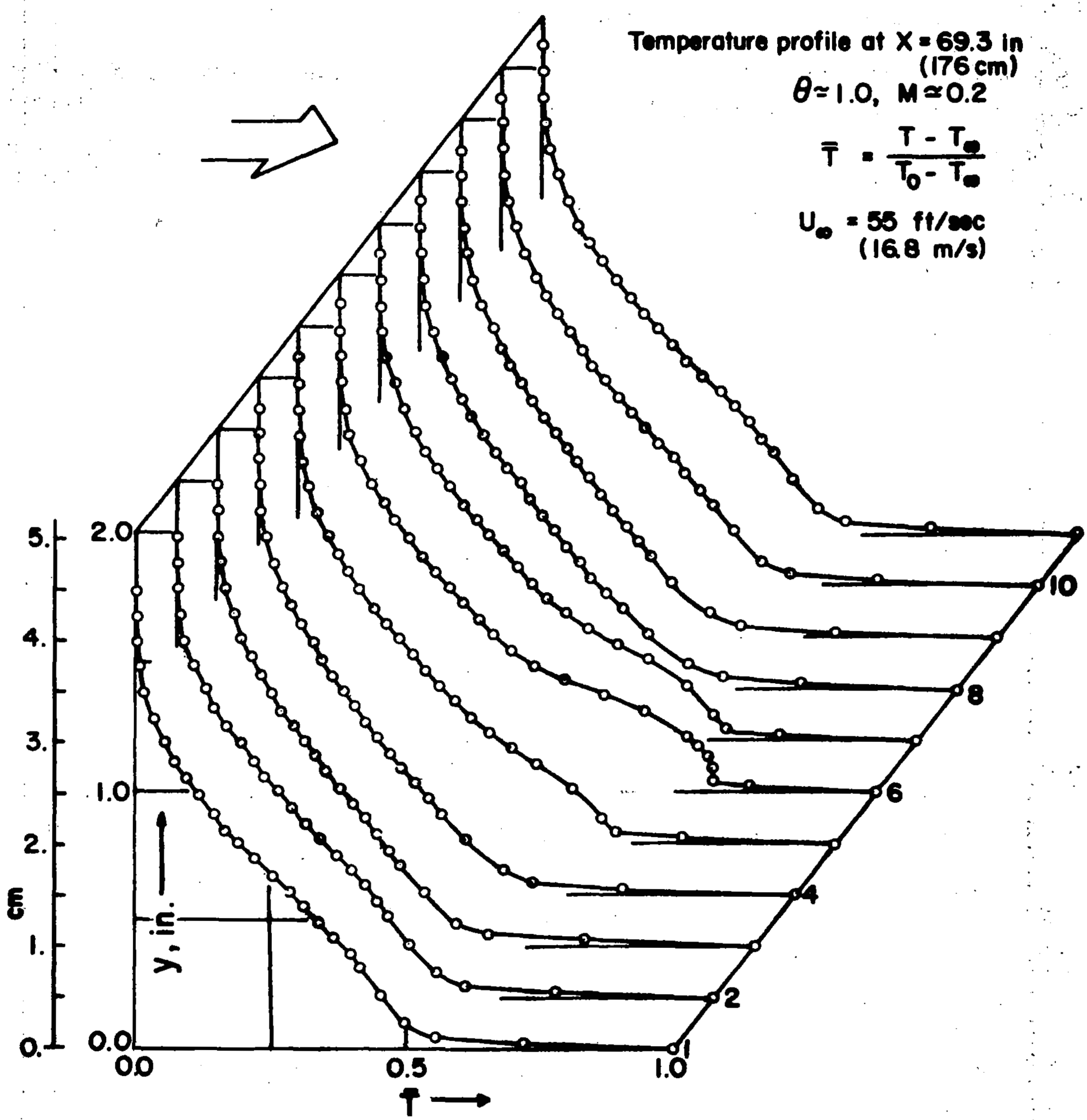

Figure 5.23 Temperature profiles across the hole in lateral direction.

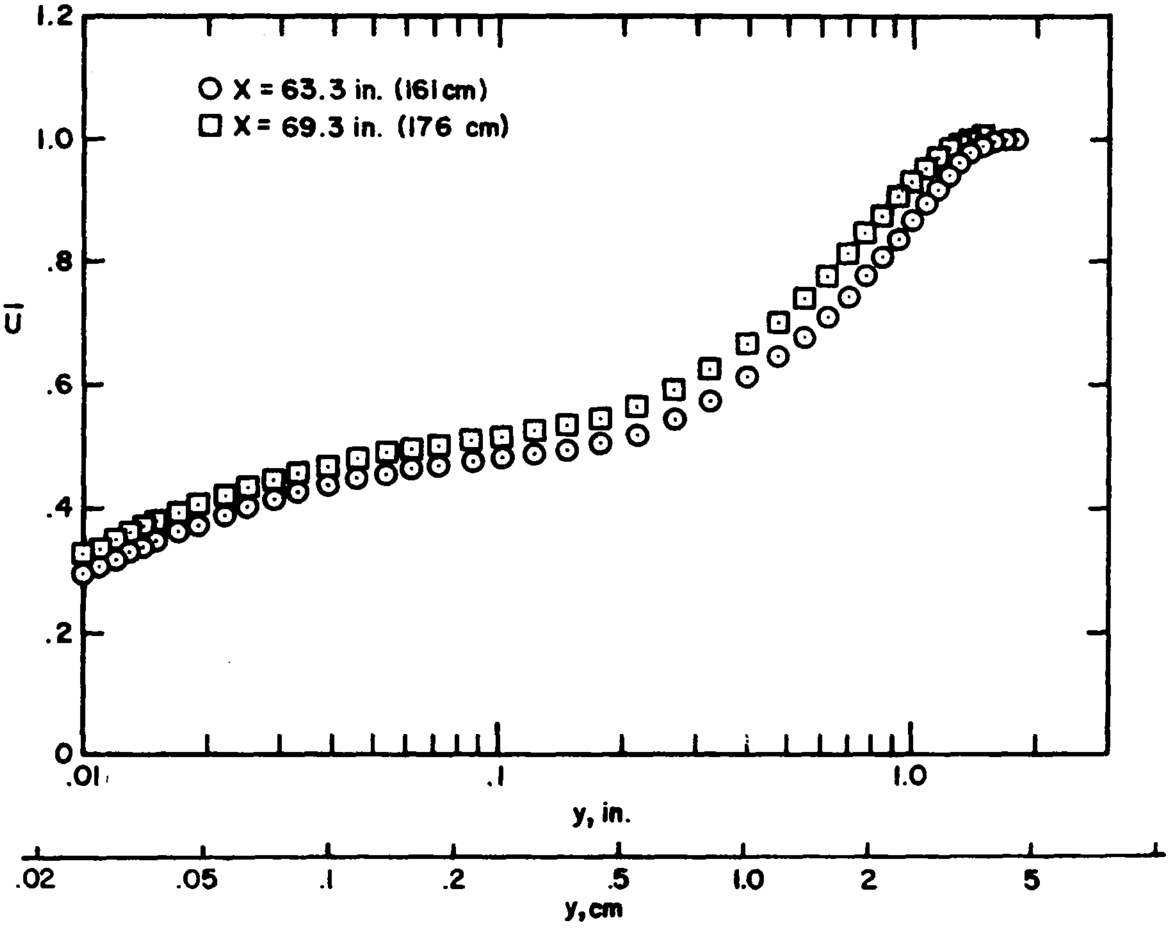

Figure 5.24 Laterally averaged velocity profile.

Error

An error occurred while processing this page. See the system log for more details.

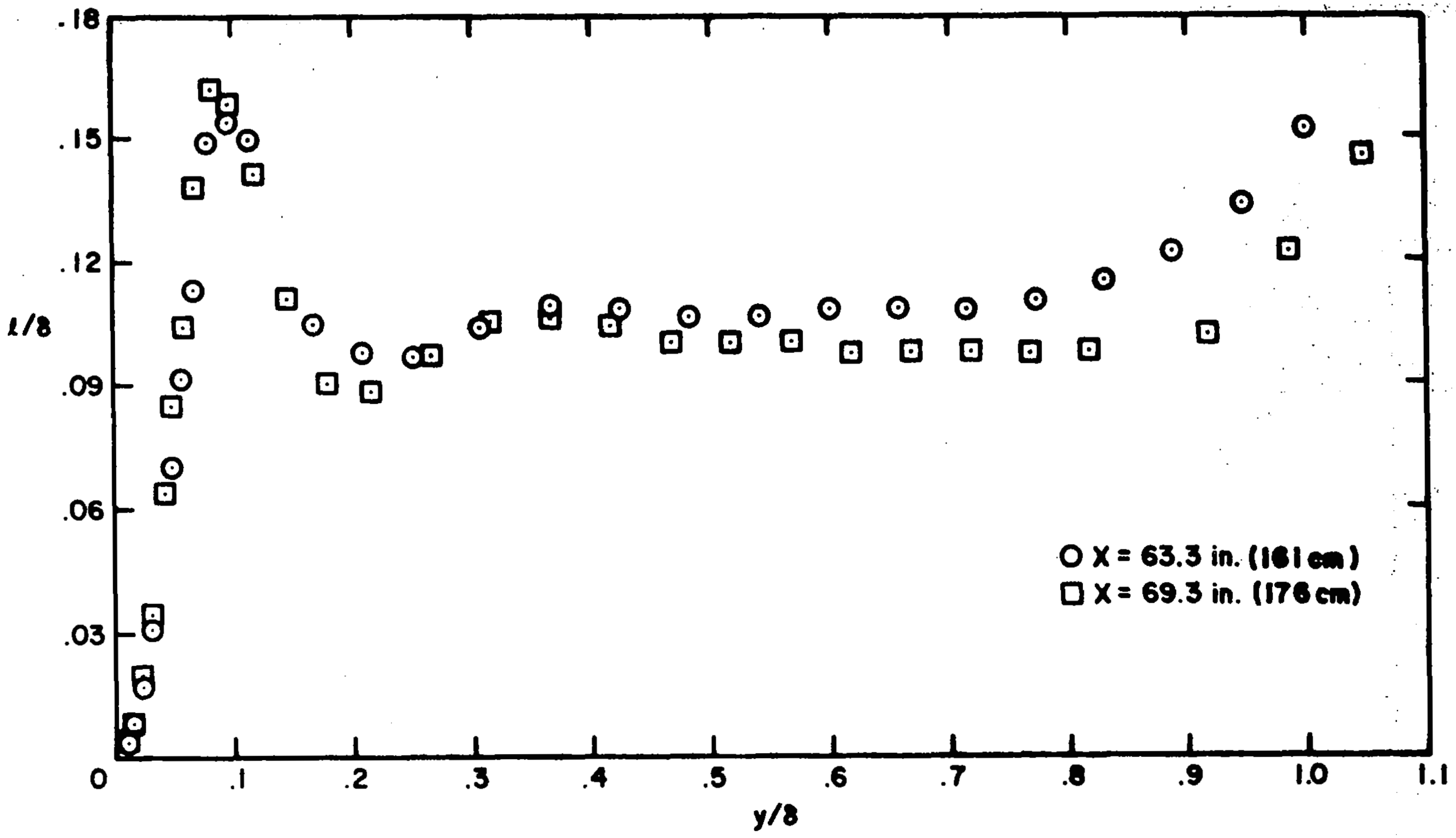

Figure 5.26 Mixing length distribution from laterally averaged velocity profiles at M = 0.2 ,

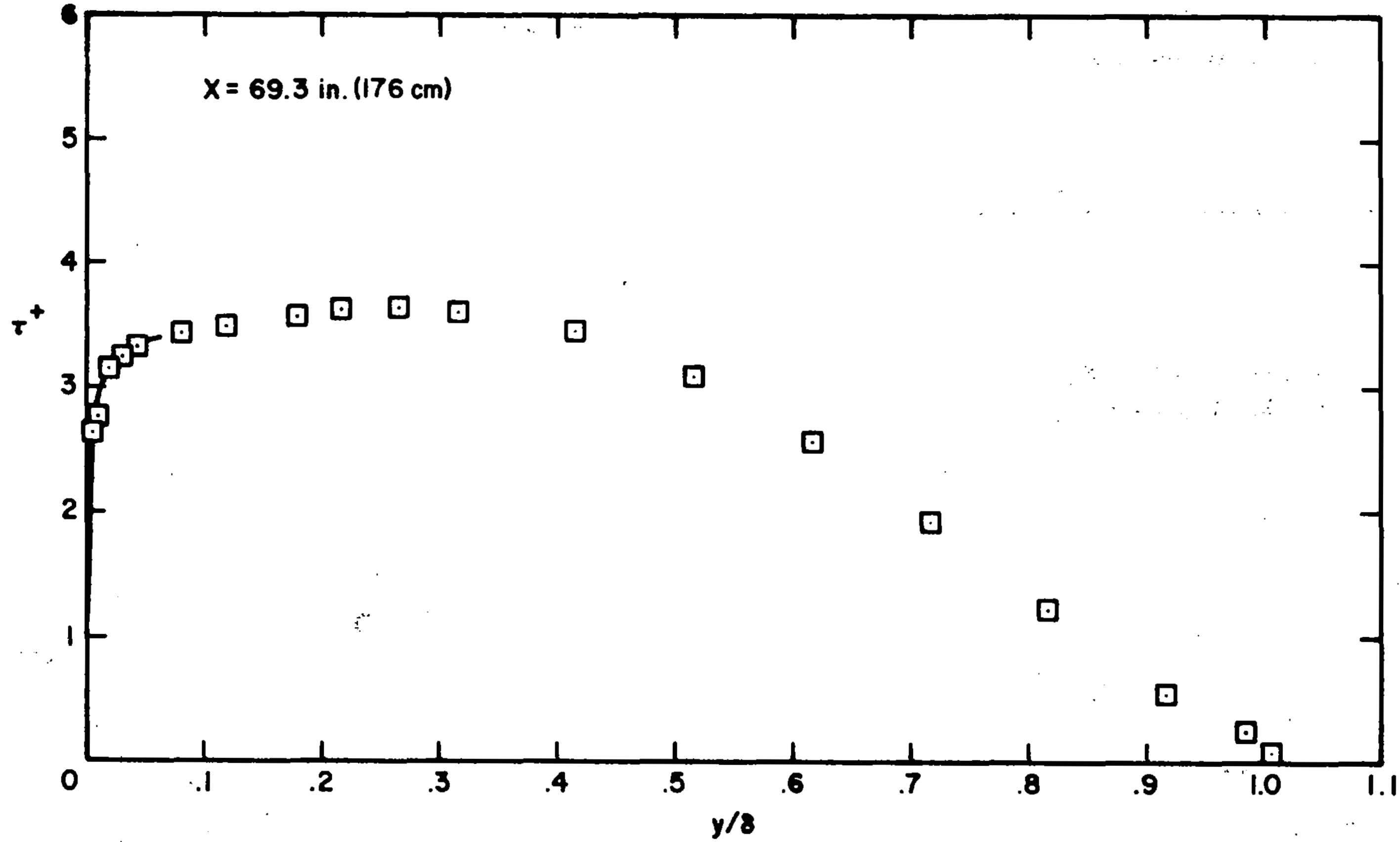

Figure 5.27. Shear stress distribution, laterally averaged at M = 0.2 .

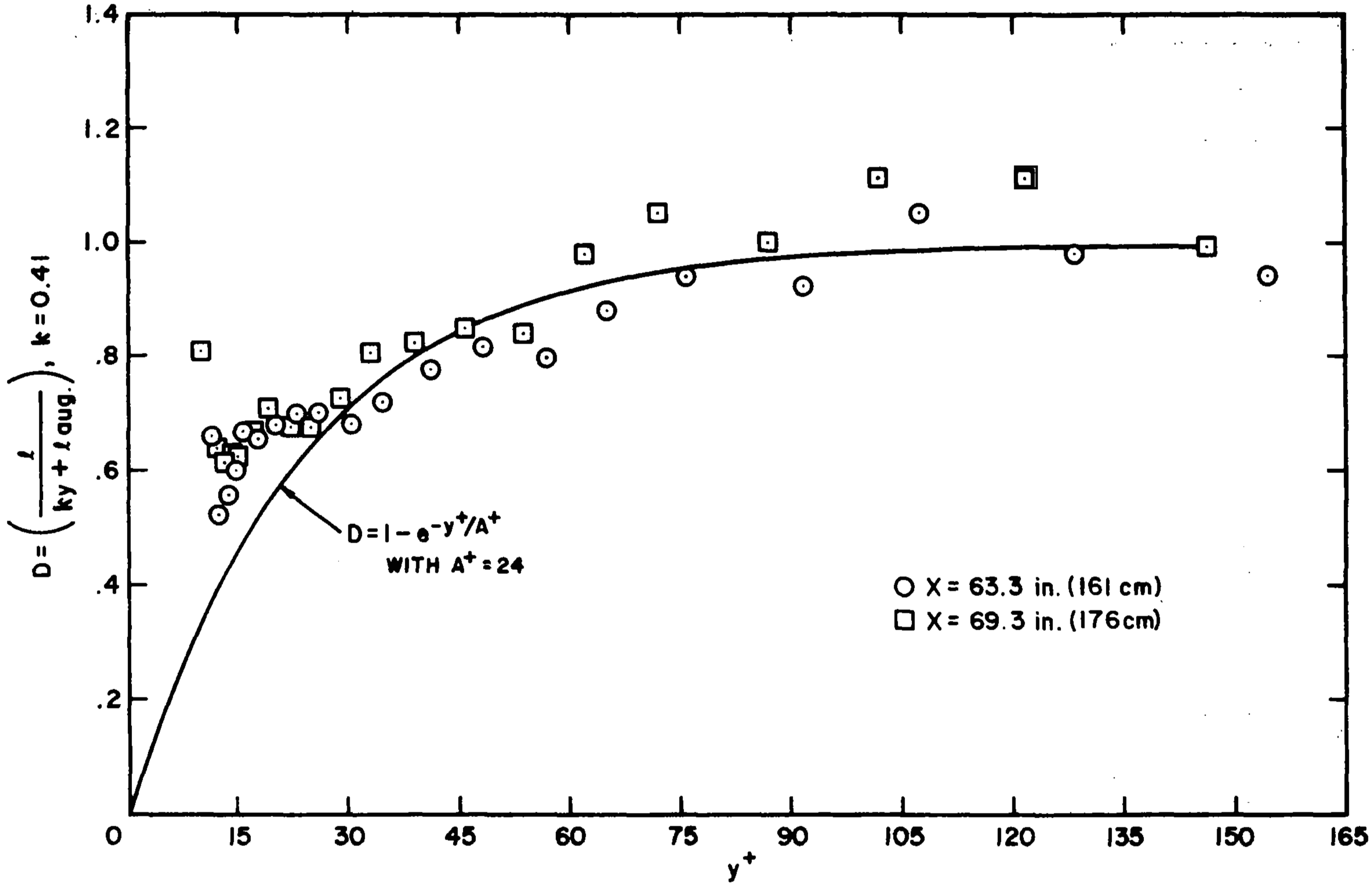

Figure 5.28 Van Driest damping function at M = 0.2 .

CHAPTER VI

PREDICTION OF THE EXPERIMENTAL DATA

Prediction of the full-coverage, film-cooled heat transfer data was made using a finite difference prediction scheme based on the computer program originated by Patankar and Spalding [10]. Several years of investigation of turbulent boundary layer heat transfer with uniform transpiration and with pressure gradient have been conducted by the Stanford HMT group [2-9] and have provided the turbulence model used in the present program. Kays [70] gives a brief description.

A. Presentation of the Modeling Problem

In Chapter IV, the basic equations for the locally-averaged properties were derived and can be summarized as

$$\frac{\partial U}{\partial x} + \frac{\partial V}{\partial y} \tag{4.6a}$$

$$U\frac{\partial U}{\partial x} + V\frac{\partial U}{dy} = \frac{\partial}{\partial y}\left(\frac{g_c\tau}{\rho}\right) + V_o U_x \frac{\partial g}{\partial y} \tag{6.1}$$

$$U\frac{\partial T}{\partial x} + V\frac{\partial T}{\partial y} = \frac{\partial}{\partial y}\left(\frac{\dot{q}''}{\rho c_p}\right) - V_o(T_2 - T_o)\frac{\partial f}{\partial y} \tag{6.2}$$

with

$$\frac{g_c\tau}{\rho} = \nu\frac{\partial U}{\partial y} - \overline{u'v'} - (\overline{\tilde{u}\tilde{v}})_{hom} \tag{6.3}$$

$$\frac{\dot{q}''}{\rho c_p} = \alpha\frac{\partial T}{\partial y} - \overline{t'v'} - (\overline{\tilde{t}\tilde{v}})_{hom} \tag{6.4}$$

and $f = g = 1.0$ at $y = 0$, $f = g = 0.0$ at $y = \infty$.

In the present program, U_∞ was kept constant, and the pressure gradient term did not appear in the momentum equation. There appear four unknown terms: $-\overline{u'v'} - (\overline{\tilde{u}\tilde{v}})_{hom}$, $-\overline{t'v'} - (\overline{\tilde{t}\tilde{v}})_{hom}$, f, and g.

These terms appear because of the non-linearity in the convective terms and present a "closure problem" (i.e., Reynolds [71]) which can be solved by proper modeling of the above terms. As was indicated by Reynolds, a higher level model, like the mean turbulence equation model or the mean Reynolds stress model, would be preferred if possible. In the present program, however, the main objective was the gross heat transfer study, and our attention was given only to the mean velocity profiles, using a pitot probe. This limited us to a mean-field type of closure model.

A.1 Model for $-\overline{u'v'} - (\overline{\tilde{u}\tilde{v}})_{hom}$ and $-\overline{t'v'} - (\overline{\tilde{t}\tilde{v}})_{hom}$

Because of its simplicity and wide applicability the mixing length model was chosen. A simple analysis in Appendix I supports the idea of applying the eddy viscosity concept to the modeling of terms, $-(\overline{\tilde{u}\tilde{v}})_{hom}$ and $-(\overline{\tilde{t}\tilde{v}})_{hom}$.

Then

$$-\overline{u'v'} - (\overline{\tilde{u}\tilde{v}})_{hom} = \ell^2 \left|\frac{\partial U}{\partial y}\right| \frac{\partial U}{\partial y} = \varepsilon_M \frac{\partial U}{\partial y} \tag{6.5}$$

$$-\overline{t'v'} - (\overline{\tilde{t}\tilde{v}})_{hom} = \varepsilon_H \frac{\partial T}{\partial y} = \frac{\varepsilon_M}{Pr_t} \frac{\partial T}{\partial y} \tag{6.6}$$

The problem becomes one of modeling of the mixing length, ℓ, and the turbulent Prandtl number, Pr_t.

As was shown in Figure 5.26, Figure 5.28 and Equation (5.18) and (5.19), the following expression was used:

$$\ell = \ell_{outer}(1 - e^{-y^+/A^+}) = (\ell_f + \ell_a)(1 - e^{-y^+/A^+}) \tag{6.7}$$

where $A^+ = 24$ was used and ℓ_f is the mixing length for the flat plate and ℓ_a denotes the augmented mixing length. Since discrete hole blowing has the value of $M \geq 0.1$, the jet always penetrates the main boundary sublayer, and the interaction between the jet and the boundary layer occurs somewhere outside the sublayer. This was the reason for a fixed value of A^+. The value of ℓ_f was the same as was used in

Kays [70].

$$\ell_f = \kappa y \qquad \text{for} \quad \kappa y < \lambda\delta_{.99}$$
$$= \lambda\delta_{.99} \qquad \text{for} \quad \kappa y \geq \lambda\delta_{.99} \tag{6.8}$$

where $\lambda = 0.08$ was used.

For ℓ_a , the empirical curve fit of Figure 5.26 was used.

$$\ell_a = \kappa_o \delta \left(\frac{y}{\delta}\right)^2 e^{-\left(\frac{y/\delta}{DPL}\right)^2} \tag{6.9}$$

where the dimensionless distance, y/δ , was used because ℓ_a is mainly due to the interaction between the jets and the outer region of the boundary layer, and the constant κ_o determines the maximum value of ℓ_a and the constant DPL gives the location of the maximum in the boundary layer. κ_o has a relationship to $(\ell_a/\delta)_{max}$, as

$$\kappa_o = \frac{e}{(DPL)^2}\left(\frac{\ell_a}{\delta}\right)_{max} \tag{6.10}$$

where e is the base for natural logarithm. Then this formulation reduces the problem of modeling into the evaluation of DPL and $(\ell_a/\delta)_{max}$.

DPL was considered as a function of M and P/D , and $(\ell_a/\delta)_{max}$ was expressed as

$$\left(\frac{\ell_a}{\delta}\right)_{max} = AKO \frac{v^+_{o,e}}{c_f/2} = AKO\left(\frac{F}{c_f/2}\right)_e \tag{6.11}$$

where $v^+_{o,e}$ is the effective v^+_o, a dimensionless blowing parameter. For the evaluation of $v^+_{o,e}$, see Section A.3 of this chapter. This linear relationship is for the convenience of use, and for the purpose of prediction.

For the turbulent Prandtl number, Pr_t , the flat plate value was used, as in Kays [70].

$$Pr_t = \frac{1}{Pr} - \frac{\frac{1}{Pr} - 0.9}{3.16} \, y^{+\,0.25} \qquad (6.12)$$

If the above expression falls below 0.86 , a simple value of 0.86 was used. Further refinements on Pr_t were not attempted because the molecular Prandtl number of air is 0.72 and Pr_t is not expected to vary considerably from flat plate values.

A.2 Model for g(y,x) and f(y,x)

The modeling of g and f requires information on the distribution of the effective body force or effective source across the boundary layer. The analysis done in Appendix I indicates that periodic perturbation at the wall will decay exponentially toward the free stream if the velocity is uniform.

Also, the following reasoning between the mixing length distribution and the effective source or effective body force can be used to determine the distribution of g and f .

From the physical point of view, the maximum in mixing length appears in the middle of the boundary layer because of the presence of the shear layer between the jet and the boundary layer; and the $\tilde{u}$, $\tilde{v}$, and $\tilde{t}$ have maximum variation around the center of the deflected jet. This means that the maximum of the mixing length will appear between the center of the deflected jet and the interface of jet boundary layer. Also, if there is an effective body force or source present due to such variation of $\tilde{u}$, $\tilde{v}$, and $\tilde{t}$, then the effective body force or the effective source should damp out beyond DPL . This discussion suggests the following distribution:

$$g(y,x) = e^{-\frac{y/\delta}{DPL}} \qquad (6.13)$$

and

$$f(y,x) = e^{-\frac{y/\delta}{DPL \cdot CPR}} \qquad (6.14)$$

In this case, CPR is mainly due to the Pr not being unity, and in this case was set to 1.0 because in air $Pr \simeq 0.72$ and the penetration distance of the jet would be almost the same for momentum and heat.

In the case of normal hole injection, $g(y,x)$ does not play a role because $U_x = 0$.

A.3 Treatment of Abrupt Change in Blowing

This is to get $v^+_{o,e}$ in Equation (6.11) from v^+_o to handle the abrupt change in blowing, and it is a purely empirical formulation. A similar approach was taken in transpiration cooling by Loyd [8].

At the step change of blowing, $v^+_{o,e}$ was set as

$$v^+_{o,e} = \left(v^+_{o,e}\right)_{\text{previous step}} + \begin{Bmatrix} CL1 \\ \text{or} \\ CL2 \end{Bmatrix} \left\{ v^+_o - (v^+_o)_{\text{previous step}} \right\}$$

where CL1 is for the positive step in blowing and 0.5 was used, and CL2 is for the negative step in blowing and 0.85 was used. After the step change, as in Loyd [8], the equation for $v^+_{o,e}$

$$\frac{dV^+_{o,e}}{dx^+} = \frac{V^+_o - V^+_{o,e}}{C_2}$$

was solved in each integrating step with C_2 of 6000.

For example, if we have step blowing through discrete holes and stop blowing after a certain distance, we have the following variation in $v^+_{o,e}$:

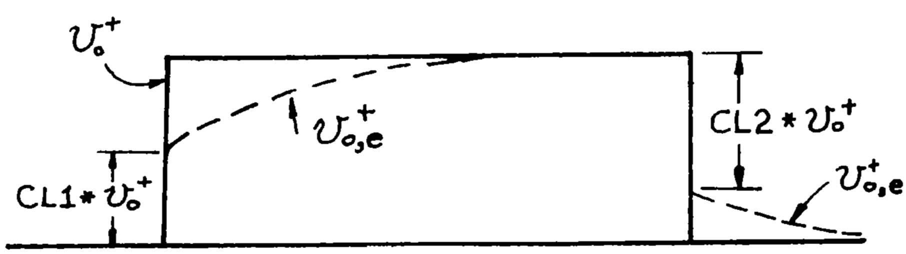

B. Prediction of Experimental Results

After the local averaging, v_o^+ was substantially higher than the transpiration cooling cases. This required an accurate handling of the sublayer equations. Appendix H explains an algorithm for obtaining a numerical solution to the sublayer equations to obtain the shear stress and heat flux at the wall.

Figure 6.1 compares the predicted local average velocity profile to that of the lateral average. It is quite satisfactory. Figure 6.2 shows the variation of DPL and $(\ell_a/\delta)_{max}$. These values were numerically determined to predict the experimental Stanton numbers. Figures 6.3 through 6.17 show the various predictions made for each test run. The overall prediction is satisfactory. The trends shown in Figure 6.2 were previously found in the analysis of Eriksen's [44]. His data analysis showed that y_o and ε_H increased as the value of M increases. In the present model, the boundary layer concept was introduced, while in Eriksen's it was not.

For the prediction of high values of M and arbitrary boundary conditions, further development must be made.

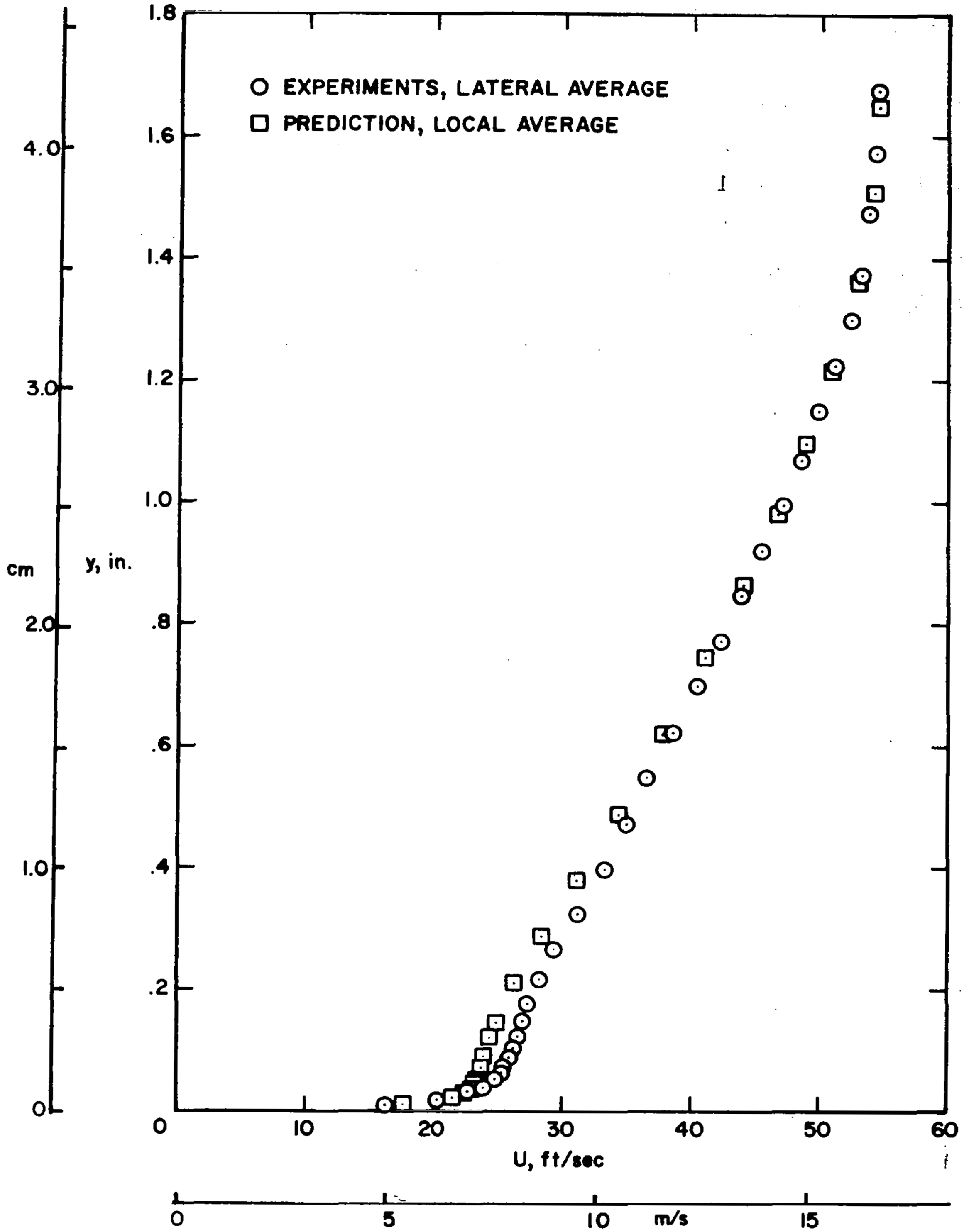

Figure 6.1 Prediction of the velocity profile.

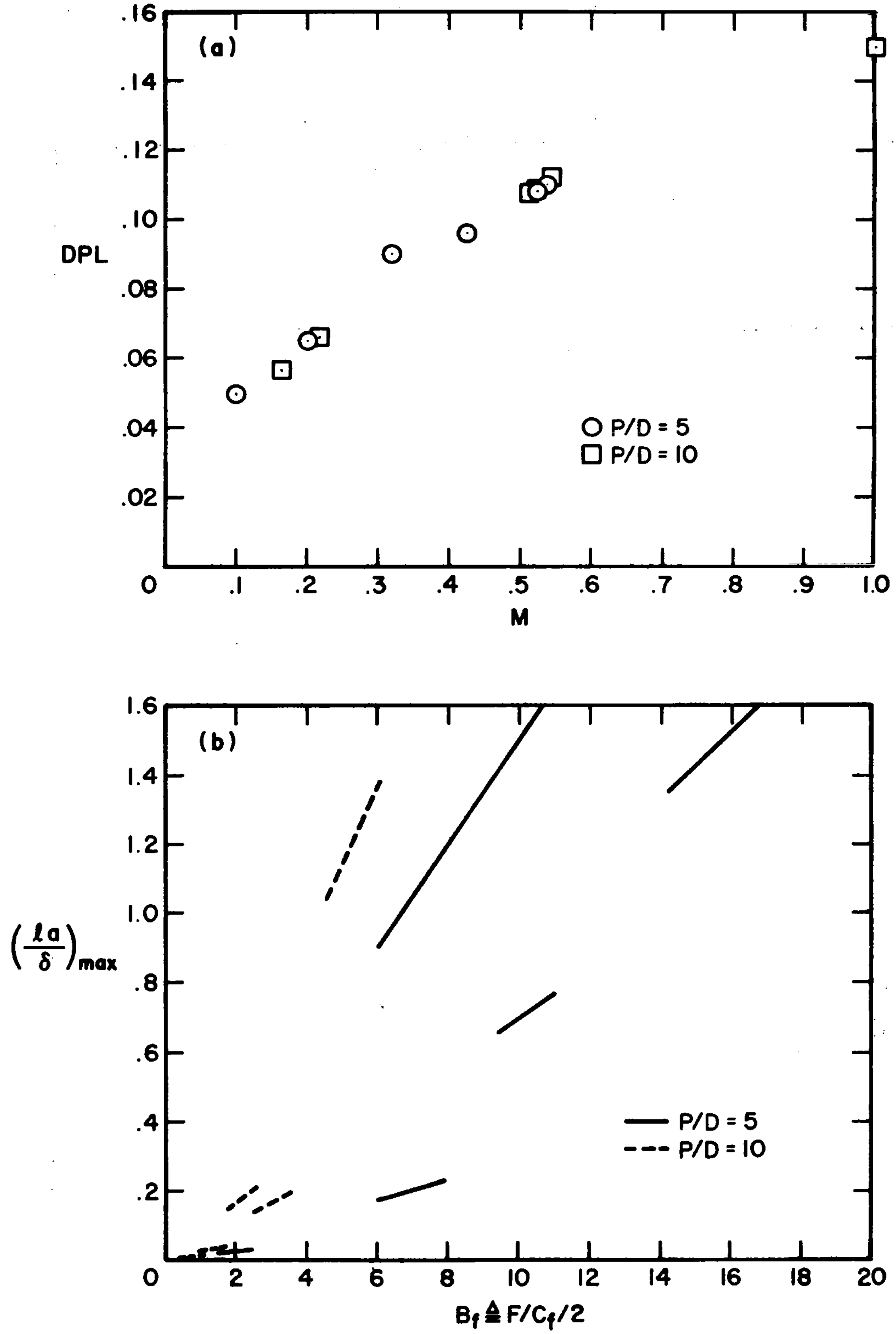

Figure 6.2 Variation of DPL and ($\ell a/\delta$)max .

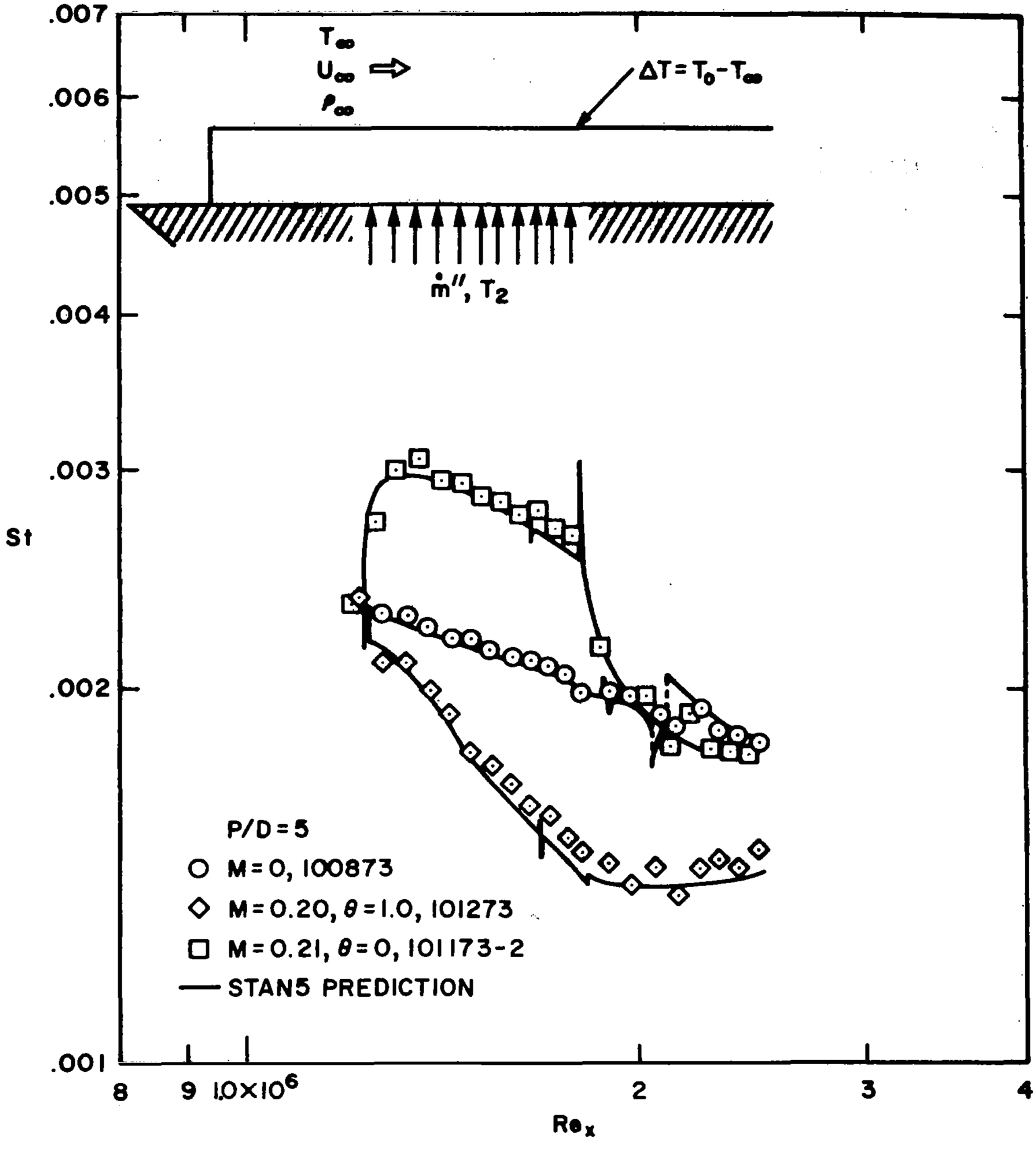

Figure 6.3 Prediction of Stanton number data on full-coverage film-cooled surface with heated starting length for M = 0.2 at U_∞ = 55 ft/sec (16.7 m/s) with P/D = 5 .

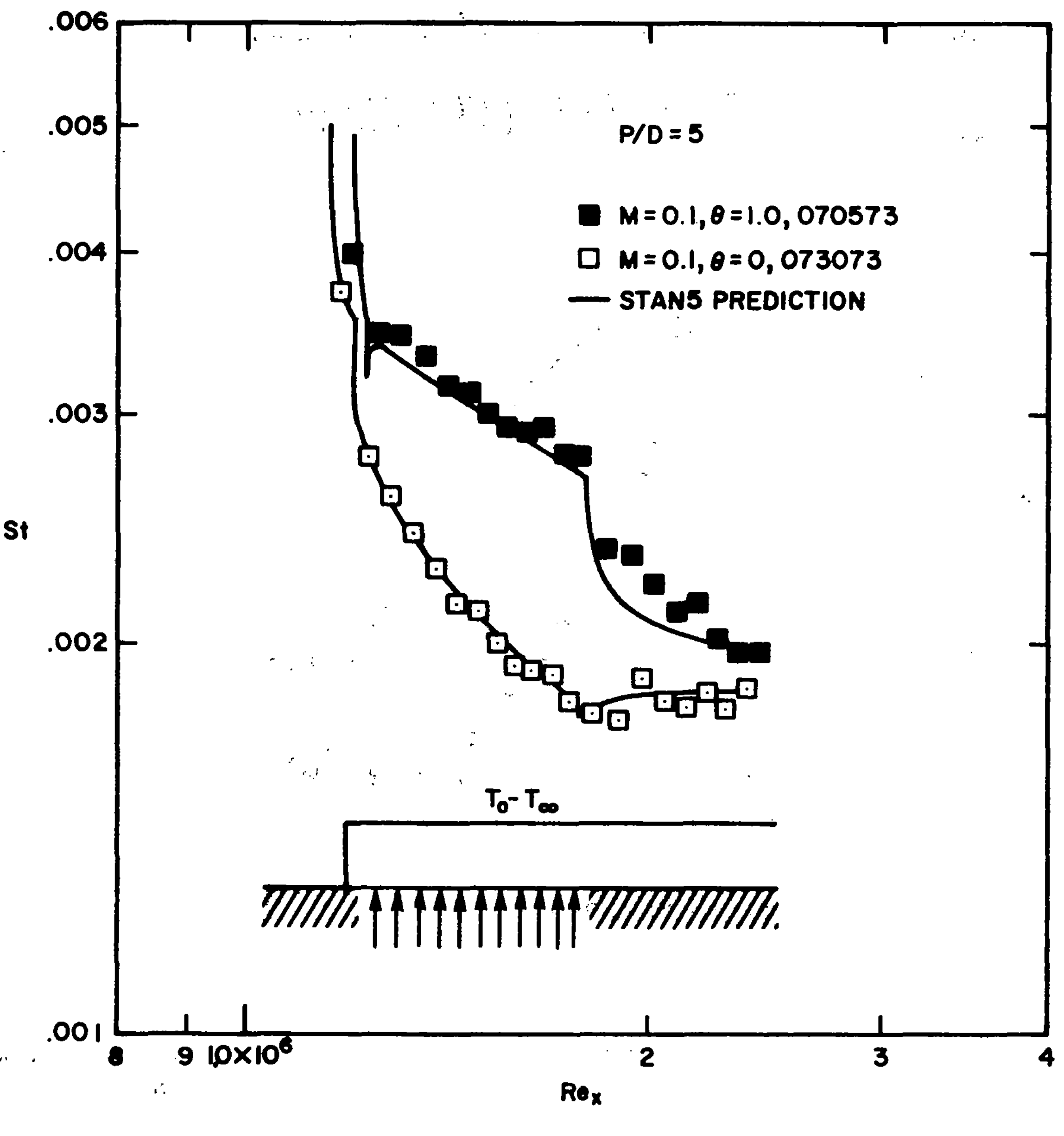

Figure 6.4 Prediction of Stanton number data on full-coverage film-cooled surface with unheated starting length for $M = 0.1$ at $U_\infty = 55$ ft/sec (16.7 m/s) with P/D = 5 .

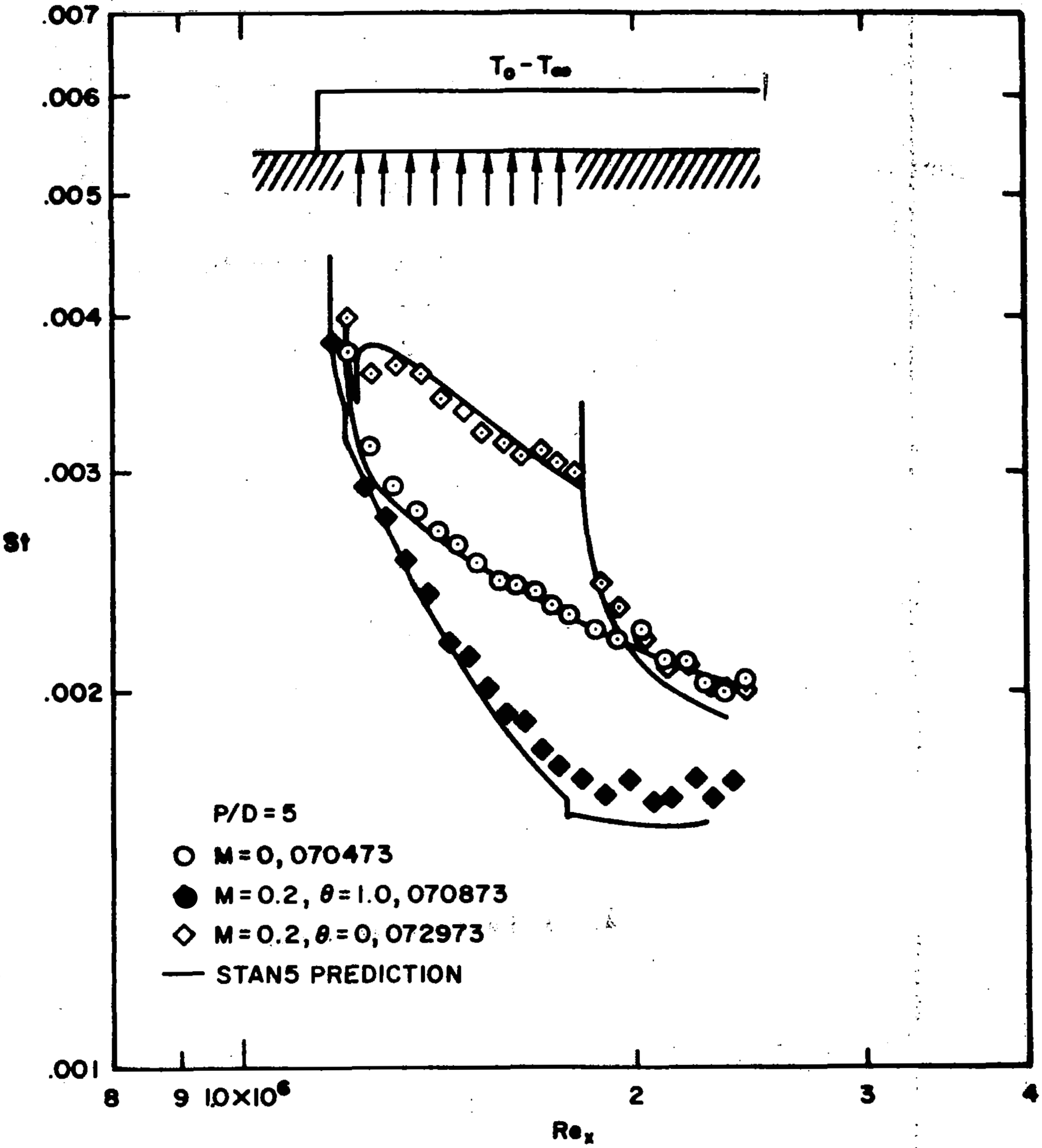

Figure 6.5 Prediction of Stanton number data on full-coverage film-cooled surface with unheated starting length for $M = 0.2$ at $U_\infty = 55$ ft/sec (16.7 m/s) with $P/D = 5$.

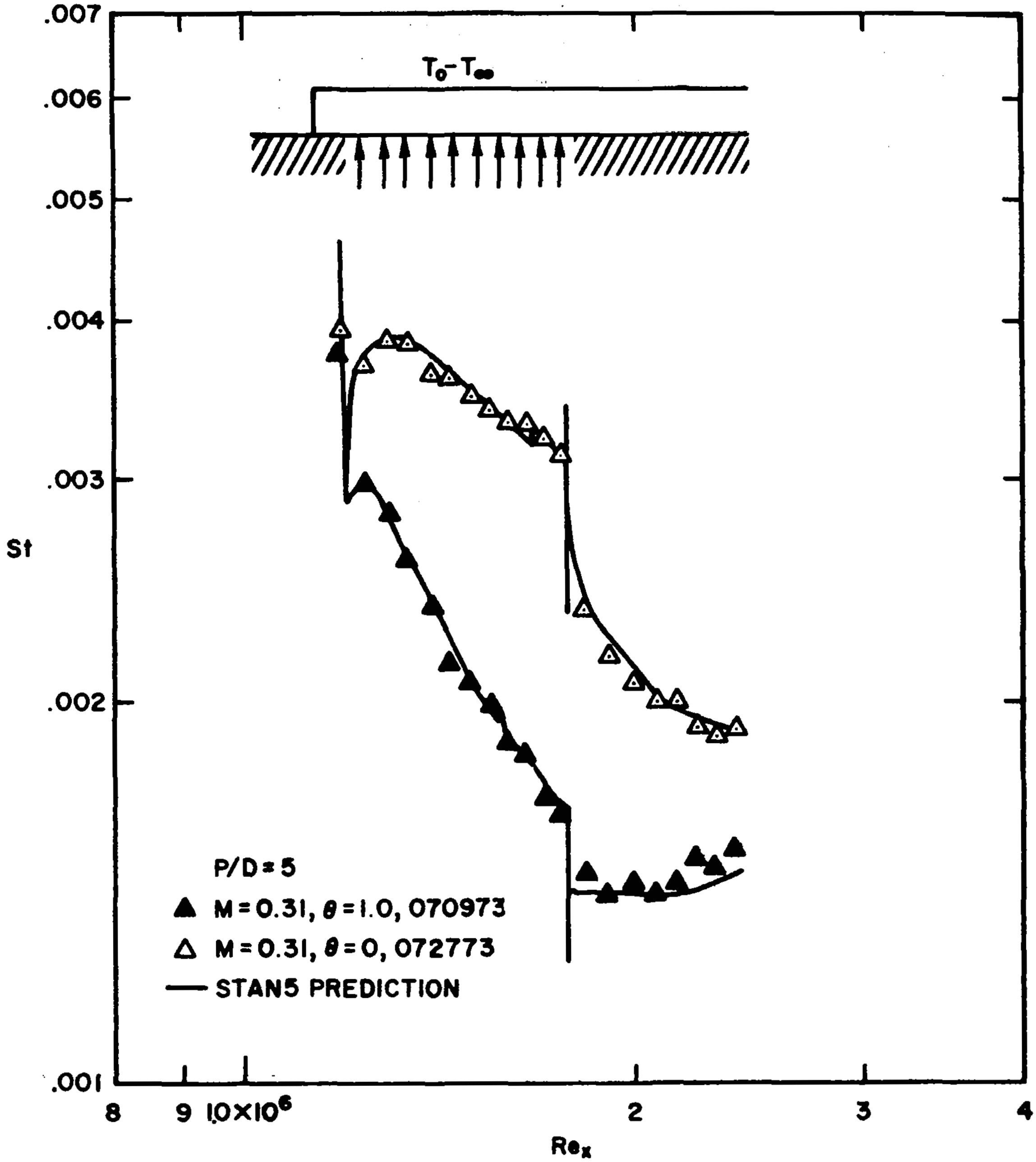

Figure 6.6 Prediction of Stanton number data on full-coverage film-cooled surface with unheated starting length for M = 0.3 at U_∞ = 55 ft/sec (16.7 m/s) with P/D = 5 .

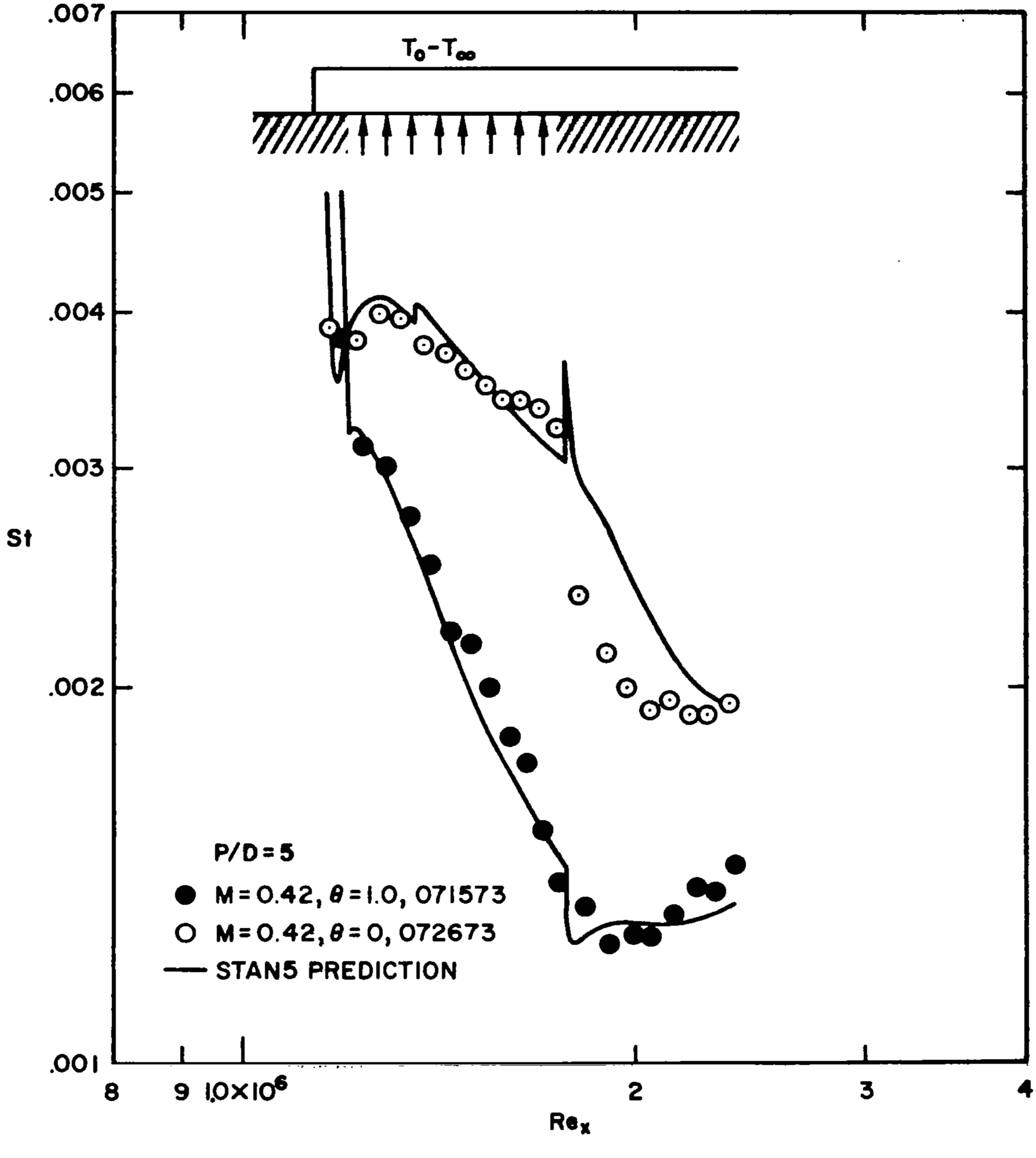

Figure 6.7 Prediction of Stanton number data on full-coverage film-cooled surface with unheated starting length for $M = 0.42$ at $U_\infty = 55$ ft/sec (16.7 m/s) with $P/D = 5$.

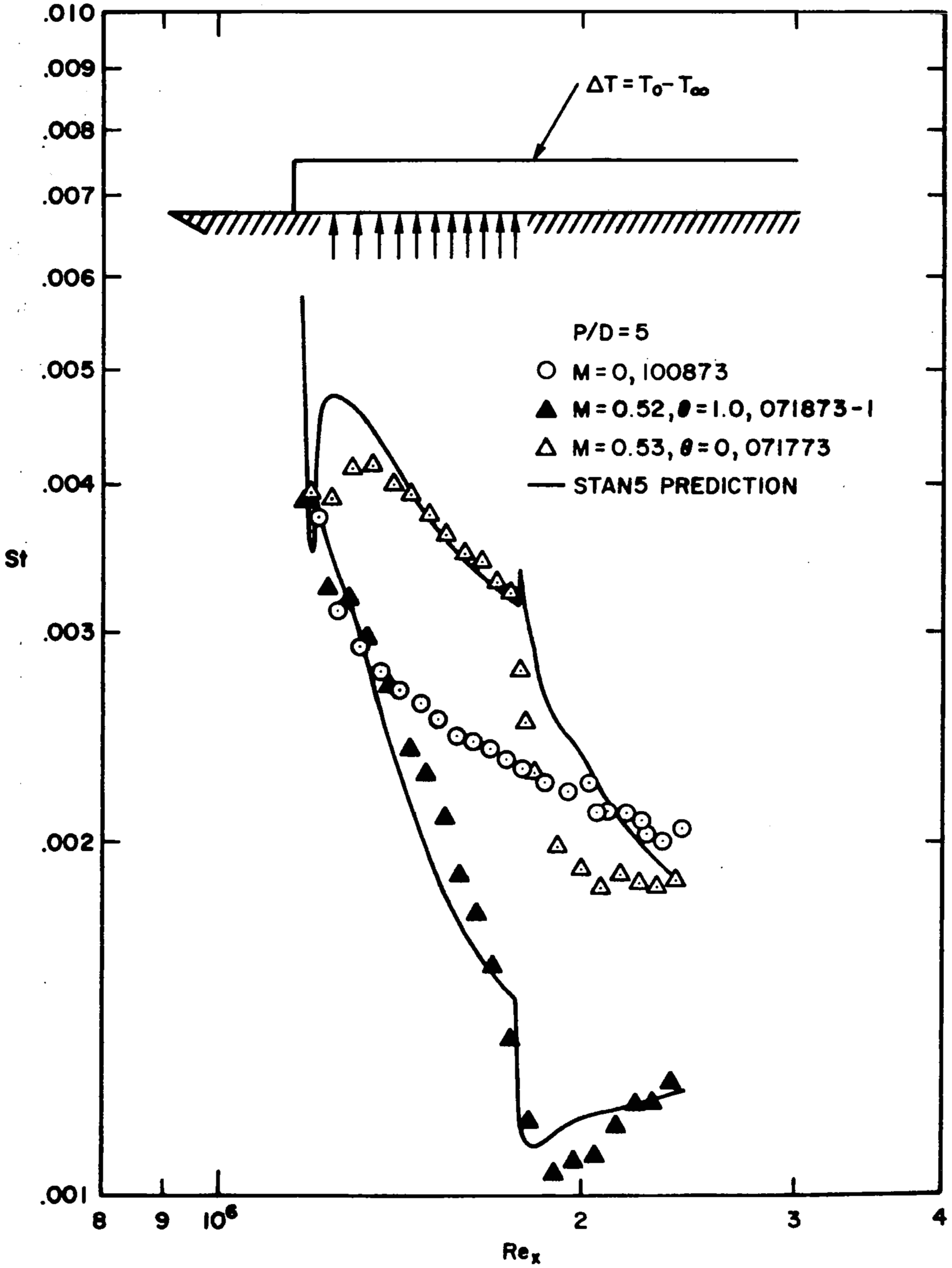

Figure 6.8 Prediction of Stanton number data on full-coverage film-cooled surface with unheated starting length for $M = 0.53$ at $U_\infty = 55$ ft/sec (16.7 m/s) with P/D = 5 .

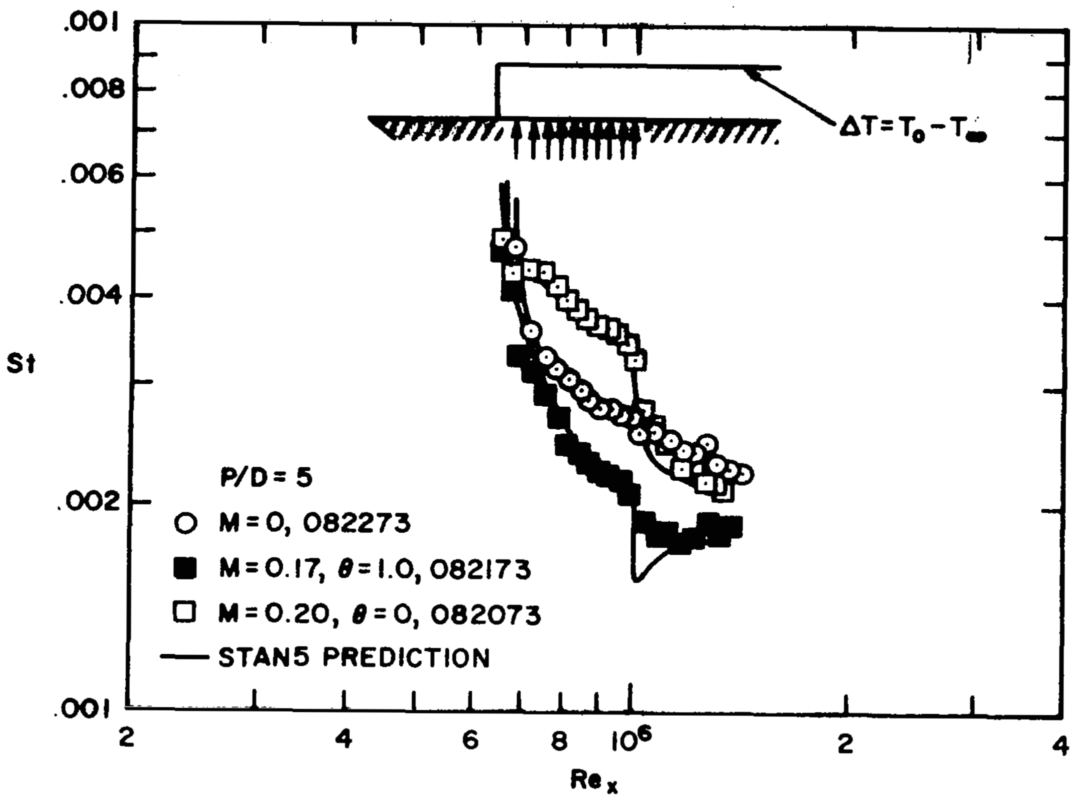

Figure 6.9 Prediction of Stanton number data on full-coverage film-cooled surface with unheated starting length for M = 0.2 at U_∞ = 32 ft/sec (9.76 m/s).

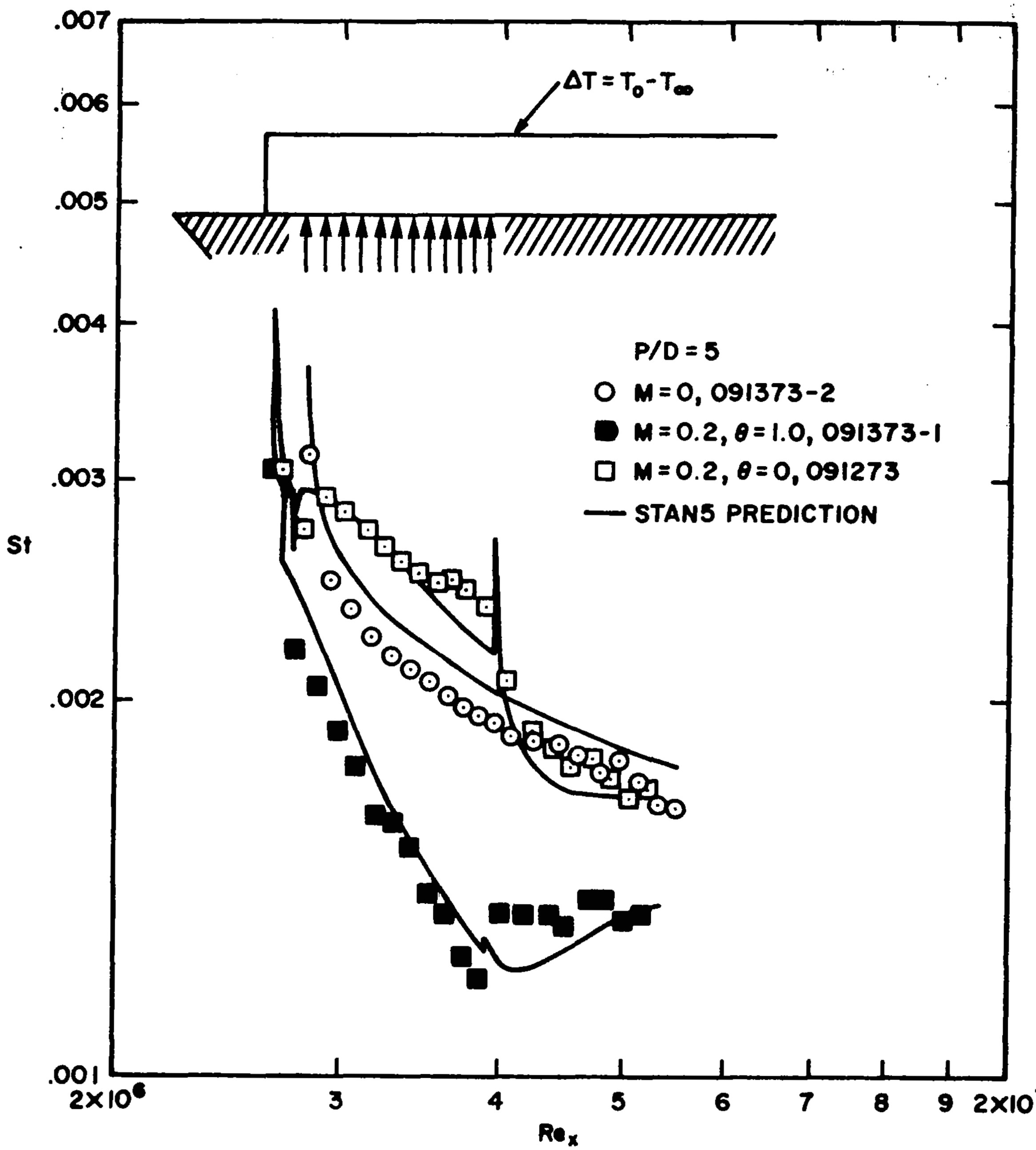

Figure 6.10 Prediction of Stanton number data on full-coverage film-cooled surface with unheated starting length for $M = 0.2$ at $U_\infty = 115$ ft/sec (35 m/s) with P/D = 5 .

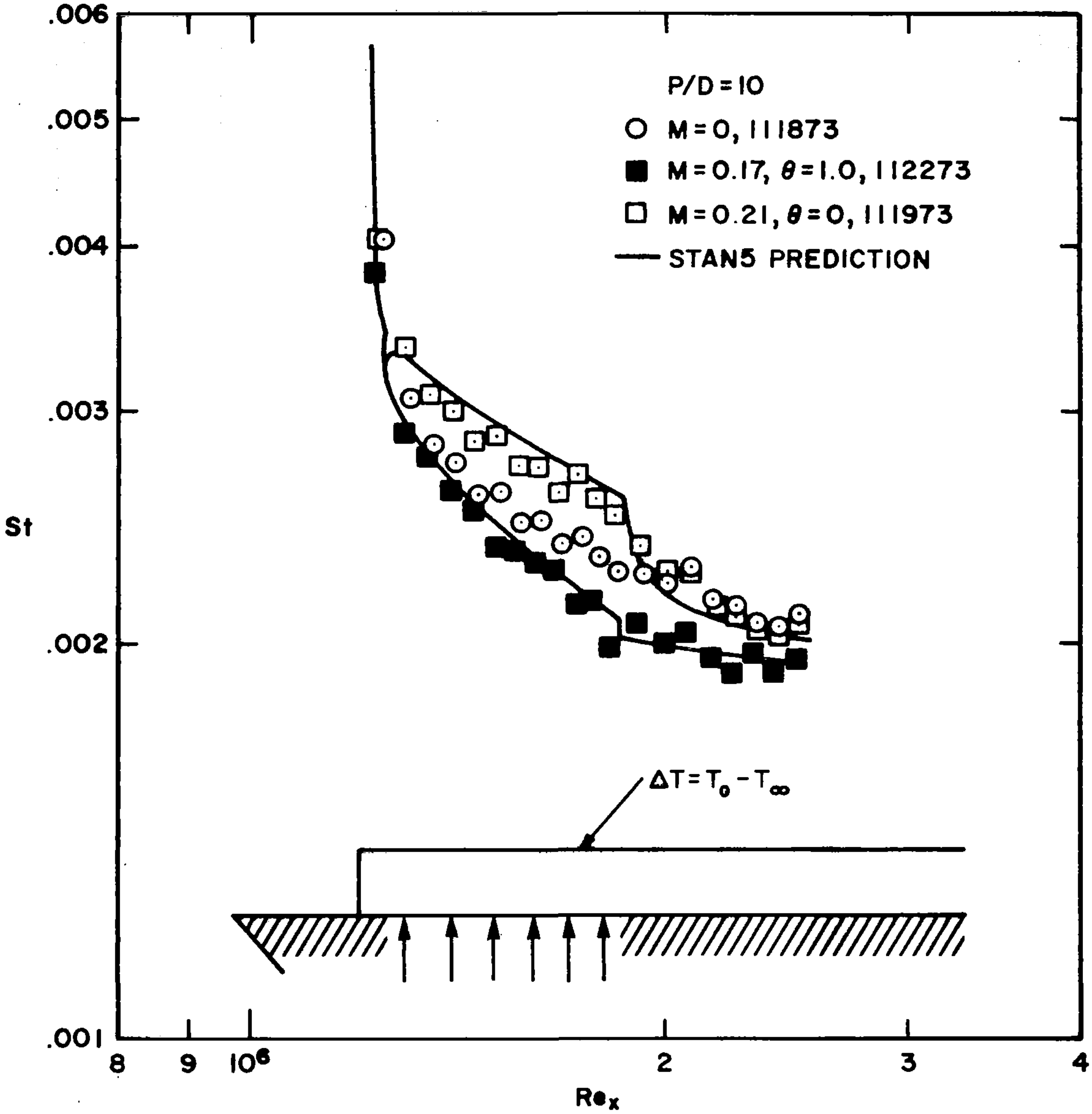

Figure 6.11 Prediction of Stanton number data on full-coverage film-cooled surface with unheated starting length for $M = 0.2$ at $U_\infty = 55$ ft/sec (16.7 m/s) with P/D = 10 .

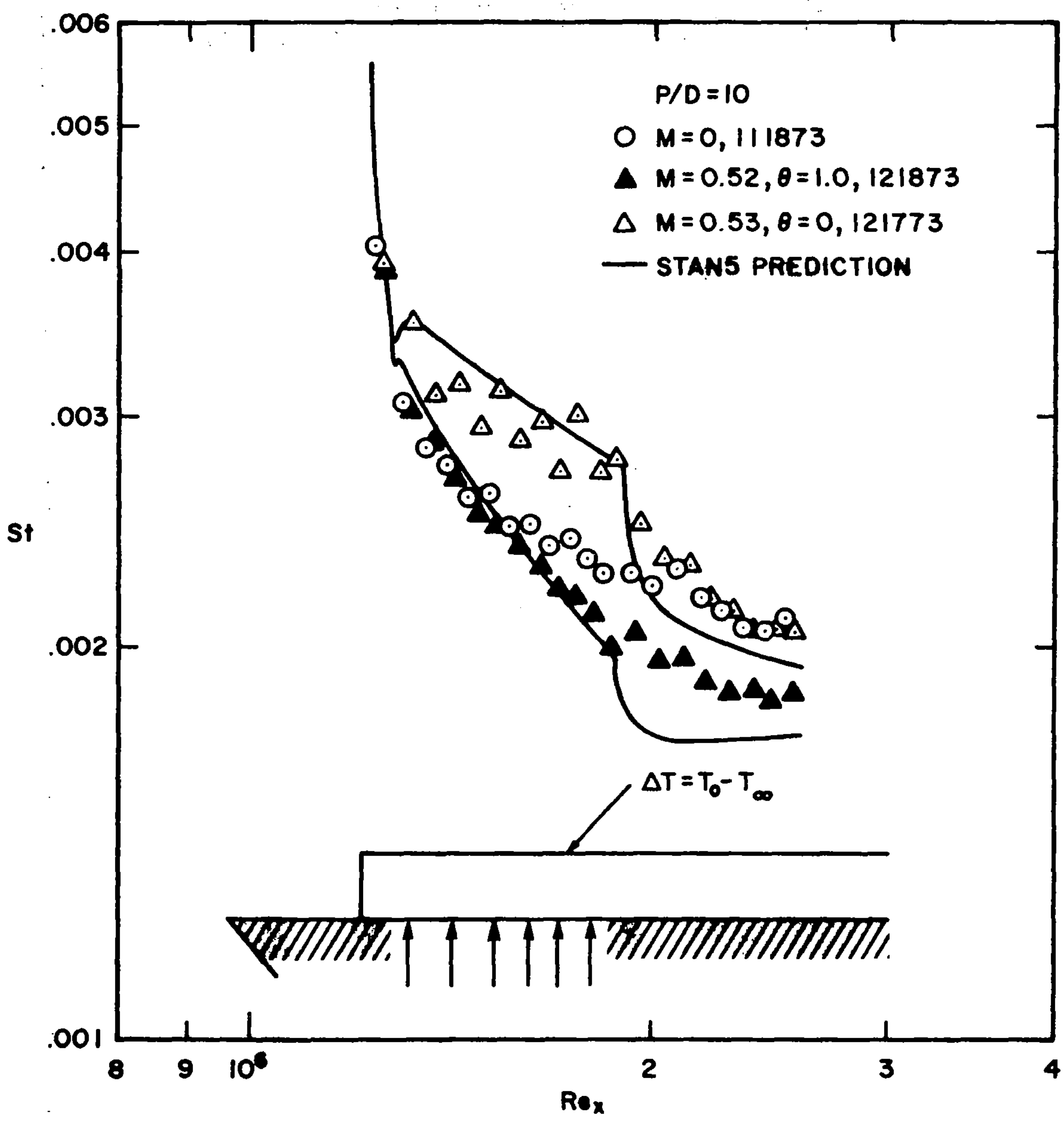

Figure 6.12 Prediction of Stanton number data on full-coverage film-cooled surface with unheated starting length for $M = 0.52$ at $U_\infty = 55$ ft/sec (16.7 m/s) with $P/D = 10$.

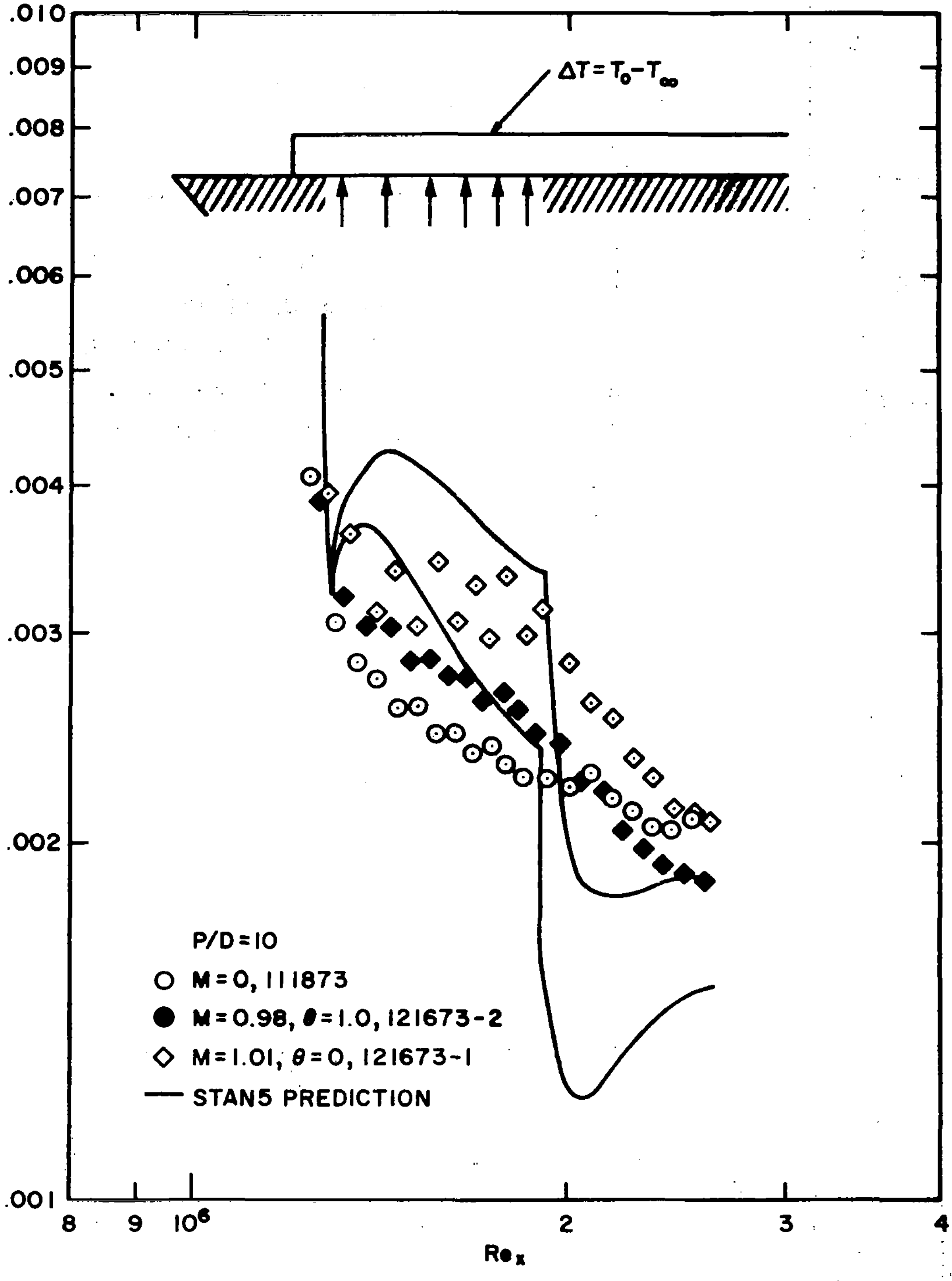

Figure 6.13 Prediction of Stanton number data on full-coverage film-cooled surface with unheated starting length for $M = 1.0$ at $U_{\infty} = 55$ ft/sec (16.7 m/s) with $P/D = 10$.

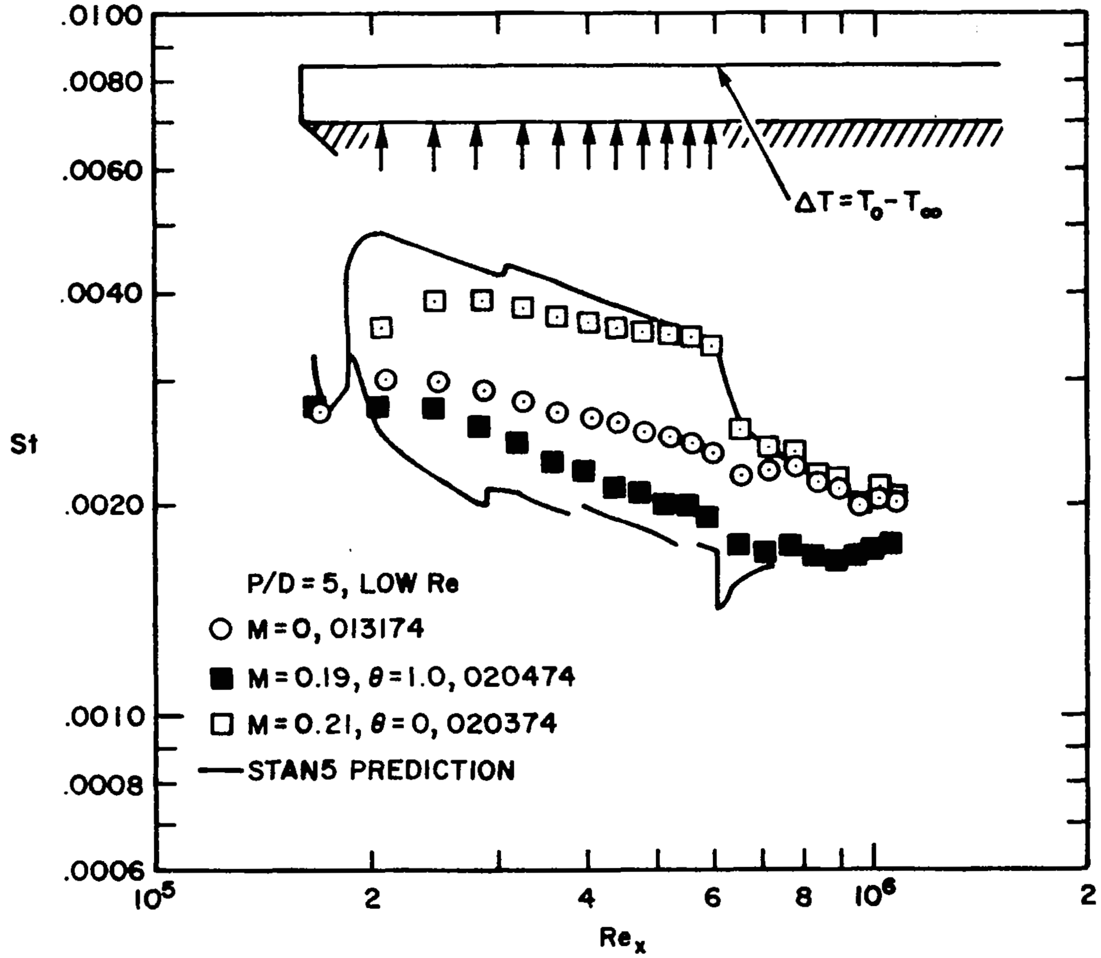

Figure 6.14 Prediction of Stanton number data on full-coverage film-cooled surface for $M = 0.2$ at $U_\infty = 39$ ft/sec (11.9 m/s) with P/D = 5 and thin boundary layer.

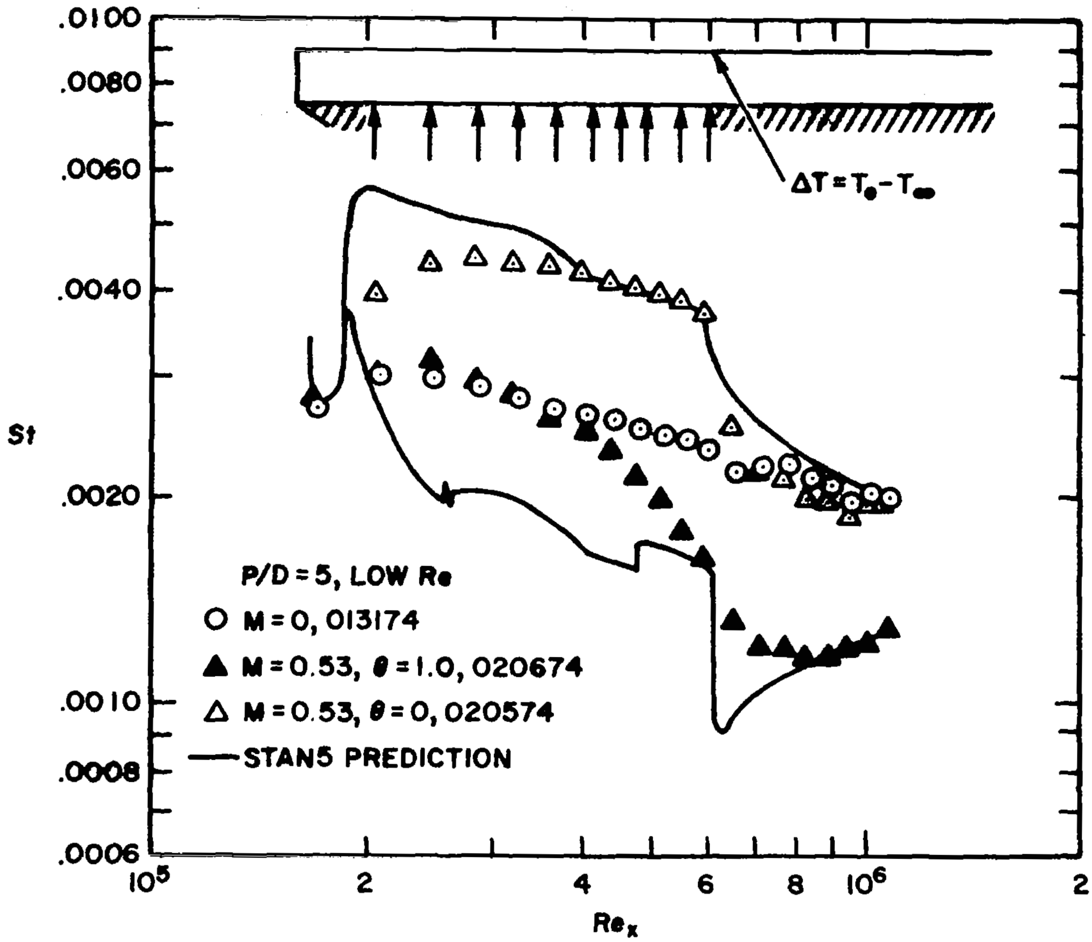

Figure 6.15 Prediction of Stanton number data on full-coverage film-cooled surface for M = 0.53 at U_∞ = 39 ft/sec (11.9 m/s) with P/D = 5 and thin boundary layer.

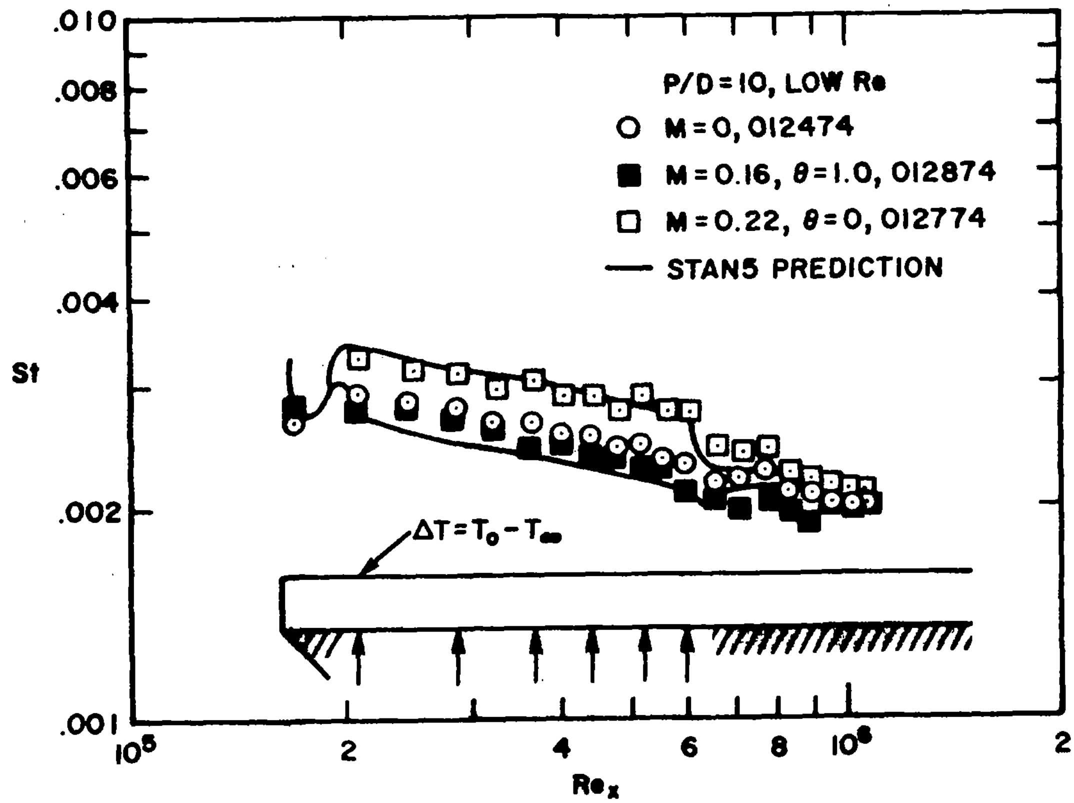

Figure 6.16 Prediction of Stanton number data on full-coverage film-cooled surface for $M = 0.2$ at $U_\infty = 39$ ft/sec (11.9 m/s) with P/D = 10 and thin boundary layer.

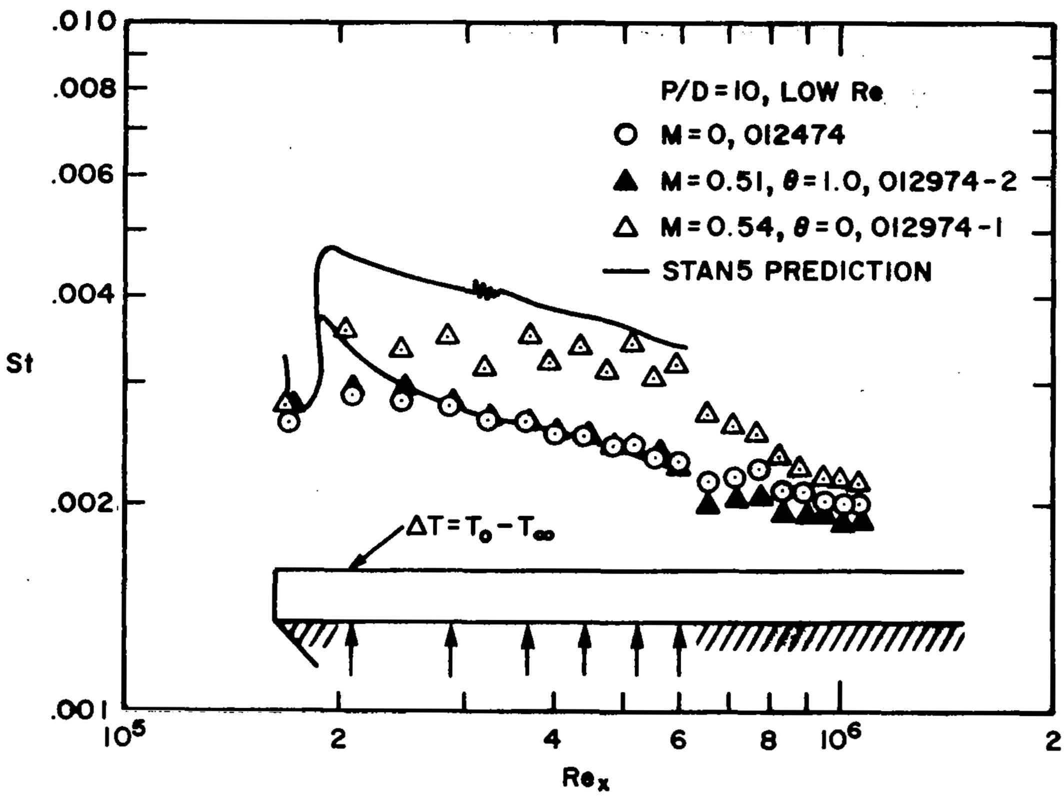

Figure 6.17 Prediction of Stanton number data on full-coverage film-cooled surface for $M = 0.52$ at $U_\infty = 39$ ft/sec (11.9 m/s) with $P/D = 10$ and thin boundary layer.

CHAPTER VII

SUMMARY AND RECOMMENDATIONS FOR FURTHER STUDY

A. Summary

1. The linear superposition method for film cooling was developed and shown to unify transpiration cooling and film cooling by using the same temperature potential, $(T_o - T_\infty)$. This allows direct comparison of Stanton number data, eliminating the calculation of wall heat flux for performance comparison. Also, with this scheme a skin friction estimation is possible for the full-coverage, film-cooled surface.

2. The concept of the local spatial average was introduced, and the proper governing equations for full-coverage film cooling were derived. This opens the way for utilization of the analytical methods developed for conventional turbulent boundary layers.

3. Heat transfer data for full-coverage film cooling with normal hole injection at $P/D = 5$ and $P/D = 10$ were taken for the fundamental cases $\theta = 0$ and $\theta = 1$.

4. For the integral equation prediction of heat transfer data, the following formulae are recommended:

$$\left.\frac{St}{St_o}\right|_{Re_{\bar{\Delta}_2}} = 1 + C_o \, Re_{\infty,D}^{-0.29} \, F^{0.43} \quad \text{for} \quad \theta = 0.0$$

$$\left.\frac{St}{St_o}\right|_{Re_{\bar{\Delta}_2}} = (1 + C_1 F)^{1.25} \left[\frac{\ln(1+B)}{B}\right]^{1.25} (1+B)^{0.25}$$

$$\text{for} \quad \theta = 1.0$$

where $C_o = 55$, $C_1 = 140$ for $P/D = 5$, and $C_o = 48$, $C_1 = 180$

for $P/D = 10$ (to be used in conjunction with the superposition scheme to obtain Stanton number for arbitrary θ).

5. A two-dimensional boundary layer program was used to predict the experimental data. This procedure accounts for the penetration of the discrete hole jets into the boundary layer and the augmentation of the turbulent mixing due to jet-main stream interaction.

6. Several observations were made for normal hole injection.
   a. Laminar-to-turbulent transition occurs quite abruptly with discrete hole blowing.
   b. The $P/D = 10$ case with a comparable F is inferior to $P/D = 5$.
   c. In the initial blowing region, there is not much cooling effect.

B. Recommendations for Further Study

1. Study of full coverage film-cooling with slant angle injection geometry.

   For the application in the turbine blade cooling, the majority of discrete holes, except near the leading edge, can be slanted with respect to the surface in the main stream direction for better performance. This is due to jets remaining closer to the wall surface. This work is in progress.

2. Study of full coverage film-cooling with complex angle injection.

   By having a complex angle injection, the area covered by a jet increases, and thus the cooling performance increases. Especially in the leading edge of the turbine blade, the normal hole injection does not help very much and the introduction of angled injection in the lateral direction is essential. This work is being pursued.

3. Detailed investigation of mean velocity, mean temperature and turbulence profiles around the discrete holes.

This study will provide the detail variation of velocity, temperature and turbulence level around the holes and also will provide a better model of local average flux terms, which can be used in the numerical prediction program. This is being pursued.

4. Three-dimensional prediction program for $\tilde{u}$, $\tilde{v}$ and $\tilde{t}$.

   Along with the experimental investigation in item 3 , this study will provide an analytical means of predicting $\tilde{u}$, $\tilde{v}$ and $\tilde{t}$.

5. Study of the effects of $dP/dX \neq 0$ and the presence of other body forces.

   In many practical applications including the gas turbine blade, the effects of non-uniform free-stream velocity and other body forces are very important.

6. Refinement of the present computer program such that the higher mass flux at the wall and the abrupt change in the boundary conditions can be handled.

7. An experiment to determine the heat transfer characteristics downstream of a step in temperature of the injected air.

   This will provide the kernel function needed to handle the general case of arbitrary secondary gas temperature by superposition. These data are the counterpart of the unheated starting length data used in dealing with the arbitrary wall temperature problem for an impermeable wall.

REFERENCES

1. Esgar, J. B., Colladay, R. S., and Kaufman, A., "An Analysis of the Capabilities and Limitations of Turbine Air Cooling Methods," NASA TND-5992, Sept. 1970.

2. Moffat, R. J., and Kays, W. M., "The Turbulent Boundary Layer on a Porous Plate: Experimental Heat Transfer with Uniform Blowing and Suction," Report No. HMT-1, Thermosciences Division, Dept. of Mech. Engrg., Stanford Univ., 1967.

3. Simpson, R. L., Kays, W. M., and Moffat, R. J., "The Turbulent Boundary Layer on a Porous Plate: An Experimental Study of the Fluid Dynamics with Injection and Suction," Report No. HMT-2, Thermosciences Division, Dept. of Mech. Engrg., Stanford Univ., 1967.

4. Whitten, D. G., Kays, W. M., and Moffat, R. J., "The Turbulent Boundary Layer on a Porous Plate: Experimental Heat Transfer with Variable Suction, Blowing and Surface Temperature," Report No. HMT-3, Thermosciences Division, Dept. of Mech. Engrg., Stanford Univ., 1967.

5. Julien, H. L., Kays, W. M., and Moffat, R. J., "The Turbulent Boundary Layer on a Porous Plate: Experimental Study of the Effects of a Favorable Pressure Gradient," Report No. HMT-4, Thermosciences Division, Dept. of Mech. Engrg., Stanford Univ., 1969.

6. Thielbahr, W. H., Kays, W. M., and Moffat, R. J., "The Turbulent Boundary Layer: Experimental Heat Transfer with Blowing, Suction, and Favorable Pressure Gradient," Report No. HMT-5, Thermosciences Division, Dept. of Mech. Engrg., Stanford Univ., 1969.

7. Kearney, D. W., Moffat, R. J., and Kays, W. M., "The Turbulent Boundary Layer: Experimental Heat Transfer with Strong Favorable Pressure Gradients and Blowing," Report No. HMT-12, Thermosciences Division, Dept. of Mech. Engrg., Stanford Univ., 1970.

8. Loyd, R. J., Moffat, R. J., and Kays, W. M., "The Turbulent Boundary Layer on a Porous Plate: An Experimental Study of the Fluid Dynamics with Strong Favorable Pressure Gradients and Blowing," Report No. HMT-13, Thermosciences Division, Dept. of Mech. Engrg., Stanford Univ., 1970.

9. Andersen, P. S., Kays, W. M., and Moffat, R. J., "The Turbulent Boundary Layer on a Porous Plate: An Experimental Study of the Fluid Mechanics for Adverse Free-Stream Pressure Gradients," Report No. HMT-15, Thermosciences Division, Dept. of Mech. Engrg., Stanford Univ., 1972.

10. Spalding, D. B., and Patankar, S. V., Heat and Mass Transfer in Boundary Layers, Morgan-Granpian, London, 1967.

11. Wieghardt, K., "Hot-Air Discharge for De-icing," AAF Translation, Report No. F-TS-919-Re, Wright Field, 1946.

12. Seban, R. A., "Heat Transfer and Effectiveness for a Turbulent Boundary Layer with Tangential Fluid Injection," ASME Series C, JHT, Vol. 82, 1960, pp. 303-313.

13. Seban, R. A., and Back, L. H., "Effectiveness and Heat Transfer for a Turbulent Boundary Layer with Tangential Injection and Variable Free-Stream Velocity," ASME Ser. C, JHT, Vol. 84, 1962, pp. 235-244.

14. Hartnett, J. P., Birkebak, R. C., and Eckert, E. R. G., "Velocity Distribution, Temperature Distributions, Effectiveness and Heat Transfer for Air Injected through a Tangential Slot into a Turbulent Boundary Layer," ASME Ser. C, JHT, Vol. 83, 1961, pp. 293-306.

15. Papell, S. S., "Effect on Gaseous Film Cooling of Coolant Injection through Angled Slots and Normal Holes," NASA TN D-299, Sept. 1960.

16. Haji-Sheikh, A., "Flow Parameters on a Film-Cooled Surface," 4th International Heat Transfer Conference, Versailles, France, Aug. 1970, FC 1.10.

17. Artt, D. W., Brown, A., and Miller, P. P., "An Experimental Investigation into Film Cooling with Particular Application to Cooled Turbine Blades," 4th International Heat Transfer Conference, Versailles, France, Aug. 1970, FC 1.7.

18. Repukhov, V. M., Popovich, Ye. G., and Danileyko, V. M., "Effectiveness of Film-Cooling of a Flat Wall by Air Injection through a Slot Normal to the Film-Cooled Surface," Heat Transfer-Soviet Research, Vol. 2, No. 1, Jan. 1970, pp. 128-133.

19. Metzger, D. E., Carper, H. J., and Swank, L. R., "Heat Transfer with Film Cooling Near Non-tangential Injection Slots," ASME Transactions, J. of Eng. Power, 1968, pp. 157-163.

20. Kacker, S. C., and Whitelaw, J. H., "The Effect of Slot Height and Slot Turbulence Intensity on the Effectiveness of the Uniform Density, Two-Dimensional Wall Jet," ASME Ser. C, JHT, Vol. 90, 1968, pp. 469-475.

21. Pai, B. R., and Whitelaw, J. H., "The Influence of Strong Pressure Gradient on Film Cooling Effectiveness," 4th International Heat Transfer Conference, Versailles, France, Aug. 1970, FC 1.11.

22. Carson, L. W., and Talmor, E., "Gaseous Film Cooling at Various Degrees of Hot Gas Acceleration and Turbulence Levels," Int. J. Heat and Mass Transfer, Vol. 11, 1968, pp. 1695-1713.

23. Goldstein, R. J., Shavit, G., and Chen, T. S., "Film-Cooling Effectiveness with Injection through a Porous Section," ASME Ser. C, JHT, Vol. 87, 1965, pp. 353-361.

24. Escudier, M. P., and Whitelaw, J. H., "The Influence of Strong Adverse Pressure Gradient on the Effectiveness of Film Cooling," Int. J. Heat and Mass Transfer, Vol. 11, 1968, pp. 1289-1292.

25. Nishiwaki, N., Hirata, M., and Tsuchida, A., "Heat Transfer on a Surface Covered by Cold Air Film," Int. Development in Heat Transfer, ASME, N. Y., 1961, pp. 675-681.

26. Papell, S. S., and Trout, A. M., "Experimental Investigation of Air Film Cooling Applied to an Adiabatic Wall by Means of an Axially Discharging Slot," NASA TN D-9, Aug. 1959.

27. Samuel, A. E., and Joubert, P. N., "Film Cooling of an Adiabatic Flat Plate in Zero Pressure Gradient in the Presence of a Hot Mainstream and Cold Tangential Secondary Injection," J. Heat Transfer, Vol. 87, 1965, pp. 409-419.

28. Chin, J. H., Skirvin, S. C., Hayes, L. E., and Burggraf, F., "Film Cooling with Multiple Slots and Louvers," ASME Ser. C, JHT, Vol. 83, 1961, pp. 281-292.

29. Goldstein, R. G., Eckert, E. R. G., and Ramsey, J. W., "Film Cooling with Injection through Holes; Adiabatic Temperature Downstream of a Circular Hole," ASME, J. Engrg. Power, 1968, pp. 384-395.

30. Goldstein, R. G., Eckert, E. R. G., Eriksen, V. L., and Ramsey, J. W., "Film Cooling Following Injection through Inclined Circular Tubes," NASA CR-72612, Nov. 1969.

31. Metzger, D.E., and Fletcher, D.D.,"Surface Heat Transfer Immediately Downstream of Flush, Non-tangential Injection Holes and Slots," AIAA, 5th Propulsion Joint Specialist Conference, USAF Academy, Colorado Springs, Colo., June 1969, Paper 69-523.

32. Eriksen, V. L., "Film Cooling Effectiveness and Heat Transfer with Injection through Holes," NASA CR-72991, Aug. 1971.

33. LeBrocq, R. V., Launder, B. E., and Priddin, C. H., "Discrete Hole Injection as a Means of Transpiration Cooling -- An Experimental Study," HTS/70/37, Department of Mech. Engrg., Imperial College of Science and Technology, June 1971.

34. Launder, B. E., and York, J., "Discrete Hole Cooling in the Presence of Free Stream Turbulence and Strong Favorable Pressure Gradient," HTS/73/9, Department of Mech. Engrg., Imperial College of Science and Technology, Jan. 1973.

35. Burggraf, F., and Huffmeier, R. W., "Film Effectiveness and Heat Transfer Coefficients for Injection from One and Two Rows of Holes at 35° to the Surface," AEG-Technical Information Series Report No. R70AEG351, General Electric Co., Lynn, Mass., Cincinnati, Ohio, August, 1970.

36. Nina, M. N. R., and Whitelaw, J. H., "The Effectiveness of Film Cooling with Three-Dimensional Slot Geometry," Gas Turbine Conference and Products Show, Houston, Texas, March, 1971, ASME Paper No. 71-GT-11.

37. Ramsey, J. W., and Goldstein, R. J., "Interaction of a Heated Jet with a Deflecting Stream," NASA CR-72613, April 1970.

38. Metzger, D. E., Takeuchi, D. I., and Kuenstler, P. A., "Effectiveness and Heat Transfer with Full-Coverage Film Cooling," Trans. of ASME, J. Eng. Pwr., July 1973, pp. 180-184.

39. Stollery, J. L., and El-Ehwany, A. A. M., "A Note on the Use of a Boundary Layer Model for Correlating Film Cooling Data," Int. J. Heat Mass Transfer, Vol. 8, 1965, pp. 55-65.

40. Libbrizzi, J., and Cresci, R. J., "Transpiration Cooling of a Turbulent Boundary Layer in an Axisymmetric Nozzle," AIAA Journal, Vol. 2, 1964, pp. 617-624.

41. Kutateladze, S. S., and Leont'ev, A. I., "Film Cooling with a Turbulent Gaseous Boundary Layer," Thermal Physics at High Temperature, Vol. 1, 1963, pp. 281-290.

42. Nicoll, W. B., and Whitelaw, J. H., "The Effectiveness of the Uniform Density, Two-Dimensional Wall Jet," Int. J. Heat Mass Transfer, Vol. 10, 1967, pp. 623-639.

43. Pai, B. R., and Whitelaw, J. H., "The Prediction of Wall Temperature in the Presence of Film Cooling," Int. J. Heat Mass Transfer, Vol. 14, 1971, pp. 409-426.

44. Patankar, S. V., Rastogi, A. K., and Whitelaw, J. H., "The Effectiveness of Three-Dimensional Film-Cooling Slots -- II. Predictions," Int. J. Heat Mass Transfer, Vol. 16, pp. 1673-1681.

45. Eriksen, V. L.; Eckert, E. R. G., and Goldstein, R. G., "A Model for Analysis of the Temperature Field Downstream of a Heated Jet Injected into an Isothermal Crossflow at an Angle of 90°," NASA CR-72990, July, 1971.

46. Herring, H. J., "A Method of Predicting the Behavior of a Turbulent Boundary Layer with Discrete Transpiration Jets," ASME Paper No. 74-GT-48, 1974.

47. Mayle, R. E., and Camarata, F. J., "Multihole Cooling Film Effectiveness and Heat Transfer," AIAA/ASME 1974 Thermophysics and Heat Transfer Conference, Boston, Mass., July 15-17, 1974, AIAA Paper No. 74-675/ ASME Paper No. 74-HT-9.

48. Blair, M. F., and Lander, R. D., "New Techniques for Measuring Film Cooling Effectiveness and Heat Transfer," ASME Paper No. 74-HT-8, Presented at AIAA/ASME 1974 Thermophysics and Heat Transfer Conference, Boston, Mass., July 15-17, 1974.

49. Pedersen, D. R., "Effect of Density Ratio on Film Cooling Effectiveness for Injection through a Row of Holes and for a Porous Slot," Ph.D. Thesis, Department of Mech. Engrg., University of Minnesota, March, 1972.

50. Wilson, D. J., Eriksen, V. L., and Goldstein, R. J., "Predicting Heat Transfer Coefficients with Film Cooling from a Row of Holes," Tech. Brief, J. Heat Transfer, ASME Ser. C, Vol. 96, May 1974, pp. 258-260.

51. Goldstein, R. J., Eckert, E. R. G., and Burggraf, F., "Effects of Hole Geometry and Density on Three-Dimensional Film Cooling," Int. J. Heat Mass Transfer, Vol. 17, 1974, pp. 595-607.

52. McCuen, P., "Heat Transfer with Laminar and Turbulent Flow Between Parallel Plane with Constant and Variable Wall Temperature and Heat Flux," Ph.D. Thesis, Thermosciences Division, Mech. Engrg. Dept., Stanford Univ., 1962.

53. Morretti, P. A., "Heat Transfer through an Incompressible Turbulent Boundary Layer with Varying Free-Stream Velocity and Varying Surface Temperature," Ph.D. Thesis, Thermosciences Division, Mechanical Engineering Dept., Stanford Univ., 1965.

54. London, A. L., Klopfer, G., and Wolf, S., "Oblique Flow Headers for Heat Exchangers," ASME Trans., J. of Engr. for Power, Vol. 90, July 1968, pp. 271-286.

55. Schubauer, G. E., Spangenberg, W. G., and Klebanoff, P. S., "Aerodynamic Characteristics of Damping Screens," NACA TN 2001, Jan. 1950.

56. Rause, H., and Hassan, M. M., "Cavitation Free Inlets and Contractions," Mech. Engrg., 71, 3, 213-216, 1949.

57. Moffat, R. J., "Temperature Measurement in Solids," ISA Paper 68-514, 1968.

58. Blackwell, B. F., "The Turbulent Boundary Layer on a Porous Plate: An Experimental Study of the Heat Transfer Behavior with Adverse Pressure Gradient," Report No. HMT-16, Thermosciences Division, Mech. Engrg. Dept., Stanford Univ., 1972.

59. Healzer, J. M., "The Turbulent Boundary Layer on a Rough Porous Plate: Experimental Heat Transfer with Uniform Blowing," Report No. HMT-18, Thermosciences Division, Dept. of Mech. Engrg., Stanford Univ. 1974.

60. Reynolds, W. C., Kays, W. M., and Kline, S. J., "Heat Transfer in the Turbulent Incompressible Boundary Layer, Part I," NASA Memo 12-1-58W, 1958.

61. Kays, W. M., Computer Program STAN5, Mech. Engrg. Dept., Stanford Univ., 1974.

62. Kline, S. J., and McClintock, F. A., "Describing Uncertainties in Single Sample Experiments," Mechanical Engineering, Jan 1953.

63. Keffer, J. F., and Bains, W. D., "The Round Turbulent Jet in a Crosswind," Journal of Fluid Mechanics, Vol. 15, 1963, pp. 481-496.

64. Platten, J. L., and Keffer, J. F., "Deflected Turbulent Jet Flows," Journal of Applied Mechanics, ASME Transactions, Dec., 1971, pp. 756-758.

65. Kamotani, Y., and Greber, I., "Experiments on a Turbulent Jet in a Cross Flow," NASA CR-72893, June 1971.

66. Lee, C. C., "A Review of Research on the Interaction of a Jet with an External Stream," Brown Engrg. Co., Inc., Rep. No. 184-AD-630294, Huntsville, Ala. Res. Labs., 1966.

67. Abramovich, G. N., The Theory of Turbulent Jets, MIT Press, 1963, pp. 3-25, 195-201, 541-556.

68. Kays, W. M., Convective Heat and Mass Transfer, McGraw-Hill Book Co., 1966.

69. Millikan, C. B., "A Critical Discussion of Turbulent Flows in Channels and Circular Tubes," Proc. 5th International Congress of Applied Mechanics, Cambridge, Mass., 1938.

70. Kays, W. M., "Heat Transfer to the Transpired Turbulent Boundary Layer," Report No. HMT-14, Thermosciences Div., Dept. of Mech. Engrg., Stanford Univ., June 1971.

71. Reynolds, W. C., "Computation of Turbulent Flows -- State-of-the-Art, 1970," Report MD-27, Thermosciences Division, Dept. of Mech. Engrg., Stanford Univ., 1970.

APPENDIX A

STANTON NUMBER DATA

This is the tabulation of all the Stanton numbers along with velocity and temperature profiles which give the initial conditions at the starting point of blowing (in the middle of the 1st plate).

<u>Special Nomenclature</u>

DREEN	$\delta Re_{\overline{\Delta}_2}$, uncertainty in $Re_{\overline{\Delta}_2}$
DST	δSt , uncertainty in St
DTH	$\delta\theta$, uncertainty in θ
ETA	$1-St(\theta = 1.0)/St(\theta = 0.0)$
F-COL	F at $\theta = 0.0$
F-HOT	F at $\theta = 1.0$
PHI-1	ϕ_1 defined in Chapter V (see Equation 5.12)
RED2	$Re_{\overline{\delta}_2}$
RE DEL2	$Re_{\overline{\Delta}_2}$
REENTH	$Re_{\overline{\Delta}_2}$
REX	Re_x
REXCOL	Re_x for $\theta = 0.0$
REXHOT	Re_x for $\theta = 1.0$
STCR	$St(\theta = 0)/St_o$
STHR	$St(\theta = 1.0)/St_o$
XVO	X_{vo} , virtual origin of turbulent boundary layer

RUN NUMBER 062873 FLAT PLATE VELOCITY PROFILE

DISCRETE HOLE RIG *** NAS-3-14336

VELOCITY PROFILE

UINF= 55.1 FT/SEC X= 53.0 INCHES PORT= 19
TINF= 70.9 DEG F PINF= 2100. PSF

Y(INCHES)	U(FT/SEC)	Y+	U+	UBAR	DU
0.010	23.72	11.4	10.49	0.4302	0.19
0.012	25.08	13.7	11.09	0.4549	0.18
0.014	26.46	16.0	11.70	0.4799	0.17
0.016	27.58	18.3	12.20	0.5002	0.16
0.018	28.50	20.6	12.60	0.5169	0.16
0.020	29.18	22.9	12.91	0.5292	0.16
0.022	29.87	25.1	13.21	0.5418	0.15
0.024	30.38	27.4	13.43	0.5509	0.15
0.026	30.85	29.7	13.64	0.5594	0.15
0.028	31.24	32.0	13.81	0.5665	0.15
0.031	31.74	35.4	14.04	0.5756	0.14
0.034	32.24	38.9	14.26	0.5846	0.14
0.038	32.89	43.4	14.54	0.5964	0.14
0.044	33.55	50.3	14.84	0.6084	0.14
0.049	33.95	56.0	15.01	0.6157	0.13
0.056	34.61	64.0	15.31	0.6277	0.13
0.063	35.26	72.0	15.59	0.6395	0.13
0.073	35.77	83.4	15.82	0.6488	0.13
0.083	36.44	94.9	16.12	0.6609	0.12
0.094	37.00	107.4	16.36	0.6710	0.12
0.114	37.91	130.3	16.76	0.6875	0.12
0.139	39.24	158.9	17.35	0.7117	0.12
0.164	40.19	187.4	17.78	0.7289	0.11
0.189	41.05	216.0	18.15	0.7445	0.11
0.239	42.64	273.2	18.86	0.7733	0.11
0.289	44.21	330.3	19.55	0.8017	0.10
0.339	45.52	387.5	20.13	0.8256	0.10
0.389	46.80	444.6	20.70	0.8488	0.10
0.439	48.04	501.7	21.25	0.8713	0.09
0.489	49.24	558.9	21.78	0.8930	0.09
0.589	51.18	673.2	22.64	0.9283	0.09
0.689	52.96	787.5	23.42	0.9604	0.09
0.789	54.07	901.8	23.91	0.9807	0.08
0.889	54.80	1016.1	24.23	0.9938	0.08
1.039	55.17	1187.5	24.40	1.0005	0.08
1.189	55.14	1358.9	24.39	1.0000	0.08

REX= 0.12701E 07 RED2= 2827. XVO= 7.43 IN.
DEL1= 0.136 IN. DEL2= 0.101IN. H= 1.34
CF2= 0.16817E-02 DXVO= 0.67 DDEL1=0.002 DDEL2=0.001 DCF/2=0.130 IN RATIO

STANTON NUMBER DATA RUN 070473 *** DISCRETE HOLE RIG *** NAS-3-14336

TINF= 83.3 UINF= 53.9 XVO= 4.600 RHO= 0.07231 CP= 0.242 VISC= 0.17101E-03 PR=0.715
DISTANCE FROM ORIGIN OF BL TO 1ST PLATE=44.700 P/D= 5
UNCERTAINTY IN REX=26262.

** M=0., FLAT PLATE RUN, HIGH RE, STEP T-WALL AT THE 1ST PLATE

PLATE	X	REX	TO	REENTH	STANTON NO	DST	DREEN	M	F	T2	THETA	DTH
1	50.30	0.12002E 07	107.2	0.98007E 02	0.37319E-02	0.667E-04	2.					
2	52.30	0.12527E 07	107.5	0.27787E 03	0.31169E-02	0.619E-04	3.	0.00	0.0000	107.5	1.000	0.015
3	54.30	0.13052E 07	107.3	0.43599E 03	0.29041E-02	0.610E-04	4.	0.00	0.0000	107.3	1.000	0.015
4	56.30	0.13577E 07	107.3	0.58507E 03	0.27726E-02	0.604E-04	5.	0.00	0.0000	107.3	1.000	0.015
5	58.30	0.14103E 07	107.3	0.72797E 03	0.26684E-02	0.598E-04	5.	0.00	0.0000	107.3	1.000	0.015
6	60.30	0.14628E 07	107.5	0.86638E 03	0.26023E-02	0.589E-04	6.	0.00	0.0000	107.5	1.000	0.015
7	62.30	0.15153E 07	107.3	0.10010E 04	0.25218E-02	0.589E-04	6.	0.00	0.0000	107.3	1.000	0.015
8	64.30	0.15678E 07	107.4	0.11312E 04	0.24381E-02	0.584E-04	6.	0.00	0.0000	107.4	1.000	0.015
9	66.30	0.16204E 07	107.3	0.12587E 04	0.24179E-02	0.584E-04	7.	0.00	0.0000	107.3	1.000	0.015
10	68.30	0.16729E 07	107.3	0.13847E 04	0.23779E-02	0.583E-04	7.	0.00	0.0000	107.3	1.000	0.015
11	70.30	0.17254E 07	107.2	0.15082E 04	0.23267E-02	0.581E-04	7.	0.00	0.0000	107.2	1.000	0.015
12	72.30	0.17779E 07	107.6	0.16294E 04	0.22865E-02	0.571E-04	8.	0.00	0.0000	107.6	1.000	0.015
13	73.82	0.18178E 07	107.1	0.17208E 04	0.23159E-02	0.403E-04	8.					
14	74.85	0.18449E 07	106.8	0.17818E 04	0.21927E-02	0.417E-04	8.					
15	75.88	0.18719E 07	107.3	0.18416E 04	0.22168E-02	0.422E-04	8.					
16	76.91	0.18991E 07	107.3	0.19012F 04	0.21859E-02	0.414E-04	8.					
17	77.95	0.19263E 07	107.5	0.19600E 04	0.21574E-02	0.412E-04	8.					
18	78.98	0.19534E 07	107.4	0.20187E 04	0.21819E-02	0.416E-04	8.					
19	80.01	0.19804E 07	107.3	0.20775E 04	0.21563E-02	0.404E-04	8.					
20	81.04	0.20075E 07	107.5	0.21347E 04	0.20724E-02	0.391E-04	8.					
21	82.07	0.20345E 07	107.4	0.21929E 04	0.22212E-02	0.415E-04	8.					
22	83.10	0.20616E 07	107.5	0.22513E 04	0.20946E-02	0.408E-04	8.					
23	84.13	0.20886E 07	107.3	0.23074E 04	0.20498E-02	0.402E-04	8.					
24	85.16	0.21158E 07	107.4	0.23637E 04	0.21048E-02	0.417E-04	8.					
25	86.20	0.21430E 07	106.7	0.24192E 04	0.19909E-02	0.403E-04	8.					
26	87.23	0.21700E 07	106.5	0.24749E 04	0.21226E-02	0.420E-04	9.					
27	88.26	0.21971E 07	107.4	0.25319E 04	0.20928E-02	0.412E-04	9.					
28	89.29	0.22241E 07	107.6	0.25878E 04	0.20300E-02	0.400E-04	9.					
29	90.32	0.22512E 07	107.1	0.26432E 04	0.20636E-02	0.400E-04	9.					
30	91.35	0.22782E 07	107.9	0.26983E 04	0.20082E-02	0.402E-04	9.					
31	92.38	0.23053E 07	107.8	0.27535E 04	0.20668E-02	0.402E-04	9.					
32	93.41	0.23324E 07	107.6	0.28076E 04	0.19289E-02	0.390E-04	9.					
33	94.45	0.23596E 07	107.5	0.28605E 04	0.19762E-02	0.393E-04	9.					
34	95.48	0.23867E 07	106.8	0.29143E 04	0.19957E-02	0.393E-04	9.					
35	96.51	0.24137E 07	107.3	0.29686E 04	0.20138E-02	0.416E-04	9.					
36	97.54	0.24408E 07	106.7	0.30233E 04	0.20286E-02	0.455E-04	9.					

STANTON NUMBER DATA RUN 073073 *** DISCRETE HOLE RIG *** NAS-3-14336

TINF= 79.8 UINF= 53.3 XVO= 4.600 RHO= 0.07296 CP= 0.242 VISC= 0.16869E-03 PR=0.715
DISTANCE FROM ORIGIN OF BL TO 1ST PLATE=44.700 P/D= 5
UNCERTAINTY IN REX=26336. UNCERTAINTY IN F=0.03027 IN RATIO

** M=0.1, COLD RUN, HIGH RE, STEP T-WALL AT 1ST PLATE.

PLATE	X	REX	TO	REENTH	STANTON NO	DST	DREEN	M	F	T2	THETA	DTH
1	50.30	0.12035E 07	103.5	0.10459E 03	0.39714E-02	0.692E-04	2.					
2	52.30	0.12562E 07	103.5	0.31052E 03	0.33502E-02	0.648E-04	3.	0.10	0.0033	83.4	0.152	0.011
3	54.30	0.13089E 07	103.5	0.51165E 03	0.32989E-02	0.645E-04	4.	0.09	0.0029	83.8	0.169	0.011
4	56.30	0.13616E 07	103.5	0.70897E 03	0.31598E-02	0.635E-04	5.	0.10	0.0033	83.7	0.163	0.011
5	58.30	0.14142E 07	103.5	0.89973E 03	0.30206E-02	0.627E-04	6.	0.09	0.0030	84.0	0.174	0.011
6	60.30	0.14669E 07	103.6	0.10849E 04	0.29460E-02	0.621E-04	7.	0.10	0.0033	83.7	0.163	0.011
7	62.30	0.15196E 07	103.6	0.12658E 04	0.28552E-02	0.615E-04	7.	0.09	0.0028	84.2	0.186	0.011
8	64.30	0.15722E 07	103.6	0.14420E 04	0.27563E-02	0.610E-04	8.	0.10	0.0031	84.0	0.178	0.011
9	66.30	0.16249E 07	103.6	0.16159E 04	0.27358E-02	0.609E-04	8.	0.09	0.0030	84.3	0.187	0.011
10	68.30	0.16776E 07	103.6	0.17899E 04	0.27316E-02	0.609E-04	8.	0.10	0.0033	84.0	0.177	0.011
11	70.30	0.17303E 07	103.5	0.19616E 04	0.26369E-02	0.606E-04	9.	0.09	0.0030	84.3	0.190	0.011
12	72.30	0.17829E 07	103.5	0.21305E 04	0.25764E-02	0.601E-04	9.	0.10	0.0033	84.3	0.191	0.011
13	73.82	0.18230E 07	103.1	0.22487E 04	0.24726E-02	0.429E-04	10.					
14	74.85	0.18501E 07	102.9	0.23139E 04	0.23230E-02	0.438E-04	10.					
15	75.88	0.18772E 07	103.6	0.23759E 04	0.22435E-02	0.429E-04	10.					
16	76.91	0.19045E 07	103.8	0.24357E 04	0.21642E-02	0.413E-04	10.					
17	77.95	0.19317E 07	104.0	0.24933E 04	0.20767E-02	0.404E-04	10.					
18	78.98	0.19588E 07	103.5	0.25517E 04	0.22232E-02	0.424E-04	10.					
19	80.01	0.19860E 07	103.8	0.26103E 04	0.20886E-02	0.398E-04	10.					
20	81.04	0.20131E 07	104.1	0.26661E 04	0.20262E-02	0.386E-04	10.					
21	82.07	0.20402E 07	103.8	0.27228E 04	0.21499E-02	0.406E-04	10.					
22	83.10	0.20673E 07	104.0	0.27797E 04	0.20402E-02	0.402E-04	10.					
23	84.13	0.20945E 07	103.7	0.28346E 04	0.19975E-02	0.398E-04	10.					
24	85.16	0.21217E 07	103.7	0.28895E 04	0.20511E-02	0.417E-04	10.					
25	86.20	0.21490E 07	102.4	0.29432E 04	0.18984E-02	0.400E-04	10.					
26	87.23	0.21761E 07	102.9	0.29975E 04	0.21020E-02	0.422E-04	10.					
27	88.26	0.22032E 07	103.7	0.30542E 04	0.20733E-02	0.412E-04	10.					
28	89.29	0.22304E 07	104.0	0.31095E 04	0.20028E-02	0.399E-04	10.					
29	90.32	0.22575E 07	103.5	0.31660E 04	0.21560E-02	0.413E-04	10.					
30	91.35	0.22846E 07	104.4	0.32220E 04	0.19668E-02	0.399E-04	10.					
31	92.38	0.23117E 07	104.2	0.32761E 04	0.20183E-02	0.398E-04	10.					
32	93.41	0.23390E 07	104.0	0.33294E 04	0.19060E-02	0.389E-04	10.					
33	94.45	0.23663E 07	103.9	0.33815E 04	0.19312E-02	0.390E-04	10.					
34	95.48	0.23934E 07	103.1	0.34341E 04	0.19441E-02	0.390E-04	10.					
35	96.51	0.24205E 07	103.6	0.34873E 04	0.19698E-02	0.413E-04	10.					
36	97.54	0.24476E 07	103.1	0.35402E 04	0.19242E-02	0.448E-04	10.					

STANTON NUMBER DATA RUN 070573 *** DISCRETE HOLE RIG *** NAS-3-14336

TINF= 84.1 UINF= 53.2 XVO= 4.600 RHO= 0.07218 CP= 0.242 VISC= 0.17163E-03 PR=0.714
DISTANCE FROM ORIGIN OF BL TO 1ST PLATE=44.700 P/D= 5
UNCERTAINTY IN REX=25812. UNCERTAINTY IN F=0.03028 IN RATIO

** M=0.1, HOT RUN, HIGH RE, STEP T-WALL AT 1ST PLATE.

PLATE	X	REX	TO	REENTH	STANTON NO	DST	DREEN	M	F	T2	THETA	DTH
1	50.30	0.11796E 07	108.8	0.95738E 02	0.37091E-02	0.652E-04	2.					
2	52.30	0.12312E 07	109.0	0.32633E 03	0.29765E-02	0.602E-04	4.	0.10	0.0032	101.4	0.695	0.012
3	54.30	0.12829E 07	108.9	0.58545E 03	0.28329E-02	0.596E-04	5.	0.09	0.0028	101.9	0.716	0.012
4	56.30	0.13345E 07	109.0	0.83782E 03	0.26686E-02	0.585E-04	6.	0.10	0.0032	101.9	0.717	0.012
5	58.30	0.13861E 07	108.9	0.10891E 04	0.25133E-02	0.579E-04	7.	0.10	0.0031	102.1	0.727	0.012
6	60.30	0.14377E 07	109.1	0.13352E 04	0.24249E-02	0.570E-04	8.	0.10	0.0034	101.4	0.691	0.012
7	62.30	0.14894E 07	109.0	0.15676E 04	0.23496E-02	0.568E-04	9.	0.08	0.0026	102.5	0.740	0.012
8	64.30	0.15410E 07	109.0	0.17944E 04	0.22117E-02	0.562E-04	9.	0.10	0.0031	102.8	0.750	0.013
9	66.30	0.15926E 07	109.1	0.20210E 04	0.21576E-02	0.558E-04	10.	0.09	0.0028	102.9	0.752	0.013
10	68.30	0.16442E 07	109.0	0.22472E 04	0.21158E-02	0.557E-04	11.	0.10	0.0031	103.4	0.774	0.013
11	70.30	0.16959E 07	109.1	0.24745E 04	0.20422E-02	0.553E-04	11.	0.08	0.0027	104.5	0.816	0.013
12	72.30	0.17475E 07	109.4	0.27034E 04	0.19235E-02	0.542E-04	12.	0.10	0.0031	105.6	0.852	0.013
13	73.82	0.17867E 07	108.4	0.28491E 04	0.20557E-02	0.364E-04	12.					
14	74.85	0.18133E 07	108.1	0.29022E 04	0.19340E-02	0.382E-04	12.					
15	75.88	0.18399E 07	108.8	0.29532E 04	0.18950E-02	0.381E-04	12.					
16	76.91	0.18666E 07	108.6	0.30039E 04	0.19174E-02	0.380E-04	12.					
17	77.95	0.18933E 07	108.8	0.30545E 04	0.18830E-02	0.376E-04	12.					
18	78.98	0.19199E 07	108.8	0.31046E 04	0.18801E-02	0.378E-04	12.					
19	80.01	0.19465E 07	108.7	0.31547E 04	0.18878E-02	0.369E-04	12.					
20	81.04	0.19731E 07	108.8	0.32044E 04	0.18482E-02	0.362E-04	12.					
21	82.07	0.19997E 07	108.7	0.32549E 04	0.19455E-02	0.379E-04	12.					
22	83.10	0.20262E 07	108.7	0.33058E 04	0.18782E-02	0.380E-04	12.					
23	84.13	0.20528E 07	108.7	0.33549E 04	0.18125E-02	0.373E-04	12.					
24	85.16	0.20795E 07	108.8	0.34038E 04	0.18608E-02	0.387E-04	12.					
25	86.20	0.21063E 07	108.0	0.34524E 04	0.17905E-02	0.378E-04	12.					
26	87.23	0.21329E 07	107.6	0.35020E 04	0.19317E-02	0.397E-04	12.					
27	88.26	0.21594E 07	108.7	0.35525E 04	0.18628E-02	0.385E-04	12.					
28	89.29	0.21860E 07	109.0	0.36016E 04	0.18297E-02	0.375E-04	13.					
29	90.32	0.22126E 07	108.5	0.36508E 04	0.18670E-02	0.375E-04	13.					
30	91.35	0.22392E 07	109.0	0.37004E 04	0.18601E-02	0.383E-04	13.					
31	92.38	0.22658E 07	109.0	0.37501E 04	0.18746E-02	0.380E-04	13.					
32	93.41	0.22925E 07	108.7	0.37990E 04	0.18008E-02	0.375E-04	13.					
33	94.45	0.23192E 07	108.7	0.38471E 04	0.18124E-02	0.374E-04	13.					
34	95.48	0.23458E 07	108.0	0.38955E 04	0.18245E-02	0.372E-04	13.					
35	96.51	0.23724E 07	108.4	0.39445E 04	0.18572E-02	0.397E-04	13.					
36	97.54	0.23990E 07	107.9	0.39939E 04	0.18520E-02	0.430E-04	13.					

FOLLOWING IS THE DATA FOR THETA=0 AND THETA=1, WHICH WAS OBTAINED BY LINEAR SUPERPOSITION THEORY.
THIS DATA WAS PRODUCED FROM RUN 073073 AND RUN 070573
FOR THE DETAIL CHANGES OF PROPERTIES AND BOUNDARY CONDITIONS, PLEASE SEE THE ABOVE TWO RUNS

PLATE	REXCOL	RE DEL2	ST(TH=0)	REXHOT	RE DEL2	ST(TH=1)	ETA	STCR	F-COL	STHR	F-HOT	PHI-1
1	1203538.0	104.6	0.003971	1179611.0	95.7	0.003709	UUUUU	UUUUU	0.0000	UUUUUUU	0.0000	UUUUU
2	1256209.0	300.2	0.003454	1231235.0	346.4	0.002767	0.199	0.898	0.0033	0.985	0.0032	1.487
3	1308880.0	481.8	0.003443	1282859.0	639.6	0.002591	0.248	1.002	0.0029	0.980	0.0028	1.440
4	1361552.0	659.5	0.003305	1334483.0	922.9	0.002418	0.268	1.036	0.0033	0.953	0.0032	1.496
5	1414223.0	830.3	0.003181	1386107.0	1206.5	0.002263	0.289	1.053	0.0030	0.920	0.0031	1.462
6	1466894.0	995.9	0.003107	1437732.0	1487.0	0.002121	0.317	1.075	0.0033	0.885	0.0034	1.479
7	1519565.0	1157.4	0.003025	1489356.0	1749.6	0.002112	0.302	1.086	0.0028	0.901	0.0026	1.376
8	1572237.0	1314.1	0.002926	1540980.0	2001.4	0.001974	0.325	1.084	0.0031	0.858	0.0031	1.428
9	1624908.0	1468.2	0.002928	1592604.0	2253.0	0.001904	0.350	1.115	0.0030	0.842	0.0028	1.363
10	1677579.0	1622.1	0.002914	1644228.0	2502.5	0.001882	0.354	1.137	0.0033	0.845	0.0031	1.432
11	1730250.0	1773.0	0.002817	1695852.0	2750.5	0.001868	0.337	1.124	0.0030	0.850	0.0027	1.383
12	1782922.0	1920.0	0.002765	1747476.0	2996.1	0.001778	0.357	1.125	0.0033	0.820	0.0031	1.420
13	1822952.0	2028.2	0.002600	1786711.0	3147.4	0.001872	0.280	1.073		0.872		
14	1850078.0	2096.6	0.002442	1813297.0	3195.8	0.001763	0.278	1.017		0.826		
15	1877203.0	2161.7	0.002350	1839884.0	3242.5	0.001742	0.259	0.987		0.820		
16	1904460.0	2224.0	0.002240	1866599.0	3289.7	0.001809	0.192	0.948		0.857		
17	1931718.0	2283.5	0.002136	1893314.0	3337.7	0.001798	0.158	0.912		0.856		
18	1958844.0	2344.1	0.002328	1919901.0	3384.7	0.001729	0.257	1.001		0.828		
19	1985969.0	2404.9	0.002150	1946487.0	3431.6	0.001800	0.163	0.932		0.866		
20	2013095.0	2462.3	0.002081	1973074.0	3479.2	0.001770	0.149	0.908		0.856		
21	2040221.0	2520.6	0.002212	1999660.0	3527.4	0.001856	0.161	0.972		0.902		
22	2067347.0	2579.1	0.002090	2026247.0	3576.2	0.001807	0.135	0.924		0.882		
23	2094472.0	2635.3	0.002054	2052833.0	3623.2	0.001731	0.157	0.915		0.849		
24	2121729.0	2691.9	0.002109	2079548.0	3669.9	0.001777	0.157	0.945		0.875		
25	2148987.0	2746.7	0.001932	2106264.0	3716.8	0.001743	0.098	0.871		0.862		
26	2176113.0	2802.2	0.002154	2132850.0	3764.7	0.001857	0.138	0.977		0.922		
27	2203238.0	2860.5	0.002138	2159437.0	3813.0	0.001770	0.172	0.975		0.883		
28	2230364.0	2917.5	0.002056	2186023.0	3859.9	0.001754	0.147	0.943		0.878		
29	2257490.0	2975.9	0.002245	2212610.0	3906.4	0.001740	0.225	1.035		0.875		
30	2284616.0	3033.5	0.001999	2239196.0	3953.7	0.001813	0.093	0.927		0.915		
31	2311741.0	3088.6	0.002062	2265783.0	4001.9	0.001811	0.122	0.961		0.918		
32	2338998.0	3143.0	0.001938	2292498.0	4049.4	0.001755	0.095	0.908		0.892		
33	2366256.0	3196.0	0.001968	2319213.0	4096.1	0.001760	0.105	0.927		0.899		
34	2393382.0	3249.6	0.001981	2345800.0	4143.1	0.001772	0.105	0.937		0.908		
35	2420507.0	3303.7	0.002004	2372386.0	4190.8	0.001808	0.098	0.953		0.929		
36	2447633.0	3357.4	0.001946	2398973.0	4239.1	0.001820	0.065	0.930		0.939		

STANTON NUMBER DATA RUN 072973 *** DISCRETE HOLE RIG *** NAS-3-14336

TINF= 77.7 UINF= 53.2 XVO= 4.600 RHO= 0.07321 CP= 0.242 VISC= 0.16767E-03 PR=0.715
DISTANCE FROM ORIGIN OF BL TO 1ST PLATE=44.700 P/D= 5
UNCERTAINTY IN REX=26451. UNCERTAINTY IN F=0.03027 IN RATIO

** M=0.2, COLD RUN, HIGH RE, STEP T-WALL AT 1ST PLATE.

PLATE	X	REX	TO	REENTH	STANTON NO	DST	DREEN	M	F	T2	THETA	DTH
1	50.30	0.12088E 07	100.6	0.10533E 03	0.39819E-02	0.716E-04	2.					
2	52.30	0.12617E 07	100.6	0.32113E 03	0.35832E-02	0.686E-04	4.	0.20	0.0066	79.8	0.090	0.011
3	54.30	0.13146E 07	100.6	0.54358E 03	0.36436E-02	0.691E-04	5.	0.21	0.0067	79.7	0.088	0.011
4	56.30	0.13675E 07	100.6	0.76611E 03	0.35372E-02	0.682E-04	7.	0.20	0.0065	80.0	0.098	0.011
5	58.30	0.14204E 07	100.6	0.98322E 03	0.33879E-02	0.673E-04	8.	0.21	0.0067	79.9	0.096	0.011
6	60.30	0.14733E 07	100.6	0.11934E 04	0.32861E-02	0.664E-04	9.	0.20	0.0065	79.9	0.096	0.011
7	62.30	0.15262E 07	100.6	0.13989E 04	0.31704E-02	0.657E-04	9.	0.21	0.0067	80.1	0.102	0.011
8	64.30	0.15791E 07	100.6	0.16013E 04	0.30941E-02	0.652E-04	10.	0.20	0.0066	80.2	0.107	0.011
9	66.30	0.16320E 07	100.7	0.18002E 04	0.30467E-02	0.648E-04	11.	0.20	0.0066	80.1	0.103	0.011
10	68.30	0.16850E 07	100.6	0.19973E 04	0.30372E-02	0.650E-04	11.	0.20	0.0066	80.1	0.104	0.011
11	70.30	0.17379E 07	100.6	0.21929E 04	0.30051E-02	0.647E-04	12.	0.20	0.0066	80.0	0.101	0.011
12	72.30	0.17908E 07	100.7	0.23864E 04	0.29064E-02	0.638E-04	13.	0.20	0.0066	80.3	0.112	0.011
13	73.82	0.18310E 07	99.9	0.25196E 04	0.26925E-02	0.470E-04	13.					
14	74.85	0.18582E 07	99.7	0.25904E 04	0.24939E-02	0.473E-04	13.					
15	75.88	0.18855E 07	100.6	0.26565E 04	0.23569E-02	0.454E-04	13.					
16	76.91	0.19128E 07	100.8	0.27192E 04	0.22362E-02	0.432E-04	13.					
17	77.95	0.19402E 07	101.1	0.27787E 04	0.21285E-02	0.419E-04	13.					
18	78.98	0.19675E 07	100.7	0.28384E 04	0.22458E-02	0.435E-04	13.					
19	80.01	0.19947E 07	101.0	0.28976E 04	0.20953E-02	0.406E-04	13.					
20	81.04	0.20219E 07	101.3	0.29537E 04	0.20216E-02	0.392E-04	13.					
21	82.07	0.20492E 07	101.0	0.30104E 04	0.21312E-02	0.411E-04	13.					
22	83.10	0.20764E 07	101.2	0.30671E 04	0.20287E-02	0.408E-04	13.					
23	84.13	0.21037E 07	101.0	0.31217E 04	0.19765E-02	0.402E-04	13.					
24	85.16	0.21311E 07	101.0	0.31763E 04	0.20241E-02	0.421E-04	13.					
25	86.20	0.21584E 07	99.6	0.32302E 04	0.19288E-02	0.411E-04	13.					
26	87.23	0.21857E 07	100.2	0.32854E 04	0.21156E-02	0.431E-04	13.					
27	88.26	0.22129E 07	100.9	0.33420E 04	0.20336E-02	0.414E-04	13.					
28	89.29	0.22402E 07	101.2	0.33968E 04	0.19906E-02	0.404E-04	13.					
29	90.32	0.22674E 07	100.7	0.34533E 04	0.21466E-02	0.419E-04	13.					
30	91.35	0.22947E 07	101.5	0.35095E 04	0.19731E-02	0.406E-04	13.					
31	92.38	0.23219E 07	101.4	0.35637E 04	0.20016E-02	0.403E-04	13.					
32	93.41	0.23493E 07	101.1	0.36170E 04	0.19060E-02	0.397E-04	14.					
33	94.45	0.23767E 07	101.0	0.36695E 04	0.19482E-02	0.399E-04	14.					
34	95.48	0.24039E 07	100.3	0.37226E 04	0.19411E-02	0.397E-04	14.					
35	96.51	0.24311E 07	100.8	0.37758E 04	0.19626E-02	0.420E-04	14.					
36	97.54	0.24584E 07	100.2	0.38291E 04	0.19459E-02	0.460E-04	14.					

STANTON NUMBER DATA RUN 070873 *** DISCRETE HOLE RIG *** NAS-3-14336

TINF= 81.5 UINF= 52.5 XVO= 4.600 RHO= 0.07272 CP= 0.242 VISC= 0.16982E-03 PR=0.714
DISTANCE FROM ORIGIN OF BL TO 1ST PLATE=44.700 P/D= 5
UNCERTAINTY IN REX=25777. UNCERTAINTY IN F=0.03029 IN RATIO

** M=0.2, HOT RUN, HIGH RE, STEP T-WALL AT 1ST PLATE.

PLATE	X	REX	TO	REENTH	STANTON NO	DST	DREEN	M	F	T2	THETA	DTH
1	50.30	0.11780E 07	106.2	0.97551E 02	0.37844E-02	0.662E-04	2.					
2	52.30	0.12296E 07	106.2	0.46963E 03	0.28529E-02	0.601E-04	7.	0.23	0.0074	107.6	1.053	0.015
3	54.30	0.12811E 07	106.2	0.10035E 04	0.26727E-02	0.591E-04	12.	0.21	0.0070	107.8	1.061	0.015
4	56.30	0.13327E 07	106.3	0.15065E 04	0.24589E-02	0.579E-04	15.	0.21	0.0067	107.5	1.050	0.015
5	58.30	0.13842E 07	106.3	0.19748E 04	0.22755E-02	0.570E-04	17.	0.18	0.0060	108.2	1.077	0.015
6	60.30	0.14358E 07	106.2	0.24382E 04	0.21128E-02	0.564E-04	19.	0.21	0.0069	107.2	1.037	0.015
7	62.30	0.14873E 07	106.3	0.28897E 04	0.20358E-02	0.558E-04	21.	0.18	0.0058	108.1	1.070	0.015
8	64.30	0.15389E 07	106.2	0.33210E 04	0.18799E-02	0.554E-04	23.	0.19	0.0060	108.6	1.097	0.015
9	66.30	0.15905E 07	106.2	0.37511E 04	0.17950E-02	0.551E-04	24.	0.18	0.0059	108.2	1.079	0.015
10	68.30	0.16420E 07	106.3	0.41878E 04	0.17717E-02	0.549E-04	26.	0.20	0.0065	108.1	1.073	0.015
11	70.30	0.16936E 07	106.0	0.46207E 04	0.16633E-02	0.551E-04	27.	0.18	0.0059	108.1	1.084	0.015
12	72.30	0.17451E 07	106.1	0.50515E 04	0.15575E-02	0.545E-04	28.	0.19	0.0063	109.2	1.126	0.015
13	73.82	0.17843E 07	105.7	0.52980E 04	0.17524E-02	0.329E-04	29.					
14	74.85	0.18108E 07	105.5	0.53435E 04	0.16696E-02	0.353E-04	29.					
15	75.88	0.18374E 07	106.1	0.53872E 04	0.16197E-02	0.351E-04	29.					
16	76.91	0.18641E 07	106.0	0.54304E 04	0.16338E-02	0.348E-04	29.					
17	77.95	0.18908E 07	106.3	0.54732E 04	0.15860E-02	0.344E-04	29.					
18	78.98	0.19173E 07	106.3	0.55152E 04	0.15735E-02	0.344E-04	29.					
19	80.01	0.19439E 07	106.1	0.55574E 04	0.16044E-02	0.337E-04	29.					
20	81.04	0.19704E 07	106.2	0.55996E 04	0.15673E-02	0.330E-04	29.					
21	82.07	0.19970E 07	106.2	0.56421E 04	0.16322E-02	0.344E-04	29.					
22	83.10	0.20235E 07	106.2	0.56852E 04	0.16055E-02	0.350E-04	29.					
23	84.13	0.20501E 07	106.1	0.57271E 04	0.15520E-02	0.344E-04	29.					
24	85.16	0.20767E 07	106.4	0.57687E 04	0.15765E-02	0.354E-04	29.					
25	86.20	0.21034E 07	105.7	0.58100E 04	0.15285E-02	0.348E-04	29.					
26	87.23	0.21300E 07	105.3	0.58512E 04	0.15760E-02	0.356E-04	29.					
27	88.26	0.21565E 07	106.2	0.58932E 04	0.15847E-02	0.353E-04	29.					
28	89.29	0.21831E 07	106.3	0.59355E 04	0.15958E-02	0.349E-04	29.					
29	90.32	0.22096E 07	105.9	0.59785E 04	0.16361E-02	0.350E-04	29.					
30	91.35	0.22362E 07	106.3	0.60222E 04	0.16534E-02	0.361E-04	29.					
31	92.38	0.22627E 07	106.4	0.60656E 04	0.16144E-02	0.354E-04	29.					
32	93.41	0.22894E 07	105.8	0.61084E 04	0.16074E-02	0.357E-04	29.					
33	94.45	0.23161E 07	106.0	0.61510E 04	0.15940E-02	0.352E-04	29.					
34	95.48	0.23426E 07	105.4	0.61934E 04	0.15929E-02	0.348E-04	29.					
35	96.51	0.23692E 07	105.7	0.62363E 04	0.16381E-02	0.375E-04	29.					
36	97.54	0.23957E 07	105.2	0.62799E 04	0.16413E-02	0.404E-04	29.					

FOLLOWING IS THE DATA FOR THETA=0 AND THETA=1, WHICH WAS OBTAINED BY LINEAR SUPERPOSITION THEORY.
THIS DATA WAS PRODUCED FROM RUN 072973 AND RUN 070873
FOR THE DETAIL CHANGES OF PROPERTIES AND BOUNDARY CONDITIONS, PLEASE SEE THE ABOVE TWO RUNS

PLATE	REXCOL	RE DEL2	ST(TH=0)	REXHOT	RE DEL2	ST(TH=1)	ETA	STCR	F-COL	STHR	F-HOT	PHI-1
1	1208827.0	105.3	0.003982	1178016.0	97.6	0.003784	UUUUU	UUUUU	0.0000	UUUUUUU	0.0000	UUUUU
2	1261729.0	307.2	0.003651	1229571.0	460.5	0.002893	0.208	0.950	0.0066	1.029	0.0074	2.075
3	1314632.0	502.5	0.003732	1281125.0	975.9	0.002734	0.267	1.087	0.0067	1.033	0.0070	2.079
4	1367535.0	697.7	0.003648	1332679.0	1462.4	0.002516	0.310	1.144	0.0065	0.991	0.0067	2.027
5	1420437.0	886.7	0.003497	1384234.0	1913.9	0.002363	0.324	1.159	0.0067	0.961	0.0060	1.927
6	1473340.0	1069.3	0.003406	1435788.0	2362.3	0.002159	0.366	1.180	0.0065	0.901	0.0059	2.006
7	1526243.0	1246.5	0.003291	1487342.0	2799.9	0.002118	0.356	1.183	0.0067	0.903	0.0058	1.877
8	1579146.0	1418.8	0.003225	1538897.0	3210.9	0.001999	0.380	1.196	0.0066	0.869	0.0060	1.883
9	1632048.0	1588.2	0.003179	1590451.0	3619.6	0.001896	0.403	1.212	0.0066	0.838	0.0059	1.851
10	1684951.0	1756.3	0.003173	1642006.0	4037.0	0.001868	0.411	1.239	0.0066	0.838	0.0065	1.944
11	1737854.0	1923.3	0.003143	1693560.0	4450.3	0.001777	0.434	1.255	0.0066	0.809	0.0059	1.836
12	1790756.0	2087.3	0.003056	1745114.0	4855.1	0.001726	0.435	1.244	0.0066	0.796	0.0063	1.891
13	1830963.0	2206.1	0.002789	1784296.0	5086.3	0.001823	0.346	1.152		0.849		
14	1858207.0	2279.4	0.002578	1810846.0	5133.6	0.001732	0.328	1.074		0.811		
15	1885452.0	2347.7	0.002433	1837397.0	5178.9	0.001675	0.311	1.022		0.789		
16	1912829.0	2412.2	0.002298	1864076.0	5223.5	0.001679	0.269	0.974		0.795		
17	1940206.0	2473.3	0.002184	1890755.0	5267.4	0.001627	0.255	0.933		0.775		
18	1967451.0	2534.7	0.002315	1917306.0	5310.6	0.001624	0.298	0.996		0.777		
19	1994696.0	2595.5	0.002146	1943856.0	5354.0	0.001641	0.235	0.930		0.790		
20	2021941.0	2653.0	0.002068	1970406.0	5397.1	0.001602	0.226	0.903		0.774		
21	2049186.0	2711.0	0.002182	1996957.0	5440.6	0.001670	0.235	0.960		0.811		
22	2076431.0	2769.0	0.002072	2023508.0	5484.6	0.001637	0.210	0.917		0.799		
23	2103676.0	2824.8	0.002020	2050058.0	5527.4	0.001584	0.216	0.900		0.777		
24	2131053.0	2880.6	0.002070	2076737.0	5569.8	0.001610	0.222	0.928		0.793		
25	2158430.0	2935.7	0.001970	2103417.0	5612.0	0.001559	0.209	0.889		0.771		
26	2185675.0	2992.2	0.002171	2129967.0	5654.2	0.001617	0.255	0.985		0.803		
27	2212920.0	3050.2	0.002080	2156518.0	5697.2	0.001619	0.222	0.949		0.807		
28	2240165.0	3106.2	0.002031	2183068.0	5740.3	0.001626	0.200	0.933		0.814		
29	2267410.0	3163.9	0.002199	2209619.0	5784.1	0.001675	0.238	1.015		0.842		
30	2294655.0	3221.3	0.002006	2236169.0	5828.7	0.001678	0.164	0.931		0.847		
31	2321900.0	3276.5	0.002041	2262720.0	5872.8	0.001644	0.195	0.952		0.833		
32	2349277.0	3330.7	0.001937	2289399.0	5916.4	0.001630	0.158	0.908		0.829		
33	2376654.0	3384.2	0.001985	2316079.0	5959.6	0.001621	0.183	0.935		0.827		
34	2403899.0	3438.2	0.001977	2342629.0	6002.6	0.001619	0.181	0.936		0.829		
35	2431144.0	3492.4	0.001996	2369179.0	6046.2	0.001663	0.167	0.950		0.855		
36	2458389.0	3546.6	0.001977	2395730.0	6090.5	0.001664	0.158	0.945		0.858		

STANTON NUMBER DATA RUN 072773 *** DISCRETE HOLE RIG *** NAS-3-14336

TINF= 81.0 UINF= 52.8 XVO= 4.600 RHO= 0.07246 CP= 0.242 VISC= 0.17002E-03 PR=0.716
DISTANCE FROM ORIGIN OF BL TO 1ST PLATE=44.700 P/D= 5
UNCERTAINTY IN REX=25900. UNCERTAINTY IN F=0.03028 IN RATIO

** M=0.3, COLD RUN, HIGH RE, STEP T-WALL AT 1ST PLATE.

PLATE	X	REX	TO	REENTH	STANTON NO	DST	DREEN	M	F	T2	THETA	DTH
1	50.30	0.11836E 07	104.3	0.10103E 03	0.39009E-02	0.705E-04	2.					
2	52.30	0.12355E 07	104.2	0.32125E 03	0.36663E-02	0.690E-04	4.	0.31	0.0102	83.1	0.092	0.011
3	54.30	0.12873E 07	104.2	0.56348E 03	0.38311E-02	0.703E-04	7.	0.31	0.0101	83.1	0.091	0.011
4	56.30	0.13391E 07	104.3	0.80875E 03	0.37606E-02	0.696E-04	8.	0.32	0.0102	83.2	0.094	0.011
5	58.30	0.13909E 07	104.3	0.10481E 04	0.35840E-02	0.683E-04	10.	0.31	0.0101	83.2	0.093	0.011
6	60.30	0.14427E 07	104.3	0.12804E 04	0.35202E-02	0.678E-04	11.	0.31	0.0101	83.1	0.092	0.011
7	62.30	0.14945E 07	104.2	0.15109E 04	0.34100E-02	0.672E-04	12.	0.31	0.0100	83.4	0.104	0.011
8	64.30	0.15463E 07	104.2	0.17384E 04	0.33030E-02	0.665E-04	13.	0.31	0.0100	83.4	0.104	0.011
9	66.30	0.15981E 07	104.2	0.19612E 04	0.32387E-02	0.661E-04	14.	0.31	0.0100	83.4	0.103	0.011
10	68.30	0.16499E 07	104.3	0.21814E 04	0.32203E-02	0.659E-04	14.	0.31	0.0100	83.4	0.102	0.011
11	70.30	0.17017E 07	104.2	0.23988E 04	0.31445E-02	0.656E-04	15.	0.31	0.0100	83.3	0.101	0.011
12	72.30	0.17535E 07	104.2	0.26119E 04	0.30343E-02	0.649E-04	16.	0.31	0.0100	83.4	0.104	0.011
13	73.82	0.17928E 07	103.0	0.27533E 04	0.26905E-02	0.472E-04	16.					
14	74.85	0.18195E 07	102.9	0.28218E 04	0.24355E-02	0.470E-04	16.					
15	75.88	0.18462E 07	103.9	0.28845E 04	0.22603E-02	0.446E-04	16.					
16	76.91	0.18730E 07	104.1	0.29434E 04	0.21492E-02	0.424E-04	16.					
17	77.95	0.18998E 07	104.3	0.29992E 04	0.20349E-02	0.410E-04	16.					
18	78.98	0.19265E 07	104.1	0.30543E 04	0.20881E-02	0.418E-04	16.					
19	80.01	0.19532E 07	104.3	0.31087E 04	0.19860E-02	0.395E-04	16.					
20	81.04	0.19798E 07	104.5	0.31606E 04	0.18979E-02	0.381E-04	17.					
21	82.07	0.20065E 07	104.3	0.32127E 04	0.20072E-02	0.399E-04	17.					
22	83.10	0.20332E 07	104.6	0.32647E 04	0.18828E-02	0.393E-04	17.					
23	84.13	0.20599E 07	104.4	0.33144E 04	0.18394E-02	0.389E-04	17.					
24	85.16	0.20867E 07	104.3	0.33646E 04	0.19231E-02	0.409E-04	17.					
25	86.20	0.21135E 07	103.4	0.34145E 04	0.18138E-02	0.396E-04	17.					
26	87.23	0.21402E 07	103.8	0.34653E 04	0.19898E-02	0.416E-04	17.					
27	88.26	0.21668E 07	104.4	0.35175E 04	0.19182E-02	0.402E-04	17.					
28	89.29	0.21935E 07	104.6	0.35680E 04	0.18638E-02	0.391E-04	17.					
29	90.32	0.22202E 07	104.2	0.36197E 04	0.20087E-02	0.404E-04	17.					
30	91.35	0.22469E 07	104.9	0.36713E 04	0.18500E-02	0.394E-04	17.					
31	92.38	0.22735E 07	104.7	0.37214E 04	0.18995E-02	0.394E-04	17.					
32	93.41	0.23003E 07	104.6	0.37708E 04	0.17998E-02	0.387E-04	17.					
33	94.45	0.23272E 07	104.6	0.38191E 04	0.18230E-02	0.387E-04	17.					
34	95.48	0.23538E 07	103.7	0.38682E 04	0.18530E-02	0.389E-04	17.					
35	96.51	0.23805E 07	104.1	0.39179E 04	0.18634E-02	0.413E-04	17.					
36	97.54	0.24072E 07	103.5	0.39676E 04	0.18584E-02	0.454E-04	17.					

STANTON NUMBER DATA RUN 070973 *** DISCRETE HOLE RIG *** NAS-3-14336

TINF= 80.0 UINF= 52.7 XVO= 4.600 RHO= 0.07274 CP= 0.242 VISC= 0.16921E-03 PR=0.715
DISTANCE FROM ORIGIN OF BL TO 1ST PLATE=44.700 P/D= 5
UNCERTAINTY IN REX=25974. UNCERTAINTY IN F=0.03028 IN RATIO

** M=0.3, HOT RUN, HIGH RE, STEP T-WALL AT 1ST PLATE.

PLATE	X	REX	TO	REENTH	STANTON NO	DST	DREEN	M	F	T2	THETA	DTH
1	50.30	0.11870E 07	107.2	0.97674E 02	0.37604E-02	0.601E-04	2.					
2	52.30	0.12390E 07	107.1	0.53160E 03	0.29231E-02	0.553E-04	9.	0.29	0.0095	108.5	1.052	0.013
3	54.30	0.12909E 07	107.3	0.12260E 04	0.27180E-02	0.539E-04	16.	0.32	0.0103	109.3	1.073	0.013
4	56.30	0.13429E 07	107.3	0.19245E 04	0.24890E-02	0.528E-04	21.	0.31	0.0100	109.0	1.061	0.013
5	58.30	0.13948E 07	107.1	0.26151E 04	0.22335E-02	0.521E-04	25.	0.32	0.0103	109.6	1.093	0.014
6	60.30	0.14468E 07	107.2	0.32941E 04	0.21085E-02	0.513E-04	28.	0.32	0.0103	107.9	1.025	0.013
7	62.30	0.14987E 07	107.0	0.39455E 04	0.19442E-02	0.509E-04	31.	0.30	0.0097	109.3	1.085	0.014
8	64.30	0.15507E 07	107.1	0.45893E 04	0.18190E-02	0.504E-04	34.	0.30	0.0096	109.8	1.102	0.014
9	66.30	0.16026E 07	107.1	0.52169E 04	0.17582E-02	0.501E-04	36.	0.29	0.0094	108.8	1.063	0.013
10	68.30	0.16545E 07	107.2	0.58640E 04	0.17176E-02	0.499E-04	38.	0.33	0.0108	108.8	1.060	0.013
11	70.30	0.17065E 07	107.0	0.65242E 04	0.16126E-02	0.498E-04	41.	0.32	0.0103	107.9	1.035	0.013
12	72.30	0.17584E 07	107.1	0.71595E 04	0.15429E-02	0.493E-04	43.	0.31	0.0101	108.5	1.049	0.013
13	73.82	0.17979E 07	106.8	0.74956E 04	0.15136E-02	0.281E-04	44.					
14	74.85	0.18247E 07	106.5	0.75353E 04	0.14529E-02	0.307E-04	44.					
15	75.88	0.18514E 07	107.1	0.75734E 04	0.13917E-02	0.304E-04	44.					
16	76.91	0.18783E 07	107.1	0.76106E 04	0.13876E-02	0.300E-04	44.					
17	77.95	0.19052E 07	107.3	0.76474E 04	0.13550E-02	0.298E-04	44.					
18	78.98	0.19319E 07	107.3	0.76835E 04	0.13471E-02	0.298E-04	44.					
19	80.01	0.19587E 07	107.2	0.77197E 04	0.13543E-02	0.289E-04	44.					
20	81.04	0.19855E 07	107.3	0.77556E 04	0.13224E-02	0.283E-04	44.					
21	82.07	0.20122E 07	107.2	0.77919E 04	0.13893E-02	0.296E-04	44.					
22	83.10	0.20390E 07	107.1	0.78289E 04	0.13750E-02	0.304E-04	44.					
23	84.13	0.20657E 07	107.1	0.78651E 04	0.13288E-02	0.300E-04	44.					
24	85.16	0.20926E 07	107.2	0.79011E 04	0.13613E-02	0.311E-04	44.					
25	86.20	0.21195E 07	106.5	0.79371E 04	0.13249E-02	0.306E-04	44.					
26	87.23	0.21462E 07	106.0	0.79732E 04	0.13693E-02	0.313E-04	44.					
27	88.26	0.21730E 07	107.0	0.80101E 04	0.13883E-02	0.312E-04	44.					
28	89.29	0.21997E 07	107.1	0.80475E 04	0.14047E-02	0.309E-04	44.					
29	90.32	0.22265E 07	106.7	0.80860E 04	0.14678E-02	0.311E-04	44.					
30	91.35	0.22532E 07	107.1	0.81252E 04	0.14596E-02	0.320E-04	44.					
31	92.38	0.22800E 07	107.1	0.81641E 04	0.14425E-02	0.315E-04	44.					
32	93.41	0.23069E 07	106.5	0.82028E 04	0.14475E-02	0.320E-04	44.					
33	94.45	0.23338E 07	106.6	0.82414E 04	0.14390E-02	0.315E-04	44.					
34	95.48	0.23605E 07	106.0	0.82801E 04	0.14476E-02	0.312E-04	44.					
35	96.51	0.23873E 07	106.3	0.83195E 04	0.14963E-02	0.339E-04	44.					
36	97.54	0.24140E 07	105.8	0.83596E 04	0.14946E-02	0.367E-04	44.					

FOLLOWING IS THE DATA FOR THETA=0 AND THETA=1, WHICH WAS OBTAINED BY LINEAR SUPERPOSITION THEORY.
THIS DATA WAS PRODUCED FROM RUN 072773 . AND RUN 070973
FOR THE DETAIL CHANGES OF PROPERTIES AND BOUNDARY CONDITIONS, PLEASE SEE THE ABOVE TWO RUNS

PLATE	REXCOL	RE DEL2	ST(TH=0)	REXHOT	RE DEL2	ST(TH=1)	ETA	STCR	F-COL	STHR	F-HOT	PHI-1
1	1183649.0	101.0	0.003901	1187013.0	97.7	0.003760	UUUUU	UUUUU	0.0000	UUUUUUU	0.0000	UUUUU
2	1235450.0	298.9	0.003737	1238961.0	519.8	0.002963	0.207	0.969	0.0102	1.057	0.0095	2.362
3	1287251.0	497.6	0.003934	1290909.0	1185.0	0.002801	0.288	1.142	0.0101	1.061	0.0103	2.532
4	1339052.0	700.1	0.003884	1342857.0	1852.3	0.002569	0.339	1.214	0.0102	1.014	0.0100	2.487
5	1390853.0	896.7	0.003710	1394806.0	2507.5	0.002360	0.364	1.226	0.0101	0.961	0.0103	2.497
6	1442654.0	1087.6	0.003660	1446754.0	3159.2	0.002146	0.414	1.264	0.0101	0.897	0.0103	2.449
7	1494454.0	1274.7	0.003565	1498702.0	3786.9	0.002071	0.419	1.277	0.0100	0.885	0.0097	2.380
8	1546255.0	1456.6	0.003457	1550650.0	4391.2	0.001971	0.430	1.278	0.0100	0.858	0.0095	2.358
9	1598056.0	1634.2	0.003397	1602598.0	4984.4	0.001855	0.454	1.290	0.0100	0.822	0.0094	2.316
10	1649857.0	1809.7	0.003381	1654546.0	5604.3	0.001812	0.464	1.316	0.0100	0.815	0.0108	2.498
11	1701658.0	1983.0	0.003311	1706494.0	6242.3	0.001669	0.496	1.317	0.0100	0.762	0.0103	2.390
12	1753459.0	2151.6	0.003198	1758442.0	6858.9	0.001620	0.493	1.298	0.0100	0.749	0.0101	2.361
13	1792828.0	2271.9	0.002810	1797923.0	7185.1	0.001591	0.434	1.156		0.742		
14	1819505.0	2343.3	0.002535	1824676.0	7226.7	0.001517	0.401	1.053		0.712		
15	1846182.0	2408.5	0.002349	1851429.0	7266.5	0.001449	0.383	0.984		0.684		
16	1872989.0	2469.6	0.002227	1878312.0	7305.1	0.001438	0.354	0.940		0.682		
17	1899796.0	2527.5	0.002104	1905195.0	7343.1	0.001400	0.335	0.896		0.668		
18	1926473.0	2584.5	0.002163	1931949.0	7380.6	0.001396	0.355	0.928		0.670		
19	1953151.0	2640.7	0.002050	1958702.0	7417.9	0.001396	0.319	0.886		0.673		
20	1979828.0	2694.2	0.001956	1985455.0	7454.9	0.001360	0.305	0.851		0.659		
21	2006506.0	2748.0	0.002070	2012209.0	7492.2	0.001430	0.309	0.907		0.696		
22	2033184.0	2801.5	0.001934	2038962.0	7530.2	0.001408	0.272	0.853		0.689		
23	2059861.0	2852.6	0.001891	2065715.0	7567.3	0.001362	0.280	0.840		0.669		
24	2086668.0	2904.3	0.001980	2092598.0	7604.3	0.001398	0.294	0.885		0.690		
25	2113475.0	2955.6	0.001864	2119481.0	7641.2	0.001357	0.272	0.838		0.673		
26	2140152.0	3007.9	0.002053	2146234.0	7678.3	0.001410	0.313	0.929		0.702		
27	2166829.0	3061.7	0.001972	2172988.0	7716.2	0.001423	0.278	0.897		0.711		
28	2193507.0	3113.5	0.001910	2199741.0	7754.5	0.001435	0.249	0.874		0.720		
29	2220185.0	3166.6	0.002064	2226494.0	7793.8	0.001503	0.272	0.949		0.757		
30	2246862.0	3219.4	0.001890	2253248.0	7833.9	0.001485	0.214	0.874		0.751		
31	2273540.0	3270.6	0.001946	2280001.0	7873.5	0.001473	0.243	0.905		0.748		
32	2300346.0	3321.1	0.001836	2306884.0	7912.9	0.001471	0.199	0.858		0.749		
33	2327153.0	3370.5	0.001862	2333767.0	7952.2	0.001464	0.214	0.875		0.749		
34	2353831.0	3420.7	0.001894	2360520.0	7991.6	0.001474	0.222	0.894		0.757		
35	2380508.0	3471.3	0.001901	2387273.0	8031.7	0.001520	0.200	0.901		0.783		
36	2407185.0	3522.0	0.001895	2414027.0	8072.4	0.001518	0.199	0.903		0.785		

STANTON NUMBER DATA RUN 072673 *** DISCRETE HOLE RIG *** NAS-3-14336

TINF= 79.3 UINF= 51.9 XVO= 4.600 RHO= 0.07261 CP= 0.242 VISC= 0.16932E-03 PR=0.716
DISTANCE FROM ORIGIN OF BL TO 1ST PLATE=44.700 P/D= 5
UNCERTAINTY IN REX=25547. UNCERTAINTY IN F=0.03030 IN RATIO

** M=0.4, COLD RUN, HIGH RE, STEP T-WALL AT 1ST PLATE.

PLATE	X	REX	TO	REENTH	STANTON NO	DST	DREEN	M	F	T2	THETA	DTH
1	50.30	0.11675E 07	102.7	0.99173E 02	0.38820E-02	0.709E-04	2.					
2	52.30	0.12186E 07	102.8	0.33023E 03	0.37816E-02	0.699E-04	5.	0.42	0.0136	81.7	0.101	0.011
3	54.30	0.12697E 07	102.8	0.59744E 03	0.39629E-02	0.712E-04	8.	0.42	0.0137	81.6	0.097	0.011
4	56.30	0.13208E 07	102.8	0.86742E 03	0.38891E-02	0.708E-04	10.	0.41	0.0134	81.8	0.103	0.011
5	58.30	0.13719E 07	102.8	0.11322E 04	0.37144E-02	0.695E-04	12.	0.42	0.0136	81.7	0.101	0.011
6	60.30	0.14230E 07	102.8	0.13912E 04	0.36233E-02	0.689E-04	13.	0.42	0.0135	81.8	0.105	0.011
7	62.30	0.14741E 07	102.7	0.16491E 04	0.35063E-02	0.683E-04	15.	0.43	0.0138	82.0	0.112	0.011
8	64.30	0.15252E 07	102.8	0.19040E 04	0.33910E-02	0.672E-04	16.	0.42	0.0135	82.0	0.113	0.011
9	66.30	0.15763E 07	102.9	0.21532E 04	0.33238E-02	0.666E-04	17.	0.42	0.0137	81.9	0.110	0.011
10	68.30	0.16273E 07	102.9	0.23990E 04	0.32736E-02	0.664E-04	18.	0.42	0.0135	82.0	0.112	0.011
11	70.30	0.16784E 07	102.9	0.26413E 04	0.32298E-02	0.661E-04	19.	0.42	0.0136	81.9	0.108	0.011
12	72.30	0.17295E 07	102.9	0.28784E 04	0.30779E-02	0.649E-04	20.	0.41	0.0134	82.0	0.113	0.011
13	73.82	0.17684E 07	101.7	0.30312E 04	0.26996E-02	0.471E-04	20.					
14	74.85	0.17947E 07	101.6	0.30989E 04	0.24432E-02	0.469E-04	20.					
15	75.88	0.18210E 07	102.6	0.31607E 04	0.22467E-02	0.442E-04	20.					
16	76.91	0.18474E 07	102.9	0.32180E 04	0.21049E-02	0.417E-04	20.					
17	77.95	0.18739E 07	103.2	0.32716E 04	0.19651E-02	0.400E-04	20.					
18	78.98	0.19002E 07	102.9	0.33243E 04	0.20366E-02	0.409E-04	20.					
19	80.01	0.19265E 07	103.3	0.33759E 04	0.18778E-02	0.379E-04	20.					
20	81.04	0.19528E 07	103.4	0.34249E 04	0.18422E-02	0.370E-04	20.					
21	82.07	0.19791E 07	103.3	0.34744E 04	0.19199E-02	0.385E-04	20.					
22	83.10	0.20054E 07	103.5	0.35237E 04	0.18222E-02	0.383E-04	20.					
23	84.13	0.20318E 07	103.2	0.35713E 04	0.17923E-02	0.380E-04	20.					
24	85.16	0.20582E 07	103.2	0.36193E 04	0.18452E-02	0.399E-04	20.					
25	86.20	0.20846E 07	102.1	0.36671E 04	0.17870E-02	0.392E-04	20.					
26	87.23	0.21110E 07	102.6	0.37162E 04	0.19366E-02	0.407E-04	20.					
27	88.26	0.21373E 07	103.1	0.37664E 04	0.18790E-02	0.395E-04	21.					
28	89.29	0.21636E 07	103.4	0.38153E 04	0.18356E-02	0.387E-04	21.					
29	90.32	0.21899E 07	102.8	0.38658E 04	0.19941E-02	0.401E-04	21.					
30	91.35	0.22162E 07	103.6	0.39163E 04	0.18366E-02	0.393E-04	21.					
31	92.38	0.22425E 07	103.4	0.39652E 04	0.18797E-02	0.392E-04	21.					
32	93.41	0.22690E 07	103.1	0.40138E 04	0.18068E-02	0.388E-04	21.					
33	94.45	0.22954E 07	103.1	0.40618E 04	0.18387E-02	0.389E-04	21.					
34	95.48	0.23217E 07	102.4	0.41103E 04	0.18410E-02	0.387E-04	21.					
35	96.51	0.23480E 07	102.8	0.41592E 04	0.18726E-02	0.413E-04	21.					
36	97.54	0.23743E 07	102.1	0.42085E 04	0.18713E-02	0.456E-04	21.					

STANTON NUMBER DATA RUN 071573 *** DISCRETE HOLE RIG *** NAS-3-14336

TINF= 81.8 UINF= 52.7 XVO= 4.600 RHO= 0.07269 CP= 0.242 VISC= 0.16980E-03 PR=0.715
DISTANCE FROM ORIGIN OF BL TO 1ST PLATE=44.700 P/D= 5
UNCERTAINTY IN REX=25871. UNCERTAINTY IN F=0.03028 IN RATIO

** M=0.4, HOT RUN, HIGH RE, STEP T-WALL AT 1ST PLATE.

PLATE	X	REX	TB	REENTH	STANTON NO	DST	DREEN	M	F	T2	THETA	DTH
1	50.30	0.11823E 07	107.1	0.98412E 02	0.38040E-02	0.647E-04	2.					
2	52.30	0.12340E 07	107.0	0.64181E 03	0.30700E-02	0.601E-04	13.	0.42	0.0135	108.2	1.048	0.014
3	54.30	0.12858E 07	107.0	0.15545E 04	0.28776E-02	0.592E-04	22.	0.42	0.0137	109.7	1.108	0.015
4	56.30	0.13375E 07	107.0	0.24654E 04	0.26097E-02	0.575E-04	29.	0.41	0.0132	109.5	1.096	0.015
5	58.30	0.13893E 07	107.1	0.33545E 04	0.23449E-02	0.561E-04	34.	0.41	0.0134	109.9	1.112	0.015
6	60.30	0.14410E 07	107.0	0.42362E 04	0.21595E-02	0.554E-04	39.	0.44	0.0143	107.7	1.025	0.014
7	62.30	0.14927E 07	107.0	0.51142E 04	0.20217E-02	0.548E-04	43.	0.43	0.0139	109.2	1.086	0.015
8	64.30	0.15445E 07	107.0	0.59691E 04	0.18369E-02	0.541E-04	46.	0.39	0.0128	109.7	1.107	0.015
9	66.30	0.15962E 07	107.0	0.67775E 04	0.17217E-02	0.536E-04	49.	0.40	0.0129	108.4	1.054	0.014
10	68.30	0.16480E 07	107.0	0.75908E 04	0.16359E-02	0.533E-04	52.	0.43	0.0138	108.2	1.048	0.014
11	70.30	0.16997E 07	106.9	0.84042E 04	0.15170E-02	0.531E-04	55.	0.43	0.0138	106.8	0.998	0.014
12	72.30	0.17515E 07	107.1	0.91844E 04	0.13596E-02	0.523E-04	58.	0.41	0.0134	107.3	1.009	0.014
13	73.82	0.17908E 07	106.1	0.95889E 04	0.15060E-02	0.295E-04	59.					
14	74.85	0.18174E 07	106.0	0.96273E 04	0.13714E-02	0.320E-04	59.					
15	75.88	0.18441E 07	106.8	0.96622E 04	0.12461E-02	0.310E-04	59.					
16	76.91	0.18708E 07	106.8	0.96954E 04	0.12430E-02	0.304E-04	59.					
17	77.95	0.18976E 07	107.1	0.97278E 04	0.11859E-02	0.299E-04	59.					
18	78.98	0.19243E 07	107.2	0.97592E 04	0.11707E-02	0.299E-04	59.					
19	80.01	0.19509E 07	106.9	0.97910E 04	0.12118E-02	0.291E-04	59.					
20	81.04	0.19776E 07	107.2	0.98227E 04	0.11616E-02	0.283E-04	59.					
21	82.07	0.20042E 07	107.1	0.98543E 04	0.12055E-02	0.294E-04	59.					
22	83.10	0.20309E 07	107.0	0.98866E 04	0.12214E-02	0.307E-04	59.					
23	84.13	0.20575E 07	106.9	0.99187E 04	0.11804E-02	0.303E-04	59.					
24	85.16	0.20843E 07	107.1	0.99504E 04	0.11982E-02	0.314E-04	59.					
25	86.20	0.21111E 07	106.2	0.99817E 04	0.11518E-02	0.311E-04	59.					
26	87.23	0.21377E 07	105.5	0.10014E 05	0.12760E-02	0.327E-04	59.					
27	88.26	0.21643E 07	106.7	0.10048E 05	0.12600E-02	0.320E-04	59.					
28	89.29	0.21910E 07	107.0	0.10081E 05	0.12532E-02	0.312E-04	59.					
29	90.32	0.22176E 07	106.5	0.10117E 05	0.13742E-02	0.320E-04	59.					
30	91.35	0.22443E 07	106.9	0.10153E 05	0.13269E-02	0.325E-04	59.					
31	92.38	0.22709E 07	107.0	0.10188E 05	0.13113E-02	0.320E-04	59.					
32	93.41	0.22977E 07	106.4	0.10223E 05	0.13220E-02	0.326E-04	59.					
33	94.45	0.23245E 07	106.5	0.10258E 05	0.13164E-02	0.321E-04	59.					
34	95.48	0.23511E 07	105.8	0.10294E 05	0.13403E-02	0.320E-04	59.					
35	96.51	0.23778E 07	106.1	0.10330E 05	0.13706E-02	0.347E-04	59.					
36	97.54	0.24044E 07	105.6	0.10366E 05	0.13872E-02	0.374E-04	59.					

FOLLOWING IS THE DATA FOR THETA=0 AND THETA=1, WHICH WAS OBTAINED BY LINEAR SUPERPOSITION THEORY.
THIS DATA WAS PRODUCED FROM RUN 072673 AND RUN 071573
FOR THE DETAIL CHANGES OF PROPERTIES AND BOUNDARY CONDITIONS, PLEASE SEE THE ABOVE TWO RUNS

PLATE	REXCOL	RE DEL2	ST(TH=0)	REXHOT	RE DEL2	ST(TH=1)	ETA	STCR	F-COL	STHR	F-HOT	PHI-1
1	1167500.0	99.2	0.003882	1182294.0	98.4	0.003804	UUUUU	UUUUU	0.0000	UUUUUUU	0.0000	UUUUU
2	1218594.0	296.9	0.003858	1234036.0	625.9	0.003106	0.195	0.997	0.0136	1.107	0.0135	2.867
3	1269688.0	499.4	0.004067	1285778.0	1487.4	0.002993	0.264	1.177	0.0137	1.133	0.0137	3.020
4	1320782.0	706.0	0.004022	1337519.0	2333.3	0.002733	0.320	1.253	0.0134	1.078	0.0132	2.959
5	1371876.0	907.2	0.003852	1389261.0	3158.0	0.002496	0.352	1.269	0.0136	1.016	0.0134	2.946
6	1422971.0	1102.4	0.003790	1441002.0	3996.4	0.002200	0.420	1.305	0.0135	0.919	0.0143	2.966
7	1474065.0	1293.1	0.003676	1492744.0	4838.5	0.002153	0.414	1.313	0.0138	0.919	0.0139	2.951
8	1525159.0	1478.2	0.003568	1544486.0	5635.1	0.002004	0.438	1.315	0.0135	0.872	0.0128	2.779
9	1576253.0	1659.1	0.003511	1596227.0	6397.1	0.001813	0.484	1.330	0.0137	0.802	0.0129	2.725
10	1627347.0	1837.4	0.003470	1647969.0	7179.8	0.001720	0.504	1.346	0.0135	0.773	0.0138	2.823
11	1678441.0	2013.9	0.003438	1699710.0	7978.8	0.001513	0.560	1.363	0.0136	0.689	0.0138	2.719
12	1729535.0	2185.8	0.003295	1751452.0	8757.0	0.001377	0.582	1.333	0.0134	0.636	0.0134	2.604
13	1768367.0	2307.3	0.002833	1790776.0	9159.8	0.001584	0.441	1.162		0.738		
14	1794680.0	2378.4	0.002563	1817422.0	9200.2	0.001442	0.437	1.061		0.676		
15	1820994.0	2443.2	0.002359	1844069.0	9236.9	0.001312	0.444	0.985		0.618		
16	1847435.0	2503.3	0.002201	1870845.0	9271.8	0.001300	0.410	0.927		0.616		
17	1873876.0	2559.3	0.002052	1897622.0	9305.6	0.001237	0.397	0.871		0.590		
18	1900189.0	2614.5	0.002133	1924269.0	9338.5	0.001228	0.425	0.912		0.588		
19	1926503.0	2668.3	0.001952	1950915.0	9371.6	0.001256	0.357	0.841		0.605		
20	1952816.0	2719.3	0.001918	1977562.0	9404.5	0.001206	0.371	0.832		0.584		
21	1979130.0	2770.9	0.002000	2004210.0	9437.3	0.001252	0.374	0.874		0.609		
22	2005444.0	2822.1	0.001889	2030856.0	9470.8	0.001261	0.333	0.831		0.616		
23	2031757.0	2871.5	0.001861	2057503.0	9503.9	0.001221	0.344	0.824		0.599		
24	2058198.0	2921.3	0.001918	2084279.0	9536.7	0.001241	0.353	0.854		0.612		
25	2084639.0	2971.0	0.001858	2111056.0	9569.2	0.001194	0.358	0.833		0.591		
26	2110953.0	3022.0	0.002010	2137703.0	9602.7	0.001319	0.344	0.907		0.656		
27	2137266.0	3074.1	0.001948	2164349.0	9637.7	0.001301	0.332	0.884		0.649		
28	2163580.0	3124.8	0.001901	2190996.0	9672.2	0.001291	0.321	0.867		0.647		
29	2189893.0	3177.0	0.002063	2217644.0	9708.3	0.001415	0.314	0.946		0.712		
30	2216207.0	3229.2	0.001894	2244290.0	9745.4	0.001360	0.282	0.873		0.687		
31	2242520.0	3279.7	0.001943	2270937.0	9781.5	0.001349	0.306	0.901		0.684		
32	2268961.0	3329.8	0.001861	2297713.0	9817.5	0.001354	0.273	0.867		0.689		
33	2295402.0	3379.3	0.001897	2324490.0	9853.6	0.001351	0.288	0.888		0.690		
34	2321716.0	3429.3	0.001897	2351137.0	9889.9	0.001373	0.276	0.893		0.704		
35	2348029.0	3479.7	0.001929	2377783.0	9927.0	0.001404	0.272	0.912		0.722		
36	2374343.0	3530.5	0.001925	2404430.0	9964.6	0.001419	0.263	0.915		0.733		

STANTON NUMBER DATA RUN 071773 *** DISCRETE HOLE RIG *** NAS-3-14336

TINF= 77.8 UINF= 52.1 XVO= 4.600 RHO= 0.07319 CP= 0.242 VISC= 0.16782E-03 PR=0.715
DISTANCE FROM ORIGIN OF BL TO 1ST PLATE=44.700 P/D= 5
UNCERTAINTY IN REX=25870. UNCERTAINTY IN F=0.03029 IN RATIO

** M=0.5, COLD RUN, HIGH RE, STEP T-WALL AT 1ST PLATE

PLATE	X	REX	TO	REENTH	STANTON NO	DST	DREEN	M	F	T2	THETA	DTH
1	50.30	0.11822E 07	102.3	0.10157E 03	0.39262E-02	0.677E-04	2.					
2	52.30	0.12340E 07	102.4	0.33569E 03	0.38961E-02	0.673E-04	6.	0.54	0.0174	79.5	0.071	0.010
3	54.30	0.12857E 07	102.3	0.60507E 03	0.41236E-02	0.692E-04	9.	0.52	0.0168	79.5	0.069	0.010
4	56.30	0.13375E 07	102.4	0.88007E 03	0.41163E-02	0.688E-04	11.	0.53	0.0172	79.5	0.071	0.010
5	58.30	0.13892E 07	102.3	0.11515E 04	0.39522E-02	0.679E-04	13.	0.52	0.0170	79.5	0.071	0.010
6	60.30	0.14409E 07	102.5	0.14167E 04	0.38749E-02	0.670E-04	15.	0.53	0.0171	79.5	0.072	0.010
7	62.30	0.14927E 07	102.4	0.16797E 04	0.37101E-02	0.660E-04	17.	0.52	0.0170	79.8	0.080	0.010
8	64.30	0.15444E 07	102.3	0.19388E 04	0.35499E-02	0.651E-04	18.	0.53	0.0173	79.8	0.081	0.010
9	66.30	0.15962E 07	102.3	0.21894E 04	0.34287E-02	0.643E-04	19.	0.53	0.0173	79.6	0.076	0.010
10	68.30	0.16479E 07	102.3	0.24327E 04	0.33756E-02	0.639E-04	21.	0.53	0.0170	79.6	0.076	0.010
11	70.30	0.16996E 07	102.4	0.26701E 04	0.32328E-02	0.628E-04	22.	0.53	0.0170	79.6	0.075	0.010
12	72.30	0.17514E 07	102.3	0.29034E 04	0.31595E-02	0.626E-04	23.	0.53	0.0170	79.7	0.080	0.010
13	73.82	0.17907E 07	100.6	0.30563E 04	0.27083E-02	0.463E-04	23.					
14	74.85	0.18173E 07	100.5	0.31249E 04	0.24295E-02	0.459E-04	23.					
15	75.88	0.18440E 07	101.6	0.31867E 04	0.22042E-02	0.429E-04	23.					
16	76.91	0.18708E 07	101.9	0.32433E 04	0.20400E-02	0.401E-04	23.					
17	77.95	0.18975E 07	102.2	0.32960E 04	0.19126E-02	0.384E-04	23.					
18	78.98	0.19242E 07	102.2	0.33470E 04	0.19055E-02	0.384E-04	23.					
19	80.01	0.19508E 07	102.3	0.33967E 04	0.18225E-02	0.363E-04	23.					
20	81.04	0.19775E 07	102.5	0.34444E 04	0.17555E-02	0.352E-04	24.					
21	82.07	0.20041E 07	102.4	0.34922E 04	0.18300E-02	0.366E-04	24.					
22	83.10	0.20308E 07	102.6	0.35399E 04	0.17456E-02	0.366E-04	24.					
23	84.13	0.20574E 07	102.4	0.35860E 04	0.17049E-02	0.361E-04	24.					
24	85.16	0.20842E 07	102.4	0.36322E 04	0.17635E-02	0.380E-04	24.					
25	86.20	0.21110E 07	101.1	0.36782E 04	0.16810E-02	0.375E-04	24.					
26	87.23	0.21376E 07	100.6	0.37241E 04	0.17635E-02	0.387E-04	24.					
27	88.26	0.21643E 07	101.9	0.37718E 04	0.18111E-02	0.386E-04	24.					
28	89.29	0.21909E 07	102.4	0.38196E 04	0.17724E-02	0.372E-04	24.					
29	90.32	0.22176E 07	101.9	0.38688E 04	0.19173E-02	0.383E-04	24.					
30	91.35	0.22442E 07	102.7	0.39181E 04	0.17777E-02	0.377E-04	24.					
31	92.38	0.22708E 07	102.5	0.39659E 04	0.18072E-02	0.375E-04	24.					
32	93.41	0.22976E 07	102.2	0.40131E 04	0.17285E-02	0.371E-04	24.					
33	94.45	0.23244E 07	102.1	0.40598E 04	0.17731E-02	0.372E-04	24.					
34	95.48	0.23510E 07	101.5	0.41070E 04	0.17674E-02	0.369E-04	24.					
35	96.51	0.23777E 07	101.8	0.41548E 04	0.18151E-02	0.397E-04	24.					
36	97.54	0.24043E 07	101.2	0.42030E 04	0.17969E-02	0.439E-04	24.					

STANTON NUMBER DATA RUN 071873-1 *** DISCRETE HOLE RIG *** NAS-3-14336

TINF= 80.3 UINF= 52.0 XVO= 4.600 RHO= 0.07296 CP= 0.242 VISC= 0.16893E-03 PR=0.715
DISTANCE FROM ORIGIN OF BL TO 1ST PLATE=44.700 P/D= 5
UNCERTAINTY IN REX=25655. UNCERTAINTY IN F=0.03030 IN RATIO

** M=0.5, HOT RUN, HIGH RE, STEP T-WALL AT 1ST PLATE

PLATE	X	REX	TO	REENTH	STANTON NO	DST	DREEN	M	F	T2	THETA	DTH
1	50.30	0.11724E 07	108.0	0.99059E 02	0.38612E-02	0.603E-04	2.					
2	52.30	0.12237E 07	108.0	0.75690E 03	0.31864E-02	0.562E-04	16.	0.52	0.0168	111.0	1.108	0.013
3	54.30	0.12750E 07	108.0	0.18926E 04	0.30535E-02	0.556E-04	28.	0.53	0.0171	111.8	1.140	0.014
4	56.30	0.13264E 07	108.0	0.30417E 04	0.27443E-02	0.539E-04	36.	0.52	0.0169	112.4	1.161	0.014
5	58.30	0.13777E 07	108.0	0.41795E 04	0.24633E-02	0.526E-04	43.	0.52	0.0168	112.6	1.167	0.014
6	60.30	0.14290E 07	107.9	0.52762E 04	0.22447E-02	0.517E-04	49.	0.53	0.0170	110.2	1.084	0.013
7	62.30	0.14803E 07	108.1	0.63551E 04	0.20459E-02	0.505E-04	54.	0.52	0.0169	112.0	1.141	0.014
8	64.30	0.15316E 07	108.1	0.74430E 04	0.18083E-02	0.497E-04	59.	0.51	0.0165	112.7	1.167	0.014
9	66.30	0.15829E 07	108.0	0.85025E 04	0.16423E-02	0.492E-04	63.	0.51	0.0166	111.3	1.121	0.014
10	68.30	0.16342E 07	108.1	0.95391E 04	0.15273E-02	0.487E-04	67.	0.52	0.0168	111.2	1.112	0.013
11	70.30	0.16855E 07	108.0	0.10540E 05	0.14567E-02	0.487E-04	70.	0.51	0.0165	109.4	1.053	0.013
12	72.30	0.17368E 07	108.0	0.11495E 05	0.12663E-02	0.482E-04	73.	0.51	0.0164	109.1	1.040	0.013
13	73.82	0.17758E 07	107.5	0.11982E 05	0.12116E-02	0.246E-04	75.					
14	74.85	0.18023E 07	107.4	0.12012E 05	0.11068E-02	0.272E-04	75.					
15	75.88	0.18287E 07	108.2	0.12040E 05	0.10103E-02	0.267E-04	75.					
16	76.91	0.18552E 07	108.2	0.12067E 05	0.97954E-03	0.260E-04	75.					
17	77.95	0.18818E 07	108.4	0.12092E 05	0.94613E-03	0.258E-04	75.					
18	78.98	0.19082E 07	108.5	0.12117E 05	0.92483E-03	0.258E-04	75.					
19	80.01	0.19346E 07	108.3	0.12142E 05	0.95064E-03	0.249E-04	75.					
20	81.04	0.19611E 07	108.4	0.12167E 05	0.93190E-03	0.244E-04	75.					
21	82.07	0.19875E 07	108.4	0.12192E 05	0.95834E-03	0.253E-04	75.					
22	83.10	0.20139E 07	108.3	0.12217E 05	0.97901E-03	0.265E-04	75.					
23	84.13	0.20403E 07	108.3	0.12243E 05	0.93775E-03	0.262E-04	75.					
24	85.16	0.20669E 07	108.3	0.12268E 05	0.97765E-03	0.274E-04	75.					
25	86.20	0.20934E 07	107.5	0.12293E 05	0.92275E-03	0.269E-04	75.					
26	87.23	0.21199E 07	106.9	0.12319E 05	0.10159E-02	0.280E-04	75.					
27	88.26	0.21463E 07	107.9	0.12346E 05	0.10409E-02	0.278E-04	75.					
28	89.29	0.21727E 07	108.2	0.12373E 05	0.10354E-02	0.272E-04	75.					
29	90.32	0.21991E 07	107.7	0.12402E 05	0.11445E-02	0.277E-04	75.					
30	91.35	0.22256E 07	108.1	0.12432E 05	0.11022E-02	0.284E-04	75.					
31	92.38	0.22520E 07	108.1	0.12461E 05	0.11030E-02	0.280E-04	75.					
32	93.41	0.22785E 07	107.6	0.12490E 05	0.11030E-02	0.285E-04	75.					
33	94.45	0.23051E 07	107.6	0.12520E 05	0.11141E-02	0.281E-04	75.					
34	95.48	0.23315E 07	107.1	0.12549E 05	0.11208E-02	0.278E-04	75.					
35	96.51	0.23579E 07	107.3	0.12579E 05	0.11591E-02	0.303E-04	75.					
36	97.54	0.23844E 07	106.8	0.12610E 05	0.11549E-02	0.328E-04	75.					

FOLLOWING IS THE DATA FOR THETA=0 AND THETA=1, WHICH WAS OBTAINED BY LINEAR SUPERPOSITION THEORY.
THIS DATA WAS PRODUCED FROM RUN 071773 AND RUN 071873-1
FOR THE DETAIL CHANGES OF PROPERTIES AND BOUNDARY CONDITIONS, PLEASE SEE THE ABOVE TWO RUNS

PLATE	REXCOL	RE DEL2	ST(TH=0)	REXHOT	RE DEL2	ST(TH=1)	ETA	STCR	F-COL	STHR	F-HOT	PHI-1
1	1182247.0	101.6	0.003926	1172427.0	99.1	0.003861	UUUUU	UUUUU	0.0000	UUUUUUU	0.0000	UUUUU
2	1233986.0	305.2	0.003944	1223736.0	712.4	0.003260	0.173	1.021	0.0174	1.159	0.0168	3.286
3	1285726.0	515.7	0.004193	1275046.0	1746.0	0.003193	0.238	1.216	0.0168	1.206	0.0171	3.488
4	1337465.0	733.0	0.004206	1326356.0	2773.4	0.002946	0.299	1.314	0.0172	1.160	0.0169	3.483
5	1389205.0	946.5	0.004048	1377666.0	3781.0	0.002690	0.336	1.336	0.0170	1.093	0.0168	3.444
6	1440944.0	1154.4	0.003990	1428975.0	4778.6	0.002380	0.404	1.377	0.0171	0.992	0.0170	3.383
7	1492684.0	1356.9	0.003836	1480285.0	5768.8	0.002267	0.409	1.373	0.0170	0.966	0.0169	3.375
8	1544423.0	1551.3	0.003679	1531595.0	6737.3	0.002077	0.436	1.359	0.0173	0.902	0.0165	3.269
9	1596163.0	1738.5	0.003558	1582904.0	7686.7	0.001849	0.480	1.351	0.0173	0.817	0.0166	3.186
10	1647902.0	1921.4	0.003511	1634214.0	8634.0	0.001728	0.508	1.366	0.0170	0.775	0.0168	3.171
11	1699641.0	2099.4	0.003368	1685524.0	9572.1	0.001553	0.539	1.339	0.0170	0.706	0.0165	3.062
12	1751381.0	2272.3	0.003317	1736834.0	10491.8	0.001346	0.594	1.345	0.0170	0.620	0.0164	2.933
13	1790703.0	2395.7	0.002815	1775829.0	10966.1	0.001380	0.510	1.158		0.642		
14	1817349.0	2466.9	0.002524	1802254.0	11000.9	0.001256	0.502	1.047		0.588		
15	1843995.0	2531.1	0.002290	1828678.0	11032.7	0.001145	0.500	0.958		0.539		
16	1870770.0	2589.9	0.002116	1855231.0	11062.4	0.001099	0.481	0.893		0.520		
17	1897545.0	2644.5	0.001982	1881783.0	11090.9	0.001055	0.468	0.843		0.502		
18	1924191.0	2697.3	0.001976	1908208.0	11118.5	0.001035	0.476	0.847		0.495		
19	1950836.0	2748.8	0.001885	1934632.0	11146.1	0.001049	0.444	0.814		0.504		
20	1977482.0	2798.1	0.001814	1961057.0	11173.5	0.001025	0.435	0.789		0.495		
21	2004128.0	2847.6	0.001892	1987482.0	11201.0	0.001057	0.442	0.829		0.513		
22	2030774.0	2896.8	0.001800	2013906.0	11229.1	0.001065	0.408	0.794		0.520		
23	2057420.0	2944.3	0.001760	2040331.0	11256.7	0.001024	0.418	0.781		0.502		
24	2084195.0	2992.1	0.001820	2066883.0	11284.4	0.001066	0.414	0.813		0.525		
25	2110970.0	3039.5	0.001735	2093436.0	11311.8	0.001008	0.419	0.780		0.498		
26	2137616.0	3086.9	0.001817	2119861.0	11339.7	0.001100	0.394	0.821		0.546		
27	2164262.0	3136.0	0.001866	2146285.0	11369.2	0.001128	0.396	0.848		0.562		
28	2190908.0	3185.2	0.001825	2172710.0	11398.9	0.001118	0.387	0.834		0.560		
29	2217554.0	3235.9	0.001973	2199134.0	11430.0	0.001232	0.376	0.907		0.619		
30	2244200.0	3286.6	0.001826	2225559.0	11461.9	0.001178	0.355	0.844		0.594		
31	2270845.0	3335.7	0.001857	2251983.0	11493.1	0.001182	0.363	0.863		0.599		
32	2297620.0	3384.1	0.001773	2278536.0	11524.3	0.001173	0.338	0.828		0.596		
33	2324396.0	3432.1	0.001820	2305089.0	11555.5	0.001188	0.347	0.854		0.606		
34	2351041.0	3480.5	0.001814	2331513.0	11587.0	0.001194	0.342	0.855		0.611		
35	2377687.0	3529.6	0.001862	2357938.0	11619.1	0.001233	0.338	0.882		0.633		
36	2404333.0	3579.0	0.001843	2384362.0	11651.7	0.001227	0.334	0.877		0.632		

Error

An error occurred while processing this page. See the system log for more details.

STANTON NUMBER DATA RUN 072573 *** DISCRETE HOLE RIG *** NAS-3-14336

TINF= 83.4 UINF= 53.8 XVO= 4.600 RHO= 0.07210 CP= 0.242 VISC= 0.17153E-03 PR=0.715
DISTANCE FROM ORIGIN OF BL TO 1ST PLATE=44.700 P/D= 5
UNCERTAINTY IN REX=26157. UNCERTAINTY IN F=0.03027 IN RATIO

** M=0.65, HOT RUN, HIGH RE, STEP T-WALL AT 1ST PLATE

PLATE	X	REX	TO	REENTH	STANTON NO	DST	DREEN	M	F	T2	THETA	DTH
1	50.30	0.11954E 07	109.0	0.94287E 02	0.36046E-02	0.620E-04	2.					
2	52.30	0.12477E 07	109.1	0.68672E 03	0.34091E-02	0.605E-04	14.	0.63	0.0205	103.0	0.761	0.012
3	54.30	0.13000E 07	109.2	0.16912E 04	0.35108E-02	0.609E-04	25.	0.63	0.0204	103.4	0.775	0.012
4	56.30	0.13523E 07	109.1	0.27205E 04	0.33292E-02	0.600E-04	32.	0.63	0.0204	104.4	0.815	0.013
5	58.30	0.14046E 07	109.1	0.37823E 04	0.30704E-02	0.585E-04	39.	0.64	0.0208	105.1	0.844	0.013
6	60.30	0.14570E 07	109.1	0.48451E 04	0.28099E-02	0.571E-04	45.	0.63	0.0204	105.1	0.846	0.013
7	62.30	0.15093E 07	109.1	0.58841E 04	0.25736E-02	0.558E-04	50.	0.61	0.0198	105.6	0.863	0.013
8	64.30	0.15616E 07	109.0	0.69326E 04	0.23258E-02	0.547E-04	55.	0.63	0.0203	106.2	0.888	0.013
9	66.30	0.16139E 07	109.0	0.79958E 04	0.20738E-02	0.537E-04	59.	0.62	0.0202	106.4	0.899	0.013
10	68.30	0.16662E 07	109.0	0.90574E 04	0.19220E-02	0.529E-04	64.	0.63	0.0206	106.3	0.896	0.013
11	70.30	0.17185E 07	109.0	0.10108E 05	0.17927E-02	0.524E-04	68.	0.62	0.0202	106.3	0.892	0.013
12	72.30	0.17708E 07	109.0	0.11154E 05	0.15941E-02	0.518E-04	71.	0.64	0.0209	106.1	0.889	0.013
13	73.82	0.18106E 07	108.2	0.11701E 05	0.14586E-02	0.284E-04	73.					
14	74.85	0.18376E 07	108.2	0.11738E 05	0.12731E-02	0.302E-04	73.					
15	75.88	0.18645E 07	109.0	0.11771E 05	0.11556E-02	0.293E-04	73.					
16	76.91	0.18916E 07	109.1	0.11801E 05	0.10826E-02	0.281E-04	73.					
17	77.95	0.19186E 07	109.4	0.11830E 05	0.10458E-02	0.278E-04	73.					
18	78.98	0.19456E 07	109.4	0.11857E 05	0.10030E-02	0.276E-04	73.					
19	80.01	0.19725E 07	109.3	0.11884E 05	0.99680E-03	0.264E-04	73.					
20	81.04	0.19995E 07	109.5	0.11911E 05	0.96929E-03	0.258E-04	73.					
21	82.07	0.20264E 07	109.5	0.11937E 05	0.10017E-02	0.267E-04	73.					
22	83.10	0.20533E 07	109.5	0.11964E 05	0.98992E-03	0.277E-04	73.					
23	84.13	0.20803E 07	109.5	0.11990E 05	0.95891E-03	0.274E-04	73.					
24	85.16	0.21074E 07	109.5	0.12017E 05	0.99265E-03	0.286E-04	73.					
25	86.20	0.21344E 07	108.5	0.12043E 05	0.94862E-03	0.283E-04	73.					
26	87.23	0.21614E 07	108.2	0.12069E 05	0.10137E-02	0.291E-04	73.					
27	88.26	0.21883E 07	109.1	0.12097E 05	0.10593E-02	0.290E-04	73.					
28	89.29	0.22153E 07	109.4	0.12126E 05	0.10540E-02	0.284E-04	73.					
29	90.32	0.22422E 07	109.0	0.12156E 05	0.11596E-02	0.289E-04	73.					
30	91.35	0.22691E 07	109.5	0.12186E 05	0.10943E-02	0.294E-04	73.					
31	92.38	0.22961E 07	109.4	0.12216E 05	0.11187E-02	0.291E-04	73.					
32	93.41	0.23232E 07	109.0	0.12246E 05	0.10953E-02	0.294E-04	73.					
33	94.45	0.23502E 07	108.9	0.12276E 05	0.11259E-02	0.292E-04	73.					
34	95.48	0.23772E 07	108.4	0.12306E 05	0.11343E-02	0.289E-04	73.					
35	96.51	0.24041E 07	108.7	0.12337E 05	0.11575E-02	0.314E-04	73.					
36	97.54	0.24311E 07	108.2	0.12368E 05	0.11609E-02	0.342E-04	73.					

FOLLOWING IS THE DATA FOR THETA=0 AND THETA=1, WHICH WAS OBTAINED BY LINEAR SUPERPOSITION THEORY.
THIS DATA WAS PRODUCED FROM RUN 072473 AND RUN 072573
FOR THE DETAIL CHANGES OF PROPERTIES AND BOUNDARY CONDITIONS, PLEASE SEE THE ABOVE TWO RUNS

PLATE	REXCOL	RE DEL2	ST(TH=0)	REXHOT	RE DEL2	ST(TH=1)	ETA	STCR	F-COL	STHR	F-HOT	PHI-1
1	1202637.0	93.5	0.003743	1195388.0	94.3	0.003605	UUUUU	UUUUU	0.0000	UUUUUUUU	0.0000	UUUUU
2	1255269.0	299.3	0.003887	1247703.0	810.9	0.003259	0.161	1.010	0.0215	1.164	0.0205	3.588
3	1307901.0	512.7	0.004223	1300017.0	2054.6	0.003304	0.218	1.229	0.0214	1.253	0.0204	3.932
4	1360533.0	736.6	0.004282	1352332.0	3292.1	0.003113	0.273	1.342	0.0213	1.230	0.0204	3.993
5	1413165.0	958.9	0.004167	1404647.0	4526.7	0.002868	0.312	1.380	0.0212	1.170	0.0208	4.017
6	1465796.0	1174.3	0.004017	1456961.0	5745.6	0.002589	0.355	1.391	0.0212	1.084	0.0204	3.906
7	1518428.0	1382.2	0.003884	1509276.0	6926.5	0.002366	0.391	1.395	0.0210	1.012	0.0198	3.789
8	1571060.0	1581.5	0.003689	1561591.0	8095.4	0.002155	0.416	1.368	0.0216	0.939	0.0203	3.791
9	1623692.0	1773.9	0.003622	1613905.0	9262.5	0.001899	0.476	1.380	0.0214	0.842	0.0202	3.654
10	1676324.0	1962.1	0.003532	1666220.0	10424.3	0.001735	0.509	1.379	0.0213	0.782	0.0206	3.626
11	1728956.0	2145.7	0.003445	1718534.0	11577.3	0.001593	0.537	1.375	0.0212	0.728	0.0202	3.528
12	1781588.0	2324.1	0.003331	1770849.0	12730.1	0.001377	0.587	1.356	0.0216	0.637	0.0209	3.473
13	1821588.0	2449.4	0.002780	1810608.0	13329.2	0.001228	0.558	1.147		0.574		
14	1848693.0	2520.7	0.002471	1837550.0	13360.2	0.001065	0.569	1.029		0.500		
15	1875799.0	2584.2	0.002210	1864492.0	13387.6	0.000972	0.560	0.928		0.459		
16	1903035.0	2641.6	0.002020	1891565.0	13413.1	0.000919	0.545	0.855		0.437		
17	1930272.0	2694.2	0.001859	1918638.0	13437.7	0.000904	0.514	0.794		0.432		
18	1957378.0	2744.6	0.001855	1945580.0	13461.4	0.000855	0.539	0.798		0.410		
19	1984483.0	2793.5	0.001745	1972522.0	13484.7	0.000866	0.504	0.756		0.418		
20	2011589.0	2839.9	0.001674	1999464.0	13507.8	0.000847	0.494	0.731		0.411		
21	2038694.0	2886.3	0.001744	2026406.0	13530.9	0.000872	0.500	0.767		0.425		
22	2065800.0	2932.4	0.001658	2053348.0	13554.5	0.000874	0.473	0.734		0.428		
23	2092905.0	2977.0	0.001623	2080290.0	13577.6	0.000843	0.481	0.723		0.415		
24	2120142.0	3021.7	0.001677	2107362.0	13600.8	0.000873	0.479	0.752		0.432		
25	2147379.0	3066.4	0.001611	2134435.0	13623.8	0.000833	0.483	0.726		0.414		
26	2174484.0	3110.8	0.001663	2161377.0	13647.2	0.000901	0.459	0.755		0.449		
27	2201590.0	3157.2	0.001756	2188319.0	13672.0	0.000938	0.466	0.801		0.469		
28	2228695.0	3203.9	0.001687	2215261.0	13697.4	0.000944	0.440	0.774		0.474		
29	2255801.0	3251.9	0.001854	2242204.0	13724.1	0.001039	0.440	0.855		0.524		
30	2282906.0	3300.6	0.001735	2269146.0	13751.4	0.000983	0.433	0.805		0.498		
31	2310011.0	3348.1	0.001764	2296088.0	13778.2	0.001006	0.429	0.822		0.512		
32	2337248.0	3394.8	0.001679	2323160.0	13805.2	0.000994	0.408	0.787		0.507		
33	2364485.0	3441.4	0.001751	2350233.0	13832.3	0.001017	0.419	0.825		0.521		
34	2391591.0	3488.7	0.001734	2377175.0	13859.9	0.001030	0.406	0.821		0.529		
35	2418696.0	3536.1	0.001762	2404117.0	13888.0	0.001052	0.403	0.838		0.543		
36	2445801.0	3583.9	0.001759	2431059.0	13916.4	0.001057	0.399	0.841		0.547		

STANTON NUMBER DATA RUN 071873-2 *** DISCRETE HOLE RIG *** NAS-3-14336

TINF= 79.7 UINF= 52.0 XVO= 4.600 RHO= 0.07304 CP= 0.242 VISC= 0.16860E-03 PR=0.715
DISTANCE FROM ORIGIN OF BL TO 1ST PLATE=44.700 P/D= 5
UNCERTAINTY IN REX=25688. UNCERTAINTY IN F=0.03030 IN RATIO

** M=0.5, THETA=1.4, HIGH RE, STEP T-WALL AT 1ST PLATE, ** TEST FOR LINEARITY.

PLATE	X	REX	TO	REENTH	STANTON NO	DST	DREEN	M	F	T2	THETA	DTH
1	50.30	0.11740E 07	108.8	0.97243E 02	0.37855E-02	0.572E-04	2.					
2	52.30	0.12253E 07	108.8	0.84011E 03	0.29917E-02	0.526E-04	19.	0.50	0.0163	119.2	1.357	0.014
3	54.30	0.12767E 07	108.7	0.21573E 04	0.27288E-02	0.515E-04	33.	0.50	0.0163	121.4	1.437	0.015
4	56.30	0.13281E 07	108.8	0.34933E 04	0.23816E-02	0.498E-04	43.	0.51	0.0164	121.4	1.433	0.015
5	58.30	0.13795E 07	108.8	0.48143E 04	0.20550E-02	0.483E-04	51.	0.50	0.0163	121.7	1.440	0.015
6	60.30	0.14308E 07	108.8	0.60847E 04	0.18289E-02	0.475E-04	58.	0.51	0.0167	118.3	1.325	0.014
7	62.30	0.14822E 07	108.8	0.73415E 04	0.15911E-02	0.468E-04	64.	0.51	0.0167	120.6	1.406	0.015
8	64.30	0.15336E 07	108.7	0.86121E 04	0.13622E-02	0.462E-04	69.	0.49	0.0160	121.5	1.440	0.015
9	66.30	0.15850E 07	108.7	0.98431E 04	0.11955E-02	0.458E-04	74.	0.50	0.0161	119.7	1.380	0.015
10	68.30	0.16363E 07	108.7	0.11050E 05	0.10462E-02	0.455E-04	79.	0.51	0.0164	119.4	1.372	0.015
11	70.30	0.16877E 07	108.8	0.12226E 05	0.94881E-03	0.452E-04	83.	0.51	0.0165	117.2	1.291	0.014
12	72.30	0.17391E 07	108.8	0.13339E 05	0.75554E-03	0.448E-04	87.	0.49	0.0158	117.2	1.287	0.014
13	73.82	0.17781E 07	108.3	0.13892E 05	0.91048E-03	0.208E-04	88.					
14	74.85	0.18046E 07	108.2	0.13915E 05	0.82859E-03	0.240E-04	88.					
15	75.88	0.18311E 07	108.9	0.13936E 05	0.74512E-03	0.237E-04	88.					
16	76.91	0.18576E 07	108.9	0.13956E 05	0.75157E-03	0.234E-04	88.					
17	77.95	0.18842E 07	109.1	0.13976E 05	0.73226E-03	0.233E-04	88.					
18	78.98	0.19107E 07	109.2	0.13995E 05	0.71082E-03	0.234E-04	88.					
19	80.01	0.19372E 07	108.9	0.14014E 05	0.76245E-03	0.226E-04	88.					
20	81.04	0.19636E 07	109.1	0.14034E 05	0.73844E-03	0.221E-04	88.					
21	82.07	0.19901E 07	109.2	0.14054E 05	0.75510E-03	0.230E-04	88.					
22	83.10	0.20165E 07	108.8	0.14075E 05	0.81686E-03	0.244E-04	88.					
23	84.13	0.20430E 07	108.9	0.14096E 05	0.77502E-03	0.242E-04	88.					
24	85.16	0.20696E 07	109.0	0.14117E 05	0.78943E-03	0.250E-04	88.					
25	86.20	0.20962E 07	108.3	0.14137E 05	0.76989E-03	0.248E-04	88.					
26	87.23	0.21226E 07	107.5	0.14159E 05	0.88101E-03	0.260E-04	88.					
27	88.26	0.21491E 07	108.6	0.14182E 05	0.84924E-03	0.254E-04	88.					
28	89.29	0.21755E 07	108.8	0.14205E 05	0.88368E-03	0.251E-04	88.					
29	90.32	0.22020E 07	108.3	0.14229E 05	0.96924E-03	0.254E-04	88.					
30	91.35	0.22285E 07	108.6	0.14255E 05	0.95696E-03	0.264E-04	88.					
31	92.38	0.22549E 07	108.6	0.14280E 05	0.94092E-03	0.260E-04	88.					
32	93.41	0.22815E 07	108.0	0.14305E 05	0.97404E-03	0.266E-04	88.					
33	94.45	0.23081E 07	108.1	0.14331E 05	0.96284E-03	0.260E-04	88.					
34	95.48	0.23345E 07	107.5	0.14357E 05	0.98514E-03	0.259E-04	88.					
35	96.51	0.23610E 07	107.7	0.14384E 05	0.10299E-02	0.284E-04	88.					
36	97.54	0.23875E 07	107.3	0.14411E 05	0.10218E-02	0.303E-04	88.					

**** VELOCITY PROFILE AT UINF= 30 FT/SEC, M= 0

DISCRETE HOLE RIG *** NAS-3-14336

VELOCITY PROFILE

UINF= 31.7 FT/SEC X= 53.0 INCHES PORT= 19
TINF= 78.0 DEG F PINF= 2112. PSF

Y(INCHES)	U(FT/SEC)	Y+	U+	UBAR	DU
0.010	10.91	6.9	7.90	0.3443	0.42
0.011	11.45	7.5	8.30	0.3615	0.40
0.012	11.91	8.2	8.63	0.3759	0.38
0.014	13.01	9.6	9.43	0.4107	0.35
0.016	13.86	11.0	10.05	0.4376	0.33
0.018	14.72	12.3	10.67	0.4645	0.31
0.020	15.18	13.7	11.00	0.4790	0.30
0.024	16.29	16.5	11.81	0.5142	0.28
0.028	17.03	19.2	12.34	0.5374	0.27
0.032	17.64	21.9	12.78	0.5568	0.26
0.036	17.98	24.7	13.03	0.5676	0.25
0.040	18.44	27.4	13.37	0.5822	0.25
0.047	19.02	32.2	13.78	0.6002	0.24
0.054	19.49	37.0	14.12	0.6152	0.23
0.065	19.99	44.6	14.49	0.6310	0.23
0.080	20.71	54.9	15.00	0.6535	0.22
0.095	21.11	65.1	15.29	0.6662	0.22
0.110	21.50	75.4	15.58	0.6786	0.21
0.130	22.06	89.1	15.99	0.6963	0.21
0.155	22.51	106.3	16.31	0.7103	0.20
0.185	23.21	126.9	16.82	0.7324	0.20
0.215	23.69	147.4	17.17	0.7478	0.19
0.265	24.58	181.7	17.81	0.7758	0.19
0.315	25.37	216.0	18.39	0.8008	0.18
0.365	26.11	250.3	18.92	0.8242	0.17
0.415	26.83	284.6	19.45	0.8470	0.17
0.465	27.34	318.8	19.81	0.8629	0.17
0.515	28.00	353.1	20.29	0.8838	0.16
0.565	28.60	387.4	20.72	0.9025	0.16
0.615	29.07	421.7	21.07	0.9176	0.16
0.665	29.57	456.0	21.42	0.9332	0.15
0.715	30.08	490.3	21.80	0.9493	0.15
0.765	30.46	524.5	22.07	0.9613	0.15
0.815	30.80	558.8	22.32	0.9723	0.15
0.865	31.10	593.1	22.54	0.9816	0.15
0.915	31.37	627.4	22.73	0.9901	0.15
0.965	31.61	661.7	22.91	0.9977	0.14
1.015	31.64	696.0	22.92	0.9985	0.14
1.065	31.68	730.2	22.96	1.0000	0.14

REX= 0.69242E 06 RED2= 1740. XVO= 9.02 IN.
DEL1= 0.150 IN. DEL2= 0.111IN. H= 1.35
CF2= 0.18971E-02 DXVO= 0.58 DDEL1=0.002 DDEL2=0.001 DCF/2=0.128 IN RATIO

STANTON NUMBER DATA RUN 082273 *** DISCRETE HOLE RIG *** NAS-3-14336

TINF= 76.9 UINF= 31.0 XVO= 6.390 RHO= 0.07377 CP= 0.242 VISC= 0.16643E-03 PR=0.714
DISTANCE FROM ORIGIN OF BL TO 1ST PLATE=42.910 P/D= 5
UNCERTAINTY IN REX=15523.

** M=0. , FLAT PLATE RUN, HIGH RE, STEP T-WALL AT 1ST PLATE

PLATE	X	REX	TO	REENTH	STANTON NO	DST	DREEN	M	F	T2	THETA	DTH
1	50.30	0.68160E 06	103.8	0.73379E 02	0.47272E-02	0.106E-03	2.					
2	52.30	0.71265E 06	103.9	0.20124E 03	0.35096E-02	0.950E-04	3.	0.00	0.0000	103.9	1.000	0.013
3	54.30	0.74370E 06	103.9	0.30661E 03	0.32785E-02	0.931E-04	4.	0.00	0.0000	103.9	1.000	0.013
4	56.30	0.77474E 06	103.9	0.40638E 03	0.31491E-02	0.920E-04	4.	0.00	0.0000	103.9	1.000	0.013
5	58.30	0.80579E 06	103.9	0.50209E 03	0.30164E-02	0.910E-04	5.	0.00	0.0000	103.9	1.000	0.013
6	60.30	0.83583E 06	103.9	0.59429E 03	0.29233E-02	0.905E-04	5.	0.00	0.0000	103.9	1.000	0.013
7	62.30	0.86788E 06	103.8	0.68340E 03	0.28176E-02	0.898E-04	5.	0.00	0.0000	103.8	1.000	0.013
8	64.30	0.89892E 06	103.8	0.76988E 03	0.27535E-02	0.896E-04	6.	0.00	0.0000	103.8	1.000	0.013
9	66.30	0.92997E 06	103.8	0.85473E 03	0.27124E-02	0.892E-04	6.	0.00	0.0000	103.8	1.000	0.013
10	68.30	0.96101E 06	103.8	0.93828E 03	0.26700E-02	0.890E-04	6.	0.00	0.0000	103.8	1.000	0.013
11	70.30	0.99206E 06	103.8	0.10209E 04	0.26525E-02	0.888E-04	7.	0.00	0.0000	103.8	1.000	0.013
12	72.30	0.10231E 07	103.9	0.11012E 04	0.25205E-02	0.877E-04	7.	0.00	0.0000	103.9	1.000	0.013
13	73.82	0.10467E 07	103.5	0.11626E 04	0.27876E-02	0.588E-04	7.					
14	74.85	0.10627E 07	103.4	0.12058E 04	0.26047E-02	0.605E-04	7.					
15	75.88	0.10787E 07	104.0	0.12469E 04	0.25370E-02	0.600E-04	7.					
16	76.91	0.10947E 07	104.1	0.12872E 04	0.24881E-02	0.587E-04	7.					
17	77.95	0.11108E 07	104.2	0.13267E 04	0.24575E-02	0.585E-04	7.					
18	78.98	0.11268E 07	104.0	0.13667E 04	0.25321E-02	0.598E-04	7.					
19	80.01	0.11428E 07	104.0	0.14067E 04	0.24707E-02	0.575E-04	7.					
20	81.04	0.11588E 07	104.2	0.14457E 04	0.23930E-02	0.560E-04	7.					
21	82.07	0.11748E 07	104.0	0.14850E 04	0.25223E-02	0.586E-04	7.					
22	83.10	0.11908E 07	104.2	0.15243E 04	0.23881E-02	0.581E-04	7.					
23	84.13	0.12067E 07	104.0	0.15619E 04	0.23076E-02	0.571E-04	7.					
24	85.16	0.12228E 07	103.8	0.15994E 04	0.23786E-02	0.604E-04	7.					
25	86.20	0.12389E 07	102.0	0.16356E 04	0.21514E-02	0.576E-04	8.					
26	87.23	0.12549E 07	102.4	0.16721E 04	0.24004E-02	0.607E-04	8.					
27	88.26	0.12708E 07	103.7	0.17108E 04	0.24403E-02	0.603E-04	8.					
28	89.29	0.12868E 07	104.2	0.17489E 04	0.23201E-02	0.574E-04	8.					
29	90.32	0.13028E 07	103.8	0.17879E 04	0.25553E-02	0.598E-04	8.					
30	91.35	0.13188E 07	104.6	0.18267E 04	0.22803E-02	0.574E-04	8.					
31	92.38	0.13348E 07	104.5	0.18636E 04	0.23368E-02	0.572E-04	8.					
32	93.41	0.13509E 07	104.3	0.18998E 04	0.21902E-02	0.559E-04	8.					
33	94.45	0.13669E 07	104.2	0.19352E 04	0.22272E-02	0.557E-04	8.					
34	95.48	0.13829E 07	103.5	0.19709E 04	0.22284E-02	0.553E-04	8.					
35	96.51	0.13989E 07	103.9	0.20065E 04	0.22236E-02	0.586E-04	8.					
36	97.54	0.14149E 07	103.2	0.20420E 04	0.22140E-02	0.646E-04	8.					

STANTON NUMBER DATA RUN 082073 *** DISCRETE HOLE RIG *** NAS-3-14336

TINF= 78.8 UINF= 30.0 XVO= 6.390 RHO= 0.07317 CP= 0.242 VISC= 0.16824E-03 PR=0.714
DISTANCE FROM ORIGIN OF BL TO 1ST PLATE=42.910 P/D= 5
UNCERTAINTY IN REX=14863. UNCERTAINTY IN F=0.03257 IN RATIO

** M=0.2, COLD RUN, HIGH RE, STEP T-WALL AT 1ST PLATE.

PLATE	X	REX	TO	REENTH	STANTON NO	DST	DREEN	M	F	T2	THETA	DTH
1	50.30	0.65264E 06	105.0	0.72454E 02	0.48748E-02	0.115E-03	2.					
2	52.30	0.68236E 06	105.1	0.22427E 03	0.41601E-02	0.107E-03	3.	0.20	0.0066	83.5	0.178	0.010
3	54.30	0.71209E 06	105.2	0.38383E 03	0.41815E-02	0.107E-03	4.	0.21	0.0067	83.6	0.190	0.010
4	56.30	0.74181E 06	105.2	0.54295E 03	0.40722E-02	0.106E-03	5.	0.20	0.0065	83.8	0.189	0.010
5	58.30	0.77154E 06	105.1	0.69809E 03	0.38964E-02	0.105E-03	6.	0.20	0.0066	83.7	0.186	0.010
6	60.30	0.80127E 06	105.1	0.84683E 03	0.36873E-02	0.103E-03	6.	0.20	0.0065	83.7	0.184	0.010
7	62.30	0.83099E 06	105.1	0.99216E 03	0.36070E-02	0.102E-03	7.	0.21	0.0069	83.8	0.188	0.010
8	64.30	0.86072E 06	105.1	0.11360E 04	0.34868E-02	0.101E-03	7.	0.21	0.0068	83.8	0.189	0.010
9	66.30	0.89044E 06	105.1	0.12769E 04	0.34188E-02	0.100E-03	8.	0.21	0.0067	83.9	0.191	0.010
10	68.30	0.92017E 06	105.2	0.14159E 04	0.33644E-02	0.996E-04	8.	0.21	0.0067	83.9	0.192	0.010
11	70.30	0.94990E 06	105.4	0.15532E 04	0.32980E-02	0.987E-04	9.	0.21	0.0069	83.8	0.188	0.010
12	72.30	0.97962E 06	105.2	0.16877E 04	0.31757E-02	0.982E-04	9.	0.20	0.0066	84.0	0.197	0.010
13	73.82	0.10022E 07	104.6	0.17774E 04	0.30220E-02	0.654E-04	9.					
14	74.85	0.10175E 07	104.6	0.18213E 04	0.27140E-02	0.653E-04	9.					
15	75.88	0.10328E 07	105.4	0.18617E 04	0.25479E-02	0.631E-04	9.					
16	76.91	0.10482E 07	105.5	0.18998E 04	0.24356E-02	0.607E-04	9.					
17	77.95	0.10636E 07	105.7	0.19363E 04	0.23152E-02	0.592E-04	9.					
18	78.98	0.10789E 07	105.4	0.19725E 04	0.24161E-02	0.609E-04	10.					
19	80.01	0.10942E 07	105.6	0.20085E 04	0.22804E-02	0.573E-04	10.					
20	81.04	0.11095E 07	105.8	0.20428E 04	0.21894E-02	0.555E-04	10.					
21	82.07	0.11248E 07	105.6	0.20774E 04	0.23257E-02	0.582E-04	10.					
22	83.10	0.11401E 07	105.9	0.21117E 04	0.21591E-02	0.575E-04	10.					
23	84.13	0.11555E 07	105.6	0.21446E 04	0.21334E-02	0.571E-04	10.					
24	85.16	0.11708E 07	105.6	0.21774E 04	0.21489E-02	0.595E-04	10.					
25	86.20	0.11862E 07	104.0	0.22091E 04	0.19764E-02	0.574E-04	10.					
26	87.23	0.12015E 07	104.4	0.22408E 04	0.21651E-02	0.596E-04	10.					
27	88.26	0.12168E 07	105.5	0.22743E 04	0.22084E-02	0.592E-04	10.					
28	89.29	0.12321E 07	105.9	0.23075E 04	0.21221E-02	0.570E-04	10.					
29	90.32	0.12475E 07	105.6	0.23416E 04	0.23220E-02	0.589E-04	10.					
30	91.35	0.12628E 07	106.3	0.23754E 04	0.20906E-02	0.573E-04	10.					
31	92.38	0.12781E 07	106.1	0.24078E 04	0.21411E-02	0.570E-04	10.					
32	93.41	0.12935E 07	106.0	0.24398E 04	0.20361E-02	0.563E-04	10.					
33	94.45	0.13088E 07	105.9	0.24713E 04	0.20777E-02	0.560E-04	10.					
34	95.48	0.13241E 07	105.4	0.25031E 04	0.20645E-02	0.553E-04	10.					
35	96.51	0.13395E 07	105.6	0.25349E 04	0.20803E-02	0.591E-04	10.					
36	97.54	0.13548E 07	105.0	0.25665E 04	0.20418E-02	0.652E-04	10.					

STANTON NUMBER DATA RUN 082173 *** DISCRETE HOLE RIG *** NAS-3-14336

TINF= 79.1 UINF= 30.3 XVO= 6.390 RHO= 0.07350 CP= 0.242 VISC= 0.16762E-03 PR=0.714
DISTANCE FROM ORIGIN OF BL TO 1ST PLATE=42.910 P/D= 5
UNCERTAINTY IN REX=15072. UNCERTAINTY IN F=0.03245 IN RATIO

** M=0.2, HOT RUN, HIGH RE, STEP T-WALL AT 1ST PLATE.

PLATE	X	REX	TO	REENTH	STANTON NO	DST	DREEN	M	F	T2	THETA	DTH
1	50.30	0.66182E 06	108.2	0.70832E 02	0.46995E-02	0.104E-03	2.					
2	52.30	0.69196E 06	108.2	0.26170E 03	0.35162E-02	0.922E-04	4.	0.18	0.0057	101.6	0.774	0.011
3	54.30	0.72211E 06	108.2	0.49703E 03	0.33932E-02	0.911E-04	5.	0.17	0.0054	102.0	0.785	0.011
4	56.30	0.75225E 06	108.3	0.72354E 03	0.31960E-02	0.892E-04	6.	0.16	0.0053	102.4	0.796	0.011
5	58.30	0.78239E 06	108.2	0.94752E 03	0.29713E-02	0.877E-04	8.	0.17	0.0056	102.6	0.806	0.011
6	60.30	0.81254E 06	108.2	0.11712E 04	0.27576E-02	0.861E-04	8.	0.18	0.0059	101.8	0.791	0.011
7	62.30	0.84268E 06	108.1	0.13862E 04	0.26396E-02	0.856E-04	9.	0.16	0.0052	102.7	0.813	0.011
8	64.30	0.87283E 06	108.1	0.15977E 04	0.25132E-02	0.848E-04	10.	0.17	0.0054	103.8	0.854	0.011
9	66.30	0.90297E 06	108.1	0.18101E 04	0.24554E-02	0.844E-04	11.	0.16	0.0053	103.6	0.847	0.011
10	68.30	0.93311E 06	108.1	0.20281E 04	0.23887E-02	0.839E-04	12.	0.18	0.0058	104.6	0.879	0.011
11	70.30	0.96326E 06	108.1	0.22525E 04	0.22831E-02	0.832E-04	12.	0.17	0.0056	105.4	0.906	0.012
12	72.30	0.99340E 06	108.2	0.24708E 04	0.20549E-02	0.816E-04	13.	0.16	0.0052	107.6	0.980	0.012
13	73.82	0.10163E 07	107.8	0.25959E 04	0.23300E-02	0.511E-04	13.					
14	74.85	0.10318E 07	107.7	0.26309E 04	0.21739E-02	0.535E-04	13.					
15	75.88	0.10474E 07	108.5	0.26634E 04	0.20084E-02	0.517E-04	13.					
16	76.91	0.10630E 07	108.5	0.26945E 04	0.19940E-02	0.508E-04	13.					
17	77.95	0.10786E 07	108.7	0.27253E 04	0.19604E-02	0.504E-04	13.					
18	78.98	0.10941E 07	108.9	0.27553E 04	0.19085E-02	0.501E-04	13.					
19	80.01	0.11096E 07	108.7	0.27853E 04	0.19455E-02	0.489E-04	13.					
20	81.04	0.11251E 07	108.9	0.28150E 04	0.18802E-02	0.477E-04	13.					
21	82.07	0.11407E 07	108.9	0.28444E 04	0.18998E-02	0.489E-04	13.					
22	83.10	0.11562E 07	108.7	0.28741E 04	0.19278E-02	0.506E-04	13.					
23	84.13	0.11717E 07	108.7	0.29034E 04	0.18395E-02	0.495E-04	13.					
24	85.16	0.11873E 07	108.9	0.29319E 04	0.18304E-02	0.509E-04	13.					
25	86.20	0.12029E 07	107.6	0.29597E 04	0.17469E-02	0.496E-04	13.					
26	87.23	0.12184E 07	107.5	0.29885E 04	0.19518E-02	0.523E-04	13.					
27	88.26	0.12340E 07	108.7	0.30181E 04	0.18627E-02	0.507E-04	14.					
28	89.29	0.12495E 07	108.9	0.30471E 04	0.18579E-02	0.497E-04	14.					
29	90.32	0.12650E 07	108.5	0.30772E 04	0.20272E-02	0.513E-04	14.					
30	91.35	0.12805E 07	109.0	0.31078E 04	0.19024E-02	0.511E-04	14.					
31	92.38	0.12961E 07	109.0	0.31371E 04	0.18709E-02	0.501E-04	14.					
32	93.41	0.13117E 07	108.5	0.31662E 04	0.18779E-02	0.507E-04	14.					
33	94.45	0.13273E 07	108.6	0.31953E 04	0.18577E-02	0.498E-04	14.					
34	95.48	0.13428E 07	108.1	0.32241E 04	0.18569E-02	0.492E-04	14.					
35	96.51	0.13583E 07	108.3	0.32532E 04	0.18828E-02	0.528E-04	14.					
36	97.54	0.13738E 07	107.7	0.32823E 04	0.18557E-02	0.574E-04	14.					

FOLLOWING IS THE DATA FOR THETA=0 AND THETA=1, WHICH WAS OBTAINED BY LINEAR SUPERPOSITION THEORY.
THIS DATA WAS PRODUCED FROM RUN 082073 AND RUN 082173
FOR THE DETAIL CHANGES OF PROPERTIES AND BOUNDARY CONDITIONS, PLEASE SEE THE ABOVE TWO RUNS

PLATE	REXCOL	RE DEL2	ST(TH=0)	REXHOT	RE DEL2	ST(TH=1)	ETA	STCR	F-COL	STHR	F-HOT	PHI-1
1	652635.8	72.5	0.004875	661816.6	70.8	0.004700	UUUUU	UUUUU	0.0000	UUUUUUU	0.0000	UUUUU
2	682361.9	209.6	0.004352	691960.9	277.6	0.003273	0.248	1.009	0.0066	1.042	0.0057	1.805
3	712088.0	339.9	0.004416	722105.1	542.1	0.003113	0.295	1.147	0.0067	1.053	0.0054	1.819
4	741814.1	470.2	0.004346	752249.4	793.7	0.002900	0.333	1.215	0.0065	1.023	0.0053	1.793
5	771540.1	596.8	0.004173	782393.6	1041.4	0.002683	0.357	1.233	0.0066	0.976	0.0056	1.807
6	801266.3	717.9	0.003973	812537.8	1291.3	0.002417	0.392	1.227	0.0065	0.903	0.0059	1.782
7	830992.3	834.8	0.003398	842682.1	1531.0	0.002351	0.397	1.249	0.0069	0.897	0.0052	1.707
8	860718.4	948.7	0.003764	872826.3	1761.6	0.002299	0.389	1.245	0.0068	0.895	0.0054	1.740
9	890444.4	1059.7	0.003699	902970.6	1991.6	0.002231	0.397	1.257	0.0067	0.883	0.0053	1.728
10	920170.6	1168.7	0.003637	933114.8	2226.5	0.002217	0.390	1.266	0.0067	0.892	0.0058	1.816
11	949896.6	1275.7	0.003563	963259.1	2464.8	0.002150	0.397	1.268	0.0069	0.877	0.0056	1.785
12	979622.7	1380.1	0.003458	993403.3	2690.2	0.002026	0.414	1.255	0.0066	0.837	0.0052	1.682
13	1002214.0	1456.1	0.003221	1016313.0	2815.2	0.002158	0.330	1.186		0.900		
14	1017523.0	1502.8	0.002870	1031837.0	2847.8	0.002040	0.289	1.066		0.856		
15	1032832.0	1545.5	0.002703	1047361.0	2878.2	0.001874	0.307	1.013		0.791		
16	1048215.0	1585.9	0.002563	1062961.0	2907.5	0.001884	0.265	0.968		0.799		
17	1063598.0	1624.1	0.002417	1078560.0	2936.6	0.001872	0.226	0.920		0.799		
18	1078907.0	1662.2	0.002562	1094084.0	2965.0	0.001782	0.304	0.983		0.764		
19	1094216.0	1700.1	0.002377	1109609.0	2993.4	0.001862	0.217	0.919		0.803		
20	1109525.0	1735.7	0.002278	1125133.0	3021.9	0.001803	0.208	0.887		0.781		
21	1124834.0	1772.0	0.002448	1140658.0	3049.8	0.001794	0.267	0.960		0.781		
22	1140143.0	1807.8	0.002226	1156182.0	3078.3	0.001870	0.160	0.878		0.818		
23	1155452.0	1841.8	0.002218	1171706.0	3106.6	0.001767	0.204	0.881		0.776		
24	1170835.0	1876.0	0.002241	1187306.0	3133.9	0.001751	0.218	0.896		0.773		
25	1186218.0	1908.8	0.002042	1202905.0	3160.6	0.001690	0.173	0.822		0.749		
26	1201527.0	1941.6	0.002227	1218429.0	3188.5	0.001899	0.147	0.901		0.845		
27	1216836.0	1976.3	0.002308	1233954.0	3217.1	0.001777	0.230	0.939		0.794		
28	1232145.0	2010.8	0.002198	1249478.0	3244.8	0.001792	0.185	0.900		0.804		
29	1247454.0	2046.1	0.002407	1265003.0	3273.9	0.001954	0.188	0.990		0.880		
30	1262763.0	2081.0	0.002145	1280527.0	3303.6	0.001856	0.135	0.887		0.839		
31	1278072.0	2114.5	0.002219	1296051.0	3332.0	0.001804	0.187	0.923		0.819		
32	1293455.0	2147.4	0.002082	1311651.0	3360.3	0.001839	0.117	0.870		0.838		
33	1308838.0	2179.8	0.002141	1327250.0	3388.6	0.001803	0.158	0.899		0.825		
34	1324147.0	2212.5	0.002124	1342774.0	3416.6	0.001805	0.150	0.897		0.829		
35	1339456.0	2245.1	0.002138	1358299.0	3444.9	0.001834	0.142	0.907		0.845		
36	1354765.0	2277.6	0.002095	1373823.0	3473.2	0.001809	0.136	0.893		0.837		

STANTON NUMBER DATA RUN 082473 *** DISCRETE HOLE RIG *** NAS-3-14336

TINF= 77.7 UINF= 31.0 XVO= 6.390 RHO= 0.07314 CP= 0.242 VISC= 0.16801E-03 PR=0.714
DISTANCE FROM ORIGIN OF BL TO 1ST PLATE=42.910 P/D= 5
UNCERTAINTY IN REX=15370. UNCERTAINTY IN F=0.03228 IN RATIO

** M=0.8, COLD RUN, HIGH RE, STEP T-WALL AT 1ST PLATE.

PLATE	X	REX	TO	REENTH	STANTON NO	DST	DREEN	M	F	T2	THETA	DTH
1	50.30	0.67488E 06	103.8	0.72093E 02	0.46906E-02	0.109E-03	2.					
2	52.30	0.70562E 06	103.8	0.24641E 03	0.45875E-02	0.108E-03	5.	0.75	0.0242	79.9	0.085	0.010
3	54.30	0.73636E 06	103.8	0.45478E 03	0.49812E-02	0.112E-03	7.	0.73	0.0237	79.8	0.081	0.010
4	56.30	0.76709E 06	103.9	0.67148E 03	0.50957E-02	0.113E-03	9.	0.75	0.0243	79.9	0.086	0.010
5	58.30	0.79783E 06	103.9	0.88933E 03	0.49268E-02	0.111E-03	11.	0.74	0.0239	79.9	0.086	0.010
6	60.30	0.82857E 06	103.9	0.10987E 04	0.47156E-02	0.109E-03	12.	0.74	0.0239	79.8	0.081	0.010
7	62.30	0.85931E 06	103.9	0.13032E 04	0.44294E-02	0.106E-03	14.	0.73	0.0237	80.1	0.094	0.010
8	64.30	0.89005E 06	103.8	0.15048E 04	0.41676E-02	0.104E-03	15.	0.75	0.0243	80.1	0.094	0.010
9	66.30	0.92079E 06	103.7	0.16993E 04	0.39869E-02	0.103E-03	16.	0.74	0.0241	80.0	0.091	0.010
10	68.30	0.95153E 06	103.8	0.18887E 04	0.38873E-02	0.102E-03	17.	0.75	0.0244	80.1	0.092	0.010
11	70.30	0.98227E 06	103.8	0.20722E 04	0.37120E-02	0.999E-04	18.	0.74	0.0240	80.0	0.088	0.010
12	72.30	0.10130E 07	103.9	0.22519E 04	0.36169E-02	0.988E-04	19.	0.75	0.0243	80.1	0.093	0.010
13	73.82	0.10364E 07	102.7	0.23671E 04	0.31386E-02	0.658E-04	19.					
14	74.85	0.10522E 07	102.7	0.24138E 04	0.27604E-02	0.650E-04	19.					
15	75.88	0.10680E 07	103.7	0.24547E 04	0.24014E-02	0.600E-04	19.					
16	76.91	0.10839E 07	104.0	0.24909E 04	0.21600E-02	0.556E-04	19.					
17	77.95	0.10998E 07	104.3	0.25237E 04	0.19817E-02	0.532E-04	19.					
18	78.98	0.11157E 07	104.3	0.25550E 04	0.19706E-02	0.532E-04	19.					
19	80.01	0.11315E 07	104.5	0.25851E 04	0.18278E-02	0.496E-04	19.					
20	81.04	0.11473E 07	104.7	0.26135E 04	0.17578E-02	0.481E-04	19.					
21	82.07	0.11632E 07	104.5	0.26420E 04	0.18377E-02	0.500E-04	19.					
22	83.10	0.11790E 07	104.7	0.26702E 04	0.17189E-02	0.502E-04	19.					
23	84.13	0.11948E 07	104.5	0.26973E 04	0.16960E-02	0.500E-04	19.					
24	85.16	0.12107E 07	104.4	0.27244E 04	0.17234E-02	0.528E-04	19.					
25	86.20	0.12266E 07	102.6	0.27510E 04	0.16375E-02	0.523E-04	19.					
26	87.23	0.12425E 07	103.0	0.27781E 04	0.17830E-02	0.535E-04	19.					
27	88.26	0.12583E 07	104.2	0.28066E 04	0.18115E-02	0.528E-04	19.					
28	89.29	0.12741E 07	104.6	0.28349E 04	0.17585E-02	0.510E-04	19.					
29	90.32	0.12900E 07	104.1	0.28647E 04	0.20067E-02	0.533E-04	19.					
30	91.35	0.13058E 07	104.8	0.28947E 04	0.17747E-02	0.521E-04	19.					
31	92.38	0.13216E 07	104.7	0.29232E 04	0.18186E-02	0.516E-04	19.					
32	93.41	0.13375E 07	104.5	0.29515E 04	0.17523E-02	0.515E-04	19.					
33	94.45	0.13534E 07	104.4	0.29796E 04	0.17979E-02	0.513E-04	19.					
34	95.48	0.13693E 07	103.8	0.30082E 04	0.18153E-02	0.510E-04	19.					
35	96.51	0.13851E 07	104.1	0.30369E 04	0.18052E-02	0.546E-04	19.					
36	97.54	0.14009E 07	103.3	0.30656E 04	0.18116E-02	0.616E-04	19.					

STANTON NUMBER DATA RUN 082773 *** DISCRETE HOLE RIG *** NAS-3-14336

TINF= 78.8 UINF= 31.0 XVO= 6.390 RHO= 0.07319 CP= 0.242 VISC= 0.16809E-03 PR=0.715
DISTANCE FROM ORIGIN OF BL TO 1ST PLATE=42.910 P/D= 5
UNCERTAINTY IN REX=15394. UNCERTAINTY IN F=0.03225 IN RATIO

** M=0.8, HOT RUN, HIGH RE, STEP T-WALL AT 1ST PLATE.

PLATE	X	REX	TO	REENTH	STANTON NO	DST	DREEN	M	F	T2	THETA	DTH
1	50.30	0.67594E 06	108.2	0.71660E 02	0.46551E-02	0.998E-04	2.					
2	52.30	0.70673E 06	108.3	0.54239E 03	0.41089E-02	0.944E-04	12.	0.73	0.0235	106.1	0.927	0.012
3	54.30	0.73752E 06	108.2	0.13651E 04	0.41592E-02	0.950E-04	21.	0.74	0.0238	107.6	0.980	0.012
4	56.30	0.76831E 06	108.4	0.22034E 04	0.40343E-02	0.935E-04	27.	0.73	0.0236	107.5	0.971	0.012
5	58.30	0.79910E 06	108.3	0.30289E 04	0.36588E-02	0.903E-04	33.	0.72	0.0235	107.8	0.982	0.012
6	60.30	0.82988E 06	108.3	0.38263E 04	0.32656E-02	0.871E-04	37.	0.75	0.0243	105.3	0.899	0.011
7	62.30	0.86067E 06	108.2	0.46155E 04	0.28641E-02	0.842E-04	41.	0.75	0.0243	107.0	0.958	0.012
8	64.30	0.89146E 06	108.3	0.54109E 04	0.25430E-02	0.819E-04	44.	0.72	0.0234	107.7	0.980	0.012
9	66.30	0.92225E 06	108.3	0.61734E 04	0.22953E-02	0.803E-04	48.	0.71	0.0232	106.4	0.938	0.012
10	68.30	0.95303E 06	108.2	0.69318E 04	0.21325E-02	0.795E-04	51.	0.76	0.0245	106.5	0.942	0.012
11	70.30	0.98382E 06	108.2	0.76970E 04	0.19337E-02	0.784E-04	53.	0.78	0.0252	105.1	0.895	0.011
12	72.30	0.10146E 07	108.3	0.84379E 04	0.17535E-02	0.773E-04	56.	0.75	0.0244	105.3	0.900	0.011
13	73.82	0.10380E 07	107.6	0.88158E 04	0.17046E-02	0.408E-04	57.					
14	74.85	0.10539E 07	107.7	0.88407E 04	0.14383E-02	0.431E-04	57.					
15	75.88	0.10697E 07	108.5	0.88619E 04	0.12260E-02	0.412E-04	57.					
16	76.91	0.10857E 07	108.7	0.88806E 04	0.11308E-02	0.396E-04	57.					
17	77.95	0.11016E 07	108.9	0.88980E 04	0.10635E-02	0.390E-04	57.					
18	78.98	0.11174E 07	109.0	0.89147E 04	0.10376E-02	0.391E-04	57.					
19	80.01	0.11333E 07	109.0	0.89309E 04	0.10149E-02	0.370E-04	57.					
20	81.04	0.11492E 07	109.1	0.89467E 04	0.97625E-03	0.361E-04	57.					
21	82.07	0.11650E 07	109.1	0.89626E 04	0.10168E-02	0.376E-04	57.					
22	83.10	0.11809E 07	109.0	0.89786E 04	0.10003E-02	0.391E-04	57.					
23	84.13	0.11967E 07	108.9	0.89943E 04	0.97517E-03	0.389E-04	57.					
24	85.16	0.12127E 07	109.0	0.90098E 04	0.97663E-03	0.406E-04	57.					
25	86.20	0.12286E 07	107.7	0.90248E 04	0.92200E-03	0.401E-04	57.					
26	87.23	0.12444E 07	107.7	0.90406E 04	0.10706E-02	0.414E-04	57.					
27	88.26	0.12603E 07	108.7	0.90575E 04	0.10602E-02	0.407E-04	57.					
28	89.29	0.12762E 07	109.0	0.90743E 04	0.10469E-02	0.396E-04	57.					
29	90.32	0.12920E 07	108.6	0.90923E 04	0.12228E-02	0.407E-04	57.					
30	91.35	0.13079E 07	109.0	0.91108E 04	0.11113E-02	0.412E-04	57.					
31	92.38	0.13237E 07	109.0	0.91284E 04	0.11092E-02	0.405E-04	57.					
32	93.41	0.13397E 07	108.7	0.91462E 04	0.11253E-02	0.413E-04	57.					
33	94.45	0.13556E 07	108.6	0.91641E 04	0.11322E-02	0.404E-04	57.					
34	95.48	0.13714E 07	108.2	0.91823E 04	0.11601E-02	0.401E-04	57.					
35	96.51	0.13873E 07	108.3	0.92009E 04	0.11790E-02	0.439E-04	57.					
36	97.54	0.14032E 07	107.7	0.92195E 04	0.11667E-02	0.477E-04	57.					

FOLLOWING IS THE DATA FOR THETA=0 AND THETA=1, WHICH WAS OBTAINED BY LINEAR SUPERPOSITION THEORY.
THIS DATA WAS PRODUCED FROM RUN 082473 AND RUN 082773
FOR THE DETAIL CHANGES OF PROPERTIES AND BOUNDARY CONDITIONS, PLEASE SEE THE ABOVE TWO RUNS

PLATE	REXCOL	RE DEL2	ST(TH=0)	REXHOT	RE DEL2	ST(TH=1)	ETA	STCR	F-COL	STHR	F-HOT	PHI-1
1	674877.1	72.1	0.004691	675944.3	71.7	0.004655	UUUUU	UUUUU	0.0000	UUUUUUU	0.0000	UUUUU
2	705616.3	215.4	0.004636	706732.1	568.2	0.004067	0.123	1.083	0.0242	1.301	0.0235	3.932
3	736355.3	364.4	0.005055	737519.8	1423.7	0.004141	0.181	1.322	0.0237	1.408	0.0238	4.242
4	767094.4	522.0	0.005199	768307.5	2279.1	0.003999	0.231	1.464	0.0243	1.417	0.0236	4.328
5	797833.6	679.5	0.005048	799095.3	3120.9	0.003633	0.280	1.503	0.0239	1.328	0.0235	4.270
6	828572.7	831.8	0.004859	829882.9	3959.4	0.003087	0.365	1.512	0.0239	1.159	0.0243	4.177
7	859311.8	977.1	0.004599	860670.7	4798.0	0.002788	0.394	1.485	0.0237	1.070	0.0243	4.100
8	890050.9	1114.5	0.004341	891458.4	5614.6	0.002506	0.423	1.446	0.0243	0.980	0.0234	3.922
9	920790.1	1245.3	0.004170	922246.1	6404.2	0.002171	0.479	1.427	0.0241	0.864	0.0232	3.751
10	951529.2	1372.1	0.004077	953033.9	7202.9	0.002013	0.506	1.430	0.0244	0.813	0.0245	3.842
11	982268.3	1494.8	0.003905	983821.6	8025.2	0.001703	0.564	1.400	0.0240	0.698	0.0252	3.738
12	1013007.0	1613.7	0.003832	1014609.0	8837.3	0.001522	0.603	1.401	0.0243	0.632	0.0244	3.568
13	1036369.0	1698.6	0.003287	1038008.0	9248.4	0.001609	0.511	1.219		0.674		
14	1052199.0	1747.6	0.002897	1053863.0	9271.9	0.001350	0.534	1.084		0.569		
15	1068030.0	1790.6	0.002523	1069719.0	9291.7	0.001147	0.545	0.952		0.486		
16	1083937.0	1828.5	0.002266	1085651.0	9309.3	0.001062	0.531	0.862		0.453		
17	1099845.0	1862.9	0.002077	1101584.0	9325.7	0.001002	0.517	0.796		0.430		
18	1115675.0	1895.8	0.002067	1117440.0	9341.4	0.000975	0.528	0.799		0.420		
19	1131506.0	1927.3	0.001912	1133295.0	9356.7	0.000961	0.498	0.744		0.416		
20	1147337.0	1957.0	0.001839	1149151.0	9371.7	0.000924	0.497	0.721		0.402		
21	1163168.0	1986.8	0.001923	1165007.0	9386.6	0.000962	0.500	0.759		0.421		
22	1178998.0	2016.3	0.001793	1180863.0	9401.8	0.000952	0.469	0.713		0.418		
23	1194829.0	2044.5	0.001770	1196718.0	9416.8	0.000927	0.476	0.708		0.409		
24	1210736.0	2072.8	0.001801	1212651.0	9431.5	0.000927	0.485	0.725		0.411		
25	1226644.0	2100.6	0.001711	1228583.0	9445.8	0.000874	0.489	0.693		0.389		
26	1242474.0	2128.9	0.001857	1244439.0	9460.8	0.001023	0.449	0.757		0.458		
27	1258305.0	2158.6	0.001889	1260295.0	9476.9	0.001010	0.465	0.774		0.454		
28	1274136.0	2188.1	0.001832	1276150.0	9492.9	0.000999	0.455	0.755		0.451		
29	1289966.0	2219.2	0.002088	1292006.0	9510.1	0.001170	0.439	0.865		0.530		
30	1305797.0	2250.3	0.001843	1307862.0	9527.9	0.001067	0.421	0.768		0.485		
31	1321628.0	2279.9	0.001892	1323718.0	9544.8	0.001062	0.439	0.793		0.484		
32	1337535.0	2309.3	0.001817	1339650.0	9561.8	0.001083	0.404	0.765		0.496		
33	1353443.0	2338.5	0.001867	1355583.0	9579.0	0.001088	0.417	0.790		0.500		
34	1369273.0	2368.2	0.001883	1371438.0	9596.5	0.001116	0.407	0.801		0.515		
35	1385104.0	2398.0	0.001870	1387294.0	9614.4	0.001137	0.392	0.799		0.526		
36	1400934.0	2427.7	0.001878	1403150.0	9632.4	0.001124	0.402	0.806		0.522		

STANTON NUMBER DATA RUN 082973 *** DISCRETE HOLE RIG *** NAS-3-14336

TINF= 80.4 UINF= 31.1 XVO= 6.390 RHO= 0.07257 CP= 0.242 VISC= 0.16969E-03 PR=0.715
DISTANCE FROM ORIGIN OF BL TO 1ST PLATE=42.910 P/D= 5
UNCERTAINTY IN REX=15277. UNCERTAINTY IN F=0.03228 IN RATIO

** M=1.0, COLD RUN, HIGH RE, STEP T-WALL AT 1ST PLATE.

PLATE	X	REX	TO	REENTH	STANTON NO	DST	DREEN	M	F	T2	THETA	DTH
1	50.30	0.67080E 06	107.5	0.70759E 02	0.46318E-02	0.106E-03	2.					
2	52.30	0.70136E 06	107.5	0.24483E 03	0.46361E-02	0.106E-03	5.	0.95	0.0306	82.3	0.069	0.009
3	54.30	0.73191E 06	107.5	0.45789E 03	0.51144E-02	0.111E-03	9.	0.95	0.0309	82.2	0.067	0.009
4	56.30	0.76246E 06	107.5	0.68332E 03	0.54325E-02	0.114E-03	11.	0.95	0.0309	82.3	0.069	0.009
5	58.30	0.79302E 06	107.5	0.91145E 03	0.52269E-02	0.112E-03	13.	0.94	0.0306	82.3	0.070	0.009
6	60.30	0.82357E 06	107.4	0.11281E 04	0.49019E-02	0.109E-03	15.	0.95	0.0307	82.1	0.062	0.009
7	62.30	0.85413E 06	107.4	0.13392E 04	0.46186E-02	0.106E-03	16.	0.95	0.0309	82.4	0.077	0.009
8	64.30	0.88468E 06	107.4	0.15492E 04	0.43010E-02	0.103E-03	17.	0.95	0.0308	82.5	0.079	0.009
9	66.30	0.91523E 06	107.5	0.17508E 04	0.41065E-02	0.101E-03	19.	0.96	0.0310	82.4	0.076	0.009
10	68.30	0.94579E 06	107.5	0.19459E 04	0.39612E-02	0.994E-04	20.	0.97	0.0314	82.4	0.075	0.009
11	70.30	0.97634E 06	107.5	0.21361E 04	0.38148E-02	0.980E-04	21.	0.96	0.0310	82.4	0.074	0.009
12	72.30	0.10069E 07	107.5	0.23233E 04	0.37473E-02	0.973E-04	22.	0.95	0.0306	82.5	0.078	0.009
13	73.82	0.10301E 07	105.5	0.24407E 04	0.30146E-02	0.633E-04	23.					
14	74.85	0.10458E 07	105.3	0.24859E 04	0.27151E-02	0.645E-04	23.					
15	75.88	0.10616E 07	106.3	0.25254E 04	0.23009E-02	0.588E-04	23.					
16	76.91	0.10774E 07	106.7	0.25597E 04	0.20581E-02	0.544E-04	23.					
17	77.95	0.10932E 07	107.0	0.25906E 04	0.18563E-02	0.518E-04	23.					
18	78.98	0.11089E 07	106.8	0.26202E 04	0.19087E-02	0.527E-04	23.					
19	80.01	0.11247E 07	107.1	0.26489E 04	0.17320E-02	0.486E-04	23.					
20	81.04	0.11404E 07	107.3	0.26757E 04	0.16699E-02	0.471E-04	23.					
21	82.07	0.11561E 07	107.2	0.27027E 04	0.17556E-02	0.492E-04	23.					
22	83.10	0.11719E 07	107.4	0.27294E 04	0.16380E-02	0.494E-04	23.					
23	84.13	0.11876E 07	107.2	0.27548E 04	0.15810E-02	0.489E-04	23.					
24	85.16	0.12034E 07	107.0	0.27800E 04	0.16201E-02	0.521E-04	23.					
25	86.20	0.12192E 07	105.0	0.28051E 04	0.15663E-02	0.523E-04	23.					
26	87.23	0.12350E 07	105.6	0.28305E 04	0.16574E-02	0.525E-04	23.					
27	88.26	0.12507E 07	106.8	0.28568E 04	0.16924E-02	0.516E-04	23.					
28	89.29	0.12664E 07	107.2	0.28829E 04	0.16202E-02	0.495E-04	23.					
29	90.32	0.12822E 07	106.9	0.29102E 04	0.18451E-02	0.513E-04	23.					
30	91.35	0.12979E 07	107.6	0.29373E 04	0.15945E-02	0.500E-04	23.					
31	92.38	0.13137E 07	107.4	0.29631E 04	0.16722E-02	0.499E-04	23.					
32	93.41	0.13295E 07	107.3	0.29887E 04	0.15867E-02	0.496E-04	23.					
33	94.45	0.13453E 07	107.1	0.30142E 04	0.16428E-02	0.494E-04	23.					
34	95.48	0.13610E 07	106.6	0.30403E 04	0.16687E-02	0.493E-04	23.					
35	96.51	0.13767E 07	106.8	0.30662E 04	0.16303E-02	0.527E-04	23.					
36	97.54	0.13925E 07	106.0	0.30921E 04	0.16584E-02	0.606E-04	23.					

STANTON NUMBER DATA RUN 083073 *** DISCRETE HOLE RIG *** NAS-3-14336

TINF= 82.6 UINF= 31.7 XVO= 6.390 RHO= 0.07240 CP= 0.242 VISC= 0.17081E-03 PR=0.714
DISTANCE FROM ORIGIN OF BL TO 1ST PLATE=42.910 P/D= 5
UNCERTAINTY IN REX=15482. UNCERTAINTY IN F=0.03212 IN RATIO

** M=1.0, HOT RUN, HIGH RE, STEP T-WALL AT 1ST PLATE.

PLATE	X	REX	TO	REENTH	STANTON NO	DST	DREEN	M	F	T2	THETA	DTH
1	50.30	0.67981E 06	109.9	0.70449E 02	0.45504E-02	0.103E-03	2.					
2	52.30	0.71077E 06	109.8	0.66866E 03	0.41817E-02	0.995E-04	16.	0.91	0.0295	110.2	1.015	0.013
3	54.30	0.74174E 06	109.7	0.17421E 04	0.44784E-02	0.102E-03	29.	0.91	0.0296	110.8	1.040	0.013
4	56.30	0.77270E 06	109.7	0.28354E 04	0.43950E-02	0.102E-03	37.	0.90	0.0293	111.2	1.058	0.013
5	58.30	0.80366E 06	109.8	0.39253E 04	0.39181E-02	0.971E-04	44.	0.91	0.0295	111.3	1.054	0.013
6	60.30	0.83463E 06	109.8	0.49632E 04	0.33478E-02	0.924E-04	50.	0.91	0.0295	109.0	0.972	0.013
7	62.30	0.86559E 06	109.7	0.59805E 04	0.28925E-02	0.891E-04	55.	0.92	0.0297	110.7	1.037	0.013
8	64.30	0.89656E 06	109.7	0.70240E 04	0.25573E-02	0.870E-04	60.	0.90	0.0292	111.5	1.065	0.014
9	66.30	0.92752E 06	109.7	0.80445E 04	0.21980E-02	0.848E-04	64.	0.91	0.0294	110.3	1.021	0.013
10	68.30	0.95848E 06	109.7	0.90469E 04	0.20452E-02	0.839E-04	68.	0.93	0.0300	110.1	1.015	0.013
11	70.30	0.98945E 06	109.7	0.10013E 05	0.17952E-02	0.827E-04	72.	0.91	0.0295	108.4	0.950	0.013
12	72.30	0.10204E 07	109.7	0.10918E 05	0.17191E-02	0.824E-04	75.	0.90	0.0292	107.6	0.921	0.013
13	73.82	0.10439E 07	108.8	0.11371E 05	0.11869E-02	0.362E-04	76.					
14	74.85	0.10599E 07	108.7	0.11390E 05	0.11071E-02	0.427E-04	76.					
15	75.88	0.10758E 07	109.3	0.11406E 05	0.92543E-03	0.416E-04	76.					
16	76.91	0.10919E 07	109.5	0.11420E 05	0.84840E-03	0.404E-04	76.					
17	77.95	0.11079E 07	109.6	0.11433E 05	0.78265E-03	0.400E-04	76.					
18	78.98	0.11238E 07	109.6	0.11445E 05	0.78392E-03	0.404E-04	76.					
19	80.01	0.11398E 07	109.6	0.11458E 05	0.75751E-03	0.380E-04	76.					
20	81.04	0.11557E 07	109.7	0.11470E 05	0.74852E-03	0.373E-04	76.					
21	82.07	0.11717E 07	109.7	0.11482E 05	0.76362E-03	0.387E-04	76.					
22	83.10	0.11876E 07	109.7	0.11494E 05	0.74530E-03	0.406E-04	76.					
23	84.13	0.12036E 07	109.5	0.11506E 05	0.75448E-03	0.408E-04	76.					
24	85.16	0.12196E 07	109.6	0.11518E 05	0.72885E-03	0.421E-04	76.					
25	86.20	0.12356E 07	108.6	0.11529E 05	0.68232E-03	0.420E-04	76.					
26	87.23	0.12516E 07	108.5	0.11541E 05	0.81375E-03	0.430E-04	76.					
27	88.26	0.12675E 07	109.4	0.11553E 05	0.75625E-03	0.417E-04	76.					
28	89.29	0.12834E 07	109.6	0.11566E 05	0.76915E-03	0.408E-04	76.					
29	90.32	0.12994E 07	109.3	0.11579E 05	0.92472E-03	0.413E-04	76.					
30	91.35	0.13153E 07	109.7	0.11593E 05	0.82069E-03	0.423E-04	76.					
31	92.38	0.13313E 07	109.7	0.11606E 05	0.81250E-03	0.414E-04	76.					
32	93.41	0.13473E 07	109.4	0.11619E 05	0.82940E-03	0.424E-04	76.					
33	94.45	0.13633E 07	109.4	0.11633E 05	0.85013E-03	0.413E-04	76.					
34	95.48	0.13793E 07	109.0	0.11646E 05	0.85659E-03	0.408E-04	76.					
35	96.51	0.13952E 07	109.0	0.11660E 05	0.87666E-03	0.450E-04	76.					
36	97.54	0.14112E 07	108.6	0.11674E 05	0.84975E-03	0.481E-04	76.					

FOLLOWING IS THE DATA FOR THETA=0 AND THETA=1, WHICH WAS OBTAINED BY LINEAR SUPERPOSITION THEORY.
THIS DATA WAS PRODUCED FROM RUN 082973 AND RUN 083073
FOR THE DETAIL CHANGES OF PROPERTIES AND BOUNDARY CONDITIONS, PLEASE SEE THE ABOVE TWO RUNS

PLATE	REXCOL	RE DEL2	ST(TH=0)	REXHOT	RE DEL2	ST(TH=1)	ETA	STCR	F-COL	STHR	F-HOT	PHI-1
1	670803.8	70.8	0.004632	679809.4	70.4	0.004550	UUUUU	UUUUU	0.0000	UUUUUUU	0.0000	UUUUU
2	701357.4	212.9	0.004670	710773.2	662.1	0.004189	0.103	1.089	0.0306	1.341	0.0295	4.529
3	731910.9	363.0	0.005158	741737.0	1711.1	0.004504	0.127	1.347	0.0309	1.533	0.0296	4.975
4	762464.5	525.9	0.005505	772700.8	2761.2	0.004456	0.191	1.548	0.0309	1.580	0.0293	5.129
5	793018.1	691.3	0.005320	803664.5	3802.3	0.003990	0.250	1.581	0.0306	1.460	0.0295	5.078
6	823571.7	849.0	0.005009	834628.3	4828.5	0.003301	0.341	1.556	0.0307	1.240	0.0295	4.823
7	854125.3	998.2	0.004757	865592.1	5841.8	0.002958	0.378	1.533	0.0309	1.136	0.0297	4.751
8	884678.9	1138.8	0.004441	896555.9	6841.7	0.002672	0.398	1.477	0.0308	1.046	0.0292	4.614
9	915232.4	1271.7	0.004259	927519.6	7825.5	0.002241	0.474	1.456	0.0310	0.892	0.0294	4.422
10	945786.1	1399.6	0.004114	958483.4	8812.2	0.002076	0.495	1.441	0.0314	0.840	0.0300	4.433
11	976339.6	1523.3	0.003986	989447.2	9792.4	0.001680	0.579	1.427	0.0310	0.689	0.0295	4.146
12	1006893.0	1644.3	0.003935	1020410.0	10751.9	0.001529	0.611	1.437	0.0306	0.635	0.0292	4.046
13	1030114.0	1729.3	0.003155	1043943.0	11237.7	0.001213	0.616	1.168		0.509		
14	1045849.0	1776.5	0.002839	1059889.0	11256.4	0.001130	0.602	1.061		0.477		
15	1061584.0	1817.8	0.002407	1075836.0	11273.0	0.000945	0.607	0.907		0.401		
16	1077395.0	1853.7	0.002151	1091859.0	11287.4	0.000866	0.598	0.817		0.369		
17	1093207.0	1886.0	0.001939	1107883.0	11300.7	0.000798	0.588	0.743		0.342		
18	1108942.0	1917.0	0.001995	1123829.0	11313.5	0.000800	0.599	0.770		0.345		
19	1124677.0	1946.9	0.001807	1139776.0	11326.0	0.000771	0.573	0.703		0.334		
20	1140412.0	1974.9	0.001741	1155722.0	11338.3	0.000762	0.562	0.682		0.332		
21	1156147.0	2003.0	0.001832	1171669.0	11350.6	0.000778	0.575	0.722		0.341		
22	1171882.0	2030.9	0.001707	1187615.0	11362.8	0.000758	0.556	0.678		0.333		
23	1187617.0	2057.3	0.001645	1203561.0	11375.0	0.000766	0.534	0.657		0.339		
24	1203429.0	2083.5	0.001689	1219585.0	11387.0	0.000742	0.561	0.679		0.329		
25	1219240.0	2109.7	0.001634	1235609.0	11398.5	0.000695	0.575	0.661		0.310		
26	1234975.0	2136.1	0.001722	1251555.0	11410.6	0.000826	0.521	0.701		0.370		
27	1250710.0	2163.6	0.001765	1267501.0	11423.4	0.000770	0.564	0.722		0.346		
28	1266445.0	2190.8	0.001686	1283448.0	11435.7	0.000781	0.537	0.694		0.353		
29	1282181.0	2219.2	0.001916	1299394.0	11449.5	0.000938	0.510	0.793		0.425		
30	1297916.0	2247.3	0.001654	1315340.0	11463.6	0.000832	0.497	0.688		0.378		
31	1313651.0	2274.0	0.001738	1331287.0	11476.8	0.000825	0.526	0.727		0.377		
32	1329462.0	2300.7	0.001645	1347310.0	11490.1	0.000840	0.489	0.692		0.385		
33	1345274.0	2327.0	0.001704	1363334.0	11503.7	0.000861	0.494	0.720		0.396		
34	1361009.0	2354.1	0.001731	1379280.0	11517.5	0.000868	0.498	0.735		0.401		
35	1376744.0	2381.0	0.001688	1395227.0	11531.5	0.000887	0.474	0.720		0.411		
36	1392479.0	2407.9	0.001721	1411173.0	11545.5	0.000861	0.499	0.738		0.401		

*** VELOCITY PROFILE AT UINF= 100FT/SEC, M=0

DISCRETE HOLE RIG *** NAS-3-14336

VELOCITY PROFILE

UINF=115.4 FT/SEC X= 53.0 INCHES PORT= 19
TINF= 79.2 DEG F PINF= 2104. PSF

Y(INCHES)	U(FT/SEC)	Y+	U+	UBAR	DU
0.010	62.46	22.5	13.70	0.5412	0.07
0.011	63.38	24.7	13.90	0.5491	0.07
0.012	63.74	27.0	13.98	0.5523	0.07
0.014	64.77	31.5	14.21	0.5612	0.07
0.016	65.85	36.0	14.44	0.5706	0.07
0.018	66.56	40.5	14.60	0.5767	0.07
0.021	67.84	47.2	14.88	0.5878	0.07
0.024	68.77	53.9	15.08	0.5959	0.07
0.027	69.62	60.7	15.27	0.6033	0.07
0.031	71.05	69.7	15.59	0.6157	0.06
0.035	72.03	78.7	15.80	0.6241	0.06
0.040	72.87	89.9	15.98	0.6314	0.06
0.045	73.95	101.1	16.22	0.6407	0.06
0.052	75.12	116.9	16.48	0.6509	0.06
0.060	76.56	134.8	16.79	0.6634	0.06
0.070	78.04	157.3	17.12	0.6762	0.06
0.080	79.27	179.8	17.39	0.6868	0.06
0.090	80.51	202.3	17.66	0.6976	0.06
0.105	82.23	236.0	18.04	0.7125	0.06
0.120	83.56	269.7	18.33	0.7240	0.06
0.135	85.01	303.4	18.65	0.7366	0.05
0.155	86.82	348.3	19.05	0.7523	0.05
0.175	88.08	393.3	19.32	0.7632	0.05
0.200	89.70	449.5	19.68	0.7773	0.05
0.230	91.68	516.9	20.11	0.7944	0.05
0.260	93.50	584.3	20.51	0.8102	0.05
0.290	95.28	651.7	20.90	0.8256	0.05
0.320	96.63	719.2	21.20	0.8373	0.05
0.360	98.60	809.1	21.63	0.8544	0.05
0.395	100.26	887.7	21.99	0.8688	0.05
0.435	102.23	977.6	22.43	0.8858	0.04
0.485	104.22	1090.0	22.86	0.9030	0.04
0.535	106.00	1202.3	23.25	0.9185	0.04
0.585	108.08	1314.7	23.71	0.9365	0.04
0.635	109.47	1427.1	24.01	0.9485	0.04
0.685	110.94	1539.4	24.33	0.9613	0.04
0.735	112.32	1651.8	24.64	0.9732	0.04
0.785	113.02	1764.2	24.79	0.9793	0.04
0.835	113.95	1876.5	25.00	0.9874	0.04
0.885	114.77	1988.9	25.18	0.9944	0.04
0.935	115.10	2101.3	25.25	0.9973	0.04
0.985	115.36	2213.7	25.30	0.9995	0.04
1.035	115.41	2326.0	25.32	1.0000	0.04

REX= 0.28179E 07 RED2= 5347. XVO= 3.47 IN.
DEL1= 0.121 IN. DEL2= 0.094IN. H= 1.29
CF2= 0.15603E-02 DXVO= 0.76 DDEL1=0.002 DDEL2=0.001 DCF/2=0.156 IN RATIO

STANTON NUMBER DATA RUN 091373-2 *** DISCRETE HOLE RIG *** NAS-3-14336

TINF= 80.0 UINF=116.1 XVC= 0.830 RHO= 0.07275 CP= 0.242 VISC= 0.16920E-03 PR=0.715
DISTANCE FROM ORIGIN OF BL TO 1ST PLATE=48.470 P/D= 5 TADIAB= 81.0
UNCERTAINTY IN REX=57159.

** M=0.0, FLAT PLATE RUN, HIGH RE, STEP T-WALL AT 1ST PLATE.

PLATE	X	REX	TO	REENTH	STANTON NO	DST	DREEN	M	F	T2	THETA	DTH
1	50.30	0.28277E 07	102.7	0.18490E 03	0.32348E-02	0.444E-04	3.					
2	52.30	0.29420E 07	102.8	0.52003E 03	0.26283E-02	0.391E-04	4.	0.00	0.0000	102.8	1.000	0.015
3	54.30	0.30563E 07	102.9	0.81253E 03	0.24889E-02	0.378E-04	6.	0.00	0.0000	102.9	1.000	0.015
4	56.30	0.31706E 07	102.9	0.10900E 04	0.23660E-02	0.368E-04	6.	0.00	0.0000	102.9	1.000	0.015
5	58.30	0.32849E 07	102.8	0.13561E 04	0.22882E-02	0.364E-04	7.	0.00	0.0000	102.8	1.000	0.016
6	60.30	0.33993E 07	102.9	0.16145E 04	0.22335E-02	0.359E-04	8.	0.00	0.0000	102.9	1.000	0.015
7	62.30	0.35136E 07	102.8	0.18668E 04	0.21805E-02	0.356E-04	8.	0.00	0.0000	102.8	1.000	0.015
8	64.30	0.36279E 07	102.9	0.21128E 04	0.21239E-02	0.351E-04	9.	0.00	0.0000	102.9	1.000	0.015
9	66.30	0.37422E 07	102.9	0.23534E 04	0.20838E-02	0.348E-04	9.	0.00	0.0000	102.9	1.000	0.015
10	68.30	0.38565E 07	102.8	0.25901E 04	0.20577E-02	0.347E-04	10.	0.00	0.0000	102.8	1.000	0.016
11	70.30	0.39709E 07	102.8	0.28239E 04	0.20328E-02	0.346E-04	10.	0.00	0.0000	102.8	1.000	0.016
12	72.30	0.40852E 07	103.0	0.30526E 04	0.19684E-02	0.337E-04	11.	0.00	0.0000	103.0	1.000	0.015
13	73.82	0.41721E 07	102.8	0.32249E 04	0.20276E-02	0.322E-04	11.					
14	74.85	0.42309E 07	102.4	0.33422E 04	0.19541E-02	0.321E-04	11.					
15	75.88	0.42898E 07	103.3	0.34574E 04	0.19542E-02	0.320E-04	11.					
16	76.91	0.43490E 07	103.3	0.35714E 04	0.19149E-02	0.311E-04	11.					
17	77.95	0.44081E 07	103.4	0.36837E 04	0.18929E-02	0.309E-04	11.					
18	78.98	0.44670E 07	103.2	0.37968E 04	0.19458E-02	0.317E-04	11.					
19	80.01	0.45259E 07	103.3	0.39099E 04	0.18904E-02	0.306E-04	11.					
20	81.04	0.45847E 07	103.5	0.40199E 04	0.18422E-02	0.299E-04	12.					
21	82.07	0.46436E 07	103.2	0.41305E 04	0.19103E-02	0.310E-04	12.					
22	83.10	0.47025E 07	103.5	0.42413E 04	0.18494E-02	0.304E-04	12.					
23	84.13	0.47614E 07	103.1	0.43483E 04	0.17825E-02	0.296E-04	12.					
24	85.16	0.48205E 07	103.1	0.44553E 04	0.18479E-02	0.314E-04	12.					
25	86.20	0.48797E 07	100.8	0.45584E 04	0.16504E-02	0.296E-04	12.					
26	87.23	0.49386E 07	101.2	0.46607E 04	0.18201E-02	0.318E-04	12.					
27	88.26	0.49974E 07	102.9	0.47698E 04	0.18816E-02	0.316E-04	12.					
28	89.29	0.50563E 07	103.5	0.48791E 04	0.18285E-02	0.303E-04	12.					
29	90.32	0.51152E 07	102.8	0.49898E 04	0.19246E-02	0.314E-04	12.					
30	91.35	0.51741E 07	104.0	0.50996E 04	0.18034E-02	0.298E-04	12.					
31	92.38	0.52329E 07	103.8	0.52053E 04	0.17837E-02	0.293E-04	13.					
32	93.41	0.52921E 07	103.4	0.53081E 04	0.17020E-02	0.285E-04	13.					
33	94.45	0.53512E 07	103.2	0.54094E 04	0.17372E-02	0.291E-04	13.					
34	95.48	0.54101E 07	102.3	0.55113E 04	0.17187E-02	0.290E-04	13.					
35	96.51	0.54690E 07	103.0	0.56135E 04	0.17489E-02	0.300E-04	13.					
36	97.54	0.55279E 07	102.7	0.57158E 04	0.17210E-02	0.313E-04	13.					

STANTON NUMBER DATA RUN 091273 *** DISCRETE HOLE RIG *** NAS-3-14336

TINF= 78.8 UINF=110.4 XVO= 0.830 RHO= 0.07270 CP= 0.242 VISC= 0.16907E-03 PR=0.715
DISTANCE FROM ORIGIN OF BL TO 1ST PLATE=48.470 P/D= 5 TADIAB= 79.7
UNCERTAINTY IN REX=54423. UNCERTAINTY IN F=0.03001 IN RATIO

** M=0.2, COLD RUN, HIGH RE, STEP T-WALL AT 1ST PLATE.

PLATE	X	REX	TO	REENTH	STANTON NO	DST	DREEN	M	F	T2	THETA	DTH
1	50.30	0.26923E 07	99.9	0.17478E 03	0.32114E-02	0.486E-04	3.					
2	52.30	0.28011E 07	99.9	0.54803E 03	0.28501E-02	0.452E-04	7.	0.21	0.0069	81.2	0.115	0.012
3	54.30	0.29100E 07	100.0	0.94960E 03	0.29780E-02	0.462E-04	10.	0.21	0.0068	81.1	0.111	0.012
4	56.30	0.30188E 07	99.9	0.13524E 04	0.28930E-02	0.455E-04	12.	0.20	0.0065	81.3	0.119	0.012
5	58.30	0.31277E 07	99.9	0.17471E 04	0.28106E-02	0.448E-04	14.	0.21	0.0067	81.2	0.115	0.012
6	60.30	0.32365E 07	99.9	0.21290E 04	0.27033E-02	0.440E-04	16.	0.21	0.0067	81.1	0.108	0.012
7	62.30	0.33454E 07	99.8	0.25059E 04	0.26402E-02	0.435E-04	18.	0.21	0.0067	81.5	0.128	0.012
8	64.30	0.34542E 07	99.8	0.28833E 04	0.25512E-02	0.428E-04	19.	0.21	0.0068	81.5	0.132	0.012
9	66.30	0.35631E 07	99.9	0.32539E 04	0.25253E-02	0.424E-04	21.	0.21	0.0067	81.4	0.126	0.012
10	68.30	0.36719E 07	99.9	0.36204E 04	0.25151E-02	0.423E-04	22.	0.21	0.0069	81.4	0.124	0.012
11	70.30	0.37808E 07	100.0	0.39822E 04	0.24815E-02	0.419E-04	23.	0.21	0.0067	81.3	0.119	0.012
12	72.30	0.38896E 07	100.0	0.43363E 04	0.23948E-02	0.411E-04	24.	0.21	0.0067	81.4	0.125	0.012
13	73.82	0.39723E 07	101.1	0.45809E 04	0.24553E-02	0.392E-04	25.					
14	74.85	0.40284E 07	101.4	0.47113E 04	0.21944E-02	0.356E-04	25.					
15	75.88	0.40844E 07	103.0	0.48315E 04	0.20883E-02	0.335E-04	25.					
16	76.91	0.41408E 07	103.1	0.49454E 04	0.19703E-02	0.314E-04	25.					
17	77.95	0.41971E 07	103.4	0.50543E 04	0.19098E-02	0.305E-04	25.					
18	78.98	0.42531E 07	103.4	0.51613E 04	0.19047E-02	0.304E-04	25.					
19	80.01	0.43092E 07	103.4	0.52670E 04	0.18604E-02	0.295E-04	25.					
20	81.04	0.43653E 07	103.6	0.53699E 04	0.18084E-02	0.287E-04	25.					
21	82.07	0.44213E 07	103.4	0.54728E 04	0.18589E-02	0.295E-04	25.					
22	83.10	0.44774E 07	103.7	0.55758E 04	0.18084E-02	0.291E-04	25.					
23	84.13	0.45334E 07	103.4	0.56744E 04	0.17058E-02	0.278E-04	25.					
24	85.16	0.45898E 07	103.3	0.57726E 04	0.17954E-02	0.301E-04	25.					
25	86.20	0.46461E 07	100.6	0.58683E 04	0.16127E-02	0.285E-04	25.					
26	87.23	0.47021E 07	101.2	0.59636E 04	0.17847E-02	0.305E-04	25.					
27	88.26	0.47582E 07	103.1	0.60653E 04	0.18400E-02	0.303E-04	25.					
28	89.29	0.48142E 07	103.7	0.61670E 04	0.17851E-02	0.290E-04	25.					
29	90.32	0.48703E 07	103.0	0.62700E 04	0.18853E-02	0.300E-04	25.					
30	91.35	0.49264E 07	104.2	0.63725E 04	0.17666E-02	0.286E-04	25.					
31	92.38	0.49824E 07	104.1	0.64714E 04	0.17563E-02	0.282E-04	25.					
32	93.41	0.50387E 07	103.5	0.65679E 04	0.16858E-02	0.276E-04	26.					
33	94.45	0.50951E 07	103.4	0.66632E 04	0.17073E-02	0.280E-04	26.					
34	95.48	0.51511E 07	102.4	0.67588E 04	0.17001E-02	0.279E-04	26.					
35	96.51	0.52072E 07	103.1	0.68550E 04	0.17278E-02	0.290E-04	26.					
36	97.54	0.52632E 07	102.7	0.69518E 04	0.17222E-02	0.310E-04	26.					

STANTON NUMBER DATA RUN 091373-1 *** DISCRETE HOLE RIG *** NAS-3-14336

TINF= 82.7 UINF=110.1 XVO= 0.830 RHO= 0.07231 CP= 0.242 VISC= 0.17095E-03 PR=0.715
DISTANCE FROM ORIGIN OF BL TO 1ST PLATE=48.470 P/D= 5 TADIAB= 83.6
UNCERTAINTY IN REX=53661. UNCERTAINTY IN F=0.03002 IN RATIO

** M=0.2, HOT RUN, HIGH RE, STEP T-WALL AT 1ST PLATE.

PLATE	X	REX	TO	REENTH	STANTON NO	DST	DREEN	M	F	T2	THETA	DTH
1	50.30	0.26546E 07	105.8	0.17124E 03	0.31910E-02	0.444E-04	3.					
2	52.30	0.27619E 07	105.8	0.81066E 03	0.23607E-02	0.376E-04	12.	0.21	0.0070	103.8	0.914	0.015
3	54.30	0.28693E 07	105.8	0.17465E 04	0.22171E-02	0.365E-04	21.	0.21	0.0069	104.4	0.936	0.015
4	56.30	0.29766E 07	105.8	0.26502E 04	0.20457E-02	0.354E-04	27.	0.20	0.0065	104.4	0.939	0.015
5	58.30	0.30839E 07	105.7	0.35328E 04	0.19100E-02	0.346E-04	32.	0.21	0.0068	104.5	0.946	0.015
6	60.30	0.31912E 07	105.9	0.44058E 04	0.18201E-02	0.338E-04	36.	0.21	0.0069	103.3	0.888	0.014
7	62.30	0.32985E 07	105.8	0.52736E 04	0.17240E-02	0.333E-04	39.	0.21	0.0068	104.7	0.953	0.015
8	64.30	0.34059E 07	105.8	0.61558E 04	0.16132E-02	0.326E-04	43.	0.21	0.0067	105.5	0.987	0.015
9	66.30	0.35132E 07	105.8	0.70078E 04	0.15627E-02	0.323E-04	46.	0.20	0.0066	104.1	0.927	0.015
10	68.30	0.36205E 07	105.8	0.78357E 04	0.15364E-02	0.321E-04	49.	0.21	0.0069	103.5	0.900	0.015
11	70.30	0.37278E 07	105.7	0.86453E 04	0.15044E-02	0.321E-04	51.	0.21	0.0068	102.3	0.850	0.014
12	72.30	0.38352E 07	106.0	0.94203E 04	0.14561E-02	0.315E-04	54.	0.21	0.0067	102.3	0.842	0.014
13	73.82	0.39167E 07	105.6	0.98466E 04	0.16050E-02	0.263E-04	55.					
14	74.85	0.39720E 07	105.4	0.99327E 04	0.15080E-02	0.263E-04	55.					
15	75.88	0.40273E 07	106.2	0.10015E 05	0.14812E-02	0.259E-04	55.					
16	76.91	0.40828E 07	106.2	0.10097E 05	0.14615E-02	0.253E-04	55.					
17	77.95	0.41383E 07	106.4	0.10177E 05	0.14330E-02	0.250E-04	55.					
18	78.98	0.41936E 07	106.3	0.10257E 05	0.14526E-02	0.253E-04	55.					
19	80.01	0.42489E 07	106.2	0.10337E 05	0.14456E-02	0.248E-04	55.					
20	81.04	0.43042E 07	106.3	0.10416E 05	0.14147E-02	0.243E-04	55.					
21	82.07	0.43594E 07	106.2	0.10495E 05	0.14521E-02	0.250E-04	55.					
22	83.10	0.44147E 07	106.3	0.10575E 05	0.14371E-02	0.252E-04	55.					
23	84.13	0.44700E 07	106.2	0.10653E 05	0.13690E-02	0.244E-04	55.					
24	85.16	0.45255E 07	106.2	0.10730E 05	0.14245E-02	0.259E-04	55.					
25	86.20	0.45810E 07	104.2	0.10806E 05	0.12964E-02	0.248E-04	55.					
26	87.23	0.46363E 07	104.4	0.10880E 05	0.13850E-02	0.258E-04	55.					
27	88.26	0.46916E 07	105.8	0.10959E 05	0.14822E-02	0.265E-04	55.					
28	89.29	0.47469E 07	106.3	0.11040E 05	0.14529E-02	0.256E-04	55.					
29	90.32	0.48021E 07	105.7	0.11123E 05	0.15436E-02	0.266E-04	55.					
30	91.35	0.48574E 07	106.5	0.11207E 05	0.14742E-02	0.260E-04	55.					
31	92.38	0.49127E 07	106.4	0.11287E 05	0.14451E-02	0.254E-04	55.					
32	93.41	0.49682E 07	105.9	0.11367E 05	0.14202E-02	0.254E-04	55.					
33	94.45	0.50237E 07	105.9	0.11445E 05	0.14256E-02	0.254E-04	55.					
34	95.48	0.50790E 07	105.1	0.11524E 05	0.14219E-02	0.254E-04	55.					
35	96.51	0.51343E 07	105.6	0.11604E 05	0.14492E-02	0.266E-04	55.					
36	97.54	0.51896E 07	105.2	0.11684E 05	0.14445E-02	0.282E-04	55.					

FOLLOWING IS THE DATA FOR THETA=0 AND THETA=1, WHICH WAS OBTAINED BY LINEAR SUPERPOSITION THEORY.
THIS DATA WAS PRODUCED FROM RUN 091273 AND RUN 091373-1
FOR THE DETAIL CHANGES OF PROPERTIES AND BOUNDARY CONDITIONS, PLEASE SEE THE ABOVE TWO RUNS

PLATE	REXCOL	RE DEL2	ST(TH=0)	REXHOT	RE DEL2	ST(TH=1)	ETA	STCR	F-COL	STHR	F-HOT	PHI-1
1	2692300.0	174.8	0.003211	2654612.0	171.2	0.003191	UUUUU	UUUUU	0.0000	UUUUUUU	0.0000	UUUUU
2	2801146.0	508.5	0.002920	2761934.0	840.1	0.002308	0.210	0.876	0.0069	0.958	0.0070	2.078
3	2909992.0	835.1	0.003080	2869256.0	1826.1	0.002158	0.299	1.035	0.0068	0.951	0.0069	2.126
4	3018638.0	1166.8	0.003016	2976578.0	2768.2	0.001983	0.342	1.091	0.0065	0.910	0.0065	2.049
5	3127684.0	1490.7	0.002935	3083900.0	3685.1	0.001851	0.369	1.122	0.0067	0.877	0.0068	2.086
6	3236529.0	1804.2	0.002826	3191222.0	4609.3	0.001693	0.401	1.130	0.0067	0.823	0.0069	2.064
7	3345375.0	2109.4	0.002782	3298545.0	5526.3	0.001672	0.399	1.154	0.0067	0.830	0.0068	2.085
8	3454221.0	2407.5	0.002695	3405867.0	6426.7	0.001599	0.407	1.153	0.0068	0.809	0.0067	2.057
9	3563067.0	2699.8	0.002676	3513189.0	7303.6	0.001475	0.449	1.177	0.0067	0.759	0.0066	1.995
10	3671913.0	2990.9	0.002672	3620511.0	8182.9	0.001410	0.472	1.204	0.0069	0.737	0.0069	2.035
11	3780758.0	3280.0	0.002641	3727833.0	9067.2	0.001304	0.506	1.216	0.0067	0.691	0.0068	1.979
12	3889604.0	3562.9	0.002558	3835155.0	9932.5	0.001249	0.512	1.202	0.0067	0.670	0.0067	1.947
13	3972327.0	3774.7	0.002583	3916720.0	10402.2	0.001516	0.413	1.231		0.821		
14	4028383.0	3911.6	0.002298	3971991.0	10483.9	0.001436	0.375	1.105		0.782		
15	4084438.0	4037.3	0.002180	4027262.0	10562.9	0.001418	0.350	1.057		0.777		
16	4140765.0	4155.9	0.002047	4082800.0	10641.0	0.001408	0.312	1.001		0.776		
17	4197093.0	4268.9	0.001982	4138340.0	10718.3	0.001383	0.302	0.977		0.766		
18	4253149.0	4379.9	0.001973	4193611.0	10795.4	0.001405	0.288	0.980		0.782		
19	4309204.0	4489.2	0.001923	4248881.0	10873.1	0.001402	0.271	0.962		0.784		
20	4365260.0	4595.6	0.001868	4304152.0	10949.9	0.001373	0.265	0.941		0.772		
21	4421316.0	4701.9	0.001920	4359424.0	11026.9	0.001409	0.266	0.975		0.796		
22	4477372.0	4808.1	0.001864	4414695.0	11104.6	0.001398	0.250	0.953		0.793		
23	4533427.0	4909.7	0.001757	4469966.0	11180.2	0.001334	0.241	0.903		0.760		
24	4589754.0	5010.9	0.001851	4525504.0	11255.4	0.001386	0.252	0.958		0.793		
25	4646082.0	5109.5	0.001660	4581043.0	11328.7	0.001263	0.239	0.865		0.726		
26	4702138.0	5207.8	0.001845	4636314.0	11400.8	0.001343	0.272	0.966		0.776		
27	4758193.0	5312.8	0.001894	4691585.0	11477.9	0.001445	0.237	0.998		0.838		
28	4814249.0	5417.4	0.001835	4746856.0	11557.1	0.001418	0.227	0.972		0.826		
29	4870305.0	5523.3	0.001937	4802128.0	11638.1	0.001508	0.221	1.032		0.881		
30	4926360.0	5628.4	0.001811	4857398.0	11719.8	0.001444	0.203	0.970		0.847		
31	4982416.0	5729.8	0.001803	4912669.0	11798.8	0.001412	0.217	0.971		0.832		
32	5038743.0	5828.9	0.001726	4968208.0	11876.4	0.001392	0.193	0.934		0.823		
33	5095071.0	5926.4	0.001750	5023747.0	11953.5	0.001396	0.202	0.952		0.828		
34	5151127.0	6024.4	0.001742	5079018.0	12030.7	0.001393	0.201	0.952		0.829		
35	5207182.0	6122.9	0.001770	5134289.0	12108.5	0.001420	0.198	0.972		0.848		
36	5263238.0	6222.1	0.001764	5189560.0	12187.0	0.001415	0.198	0.973		0.848		

100874 *** FOLLOWING PROFILES ARE FOR HEATED STARTING RUN

DISCRETE HOLE RIG *** NAS-3-14336

VELOCITY PROFILE

UINF= 54.4 FT/SEC   X= 50.3 INCHES   PORT= 19
TINF= 74.9 DEG F   PINF= 2118. PSF

Y(INCHES)	U(FT/SEC)	Y+	U+	UBAR	DU
0.010	23.58	11.3	10.52	0.4336	0.19
0.011	24.20	12.4	10.80	0.4448	0.19
0.012	24.89	13.5	11.11	0.4576	0.18
0.013	25.46	14.7	11.36	0.4681	0.18
0.014	26.16	15.8	11.68	0.4810	0.17
0.015	26.68	16.9	11.91	0.4905	0.17
0.016	27.16	18.0	12.12	0.4993	0.17
0.018	28.06	20.3	12.52	0.5160	0.16
0.020	29.01	22.6	12.94	0.5333	0.16
0.023	29.80	25.9	13.30	0.5479	0.15
0.027	30.87	30.5	13.78	0.5675	0.15
0.031	31.44	35.0	14.03	0.5781	0.14
0.037	32.39	41.7	14.45	0.5955	0.14
0.044	33.20	49.6	14.82	0.6105	0.14
0.051	33.72	57.5	15.05	0.6200	0.13
0.059	34.39	66.5	15.35	0.6322	0.13
0.067	35.02	75.6	15.63	0.6439	0.13
0.076	35.59	85.7	15.88	0.6543	0.13
0.086	36.15	97.0	16.13	0.6646	0.13
0.096	36.77	108.3	16.41	0.6760	0.12
0.111	37.45	125.2	16.71	0.6885	0.12
0.131	38.30	147.8	17.09	0.7041	0.12
0.156	39.33	175.9	17.55	0.7230	0.12
0.186	40.43	209.8	18.04	0.7434	0.11
0.221	41.55	249.3	18.54	0.7639	0.11
0.261	42.88	294.4	19.14	0.7884	0.11
0.311	44.12	350.8	19.69	0.8112	0.10
0.361	45.48	407.2	20.30	0.8362	0.10
0.411	46.68	463.6	20.83	0.8582	0.10
0.461	47.96	519.9	21.40	0.8817	0.09
0.511	48.92	576.3	21.83	0.8995	0.09
0.561	49.83	632.7	22.24	0.9162	0.09
0.611	50.83	689.1	22.68	0.9345	0.09
0.661	51.67	745.5	23.06	0.9499	0.09
0.711	52.37	801.9	23.37	0.9628	0.09
0.761	52.98	858.3	23.64	0.9740	0.09
0.811	53.50	914.7	23.88	0.9836	0.08
0.861	53.87	971.1	24.04	0.9904	0.08
0.911	54.12	1027.5	24.15	0.9950	0.08
0.961	54.33	1083.9	24.25	0.9989	0.08
1.011	54.39	1140.3	24.27	1.0000	0.08

TEMPERATURE PROFILE

Y(INCHES)	T(DEG F)	TBAR
0.0065	93.07	0.7131
0.0075	92.22	0.6804
0.0085	91.06	0.6352
0.0095	90.15	0.6001
0.0105	89.34	0.5685
0.0115	88.64	0.5413
0.0135	87.58	0.5005
0.0155	86.77	0.4688
0.0175	86.06	0.4416
0.0205	85.27	0.4110
0.0235	84.69	0.3883
0.0275	84.16	0.3679
0.0325	83.66	0.3485
0.0395	83.08	0.3258
0.0495	82.43	0.3008
0.0645	81.79	0.2758
0.0845	81.11	0.2497
0.1095	80.44	0.2235
0.1445	79.73	0.1962
0.1945	78.91	0.1643
0.2545	78.09	0.1324
0.3295	77.26	0.1004
0.4045	76.59	0.0742
0.4795	76.03	0.0525
0.5545	75.61	0.0365
0.6295	75.29	0.0240
0.6795	75.11	0.0171
0.7295	74.97	0.0114
0.7795	74.88	0.0080
0.8295	74.82	0.0057
0.8795	74.73	0.0023
0.9295	74.67	0.0000

END2= 0.068IN.   REEN= 1820.   TO=100.47 F
DEND2=0.001   DREEN= 25.

REX= 0.12471E 07   RED2= 2786.   XVO= 4.75 IN.
DEL1= 0.136 IN.   DEL2= 0.102IN.   H= 1.33
CF2= 0.16972E-02   DXVO= 0.68   DDEL1=0.002   DDEL2=0.001   DCF/2=0.100 IN RATIO

STANTON NUMBER DATA RUN 100873 *** DISCRETE HOLE RIG *** NAS-3-14336

TINF= 74.5 UINF= 53.2 XVO= 4.750 RHO= 0.07355 CP= 0.242 VISC= 0.16598E-03 PR=0.717
DISTANCE FROM ORIGIN OF BL TO 1ST PLATE=44.550 P/D= 5
UNCERTAINTY IN REX=26701.

** M=0.0, FLAT PLATE RUN, HIGH RE, STEP T-WALL AT 24 IN UPSREAM OF 1ST PLATE

PLATE	X	REX	TO	REENTH	STANTON NO	DST	DREEN	M	F	T2	THETA	DTH
1	50.30	0.12162E 07	100.5	0.18157E 04	0.24234E-02	0.541E-04	80.					
2	52.30	0.12697E 07	100.4	0.19431E 04	0.23464E-02	0.539E-04	80.	0.00	0.0000	100.4	1.000	0.014
3	54.30	0.13231E 07	100.4	0.20681E 04	0.23355E-02	0.538E-04	80.	0.00	0.0000	100.4	1.000	0.014
4	56.30	0.13765E 07	100.3	0.21916E 04	0.22918E-02	0.537E-04	80.	0.00	0.0000	100.3	1.000	0.014
5	58.30	0.14299E 07	100.2	0.23128E 04	0.22479E-02	0.537E-04	80.	0.00	0.0000	100.2	1.000	0.014
6	60.30	0.14833E 07	100.3	0.24327E 04	0.22414E-02	0.536E-04	80.	0.00	0.0000	100.3	1.000	0.014
7	62.30	0.15367E 07	100.4	0.25515E 04	0.22057E-02	0.533E-04	80.	0.00	0.0000	100.4	1.000	0.014
8	64.30	0.15901E 07	100.3	0.26685E 04	0.21784E-02	0.532E-04	80.	0.00	0.0000	100.3	1.000	0.014
9	66.30	0.16435E 07	100.4	0.27843E 04	0.21586E-02	0.531E-04	80.	0.00	0.0000	100.4	1.000	0.014
10	68.30	0.16969E 07	100.2	0.28990E 04	0.21372E-02	0.534E-04	80.	0.00	0.0000	100.2	1.000	0.014
11	70.30	0.17503E 07	100.1	0.30123E 04	0.21062E-02	0.533E-04	80.	0.00	0.0000	100.1	1.000	0.014
12	72.30	0.18037E 07	100.2	0.31228E 04	0.20321E-02	0.528E-04	80.	0.00	0.0000	100.2	1.000	0.014
13	73.82	0.18443E 07	100.1	0.32065E 04	0.21348E-02	0.363E-04	80.					
14	74.85	0.18718E 07	100.0	0.32639E 04	0.20345E-02	0.375E-04	80.					
15	75.88	0.18993E 07	100.7	0.33199E 04	0.20310E-02	0.377E-04	80.					
16	76.91	0.19269E 07	100.7	0.33753E 04	0.19952E-02	0.369E-04	80.					
17	77.95	0.19545E 07	100.8	0.34298E 04	0.19673E-02	0.367E-04	80.					
18	78.98	0.19820E 07	100.6	0.34848E 04	0.20280E-02	0.376E-04	80.					
19	80.01	0.20095E 07	100.6	0.35402E 04	0.19937E-02	0.363E-04	80.					
20	81.04	0.20371E 07	100.9	0.35940E 04	0.19151E-02	0.352E-04	80.					
21	82.07	0.20646E 07	100.6	0.36486E 04	0.20484E-02	0.372E-04	80.					
22	83.10	0.20921E 07	100.8	0.37037E 04	0.19514E-02	0.369E-04	80.					
23	84.13	0.21196E 07	100.6	0.37563E 04	0.18739E-02	0.361E-04	80.					
24	85.16	0.21472E 07	100.3	0.38084E 04	0.19097E-02	0.387E-04	80.					
25	86.20	0.21748E 07	97.8	0.38571E 04	0.16289E-02	0.363E-04	80.					
26	87.23	0.22023E 07	98.1	0.39055E 04	0.18807E-02	0.387E-04	80.					
27	88.26	0.22298E 07	100.0	0.39586E 04	0.19820E-02	0.389E-04	80.					
28	89.29	0.22573E 07	100.7	0.40125E 04	0.19307E-02	0.370E-04	80.					
29	90.32	0.22848E 07	100.2	0.40662E 04	0.19722E-02	0.368E-04	80.					
30	91.35	0.23123E 07	101.1	0.41197E 04	0.19089E-02	0.369E-04	80.					
31	92.38	0.23398E 07	101.0	0.41727E 04	0.19432E-02	0.367E-04	80.					
32	93.41	0.23675E 07	100.8	0.42246E 04	0.18265E-02	0.358E-04	80.					
33	94.45	0.23951E 07	100.6	0.42756E 04	0.18800E-02	0.361E-04	80.					
34	95.48	0.24226E 07	100.1	0.43276E 04	0.18966E-02	0.360E-04	80.					
35	96.51	0.24501E 07	100.5	0.43796E 04	0.18798E-02	0.377E-04	80.					
36	97.54	0.24776E 07	99.9	0.44311E 04	0.18593E-02	0.413E-04	81.					

STANTON NUMBER DATA RUN 101173-2 *** DISCRETE HOLE RIG *** NAS-3-14336

TINF= 75.6 UINF= 52.7 XVO= 4.750 RHO= 0.07333 CP= 0.242 VISC= 0.16699E-03 PR=0.715
DISTANCE FROM ORIGIN OF BL TO 1ST PLATE=44.550 P/D= 5
UNCERTAINTY IN REX=26321. UNCERTAINTY IN F=0.03028 IN RATIO

** M=0.2, COLD RUN, HIGH RE, STEP T-WALL AT 24 IN. UPSTREAM OF 1ST PLATE.

PLATE	X	REX	TO	REENTH	STANTON NO	DST	DREEN	M	F	T2	THETA	DTH
1	50.30	0.11989E 07	101.9	0.17898E 04	0.23837E-02	0.537E-04	79.					
2	52.30	0.12515E 07	101.9	0.19604E 04	0.26997E-02	0.554E-04	79.	0.22	0.0070	80.8	0.199	0.010
3	54.30	0.13042E 07	101.9	0.21815E 04	0.29464E-02	0.567E-04	79.	0.21	0.0069	80.8	0.197	0.010
4	56.30	0.13568E 07	101.9	0.24087E 04	0.29550E-02	0.567E-04	79.	0.21	0.0068	80.8	0.201	0.010
5	58.30	0.14095E 07	101.9	0.26338E 04	0.28569E-02	0.561E-04	79.	0.21	0.0068	80.9	0.201	0.010
6	60.30	0.14621E 07	101.9	0.28553E 04	0.28161E-02	0.560E-04	79.	0.21	0.0068	80.9	0.201	0.010
7	62.30	0.15148E 07	101.9	0.30752E 04	0.27433E-02	0.556E-04	79.	0.21	0.0068	81.1	0.209	0.010
8	64.30	0.15674E 07	101.9	0.32946E 04	0.26910E-02	0.554E-04	80.	0.21	0.0069	81.1	0.212	0.010
9	66.30	0.16200E 07	101.9	0.35114E 04	0.26444E-02	0.551E-04	80.	0.21	0.0069	81.1	0.209	0.010
10	68.30	0.16727E 07	101.9	0.37260E 04	0.26468E-02	0.552E-04	80.	0.21	0.0069	81.0	0.208	0.010
11	70.30	0.17253E 07	101.9	0.39385E 04	0.25861E-02	0.548E-04	80.	0.21	0.0069	80.9	0.204	0.010
12	72.30	0.17780E 07	102.0	0.41491E 04	0.25081E-02	0.543E-04	80.	0.21	0.0068	81.3	0.219	0.010
13	73.82	0.18180E 07	101.1	0.42866E 04	0.23680E-02	0.391E-04	80.					
14	74.85	0.18451E 07	101.2	0.43479E 04	0.21468E-02	0.390E-04	80.					
15	75.88	0.18722E 07	102.0	0.44050E 04	0.20664E-02	0.382E-04	80.					
16	76.91	0.18994E 07	102.2	0.44599E 04	0.19756E-02	0.366E-04	80.					
17	77.95	0.19267E 07	102.4	0.45125E 04	0.18997E-02	0.357E-04	80.					
18	78.98	0.19538E 07	102.3	0.45644E 04	0.19263E-02	0.361E-04	80.					
19	80.01	0.19809E 07	102.4	0.46158E 04	0.18617E-02	0.345E-04	80.					
20	81.04	0.20080E 07	102.6	0.46655E 04	0.17996E-02	0.335E-04	80.					
21	82.07	0.20351E 07	102.4	0.47159E 04	0.19116E-02	0.352E-04	80.					
22	83.10	0.20622E 07	102.6	0.47662E 04	0.17946E-02	0.348E-04	80.					
23	84.13	0.20893E 07	102.4	0.48142E 04	0.17447E-02	0.343E-04	80.					
24	85.16	0.21166E 07	102.1	0.48617E 04	0.17549E-02	0.365E-04	80.					
25	86.20	0.21438E 07	99.7	0.49065E 04	0.15458E-02	0.348E-04	80.					
26	87.23	0.21709E 07	100.2	0.49517E 04	0.17845E-02	0.370E-04	80.					
27	88.26	0.21980E 07	102.0	0.50012E 04	0.18625E-02	0.369E-04	80.					
28	89.29	0.22252E 07	102.6	0.50508E 04	0.17936E-02	0.350E-04	80.					
29	90.32	0.22523E 07	102.0	0.51004E 04	0.18585E-02	0.351E-04	80.					
30	91.35	0.22794E 07	102.9	0.51497E 04	0.17725E-02	0.351E-04	80.					
31	92.38	0.23065E 07	102.8	0.51986E 04	0.18305E-02	0.351E-04	80.					
32	93.41	0.23337E 07	102.6	0.52468E 04	0.17217E-02	0.343E-04	80.					
33	94.45	0.23610E 07	102.5	0.52941E 04	0.17643E-02	0.344E-04	80.					
34	95.48	0.23881E 07	101.8	0.53425E 04	0.18069E-02	0.346E-04	80.					
35	96.51	0.24152E 07	102.2	0.53915E 04	0.17979E-02	0.366E-04	80.					
36	97.54	0.24423E 07	101.5	0.54399E 04	0.17700E-02	0.403E-04	80.					

STANTON NUMBER DATA RUN 101273 *** DISCRETE HOLE RIG *** NAS-3-14336

TINF= 72.8 UINF= 53.0 XVO= 4.750 RHO= 0.07393 CP= 0.242 VISC= 0.16503E-03 PR=0.715
DISTANCE FROM ORIGIN OF BL TO 1ST PLATE=44.550 P/D= 5
UNCERTAINTY IN REX=26743. UNCERTAINTY IN F=0.03027 IN RATIO

** M=0.2, HOT RUN, HIGH RE, STEP T-WALL AT 24 IN. UPSTREAM OF 1ST PLATE.

PLATE	X	REX	TO	REENTH	STANTON NO	DST	DREEN	M	F	T2	THETA	DTH
1	50.30	0.12181E 07	103.6	0.18185E 04	0.24269E-02	0.461E-04	80.					
2	52.30	0.12716E 07	103.6	0.21192E 04	0.21732E-02	0.450E-04	80.	0.21	0.0069	102.5	0.965	0.011
3	54.30	0.13251E 07	103.6	0.26043E 04	0.21857E-02	0.451E-04	81.	0.23	0.0074	102.6	0.967	0.011
4	56.30	0.13786E 07	103.5	0.30849E 04	0.21008E-02	0.449E-04	81.	0.21	0.0068	102.3	0.960	0.011
5	58.30	0.14321E 07	103.5	0.35412E 04	0.19802E-02	0.445E-04	82.	0.20	0.0066	102.9	0.980	0.011
6	60.30	0.14855E 07	103.6	0.39867E 04	0.18958E-02	0.440E-04	82.	0.21	0.0067	102.2	0.954	0.011
7	62.30	0.15390E 07	103.6	0.44064E 04	0.18110E-02	0.437E-04	83.	0.18	0.0057	102.9	0.979	0.011
8	64.30	0.15925E 07	103.6	0.48158E 04	0.17252E-02	0.434E-04	83.	0.19	0.0061	103.6	1.001	0.011
9	66.30	0.16460E 07	103.5	0.52289E 04	0.16729E-02	0.433E-04	83.	0.18	0.0060	103.1	0.987	0.011
10	68.30	0.16995E 07	103.5	0.56450E 04	0.16462E-02	0.433E-04	84.	0.20	0.0064	103.2	0.991	0.011
11	70.30	0.17530E 07	103.4	0.60595E 04	0.15863E-02	0.432E-04	84.	0.19	0.0060	103.0	0.985	0.011
12	72.30	0.18065E 07	103.4	0.64734E 04	0.14937E-02	0.429E-04	84.	0.19	0.0063	104.4	1.030	0.012
13	73.82	0.18471E 07	103.2	0.67087E 04	0.16385E-02	0.273E-04	85.					
14	74.85	0.18747E 07	103.0	0.67528E 04	0.15639E-02	0.288E-04	85.					
15	75.88	0.19022E 07	103.9	0.67952E 04	0.15111E-02	0.287E-04	85.					
16	76.91	0.19299E 07	103.9	0.68367E 04	0.14993E-02	0.281E-04	85.					
17	77.95	0.19576E 07	104.1	0.68778E 04	0.14772E-02	0.279E-04	85.					
18	78.98	0.19851E 07	104.2	0.69182E 04	0.14534E-02	0.278E-04	85.					
19	80.01	0.20126E 07	104.0	0.69586E 04	0.14795E-02	0.272E-04	85.					
20	81.04	0.20402E 07	104.2	0.69988E 04	0.14345E-02	0.266E-04	85.					
21	82.07	0.20677E 07	104.2	0.70392E 04	0.14948E-02	0.277E-04	85.					
22	83.10	0.20953E 07	104.0	0.70801E 04	0.14756E-02	0.282E-04	95.					
23	84.13	0.21228E 07	103.9	0.71201E 04	0.14235E-02	0.277E-04	85.					
24	85.16	0.21505E 07	104.0	0.71594E 04	0.14252E-02	0.291E-04	85.					
25	86.20	0.21782E 07	102.1	0.71969E 04	0.12929E-02	0.276E-04	85.					
26	87.23	0.22057E 07	102.4	0.72358E 04	0.15318E-02	0.298E-04	85.					
27	88.26	0.22333E 07	103.9	0.72775E 04	0.14915E-02	0.292E-04	85.					
28	89.29	0.22608E 07	104.1	0.73186E 04	0.14880E-02	0.285E-04	85.					
29	90.32	0.22884E 07	103.6	0.73600E 04	0.15148E-02	0.283E-04	85.					
30	91.35	0.23159E 07	104.1	0.74018E 04	0.15152E-02	0.292E-04	85.					
31	92.38	0.23434E 07	104.1	0.74437E 04	0.15271E-02	0.290E-04	85.					
32	93.41	0.23711E 07	103.6	0.74854E 04	0.14928E-02	0.289E-04	85.					
33	94.45	0.23988E 07	103.7	0.75265E 04	0.14911E-02	0.287E-04	85.					
34	95.48	0.24264E 07	103.0	0.75683E 04	0.15403E-02	0.237E-04	85.					
35	96.51	0.24539E 07	103.3	0.76109E 04	0.15445E-02	0.306E-04	95.					
36	97.54	0.24814E 07	102.7	0.76534E 04	0.15375E-02	0.336E-04	85.					

FOLLOWING IS THE DATA FOR THETA=0 AND THETA=1, WHICH WAS OBTAINED BY LINEAR SUPERPOSITION THEORY.
THIS DATA WAS PRODUCED FROM RUN 101173-2 AND RUN 101273
FOR THE DETAIL CHANGES OF PROPERTIES AND BOUNDARY CONDITIONS, PLEASE SEE THE ABOVE TWO RUNS

PLATE	REXCOL	RE DEL2	ST(TH=0)	REXHOT	RE DEL2	ST(TH=1)	FTA	STCR	F-COL	STHR	F-HOT	PHT-1
1	1198907.0	1789.8	0.002384	1218122.0	1818.5	0.002427	UUUUU	UUUUU	0.0000	UUUUUUU	0.0000	UUUUU
2	1251549.0	1927.2	0.002836	1271607.0	2125.1	0.002149	0.242	1.209	0.0070	0.916	0.0069	2.044
3	1304190.0	2084.5	0.003141	1325092.0	2621.6	0.002153	0.314	1.345	0.0069	0.922	0.0074	2.123
4	1356831.0	2250.9	0.003181	1378577.0	3113.9	0.002056	0.354	1.388	0.0068	0.897	0.0068	2.036
5	1409473.0	2415.8	0.003083	1432062.0	3579.2	0.001957	0.365	1.371	0.0068	0.871	0.0066	1.984
6	1462114.0	2577.5	0.003061	1485547.0	4034.3	0.001840	0.399	1.366	0.0068	0.821	0.0067	1.942
7	1514756.0	2737.0	0.002997	1539032.0	4463.3	0.001785	0.404	1.359	0.0068	0.909	0.0057	1.810
8	1567397.0	2393.5	0.002950	1592518.0	4875.2	0.001726	0.415	1.354	0.0069	0.792	0.0061	1.859
9	1620038.0	3047.6	0.002905	1646003.0	5289.9	0.001656	0.430	1.346	0.0069	0.767	0.0060	1.813
10	1672680.0	3200.7	0.002913	1699488.0	5708.9	0.001635	0.439	1.363	0.0069	0.765	0.0064	1.880
11	1725321.0	3352.4	0.002848	1752973.0	6126.6	0.001567	0.450	1.352	0.0069	0.744	0.0060	1.813
12	1777963.0	3500.5	0.002781	1806458.0	6538.4	0.001531	0.449	1.369	0.0068	0.754	0.0063	1.895
13	1817970.0	3608.5	0.002561	1847107.0	6769.4	0.001621	0.367	1.200		0.759		
14	1845080.0	3674.5	0.002301	1874651.0	6813.1	0.001550	0.326	1.131		0.762		
15	1872191.0	3735.7	0.002213	1902196.0	6855.1	0.001498	0.323	1.090		0.738		
16	1899432.0	3794.3	0.002102	1929874.0	6896.3	0.001488	0.292	1.053		0.746		
17	1926674.0	3850.1	0.002011	1957553.0	6937.1	0.001467	0.271	1.022		0.746		
18	1953785.0	3905.3	0.002051	1985098.0	6977.2	0.001442	0.297	1.012		0.711		
19	1980895.0	3959.7	0.001963	2012643.0	7017.3	0.001470	0.251	0.985		0.738		
20	2008005.0	4012.1	0.001896	2040187.0	7057.3	0.001426	0.248	0.990		0.745		
21	2035116.0	4065.3	0.002022	2067733.0	7097.4	0.001485	0.266	0.987		0.725		
22	2062226.0	4118.2	0.001879	2095277.0	7138.1	0.001468	0.219	0.963		0.752		
23	2089336.0	4168.5	0.001830	2122822.0	7177.9	0.001416	0.226	0.976		0.756		
24	2116578.0	4218.4	0.001842	2150500.0	7217.0	0.001417	0.231	0.965		0.742		
25	2143820.0	4265.3	0.001613	2178179.0	7254.3	0.001287	0.202	0.990		0.790		
26	2170930.0	4312.3	0.001851	2205724.0	7293.0	0.001526	0.176	0.984		0.811		
27	2198041.0	4364.0	0.001961	2233268.0	7334.5	0.001483	0.244	0.989		0.748		
28	2225151.0	4416.1	0.001874	2260813.0	7375.4	0.001481	0.210	0.971		0.767		
29	2252262.0	4468.0	0.001949	2288358.0	7416.6	0.001507	0.227	0.988		0.764		
30	2279372.0	4519.4	0.001841	2315903.0	7458.2	0.001509	0.180	0.964		0.791		
31	2306482.0	4570.3	0.001911	2343448.0	7499.9	0.001520	0.205	0.983		0.782		
32	2333724.0	4620.4	0.001782	2371126.0	7541.4	0.001487	0.165	0.976		0.814		
33	2360966.0	4669.5	0.001837	2398805.0	7582.4	0.001485	0.192	0.977		0.790		
34	2388076.0	4719.9	0.001877	2426350.0	7624.0	0.001534	0.183	0.990		0.809		
35	2415186.0	4770.7	0.001865	2453894.0	7666.4	0.001538	0.175	0.992		0.818		
36	2442297.0	4820.9	0.001831	2481439.0	7708.7	0.001532	0.164	0.985		0.824		

STANTON NUMBER DATA RUN 101573 *** DISCRETE HOLE RIG *** NAS-3-14336

TINF= 73.8 UINF= 52.7 XVO= 0.000 RHO= 0.07385 CP= 0.242 VISC= 0.16534E-03 PR=0.716
DISTANCE FROM ORIGIN OF BL TO 1ST PLATE=49.300 P/D= 5
UNCERTAINTY IN REX=26743. UNCERTAINTY IN F=0.03028 IN RATIO

** M=0.2,HIGH RE, ADIABATIC WALL EFFECTIVENESS RUN.

PLATE	X	REX	TO	X/D	ETA	M	F	T2
2	52.30	0.12716E 07	2.5	0.22	0.2224	0.01		
3	54.30	0.13251E 07	7.4	0.29	0.2297	0.01		
4	56.30	0.13786E 07	12.3	0.34	0.2133	0.01		
5	58.30	0.14321E 07	17.2	0.36	0.2024	0.01		
6	60.30	0.14855E 07	22.2	0.39	0.2130	0.01		
7	62.30	0.15390E 07	27.1	0.40	0.1801	0.01		
8	64.30	0.15925E 07	32.0	0.40	0.1905	0.01		
9	66.30	0.16460E 07	36.9	0.42	0.1873	0.01		
10	68.30	0.16995E 07	41.9	0.44	0.2029	0.01		
11	70.30	0.17530E 07	46.8	0.45	0.1911	0.01		
12	72.30	0.18065E 07	51.7	0.44	0.1966	0.01		
13	73.82	0.18471E 07	55.5	0.43				
14	74.85	0.18747E 07	58.0	0.40				
15	75.88	0.19022E 07	60.5	0.39				
16	76.91	0.19299E 07	63.1	0.37				
17	77.95	0.19576E 07	65.6	0.36				
18	78.98	0.19851E 07	68.2	0.37				
19	80.01	0.20126E 07	70.7	0.35				
20	81.04	0.20402E 07	73.3	0.34				
21	82.07	0.20677E 07	75.8	0.34				
22	83.10	0.20953E 07	78.3	0.33				
23	84.13	0.21228E 07	80.9	0.34				
24	85.16	0.21505E 07	83.4	0.34				
25	86.20	0.21782E 07	86.0	0.33				
26	87.23	0.22057E 07	88.5	0.32				
27	88.26	0.22333E 07	91.0	0.33				
28	89.29	0.22608E 07	93.6	0.33				
29	90.32	0.22884E 07	96.1	0.33				
30	91.35	0.23159E 07	98.6	0.31				
31	92.38	0.23434E 07	101.2	0.31				
32	93.41	0.23711E 07	103.7	0.30				
33	94.45	0.23988E 07	106.3	0.30				
34	95.48	0.24264E 07	108.8	0.30				
35	96.51	0.24539E 07	111.4	0.30				
36	97.54	0.24814E 07	113.9	0.29				

STANTON NUMBER DATA RUN 111873 *** DISCRETE HOLE RIG *** NAS-3-14336

TINF= 72.9 UINF= 53.4 XVO= 4.610 RHO= 0.07457 CP= 0.241 VISC= 0.16387E-03 PR=0.714
DISTANCE FROM ORIGIN OF BL TO 1ST PLATE=44.690 P/D=10
UNCERTAINTY IN REX=27139.

** M=0.0, FLAT PLATE RUN, HIGH RE, STEP T-WALL AT 1ST PLATE

PLATE	X	REX	TO	REENTH	STANTON NO	DST	DREEN	M	F	T2	THETA	DTH
1	50.30	0.12400E 07	101.3	0.11106E 03	0.40922E-02	0.585E-04	2.					
2	52.30	0.12943E 07	101.4	0.30568E 03	0.30791E-02	0.523E-04	3.	0.00	0.0000	101.4	1.000	0.012
3	54.30	0.13486E 07	101.3	0.46610E 03	0.28318E-02	0.512E-04	3.	0.00	0.0000	101.3	1.000	0.012
4	56.30	0.14028E 07	101.2	0.61764E 03	0.27520E-02	0.509E-04	4.	0.00	0.0000	101.2	1.000	0.012
5	58.30	0.14571E 07	101.3	0.76266E 03	0.25916E-02	0.500E-04	5.	0.00	0.0000	101.3	1.000	0.012
6	60.30	0.15114E 07	101.4	0.90393E 03	0.26138E-02	0.499E-04	5.	0.00	0.0000	101.4	1.000	0.012
7	62.30	0.15657E 07	101.3	0.10420E 04	0.24733E-02	0.494E-04	5.	0.00	0.0000	101.3	1.000	0.012
8	64.30	0.16200E 07	101.2	0.11764E 04	0.24796E-02	0.495E-04	6.	0.00	0.0000	101.2	1.000	0.012
9	66.30	0.16742E 07	101.3	0.13084E 04	0.23825E-02	0.490E-04	6.	0.00	0.0000	101.3	1.000	0.012
10	68.30	0.17285E 07	101.3	0.14386E 04	0.24155E-02	0.491E-04	6.	0.00	0.0000	101.3	1.000	0.012
11	70.30	0.17828E 07	101.3	0.15672E 04	0.23247E-02	0.488E-04	7.	0.00	0.0000	101.3	1.000	0.012
12	72.30	0.18371E 07	101.3	0.16920E 04	0.22706E-02	0.484E-04	7.	0.00	0.0000	101.3	1.000	0.012
13	73.82	0.18783E 07	100.5	0.17867E 04	0.23659E-02	0.374E-04	7.					
14	74.85	0.19063E 07	100.2	0.18513E 04	0.22486E-02	0.383E-04	7.					
15	75.88	0.19342E 07	100.9	0.19145E 04	0.22712E-02	0.389E-04	7.					
16	76.91	0.19623E 07	100.9	0.19777E 04	0.22433E-02	0.381E-04	7.					
17	77.95	0.19904E 07	101.0	0.20401E 04	0.22151E-02	0.379E-04	7.					
18	78.98	0.20184E 07	100.9	0.21023E 04	0.22330E-02	0.383E-04	7.					
19	80.01	0.20463E 07	100.8	0.21647E 04	0.22259E-02	0.374E-04	7.					
20	81.04	0.20743E 07	101.0	0.22257E 04	0.21338E-02	0.362E-04	7.					
21	82.07	0.21022E 07	100.8	0.22877E 04	0.22930E-02	0.385E-04	7.					
22	83.10	0.21302E 07	100.9	0.23504E 04	0.21875E-02	0.379E-04	7.					
23	84.13	0.21581E 07	100.8	0.24106E 04	0.21203E-02	0.371E-04	8.					
24	85.16	0.21862E 07	100.9	0.24708E 04	0.21799E-02	0.382E-04	8.					
25	86.20	0.22143E 07	100.8	0.25306E 04	0.20942E-02	0.369E-04	8.					
26	87.23	0.22423E 07	100.8	0.25913E 04	0.22425E-02	0.386E-04	8.					
27	88.26	0.22702E 07	101.0	0.26525E 04	0.21275E-02	0.372E-04	8.					
28	89.29	0.22982E 07	101.1	0.27114E 04	0.20825E-02	0.367E-04	8.					
29	90.32	0.23261E 07	100.4	0.27703E 04	0.21252E-02	0.368E-04	8.					
30	91.35	0.23541E 07	101.3	0.28289E 04	0.20633E-02	0.369E-04	8.					
31	92.38	0.23820E 07	101.4	0.28877E 04	0.21424E-02	0.372E-04	8.					
32	93.41	0.24101E 07	101.1	0.29455E 04	0.19899E-02	0.358E-04	8.					
33	94.45	0.24382E 07	100.9	0.30021E 04	0.20538E-02	0.363E-04	8.					
34	95.48	0.24662E 07	100.2	0.30606E 04	0.21220E-02	0.368E-04	8.					
35	96.51	0.24941E 07	100.8	0.31195E 04	0.20911E-02	0.383E-04	8.					
36	97.54	0.25221E 07	100.0	0.31781E 04	0.20975E-02	0.425E-04	8.					

STANTON NUMBER DATA RUN 111973 *** DISCRETE HOLE RIG *** NAS-3-14336

TINF= 72.4 UINF= 53.1 XVO= 4.610 RHO= 0.07479 CP= 0.241 VISC= 0.16327E-03 PR=0.714
DISTANCE FROM ORIGIN OF BL TO 1ST PLATE=44.690 P/D=10
UNCERTAINTY IN REX=27090. UNCERTAINTY IN F=0.03026 IN RATIO

** M=0.2, COLD RUN, HIGH RE,STEP T-WALL AT 1ST PLATE.

PLATE	X	REX	TO	REENTH	STANTON NO	DST	DREEN	M	F	T2	THETA	DTH
1	50.30	0.12377E 07	101.7	0.11060E 03	0.40827E-02	0.569E-04	2.					
2	52.30	0.12919E 07	101.8	0.32158E 03	0.33224E-02	0.523E-04	3.	0.20	0.0017	75.8	0.116	0.009
3	54.30	0.13461E 07	101.8	0.50464E 03	0.30516E-02	0.508E-04	4.	0.00	0.0017	101.8	0.116	0.012
4	56.30	0.14003E 07	101.8	0.67886E 03	0.29815E-02	0.503E-04	4.	0.22	0.0018	75.7	0.113	0.009
5	58.30	0.14544E 07	101.8	0.84663E 03	0.28135E-02	0.495E-04	5.	0.00	0.0018	101.8	0.113	0.012
6	60.30	0.15086E 07	101.9	0.10101E 04	0.28428E-02	0.495E-04	5.	0.20	0.0017	75.8	0.115	0.009
7	62.30	0.15628E 07	101.8	0.11703E 04	0.26910E-02	0.489E-04	6.	0.00	0.0017	101.8	0.115	0.012
8	64.30	0.16170E 07	101.8	0.13285E 04	0.26848E-02	0.489E-04	6.	0.21	0.0017	76.5	0.139	0.009
9	66.30	0.16712E 07	102.0	0.14831E 04	0.25588E-02	0.480E-04	6.	0.00	0.0017	102.0	0.139	0.012
10	68.30	0.17253E 07	102.0	0.16366E 04	0.26469E-02	0.484E-04	7.	0.21	0.0017	76.4	0.136	0.009
11	70.30	0.17795E 07	102.0	0.17891E 04	0.25194E-02	0.478E-04	7.	0.00	0.0017	102.0	0.136	0.012
12	72.30	0.18337E 07	101.9	0.19370E 04	0.24625E-02	0.477E-04	7.	0.21	0.0017	76.6	0.141	0.009
13	73.82	0.18749E 07	100.9	0.20491E 04	0.25479E-02	0.391E-04	7.					
14	74.85	0.19028E 07	100.6	0.21178E 04	0.23652E-02	0.390E-04	7.					
15	75.88	0.19307E 07	101.6	0.21800E 04	0.23288E-02	0.389E-04	7.					
16	76.91	0.19587E 07	101.6	0.22443E 04	0.22758E-02	0.377E-04	7.					
17	77.95	0.19867E 07	101.9	0.23071E 04	0.22176E-02	0.371E-04	8.					
18	78.98	0.20147E 07	101.8	0.23691E 04	0.22261E-02	0.372E-04	8.					
19	80.01	0.20426E 07	101.7	0.24310E 04	0.22023E-02	0.362E-04	8.					
20	81.04	0.20705E 07	102.0	0.24911E 04	0.21032E-02	0.350E-04	8.					
21	82.07	0.20984E 07	101.8	0.25519E 04	0.22448E-02	0.369E-04	8.					
22	83.10	0.21263E 07	101.9	0.26132E 04	0.21459E-02	0.365E-04	8.					
23	84.13	0.21542E 07	101.7	0.26722E 04	0.20815E-02	0.356E-04	8.					
24	85.16	0.21822E 07	101.9	0.27310E 04	0.21254E-02	0.365E-04	8.					
25	86.20	0.22102E 07	101.9	0.27895E 04	0.20612E-02	0.355E-04	8.					
26	87.23	0.22381E 07	101.8	0.28490E 04	0.22023E-02	0.371E-04	8.					
27	88.26	0.22660E 07	102.0	0.29089E 04	0.20835E-02	0.357E-04	8.					
28	89.29	0.22939E 07	102.1	0.29663E 04	0.20250E-02	0.351E-04	8.					
29	90.32	0.23218E 07	101.4	0.30237E 04	0.20861E-02	0.353E-04	8.					
30	91.35	0.23497E 07	102.4	0.30809E 04	0.20081E-02	0.353E-04	8.					
31	92.38	0.23777E 07	102.4	0.31383E 04	0.20987E-02	0.357E-04	8.					
32	93.41	0.24057E 07	102.1	0.31949E 04	0.19529E-02	0.343E-04	8.					
33	94.45	0.24337E 07	102.0	0.32501E 04	0.20024E-02	0.348E-04	8.					
34	95.48	0.24616E 07	101.2	0.33070E 04	0.20697E-02	0.351E-04	8.					
35	96.51	0.24895E 07	101.9	0.33647E 04	0.20594E-02	0.369E-04	8.					
36	97.54	0.25174E 07	101.0	0.34218E 04	0.20323E-02	0.411E-04	8.					

STANTON NUMBER DATA RUN 112273 *** DISCRETE HOLE RIG *** NAS-3-14336

TINF= 71.0 UINF= 53.1 XVO= 4.610 RHO= 0.07420 CP= 0.241 VISC= 0.16419E-03 PR=0.714
DISTANCE FROM ORIGIN OF BL TO 1ST PLATE=44.690 P/D=10
UNCERTAINTY IN REX=26960. UNCERTAINTY IN F=0.03026 IN RATIO

** M=0.2, HOT RUN, HIGH RE,STEP T-WALL AT 1ST PLATE.

PLATE	X	REX	TO	REENTH	STANTON NO	DST	DREEN	M	F	T2	THETA	DTH
1	50.30	0.12318E 07	100.6	0.10260E 03	0.38056E-02	0.550E-04	2.					
2	52.30	0.12857E 07	100.6	0.35501E 03	0.28868E-02	0.498E-04	3.	0.17	0.0014	99.4	0.958	0.012
3	54.30	0.13396E 07	100.6	0.57974E 03	0.27786E-02	0.492E-04	4.	0.00	0.0014	100.6	0.958	0.012
4	56.30	0.13935E 07	100.7	0.79850E 03	0.26137E-02	0.484E-04	5.	0.17	0.0014	100.3	0.986	0.012
5	58.30	0.14475E 07	100.6	0.10104E 04	0.25230E-02	0.481E-04	5.	0.00	0.0014	100.6	0.986	0.012
6	60.30	0.15014E 07	100.7	0.12129E 04	0.24101E-02	0.474E-04	6.	0.18	0.0014	97.6	0.898	0.011
7	62.30	0.15553E 07	100.5	0.14117E 04	0.23859E-02	0.477E-04	6.	0.00	0.0014	100.5	0.898	0.012
8	64.30	0.16092E 07	100.5	0.16048E 04	0.22719E-02	0.471E-04	7.	0.14	0.0012	102.7	1.072	0.012
9	66.30	0.16631E 07	100.6	0.17942E 04	0.22506E-02	0.468E-04	7.	0.00	0.0012	100.6	1.072	0.012
10	68.30	0.17171E 07	100.7	0.19907E 04	0.21251E-02	0.463E-04	8.	0.17	0.0014	101.7	1.035	0.012
11	70.30	0.17710E 07	100.7	0.21842E 04	0.21393E-02	0.463E-04	8.	0.00	0.0014	100.7	1.035	0.012
12	72.30	0.18249E 07	100.7	0.23676E 04	0.18999E-02	0.453E-04	8.	0.15	0.0012	105.1	1.147	0.013
13	73.82	0.18659E 07	99.9	0.25064E 04	0.22328E-02	0.350E-04	9.					
14	74.85	0.18936E 07	99.4	0.25666E 04	0.20999E-02	0.357E-04	9.					
15	75.88	0.19214E 07	100.4	0.26053E 04	0.20620E-02	0.356E-04	9.					
16	76.91	0.19493E 07	100.4	0.26626E 04	0.20604E-02	0.351E-04	9.					
17	77.95	0.19772E 07	100.6	0.27194E 04	0.20304E-02	0.347E-04	9.					
18	78.98	0.20050E 07	100.8	0.27754E 04	0.19955E-02	0.345E-04	9.					
19	80.01	0.20327E 07	100.5	0.28313E 04	0.20276E-02	0.340E-04	9.					
20	81.04	0.20605E 07	100.7	0.28869E 04	0.19689E-02	0.332E-04	9.					
21	82.07	0.20883E 07	100.9	0.29424E 04	0.20264E-02	0.344E-04	9.					
22	83.10	0.21161E 07	100.5	0.29988E 04	0.20331E-02	0.350E-04	9.					
23	84.13	0.21438E 07	100.6	0.30540E 04	0.19316E-02	0.338E-04	9.					
24	85.16	0.21717E 07	101.0	0.31079E 04	0.19487E-02	0.345E-04	9.					
25	86.20	0.21996E 07	100.7	0.31621E 04	0.19477E-02	0.340E-04	9.					
26	87.23	0.22274E 07	100.6	0.32180E 04	0.20782E-02	0.355E-04	9.					
27	88.26	0.22552E 07	101.2	0.32732E 04	0.18905E-02	0.335E-04	9.					
28	89.29	0.22829E 07	101.0	0.33262E 04	0.19209E-02	0.336E-04	9.					
29	90.32	0.23107E 07	100.6	0.33792E 04	0.18957E-02	0.330E-04	9.					
30	91.35	0.23385E 07	100.9	0.34328E 04	0.19559E-02	0.344E-04	9.					
31	92.38	0.23662E 07	101.2	0.34871E 04	0.19511E-02	0.343E-04	9.					
32	93.41	0.23941E 07	100.4	0.35408E 04	0.19130E-02	0.339E-04	9.					
33	94.45	0.24220E 07	100.7	0.35936E 04	0.18896E-02	0.336E-04	9.					
34	95.48	0.24498E 07	100.0	0.36472E 04	0.19629E-02	0.339E-04	9.					
35	96.51	0.24776E 07	100.5	0.37017E 04	0.19560E-02	0.356E-04	9.					
36	97.54	0.25053E 07	99.9	0.37559E 04	0.19430E-02	0.387E-04	9.					

FOLLOWING IS THE DATA FOR THETA=0 AND THETA=1, WHICH WAS OBTAINED BY LINEAR SUPERPOSITION THEORY.
THIS DATA WAS PRODUCED FROM RUN 111973 AND RUN 112273
FOR THE DETAIL CHANGES OF PROPERTIES AND BOUNDARY CONDITIONS, PLEASE SEE THE ABOVE TWO RUNS

PLATE	REXCOL	RE DEL2	ST(TH=0)	REXHOT	RE DEL2	ST(TH=1)	ETA	STCR	F-COL	STHR	F-HOT	PHI-1
1	1237721.0	110.6	0.004083	1231780.0	102.6	0.003806	UUUUU	UUUUU	0.0000	UUUUUUU	0.0000	UUUUU
2	1291900.0	312.8	0.003382	1285699.0	357.6	0.002865	0.153	0.884	0.0017	1.029	0.0014	1.262
3	1346080.0	488.1	0.003089	1339618.0	584.5	0.002765	0.105	0.904	0.0017	1.055	0.0014	1.303
4	1400259.0	653.9	0.003029	1393537.0	803.8	0.002608	0.139	0.955	0.0018	1.037	0.0014	1.292
5	1454438.0	813.1	0.002851	1447456.0	1016.4	0.002518	0.117	0.950	0.0018	1.033	0.0014	1.296
6	1508617.0	969.1	0.002906	1501375.0	1225.2	0.002353	0.190	1.012	0.0017	0.991	0.0014	1.269
7	1562796.0	1121.9	0.002736	1555294.0	1429.3	0.002346	0.142	0.988	0.0017	1.009	0.0014	1.294
8	1616975.0	1270.4	0.002746	1609213.0	1617.7	0.002304	0.161	1.023	0.0017	1.010	0.0012	1.249
9	1671154.0	1415.4	0.002605	1663132.0	1804.1	0.002274	0.127	0.998	0.0017	1.014	0.0012	1.257
10	1725333.0	1559.8	0.002726	1717051.0	1999.1	0.002145	0.213	1.070	0.0017	0.972	0.0014	1.264
11	1779512.0	1703.5	0.002577	1770970.0	2190.9	0.002154	0.164	1.034	0.0017	0.98[illegible]	0.0014	1.286
12	1833692.0	1842.1	0.002541	1824889.0	2367.4	0.001982	0.220	1.040	0.0017	0.922	0.0012	1.181
13	1874868.0	1947.2	0.002593	1865868.0	2501.2	0.002234	0.138	1.076		1.049		
14	1902770.0	2017.0	0.002403	1893636.0	2561.5	0.002101	0.126	1.006		0.993		
15	1930672.0	2083.6	0.002367	1921404.0	2602.6	0.002063	0.128	0.999		0.980		
16	1958710.0	2148.9	0.002307	1949307.0	2659.9	0.002061	0.106	0.982		0.985		
17	1986747.0	2212.4	0.002244	1977210.0	2716.8	0.002031	0.095	0.963		0.976		
18	2014650.0	2275.3	0.002259	2004979.0	2772.8	0.001997	0.116	0.977		0.964		
19	2042552.0	2338.0	0.002227	2032747.0	2828.7	0.002028	0.089	0.970		0.985		
20	2070454.0	2398.8	0.002122	2060515.0	2884.3	0.001969	0.072	0.931		0.961		
21	2098357.0	2460.2	0.002276	2088284.0	2939.9	0.002027	0.109	1.006		0.994		
22	2126259.0	2522.2	0.002162	2116052.0	2996.3	0.002034	0.059	0.962		1.001		
23	2154161.0	2581.7	0.002103	2143820.0	3051.5	0.001932	0.081	0.942		0.956		
24	2182198.0	2641.2	0.002151	2171723.0	3105.4	0.001950	0.093	0.969		0.969		
25	2210236.0	2700.2	0.002077	2199626.0	3159.6	0.001948	0.062	0.942		0.972		
26	2238138.0	2760.2	0.002220	2227395.0	3215.6	0.002079	0.064	1.013		1.042		
27	2266041.0	2820.7	0.002111	2255163.0	3270.8	0.001891	0.104	0.968		0.952		
28	2293943.0	2878.7	0.002040	2282931.0	3323.8	0.001921	0.058	0.941		0.971		
29	2321845.0	2936.7	0.002113	2310700.0	3376.8	0.001897	0.103	0.980		0.962		
30	2349748.0	2994.4	0.002016	2338468.0	3430.4	0.001956	0.030	0.940		0.996		
31	2377650.0	3052.1	0.002120	2366236.0	3484.7	0.001952	0.079	0.994		0.998		
32	2405687.0	3109.1	0.001959	2394139.0	3538.4	0.001913	0.023	0.923		0.982		
33	2433725.0	3164.7	0.002018	2422042.0	3591.3	0.001890	0.064	0.956		0.973		
34	2461627.0	3222.0	0.002085	2449811.0	3644.9	0.001963	0.058	0.992		1.015		
35	2489529.0	3280.1	0.002074	2477579.0	3699.4	0.001956	0.057	0.992		1.015		
36	2517432.0	3337.6	0.002045	2505347.0	3753.6	0.001943	0.050	0.982		1.011		

STANTON NUMBER DATA RUN 121773 *** DISCRETE HOLE RIG *** NAS-3-14336

TINF= 66.8 UINF= 53.3 XVO= 4.610 RHO= 0.07542 CP= 0.242 VISC= 0.16048E-03 PR=0.715
DISTANCE FROM ORIGIN OF BL TO 1ST PLATE=44.690 P/D=10
UNCERTAINTY IN REX=27663. UNCERTAINTY IN F=0.03025 IN RATIO

** M=0.5, COLD RUN, HIGH RE,STEP T-WALL AT 1ST PLATE.

PLATE	X	REX	TO	REENTH	STANTON NO	DST	DREEN	M	F	T2	THETA	DTH
1	50.30	0.12639E 07	94.9	0.10925E 03	0.39492E-02	0.579E-04	2.					
2	52.30	0.13192E 07	94.9	0.34363E 03	0.34204E-02	0.547E-04	3.	0.53	0.0043	70.5	0.129	0.009
3	54.30	0.13746E 07	95.0	0.55467E 03	0.31052E-02	0.527E-04	4.	0.00	0.0043	95.0	0.129	0.013
4	56.30	0.14299E 07	94.8	0.75571E 03	0.30905E-02	0.528E-04	5.	0.52	0.0042	70.4	0.128	0.009
5	58.30	0.14852E 07	94.9	0.95139E 03	0.29117E-02	0.517E-04	6.	0.00	0.0042	94.9	0.128	0.013
6	60.30	0.15405E 07	94.8	0.11444E 04	0.30122E-02	0.524E-04	7.	0.51	0.0041	70.4	0.127	0.009
7	62.30	0.15959E 07	94.9	0.13354E 04	0.28367E-02	0.513E-04	7.	0.00	0.0041	94.9	0.127	0.013
8	64.30	0.16512E 07	94.8	0.15257E 04	0.28621E-02	0.516E-04	8.	0.53	0.0043	70.7	0.137	0.009
9	66.30	0.17065E 07	94.9	0.17119E 04	0.26882E-02	0.506E-04	8.	0.00	0.0043	94.9	0.137	0.013
10	68.30	0.17618E 07	94.8	0.18968E 04	0.28570E-02	0.516E-04	9.	0.52	0.0042	70.6	0.135	0.009
11	70.30	0.18172E 07	94.8	0.20812E 04	0.26713E-02	0.506E-04	9.	0.00	0.0042	94.8	0.135	0.013
12	72.30	0.18725E 07	94.9	0.22597E 04	0.26612E-02	0.505E-04	10.	0.50	0.0041	70.7	0.138	0.009
13	73.82	0.19145E 07	94.4	0.23964E 04	0.27720E-02	0.426E-04	10.					
14	74.85	0.19430E 07	94.1	0.24720E 04	0.25313E-02	0.415E-04	10.					
15	75.88	0.19715E 07	95.2	0.25351E 04	0.24539E-02	0.407E-04	10.					
16	76.91	0.20002E 07	95.4	0.26040E 04	0.23726E-02	0.391E-04	10.					
17	77.95	0.20288E 07	95.6	0.26707E 04	0.23040E-02	0.382E-04	10.					
18	78.98	0.20573E 07	95.7	0.27364E 04	0.23007E-02	0.382E-04	10.					
19	80.01	0.20858E 07	95.6	0.28014E 04	0.22553E-02	0.370E-04	10.					
20	81.04	0.21143E 07	95.8	0.28645E 04	0.21710E-02	0.358E-04	10.					
21	82.07	0.21428E 07	95.7	0.29281E 04	0.22871E-02	0.375E-04	10.					
22	83.10	0.21713E 07	95.9	0.29917E 04	0.21739E-02	0.368E-04	10.					
23	84.13	0.21998E 07	95.6	0.30525E 04	0.20894E-02	0.358E-04	10.					
24	85.16	0.22284E 07	95.8	0.31130E 04	0.21498E-02	0.369E-04	10.					
25	86.20	0.22570E 07	95.7	0.31738E 04	0.21114E-02	0.361E-04	10.					
26	87.23	0.22855E 07	95.6	0.32355E 04	0.22174E-02	0.374E-04	10.					
27	88.26	0.23140E 07	95.9	0.32972E 04	0.21057E-02	0.361E-04	10.					
28	89.29	0.23425E 07	95.9	0.33564E 04	0.20469E-02	0.354E-04	10.					
29	90.32	0.23710E 07	95.3	0.34158E 04	0.21152E-02	0.358E-04	10.					
30	91.35	0.23995E 07	95.9	0.34750E 04	0.20351E-02	0.356E-04	10.					
31	92.38	0.24280E 07	96.3	0.35342E 04	0.21218E-02	0.362E-04	10.					
32	93.41	0.24566E 07	96.0	0.35929E 04	0.19887E-02	0.348E-04	10.					
33	94.45	0.24852E 07	95.9	0.36502E 04	0.20308E-02	0.352E-04	10.					
34	95.48	0.25137E 07	95.2	0.37090E 04	0.20929E-02	0.355E-04	11.					
35	96.51	0.25422E 07	95.8	0.37684E 04	0.20683E-02	0.370E-04	11.					
36	97.54	0.25707E 07	95.0	0.38269E 04	0.20347E-02	0.408E-04	11.					

STANTON NUMBER DATA RUN 121873 *** DISCRETE HOLE RIG *** NAS-3-14336

TINF= 67.4 UINF= 53.4 XVO= 4.610 RHO= 0.07520 CP= 0.242 VISC= 0.16112E-03 PR=0.715
DISTANCE FROM ORIGIN OF BL TO 1ST PLATE=44.690 P/D=10
UNCERTAINTY IN REX=27593. UNCERTAINTY IN F=0.03025 IN RATIO

** M=0.5, HOT RUN, HIGH RE,STEP T-WALL AT 1ST PLATE.

PLATE	X	REX	TO	REENTH	STANTON NO	DST	DREEN	M	F	T2	THETA	DTH
1	50.30	0.12607E 07	96.8	0.10582E 03	0.38349E-02	0.549E-04	2.					
2	52.30	0.13159E 07	96.9	0.52253E 03	0.30321E-02	0.502E-04	5.	0.51	0.0041	96.9	1.000	0.012
3	54.30	0.13711E 07	96.9	0.91208E 03	0.28506E-02	0.492E-04	7.	0.00	0.0041	96.9	1.000	0.012
4	56.30	0.14263E 07	97.0	0.12811E 04	0.27137E-02	0.484E-04	9.	0.51	0.0042	95.1	0.937	0.012
5	58.30	0.14815E 07	96.8	0.16420E 04	0.25571E-02	0.479E-04	11.	0.00	0.0042	96.9	0.937	0.012
6	60.30	0.15367E 07	97.0	0.20206E 04	0.24958E-02	0.474E-04	12.	0.56	0.0045	95.8	0.960	0.012
7	62.30	0.15919E 07	96.8	0.23950E 04	0.24033E-02	0.472E-04	13.	0.00	0.0045	96.8	0.960	0.012
8	64.30	0.16470E 07	96.9	0.27380E 04	0.23212E-02	0.467E-04	15.	0.48	0.0039	96.6	0.991	0.012
9	66.30	0.17022E 07	96.8	0.30763E 04	0.22295E-02	0.465E-04	15.	0.00	0.0039	96.8	0.991	0.012
10	68.30	0.17574E 07	97.0	0.34362E 04	0.22275E-02	0.462E-04	16.	0.54	0.0044	96.2	0.975	0.012
11	70.30	0.18126E 07	96.8	0.37938E 04	0.21459E-02	0.460E-04	17.	0.00	0.0044	96.8	0.975	0.012
12	72.30	0.18678E 07	97.0	0.41424E 04	0.20023E-02	0.453E-04	19.	0.52	0.0042	97.4	1.015	0.012
13	73.82	0.19097E 07	96.9	0.44078E 04	0.22974E-02	0.355E-04	19.					
14	74.85	0.19382E 07	96.6	0.44705E 04	0.21140E-02	0.351E-04	19.					
15	75.88	0.19666E 07	97.6	0.44696E 04	0.20643E-02	0.348E-04	19.					
16	76.91	0.19951E 07	97.7	0.45278E 04	0.20251E-02	0.338E-04	19.					
17	77.95	0.20237E 07	98.0	0.45848E 04	0.19800E-02	0.333E-04	19.					
18	78.98	0.20521E 07	98.1	0.46409E 04	0.19603E-02	0.332E-04	19.					
19	80.01	0.20805E 07	97.9	0.46968E 04	0.19710E-02	0.326E-04	19.					
20	81.04	0.21090E 07	98.1	0.47517E 04	0.18916E-02	0.316E-04	19.					
21	82.07	0.21374E 07	98.1	0.48068E 04	0.19765E-02	0.329E-04	19.					
22	83.10	0.21658E 07	98.0	0.48624E 04	0.19354E-02	0.331E-04	19.					
23	84.13	0.21942E 07	97.9	0.49161E 04	0.18387E-02	0.320E-04	19.					
24	85.16	0.22228E 07	98.1	0.49691E 04	0.18848E-02	0.329E-04	19.					
25	86.20	0.22513E 07	98.0	0.50225E 04	0.18663E-02	0.324E-04	19.					
26	87.23	0.22798E 07	97.8	0.50773E 04	0.19865E-02	0.337E-04	19.					
27	88.26	0.23082E 07	98.3	0.51319E 04	0.18487E-02	0.322E-04	19.					
28	89.29	0.23366E 07	98.2	0.51842E 04	0.18278E-02	0.319E-04	19.					
29	90.32	0.23650E 07	97.6	0.52369E 04	0.18774E-02	0.321E-04	19.					
30	91.35	0.23934E 07	98.1	0.52900E 04	0.18570E-02	0.326E-04	19.					
31	92.38	0.24219E 07	98.4	0.53432E 04	0.18823E-02	0.326E-04	19.					
32	93.41	0.24504E 07	97.9	0.53957E 04	0.18101E-02	0.319E-04	19.					
33	94.45	0.24790E 07	98.0	0.54475E 04	0.18287E-02	0.321E-04	19.					
34	95.48	0.25074E 07	97.2	0.55004E 04	0.18881E-02	0.323E-04	19.					
35	96.51	0.25358E 07	97.8	0.55537E 04	0.18615E-02	0.338E-04	19.					
36	97.54	0.25642E 07	97.0	0.56065E 04	0.18451E-02	0.370E-04	19.					

FOLLOWING IS THE DATA FOR THETA=0 AND THETA=1, WHICH WAS OBTAINED BY LINEAR SUPERPOSITION THEORY.
THIS DATA WAS PRODUCED FROM RUN 121773 AND RUN 121873
FOR THE DETAIL CHANGES OF PROPERTIES AND BOUNDARY CONDITIONS, PLEASE SEE THE ABOVE TWO RUNS

PLATE	REXCOL	RE DEL2	ST(TH=0)	REXHOT	RE DEL2	ST(TH=1)	ETA	STCR	F-COL	STHR	F-HOT	PHI-1
1	1263917.0	109.2	0.003949	1260738.0	105.8	0.003835	UUUUU	UUUUU	0.0000	UUUUUUU	0.0000	UUUUU
2	1319243.0	314.7	0.003478	1315925.0	522.6	0.003032	0.128	0.913	0.0043	1.094	0.0041	1.732
3	1374568.0	497.9	0.003143	1371112.0	912.2	0.002851	0.093	0.924	0.0043	1.093	0.0041	1.767
4	1429894.0	672.0	0.003150	1426298.0	1294.8	0.002685	0.148	0.997	0.0042	1.073	0.0042	1.777
5	1485220.0	841.2	0.002968	1481485.0	1668.5	0.002530	0.148	0.993	0.0042	1.043	0.0042	1.765
6	1540546.0	1008.8	0.003091	1536672.0	2055.6	0.002471	0.201	1.081	0.0041	1.045	0.0045	1.838
7	1595872.0	1174.6	0.002903	1591858.0	2438.6	0.002383	0.179	1.053	0.0041	1.030	0.0045	1.836
8	1651197.0	1336.5	0.002949	1647045.0	2782.8	0.002316	0.215	1.104	0.0043	1.021	0.0039	1.739
9	1706523.0	1494.4	0.002761	1702231.0	3122.7	0.002225	0.194	1.063	0.0043	0.997	0.0039	1.725
10	1761849.0	1652.6	0.002958	1757418.0	3488.0	0.002209	0.253	1.166	0.0042	1.006	0.0044	1.828
11	1817175.0	1810.7	0.002756	1812605.0	3850.6	0.002131	0.227	1.111	0.0042	0.984	0.0044	1.814
12	1872500.0	1963.4	0.002765	1867791.0	4195.7	0.002013	0.272	1.137	0.0041	0.942	0.0042	1.740
13	1914548.0	2080.5	0.002846	1909733.0	4458.5	0.002284	0.197	1.186		1.078		
14	1943041.0	2158.1	0.002596	1938154.0	4520.9	0.002102	0.190	1.092		0.998		
15	1971534.0	2231.0	0.002515	1966576.0	4520.6	0.002053	0.183	1.067		0.981		
16	2000164.0	2301.5	0.002427	1995134.0	4578.5	0.002015	0.169	1.038		0.968		
17	2028796.0	2369.7	0.002355	2023694.0	4635.2	0.001971	0.163	1.015		0.952		
18	2057288.0	2436.9	0.002354	2052115.0	4691.0	0.001951	0.171	1.023		0.947		
19	2085781.0	2503.2	0.002300	2080536.0	4746.7	0.001963	0.146	1.007		0.958		
20	2114274.0	2567.6	0.002215	2108957.0	4801.4	0.001884	0.149	0.976		0.924		
21	2142767.0	2632.5	0.002336	2137378.0	4856.2	0.001968	0.157	1.037		0.970		
22	2171260.0	2697.4	0.002211	2165799.0	4911.7	0.001929	0.128	0.988		0.955		
23	2199752.0	2759.3	0.002129	2194220.0	4965.2	0.001832	0.139	0.958		0.911		
24	2228383.0	2820.9	0.002191	2222779.0	5018.0	0.001878	0.143	0.992		0.938		
25	2257014.0	2882.8	0.002150	2251338.0	5071.1	0.001860	0.135	0.979		0.933		
26	2285507.0	2945.6	0.002253	2279759.0	5125.8	0.001980	0.121	1.033		0.997		
27	2314000.0	3008.4	0.002146	2308181.0	5180.1	0.001842	0.142	0.989		0.932		
28	2342493.0	3068.6	0.002081	2336602.0	5232.2	0.001822	0.125	0.965		0.925		
29	2370986.0	3129.0	0.002152	2365023.0	5284.8	0.001871	0.131	1.003		0.954		
30	2399478.0	3189.2	0.002063	2393444.0	5337.8	0.001852	0.102	0.967		0.948		
31	2427971.0	3249.4	0.002159	2421865.0	5390.8	0.001876	0.131	1.017		0.964		
32	2456602.0	3308.9	0.002017	2450424.0	5443.2	0.001805	0.105	0.955		0.931		
33	2485233.0	3367.1	0.002062	2478983.0	5494.8	0.001823	0.116	0.981		0.944		
34	2513726.0	3426.8	0.002125	2507404.0	5547.5	0.001882	0.114	1.016		0.978		
35	2542219.0	3487.1	0.002101	2535825.0	5600.7	0.001856	0.117	1.009		0.967		
36	2570711.0	3546.5	0.002064	2564247.0	5653.3	0.001840	0.109	0.996		0.962		

STANTON NUMBER DATA RUN 121673-1 *** DISCRETE HOLE RIG *** NAS-3-14336

TINF= 61.7 UINF= 53.5 XVO= 4.610 RHO= 0.07598 CP= 0.241 VISC= 0.15822E-03 PR=0.716
DISTANCE FROM ORIGIN OF BL TO 1ST PLATE=44.690 P/D=10
UNCERTAINTY IN REX=28173. UNCERTAINTY IN F=0.03025 IN RATIO

** M=1.0, COLD RUN, HIGH RE,STEP T-WALL AT 1ST PLATE.

PLATE	X	REX	TO	REENTH	STANTON NO	DST	DREEN	M	F	T2	THETA	DTH
1	50.30	0.12872E 07	90.4	0.11088E 03	0.39357E-02	0.563E-04	2.					
2	52.30	0.13436E 07	90.3	0.38899E 03	0.34172E-02	0.532E-04	4.	1.02	0.0083	66.1	0.152	0.009
3	54.30	0.13999E 07	90.4	0.64400E 03	0.31156E-02	0.514E-04	6.	0.00	0.0083	90.4	0.152	0.012
4	56.30	0.14563E 07	90.4	0.89018E 03	0.32276E-02	0.520E-04	7.	1.01	0.0082	65.9	0.147	0.009
5	58.30	0.15126E 07	90.4	0.11341E 04	0.30349E-02	0.509E-04	8.	0.00	0.0082	90.4	0.147	0.012
6	60.30	0.15690E 07	90.4	0.13829E 04	0.32167E-02	0.519E-04	10.	1.02	0.0083	66.2	0.156	0.009
7	62.30	0.16253E 07	90.4	0.16318E 04	0.30397E-02	0.509E-04	10.	0.00	0.0083	90.4	0.156	0.012
8	64.30	0.16817E 07	90.5	0.18893E 04	0.30944E-02	0.511E-04	11.	1.02	0.0083	66.9	0.181	0.009
9	66.30	0.17380E 07	90.5	0.21435E 04	0.29238E-02	0.502E-04	12.	0.00	0.0083	90.5	0.181	0.012
10	68.30	0.17943E 07	90.4	0.24004E 04	0.31100E-02	0.513E-04	13.	1.01	0.0082	67.1	0.189	0.009
11	70.30	0.18507E 07	90.4	0.26574E 04	0.29258E-02	0.503E-04	14.	0.00	0.0082	90.4	0.189	0.012
12	72.30	0.19070E 07	90.5	0.29141E 04	0.29219E-02	0.502E-04	15.	0.98	0.0079	67.6	0.206	0.009
13	73.82	0.19499E 07	69.4	0.31106E 04	0.30618E-02	0.459E-04	15.					
14	74.85	0.19789E 07	89.0	0.31963E 04	0.28389E-02	0.449E-04	15.					
15	75.88	0.20079E 07	90.2	0.32542E 04	0.27750E-02	0.443E-04	15.					
16	76.91	0.20371E 07	90.4	0.33334E 04	0.26784E-02	0.424E-04	15.					
17	77.95	0.20662E 07	90.8	0.34099E 04	0.25882E-02	0.412E-04	15.					
18	78.98	0.20952E 07	90.8	0.34849E 04	0.25739E-02	0.410E-04	15.					
19	80.01	0.21243E 07	90.8	0.35589E 04	0.25176E-02	0.397E-04	15.					
20	81.04	0.21533E 07	91.1	0.36303E 04	0.24009E-02	0.381E-04	15.					
21	82.07	0.21823E 07	91.0	0.37016E 04	0.25065E-02	0.396E-04	15.					
22	83.10	0.22113E 07	91.3	0.37724E 04	0.23703E-02	0.385E-04	15.					
23	84.13	0.22403E 07	91.1	0.38396E 04	0.22499E-02	0.370E-04	15.					
24	85.16	0.22695E 07	91.2	0.39060E 04	0.23225E-02	0.382E-04	15.					
25	86.20	0.22986E 07	91.3	0.39725E 04	0.22599E-02	0.372E-04	15.					
26	87.23	0.23277E 07	91.2	0.40393E 04	0.23352E-02	0.380E-04	15.					
27	88.26	0.23567E 07	91.5	0.41057E 04	0.22357E-02	0.368E-04	15.					
28	89.29	0.23857E 07	91.6	0.41695E 04	0.21572E-02	0.359E-04	15.					
29	90.32	0.24147E 07	91.0	0.42330E 04	0.22105E-02	0.361E-04	15.					
30	91.35	0.24437E 07	91.8	0.42958E 04	0.21160E-02	0.357E-04	15.					
31	92.38	0.24728E 07	92.1	0.43585E 04	0.21980E-02	0.362E-04	15.					
32	93.41	0.25019E 07	91.8	0.44201E 04	0.20470E-02	0.345E-04	15.					
33	94.45	0.25311E 07	91.8	0.44800E 04	0.20736E-02	0.348E-04	15.					
34	95.48	0.25601E 07	91.0	0.45413E 04	0.21432E-02	0.352E-04	15.					
35	96.51	0.25891E 07	91.6	0.46027E 04	0.20855E-02	0.363E-04	15.					
36	97.54	0.26181E 07	90.8	0.46628E 04	0.20546E-02	0.400E-04	15.					

STANTON NUMBER DATA RUN 121673-2 *** DISCRETE HOLE RIG *** NAS-3-14336

TINF= 65.7 UINF= 53.3 XVO= 4.610 RHO= 0.07538 CP= 0.241 VISC= 0.16035E-03 PR=0.715
DISTANCE FROM ORIGIN OF BL TO 1ST PLATE=44.690 P/D=10
UNCERTAINTY IN REX=27693. UNCERTAINTY IN F=0.03025 IN RATIO

** M=1.0, HOT RUN, HIGH RE, STEP T-WALL AT 1ST PLATE.

PLATE	X	REX	TO	REENTH	STANTON NO	DST	DREEN	M	F	T2	THETA	DTH
1	50.30	0.12653E 07	91.6	0.10735E 03	0.38763E-02	0.620E-04	2.					
2	52.30	0.13207E 07	91.4	0.71937E 03	0.32681E-02	0.583E-04	8.	0.99	0.0080	89.8	0.935	0.013
3	54.30	0.13761E 07	91.5	0.13082E 04	0.30382E-02	0.568E-04	13.	0.00	0.0080	91.5	0.935	0.014
4	56.30	0.14314E 07	91.4	0.19073E 04	0.30405E-02	0.569E-04	16.	1.00	0.0081	90.4	0.960	0.013
5	58.30	0.14868E 07	91.4	0.25016E 04	0.28641E-02	0.559E-04	20.	0.00	0.0081	91.4	0.960	0.014
6	60.30	0.15422E 07	91.4	0.31048E 04	0.28730E-02	0.561E-04	22.	0.98	0.0080	91.5	1.006	0.014
7	62.30	0.15976E 07	91.4	0.37059E 04	0.27871E-02	0.555E-04	25.	0.00	0.0080	91.4	1.006	0.014
8	64.30	0.16530E 07	91.4	0.43050E 04	0.27515E-02	0.554E-04	27.	0.97	0.0079	92.0	1.024	0.014
9	66.30	0.17084E 07	91.4	0.48995E 04	0.26232E-02	0.548E-04	29.	0.00	0.0079	91.4	1.024	0.014
10	68.30	0.17638E 07	91.4	0.54936E 04	0.26807E-02	0.551E-04	31.	0.96	0.0078	92.4	1.039	0.014
11	70.30	0.18191E 07	91.5	0.60866E 04	0.25841E-02	0.543E-04	33.	0.00	0.0078	91.5	1.039	0.014
12	72.30	0.18745E 07	91.5	0.66733E 04	0.24600E-02	0.536E-04	35.	0.96	0.0078	92.4	1.035	0.014
13	73.82	0.19166E 07	90.3	0.71187E 04	0.26918E-02	0.438E-04	35.					
14	74.85	0.19451E 07	89.7	0.71930E 04	0.25107E-02	0.443E-04	35.					
15	75.88	0.19737E 07	90.7	0.71484E 04	0.24377E-02	0.434E-04	35.					
16	76.91	0.20023E 07	90.9	0.72171E 04	0.23731E-02	0.419E-04	35.					
17	77.95	0.20310E 07	91.1	0.72840E 04	0.23155E-02	0.411E-04	35.					
18	78.98	0.20595E 07	91.3	0.73494E 04	0.22661E-02	0.405E-04	35.					
19	80.01	0.20880E 07	91.2	0.74139E 04	0.22506E-02	0.395E-04	35.					
20	81.04	0.21166E 07	91.4	0.74767E 04	0.21463E-02	0.379E-04	35.					
21	82.07	0.21451E 07	91.4	0.75390E 04	0.22178E-02	0.392E-04	36.					
22	83.10	0.21736E 07	91.4	0.76015E 04	0.21581E-02	0.392E-04	36.					
23	84.13	0.22021E 07	91.3	0.76610E 04	0.20106E-02	0.374E-04	36.					
24	85.16	0.22308E 07	91.6	0.77191E 04	0.20539E-02	0.383E-04	36.					
25	86.20	0.22595E 07	91.6	0.77772E 04	0.20161E-02	0.375E-04	36.					
26	87.23	0.22880E 07	91.4	0.78365E 04	0.21413E-02	0.389E-04	36.					
27	88.26	0.23165E 07	91.8	0.78954E 04	0.19803E-02	0.370E-04	36.					
28	89.29	0.23450E 07	91.8	0.79513E 04	0.19365E-02	0.364E-04	36.					
29	90.32	0.23736E 07	91.3	0.80072E 04	0.19751E-02	0.365E-04	36.					
30	91.35	0.24021E 07	91.8	0.80628E 04	0.19219E-02	0.367E-04	36.					
31	92.38	0.24306E 07	92.2	0.81183E 04	0.19625E-02	0.367E-04	36.					
32	93.41	0.24593E 07	91.8	0.81728E 04	0.18579E-02	0.357E-04	36.					
33	94.45	0.24879E 07	91.8	0.82263E 04	0.18860E-02	0.357E-04	36.					
34	95.48	0.25164E 07	91.2	0.82808E 04	0.19286E-02	0.359E-04	36.					
35	96.51	0.25450E 07	91.7	0.83353E 04	0.18925E-02	0.374E-04	36.					
36	97.54	0.25735E 07	91.1	0.83888E 04	0.18542E-02	0.401E-04	36.					

FOLLOWING IS THE DATA FOR THETA=0 AND THETA=1, WHICH WAS OBTAINED BY LINEAR SUPERPOSITION THEORY.
THIS DATA WAS PRODUCED FROM RUN 121673-1 AND RUN 121673-2
FOR THE DETAIL CHANGES OF PROPERTIES AND BOUNDARY CONDITIONS, PLEASE SEE THE ABOVE TWO RUNS

PLATE	REXCOL	RE DEL2	ST(TH=0)	REXHOT	RE DEL2	ST(TH=1)	ETA	STCR	F-COL	STHR	F-HOT	PHI-1
1	1287231.0	110.9	0.003936	1265285.0	107.3	0.003876	UUUUU	UUUUU	0.0000	UUUUUUU	0.0000	UUUUU
2	1343577.0	318.9	0.003446	1320670.0	748.0	0.003256	0.055	0.908	0.0083	1.176	0.0080	2.330
3	1399924.0	504.1	0.003131	1376056.0	1365.3	0.003032	0.032	0.924	0.0083	1.163	0.0080	2.377
4	1456270.0	684.2	0.003261	1431442.0	1981.7	0.003031	0.070	1.037	0.0082	1.212	0.0081	2.490
5	1512616.0	862.5	0.003066	1486827.0	2593.3	0.002856	0.068	1.030	0.0082	1.179	0.0081	2.486
6	1568962.0	1041.2	0.003280	1542213.0	3193.7	0.002875	0.123	1.152	0.0083	1.217	0.0080	2.543
7	1625309.0	1220.6	0.003086	1597599 0	3792.3	0.002789	0.096	1.124	0.0083	1.207	0.0080	2.556
8	1681655.0	1396.8	0.003168	1652984.0	4381.3	0.002761	0.128	1.191	0.0083	1.218	0.0079	2.574
9	1738001.0	1570.2	0.002988	1708370.0	4965.8	0.002632	0.119	1.154	0.0083	1.181	0.0079	2.550
10	1794348.0	1744.7	0.003206	1763756.0	5544.1	0.002700	0.158	1.269	0.0082	1.230	0.0078	2.613
11	1850694.0	1919.6	0.003002	1819141.0	6121.5	0.002600	0.134	1.214	0.0082	1.201	0.0078	2.596
12	1907040.0	2089.7	0.003036	1874527.0	6694.1	0.002479	0.183	1.253	0.0079	1.161	0.0078	2.567
13	1949864.0	2220.8	0.003137	1916620.0	7128.6	0.002690	0.142	1.313		1.271		
14	1978882.0	2308.6	0.002906	1945144.0	7202.8	0.002509	0.136	1.227		1.192		
15	2007900.0	2392.1	0.002844	1973667.0	7162.1	0.002436	0.143	1.211		1.164		
16	2037059.0	2473.3	0.002741	2002329.0	7230.7	0.002372	0.135	1.177		1.140		
17	2066218.0	2551.5	0.002644	2030991.0	7297.6	0.002314	0.125	1.144		1.118		
18	2095237.0	2628.2	0.002637	2059515.0	7363.0	0.002265	0.141	1.150		1.100		
19	2124255.0	2703.9	0.002572	2088038.0	7427.5	0.002249	0.125	1.130		1.098		
20	2153273.0	2776.8	0.002453	2116562.0	7490.2	0.002145	0.125	1.086		1.053		
21	2182292.0	2849.7	0.002565	2145086.0	7552.5	0.002217	0.136	1.143		1.093		
22	2211310.0	2922.1	0.002414	2173609.0	7615.0	0.002157	0.106	1.083		1.069		
23	2240329.0	2990.5	0.002299	2202133.0	7674.5	0.002010	0.126	1.038		1.000		
24	2269488.0	3058.4	0.002377	2230795.0	7732.5	0.002053	0.136	1.080		1.026		
25	2298647.0	3126.5	0.002310	2259457.0	7790.6	0.002015	0.127	1.056		1.012		
26	2327665.0	3194.6	0.002375	2287981.0	7849.9	0.002140	0.099	1.092		1.079		
27	2356684.0	3262.3	0.002288	2316504.0	7908.7	0.001979	0.135	1.058		1.002		
28	2385702.0	3327.5	0.002202	2345028.0	7964.6	0.001936	0.121	1.025		0.984		
29	2414721.0	3392.3	0.002258	2373552.0	8020.4	0.001974	0.126	1.057		1.007		
30	2443739.0	3456.4	0.002156	2402075.0	8076.1	0.001921	0.109	1.014		0.984		
31	2472757.0	3520.4	0.002246	2430599.0	8131.5	0.001961	0.127	1.062		1.009		
32	2501916.0	3583.3	0.002086	2459261.0	8186.0	0.001857	0.110	0.991		0.959		
33	2531075.0	3644.3	0.002112	2487923.0	8239.5	0.001885	0.107	1.009		0.977		
34	2560094.0	3706.7	0.002187	2516446.0	8293.9	0.001928	0.119	1.050		1.002		
35	2589112.0	3769.4	0.002125	2544970.0	8348.4	0.001892	0.110	1.025		0.987		
36	2618130.0	3830.7	0.002095	2573493.0	8401.9	0.001853	0.116	1.015		0.970		

FOLLOWING PROFILES ARE FOR P/D=10 WITH FORE PLATE HEATED

DISCRETE HOLE RIG *** NAS-3-14336

VELOCITY PROFILE

UINF= 38.9 FT/SEC X= 50.3 INCHES PORT= 19
TINF= 66.2 DEG F PINF= 2122. PSF

Y(INCHES)	U(FT/SEC)	Y+	U+	UBAR	DU
0.010	18.06	9.4	9.99	0.4637	0.25
0.011	18.62	10.3	10.30	0.4783	0.24
0.012	19.13	11.3	10.58	0.4914	0.23
0.013	19.67	12.2	10.88	0.5051	0.23
0.014	20.22	13.1	11.19	0.5194	0.22
0.015	20.48	14.1	11.33	0.5260	0.22
0.020	21.91	18.8	12.12	0.5628	0.20
0.025	22.77	23.5	12.60	0.5849	0.19
0.035	24.38	32.8	13.48	0.6261	0.18
0.050	26.28	46.9	14.53	0.6749	0.17
0.070	28.65	65.7	15.85	0.7359	0.15
0.095	31.53	89.2	17.44	0.8099	0.14
0.120	34.11	112.6	18.86	0.8760	0.13
0.145	36.11	136.1	19.97	0.9275	0.12
0.170	37.46	159.5	20.72	0.9621	0.12
0.195	38.19	183.0	21.12	0.9808	0.12
0.220	38.69	206.5	21.40	0.9936	0.11
0.245	38.86	229.9	21.49	0.9980	0.11
0.270	38.94	253.4	21.53	1.0000	0.11

TEMPERATURE PROFILE

Y(INCHES)	T(DEG F)	TBAR
0.0065	96.73	0.8738
0.0075	93.88	0.7775
0.0085	93.04	0.7490
0.0095	92.40	0.7274
0.0105	91.67	0.7028
0.0115	91.09	0.6831
0.0165	88.64	0.6003
0.0265	85.74	0.5025
0.0415	83.46	0.4254
0.0615	80.14	0.3134
0.0865	76.70	0.1972
0.1115	74.17	0.1116
0.1365	72.61	0.0588
0.1615	71.72	0.0289
0.1665	71.28	0.0140
0.2365	70.95	0.0030
0.3665	70.86	0.0000

REX= 0.16357E 06 RED2= 548. XVO= 42.21 IN.
DEL1= 0.039 IN. DEL2= 0.027IN. H= 1.45
CF2= 0.21565E-02 DXVO= 0.30 DDEL1=0.001 DDEL2=0.001
DCF/2=0.205 IN RATIO

END2= 0.031IN. REEN= 592.
DEND2=0.001 DREEN= 18.
TO=100.47 F

STANTON NUMBER DATA RUN 013174 *** DISCRETE HOLE RIG *** NAS-3-14336

TINF= 69.0 UINF= 37.8 XVO=41.550 RHO= 0.07492 CP= 0.242 VISC= 0.16207E-03 PR=0.715
DISTANCE FROM ORIGIN OF BL TO 1ST PLATE= 7.750 P/D= 5
UNCERTAINTY IN REX=19434.

** M=0.0, FLAT PLATE RUN, LOW RE, STEP T-WALL AT VIRTUAL ORIGIN OF BL.

PLATE	X	REX	TO	REENTH	STANTON NO	DST	DREEN	M	F	T2	THETA	DTH
1	50.30	0.17005E 06	98.6	0.65688E 03	0.26953E-02	0.660E-04	58.					
2	52.30	0.20892E 06	98.6	0.76795E 03	0.30199E-02	0.678E-04	58.	0.00	0.0000	98.6	1.000	0.012
3	54.30	0.24779E 06	98.6	0.88494E 03	0.30001E-02	0.678E-04	58.	0.00	0.0000	98.6	1.000	0.012
4	56.30	0.28666E 06	98.6	0.99958E 03	0.28987E-02	0.671E-04	58.	0.00	0.0000	98.6	1.000	0.012
5	58.30	0.32552E 06	98.6	0.11103E 04	0.27969E-02	0.666E-04	58.	0.00	0.0000	98.6	1.000	0.012
6	60.30	0.36439E 06	98.6	0.12171E 04	0.27010E-02	0.661E-04	58.	0.00	0.0000	98.6	1.000	0.012
7	62.30	0.40326E 06	98.6	0.13213E 04	0.26572E-02	0.659E-04	58.	0.00	0.0000	98.6	1.000	0.012
8	64.30	0.44213E 06	98.5	0.14235E 04	0.26051E-02	0.657E-04	59.	0.00	0.0000	98.5	1.000	0.012
9	66.30	0.48100E 06	98.6	0.15230E 04	0.25157E-02	0.651E-04	59.	0.00	0.0000	98.6	1.000	0.012
10	68.30	0.51987E 06	98.6	0.16203E 04	0.24870E-02	0.649E-04	59.	0.00	0.0000	98.6	1.000	0.012
11	70.30	0.55874E 06	98.7	0.17160E 04	0.24389E-02	0.646E-04	59.	0.00	0.0000	98.7	1.000	0.012
12	72.30	0.59760E 06	98.6	0.18091E 04	0.23502E-02	0.642E-04	59.	0.00	0.0000	98.6	1.000	0.012
13	73.82	0.62714E 06	96.0	0.18763E 04	0.21564E-02	0.406E-04	59.					
14	74.85	0.64716E 06	95.2	0.19194E 04	0.21418E-02	0.457E-04	59.					
15	75.88	0.66718E 06	95.7	0.19627E 04	0.21798E-02	0.467E-04	59.					
16	76.91	0.68729E 06	95.8	0.20062E 04	0.21611E-02	0.461E-04	59.					
17	77.95	0.70741E 06	95.8	0.20495E 04	0.21564E-02	0.461E-04	59.					
18	78.98	0.72742E 06	95.8	0.20934E 04	0.22238E-02	0.472E-04	59.					
19	80.01	0.74744E 06	95.7	0.21377E 04	0.21958E-02	0.456E-04	59.					
20	81.04	0.76746E 06	95.8	0.21808E 04	0.21081E-02	0.443E-04	59.					
21	82.07	0.78748E 06	95.7	0.22245E 04	0.22523E-02	0.467E-04	59.					
22	83.10	0.80749E 06	95.8	0.22685E 04	0.21366E-02	0.466E-04	59.					
23	84.13	0.82751E 06	95.5	0.23106E 04	0.20656E-02	0.458E-04	59.					
24	85.16	0.84763E 06	95.4	0.23527E 04	0.21425E-02	0.474E-04	59.					
25	86.20	0.86774E 06	95.6	0.23948E 04	0.20543E-02	0.464E-04	59.					
26	87.23	0.88776E 06	94.6	0.24365E 04	0.21038E-02	0.472E-04	59.					
27	88.26	0.90777E 06	95.3	0.24786E 04	0.21034E-02	0.471E-04	59.					
28	89.29	0.92779E 06	95.2	0.25201E 04	0.20372E-02	0.459E-04	59.					
29	90.32	0.94781E 06	94.9	0.25616E 04	0.21043E-02	0.464E-04	59.					
30	91.35	0.96783E 06	94.8	0.26026E 04	0.19805E-02	0.462E-04	59.					
31	92.38	0.98794E 06	95.8	0.26439E 04	0.21457E-02	0.473E-04	59.					
32	93.41	0.10080E 07	95.8	0.26854E 04	0.19979E-02	0.454E-04	59.					
33	94.45	0.10281E 07	95.8	0.27258E 04	0.20274E-02	0.451E-04	59.					
34	95.48	0.10481E 07	95.2	0.27674E 04	0.21304E-02	0.459E-04	59.					
35	96.51	0.10681E 07	95.6	0.28093E 04	0.20461E-02	0.477E-04	59.					
36	97.54	0.10881E 07	94.8	0.28499E 04	0.20115E-02	0.520E-04	59.					

STANTON NUMBER DATA RUN 020374 *** DISCRETE HOLE RIG *** NAS-3-14336

TINF= 67.3 UINF= 37.2 XVO=41.550 RHO= 0.07555 CP= 0.241 VISC= 0.16042E-03 PR=0.715
DISTANCE FROM ORIGIN OF BL TO 1ST PLATE= 7.750 P/D= 5
UNCERTAINTY IN REX=19337. UNCERTAINTY IN F=0.03105 IN RATIO

** M=0.2, COLD RUN, LOW RE, STEP T-WALL AT VIRTUAL ORIGIN OF BL.

PLATE	X	REX	TO	REENTH	STANTON NO	DST	DREEN	M	F	T2	THETA	DTH
1	50.30	0.16919E 06	96.0	0.65357E 03	0.27183E-02	0.685E-04	58.					
2	52.30	0.20787E 06	95.9	0.80387E 03	0.33612E-02	0.726E-04	58.	0.21	0.0068	74.4	0.248	0.009
3	54.30	0.24654E 06	95.9	0.10039E 04	0.36065E-02	0.742E-04	58.	0.21	0.0068	74.4	0.249	0.009
4	56.30	0.28521E 06	96.0	0.12084E 04	0.35828E-02	0.739E-04	58.	0.21	0.0069	74.4	0.246	0.009
5	58.30	0.32389E 06	95.9	0.14103E 04	0.34802E-02	0.733E-04	58.	0.21	0.0069	74.3	0.244	0.009
6	60.30	0.36256E 06	95.9	0.16072E 04	0.33727E-02	0.726E-04	58.	0.21	0.0068	74.2	0.243	0.009
7	62.30	0.40123E 06	95.9	0.18014E 04	0.33214E-02	0.724E-04	58.	0.21	0.0068	74.4	0.249	0.009
8	64.30	0.43991E 06	96.0	0.19936E 04	0.32117E-02	0.715E-04	59.	0.21	0.0070	74.3	0.246	0.009
9	66.30	0.47858E 06	96.0	0.21822E 04	0.31672E-02	0.712E-04	59.	0.21	0.0069	74.3	0.243	0.009
10	68.30	0.51725E 06	96.0	0.23683E 04	0.31479E-02	0.710E-04	59.	0.21	0.0069	74.2	0.239	0.009
11	70.30	0.55593E 06	96.0	0.25523E 04	0.31080E-02	0.708E-04	59.	0.21	0.0069	74.0	0.234	0.009
12	72.30	0.59460E 06	95.9	0.27341E 04	0.30627E-02	0.707E-04	59.	0.22	0.0071	73.8	0.227	0.009
13	73.82	0.62399E 06	93.0	0.28502E 04	0.25677E-02	0.473E-04	59.					
14	74.85	0.64391E 06	92.2	0.28998E 04	0.24122E-02	0.507E-04	59.					
15	75.88	0.66382E 06	92.9	0.29473E 04	0.23476E-02	0.503E-04	59.					
16	76.91	0.68384E 06	93.1	0.29934E 04	0.22831E-02	0.489E-04	59.					
17	77.95	0.70385E 06	93.3	0.30381E 04	0.21968E-02	0.478E-04	59.					
18	78.98	0.72377E 06	93.3	0.30823E 04	0.22392E-02	0.485E-04	59.					
19	80.01	0.74368E 06	93.2	0.31266E 04	0.21987E-02	0.467E-04	59.					
20	81.04	0.76360E 06	93.5	0.31693E 04	0.20836E-02	0.449E-04	59.					
21	82.07	0.78352E 06	93.3	0.32123E 04	0.22264E-02	0.473E-04	59.					
22	83.10	0.80343E 06	93.5	0.32554E 04	0.21036E-02	0.472E-04	59.					
23	84.13	0.82335E 06	93.2	0.32966E 04	0.20278E-02	0.463E-04	59.					
24	85.16	0.84336E 06	93.1	0.33377E 04	0.20917E-02	0.478E-04	59.					
25	86.20	0.86338E 06	93.2	0.33787E 04	0.20213E-02	0.469E-04	59.					
26	87.23	0.88329E 06	92.3	0.34193E 04	0.20531E-02	0.476E-04	59.					
27	88.26	0.90321E 06	92.9	0.34602E 04	0.20477E-02	0.475E-04	59.					
28	89.29	0.92313E 06	92.8	0.35007E 04	0.20110E-02	0.466E-04	59.					
29	90.32	0.94304E 06	92.5	0.35413E 04	0.20690E-02	0.471E-04	59.					
30	91.35	0.96296E 06	92.3	0.35810E 04	0.19111E-02	0.467E-04	59.					
31	92.38	0.98288E 06	93.4	0.36212E 04	0.21169E-02	0.481E-04	59.					
32	93.41	0.10029E 07	93.4	0.36618E 04	0.19522E-02	0.459E-04	59.					
33	94.45	0.10229E 07	93.4	0.37011E 04	0.19927E-02	0.457E-04	59.					
34	95.48	0.10428E 07	92.9	0.37417E 04	0.20803E-02	0.463E-04	59.					
35	96.51	0.10627E 07	93.2	0.37824E 04	0.19981E-02	0.483E-04	59.					
36	97.54	0.10827E 07	92.4	0.38219E 04	0.19703E-02	0.529E-04	59.					

STANTON NUMBER DATA RUN 020474 *** DISCRETE HOLE RIG *** NAS-3-14336

TINF= 72.7 UINF= 37.5 XVO=41.550 RHO= 0.07454 CP= 0.242 VISC= 0.16373E-03 PR=0.715
DISTANCE FROM ORIGIN OF BL TO 1ST PLATE= 7.750 P/D= 5
UNCERTAINTY IN REX=19103. UNCERTAINTY IN F=0.03104 IN RATIO

** M=0.2, HOT RUN, LOW RE, STEP T-WALL AT VIRTUAL ORIGIN OF BL.

PLATE	X	REX	TO	REENTH	STANTON NO	DST	DREEN	M	F	T2	THETA	DTH
1	50.30	0.16715E 06	101.6	0.64567E 03	0.26927E-02	0.682E-04	57.					
2	52.30	0.20535E 06	101.4	0.87987E 03	0.28016E-02	0.691E-04	58.	0.22	0.0073	99.5	0.932	0.012
3	54.30	0.24356E 06	101.5	0.12340E 04	0.28278E-02	0.691E-04	58.	0.20	0.0066	99.4	0.927	0.012
4	56.30	0.28176E 06	101.5	0.15736E 04	0.26711E-02	0.683E-04	58.	0.20	0.0066	99.4	0.927	0.012
5	58.30	0.31997E 06	101.4	0.19015E 04	0.25265E-02	0.676E-04	58.	0.19	0.0062	99.8	0.945	0.012
6	60.30	0.35818E 06	101.4	0.22165E 04	0.23867E-02	0.669E-04	59.	0.19	0.0062	99.4	0.931	0.012
7	62.30	0.39638E 06	101.4	0.25118E 04	0.22980E-02	0.665E-04	59.	0.16	0.0053	99.9	0.948	0.012
8	64.30	0.43459E 06	101.5	0.27975E 04	0.21467E-02	0.657E-04	59.	0.17	0.0057	100.6	0.971	0.012
9	66.30	0.47279E 06	101.5	0.30888E 04	0.21133E-02	0.656E-04	59.	0.18	0.0057	100.5	0.965	0.012
10	68.30	0.51100E 06	101.4	0.33904E 04	0.20228E-02	0.652E-04	60.	0.19	0.0063	100.7	0.975	0.012
11	70.30	0.54920E 06	101.4	0.36964E 04	0.19811E-02	0.651E-04	60.	0.18	0.0058	101.5	1.003	0.012
12	72.30	0.58741E 06	101.6	0.39965E 04	0.18188E-02	0.641E-04	60.	0.18	0.0057	103.4	1.062	0.013
13	73.82	0.61644E 06	99.6	0.41656E 04	0.19161E-02	0.382E-04	60.					
14	74.85	0.63612E 06	98.9	0.42028E 04	0.18533E-02	0.427E-04	60.					
15	75.88	0.65580E 06	99.6	0.42385E 04	0.17785E-02	0.424E-04	60.					
16	76.91	0.67557E 06	99.6	0.42740E 04	0.18237E-02	0.423E-04	60.					
17	77.95	0.69534E 06	99.8	0.43096E 04	0.17849E-02	0.419E-04	60.					
18	78.98	0.71501E 06	100.1	0.43442E 04	0.17346E-02	0.416E-04	60.					
19	80.01	0.73469E 06	99.7	0.43792E 04	0.18148E-02	0.410E-04	60.					
20	81.04	0.75436E 06	100.0	0.44141E 04	0.17344E-02	0.398E-04	60.					
21	82.07	0.77404E 06	100.1	0.44485E 04	0.17581E-02	0.409E-04	60.					
22	83.10	0.79372E 06	99.7	0.44835E 04	0.17960E-02	0.426E-04	60.					
23	84.13	0.81339E 06	99.7	0.45179E 04	0.16927E-02	0.415E-04	60.					
24	85.16	0.83316E 06	99.9	0.45513E 04	0.16981E-02	0.422E-04	60.					
25	86.20	0.85293E 06	99.9	0.45847E 04	0.16949E-02	0.420E-04	60.					
26	87.23	0.87261E 06	99.0	0.46192E 04	0.18048E-02	0.435E-04	60.					
27	88.26	0.89229E 06	99.8	0.46534E 04	0.16732E-02	0.419E-04	60.					
28	89.29	0.91196E 06	99.7	0.46867E 04	0.16984E-02	0.416E-04	60.					
29	90.32	0.93164E 06	99.4	0.47205E 04	0.17346E-02	0.418E-04	60.					
30	91.35	0.95131E 06	99.2	0.47543E 04	0.16974E-02	0.428E-04	60.					
31	92.38	0.97099E 06	100.0	0.47883E 04	0.17538E-02	0.428E-04	60.					
32	93.41	0.99076E 06	99.6	0.48228E 04	0.17487E-02	0.428E-04	60.					
33	94.45	0.10105E 07	99.7	0.48569E 04	0.17160E-02	0.418E-04	60.					
34	95.48	0.10302E 07	99.2	0.48917E 04	0.18171E-02	0.424E-04	60.					
35	96.51	0.10499E 07	99.5	0.49269E 04	0.17573E-02	0.447E-04	60.					
36	97.54	0.10696E 07	98.8	0.49614E 04	0.17476E-02	0.480E-04	60.					

FOLLOWING IS THE DATA FOR THETA=0 AND THETA=1, WHICH WAS OBTAINED BY LINEAR SUPERPOSITION THEORY.
THIS DATA WAS PRODUCED FROM RUN 020374 AND RUN 020474
FOR THE DETAIL CHANGES OF PROPERTIES AND BOUNDARY CONDITIONS, PLEASE SEE THE ABOVE TWO RUNS

PLATE	REXCOL	RE DEL2	ST(TH=0)	REXHOT	RE DEL2	ST(TH=1)	ETA	STCR	F-COL	STHR	F-HOT	PHI-1
1	169194.8	653.6	0.002718	167148.5	645.7	0.002693	UUUUU	UUUUU	0.0000	UUUUUUU	0.0000	UUUUU
2	207867.8	775.0	0.003564	205353.9	988.2	0.002746	0.229	1.223	0.0068	0.940	0.0073	1.921
3	246540.9	919.2	0.003892	243559.3	1258.3	0.002744	0.295	1.382	0.0068	0.972	0.0066	1.911
4	285214.0	1070.1	0.003913	281764.6	1612.8	0.002573	0.342	1.430	0.0069	0.938	0.0066	1.895
5	323887.1	1219.5	0.003812	319970.0	1953.2	0.002451	0.357	1.429	0.0069	0.917	0.0062	1.836
6	362560.1	1365.2	0.003720	358175.4	2279.6	0.002288	0.385	1.426	0.0068	0.875	0.0062	1.805
7	401233.3	1508.4	0.003686	396380.8	2584.9	0.002222	0.397	1.442	0.0068	0.867	0.0053	1.697
8	439906.3	1648.7	0.003572	434586.1	2876.7	0.002105	0.411	1.424	0.0070	0.837	0.0057	1.723
9	478579.4	1785.9	0.003522	472791.5	3173.1	0.002063	0.414	1.427	0.0069	0.834	0.0057	1.738
10	517252.5	1921.9	0.003514	510996.9	3479.7	0.001985	0.435	1.446	0.0069	0.815	0.0063	1.812
11	555925.6	2056.6	0.003452	549202.3	3787.7	0.001986	0.425	1.442	0.0069	0.827	0.0058	1.774
12	594598.7	2189.1	0.003401	587407.6	4082.5	0.001912	0.438	1.440	0.0071	0.807	0.0057	1.741
13	623990.3	2282.7	0.002787	616443.8	4246.3	0.001882	0.325	1.191		0.803		
14	643906.9	2336.4	0.002601	636119.5	4282.8	0.001824	0.299	1.118		0.783		
15	663823.5	2387.7	0.002539	655795.3	4318.0	0.001749	0.311	1.099		0.755		
16	683836.6	2437.3	0.002438	675566.3	4353.0	0.001800	0.262	1.061		0.782		
17	703850.0	2484.9	0.002336	695337.7	4388.1	0.001764	0.245	1.023		0.770		
18	723766.6	2532.2	0.002409	715013.4	4422.3	0.001708	0.291	1.061		0.750		
19	743683.3	2579.4	0.002328	734689.2	4456.8	0.001795	0.229	1.031		0.793		
20	763599.9	2624.6	0.002201	754364.9	4491.4	0.001716	0.220	0.980		0.762		
21	783516.8	2670.3	0.002384	774040.9	4525.3	0.001734	0.273	1.066		0.774		
22	803433.4	2716.1	0.002207	793716.7	4560.0	0.001780	0.194	0.992		0.798		
23	823350.0	2759.4	0.002141	813392.4	4594.0	0.001675	0.217	0.967		0.755		
24	843363.1	2802.9	0.002224	833163.5	4627.0	0.001678	0.246	1.010		0.760		
25	863376.5	2846.4	0.002131	852934.9	4660.1	0.001678	0.213	0.972		0.763		
26	883293.1	2888.9	0.002137	872610.6	4694.2	0.001792	0.161	0.979		0.819		
27	903209.8	2931.9	0.002174	892286.3	4728.2	0.001654	0.239	1.000		0.759		
28	923126.3	2974.7	0.002116	911962.1	4761.0	0.001682	0.205	0.978		0.776		
29	943043.3	3017.5	0.002182	931638.1	4794.5	0.001717	0.213	1.013		0.795		
30	962959.9	3059.0	0.001983	951313.9	4828.0	0.001686	0.150	0.924		0.784		
31	982876.5	3101.1	0.002239	970989.6	4861.7	0.001735	0.225	1.048		0.810		
32	1002889.0	3143.6	0.002021	990760.7	4895.9	0.001738	0.140	0.950		0.815		
33	1022903.0	3184.6	0.002086	1010532.0	4929.8	0.001702	0.184	0.984		0.801		
34	1042819.0	3227.0	0.002169	1030207.0	4964.3	0.001803	0.169	1.027		0.852		
35	1062736.0	3269.3	0.002079	1049883.0	4999.3	0.001745	0.161	0.989		0.828		
36	1082652.0	3310.5	0.002045	1069559.0	5033.6	0.001736	0.151	0.976		0.826		

STANTON NUMBER DATA RUN 020574 *** DISCRETE HOLE RIG *** NAS-3-14336

TINF= 67.8 UINF= 36.8 XVO=41.550 RHO= 0.07539 CP= 0.241 VISC= 0.16124E-03 PR=0.713
DISTANCE FROM ORIGIN OF BL TO 1ST PLATE= 7.750 P/D= 5
UNCERTAINTY IN REX=19011. UNCERTAINTY IN F=0.03110 IN RATIO

** M=0.5, COLD RUN, LOW RE, STEP T-WALL AT VIRTUAL ORIGIN OF BL.

PLATE	X	REX	TO	REENTH	STANTON NO	DST	DREEN	M	F	T2	THETA	DTH
1	50.30	0.16634E 06	96.0	0.64256E 03	0.28214E-02	0.713E-04	57.					
2	52.30	0.20436E 06	96.0	0.81190E 03	0.38987E-02	0.783E-04	57.	0.53	0.0172	71.4	0.127	0.009
3	54.30	0.24239E 06	96.1	0.10504E 04	0.43089E-02	0.812E-04	57.	0.55	0.0178	71.2	0.121	0.009
4	56.30	0.28041E 06	96.1	0.12955E 04	0.43717E-02	0.816E-04	58.	0.51	0.0167	71.3	0.124	0.009
5	58.30	0.31843E 06	96.1	0.15392E 04	0.42974E-02	0.812E-04	58.	0.54	0.0174	71.2	0.120	0.009
6	60.30	0.35645E 06	96.2	0.17802E 04	0.42226E-02	0.804E-04	58.	0.54	0.0174	71.2	0.119	0.009
7	62.30	0.39447E 06	96.1	0.20205E 04	0.41215E-02	0.798E-04	58.	0.54	0.0176	71.4	0.127	0.009
8	64.30	0.43249E 06	96.1	0.22592E 04	0.39801E-02	0.788E-04	58.	0.53	0.0171	71.5	0.130	0.009
9	66.30	0.47051E 06	96.1	0.24928E 04	0.38698E-02	0.779E-04	59.	0.55	0.0177	71.4	0.125	0.009
10	68.30	0.50853E 06	96.1	0.27217E 04	0.37821E-02	0.772E-04	59.	0.53	0.0171	71.4	0.127	0.009
11	70.30	0.54656E 06	96.1	0.29456E 04	0.36619E-02	0.764E-04	59.	0.54	0.0176	71.3	0.123	0.009
12	72.30	0.58458E 06	96.0	0.31641E 04	0.35561E-02	0.759E-04	59.	0.52	0.0169	71.4	0.125	0.009
13	73.82	0.61347E 06	92.7	0.33001E 04	0.28640E-02	0.524E-04	59.					
14	74.85	0.63305E 06	92.1	0.33538E 04	0.26074E-02	0.546E-04	59.					
15	75.88	0.65264E 06	93.1	0.34028E 04	0.23917E-02	0.520E-04	59.					
16	76.91	0.67231E 06	93.4	0.34482E 04	0.22419E-02	0.492E-04	59.					
17	77.95	0.69199E 06	93.6	0.34907E 04	0.20928E-02	0.473E-04	59.					
18	78.98	0.71157E 06	93.7	0.35315E 04	0.20748E-02	0.472E-04	59.					
19	80.01	0.73115E 06	93.8	0.35714E 04	0.19944E-02	0.447E-04	59.					
20	81.04	0.75073E 06	94.1	0.36095E 04	0.18844E-02	0.430E-04	59.					
21	82.07	0.77031E 06	93.9	0.36476E 04	0.20068E-02	0.451E-04	59.					
22	83.10	0.78989E 06	94.1	0.36858E 04	0.18904E-02	0.451E-04	59.					
23	84.13	0.80947E 06	93.8	0.37222E 04	0.18285E-02	0.446E-04	59.					
24	85.16	0.82915E 06	93.7	0.37587E 04	0.18907E-02	0.460E-04	59.					
25	86.20	0.84883E 06	93.8	0.37949E 04	0.18052E-02	0.451E-04	59.					
26	87.23	0.86841E 06	92.8	0.38313E 04	0.19029E-02	0.466E-04	59.					
27	88.26	0.88799E 06	93.4	0.38684E 04	0.18816E-02	0.462E-04	60.					
28	89.29	0.90757E 06	93.4	0.39047E 04	0.18219E-02	0.450E-04	60.					
29	90.32	0.92715E 06	93.0	0.39416E 04	0.19482E-02	0.462E-04	60.					
30	91.35	0.94673E 06	92.9	0.39783E 04	0.17955E-02	0.460E-04	60.					
31	92.38	0.96631E 06	93.9	0.40152E 04	0.19672E-02	0.469E-04	60.					
32	93.41	0.98599E 06	93.9	0.40525E 04	0.18361E-02	0.452E-04	60.					
33	94.45	0.10057E 07	93.9	0.40890E 04	0.18877E-02	0.451E-04	60.					
34	95.48	0.10252E 07	93.3	0.41270E 04	0.19903E-02	0.458E-04	60.					
35	96.51	0.10448E 07	93.6	0.41652E 04	0.19077E-02	0.481E-04	60.					
36	97.54	0.10644E 07	92.7	0.42024E 04	0.18816E-02	0.533E-04	60.					

STANTON NUMBER DATA RUN 020674 *** DISCRETE HOLE RIG *** NAS-3-14336

TINF= 69.7 UINF= 37.1 XVO=41.550 RHO= 0.07535 CP= 0.241 VISC= 0.16160E-03 PR=0.713
DISTANCE FROM ORIGIN OF BL TO 1ST PLATE= 7.750 P/D= 5
UNCERTAINTY IN REX=19128. UNCERTAINTY IN F=0.03107 IN RATIO

** M=0.5, HOT RUN, LOW RE, STEP T-WALL AT VIRTUAL ORIGIN OF BL.

PLATE	X	REX	TO	REENTH	STANTON NO	DST	DREEN	M	F	T2	THETA	DTH
1	50.30	0.16737E 06	102.7	0.64652E 03	0.27910E-02	0.617E-04	57.					
2	52.30	0.20562E 06	102.5	0.10799E 04	0.30348E-02	0.633E-04	58.	0.50	0.0163	103.5	1.032	0.011
3	54.30	0.24388E 06	102.6	0.18682E 04	0.30587E-02	0.634E-04	61.	0.53	0.0171	104.9	1.070	0.011
4	56.30	0.28214E 06	102.6	0.26643E 04	0.28590E-02	0.622E-04	63.	0.51	0.0165	104.4	1.057	0.011
5	58.30	0.32039E 06	102.5	0.34473E 04	0.26869E-02	0.613E-04	65.	0.52	0.0168	104.9	1.073	0.011
6	60.30	0.35865E 06	102.5	0.42452E 04	0.25513E-02	0.607E-04	67.	0.55	0.0178	103.8	1.039	0.011
7	62.30	0.39690E 06	102.4	0.50506E 04	0.23923E-02	0.600E-04	69.	0.54	0.0176	104.4	1.062	0.011
8	64.30	0.43516E 06	102.4	0.58236E 04	0.22056E-02	0.591E-04	71.	0.49	0.0160	104.7	1.070	0.011
9	66.30	0.47341E 06	102.6	0.65596E 04	0.20598E-02	0.581E-04	72.	0.51	0.0165	103.7	1.033	0.011
10	68.30	0.51167E 06	102.4	0.73070E 04	0.19229E-02	0.579E-04	74.	0.54	0.0176	103.2	1.024	0.011
11	70.30	0.54992E 06	102.4	0.80650E 04	0.17874E-02	0.574E-04	76.	0.55	0.0179	102.3	0.997	0.011
12	72.30	0.58818E 06	102.6	0.88061E 04	0.16458E-02	0.565E-04	77.	0.54	0.0175	102.5	0.997	0.011
13	73.82	0.61725E 06	101.1	0.91859E 04	0.15226E-02	0.307E-04	78.					
14	74.85	0.63696E 06	100.7	0.92145E 04	0.13743E-02	0.336E-04	78.					
15	75.88	0.65666E 06	101.5	0.92405E 04	0.12690E-02	0.331E-04	78.					
16	76.91	0.67646E 06	101.7	0.92653E 04	0.12360E-02	0.322E-04	78.					
17	77.95	0.69625E 06	101.9	0.92892E 04	0.11885E-02	0.318E-04	78.					
18	78.98	0.71595E 06	102.1	0.93124E 04	0.11708E-02	0.318E-04	78.					
19	80.01	0.73566E 06	101.9	0.93355E 04	0.11730E-02	0.305E-04	78.					
20	81.04	0.75536E 06	102.1	0.93582E 04	0.11222E-02	0.297E-04	78.					
21	82.07	0.77506E 06	102.1	0.93807E 04	0.11654E-02	0.309E-04	78.					
22	83.10	0.79476E 06	102.0	0.94036E 04	0.11512E-02	0.319E-04	78.					
23	84.13	0.81446E 06	101.9	0.94259E 04	0.11100E-02	0.316E-04	78.					
24	85.16	0.83426E 06	102.0	0.94480E 04	0.11291E-02	0.324E-04	78.					
25	86.20	0.85406E 06	102.0	0.94701E 04	0.11100E-02	0.320E-04	78.					
26	87.23	0.87376E 06	101.1	0.94929E 04	0.12062E-02	0.331E-04	78.					
27	88.26	0.89346E 06	101.8	0.95160E 04	0.11356E-02	0.324E-04	78.					
28	89.29	0.91316E 06	101.7	0.95386E 04	0.11583E-02	0.322E-04	78.					
29	90.32	0.93286E 06	101.3	0.95621E 04	0.12175E-02	0.325E-04	78.					
30	91.35	0.95257E 06	101.1	0.95857E 04	0.11753E-02	0.334E-04	78.					
31	92.38	0.97227E 06	101.8	0.96095E 04	0.12472E-02	0.335E-04	78.					
32	93.41	0.99206E 06	101.5	0.96340E 04	0.12360E-02	0.335E-04	78.					
33	94.45	0.10119E 07	101.6	0.96584E 04	0.12370E-02	0.329E-04	78.					
34	95.48	0.10316E 07	101.1	0.96837E 04	0.13225E-02	0.332E-04	78.					
35	96.51	0.10513E 07	101.3	0.97094E 04	0.12899E-02	0.356E-04	78.					
36	97.54	0.10710E 07	100.5	0.97346E 04	0.12578E-02	0.386E-04	78.					

FOLLOWING IS THE DATA FOR THETA=0 AND THETA=1, WHICH WAS OBTAINED BY LINEAR SUPERPOSITION THEORY.
THIS DATA WAS PRODUCED FROM RUN 020574 AND RUN 020674
FOR THE DETAIL CHANGES OF PROPERTIES AND BOUNDARY CONDITIONS, PLEASE SEE THE ABOVE TWO RUNS

PLATE	REXCOL	RE DEL2	ST(TH=0)	REXHOT	RE DEL2	ST(TH=1)	ETA	STCR	F-COL	STHR	F-HOT	PHI-1
1	166343.1	642.6	0.002821	167368.4	646.5	0.002791	UUUUU	UUUUU	0.0000	UUUUUUU	0.0000	UUUUU
2	204364.4	772.6	0.004020	205624.0	1070.6	0.003065	0.238	1.373	0.0172	1.048	0.0163	3.026
3	242385.7	934.0	0.004468	243879.6	1828.5	0.003151	0.295	1.579	0.0178	1.115	0.0171	3.253
4	280407.0	1105.8	0.004572	282135.3	2587.1	0.002952	0.354	1.664	0.0167	1.076	0.0165	3.185
5	318428.3	1278.3	0.004500	320390.9	3332.8	0.002810	0.376	1.680	0.0174	1.050	0.0168	3.228
6	356449.6	1448.2	0.004439	358646.5	4097.8	0.002622	0.409	1.695	0.0174	1.002	0.0178	3.316
7	394470.8	1615.4	0.004356	396902.2	4872.8	0.002506	0.425	1.697	0.0176	0.978	0.0176	3.295
8	432492.1	1778.6	0.004226	435157.8	5608.3	0.002338	0.447	1.677	0.0171	0.929	0.0160	3.090
9	470513.4	1937.2	0.004119	473413.4	6315.3	0.002125	0.484	1.663	0.0177	0.859	0.0165	3.074
10	508534.7	2092.5	0.004046	511669.1	7047.4	0.001973	0.512	1.659	0.0171	0.810	0.0176	3.149
11	546556.0	2244.0	0.003925	549924.7	7799.1	0.001781	0.546	1.632	0.0176	0.742	0.0179	3.107
12	584577.3	2391.4	0.003831	588180.3	8541.9	0.001640	0.572	1.615	0.0169	0.692	0.0175	3.003
13	613473.6	2494.1	0.003046	617254.7	8923.0	0.001583	0.480	1.297		0.675		
14	633054.5	2551.2	0.002775	636956.3	8952.7	0.001430	0.485	1.188		0.613		
15	652635.4	2603.3	0.002544	656657.9	8979.8	0.001320	0.481	1.096		0.569		
16	672311.3	2651.5	0.002378	676455.0	9005.5	0.001281	0.461	1.031		0.556		
17	691987.3	2696.6	0.002215	696252.4	9030.2	0.001229	0.445	0.966		0.537		
18	711568.3	2739.8	0.002197	715954.0	9054.3	0.001211	0.449	0.963		0.532		
19	731149.2	2782.0	0.002106	735655.6	9078.2	0.001210	0.425	0.928		0.534		
20	750730.1	2822.1	0.001988	755357.3	9101.5	0.001157	0.418	0.881		0.513		
21	770311.4	2862.4	0.002121	775059.2	9124.8	0.001203	0.433	0.945		0.537		
22	789892.3	2902.7	0.001991	794760.8	9148.4	0.001184	0.405	0.891		0.531		
23	809473.3	2941.1	0.001926	814462.4	9171.3	0.001142	0.407	0.867		0.515		
24	829149.1	2979.5	0.001994	834259.5	9194.1	0.001163	0.417	0.901		0.527		
25	848825.1	3017.7	0.001900	854056.9	9216.8	0.001141	0.399	0.863		0.519		
26	868406.1	3055.9	0.001997	873758.5	9240.2	0.001238	0.380	0.911		0.565		
27	887987.0	3094.9	0.001983	893460.1	9264.0	0.001169	0.410	0.909		0.537		
28	907567.9	3133.1	0.001912	913161.8	9287.2	0.001188	0.379	0.880		0.548		
29	927149.2	3171.9	0.002047	932863.7	9311.3	0.001250	0.389	0.946		0.579		
30	946730.1	3210.4	0.001880	952565.3	9335.5	0.001203	0.360	0.873		0.559		
31	966311.1	3249.1	0.002065	972266.9	9360.0	0.001280	0.380	0.962		0.597		
32	985986.9	3288.1	0.001918	992064.0	9385.0	0.001263	0.341	0.897		0.592		
33	1005662.0	3326.3	0.001976	1011861.0	9410.0	0.001266	0.359	0.928		0.596		
34	1025243.0	3366.0	0.002081	1031562.0	9435.8	0.001353	0.350	0.982		0.639		
35	1044824.0	3405.9	0.001991	1051264.0	9462.2	0.001318	0.338	0.943		0.625		
36	1064405.0	3444.7	0.001966	1070966.0	9487.8	0.001286	0.346	0.934		0.612		

STANTON NUMBER DATA RUN 012474 *** DISCRETE HOLE RIG *** NAS-3-14336

TINF= 71.5 UINF= 37.8 XVO=41.550 RHO= 0.07473 CP= 0.241 VISC= 0.16321E-03 PR=0.714
DISTANCE FROM ORIGIN OF BL TO 1ST PLATE= 7.750 P/D=10
UNCERTAINTY IN REX=19322.

** M=0.0, FLAT PLATE RUN,LOW RE, STEP T-WALL AT VIRTUAL ORIGIN OF BL.

PLATE	X	REX	TO	REENTH	STANTON NO	DST	DREEN	M	F	T2	THETA	DTH
1	50.30	0.16907E 06	100.6	0.65308E 03	0.26634E-02	0.669E-04	58.					
2	52.30	0.20771E 06	100.6	0.76108E 03	0.29259E-02	0.683E-04	58.	0.00	0.0000	100.6	1.000	0.012
3	54.30	0.24636E 06	100.7	0.87293E 03	0.28625E-02	0.678E-04	58.	0.00	0.0000	100.7	1.000	0.012
4	56.30	0.28500E 06	100.7	0.98247E 03	0.28071E-02	0.674E-04	58.	0.00	0.0000	100.7	1.000	0.012
5	58.30	0.32364E 06	100.7	0.10882E 04	0.26645E-02	0.668E-04	58.	0.00	0.0000	100.7	1.000	0.012
6	60.30	0.36229E 06	100.7	0.11909E 04	0.26517E-02	0.666E-04	58.	0.00	0.0000	100.7	1.000	0.012
7	62.30	0.40093E 06	100.7	0.12915E 04	0.25561E-02	0.662E-04	58.	0.00	0.0000	100.7	1.000	0.012
8	64.30	0.43958E 06	100.6	0.13899E 04	0.25325E-02	0.662E-04	58.	0.00	0.0000	100.6	1.000	0.012
9	66.30	0.47822E 06	100.7	0.14859E 04	0.24370E-02	0.655E-04	58.	0.00	0.0000	100.7	1.000	0.012
10	68.30	0.51686E 06	100.7	0.15806E 04	0.24629E-02	0.657E-04	58.	0.00	0.0000	100.7	1.000	0.012
11	70.30	0.55551E 06	100.7	0.16737E 04	0.23598E-02	0.652E-04	58.	0.00	0.0000	100.7	1.000	0.012
12	72.30	0.59415E 06	100.7	0.17643E 04	0.23257E-02	0.650E-04	58.	0.00	0.0000	100.7	1.000	0.012
13	73.82	0.62352E 06	98.1	0.18305E 04	0.21329E-02	0.407E-04	58.					
14	74.85	0.64342E 06	97.3	0.18727E 04	0.21054E-02	0.458E-04	58.					
15	75.88	0.66333E 06	97.7	0.19154E 04	0.21770E-02	0.472E-04	58.					
16	76.91	0.68332E 06	97.7	0.19586E 04	0.21654E-02	0.467E-04	58.					
17	77.95	0.70332E 06	97.8	0.20014E 04	0.21321E-02	0.464E-04	58.					
18	78.98	0.72322E 06	97.8	0.20446E 04	0.21992E-02	0.475E-04	58.					
19	80.01	0.74312E 06	97.7	0.20882E 04	0.21817E-02	0.460E-04	58.					
20	81.04	0.76303E 06	97.9	0.21309E 04	0.21008E-02	0.447E-04	58.					
21	82.07	0.78293E 06	97.7	0.21744E 04	0.22662E-02	0.474E-04	58.					
22	83.10	0.80283E 06	97.9	0.22182E 04	0.21274E-02	0.470E-04	58.					
23	84.13	0.82273E 06	97.5	0.22602E 04	0.20880E-02	0.466E-04	58.					
24	85.16	0.84273E 06	97.5	0.23019E 04	0.21018E-02	0.474E-04	58.					
25	86.20	0.86273E 06	97.8	0.23434E 04	0.20611E-02	0.465E-04	58.					
26	87.23	0.88263E 06	97.4	0.23856E 04	0.21714E-02	0.479E-04	58.					
27	88.26	0.90253E 06	97.6	0.24279E 04	0.20830E-02	0.470E-04	58.					
28	89.29	0.92243E 06	97.4	0.24687E 04	0.20085E-02	0.459E-04	58.					
29	90.32	0.94234E 06	97.1	0.25094E 04	0.20726E-02	0.462E-04	58.					
30	91.35	0.96224E 06	97.6	0.25500E 04	0.20104E-02	0.466E-04	58.					
31	92.38	0.98214E 06	98.0	0.25913E 04	0.21338E-02	0.472E-04	58.					
32	93.41	0.10021E 07	97.9	0.26323E 04	0.19772E-02	0.456E-04	58.					
33	94.45	0.10221E 07	97.8	0.26722E 04	0.20278E-02	0.456E-04	58.					
34	95.48	0.10420E 07	97.4	0.27132E 04	0.20856E-02	0.458E-04	58.					
35	96.51	0.10619E 07	97.7	0.27542E 04	0.20371E-02	0.481E-04	58.					
36	97.54	0.10818E 07	97.0	0.27947E 04	0.20267E-02	0.525E-04	58.					

STANTON NUMBER DATA RUN 012774 *** DISCRETE HOLE RIG *** NAS-3-14336

TINF= 68.7 UINF= 37.7 XVO=41.550 RHO= 0.07537 CP= 0.241 VISC= 0.16119E-03 PR=0.714
DISTANCE FROM ORIGIN OF BL TO 1ST PLATE= 7.750 P/D=10
UNCERTAINTY IN REX=19481. UNCERTAINTY IN F=0.03100 IN RATIO

** M=0.2, COLD RUN, LOW RE, STEP T-WALL AT VIRTUAL ORIGIN OF BL.

PLATE	X	REX	TO	REENTH	STANTON NO	DST	DREEN	M	F	T2	THETA	DTH
1	50.30	0.17046E 06	97.6	0.65845E 03	0.27721E-02	0.678E-04	58.					
2	52.30	0.20942E 06	97.4	0.79017E 03	0.31967E-02	0.707E-04	58.	0.21	0.0017	75.4	0.234	0.009
3	54.30	0.24838E 06	97.5	0.92804E 03	0.30875E-02	0.700E-04	59.	0.00	0.0017	97.5	0.234	0.012
4	56.30	0.28734E 06	97.4	0.10623E 04	0.30361E-02	0.698E-04	59.	0.22	0.0018	75.0	0.218	0.009
5	58.30	0.32630E 06	97.5	0.11929E 04	0.28973E-02	0.688E-04	59.	0.00	0.0018	97.5	0.218	0.012
6	60.30	0.36526E 06	97.5	0.13216E 04	0.29154E-02	0.690E-04	59.	0.22	0.0018	75.2	0.225	0.009
7	62.30	0.40423E 06	97.5	0.14486E 04	0.28082E-02	0.682E-04	59.	0.00	0.0018	97.5	0.225	0.012
8	64.30	0.44319E 06	97.5	0.15726E 04	0.28059E-02	0.683E-04	59.	0.20	0.0016	75.3	0.229	0.009
9	66.30	0.48215E 06	97.5	0.16942E 04	0.26861E-02	0.675E-04	59.	0.00	0.0016	97.5	0.229	0.012
10	68.30	0.52111E 06	97.4	0.18158E 04	0.27614E-02	0.682E-04	59.	0.22	0.0017	75.2	0.227	0.009
11	70.30	0.56007E 06	97.5	0.19369E 04	0.26592E-02	0.675E-04	59.	0.00	0.0017	97.5	0.227	0.012
12	72.30	0.59903E 06	97.5	0.20548E 04	0.26533E-02	0.674E-04	59.	0.22	0.0018	74.6	0.204	0.00[illegible]
13	73.82	0.62865E 06	94.6	0.21417E 04	0.24238E-02	0.449E-04	59.					
14	74.85	0.64871E 06	93.8	0.21895E 04	0.23353E-02	0.493E-04	59.					
15	75.88	0.66878E 06	94.3	0.22329E 04	0.23548E-02	0.500E-04	59.					
16	76.91	0.68894E 06	94.5	0.22797E 04	0.23067E-02	0.489E-04	59.					
17	77.95	0.70910E 06	94.6	0.23252E 04	0.22282E-02	0.481E-04	59.					
18	78.98	0.72917E 06	94.4	0.23711E 04	0.23341E-02	0.496E-04	59.					
19	80.01	0.74923E 06	94.5	0.24172E 04	0.22607E-02	0.474E-04	59.					
20	81.04	0.76930E 06	94.7	0.24614E 04	0.21362E-02	0.455E-04	59.					
21	82.07	0.78936E 06	94.5	0.25063E 04	0.23321E-02	0.486E-04	59.					
22	83.10	0.80943E 06	94.6	0.25516E 04	0.21824E-02	0.480E-04	59.					
23	84.13	0.82949E 06	94.3	0.25950E 04	0.21359E-02	0.476E-04	59.					
24	85.16	0.84965E 06	94.3	0.26384E 04	0.21880E-02	0.489E-04	59.					
25	86.20	0.86982E 06	94.5	0.26817E 04	0.21229E-02	0.477E-04	59.					
26	87.23	0.88988E 06	94.1	0.27254E 04	0.22264E-02	0.490E-04	59.					
27	88.26	0.90995E 06	94.3	0.27692E 04	0.21277E-02	0.480E-04	59.					
28	89.29	0.93001E 06	94.1	0.28113E 04	0.20667E-02	0.471E-04	59.					
29	90.32	0.95008E 06	93.8	0.28535E 04	0.21333E-02	0.476E-04	59.					
30	91.35	0.97014E 06	94.0	0.28953E 04	0.20301E-02	0.475E-04	59.					
31	92.38	0.99021E 06	94.8	0.29376E 04	0.21806E-02	0.484E-04	59.					
32	93.41	0.10104E 07	94.6	0.29801E 04	0.20490E-02	0.468E-04	59.					
33	94.45	0.10305E 07	94.7	0.30213E 04	0.20558E-02	0.463E-04	59.					
34	95.48	0.10506E 07	94.2	0.30635E 04	0.21418E-02	0.468E-04	59.					
35	96.51	0.10707E 07	94.5	0.31060E 04	0.20895E-02	0.491E-04	59.					
36	97.54	0.10907E 07	93.8	0.31479E 04	0.20829E-02	0.537E-04	59.					

STANTON NUMBER DATA RUN 012874 *** DISCRETE HOLE RIG *** NAS-3-14336

TINF= 71.9 UINF= 37.8 XVO=41.550 RHO= 0.07472 CP= 0.242 VISC= 0.16318E-03 PR=0.715
DISTANCE FROM ORIGIN OF BL TO 1ST PLATE= 7.750 P/D=10
UNCERTAINTY IN REX=19327. UNCERTAINTY IN F=0.03100 IN RATIO

** M=0.2, HOT RUN, LOW RE, STEP T-WALL AT VIRTUAL ORIGIN OF BL.

PLATE	X	REX	TO	REENTH	STANTON NO	DST	DREEN	M	F	T2	THETA	DTH
1	50.30	0.16911E 06	102.8	0.65325E 03	0.26936E-02	0.638E-04	58.					
2	52.30	0.20777E 06	102.8	0.80865E 03	0.28213E-02	0.645E-04	58.	0.17	0.0014	100.4	0.924	0.011
3	54.30	0.24642E 06	102.6	0.96722E 03	0.28585E-02	0.650E-04	58.	0.00	0.0014	102.6	0.924	0.012
4	56.30	0.28507E 06	102.7	0.11203E 04	0.26711E-02	0.638E-04	58.	0.16	0.0013	100.6	0.932	0.011
5	58.30	0.32373E 06	102.6	0.12695E 04	0.26509E-02	0.639E-04	58.	0.00	0.0013	102.6	0.932	0.012
6	60.30	0.36238E 06	102.8	0.14200E 04	0.24893E-02	0.628E-04	58.	0.18	0.0014	100.7	0.932	0.011
7	62.30	0.40104E 06	102.6	0.15679E 04	0.25124E-02	0.631E-04	58.	0.00	0.0014	102.6	0.932	0.012
8	64.30	0.43969E 06	102.8	0.17077E 04	0.23798E-02	0.622E-04	58.	0.15	0.0012	102.6	0.994	0.011
9	66.30	0.47835E 06	102.7	0.18443E 04	0.23514E-02	0.623E-04	58.	0.00	0.0012	102.7	0.994	0.012
10	68.30	0.51700E 06	102.7	0.19866E 04	0.22255E-02	0.616E-04	58.	0.16	0.0013	105.1	1.079	0.012
11	70.30	0.55565E 06	102.5	0.21267E 04	0.22433E-02	0.620E-04	58.	0.00	0.0013	102.5	1.079	0.012
12	72.30	0.59431E 06	102.8	0.22643E 04	0.19831E-02	0.604E-04	58.	0.16	0.0013	107.4	1.149	0.012
13	73.82	0.62368E 06	100.1	0.23664E 04	0.21589E-02	0.399E-04	58.					
14	74.85	0.64359E 06	99.2	0.24089E 04	0.21066E-02	0.442E-04	58.					
15	75.88	0.66350E 06	100.0	0.24359E 04	0.20483E-02	0.441E-04	58.					
16	76.91	0.68350E 06	99.9	0.24773E 04	0.21071E-02	0.442E-04	58.					
17	77.95	0.70351E 06	100.1	0.25192E 04	0.20895E-02	0.440E-04	58.					
18	78.98	0.72341E 06	100.6	0.25599E 04	0.19970E-02	0.432E-04	58.					
19	80.01	0.74332E 06	100.2	0.26006E 04	0.20882E-02	0.428E-04	58.					
20	81.04	0.76323E 06	100.4	0.26416E 04	0.20238E-02	0.418E-04	58.					
21	82.07	0.78313E 06	100.6	0.26820E 04	0.20328E-02	0.427E-04	58.					
22	83.10	0.80304E 06	100.1	0.27233E 04	0.21067E-02	0.446E-04	58.					
23	84.13	0.82295E 06	100.1	0.27642E 04	0.19992E-02	0.434E-04	58.					
24	85.16	0.84295E 06	100.5	0.28036E 04	0.19524E-02	0.434E-04	58.					
25	86.20	0.86295E 06	100.4	0.28427E 04	0.19726E-02	0.433E-04	58.					
26	87.23	0.88286E 06	99.7	0.28832E 04	0.20948E-02	0.448E-04	58.					
27	88.26	0.90277E 06	100.6	0.29230E 04	0.19019E-02	0.427E-04	58.					
28	89.29	0.92267E 06	100.4	0.29616E 04	0.19715E-02	0.429E-04	58.					
29	90.32	0.94258E 06	100.1	0.30005E 04	0.19326E-02	0.422E-04	58.					
30	91.35	0.96249E 06	100.0	0.30399E 04	0.20186E-02	0.443E-04	58.					
31	92.38	0.98240E 06	100.6	0.30797E 04	0.19745E-02	0.436E-04	58.					
32	93.41	0.10024E 07	100.0	0.31192E 04	0.19855E-02	0.438E-04	58.					
33	94.45	0.10224E 07	100.2	0.31582E 04	0.19343E-02	0.427E-04	58.					
34	95.48	0.10423E 07	99.7	0.31976E 04	0.20155E-02	0.430E-04	58.					
35	96.51	0.10622E 07	100.0	0.32376E 04	0.19952E-02	0.454E-04	59.					
36	97.54	0.10821E 07	99.4	0.32773E 04	0.19944E-02	0.485E-04	59.					

FOLLOWING IS THE DATA FOR THETA=0 AND THETA=1, WHICH WAS OBTAINED BY LINEAR SUPERPOSITION THEORY.
THIS DATA WAS PRODUCED FROM RUN 012774 AND RUN 012874
FOR THE DETAIL CHANGES OF PROPERTIES AND BOUNDARY CONDITIONS, PLEASE SEE THE ABOVE TWO RUNS

PLATE	REXCOL	RE DEL2	ST(TH=0)	REXHOT	RE DEL2	ST(TH=1)	ETA	STCR	F-COL	STHR	F-HOT	PHI-1
1	170456.9	658.5	0.002772	169111.9	653.3	0.002694	UUUUU	UUUUU	0.0000	UUUUUUU	0.0000	UUUUU
2	209418.6	777.2	0.003324	207766.0	811.9	0.002780	0.164	1.142	0.0017	0.954	0.0014	1.172
3	248380.1	903.6	0.003165	246420.2	973.2	0.002833	0.105	1.125	0.0017	1.006	0.0014	1.232
4	287341.8	1026.6	0.003148	285074.3	1128.5	0.002636	0.163	1.152	0.0018	0.963	0.0013	1.183
5	326303.3	1145.8	0.002973	323728.4	1279.9	0.002627	0.116	1.116	0.0018	0.985	0.0013	1.210
6	365264.9	1263.2	0.003051	362382.6	1433.0	0.002448	0.198	1.172	0.0018	0.939	0.0014	1.191
7	404226.5	1379.2	0.002902	401036.8	1583.2	0.002484	0.144	1.137	0.0018	0.972	0.0014	1.229
8	443188.1	1492.8	0.002933	439690.9	1722.6	0.002376	0.190	1.171	0.0016	0.947	0.0012	1.166
9	482149.7	1604.3	0.002786	478345.1	1859.4	0.002349	0.157	1.131	0.0016	0.952	0.0012	1.174
10	521111.3	1715.1	0.002905	516999.2	1998.7	0.002275	0.217	1.198	0.0017	0.936	0.0013	1.182
11	560072.9	1825.7	0.002770	555653.4	2136.6	0.002282	0.176	1.159	0.0017	0.953	0.0013	1.202
12	599034.5	1934.1	0.002798	594307.5	2269.7	0.002089	0.253	1.186	0.0018	0.884	0.0013	1.129
13	628645.4	2013.8	0.002502	623684.8	2368.4	0.002155	0.139	1.071		0.921		
14	648710.6	2063.0	0.002403	643591.6	2410.8	0.002103	0.125	1.035		0.904		
15	668775.8	2111.7	0.002445	663498.4	2439.6	0.002044	0.164	1.060		0.884		
16	688938.2	2160.0	0.002365	683501.8	2480.9	0.002104	0.111	1.031		0.915		
17	709100.9	2206.6	0.002269	703505.4	2522.7	0.002087	0.080	0.995		0.914		
18	729166.1	2253.8	0.002433	723412.2	2563.3	0.001992	0.181	1.073		0.877		
19	749231.3	2301.5	0.002311	743319.1	2604.0	0.002086	0.098	1.025		0.923		
20	769296.4	2346.5	0.002169	763225.9	2644.9	0.002022	0.068	0.967		0.900		
21	789361.9	2392.6	0.002420	783133.1	2685.3	0.002028	0.162	1.084		0.907		
22	809427.1	2439.0	0.002205	803039.9	2726.5	0.002106	0.045	0.993		0.947		
23	829492.3	2483.1	0.002176	822946.8	2767.4	0.001997	0.082	0.985		0.902		
24	849654.8	2527.6	0.002257	842950.1	2806.7	0.001949	0.137	1.026		0.885		
25	869817.4	2572.0	0.002167	862953.7	2845.7	0.001970	0.091	0.990		0.899		
26	889882.6	2616.5	0.002265	882860.6	2886.2	0.002093	0.076	1.039		0.959		
27	909947.8	2661.3	0.002194	902767.4	2926.0	0.001898	0.135	1.011		0.874		
28	930013.0	2704.4	0.002095	922674.3	2964.5	0.001970	0.060	0.970		0.911		
29	950078.5	2747.5	0.002192	942581.4	3003.4	0.001930	0.120	1.019		0.896		
30	970143.7	2789.9	0.002034	962488.3	3042.7	0.002018	0.007	0.949		0.941		
31	990208.9	2832.9	0.002241	982395.2	3082.5	0.001971	0.120	1.051		0.923		
32	1010371.0	2876.1	0.002068	1002398.0	3121.9	0.001984	0.040	0.973		0.933		
33	1030534.0	2917.9	0.002092	1022402.0	3161.0	0.001932	0.076	0.988		0.912		
34	1050599.0	2960.8	0.002179	1042308.0	3200.3	0.002013	0.076	1.034		0.954		
35	1070664.0	3004.0	0.002117	1062215.0	3240.2	0.001994	0.058	1.008		0.948		
36	1090729.0	3046.4	0.002109	1082122.0	3279.9	0.001993	0.055	1.008		0.951		

STANTON NUMBER DATA RUN 012974-1 *** DISCRETE HOLE RIG *** NAS-3-14336

TINF= 69.7 UINF= 37.2 XVO=41.550 RHO= 0.07497 CP= 0.241 VISC= 0.16217E-03 PR=0.715
DISTANCE FROM ORIGIN OF BL TO 1ST PLATE= 7.750 P/D=10
UNCERTAINTY IN REX=19109. UNCERTAINTY IN F=0.03107 IN RATIO

** M=0.5, COLD RUN, LOW RE, STEP T-WALL AT VIRTUAL ORIGIN OF BL.

PLATE	X	REX	TO	REENTH	STANTON NO	DST	DREEN	M	F	T2	THETA	DTH
1	50.30	0.16720E 06	97.3	0.64588E 03	0.27704E-02	0.717E-04	57.					
2	52.30	0.20542E 06	97.2	0.79130E 03	0.34398E-02	0.761E-04	57.	0.56	0.0045	73.9	0.155	0.009
3	54.30	0.24364E 06	97.2	0.94662E 03	0.32887E-02	0.751E-04	57.	0.00	0.0045	97.2	0.155	0.013
4	56.30	0.28186E 06	97.1	0.10977E 04	0.33779E-02	0.760E-04	57.	0.54	0.0044	73.5	0.142	0.009
5	58.30	0.32007E 06	97.2	0.12464E 04	0.31683E-02	0.743E-04	58.	0.00	0.0044	97.2	0.142	0.013
6	60.30	0.35829E 06	97.1	0.13962E 04	0.33691E-02	0.759E-04	58.	0.54	0.0044	73.7	0.149	0.009
7	62.30	0.39651E 06	97.2	0.15461E 04	0.31770E-02	0.744E-04	58.	0.00	0.0044	97.2	0.149	0.013
8	64.30	0.43473E 06	97.1	0.16946E 04	0.32523E-02	0.752E-04	58.	0.54	0.0043	73.9	0.154	0.009
9	66.30	0.47294E 06	97.2	0.18405E 04	0.30411E-02	0.736E-04	58.	0.00	0.0043	97.2	0.154	0.013
10	68.30	0.51116E 06	97.1	0.19874E 04	0.32388E-02	0.749E-04	58.	0.55	0.0044	74.0	0.159	0.009
11	70.30	0.54938E 06	97.2	0.21334E 04	0.29889E-02	0.733E-04	58.	0.00	0.0044	97.2	0.159	0.013
12	72.30	0.58760E 06	97.1	0.22718E 04	0.30523E-02	0.737E-04	58.	0.54	0.0043	73.5	0.139	0.009
13	73.82	0.61664E 06	94.3	0.23753E 04	0.28137E-02	0.521E-04	58.					
14	74.85	0.63632E 06	93.6	0.24293E 04	0.26657E-02	0.556E-04	58.					
15	75.88	0.65601E 06	94.3	0.24756E 04	0.26330E-02	0.555E-04	58.					
16	76.91	0.67578E 06	94.4	0.25270E 04	0.25844E-02	0.542E-04	58.					
17	77.95	0.69556E 06	94.6	0.25768E 04	0.24767E-02	0.528E-04	58.					
18	78.98	0.71524E 06	94.6	0.26262E 04	0.25347E-02	0.538E-04	58.					
19	80.01	0.73493E 06	94.6	0.26755E 04	0.24723E-02	0.516E-04	58.					
20	81.04	0.75461E 06	94.8	0.27230E 04	0.23464E-02	0.496E-04	58.					
21	82.07	0.77429E 06	94.7	0.27708E 04	0.25023E-02	0.523E-04	58.					
22	83.10	0.79397E 06	94.8	0.28186E 04	0.23517E-02	0.516E-04	58.					
23	84.13	0.81365E 06	94.5	0.28642E 04	0.22711E-02	0.507E-04	58.					
24	85.16	0.83343E 06	94.5	0.29092E 04	0.23023E-02	0.518E-04	58.					
25	86.20	0.85321E 06	94.7	0.29538E 04	0.22204E-02	0.507E-04	58.					
26	87.23	0.87289E 06	93.8	0.29979E 04	0.22511E-02	0.514E-04	58.					
27	88.26	0.89257E 06	94.5	0.30421E 04	0.22441E-02	0.512E-04	58.					
28	89.29	0.91226E 06	94.4	0.30857E 04	0.21768E-02	0.498E-04	58.					
29	90.32	0.93194E 06	94.1	0.31292E 04	0.22370E-02	0.502E-04	58.					
30	91.35	0.95162E 06	94.2	0.31724E 04	0.21506E-02	0.504E-04	58.					
31	92.38	0.97130E 06	95.1	0.32161E 04	0.22806E-02	0.511E-04	58.					
32	93.41	0.99108E 06	95.0	0.32595E 04	0.21254E-02	0.491E-04	58.					
33	94.45	0.10109E 07	95.1	0.33016E 04	0.21451E-02	0.486E-04	58.					
34	95.48	0.10305E 07	94.5	0.33447E 04	0.22347E-02	0.493E-04	58.					
35	96.51	0.10502E 07	94.8	0.33881E 04	0.21676E-02	0.515E-04	58.					
36	97.54	0.10699E 07	94.0	0.34305E 04	0.21368E-02	0.562E-04	58.					

STANTON NUMBER DATA RUN 012974-2 *** DISCRETE HOLE RIG *** NAS-3-14336

TINF= 67.6 UINF= 37.7 XVO=41.550 RHO= 0.07528 CP= 0.241 VISC= 0.16109E-03 PR=0.715
DISTANCE FROM ORIGIN OF BL TO 1ST PLATE= 7.750 P/D=10
UNCERTAINTY IN REX=19505. UNCERTAINTY IN F=0.03100 IN RATIO

** M=0.5, HOT RUN, LOW RE, STEP T-WALL AT VIRTUAL ORIGIN OF BL.

PLATE	X	REX	TO	REENTH	STANTON NO	DST	DREEN	M	F	T2	THETA	DTH
1	50.30	0.17067E 06	98.4	0.65926E 03	0.27520E-02	0.641E-04	59.					
2	52.30	0.20968E 06	98.4	0.93820E 03	0.30245E-02	0.656E-04	59.	0.55	0.0044	97.2	0.960	0.011
3	54.30	0.24869E 06	98.4	0.12212E 04	0.29624E-02	0.652E-04	59.	0.00	0.0044	98.4	0.960	0.011
4	56.30	0.28770E 06	98.6	0.14907E 04	0.28930E-02	0.646E-04	59.	0.54	0.0044	95.6	0.904	0.011
5	58.30	0.32671E 06	98.4	0.17562E 04	0.27580E-02	0.641E-04	59.	0.00	0.0044	98.4	0.904	0.011
6	60.30	0.36572E 06	98.6	0.20176E 04	0.27178E-02	0.636E-04	59.	0.54	0.0044	95.5	0.900	0.011
7	62.30	0.40472E 06	98.4	0.22764E 04	0.26276E-02	0.634E-04	59.	0.00	0.0044	98.4	0.900	0.011
8	64.30	0.44373E 06	98.4	0.25193E 04	0.25663E-02	0.631E-04	59.	0.48	0.0039	96.6	0.941	0.011
9	66.30	0.48274E 06	98.4	0.27595E 04	0.24900E-02	0.626E-04	60.	0.00	0.0039	98.4	0.941	0.011
10	68.30	0.52175E 06	98.4	0.30065E 04	0.24890E-02	0.626E-04	60.	0.50	0.0041	96.7	0.943	0.011
11	70.30	0.56076E 06	98.5	0.32522E 04	0.24286E-02	0.622E-04	60.	0.00	0.0041	98.5	0.943	0.011
12	72.30	0.59977E 06	98.4	0.34947E 04	0.22817E-02	0.617E-04	60.	0.48	0.0039	98.1	0.990	0.011
13	73.82	0.62942E 06	95.4	0.36758E 04	0.22325E-02	0.409E-04	60.					
14	74.85	0.64951E 06	94.5	0.37202E 04	0.21816E-02	0.454E-04	60.					
15	75.88	0.66960E 06	95.3	0.37241E 04	0.20701E-02	0.446E-04	60.					
16	76.91	0.68979E 06	95.2	0.37665E 04	0.21443E-02	0.449E-04	60.					
17	77.95	0.70997E 06	95.4	0.38092E 04	0.20986E-02	0.444E-04	60.					
18	78.98	0.73006E 06	95.7	0.38512E 04	0.20774E-02	0.443E-04	60.					
19	80.01	0.75015E 06	95.5	0.38933E 04	0.21100E-02	0.434E-04	60.					
20	81.04	0.77024E 06	95.7	0.39350E 04	0.20337E-02	0.421E-04	60.					
21	82.07	0.79033E 06	95.8	0.39764E 04	0.20870E-02	0.435E-04	60.					
22	83.10	0.81042E 06	95.5	0.40183E 04	0.20798E-02	0.445E-04	60.					
23	84.13	0.83051E 06	95.4	0.40589E 04	0.19583E-02	0.432E-04	60.					
24	85.16	0.85070E 06	95.5	0.40985E 04	0.19803E-02	0.441E-04	60.					
25	86.20	0.87089E 06	95.6	0.41380E 04	0.19409E-02	0.435E-04	60.					
26	87.23	0.89098E 06	94.7	0.41779E 04	0.20334E-02	0.447E-04	60.					
27	88.26	0.91107E 06	95.6	0.42180E 04	0.19456E-02	0.437E-04	60.					
28	89.29	0.93116E 06	95.5	0.42570E 04	0.19379E-02	0.430E-04	60.					
29	90.32	0.95125E 06	95.1	0.42963E 04	0.19639E-02	0.431E-04	60.					
30	91.35	0.97134E 06	95.1	0.43355E 04	0.19339E-02	0.439E-04	60.					
31	92.38	0.99143E 06	95.8	0.43748E 04	0.19816E-02	0.439E-04	60.					
32	93.41	0.10116E 07	95.5	0.44140E 04	0.19156E-02	0.432E-04	60.					
33	94.45	0.10318E 07	95.6	0.44524E 04	0.18984E-02	0.424E-04	60.					
34	95.48	0.10519E 07	95.1	0.44914E 04	0.19775E-02	0.428E-04	60.					
35	96.51	0.10720E 07	95.3	0.45307E 04	0.19328E-02	0.451E-04	60.					
36	97.54	0.10921E 07	94.6	0.45693E 04	0.19032E-02	0.482E-04	60.					

FOLLOWING IS THE DATA FOR THETA=0 AND THETA=1, WHICH WAS OBTAINED BY LINEAR SUPERPOSITION THEORY.
THIS DATA WAS PRODUCED FROM RUN 012974-1 AND RUN 012974-2
FOR THE DETAIL CHANGES OF PROPERTIES AND BOUNDARY CONDITIONS, PLEASE SEE THE ABOVE TWO RUNS

PLATE	REXCOL	RE DEL2	ST(TH=0)	REXHOT	RE DEL2	ST(TH=1)	ETA	STCP	F-COL	STHR	F-HOT	PHI-1
1	167202.4	645.9	0.002770	170667.0	659.3	0.002752	UUUUU	UUUUU	0.0000	UUUUUUU	0.0000	UUUUU
2	205420.1	766.1	0.003520	209676.6	944.8	0.003004	0.147	1.205	0.0045	1.032	0.0044	1.682
3	243637.8	897.4	0.003352	248686.3	1234.1	0.002946	0.121	1.187	0.0045	1.048	0.0044	1.718
4	281855.4	1027.7	0.003468	287695.8	1518.5	0.002832	0.183	1.264	0.0044	1.037	0.0044	1.718
5	320073.1	1156.0	0.003245	326705.4	1798.3	0.002706	0.166	1.213	0.0044	1.016	0.0044	1.712
6	358290.8	1284.8	0.003498	365715.1	2074.1	0.002631	0.248	1.338	0.0044	1.011	0.0044	1.720
7	396508.5	1414.5	0.003286	404724.7	2347.0	0.002555	0.223	1.283	0.0044	1.001	0.0044	1.722
8	434726.2	1542.0	0.003387	443734.3	2596.3	0.002515	0.258	1.347	0.0043	1.004	0.0039	1.656
9	472943.9	1666.9	0.003149	482743.9	2843.6	0.002448	0.223	1.273	0.0043	0.994	0.0039	1.556
10	511161.6	1791.8	0.003390	521753.5	3097.7	0.002435	0.282	1.392	0.0044	1.004	0.0041	1.708
11	549379.3	1915.9	0.003102	560763.1	3350.6	0.002388	0.230	1.293	0.0044	0.999	0.0041	1.712
12	587596.9	2035.9	0.003178	599772.7	3593.7	0.002272	0.285	1.342	0.0043	0.963	0.0039	1.655
13	616642.4	2125.5	0.002925	629420.1	3775.4	0.002184	0.253	1.247		0.935		
14	636324.5	2181.5	0.002759	649510.0	3818.9	0.002142	0.224	1.184		0.923		
15	656006.6	2235.7	0.002741	669599.9	3821.5	0.002024	0.262	1.183		0.877		
16	675784.1	2289.0	0.002669	689787.2	3863.1	0.002108	0.210	1.159		0.919		
17	695561.8	2340.4	0.002549	709974.8	3905.1	0.002067	0.189	1.113		0.907		
18	715243.9	2391.3	0.002623	730064.7	3946.4	0.002040	0.222	1.152		0.900		
19	734925.9	2442.2	0.002542	750154.6	3987.8	0.002080	0.182	1.123		0.922		
20	754608.0	2491.0	0.002406	770244.5	4028.9	0.002008	0.166	1.068		0.895		
21	774290.4	2540.1	0.002582	790334.8	4069.7	0.002053	0.205	1.152		0.920		
22	793972.5	2589.2	0.002404	810424.7	4111.1	0.002057	0.144	1.078		0.926		
23	813654.6	2635.9	0.002331	830514.6	4151.2	0.001932	0.171	1.051		0.875		
24	833432.0	2682.2	0.002364	850701.8	4190.3	0.001954	0.174	1.071		0.888		
25	853209.8	2727.9	0.002274	870889.4	4229.2	0.001918	0.157	1.035		0.876		
26	872891.8	2772.9	0.002293	890979.3	4268.8	0.002015	0.121	1.048		0.925		
27	892573.9	2818.1	0.002301	911069.3	4308.4	0.001921	0.165	1.057		0.886		
28	912256.0	2862.7	0.002223	931159.1	4347.0	0.001918	0.137	1.025		0.888		
29	931938.4	2907.2	0.002289	951249.4	4385.8	0.001941	0.152	1.060		0.903		
30	951620.4	2951.3	0.002192	971339.3	4424.6	0.001916	0.126	1.019		0.895		
31	971302.6	2995.9	0.002338	991429.3	4463.5	0.001957	0.163	1.092		0.918		
32	991079.9	3040.3	0.002166	1011616.0	4502.3	0.001898	0.124	1.015		0.894		
33	1010857.0	3083.3	0.002193	1031804.0	4540.3	0.001878	0.143	1.032		0.888		
34	1030539.0	3127.4	0.002284	1051893.0	4578.8	0.001956	0.144	1.079		0.928		
35	1050221.0	3171.7	0.002213	1071983.0	4617.8	0.001913	0.135	1.049		0.911		
36	1069903.0	3215.0	0.002182	1092073.0	4655.9	0.001884	0.136	1.039		0.901		

STANTON NUMBER DATA RUN 010474 *** DISCRETE HOLE RIG *** NAS-3-14336

TINF= 65.2 UINF= 37.6 XVO=20.900 RHO= 0.07448 CP= 0.241 VISC= 0.16233E-03 PR=0.714
DISTANCE FROM ORIGIN OF BL TO 1ST PLATE=28.400 P/D=10
UNCERTAINTY IN REX=19307.

** M=0.0, LOW RE, STEP T-WALL AT VIRTUAL ORIGIN OF BL, ** NO BL TRIP.

PLATE	X	REX	TO	REENTH	STANTON NO	DST.	DREEN	M	F	T2	THETA	DTH
1	50.30	0.56762E 06	94.6	0.42089E 03	0.12509E-02	0.611E-04	58.					
2	52.30	0.60624E 06	94.2	0.47050E 03	0.13186E-02	0.621E-04	58.	0.00	0.0000	94.2	1.000	0.012
3	54.30	0.64485E 06	94.5	0.52003E 03	0.12469E-02	0.615E-04	58.	0.00	0.0000	94.5	1.000	0.012
4	56.30	0.68346E 06	94.1	0.57085E 03	0.13854E-02	0.626E-04	58.	0.00	0.0000	94.1	1.000	0.012
5	58.30	0.72208E 06	94.4	0.62311E 03	0.13215E-02	0.619E-04	58.	0.00	0.0000	94.4	1.000	0.012
6	60.30	0.76069E 06	94.1	0.67728E 03	0.14838E-02	0.629E-04	58.	0.00	0.0000	94.1	1.000	0.012
7	62.30	0.79931E 06	94.2	0.73315E 03	0.14101E-02	0.624E-04	58.	0.00	0.0000	94.2	1.000	0.012
8	64.30	0.83792E 06	94.1	0.79155E 03	0.16147E-02	0.635E-04	58.	0.00	0.0000	94.1	1.000	0.012
9	66.30	0.87653E 06	94.2	0.85291E 03	0.15638E-02	0.629E-04	58.	0.00	0.0000	94.2	1.000	0.012
10	68.30	0.91515E 06	94.2	0.91749E 03	0.17809E-02	0.638E-04	58.	0.00	0.0000	94.2	1.000	0.012
11	70.30	0.95376E 06	94.3	0.98517E 03	0.17248E-02	0.634E-04	58.	0.00	0.0000	94.3	1.000	0.012
12	72.30	0.99237E 06	94.0	0.10545E 04	0.18669E-02	0.645E-04	58.	0.00	0.0000	94.0	1.000	0.012
13	73.82	0.10217E 07	92.6	0.11023E 04	0.11800E-02	0.297E-04	58.					
14	74.85	0.10416E 07	91.8	0.11274E 04	0.13374E-02	0.370E-04	58.					
15	75.88	0.10615E 07	92.1	0.11546E 04	0.13934E-02	0.382E-04	58.					
16	76.91	0.10815E 07	91.9	0.11831E 04	0.14743E-02	0.388E-04	58.					
17	77.95	0.11015E 07	91.9	0.12131E 04	0.15351E-02	0.397E-04	58.					
18	78.98	0.11213E 07	91.7	0.12444E 04	0.16145E-02	0.409E-04	58.					
19	80.01	0.11412E 07	91.5	0.12771E 04	0.16698E-02	0.402E-04	58.					
20	81.04	0.11611E 07	91.6	0.13103E 04	0.16669E-02	0.399E-04	58.					
21	82.07	0.11810E 07	91.3	0.13457E 04	0.18881E-02	0.433E-04	58.					
22	83.10	0.12009E 07	91.3	0.13827E 04	0.18321E-02	0.442E-04	58.					
23	84.13	0.12208E 07	90.9	0.14193E 04	0.18382E-02	0.444E-04	58.					
24	85.16	0.12408E 07	90.9	0.14567E 04	0.19209E-02	0.462E-04	58.					
25	86.20	0.12607E 07	90.9	0.14952E 04	0.19488E-02	0.460E-04	58.					
26	87.23	0.12806E 07	90.6	0.15360E 04	0.21432E-02	0.484E-04	58.					
27	88.26	0.13005E 07	90.7	0.15778E 04	0.20625E-02	0.476E-04	58.					
28	89.29	0.13204E 07	90.5	0.16189E 04	0.20624E-02	0.476E-04	58.					
29	90.32	0.13403E 07	90.1	0.16609E 04	0.21521E-02	0.483E-04	58.					
30	91.35	0.13602E 07	90.5	0.17035E 04	0.21274E-02	0.492E-04	58.					
31	92.38	0.13801E 07	90.8	0.17471E 04	0.22596E-02	0.500E-04	58.					
32	93.41	0.14000E 07	90.6	0.17908E 04	0.21271E-02	0.488E-04	58.					
33	94.45	0.14200E 07	90.5	0.18339E 04	0.22077E-02	0.491E-04	58.					
34	95.48	0.14399E 07	90.0	0.18786E 04	0.22769E-02	0.496E-04	58.					
35	96.51	0.14598E 07	90.3	0.19236E 04	0.22484E-02	0.521E-04	58.					
36	97.54	0.14797E 07	89.6	0.19684E 04	0.22476E-02	0.568E-04	59.					

STANTON NUMBER DATA RUN 021074 *** DISCRETE HOLE RIG *** NAS-3-14336

TINF= 65.3 UINF= 37.5 XVO=20.900 RHO= 0.07561 CP= 0.241 VISC= 0.15990E-03 PR=0.715
DISTANCE FROM ORIGIN OF BL TO 1ST PLATE=28.400 P/D= 5
UNCERTAINTY IN REX=19546. UNCERTAINTY IN F=0.03101 IN RATIO

** M=0.2, COLD RUN, LOW RE,STEP T-WALL AT VIRTUAL ORIGIN OF BL, ** NO BL TRIP.

PLATE	X	REX	TO	REENTH	STANTON NO	DST	DREEN	M	F	T2	THETA	DTH
1	50.30	0.57466E 06	96.8	0.42611E 03	0.12240E-02	0.566E-04	59.					
2	52.30	0.61375E 06	96.7	0.52835E 03	0.23586E-02	0.610E-04	59.	0.21	0.0069	72.8	0.239	0.008
3	54.30	0.65285E 06	96.8	0.70488E 03	0.33972E-02	0.667E-04	59.	0.21	0.0068	72.8	0.239	0.008
4	56.30	0.69194E 06	96.8	0.91131E 03	0.37962E-02	0.694E-04	59.	0.23	0.0076	72.5	0.229	0.008
5	58.30	0.73103E 06	96.7	0.11233E 04	0.37093E-02	0.689E-04	59.	0.21	0.0069	72.6	0.231	0.008
6	60.30	0.77012E 06	96.8	0.13276E 04	0.35460E-02	0.677E-04	59.	0.22	0.0070	72.5	0.228	0.008
7	62.30	0.80922E 06	96.7	0.15271E 04	0.34487E-02	0.672E-04	59.	0.21	0.0068	72.8	0.238	0.008
8	64.30	0.84831E 06	96.8	0.17224E 04	0.33124E-02	0.663E-04	59.	0.21	0.0068	72.7	0.236	0.008
9	66.30	0.88740E 06	96.8	0.19137E 04	0.32592E-02	0.659E-04	59.	0.21	0.0069	72.6	0.231	0.008
10	68.30	0.92649E 06	96.8	0.21035E 04	0.32260E-02	0.656E-04	59.	0.22	0.0071	72.5	0.228	0.008
11	70.30	0.96559E 06	96.9	0.22911E 04	0.31831E-02	0.652E-04	59.	0.22	0.0070	72.4	0.225	0.008
12	72.30	0.10047E 07	96.8	0.24746E 04	0.31113E-02	0.650E-04	59.	0.21	0.0070	72.2	0.219	0.008
13	73.82	0.10344E 07	92.6	0.25912E 04	0.25752E-02	0.453E-04	59.					
14	74.85	0.10545E 07	91.6	0.26419E 04	0.24561E-02	0.494E-04	59.					
15	75.88	0.10747E 07	92.4	0.26905E 04	0.23734E-02	0.488E-04	59.					
16	76.91	0.10949E 07	92.5	0.27378E 04	0.23154E-02	0.475E-04	59.					
17	77.95	0.11151E 07	92.7	0.27837E 04	0.22361E-02	0.465E-04	59.					
18	78.98	0.11352E 07	92.7	0.28289E 04	0.22530E-02	0.469E-04	59.					
19	80.01	0.11554E 07	92.7	0.28739E 04	0.22067E-02	0.450E-04	59.					
20	81.04	0.11755E 07	92.9	0.29174E 04	0.21094E-02	0.435E-04	59.					
21	82.07	0.11956E 07	92.8	0.29611E 04	0.22329E-02	0.456E-04	59.					
22	83.10	0.12158E 07	92.9	0.30048E 04	0.21007E-02	0.453E-04	59.					
23	84.13	0.12359E 07	92.6	0.30467E 04	0.20538E-02	0.448E-04	59.					
24	85.16	0.12561E 07	92.6	0.30883E 04	0.20819E-02	0.458E-04	59.					
25	86.20	0.12764E 07	92.7	0.31298E 04	0.20315E-02	0.452E-04	59.					
26	87.23	0.12965E 07	91.8	0.31710E 04	0.20530E-02	0.456E-04	59.					
27	88.26	0.13166E 07	92.4	0.32123E 04	0.20472E-02	0.455E-04	59.					
28	89.29	0.13368E 07	92.4	0.32529E 04	0.19811E-02	0.444E-04	59.					
29	90.32	0.13569E 07	91.9	0.32938E 04	0.20791E-02	0.453E-04	59.					
30	91.35	0.13770E 07	91.8	0.33343E 04	0.19410E-02	0.450E-04	59.					
31	92.38	0.13972E 07	92.9	0.33746E 04	0.20510E-02	0.455E-04	59.					
32	93.41	0.14174E 07	92.8	0.34149E 04	0.19473E-02	0.440E-04	59.					
33	94.45	0.14376E 07	92.8	0.34545E 04	0.19839E-02	0.438E-04	59.					
34	95.48	0.14578E 07	92.3	0.34951E 04	0.20502E-02	0.441E-04	59.					
35	96.51	0.14779E 07	92.6	0.35358E 04	0.19866E-02	0.462E-04	59.					
36	97.54	0.14980E 07	91.8	0.35756E 04	0.19607E-02	0.508E-04	59.					

STANTON NUMBER DATA RUN 021174 *** DISCRETE HOLE RIG *** NAS-3-14336

TINF= 64.3 UINF= 37.8 XVO=20.900 RHO= 0.07600 CP= 0.241 VISC= 0.15887E-03 PR=0.715
DISTANCE FROM ORIGIN OF BL TO 1ST PLATE=28.400 P/D= 5
UNCERTAINTY IN REX=19837. UNCERTAINTY IN F=0.03097 IN RATIO

** M=0.2, HOT RUN, LOW RE,STEP T-WALL AT VIRTUAL ORIGIN OF BL, ** NO BL TRIP.

PLATE	X	REX	TO	REENTH	STANTON NO	DST	DREEN	M	F	T2	THETA	DTH
1	50.30	0.58322E 06	95.3	0.43246E 03	0.11728E-02	0.565E-04	60.					
2	52.30	0.62290E 06	95.4	0.61967E 03	0.15788E-02	0.575E-04	60.	0.23	0.0073	92.6	0.911	0.011
3	54.30	0.66257E 06	95.4	0.95697E 03	0.24354E-02	0.610E-04	60.	0.21	0.0069	92.7	0.912	0.011
4	56.30	0.70225E 06	95.4	0.13249E 04	0.29075E-02	0.637E-04	60.	0.23	0.0075	92.8	0.917	0.011
5	58.30	0.74192E 06	95.4	0.16913E 04	0.28334E-02	0.632E-04	61.	0.19	0.0063	93.1	0.926	0.011
6	60.30	0.78160E 06	95.4	0.20320E 04	0.25961E-02	0.620E-04	61.	0.20	0.0064	92.8	0.919	0.011
7	62.30	0.82127E 06	95.5	0.23487E 04	0.24992E-02	0.613E-04	61.	0.17	0.0054	93.1	0.925	0.011
8	64.30	0.86095E 06	95.4	0.26460E 04	0.23165E-02	0.605E-04	61.	0.17	0.0055	93.6	0.944	0.011
9	66.30	0.90062E 06	95.4	0.29484E 04	0.22360E-02	0.602E-04	62.	0.18	0.0058	93.7	0.944	0.011
10	68.30	0.94030E 06	95.4	0.32671E 04	0.21635E-02	0.598E-04	62.	0.20	0.0065	94.0	0.956	0.011
11	70.30	0.97997E 06	95.4	0.35878E 04	0.20703E-02	0.595E-04	62.	0.18	0.0059	94.6	0.977	0.011
12	72.30	0.10196E 07	95.4	0.38946E 04	0.19376E-02	0.588E-04	62.	0.17	0.0056	96.1	1.023	0.011
13	73.82	0.10498E 07	92.6	0.40655E 04	0.18616E-02	0.356E-04	63.					
14	74.85	0.10702E 07	91.6	0.41033E 04	0.18298E-02	0.405E-04	63.					
15	75.88	0.10907E 07	92.2	0.41405E 04	0.18058E-02	0.407E-04	63.					
16	76.91	0.11112E 07	92.3	0.41775E 04	0.18101E-02	0.404E-04	63.					
17	77.95	0.11317E 07	92.4	0.42143E 04	0.17936E-02	0.402E-04	63.					
18	78.98	0.11522E 07	92.6	0.42509E 04	0.17834E-02	0.403E-04	63.					
19	80.01	0.11726E 07	92.4	0.42876E 04	0.18047E-02	0.392E-04	63.					
20	81.04	0.11930E 07	92.6	0.43239E 04	0.17403E-02	0.382E-04	63.					
21	82.07	0.12135E 07	92.6	0.43601E 04	0.18063E-02	0.396E-04	63.					
22	83.10	0.12339E 07	92.5	0.43969E 04	0.17912E-02	0.406E-04	63.					
23	84.13	0.12543E 07	92.3	0.44327E 04	0.17025E-02	0.397E-04	63.					
24	85.16	0.12749E 07	92.5	0.44676E 04	0.17156E-02	0.405E-04	63.					
25	86.20	0.12954E 07	92.4	0.45029E 04	0.17348E-02	0.404E-04	63.					
26	87.23	0.13158E 07	91.8	0.45388E 04	0.17731E-02	0.410E-04	63.					
27	88.26	0.13363E 07	92.4	0.45743E 04	0.17004E-02	0.402E-04	63.					
28	89.29	0.13567E 07	92.3	0.46093E 04	0.17145E-02	0.399E-04	63.					
29	90.32	0.13771E 07	92.0	0.46447E 04	0.17510E-02	0.401E-04	63.					
30	91.35	0.13975E 07	91.8	0.46802E 04	0.17226E-02	0.410E-04	63.					
31	92.38	0.14180E 07	92.5	0.47160E 04	0.17710E-02	0.411E-04	63.					
32	93.41	0.14385E 07	92.2	0.47516E 04	0.17113E-02	0.405E-04	63.					
33	94.45	0.14590E 07	92.3	0.47868E 04	0.17316E-02	0.401E-04	63.					
34	95.48	0.14795E 07	91.9	0.48228E 04	0.17838E-02	0.401E-04	63.					
35	96.51	0.14999E 07	92.1	0.48588E 04	0.17407E-02	0.424E-04	63.					
36	97.54	0.15203E 07	91.4	0.48940E 04	0.17030E-02	0.454E-04	63.					

FOLLOWING IS THE DATA FOR THETA=0 AND THETA=1, WHICH WAS OBTAINED BY LINEAR SUPERPOSITION THEORY.
THIS DATA WAS PRODUCED FROM RUN 021074 AND RUN 021174
FOR THE DETAIL CHANGES OF PROPERTIES AND BOUNDARY CONDITIONS, PLEASE SEE THE ABOVE TWO RUNS

PLATE	REXCOL	RE DEL2	ST(TH=0)	REXHOT	RE DEL2	ST(TH=1)	ETA	STCR	F-COL	STHR	F-HOT	PHI-1
1	574661.1	426.1	0.001224	583221.2	432.5	0.001173	UUUUU	UUUUU	0.0000	UUUUUUU	0.0000	UUUUU
2	613753.6	501.6	0.002636	622896.1	630.6	0.001475	0.440	1.123	0.0069	0.630	0.0073	1.754
3	652846.2	626.1	0.003739	662570.9	988.4	0.002309	0.382	1.612	0.0068	0.999	0.0069	2.160
4	691938.8	779.2	0.004092	702245.9	1376.2	0.002800	0.316	1.786	0.0076	1.225	0.0075	2.524
5	731031.4	937.4	0.004001	741920.8	1760.4	0.002740	0.315	1.765	0.0069	1.212	0.0063	2.335
6	770123.9	1091.1	0.003860	781595.6	2116.6	0.002484	0.356	1.721	0.0070	1.111	0.0064	2.251
7	809216.5	1240.4	0.003778	821270.6	2447.4	0.002396	0.366	1.701	0.0068	1.082	0.0054	2.060
8	848309.1	1385.4	0.003645	860945.4	2755.2	0.002237	0.386	1.657	0.0068	1.020	0.0055	2.024
9	887401.7	1526.9	0.003591	900620.4	3067.0	0.002156	0.400	1.647	0.0069	0.992	0.0058	2.043
10	926494.3	1666.7	0.003559	940295.3	3394.9	0.002100	0.410	1.646	0.0071	0.974	0.0065	2.135
11	965586.8	1804.9	0.003516	979970.1	3722.0	0.002036	0.421	1.640	0.0070	0.952	0.0059	2.025
12	1004679.0	1940.7	0.003431	1019645.0	4028.9	0.001971	0.425	1.613	0.0070	0.930	0.0056	1.961
13	1034389.0	2036.1	0.002808	1049798.0	4197.3	0.001802	0.358	1.328		0.855		
14	1054522.0	2091.2	0.002660	1070230.0	4233.9	0.001778	0.332	1.263		0.847		
15	1074655.0	2143.8	0.002558	1090663.0	4270.1	0.001759	0.313	1.219		0.841		
16	1094885.0	2194.6	0.002480	1111194.0	4306.2	0.001768	0.287	1.186		0.848		
17	1115115.0	2243.5	0.002380	1131726.0	4342.3	0.001757	0.262	1.143		0.846		
18	1135248.0	2291.8	0.002406	1152159.0	4378.1	0.001745	0.275	1.159		0.843		
19	1155381.0	2339.6	0.002338	1172591.0	4414.0	0.001771	0.242	1.130		0.859		
20	1175513.0	2385.6	0.002230	1193024.0	4449.6	0.001710	0.233	1.082		0.832		
21	1195646.0	2432.0	0.002372	1213457.0	4485.2	0.001771	0.253	1.155		0.865		
22	1215779.0	2478.1	0.002202	1233889.0	4521.4	0.001766	0.198	1.075		0.865		
23	1235912.0	2522.1	0.002168	1254322.0	4556.6	0.001673	0.228	1.063		0.822		
24	1256142.0	2566.2	0.002201	1274853.0	4590.9	0.001685	0.234	1.082		0.831		
25	1276372.0	2609.8	0.002128	1295385.0	4625.7	0.001710	0.196	1.050		0.846		
26	1296505.0	2652.9	0.002144	1315818.0	4661.1	0.001750	0.184	1.061		0.868		
27	1316638.0	2696.2	0.002160	1336250.0	4696.1	0.001672	0.226	1.072		0.832		
28	1336770.0	2738.9	0.002068	1356683.0	4730.5	0.001692	0.182	1.029		0.845		
29	1356903.0	2781.7	0.002186	1377115.0	4765.4	0.001724	0.211	1.091		0.863		
30	1377036.0	2824.0	0.002012	1397548.0	4800.5	0.001704	0.153	1.008		0.856		
31	1397168.0	2865.9	0.002142	1417981.0	4835.8	0.001748	0.184	1.076		0.880		
32	1417399.0	2907.9	0.002024	1438512.0	4871.0	0.001692	0.164	1.019		0.855		
33	1437629.0	2949.1	0.002066	1459044.0	4905.8	0.001711	0.172	1.044		0.867		
34	1457762.0	2991.5	0.002137	1479476.0	4941.3	0.001762	0.176	1.082		0.895		
35	1477894.0	3033.9	0.002067	1499909.0	4976.9	0.001720	0.168	1.050		0.876		
36	1498027.0	3075.3	0.002045	1520342.0	5011.7	0.001682	0.178	1.041		0.859		

STANTON NUMBER DATA RUN 020774 *** DISCRETE HOLE RIG *** NAS-3-14336

TINF= 67.1 UINF= 37.1 XVO=41.550 RHO= 0.07569 CP= 0.241 VISC= 0.16029E-03 PR=0.714
DISTANCE FROM ORIGIN OF BL TO 1ST PLATE= 7.750 P/D= 5
UNCERTAINTY IN REX=19304. UNCERTAINTY IN F=0.03105 IN RATIO

** LOW RE, ARBITRARY BOUNDARY CONDITION RUN.

PLATE	X	REX	TO	REENTH	STANTON NO	DST	DREEN	M	F	T2	THETA	DTH
1	50.30	0.16891E 06	98.9	0.65246E 03	0.29058E-02	0.639E-04	58.					
2	52.30	0.20751E 06	100.2	0.11889E 04	0.32083E-02	0.635E-04	60.	0.59	0.0192	104.4	1.126	0.011
3	54.30	0.24612E 06	101.2	0.21573E 04	0.32709E-02	0.623E-04	63.	0.62	0.0200	104.7	1.102	0.011
4	56.30	0.28473E 06	100.8	0.29827E 04	0.28863E-02	0.607E-04	65.	0.44	0.0144	101.2	1.014	0.011
5	58.30	0.32334E 06	100.5	0.33745E 04	0.28244E-02	0.608E-04	66.	0.00	0.0000	100.5	1.000	0.011
6	60.30	0.36194E 06	100.6	0.34806E 04	0.26718E-02	0.598E-04	66.	0.00	0.0000	100.6	1.000	0.011
7	62.30	0.40055E 06	97.6	0.35748E 04	0.22088E-02	0.626E-04	66.	0.00	0.0000	97.6	1.000	0.012
8	64.30	0.43916E 06	97.3	0.36871E 04	0.20707E-02	0.624E-04	66.	0.05	0.0015	98.8	1.050	0.012
9	66.30	0.47776E 06	96.7	0.38900E 04	0.19255E-02	0.631E-04	66.	0.16	0.0051	96.2	0.984	0.012
10	68.30	0.51637E 06	94.8	0.42129E 04	0.18319E-02	0.667E-04	66.	0.23	0.0074	96.8	1.074	0.013
11	70.30	0.55498E 06	94.7	0.45865E 04	0.17798E-02	0.666E-04	67.	0.21	0.0070	97.8	1.111	0.014
12	72.30	0.59359E 06	95.0	0.48055E 04	0.18260E-02	0.661E-04	67.	0.00	0.0000	95.0	1.000	0.013
13	73.82	0.62293E 06	94.9	0.48613E 04	0.20658E-02	0.400E-04	67.					
14	74.85	0.64281E 06	94.7	0.49005E 04	0.18691E-02	0.415E-04	67.					
15	75.88	0.66269E 06	95.6	0.49371E 04	0.18126E-02	0.412E-04	67.					
16	76.91	0.68267E 06	95.6	0.49734E 04	0.18316E-02	0.408E-04	67.					
17	77.95	0.70265E 06	95.8	0.50096E 04	0.18053E-02	0.405E-04	67.					
18	78.98	0.72253E 06	96.0	0.50451E 04	0.17613E-02	0.403E-04	67.					
19	80.01	0.74242E 06	95.7	0.50807E 04	0.18184E-02	0.396E-04	67.					
20	81.04	0.76230E 06	95.9	0.51163E 04	0.17513E-02	0.385E-04	67.					
21	82.07	0.78218E 06	96.0	0.51515E 04	0.17884E-02	0.397E-04	67.					
22	83.10	0.80207E 06	95.8	0.51872E 04	0.17977E-02	0.409E-04	67.					
23	84.13	0.82195E 06	95.8	0.52219E 04	0.16879E-02	0.398E-04	67.					
24	85.16	0.84193E 06	95.9	0.52559E 04	0.17249E-02	0.408E-04	67.					
25	86.20	0.86191E 06	95.9	0.52900E 04	0.17025E-02	0.403E-04	67.					
26	87.23	0.88179E 06	95.1	0.53246E 04	0.17807E-02	0.413E-04	67.					
27	88.26	0.90167E 06	95.9	0.53592E 04	0.16949E-02	0.404E-04	67.					
28	89.29	0.92155E 06	95.8	0.53929E 04	0.16920E-02	0.398E-04	67.					
29	90.32	0.94144E 06	95.5	0.54270E 04	0.17318E-02	0.400E-04	67.					
30	91.35	0.96132E 06	95.3	0.54610E 04	0.16802E-02	0.407E-04	67.					
31	92.38	0.98120E 06	96.1	0.54950E 04	0.17399E-02	0.409E-04	67.					
32	93.41	0.10012E 07	95.7	0.55295E 04	0.17210E-02	0.406E-04	67.					
33	94.45	0.10212E 07	95.9	0.55635E 04	0.16977E-02	0.398E-04	67.					
34	95.48	0.10410E 07	95.4	0.55980E 04	0.17732E-02	0.401E-04	67.					
35	96.51	0.10609E 07	95.6	0.56329E 04	0.17239E-02	0.423E-04	67.					
36	97.54	0.10808E 07	95.0	0.56669E 04	0.16952E-02	0.453E-04	67.					

APPENDIX B

PROFILE DATA

This section includes the velocity and temperature profiles taken at X = 63.3 in. (161 cm) and X = 69.3 in. (176 cm). At X = 69.3 in. (176 cm), temperature and velocity profiles are taken, and at X = 63.3 in. (161 cm), only velocity profiles were taken. The lateral average velocity profiles are used as an input data to program SHEAR which calculates the shear stress distribution and mixing length distribution.

<u>Special Nomenclature</u>

DDEL1	uncertainty in δ_1
DDEL2	uncertainty in δ_2
DEL1	δ_1 , displacement thickness
DEL2	δ_2 , momentum deficit thickness
DEND2	uncertainty in Δ_2
DREEN	uncertainty in Re_{Δ_2}
DU	uncertainty in U
END2	Δ_2 , enthalpy thickness
RED2	Re_{δ_2}
REEN	Re_{Δ_2}
TBAR	$(T - T_\infty)/(T_o - T_\infty)$
UBAR	U/U_∞

UINF= 53.8 FT/SEC X= 69.3 INCHES PORT= 1
TINF= 69.0 DEG F PINF= 2120. PSF

VELOCITY PROFILE

Y(INCHES)	U(FT/SEC)	UBAR	DU
0.010	16.00	0.2972	0.28
0.011	16.52	0.3069	0.27
0.012	17.12	0.3180	0.26
0.013	17.79	0.3303	0.25
0.014	18.39	0.3415	0.24
0.015	18.74	0.3481	0.24
0.017	19.71	0.3660	0.23
0.019	20.43	0.3793	0.22
0.022	20.95	0.3892	0.21
0.025	21.49	0.3992	0.21
0.029	22.22	0.4126	0.20
0.033	22.79	0.4233	0.20
0.039	23.40	0.4346	0.19
0.046	24.04	0.4465	0.19
0.054	24.52	0.4553	0.18
0.062	25.05	0.4653	0.18
0.072	25.42	0.4720	0.18
0.087	25.87	0.4806	0.17
0.102	26.35	0.4894	0.17
0.122	26.56	0.4933	0.17
0.147	26.88	0.4993	0.17
0.177	27.17	0.5046	0.16
0.217	27.40	0.5089	0.16
0.267	27.96	0.5192	0.16
0.322	28.71	0.5332	0.16
0.397	29.91	0.5555	0.15
0.472	31.68	0.5883	0.14
0.547	34.11	0.6334	0.13
0.622	36.53	0.6784	0.12
0.697	38.77	0.7200	0.12
0.772	41.03	0.7621	0.11
0.847	43.00	0.7987	0.10
0.922	44.86	0.8331	0.10
0.997	46.68	0.8670	0.10
1.072	48.30	0.8970	0.09
1.147	49.71	0.9233	0.09
1.223	50.97	0.9466	0.09
1.297	52.03	0.9663	0.09
1.372	52.78	0.9803	0.08
1.472	53.43	0.9924	0.08
1.572	53.69	0.9971	0.08
1.672	53.84	1.0000	0.08

TEMPERATURE PROFILE

Y(INCHES)	T(DEG F)	TBAR
0.0215	93.97	0.7229
0.0225	93.65	0.7120
0.0235	93.24	0.6982
0.0245	92.81	0.6834
0.0255	92.49	0.6725
0.0275	91.87	0.6518
0.0295	91.44	0.6370
0.0325	90.74	0.6133
0.0365	90.12	0.5925
0.0415	89.57	0.5737
0.0485	89.02	0.5549
0.0575	88.55	0.5391
0.0685	88.08	0.5232
0.0805	87.79	0.5133
0.0955	87.38	0.4995
0.1155	87.12	0.4905
0.1405	86.77	0.4786
0.1705	86.41	0.4667
0.2105	86.03	0.4539
0.2605	85.42	0.4330
0.3105	84.98	0.4181
0.3705	84.28	0.3943
0.4305	83.49	0.3675
0.4905	82.72	0.3417
0.5505	81.85	0.3119
0.6105	80.96	0.2820
0.6705	80.08	0.2522
0.7305	79.23	0.2233
0.7905	78.35	0.1934
0.8505	77.56	0.1665
0.9105	76.91	0.1445
0.9805	76.14	0.1186
1.0505	75.44	0.0946
1.1205	74.82	0.0737
1.1905	74.26	0.0547
1.2805	73.70	0.0357
1.3805	73.17	0.0177
1.4805	72.87	0.0077
1.5805	72.72	0.0027
1.6805	72.67	0.0007
1.7805	72.65	0.0002
1.8805	72.65	0.0000

DEL1= 0.395IN. DEL2= 0.239IN. H= 1.651 DDEL1=0.003 END2= 0.212IN. REEN= 5664. TO=102.15 F
RED2=6618.4 DDEL2=0.001 DEND2=0.001 DREEN= 36.

UINF= 53.8 FT/SEC   X= 69.3 INCHES   PORT= 2
TINF= 70.7 DEG F   PINF= 2120. PSF

VELOCITY PROFILE

Y(INCHES)	U(FT/SEC)	UBAR	DU
0.010	16.86	0.3135	0.27
0.011	17.06	0.3172	0.26
0.012	17.69	0.3289	0.25
0.013	18.53	0.3444	0.24
0.014	18.85	0.3504	0.24
0.015	19.46	0.3618	0.23
0.017	20.08	0.3733	0.22
0.019	20.67	0.3842	0.22
0.022	21.60	0.4016	0.21
0.025	22.37	0.4159	0.20
0.029	23.08	0.4290	0.19
0.033	23.66	0.4398	0.19
0.039	24.45	0.4546	0.18
0.046	24.98	0.4645	0.18
0.054	25.50	0.4741	0.18
0.062	26.01	0.4836	0.17
0.072	26.44	0.4915	0.17
0.087	26.92	0.5006	0.17
0.102	27.31	0.5078	0.16
0.122	27.84	0.5176	0.16
0.147	28.28	0.5259	0.16
0.177	28.76	0.5348	0.16
0.217	29.07	0.5404	0.15
0.267	29.70	0.5521	0.15
0.322	30.34	0.5641	0.15
0.397	31.55	0.5865	0.14
0.472	33.06	0.6147	0.14
0.547	35.14	0.6533	0.13
0.622	37.09	0.6896	0.12
0.697	39.17	0.7282	0.11
0.772	41.36	0.7689	0.11
0.847	43.02	0.7998	0.10
0.922	44.90	0.8348	0.10
0.997	46.70	0.8681	0.10
1.072	48.15	0.8952	0.09
1.147	49.81	0.9260	0.09
1.222	50.99	0.9480	0.09
1.297	51.99	0.9665	0.09
1.372	52.81	0.9819	0.08
1.472	53.40	0.9928	0.08
1.572	53.71	0.9985	0.08
1.672	53.79	1.0000	0.08

TEMPERATURE PROFILE

Y(INCHES)	T(DEG F)	TBAR
0.0215	92.37	0.7042
0.0225	91.99	0.6913
0.0235	91.49	0.6743
0.0245	91.09	0.6604
0.0255	90.77	0.6494
0.0275	90.21	0.6304
0.0295	89.69	0.6125
0.0325	89.22	0.5965
0.0365	88.64	0.5765
0.0415	88.05	0.5565
0.0485	87.47	0.5365
0.0575	87.06	0.5225
0.0685	86.62	0.5075
0.0805	86.27	0.4955
0.0955	85.86	0.4815
0.1155	85.54	0.4705
0.1405	85.24	0.4605
0.1705	84.81	0.4455
0.2105	84.37	0.4305
0.2605	83.84	0.4124
0.3105	83.28	0.3934
0.3705	82.67	0.3723
0.4305	82.02	0.3503
0.4905	81.29	0.3252
0.5505	80.47	0.2971
0.6105	79.61	0.2679
0.6705	78.85	0.2418
0.7305	78.09	0.2157
0.7905	77.32	0.1895
0.8505	76.64	0.1664
0.9105	76.06	0.1462
0.9805	75.29	0.1200
1.0505	74.49	0.0928
1.1205	73.85	0.0706
1.1905	73.31	0.0525
1.2805	72.70	0.0313
1.3805	72.22	0.0151
1.4805	71.96	0.0061
1.5805	71.84	0.0020
1.6805	71.81	0.0010
1.7805	71.78	0.0000

DEL1= 0.377IN.   DEL2= 0.236IN.   H= 1.596   DDEL1=0.003   END2= 0.210IN.   REEN= 5659.   TO=101.02 F
RED2=6492.5   DDEL2=0.001   DEND2=0.001   DREEN= 36.

UINF= 53.8 FT/SEC   X= 69.3 INCHES   PORT= 3
TINF= 72.0 DEG F   PINF= 2120. PSF

VELOCITY PROFILE

Y(INCHES)	U(FT/SEC)	UBAR	DU
0.010	18.27	0.3397	0.25
0.011	18.77	0.3491	0.24
0.012	19.14	0.3560	0.23
0.013	19.85	0.3692	0.23
0.014	20.43	0.3800	0.22
0.015	20.94	0.3895	0.21
0.017	21.87	0.4067	0.21
0.019	22.57	0.4197	0.20
0.022	23.35	0.4343	0.19
0.025	24.19	0.4498	0.19
0.029	24.95	0.4640	0.18
0.033	25.52	0.4747	0.18
0.039	26.17	0.4867	0.17
0.046	26.82	0.4989	0.17
0.054	27.49	0.5112	0.16
0.062	27.83	0.5176	0.16
0.072	28.45	0.5290	0.16
0.087	29.02	0.5397	0.15
0.102	29.46	0.5479	0.15
0.122	30.16	0.5609	0.15
0.147	30.86	0.5739	0.15
0.177	31.52	0.5862	0.14
0.217	32.19	0.5986	0.14
0.267	33.20	0.6174	0.14
0.322	34.20	0.6360	0.13
0.397	35.56	0.6614	0.13
0.472	36.86	0.6854	0.12
0.547	38.37	0.7136	0.12
0.622	39.87	0.7416	0.11
0.697	41.49	0.7715	0.11
0.772	43.00	0.7997	0.10
0.847	44.66	0.8306	0.10
0.922	46.10	0.8574	0.10
0.997	47.63	0.8858	0.09
1.072	49.00	0.9112	0.09
1.147	50.24	0.9343	0.09
1.222	51.37	0.9553	0.09
1.297	52.27	0.9721	0.09
1.372	52.89	0.9836	0.09
1.472	53.42	0.9936	0.08
1.572	53.61	0.9971	0.08
1.672	53.77	1.0000	0.08

TEMPERATURE PROFILE

Y(INCHES)	T(DEG F)	TBAR
0.0215	92.02	0.6812
0.0225	91.41	0.6603
1.3195	90.88	0.6424
0.0245	90.47	0.6285
0.0255	90.27	0.6215
0.0275	89.60	0.5986
0.0295	89.13	0.5826
0.0325	88.64	0.5657
0.0365	87.96	0.5428
0.0415	87.47	0.5258
0.0485	86.85	0.5048
0.0575	86.33	0.4869
0.0685	85.89	0.4719
0.0805	85.54	0.4599
0.0955	85.13	0.4459
0.1155	84.69	0.4309
0.1405	84.34	0.4189
0.1705	83.84	0.4019
0.2105	83.31	0.3839
0.2605	82.64	0.3609
0.3105	82.11	0.3429
0.3705	81.49	0.3219
0.4305	80.76	0.2968
0.4905	80.11	0.2748
0.5505	79.44	0.2517
0.6105	78.79	0.2297
0.6705	78.09	0.2056
0.7305	77.47	0.1845
0.7905	76.88	0.1644
0.8505	76.23	0.1423
0.9105	75.64	0.1222
0.9805	75.05	0.1021
1.0505	74.46	0.0820
1.1205	73.90	0.0628
1.1905	73.43	0.0467
1.2805	72.93	0.0296
1.3805	72.49	0.0145
1.4805	72.22	0.0054
1.5805	72.11	0.0014
1.6805	72.08	0.0005
1.7805	72.06	0.0000

DEL1= 0.325IN.   DEL2= 0.219IN.   H= 1.487   DDEL1=0.003
RED2=5983.1   DDEL2=0.001

END2= 0.194IN.   REEN= 5216.   TO=101.36 F
DEND2=0.011   DREEN= 307.

UINF= 53.7 FT/SEC X= 69.3 INCHES PORT= 4
TINF= 72.1 DEG F PINF= 2120. PSF

VELOCITY PROFILE

Y(INCHES)	U(FT/SEC)	UBAR	DU
0.010	17.78	0.3309	0.25
0.011	18.40	0.3425	0.24
0.012	19.03	0.3543	0.24
0.013	19.67	0.3661	0.23
0.014	20.24	0.3768	0.22
0.015	20.82	0.3875	0.22
0.017	21.75	0.4048	0.21
0.019	22.40	0.4169	0.20
0.022	23.38	0.4352	0.19
0.025	24.12	0.4489	0.19
0.029	24.94	0.4641	0.18
0.033	25.58	0.4760	0.18
0.039	26.38	0.4910	0.17
0.046	26.96	0.5017	0.17
0.054	27.42	0.5103	0.16
0.062	27.99	0.5210	0.16
0.072	28.60	0.5322	0.16
0.087	29.25	0.5445	0.15
0.102	29.82	0.5550	0.15
0.122	30.48	0.5672	0.15
0.147	31.37	0.5839	0.14
0.177	32.09	0.5972	0.14
0.217	32.99	0.6140	0.14
0.267	33.93	0.6314	0.13
0.322	35.03	0.6520	0.13
0.397	36.35	0.6765	0.12
0.472	37.76	0.7027	0.12
0.547	39.27	0.7310	0.11
0.622	40.73	0.7581	0.11
0.697	42.31	0.7875	0.11
0.772	43.73	0.8139	0.10
0.847	45.23	0.8419	0.10
0.922	46.58	0.8670	0.10
0.997	48.02	0.8938	0.09
1.072	49.29	0.9173	0.09
1.147	50.43	0.9385	0.09
1.222	51.39	0.9564	0.09
1.297	52.28	0.9730	0.09
1.372	52.84	0.9835	0.09
1.472	53.32	0.9924	0.08
1.572	53.56	0.9969	0.08
1.672	53.65	0.9986	0.08
1.772	53.73	1.0000	0.08

DEL1= 0.312IN. DEL2= 0.213IN. H= 1.467 DDEL1=0.003
RED2=5805.2 DDEL2=0.001

TEMPERATURE PROFILE

Y(INCHES)	T(DEG F)	TBAR
0.0215	92.86	0.6780
0.0225	92.46	0.6645
0.0235	91.99	0.6490
0.0245	91.61	0.6364
0.0255	91.26	0.6248
0.0275	90.65	0.6045
0.0295	90.21	0.5899
0.0325	89.63	0.5705
0.0365	89.02	0.5502
0.0415	88.55	0.5346
0.0485	87.85	0.5114
0.0575	87.35	0.4949
0.0685	86.88	0.4793
0.0805	86.50	0.4667
0.0955	86.18	0.4560
0.1155	85.65	0.4385
0.1405	85.16	0.4220
0.1705	84.66	0.4054
0.2105	84.04	0.3850
0.2605	83.40	0.3636
0.3105	82.70	0.3402
0.3705	82.02	0.3178
0.4305	81.26	0.2925
0.4905	80.55	0.2691
0.5505	79.91	0.2476
0.6105	79.17	0.2232
0.6705	78.50	0.2008
0.7305	77.88	0.1803
0.7905	77.26	0.1597
0.8505	76.70	0.1412
0.9105	76.11	0.1216
0.9805	75.53	0.1021
1.0505	74.91	0.0815
1.1205	74.38	0.0639
1.1905	73.88	0.0472
1.2805	73.40	0.0316
1.3805	72.96	0.0169
1.4805	72.70	0.0080
1.5805	72.56	0.0035
1.6805	72.49	0.0012
1.7805	72.47	0.0005
1.8805	72.45	0.0000

END2= 0.204IN. REEN= 5442. TO=102.56 F
DEND2=0.001 DREEN= 36.

UINF= 53.7 FT/SEC X= 69.3 INCHES PORT= 5
TINF= 72.2 DEG F PINF= 2120. PSF

VELOCITY PROFILE

Y(INCHES)	U(FT/SEC)	UBAR	DU
0.010	17.17	0.3198	0.26
0.011	17.42	0.3244	0.26
0.012	17.94	0.3340	0.25
0.013	18.59	0.3460	0.24
0.014	19.01	0.3540	0.24
0.015	19.71	0.3670	0.23
0.017	20.49	0.3815	0.22
0.019	21.08	0.3926	0.21
0.022	21.96	0.4089	0.20
0.025	22.69	0.4225	0.20
0.029	23.25	0.4329	0.19
0.033	23.82	0.4434	0.19
0.039	24.40	0.4542	0.18
0.046	24.91	0.4638	0.18
0.054	25.15	0.4683	0.18
0.062	25.48	0.4744	0.18
0.072	25.58	0.4764	0.18
0.087	25.87	0.4816	0.17
0.102	26.06	0.4852	0.17
0.122	26.01	0.4844	0.17
0.147	25.95	0.4831	0.17
0.177	26.33	0.4903	0.17
0.217	27.26	0.5076	0.17
0.267	28.67	0.5338	0.16
0.322	30.68	0.5712	0.15
0.397	33.09	0.6160	0.14
0.472	35.01	0.6518	0.13
0.547	36.67	0.6827	0.12
0.622	38.55	0.7178	0.12
0.697	40.25	0.7495	0.11
0.772	42.14	0.7847	0.11
0.847	43.82	0.8158	0.10
0.922	45.40	0.8453	0.10
0.997	47.03	0.8757	0.10
1.072	43.56	0.9042	0.09
1.147	49.73	0.9258	0.09
1.222	50.88	0.9474	0.09
1.297	51.73	0.9632	0.09
1.372	52.52	0.9779	0.09
1.472	53.24	0.9913	0.08
1.572	53.54	0.9969	0.08
1.672	53.71	1.0000	0.08

TEMPERATURE PROFILE

Y(INCHES)	T(DEG F)	TBAR
0.0215	94.76	0.7141
0.0225	94.38	0.7014
0.0235	93.91	0.6856
0.0245	93.68	0.6777
0.0255	93.36	0.6669
0.0275	92.89	0.6511
0.0295	92.54	0.6393
0.0325	92.17	0.6265
0.0365	91.79	0.6137
0.0415	91.47	0.6028
0.0485	91.20	0.5940
0.0575	90.94	0.5851
0.0685	90.68	0.5762
0.0805	90.39	0.5663
0.0955	90.27	0.5624
0.1155	90.04	0.5545
0.1405	89.69	0.5427
0.1705	89.31	0.5298
0.2105	88.72	0.5101
0.2605	87.93	0.4834
0.3105	86.77	0.4438
0.3705	85.39	0.3973
0.4305	84.16	0.3557
0.4905	83.05	0.3181
0.5505	82.23	0.2903
0.6105	81.41	0.2625
0.6705	80.64	0.2367
0.7305	79.88	0.2109
0.7905	79.17	0.1870
0.8505	78.47	0.1632
0.9105	77.82	0.1413
0.9805	77.09	0.1164
1.0505	76.38	0.0925
1.1205	75.85	0.0746
1.1905	75.32	0.0566
1.2805	74.76	0.0377
1.3805	74.29	0.0217
1.4805	73.93	0.0098
1.5805	73.76	0.0038
1.6805	73.67	0.0007
1.7805	73.65	0.0001
1.8805	73.65	0.0000

DEL1= 0.369IN. DEL2= 0.231IN. H= 1.598 DDEL1=0.003 END2= 0.222IN. REEN= 5912. TO=103.21 F
RED2=6305.0 DDEL2=0.001 DEND2=0.001 DREEN= 38.

UINF= 53.7 FT/SEC X= 69.3 INCHES PORT= 6
TINF= 72.2 DEG F PINF= 2120. PSF

VELOCITY PROFILE

Y(INCHES)	U(FT/SEC)	UBAR	DU
0.010	9.07	0.1687	0.50
0.011	9.42	0.1752	0.48
0.012	10.03	0.1866	0.45
0.013	10.39	0.1934	0.43
0.014	10.50	0.1953	0.43
0.015	11.00	0.2046	0.41
0.017	11.43	0.2127	0.39
0.019	12.13	0.2256	0.37
0.022	12.61	0.2346	0.36
0.025	13.20	0.2455	0.34
0.029	13.87	0.2581	0.32
0.033	14.21	0.2644	0.32
0.039	14.67	0.2730	0.31
0.046	14.94	0.2779	0.30
0.054	15.27	0.2841	0.29
0.062	15.10	0.2809	0.30
0.072	15.03	0.2797	0.30
0.087	14.32	0.2665	0.31
0.102	13.93	0.2592	0.32
0.122	13.12	0.2440	0.34
0.147	12.44	0.2315	0.36
0.177	12.63	0.2350	0.36
0.217	14.02	0.2608	0.32
0.267	17.65	0.3284	0.25
0.322	22.46	0.4179	0.20
0.388	28.51	0.5304	0.16
0.472	32.18	0.5986	0.14
0.547	34.33	0.6388	0.13
0.622	36.33	0.6759	0.12
0.697	38.18	0.7103	0.12
0.772	40.06	0.7453	0.11
0.847	42.18	0.7847	0.11
0.922	44.12	0.8209	0.10
0.997	45.93	0.8546	0.10
1.072	47.45	0.8828	0.09
1.147	48.90	0.9099	0.09
1.222	50.10	0.9321	0.09
1.297	51.28	0.9540	0.09
1.372	52.23	0.9717	0.09
1.472	53.02	0.9864	0.08
1.572	53.49	0.9952	0.08
1.672	53.63	0.9978	0.08
1.772	53.70	0.9991	0.08
1.872	53.75	1.0000	0.08

DEL1= 0.477IN. DEL2= 0.231IN. H= 2.060 DDEL1=0.004
RED2=6319.2 DDEL2=0.001

TEMPERATURE PROFILE

Y(INCHES)	T(DEG F)	TBAR
0.0215	96.44	0.7688
0.0225	96.12	0.7580
0.0235	95.92	0.7511
0.0245	95.66	0.7423
0.0255	95.51	0.7373
0.0275	95.22	0.7275
0.0295	95.05	0.7216
0.0325	94.84	0.7147
0.0365	94.64	0.7078
0.0415	94.49	0.7029
0.0485	94.35	0.6980
0.0575	94.35	0.6980
0.0685	94.29	0.6960
0.0805	94.29	0.6960
0.0955	94.20	0.6930
0.1155	94.15	0.6911
0.1405	93.97	0.6852
0.1705	93.48	0.6684
0.2105	92.89	0.6487
0.2605	91.76	0.6103
0.3105	90.50	0.5679
0.3705	88.37	0.4958
0.4305	86.21	0.4226
0.4905	84.48	0.3641
0.5505	83.19	0.3205
0.6105	82.23	0.2878
0.6705	81.38	0.2590
0.7305	80.50	0.2292
0.7905	79.76	0.2044
0.8505	78.97	0.1775
0.9105	78.29	0.1546
0.9805	77.53	0.1288
1.0505	76.73	0.1019
1.1205	76.23	0.0849
1.1905	75.55	0.0620
1.2805	75.00	0.0431
1.3805	74.41	0.0231
1.4805	74.05	0.0112
1.5805	73.85	0.0042
1.6805	73.76	0.0012
1.7805	73.74	0.0005
1.8805	73.72	0.0000

END2= 0.197IN. REEN= 5247. TO=103.27 F
DEND2=0.001 DREEN= 28.

UINF= 53.9 FT/SEC X= 69.5 INCHES PORT= 7
TINF= 71.4 DEG F PINF= 2130. PSF

VELOCITY PROFILE

Y(INCHES)	U(FT/SEC)	UBAR	DU
0.010	15.20	0.2820	0.29
0.011	15.44	0.2864	0.29
0.012	15.98	0.2964	0.28
0.013	16.55	0.3071	0.27
0.014	17.12	0.3176	0.26
0.015	17.64	0.3273	0.25
0.017	18.57	0.3446	0.24
0.019	19.02	0.3529	0.23
0.022	19.76	0.3667	0.23
0.025	20.48	0.3800	0.22
0.029	21.17	0.3929	0.21
0.033	21.54	0.3996	0.21
0.039	21.98	0.4078	0.20
0.046	22.54	0.4182	0.20
0.054	22.94	0.4255	0.19
0.062	23.12	0.4289	0.19
0.072	22.98	0.4263	0.19
0.087	23.04	0.4275	0.19
0.102	22.96	0.4261	0.19
0.122	22.77	0.4224	0.20
0.147	22.81	0.4233	0.20
0.177	22.92	0.4252	0.19
0.217	23.85	0.4425	0.19
0.267	25.70	0.4768	0.17
0.322	28.07	0.5207	0.16
0.397	31.08	0.5766	0.14
0.472	33.39	0.6195	0.13
0.547	34.97	0.6488	0.13
0.622	36.80	0.6828	0.12
0.697	38.52	0.7146	0.12
0.772	40.65	0.7542	0.11
0.847	42.40	0.7866	0.11
0.922	44.33	0.8224	0.10
0.997	45.94	0.8524	0.10
1.072	47.45	0.8802	0.09
1.147	48.91	0.9074	0.09
1.222	50.13	C.9301	0.09
1.297	51.45	0.9545	0.09
1.372	52.24	0.9692	0.09
1.472	53.07	0.9845	0.08
1.572	53.56	0.9937	0.08
1.672	53.77	0.9976	0.08
1.772	53.90	1.0000	0.08

TEMPERATURE PROFILE

Y(INCHES)	T(DEG F)	TBAR
0.0215	95.77	0.7467
0.0225	95.54	0.7388
0.0235	95.16	0.7260
0.0245	94.81	0.7142
0.0255	94.58	0.7063
0.0275	94.23	0.6944
0.0295	93.91	0.6836
0.0325	93.85	0.6816
0.0365	93.48	0.6688
0.0415	93.16	0.6579
0.0485	92.86	0.6480
0.0575	92.72	0.6431
0.0685	92.57	0.6382
0.0805	92.40	0.6322
0.0955	92.17	0.6243
0.1155	91.96	0.6174
0.1405	91.99	0.6184
0.1705	91.38	0.5976
0.2105	90.71	0.5749
0.2605	89.74	0.5422
0.3105	88.55	0.5016
0.3705	86.85	0.4441
0.4305	85.30	0.3915
0.4905	84.04	0.3488
0.5505	82.99	0.3130
0.6105	82.17	0.2852
0.6705	81.32	0.2563
0.7305	80.52	0.2295
0.7905	79.85	0.2065
0.8505	79.11	0.1816
0.9105	78.38	0.1567
0.9805	77.59	0.1298
1.0505	76.94	0.1078
1.1205	76.29	0.0859
1.1905	75.73	0.0669
1.2805	75.11	0.0459
1.3805	74.55	0.0269
1.4805	74.14	0.0129
1.5805	73.89	0.0044
1.6805	73.80	0.0012
1.7805	73.76	0.0001
1.8805	73.76	0.0000

DEL1= 0.417IN. DEL2= 0.246IN. H= 1.698 DDEL1=0.003
RED2=6776.2 DDEL2=0.001

END2= 0.229IN. REEN= 6093. TO=103.24 F
DEND2=0.001 DREEN= 37.

UINF= 53.7 FT/SEC X= 69.3 INCHES PORT= 8
TINF= 70.2 DEG F PINF= 2106. PSF

VELOCITY PROFILE

Y(INCHES)	U(FT/SEC)	UBAR	DU
0.010	16.87	0.3140	0.27
0.011	17.90	0.3332	0.25
0.012	18.23	0.3394	0.25
0.013	18.83	0.3506	0.24
0.014	19.65	0.3658	0.23
0.015	19.96	0.3715	0.23
0.017	20.96	0.3901	0.22
0.019	21.53	0.4008	0.21
0.022	22.51	0.4191	0.20
0.025	23.05	0.4291	0.20
0.029	24.02	0.4471	0.19
0.033	24.42	0.4547	0.18
0.039	25.21	0.4693	0.18
0.046	25.67	0.4778	0.18
0.054	26.29	0.4895	0.17
0.062	26.74	0.4979	0.17
0.072	27.10	0.5045	0.17
0.087	27.88	0.5190	0.16
0.102	28.40	0.5288	0.16
0.122	29.07	0.5411	0.16
0.147	29.75	0.5538	0.15
0.177	30.60	0.5696	0.15
0.217	31.32	0.5831	0.14
0.267	32.43	0.6038	0.14
0.322	33.41	0.6220	0.14
0.397	34.70	0.6460	0.13
0.472	35.87	0.6678	0.13
0.547	37.28	0.6940	0.12
0.622	38.86	0.7235	0.12
0.697	40.44	0.7528	0.11
0.772	42.16	0.7849	0.11
0.847	43.50	0.8098	0.10
0.922	44.98	0.8373	0.10
0.997	46.51	0.8658	0.10
1.072	47.98	0.8933	0.09
1.147	49.10	0.9140	0.09
1.222	50.43	0.9388	0.09
1.297	51.36	0.9562	0.09
1.372	52.23	0.9723	0.09
1.472	53.03	0.9872	0.09
1.572	53.53	0.9966	0.08
1.672	53.61	0.9980	0.08
1.772	53.71	0.9999	0.08
1.872	53.72	1.0000	0.08

TEMPERATURE PROFILE

Y(INCHES)	T(DEG F)	TBAR
0.0215	97.40	0.7100
0.0225	96.94	0.6942
0.0235	96.67	0.6853
0.0245	96.24	0.6705
0.0255	95.98	0.6616
0.0275	95.42	0.6429
0.0295	95.10	0.6320
0.0325	94.52	0.6122
0.0365	94.00	0.5945
0.0415	93.53	0.5786
0.0485	93.16	0.5658
0.0575	92.51	0.5440
0.0685	92.02	0.5272
0.0805	91.64	0.5143
0.0955	91.20	0.4995
0.1155	90.82	0.4866
0.1405	90.18	0.4648
0.1705	89.60	0.4450
0.2105	88.99	0.4242
0.2605	88.26	0.3994
0.3105	87.64	0.3785
0.3705	86.74	0.3478
0.4305	85.95	0.3209
0.4905	85.24	0.2971
0.5505	84.57	0.2742
0.6105	83.84	0.2493
0.6705	83.19	0.2274
0.7305	82.49	0.2036
0.7905	82.02	0.1876
0.8505	81.20	0.1597
0.9105	80.67	0.1418
0.9805	79.97	0.1178
1.0505	79.38	0.0979
1.1205	78.79	0.0779
1.1905	78.29	0.0609
1.2605	77.70	0.0410
1.3805	77.23	0.0250
1.4805	76.85	0.0120
1.5805	76.64	0.0050
1.6805	76.56	0.0022
1.7805	76.53	0.0010
1.8805	76.50	0.0000

DEL1= 0.351IN. DEL2= 0.233IN. H= 1.510 DDEL1=0.003 END2= 0.221IN. REEN= 5883. TO=105.94 F
RED2=6347.4 DDEL2=0.001 DEND2=0.001 DREEN= 37.

UINF= 53.8 FT/SEC X= 69.3 INCHES PORT= 9
TINF= 71.0 DEG F PINF= 2130. PSF

VELOCITY PROFILE

Y(INCHES)	U(FT/SEC)	UBAR	DU
0.010	17.76	0.3299	0.25
0.011	18.40	0.3418	0.24
0.012	18.98	0.3525	0.24
0.013	19.61	0.3644	0.23
0.014	20.02	0.3718	0.22
0.015	20.62	0.3831	0.22
0.017	21.49	0.3993	0.21
0.019	22.32	0.4145	0.20
0.022	23.18	0.4305	0.19
0.025	24.09	0.4475	0.19
0.029	24.68	0.4585	0.18
0.033	25.29	0.4699	0.18
0.039	25.91	0.4812	0.17
0.046	26.52	0.4927	0.17
0.054	26.98	0.5011	0.17
0.062	27.58	0.5122	0.16
0.072	27.97	0.5196	0.16
0.087	28.83	0.5355	0.15
0.102	29.27	0.5438	0.15
0.122	30.01	0.5575	0.15
0.147	30.72	0.5706	0.15
0.177	31.39	0.5831	0.14
0.217	32.25	0.5991	0.14
0.267	33.41	0.6207	0.13
0.322	34.41	0.6391	0.13
0.397	35.70	0.6631	0.13
0.472	36.93	0.6860	0.12
0.547	38.43	0.7138	0.12
0.622	39.83	0.7398	0.11
0.697	41.26	0.7664	0.11
0.772	42.65	0.7923	0.10
0.847	44.17	0.8205	0.10
0.922	45.57	0.8464	0.10
0.997	46.90	0.8711	0.10
1.072	48.12	0.8939	0.09
1.147	49.46	0.9187	0.09
1.222	50.42	0.9366	0.09
1.297	51.57	0.9579	0.09
1.372	52.26	0.9707	0.09
1.472	53.03	0.9850	0.08
1.572	53.49	0.9935	0.08
1.672	53.77	0.9988	0.08
1.772	53.84	1.0000	0.08

DEL1= 0.337IN. DEL2= 0.228IN. H= 1.478 DDEL1=0.003
RED2=6288.3 DDEL2=0.001

TEMPERATURE PROFILE

Y(INCHES)	T(DEG F)	TBAR
0.0215	97.02	0.7007
0.0225	96.53	0.6840
0.0235	96.09	0.6693
0.0245	95.72	0.6565
0.0255	95.31	0.6427
0.0275	94.81	0.6260
0.0295	94.23	0.6063
0.0325	93.65	0.5866
0.0365	93.04	0.5660
0.0415	92.46	0.5463
0.0485	91.87	0.5265
0.0575	91.32	0.5078
0.0685	90.85	0.4920
0.0805	90.42	0.4772
0.0955	90.07	0.4654
0.1155	89.72	0.4536
0.1405	89.10	0.4328
0.1705	88.69	0.4190
0.2105	88.02	0.3963
0.2605	87.38	0.3745
0.3105	86.82	0.3557
0.3705	86.09	0.3310
0.4305	85.48	0.3102
0.4905	84.78	0.2865
0.5505	84.13	0.2647
0.6105	83.46	0.2419
0.6705	82.84	0.2211
0.7305	82.17	0.1983
0.7905	81.55	0.1774
0.8505	80.96	0.1576
0.9105	80.35	0.1367
0.9805	79.73	0.1159
1.0505	79.11	0.0950
1.1205	78.59	0.0771
1.1905	78.14	0.0622
1.2805	77.53	0.0413
1.3805	77.03	0.0244
1.4805	76.67	0.0124
1.5805	76.47	0.0055
1.6805	76.36	0.0020
1.7805	76.31	0.0002
1.8805	76.31	0.0000

END2= 0.216IN. REEN= 5750. TO=105.87 F
DEND2=0.001 DREEN= 37.

UINF= 53.9 FT/SEC X= 69.3 INCHES PORT= 10
TINF= 72.0 DEG F PINF= 2130. PSF

VELOCITY PROFILE

Y(INCHES)	U(FT/SEC)	UBAR	DU
0.010	17.40	0.3230	0.26
0.011	17.87	0.3317	0.25
0.012	18.42	0.3418	0.24
0.013	19.04	0.3534	0.23
0.014	19.58	0.3634	0.23
0.015	20.01	0.3714	0.22
0.017	20.82	0.3865	0.21
0.019	21.49	0.3988	0.21
0.022	22.26	0.4132	0.20
0.025	23.00	0.4269	0.19
0.029	23.83	0.4423	0.19
0.033	24.38	0.4524	0.18
0.039	24.96	0.4633	0.18
0.046	25.48	0.4729	0.18
0.054	26.19	0.4861	0.17
0.062	26.60	0.4937	0.17
0.072	26.87	0.4987	0.17
0.087	27.50	0.5104	0.16
0.102	27.91	0.5180	0.16
0.122	28.49	0.5287	0.16
0.147	29.04	0.5390	0.15
0.177	29.45	0.5465	0.15
0.217	29.91	0.5551	0.15
0.267	30.38	0.5638	0.15
0.322	31.43	0.5832	0.14
0.397	32.42	0.6017	0.14
0.472	34.02	0.6314	0.13
0.547	35.77	0.6639	0.13
0.622	37.43	0.6947	0.12
0.697	39.29	0.7292	0.11
0.772	40.94	0.7599	0.11
0.847	42.51	0.7889	0.11
0.922	44.26	0.8213	0.10
0.997	45.71	0.8482	0.10
1.072	47.20	0.8759	0.09
1.147	48.68	0.9034	0.09
1.222	49.99	0.9278	0.09
1.297	51.10	0.9483	0.09
1.372	51.95	0.9640	0.09
1.472	52.94	0.9825	0.08
1.572	53.53	0.9934	0.08
1.672	53.78	0.9981	0.08
1.772	53.88	1.0000	0.08

TEMPERATURE PROFILE

Y(INCHES)	T(DEG F)	TBAR
0.0215	96.79	0.6996
0.0225	96.30	0.6828
0.0235	95.92	0.6701
0.0245	95.57	0.6583
0.0255	95.19	0.6455
0.0275	94.67	0.6277
0.0295	94.17	0.6110
0.0325	93.62	0.5923
0.0365	93.10	0.5745
0.0415	92.60	0.5578
0.0485	91.99	0.5371
0.0575	91.47	0.5193
0.0685	91.03	0.5045
0.0805	90.77	0.4956
0.0955	90.45	0.4848
0.1155	90.07	0.4719
0.1405	89.60	0.4561
0.1705	89.25	0.4443
0.2105	88.96	0.4344
0.2605	88.29	0.4117
0.3105	87.76	0.3939
0.3705	87.15	0.3731
0.4305	86.36	0.3464
0.4905	85.71	0.3246
0.5505	84.86	0.2958
0.6105	84.10	0.2701
0.6705	83.34	0.2443
0.7305	82.64	0.2205
0.7905	81.87	0.1947
0.8505	81.23	0.1728
0.9105	80.58	0.1510
0.9805	79.88	0.1271
1.0505	79.23	0.1052
1.1205	78.59	0.0833
1.1905	78.12	0.0674
1.2805	77.47	0.0455
1.3805	76.91	0.0266
1.4805	76.53	0.0137
1.5805	76.29	0.0057
1.6805	76.18	0.0020
1.7805	76.14	0.0005
1.8805	76.12	0.0000

DEL1= 0.382IN. DEL2= 0.246IN. H= 1.554 DDEL1=0.003 END2= 0.221IN. REEN= 5889. TO=105.67 F
RED2=6771.3 DDEL2=0.001 DEND2=0.001 DREEN= 36.

UINF= 53.8 FT/SEC X= 69.5 INCHES PORT= 11
TINF= 72.0 DEG F PINF= 2130. PSF

VELOCITY PROFILE

Y(INCHES)	U(FT/SEC)	UBAR	DU
0.010	15.60	0.2898	0.29
0.011	15.97	0.2968	0.28
0.012	16.56	0.3077	0.27
0.013	17.27	0.3209	0.26
0.014	17.46	0.3244	0.26
0.015	17.90	0.3325	0.25
0.017	18.91	0.3513	0.24
0.019	19.55	0.3632	0.23
0.022	20.23	0.3759	0.22
0.025	20.95	0.3893	0.21
0.029	21.64	0.4020	0.21
0.033	22.24	0.4131	0.20
0.039	22.78	0.4231	0.20
0.046	23.42	0.4351	0.19
0.054	23.81	0.4423	0.19
0.062	24.20	0.4495	0.18
0.072	24.64	0.4577	0.18
0.087	25.27	0.4695	0.18
0.102	25.69	0.4772	0.17
0.122	25.94	0.4820	0.17
0.147	26.34	0.4894	0.17
0.177	26.58	0.4938	0.17
0.217	26.60	0.4942	0.17
0.267	27.10	0.5035	0.17
0.322	27.72	0.5149	0.16
0.397	28.98	0.5383	0.15
0.472	30.67	0.5697	0.15
0.547	32.61	0.6059	0.14
0.622	34.74	0.6453	0.13
0.697	37.03	0.6880	0.12
0.772	39.25	0.7291	0.11
0.847	41.15	0.7645	0.11
0.922	42.88	0.7967	0.10
0.997	44.65	0.8294	0.10
1.072	46.38	0.8617	0.10
1.147	47.96	0.8909	0.09
1.222	49.27	0.9153	0.09
1.297	50.53	0.9388	0.09
1.372	51.59	0.9585	0.09
1.472	52.66	0.9782	0.08
1.572	53.30	0.9902	0.08
1.672	53.67	0.9971	0.08
1.772	53.79	0.9993	0.08
1.872	53.83	1.0000	0.08

TEMPERATURE PROFILE

Y(INCHES)	T(DEG F)	TBAR
0.0215	97.43	0.7255
0.0225	97.14	0.7155
0.0235	96.65	0.6986
0.0245	96.38	0.6896
0.0255	96.06	0.6786
0.0275	95.57	0.6617
0.0295	95.10	0.6457
0.0325	94.49	0.6247
0.0365	94.00	0.6078
0.0415	93.36	0.5858
0.0485	92.84	0.5678
0.0575	92.40	0.5528
0.0685	91.93	0.5368
0.0805	91.61	0.5258
0.0955	91.32	0.5158
0.1155	91.00	0.5048
0.1405	90.65	0.4928
0.1705	90.33	0.4818
0.2105	89.98	0.4698
0.2605	89.45	0.4517
0.3105	88.90	0.4327
0.3705	98.29	0.4116
0.4305	87.61	0.3886
0.4905	86.85	0.3625
0.5505	85.95	0.3314
0.6105	85.04	0.3002
0.6705	84.22	0.2721
0.7305	83.43	0.2450
0.7905	82.61	0.2168
0.8505	81.62	0.1896
0.9105	81.11	0.1654
0.9805	80.41	0.1413
1.0505	79.64	0.1151
1.1205	78.97	0.0919
1.1905	78.38	0.0717
1.2805	77.76	0.0505
1.3805	77.17	0.0303
1.4805	76.76	0.0162
1.5805	76.50	0.0071
1.6805	76.35	0.0020
1.7805	76.30	0.0002
1.8805	76.29	0.0000

DEL1= 0.434IN. DEL2= 0.260IN. H= 1.667 DDEL1=0.003
RED2=7159.6 DDEL2=0.001

END2= 0.224IN. REEN= 5925. TO=105.43 F
DENO2=0.001 DREEN= 35.

UINF= 53.9 FT/SEC   X= 63.3 INCHES   PORT= 1
TINF= 70.6 DEG F   PINF= 2127. PSF

Y(INCHES)	U(FT/SEC)	UBAR	DU
0.010	10.08	0.1871	0.44
0.011	10.33	0.1918	0.43
0.012	10.84	0.2012	0.41
0.013	11.25	0.2088	0.40
0.014	11.72	0.2175	0.38
0.015	12.03	0.2234	0.37
0.017	12.57	0.2335	0.36
0.019	13.06	0.2425	0.34
0.022	13.74	0.2551	0.33
0.025	14.07	0.2613	0.32
0.029	14.57	0.2706	0.31
0.033	15.13	0.2809	0.30
0.039	15.56	0.2888	0.29
0.046	15.94	0.2960	0.28
0.054	16.11	0.2990	0.28
0.062	16.17	0.3003	0.28
0.072	16.14	0.2996	0.28
0.087	15.61	0.2898	0.29
0.102	15.01	0.2787	0.30
0.122	14.27	0.2649	0.31
0.147	14.18	0.2633	0.31
0.177	14.06	0.2611	0.32
0.217	16.02	0.2975	0.28
0.267	19.97	0.3709	0.22
0.322	25.19	0.4677	0.18
0.397	31.68	0.5883	0.14
0.472	35.27	0.6549	0.13
0.547	37.71	0.7002	0.12
0.622	40.09	0.7444	0.11
0.697	42.44	0.7880	0.11
0.772	44.79	0.8316	0.10
0.847	46.95	0.8716	0.10
0.922	48.94	0.9087	0.09
0.997	50.42	0.9361	0.09
1.072	51.62	0.9585	0.09
1.147	52.59	0.9765	0.08
1.222	53.24	0.9885	0.08
1.297	53.60	0.9952	0.08
1.372	53.80	0.9990	0.08
1.472	53.81	0.9991	0.08
1.572	53.87	1.0002	0.08
1.672	53.86	1.0000	0.08

DEL1= 0.394IN.   DEL2= 0.189IN.   H= 2.084   DDEL1=0.004
DDEL2=0.001   RED2=5217.8

UINF= 53.9 FT/SEC   X= 63.3 INCHES   PORT= 2
TINF= 71.0 DEG F   PINF= 2127. PSF

Y(INCHES)	U(FT/SEC)	UBAR	DU
0.010	17.15	0.3181	0.26
0.011	17.57	0.3259	0.25
0.012	18.45	0.3423	0.24
0.013	18.96	0.3518	0.24
0.014	19.76	0.3666	0.23
0.015	20.01	0.3712	0.22
0.017	20.74	0.3848	0.22
0.019	21.38	0.3966	0.21
0.022	22.15	0.4109	0.20
0.025	22.61	0.4194	0.20
0.029	23.23	0.4310	0.19
0.033	23.81	0.4417	0.19
0.039	24.47	0.4539	0.18
0.046	24.70	0.4581	0.18
0.054	25.09	0.4655	0.18
0.062	25.40	0.4713	0.18
0.072	25.46	0.4723	0.18
0.087	25.72	0.4771	0.17
0.102	25.76	0.4779	0.17
0.122	25.72	0.4771	0.17
0.147	25.79	0.4784	0.17
0.177	26.45	0.4906	0.17
0.217	27.46	0.5095	0.16
0.267	29.41	0.5455	0.15
0.322	31.95	0.5927	0.14
0.397	34.58	0.6414	0.13
0.472	36.77	0.6821	0.12
0.547	38.83	0.7202	0.12
0.622	41.03	0.7611	0.11
0.697	43.10	0.7995	0.10
0.772	45.35	0.8412	0.10
0.847	47.34	0.8782	0.09
0.922	49.08	0.9104	0.09
0.997	50.59	0.9384	0.09
1.072	51.80	0.9609	0.09
1.147	52.71	0.9778	0.08
1.222	53.18	0.9866	0.08
1.297	53.58	0.9940	0.08
1.372	53.79	0.9978	0.08
1.472	53.83	0.9985	0.08
1.572	53.90	0.9999	0.08
1.672	53.91	1.0000	0.08

DEL1= 0.319IN.   DEL2= 0.196IN.   H= 1.624   DDEL1=0.003
RED2=5420.8   DDEL2=0.001

UINF= 53.8 FT/SEC X= 63.3 INCHES PORT= 3
TINF= 71.6 DEG F PINF= 2127. PSF

Y(INCHES)	U(FT/SEC)	UBAR	DU
0.010	18.10	0.3365	0.25
0.011	18.77	0.3490	0.24
0.012	19.37	0.3600	0.23
0.013	20.20	0.3756	0.22
0.014	20.67	0.3842	0.22
0.015	21.26	0.3953	0.21
0.017	22.05	0.4099	0.20
0.019	22.85	0.4249	0.20
0.022	23.68	0.4403	0.19
0.025	24.46	0.4548	0.18
0.029	25.30	0.4703	0.13
0.033	25.93	0.4820	0.17
0.039	26.60	0.4946	0.17
0.046	27.20	0.5059	0.16
0.054	27.82	0.5173	0.16
0.062	28.50	0.5299	0.16
0.072	28.91	0.5374	0.15
0.087	29.68	0.5517	0.15
0.102	30.31	0.5636	0.15
0.122	31.17	0.5794	0.14
0.147	32.10	0.5968	0.14
0.177	33.00	0.6134	0.14
0.217	34.22	0.6361	0.13
0.267	35.40	0.6581	0.13
0.322	36.70	0.6824	0.12
0.397	38.41	0.7141	0.12
0.472	40.18	0.7470	0.11
0.547	41.94	0.7798	0.11
0.622	43.63	0.8112	0.10
0.697	45.46	0.8451	0.10
0.772	47.09	0.8755	0.10
0.847	48.52	0.9020	0.09
0.922	49.89	0.9275	0.09
0.997	51.10	0.9500	0.09
1.072	52.09	0.9685	0.09
1.147	52.84	0.9824	0.08
1.222	53.34	0.9916	0.08
1.297	53.58	0.9962	0.08
1.372	53.74	0.9991	0.08
1.472	53.78	0.9999	0.08
1.572	53.75	0.9993	0.08
1.672	53.79	1.0000	0.08

DEL1= 0.256IN. DEL2= 0.175IN. H= 1.463 DDEL1=0.003
RED2=4803.5 DDEL2=0.001

UINF= 53.8 FT/SEC X= 63.3 INCHES PORT= 4
TINF= 71.3 DEG F PINF= 2122. PSF

Y(INCHES)	U(FT/SEC)	UBAR	DU
0.010	19.29	0.3582	0.23
0.011	19.44	0.3611	0.23
0.012	20.30	0.3771	0.22
0.013	21.07	0.3913	0.21
0.014	21.64	0.4018	0.21
0.015	22.22	0.4127	0.20
0.017	23.05	0.4282	0.19
0.019	23.77	0.4414	0.19
0.022	24.78	0.4603	0.18
0.025	25.52	0.4740	0.18
0.029	26.25	0.4876	0.17
0.033	26.91	0.4997	0.17
0.039	27.58	0.5123	0.16
0.046	28.34	0.5263	0.16
0.054	28.87	0.5362	0.16
0.062	29.29	0.5440	0.15
0.072	29.95	0.5563	0.15
0.087	30.67	0.5695	0.15
0.102	31.17	0.5790	0.14
0.122	31.92	0.5928	0.14
0.147	32.72	0.6077	0.14
0.177	33.74	0.6267	0.13
0.217	35.02	0.6504	0.13
0.267	36.44	0.6768	0.12
0.322	37.71	0.7003	0.12
0.397	39.57	0.7349	0.11
0.472	41.14	0.7641	0.11
0.547	42.94	0.7974	0.10
0.622	44.49	0.8262	0.10
0.697	45.99	0.8542	0.10
0.772	47.44	0.8810	0.09
0.847	48.79	0.9063	0.09
0.922	50.00	0.9286	0.09
0.997	51.12	0.9495	0.09
1.072	52.04	0.9665	0.09
1.147	52.68	0.9784	0.09
1.222	53.32	0.9902	0.08
1.297	53.59	0.9952	0.08
1.372	53.75	0.9983	0.08
1.472	53.84	1.0000	0.08
1.572	53.85	1.0002	0.08
1.672	53.84	1.0000	0.08

DEL1= 0.244IN. DEL2= 0.170IN. H= 1.432 DDEL1=0.003
RED2=4675.1 DDEL2=0.001

UINF= 53.9 FT/SEC X= 53.3 INCHES PORT= 5
TINF= 71.0 DEG F PINF= 2122. PSF

Y(INCHES)	U(FT/SEC)	UBAR	DU
0.010	19.00	0.3525	0.24
0.011	19.51	0.3621	0.23
0.012	20.18	0.3744	0.22
0.013	20.93	0.3884	0.21
0.014	21.66	0.4018	0.21
0.015	22.13	0.4106	0.20
0.017	22.88	0.4245	0.20
0.019	23.66	0.4390	0.19
0.022	24.51	0.4549	0.18
0.025	25.01	0.4641	0.18
0.029	25.87	0.4801	0.17
0.033	26.44	0.4907	0.17
0.039	27.10	0.5030	0.17
0.046	27.79	0.5157	0.16
0.054	28.24	0.5240	0.16
0.062	28.75	0.5335	0.16
0.072	29.15	0.5410	0.15
0.087	29.69	0.5508	0.15
0.102	30.12	0.5588	0.15
0.122	30.74	0.5703	0.15
0.147	31.36	0.5818	0.14
0.177	31.80	0.5901	0.14
0.217	32.66	0.6060	0.14
0.267	33.45	0.6206	0.13
0.322	34.64	0.6428	0.13
0.397	36.16	0.6710	0.12
0.472	38.07	0.7064	0.12
0.547	40.03	0.7429	0.11
0.622	42.24	0.7838	0.11
0.697	44.15	0.8193	0.10
0.772	45.79	0.8497	0.10
0.847	47.45	0.8806	0.09
0.922	49.01	0.9095	0.09
0.997	50.27	0.9328	0.09
1.072	51.42	0.9542	0.09
1.147	52.36	0.9715	0.09
1.222	53.01	0.9836	0.08
1.297	53.51	0.9929	0.08
1.372	53.71	0.9967	0.08
1.472	53.85	0.9993	0.08
1.572	53.89	1.0000	0.08

DEL1= 0.285IN. DEL2= 0.191IN. H= 1.489 DDEL1=0.003
RED2=5260.1 DDEL2=0.001

UINF= 53.9 FT/SEC X= 63.3 INCHES PORT= 6
TINF= 71.0 DEG F PINF= 2122. PSF

Y(INCHES)	U(FT/SEC)	UBAR	DU
0.010	17.17	0.3186	0.26
0.011	17.69	0.3281	0.25
0.012	18.40	0.3414	0.24
0.013	19.01	0.3528	0.24
0.014	19.47	0.3612	0.23
0.015	20.01	0.3713	0.22
0.017	20.82	0.3863	0.22
0.019	21.66	0.4019	0.21
0.022	22.22	0.4123	0.20
0.025	22.84	0.4238	0.20
0.029	23.58	0.4376	0.19
0.033	24.19	0.4489	0.19
0.039	24.87	0.4614	0.18
0.046	25.49	0.4729	0.18
0.054	26.02	0.4828	0.17
0.062	26.48	0.4912	0.17
0.072	26.75	0.4964	0.17
0.067	27.33	0.5070	0.16
0.102	27.68	0.5135	0.16
0.122	28.05	0.5204	0.16
0.147	28.39	0.5267	0.16
0.177	28.65	0.5316	0.16
0.217	29.08	0.5396	0.15
0.267	29.79	0.5528	0.15
0.322	30.62	0.5681	0.15
0.397	32.22	0.5978	0.14
0.472	34.51	0.6402	0.13
0.547	37.07	0.6877	0.12
0.622	39.63	0.7354	0.11
0.697	42.20	0.7831	0.11
0.772	44.21	0.8203	0.10
0.847	46.01	0.8538	0.10
0.922	47.82	0.8872	0.09
0.997	49.34	0.9155	0.09
1.072	50.74	0.9415	0.09
1.147	51.92	0.9634	0.09
1.222	52.76	0.9789	0.09
1.297	53.22	0.9874	0.08
1.372	53.60	0.9944	0.08
1.472	53.80	0.9982	0.08
1.572	53.90	1.0001	0.08
1.672	53.90	1.0000	0.08

DEL1= 0.336IN. DEL2= 0.210IN. H= 1.600 DDEL1=0.003
RED2=5779.5 DDEL2=0.001

UINF= 53.8 FT/SEC X= 63.3 INCHES PORT= 7
TINF= 70.7 DEG F PINF= 2122. PSF

Y(INCHES)	U(FT/SEC)	UBAR	DU
0.010	18.47	0.3435	0.24
0.011	18.93	0.3519	0.24
0.012	19.60	0.3645	0.23
0.013	20.09	0.3736	0.22
0.014	20.81	0.3869	0.22
0.015	21.25	0.3950	0.21
0.017	22.08	0.4105	0.20
0.019	22.79	0.4237	0.20
0.022	23.52	0.4373	0.19
0.025	24.21	0.4501	0.19
0.029	24.91	0.4631	0.18
0.033	25.49	0.4739	0.18
0.039	26.25	0.4879	0.17
0.046	26.75	0.4974	0.17
0.054	27.27	0.5070	0.16
0.062	27.71	0.5152	0.16
0.072	28.10	0.5225	0.16
0.087	28.75	0.5344	0.16
0.102	29.21	0.5431	0.15
0.122	29.68	0.5519	0.15
0.147	30.22	0.5619	0.15
0.177	30.80	0.5726	0.15
0.217	31.51	0.5859	0.14
0.267	32.23	0.5992	0.14
0.322	33.05	0.6145	0.14
0.397	34.44	0.6403	0.13
0.472	36.35	0.6757	0.12
0.547	38.45	0.7149	0.12
0.622	40.55	0.7539	0.11
0.697	42.60	0.7920	0.11
0.772	44.52	0.8278	0.10
0.847	46.21	0.8592	0.10
0.922	47.87	0.8900	0.09
0.997	49.37	0.9178	0.09
1.072	50.77	0.9438	0.09
1.147	51.86	0.9641	0.09
1.222	52.73	0.9803	0.09
1.297	53.24	0.9898	0.08
1.372	53.61	0.9966	0.08
1.472	53.76	0.9995	0.08
1.572	53.77	0.9998	0.08
1.672	53.79	1.0000	0.08

DEL1= 0.310IN. DEL2= 0.203IN. H= 1.526 DDEL1=0.003
RED2=5593.0 DDEL2=0.001

UINF= 53.8 FT/SEC X= 63.3 INCHES PORT= 8
TINF= 71.9 DEG F PINF= 2122. PSF

Y(INCHES)	U(FT/SEC)	UBAR	DU
0.010	18.72	0.3476	0.24
0.011	19.46	0.3614	0.23
0.012	20.17	0.3745	0.22
0.013	21.00	0.3899	0.21
0.014	21.51	0.3995	0.21
0.015	22.05	0.4094	0.20
0.017	22.76	0.4226	0.20
0.019	23.40	0.4345	0.19
0.022	24.25	0.4503	0.19
0.025	24.96	0.4636	0.18
0.029	25.80	0.4791	0.17
0.033	26.37	0.4896	0.17
0.039	27.02	0.5018	0.17
0.046	27.59	0.5124	0.16
0.054	28.14	0.5225	0.16
0.062	28.65	0.5320	0.16
0.072	29.16	0.5415	0.15
0.087	29.88	0.5548	0.15
0.102	30.50	0.5664	0.15
0.122	31.13	0.5780	0.14
0.147	32.10	0.5961	0.14
0.177	32.87	0.6104	0.14
0.217	33.99	0.6312	0.13
0.267	35.36	0.6567	0.13
0.322	36.60	0.6797	0.12
0.397	38.25	0.7104	0.12
0.472	39.91	0.7412	0.11
0.547	41.49	0.7704	0.11
0.622	42.95	0.7977	0.10
0.697	44.52	0.8267	0.10
0.772	45.95	0.8533	0.10
0.847	47.27	0.8778	0.10
0.922	48.70	0.9044	0.09
0.997	49.97	0.9281	0.09
1.072	51.06	0.9483	0.09
1.147	51.94	0.9646	0.09
1.222	52.82	0.9808	0.09
1.297	53.23	0.9885	0.08
1.372	53.61	0.9957	0.08
1.472	53.75	0.9981	0.08
1.572	53.80	0.9992	0.08
1.672	53.85	1.0000	0.08

DEL1= 0.271IN. DEL2= 0.187IN. H= 1.447 DDEL1=0.003
RED2=5133.7 DDEL2=0.001

UINF= 53.8 FT/SEC X= 63.3 INCHES PORT= 9
TINF= 72.3 DEG F PINF= 2122. PSF

Y(INCHES)	U(FT/SEC)	UBAR	DU
0.010	17.94	0.3335	0.25
0.011	18.20	0.3384	0.25
0.012	19.49	0.3623	0.23
0.013	20.10	0.3738	0.22
0.014	20.41	0.3794	0.22
0.015	20.97	0.3898	0.21
0.017	21.94	0.4079	0.20
0.019	22.68	0.4217	0.20
0.022	23.54	0.4377	0.19
0.025	24.25	0.4509	0.19
0.029	25.04	0.4656	0.18
0.033	25.83	0.4801	0.17
0.039	26.45	0.4917	0.17
0.046	27.22	0.5061	0.17
0.054	27.82	0.5172	0.16
0.062	28.20	0.5243	0.16
0.072	28.77	0.5350	0.16
0.087	29.70	0.5521	0.15
0.102	30.11	0.5598	0.15
0.122	30.95	0.5754	0.15
0.147	31.88	0.5927	0.14
0.177	32.91	0.6119	0.14
0.217	34.19	0.6356	0.13
0.267	35.39	0.6580	0.13
0.322	36.54	0.6794	0.12
0.397	38.16	0.7094	0.12
0.472	39.88	0.7415	0.11
0.547	41.58	0.7730	0.11
0.622	43.24	0.8039	0.10
0.697	44.83	0.8335	0.10
0.772	46.24	0.8598	0.10
0.847	47.57	0.8845	0.09
0.922	48.95	0.9100	0.09
0.997	50.14	0.9321	0.09
1.072	51.05	0.9492	0.09
1.147	51.89	0.9648	0.09
1.222	52.65	0.9789	0.09
1.297	53.16	0.9884	0.08
1.372	53.55	0.9956	0.08
1.472	53.73	0.9989	0.08
1.572	53.78	0.9999	0.08
1.672	53.79	1.0000	0.08

DEL1= 0.269IN. DEL2= 0.185IN. H= 1.453 DDEL1=0.003
RED2=5061.8 DDEL2=0.001

UINF= 53.9 FT/SEC X= 63.8 INCHES PORT= 10
TINF= 67.8 DEG F PINF= 2120. PSF

Y(INCHES)	U(FT/SEC)	UBAR	DU
0.010	17.48	0.3243	0.26
0.011	18.17	0.3370	0.25
0.012	18.90	0.3506	0.24
0.013	19.37	0.3593	0.23
0.014	19.92	0.3696	0.22
0.015	20.21	0.3749	0.22
0.017	20.92	0.3881	0.21
0.019	21.50	0.3989	0.21
0.022	22.17	0.4113	0.20
0.025	22.80	0.4231	0.20
0.029	23.36	0.4335	0.19
0.033	23.82	0.4420	0.19
0.039	24.37	0.4521	0.18
0.046	24.75	0.4591	0.18
0.054	25.14	0.4664	0.18
0.062	25.44	0.4719	0.18
0.072	25.47	0.4726	0.18
0.087	25.54	0.4739	0.17
0.102	25.57	0.4743	0.17
0.122	25.76	0.4779	0.17
0.147	25.73	0.4774	0.17
0.177	26.12	0.4846	0.17
0.217	27.37	0.5078	0.16
0.267	29.28	0.5433	0.15
0.322	31.57	0.5857	0.14
0.397	34.54	0.6407	0.13
0.472	36.63	0.6795	0.12
0.547	38.62	0.7165	0.12
0.622	40.60	0.7533	0.11
0.697	42.60	0.7903	0.10
0.772	44.58	0.8272	0.10
0.847	46.39	0.8607	0.10
0.922	48.02	0.8909	0.09
0.997	49.52	0.9187	0.09
1.072	50.77	0.9419	0.09
1.147	51.78	0.9606	0.09
1.222	52.52	0.9744	0.08
1.297	53.19	0.9868	0.08
1.372	53.59	0.9943	0.08
1.472	53.83	0.9987	0.08
1.572	53.90	1.0000	0.08
1.672	53.90	1.0000	0.08

DEL1= 0.331IN. DEL2= 0.206IN. H= 1.611 DDEL1=0.003
RED2=5718.4 DDEL2=0.001

UINF= 53.9 FT/SEC X= 63.3 INCHES PORT= 11
TINF= 68.7 DEG F PINF= 2120. PSF

Y(INCHES)	U(FT/SEC)	UBAR	DU
0.010	9.64	0.1787	0.46
0.011	10.12	0.1877	0.44
0.012	10.39	0.1927	0.43
0.013	10.81	0.2005	0.41
0.014	11.40	0.2113	0.39
0.015	11.89	0.2205	0.38
0.017	12.28	0.2277	0.36
0.019	12.63	0.2341	0.35
0.022	13.14	0.2437	0.34
0.025	13.70	0.2540	0.33
0.029	14.29	0.2649	0.31
0.033	14.69	0.2724	0.30
0.039	15.18	0.2815	0.29
0.046	15.53	0.2879	0.29
0.054	15.69	0.2909	0.28
0.062	15.80	0.2930	0.28
0.072	15.67	0.2906	0.28
0.086	15.34	0.2844	0.29
0.102	14.87	0.2757	0.30
0.122	14.04	0.2604	0.32
0.147	13.70	0.2540	0.33
0.177	13.77	0.2554	0.32
0.217	15.40	0.2855	0.29
0.267	18.91	0.3507	0.24
0.322	23.79	0.4411	0.19
0.397	29.95	0.5553	0.15
0.472	33.69	0.6247	0.13
0.547	36.08	0.6691	0.12
0.622	38.30	0.7102	0.12
0.697	40.67	0.7541	0.11
0.772	42.95	0.7964	0.10
0.847	45.13	0.8368	0.10
0.922	47.08	0.8729	0.09
0.997	48.78	0.9045	0.09
1.072	50.29	0.9324	0.09
1.147	51.41	0.9532	0.09
1.222	52.29	0.9695	0.09
1.297	52.97	0.9822	0.08
1.372	53.48	0.9916	0.08
1.472	53.77	0.9970	0.08
1.572	53.93	1.0000	0.08

DEL1= 0.428IN. DEL2= 0.206IN. H= 2.075 DDEL1=0.004
RED2=5718.2 DDEL2=0.001

APPENDIX C

DATA REDUCTION PROGRAMS

(a) Stanton Number Data Reduction Program, STNO

This is the major heat transfer data reduction program

(b) Profile Data Reduction Program, PROF. (not listed)

This program uses a simple trapezoidal rule to calculate the integral parameters. This program calculates the $c_f/2$ using Clauser plot.

(c) Shear stress reduction program, SHEAR

This program calculates the shear stress and mixing length distribution with given velocity profile, $c_f/2$. $Re_{\overline{\delta}_2}$, δ_2 , δ and F . This program essentially uses the method outlined in Simpson [3].

Special Nomenclature for Program SHEAR

B	$F/c_f/2$
DEL	δ , boundary layer thickness
CF2	$c_f/2$
DEL2	δ_2, momentum deficit thickness
DUDY	numerical approximation of dU/dy
D1	Van Driest damping function based on XL1
D2	Van Driest damping function based on XL2
TAUL	laminar shear stress
TAUT	turbulent shear stress
TAU+	$\tau^+ = \tau/\tau_o$
TAULAM+	du^+/dy^+
UB	laterally averaged velocity profile
UYP	$\nu/(U_\infty\ c_f/2)$
XL1	outer layer mixing length assuming augmented mixing length has distribution as $3.32\ (y/\delta)e^{-(y/0.1\delta)}$

XL2	outer layer mixing length assuming augmented mixing length has distributions as $33.2\ (\frac{y}{\delta})^2\ e^{-100(\frac{y}{\delta})^2}$
YL	y/δ
YPL	$y^+ = yU_\tau/\nu$
YPUT	U_τ/ν

NOTE: Flat plate mixing length is curve fitted as

$$0.078\ \tanh(5.25\ y/\delta)$$

```
    $WATFIV
    C
    C      STANTON NUMBER DATA REDUCTION PROGRAM
    C      DISCRETE HOLE RIG  NAS-3-14336
    C      THIS PROGRAM USES THE LINEAR SUPERPOSITION  PRINCIPLE TO
    C      CALCULATE STANTON NUMBERS AND OTHER INTEGRAL PARAMETERS AT THETA=
    C      0. AND 1.
    C
 1         REAL  K(39),S(40)
 2         DIMENSION NRN(4),TO(45),TG(12),Q(12),SAFR(12),ST(36),T2(12)
 3         DIMENSION X(36),REX(36),D2(36),REEN(36),SM(12),F(12),T4(12),CI(12)
 4         DIMENSION VAR(12),TCAST(5),KOMMNT(40),HM(45),QDOT(36),QFLOW(12)
 5         DIMENSION TCAV(12),STNOB(36),STO(36),STCOL(36),STHOT(36),STS(36),
          1STSF(36),STCR(36),STHR(36),STSR(36),SMO(12),FO(12),THO(12),FB(12),
          2BHCOL(12),BHOT(12),REXO(36),RENCOL(36),RENHOT(36),D2COL(36),
          3D2HOT(36),DQDOT(36),DTH(12),DST(36),DREEN(36),DD2(36),DTHO(12)
 6           DIMENSION DSTO(36),ETA(36),XD(36),SF(12),SFO(12),NRNO(4)
 7         DATA X/50.3,52.3,54.3,56.3,58.3,60.3,62.3,64.3,66.3,68.3,
          1        70.3,72.3,73.82,74.85,75.88,76.915,77.95,78.98,80.01,81.04,
          2        82.07,83.1,84.13,85.165,86.2,87.23,88.26,89.29,90.32,91.35,
          3        92.38,93.415,94.45,95.48,96.51,97.54/
    C     FOLLOWING IS THE CONDUCTION LOSS CONSTANTS FOR BLOWING SECTION.
 8           DATA K/  .4762,   .3867,   .3601,   .3558,   .3683,   .3712,
          1           .3559,   .4184,   .3774,   .3861,   .3584,   .4919,
    CCC        FOLLOWING IS THE HEAT FLUX METER CALIBRATION CONSTANTS  NO 13-36.
          2           36.05,  34.78,  35.05,  33.81,  33.32,  32.33,
          3           25.02,  23.00,  28.61,  31.46,  29.31,  31.79,
          4           33.71,  34.63,  31.51,  29.49,  24.67,  30.98,
          5           32.46,  37.82,  31.97,  24.10,  36.16,  34.09,
    CCC      HEAT FLUX METER CALIBRATION CONSTANTS NO 106-108
          6           32.53,  34.18,  38.07/
    CCC   FOLLOWING IS THE AXIAL CONDUCTION LOSS CONSTANTS
 9         DATA  S/  .9928,  11*.80,  .9078,  4.712,  4.962,  5.014,  4.965,
          1           5.118,  5.183,  4.777,  4.494,  5.480,  5.020,  5.597,
          2           5.254,  5.169,  5.254,  5.356,  5.211,  5.370,  5.583,
          3           4.990,  5.435,  4.872,  5.557,  5.545,  5.585,
    CCC      NO  106-108
          4           4.983,  5.056,  4.989/
    C
    C     DQ:  ENERGY BALANCE ERROR, WATT
10         DQ=0.3
    C      DP : UNCERTAINTY IN  MANOMETER PRESSURE   , IN H2O
11         DP=0.005
    C     ASSUME ALL PROPERTIES CORRECT, AFTER TEMPERATURE-HUMIDITY CORRECTION.
    C     DT: UNCERTAINTY IN TEMPERATURE, F
12         DT=0.25
    C      DSAFR:  UNCERTAINTY IN SECONDARY FLOW RATE,RATIO
13         DSAFR=0.03
    C    DHM:  UNCEPTAINTY IN HM(I),MV
14         DHM=0.025
    C     DK:  UNCERTAINTY IN HEAT FLUX METER CALIBRATION,RATIO
15         DK=0.01
    C     DS:  UNCERTAINTY IN CONDUCTION CORRECTION ON HEAT FLUX METER,RATIO
16         DS=0.05
    C    DXVO: UNCERTAINTY IN XVO,IN
    C
    C $$$ READ RUN NUMBER, COL. 1-8
    C      TERMINATE PROGRAM WITH 9999999999 CARD, COL. 1-10
    C**   KT=0  IT STORES THE HEAT TRANSFER PARAMETERS WHICH CAN  BE USED
    C**         FOR KT=1. NO-BLOWING RUN OR COLD RUN.
```

```
C**  KT=1  IT CALCULATES ST AND OTHER INTEGRAL PARAMETERS AT THETA=0.&1.
C**        USING THE LINEAR SUPERPOSITION PRINCIPLE. HOT RUNS.
C**  **** ARRANGE DATA SUCH THAT HOT RUN FOLLOWS COLD RUN AT SAME VALUE OF M.
C**  KT=2  IT CALCULATES THE ADIABATIC WALL EFFECTIVENESS.
C**  KM=0  P/D RATIO OF 5
C**  KM=1  P/D RATIO OF 10
C**  L=0  NO-BLOWING CASE HAS A CONSTANT WALL TEMPERATURE WITHOUT ANY STEP.
C**  L=1  NO-BLOWING CASE HAS A STEP T-WALL AT THE 1ST PLATE. INTERNALLY SET
C**       IF INPUT END2 IS ZERO.
C**  L=2  NO BLOWING HAS A STEP T-WALL AT SOME PLACE IN THE FORE PLATE.
C**       ACTUAL ST TAKEN ON THE RIG IS USED FOR THE NO-BLOWING ST  #.
C**       SPECIFICATION OF L=2 IS ONLY NECESSARY AT KT=1
    5 READ (5,10)   (NRN(I),I=1,4),IOUT,KT,KM,L
   10 FORMAT (4A2,I2,I2,I2,I2)
      IF (IOUT.NE.0) GO TO 2000
C
C
C $$$ READ STATEMENT PROVIDES 80 SPACES FOR A COMMENT REGARDING
C        DATA REDUCTION.  STATEMENT WILL APPEAR ON OUTPUT SHEET
      READ (5,2) (KOMMNT(I), I=1,40)
    2 FORMAT (40A2)
C $$$ READ AMBIENT CONDITIONS: TEMP(DEG F), PRESS(IN HG), RELHUM(PCT)
      READ (5,20) TAMB,PAMB,RHUM,THEAT
   20 FORMAT (7F10.0)
C
C $$$ READ TUNNEL CONDITIONS: TINF(MV) RECOVERY TEMP,PDYN(IN H2O),
C          PSTAT(IN H2O) GAGE STATIC PRESSURE, NOTE NEG IF BELOW
C          PAMB, XVO(IN) VIRTUAL ORIGIN OF TBL, INCHES
C          FROM THE PHYSICAL STARTING POINT OF THE PLATE
      READ (5,20) TINF,PDYN,PSTAT,XVO,END2,DXVO,DEND2
      TRECOV=TINF
      IF (END2.EQ..0) L=1
C
C          POWERSTAT SETTING, SEC AIR FLOWRATE(MV) TAKEN AT SEC AIR TEMP
C $$$ READ SEC AIR TEMP(MV), PLATE TEMP(MV), PLATE POWER(WATTS),
      READ (5,25) (TG(I),TO(I),Q(I),VAR(I),SAFR(I),CI(I),I=1,12)
   25 FORMAT (6F10.0)
      READ (5,26) (TO(I),HM(I),I=13,45)
   26 FORMAT(2F10.0)
C $$$ READ CASTING TEMPERATURES
      READ (5,25) (TCAST(I), I=1,5)
C
C     WRITE OUT ALL RAW DATA
      WRITE (6,40) (NRN(I), I=1,4)
   40 FORMAT (1H1,9X,'STANTON NUMBER DATA  RUN  ',4A2,' *** DISCRETE HOL
     1E RIG *** NAS-3-14336'/)
      WRITE (6,45)
   45 FORMAT (10X,'UNITS: PAMB(DEG F),PAMB(IN HG), RHUM(PCT)'/17X,
     1 'PSTAT(IN H2O), TRECOV(MV), PDYN(IN H2O), XVO(IN), TPLATE(MV)'/17
     2X,'TGAS(MV), QDOT(WATTS), SAFR(MV),HM(MV), CI(MV), THEAT(MV)'/)
      WRITE (6,50) TAMB,PAMB,RHUM,THEAT
   50 FORMAT (10X,'TAMB='F6.1,5X,'PAMB='F6.2,5X,'RELHUM='F5.1,6X,
     1  'THEATER='F6.2/)
      WRITE (6,60) PSTAT,TRECOV,PDYN,XVO
   60 FORMAT (10X,'PSTAT='F6.2,5X,'TRECOV='F6.3,5X,'PDYN='F6.3,5X,
     1 'XVO='F6.2//)
      WRITE (6,70)
   70 FORMAT (10X,'PLATE',6X, 'TPLATE',6X,'TGAS',6X,'QDOT',4X,'VARIAC',
     1 5X,'SAFLOW',5X,'CURRENT'/)
      NP1=1
```

```
      WRITE (6,75) NP1,TO(1),Q(1),VAR(1)
   75 FORMAT (10X,I3,7X,F7.3,13X,F7.2,3X,F7.1)
      WRITE (6,80) (I,TO(I),TG(I),Q(I),VAR(I),SAFR(I),CI(I),I=2,12)
   80 FORMAT (10X,I3,7X,F7.3,3X,F7.3,3X,F7.2,3X,F7.1,3X,F8.3,3X,F8.3)
      WRITE(6,71)
   71 FORMAT(/,10X,'PLATE',6X,'TPLATE',6X,'HM')
      WRITE(6,72)(I,TO(I),HM(I),I=13,45)
   72 FORMAT(10X,I3,7X,F7.3,3X,F7.3)
      WRITE (6,85) (I,TCAST(I), I=1,5)
   85 FORMAT (/10X,5('TCAST('I1,')='F6.3,5X))
C
C     DATA REDUCTION SEGMENT
C
C     CONVERT ALL TEMPERATURES FROM MV TO DEG F
      TRECOV=TC(TRECOV)
      DO 90 I=1,12
      TO(I)=TC(TO(I))
      TG(I)=TC(TG(I))
   90 CONTINUE
      DO 89 I=13,45
   89 TO(I)=TC(TO(I))
      DO 95 I=1,5
   95 TCAST(I)=TC(TCAST(I))
C     MIXTURE COMPOSITION, GAS CONSTANT,RM, AND SPECIFIC HEAT, CP
      RHUM=RHUM/100.
      PSINF=PAMB+29.92*PSTAT/407.
CC        TO HAVE ACCURATE RESULTS:
CC      AFTER CALLING SUBROUTINES HUMID AND  VEL , AGAIN  CALL HUMID (PSINF,
CC      TINF,RHUM,P,CP,RM,W)   AND    CALL VEL (RM,P,W,PDYN,TRECOV,TINF,RHOG,
CC      UINF,VISC,CP,PR).THIS PROCEDURE MAY BE ITERATED FOR THE DESIRED ACCURACY
CC            IN OUR CASE, KINETIC TEMP IS LESS THAN ABOUT 1.0 F FOR  100.FT/SEC
CC      AND ABSOLUTE HUMIDITY, W, AND OTHER PROPERTIES DO NOT CHANGE NOTICEABLY.
CC      SO WE DO NOT NEED ANY ITERATIONS.
      CALL    HUMID (PSINF,TRECOV,RHUM,P,CP,RM,W)
C     COMPUTE FREE STREAM DENSITY,VELOCITY,STATIC TEMP,KIN.VISC
        CALL    VEL (RM,P,W,PDYN,TRECOV,TINF,RHOG,UINF,VISC,CP,PR)
C     PLATE AREAS
      A=18.*1.968750/144.
C    HOLE AREA
      AH=(3.141593*0.406250*0.406250*0.25)/144.
C     SECONDARY AIR FLOWRATE
        CALL    FLOW (KERROR,UINF,AH,W,TG,THEAT,CI,RHOG,SAFR,SM,F,KM)
C   DF: UNCERTAINTY IN  F , RATIO
      DF=SQRT(DSAFR*DSAFR+DP*DP/(4.*PDYN*PDYN))
      IF (KERROR.GT.0) GO TO 1000
C     WATTMETER CORRECTION  FOR WATTMETER CALIBRATION AND THE CIRCUITRY.
      CALL WATT (Q,VAR)
CC      CALCULATES THE MIXED MEAN 2ND GAS TEMP,HEAT LOSSES,AND EFFECTIVE CASTING
CC      TEMP.
        CALL    TEFFS (SAFR,TCAST,TO,TG,K,HM,T2,QFLOW,TCAV,KM)
CC      CORRECS THE PLATE POWER TO GET CONVECTIVE FLUXES ON BLOWING SECTION
        CALL    PLOSS (Q,TO,TCAV,TINF,A,K,S,QFLOW,QDOT)
CC      CALCULATES THE CONVECTIVE HEAT FLUXES ON THE RECOVERY REGION.
         CALL   HFM (TO,TINF,HM,K,S,QDOT)
C   DQDOT: UNCERTAINTY IN HEAT FLUX,BTU/HR.SQFT
      DO 711 I=1,12
  711 DQDOT(I)=DQ*3.4129/A
      DO 712 I=13,36
  712 DQDOT(I)=SQRT(DK*DK*K(I)*K(I)*HM(I)*HM(I)+K(I)*K(I)*DHM*DHM+DT*DT
     1*(S(I)*S(I)+S(I+1)*S(I+1))+DS*DS*(S(I)*S(I)*(TO(I)-TO(I-1))*(TO(I)
```

```
     2-TO(I-1))+S(I+1)*S(I+1)*(TO(I)-TO(I+1))*(TO(I)-TO(I+1)))))
C
C     WRITE ALL CONVERTED DATA
C
      WRITE (6,100)
  100 FORMAT (//,10X,'UNITS: TPLATE(DEGF), TGAS(DEG F), QDOT(WATTS),',
     1 /17X,'SAFLOW(CFM),QFLUX(BTU/HR/SQFT),TEFF2(DEG F)'/)
      WRITE (6,102)
  102 FORMAT (10X,'PLATE',6X, 'TPLATE',5X,'TEFF2',5X,'TGAS',6X,'QDOT',
     1  6X,'QFLUX',6X,'SAFLOW'/)
      WRITE (6,105) NP1,TO(1),Q(1),QDOT(1)
  105 FORMAT(10X,I3,7X,F7.1,23X,F7.2, 5X,F7.2)
      WRITE (6,110) (I,TO(I),T2(I),TG(I),Q(I),QDOT(I),SAFR(I),I=2,12)
  110 FORMAT(10X,I3,7X,F7.1,3X,F7.1,3X,F7.1,3X,F7.2,5X,F7.2,1X,F8.2)
      WRITE (6,106)
  106 FORMAT(/,10X,'PLATE',6X,'TPLATE',6X,'HM',5X,'QFLUX'/)
      WRITE(6,107) (I,TO(I),HM(I),QDOT(I),I=13,36)
  107 FORMAT (10X,I3,7X,F7.3,3X,F7.3,3X,F7.2)
      WRITE (6,115) (I,TCAST(I), I=1,5)
  115 FORMAT (/10X,5('TCAST('I1,')='F6.1,5X))
      XVI=X(1)-XVO-1.0
      IPD=5
      IF (KM.EQ.1) IPD=10
      WRITE (6,40) (NRN(I), I=1,4)
      WRITE (6,300) TINF,UINF,XVO,RHOG,CP,VISC,PR,XVI,IPD
  300 FORMAT (10X,'TINF='F6.1,4X,'UINF='F5.1,5X,'XVO='F6.3,   5X,'RHO=',
     1F8.5,3X,'CP='F6.3,6X,'VISC='E12.5,5X,'PR='F5.3,/10X,'DISTANCE FROM
     1 ORIGIN OF BL TO 1ST PLATE='F6.3,14X'P/D='I2)
      IF (KT.EQ.2) GO TO 402
C
C     COMPUTE HEAT TRANSFER PARAMETERS
C
C     COMPUTE THETA=(T2-TINF)/(TO-TINF)
      TH(1)=0.
      DTH(1)=0.
      SM(1)=0.
      F(1)=0.
      DO 200 I=2,12
      TH(I)=(T2(I)-TINF)/(TO(I)-TINF)
C   DTH(I): UNCERTAINTY IN TH(I)
  200 DTH(I)=DT*SQRT(1.+TH(I)*TH(I))/(TO(I)-TINF)
      IF (KM.EQ.0) GO TO 201
      DO 202 I=3,11,2
      TH(I)=TH(I-1)
  202 F(I)=F(I-1)
C     X REYNOLDS NUMBER BASED ON VIRTUAL ORIGIN TBL
  201 FACT=UINF/(VISC*12.)
      DREX=FACT*DXVO
      DO 210 I=1,36
  210 REX(I)=FACT*(X(I)-XVO)
C     COMPUTE STANTON NUMBERS
      DENOM=RHOG*UINF*CP*3600.
      DO 220 I=1,36
      ST(I)=QDOT(I)/(DENOM*(TO(I)-TINF))
CC    VARIABLE PROPERTY CORRECTION.
      ST(I)=ST(I)*((TO(I)+459.67)/(TINF+459.67))**(.4)
C    DST(I):  UNCERTAINTY IN ST(I)
      DST(I)=ST(I)*SQRT(DQDOT(I)*DQDOT(I)/(QDOT(I)*QDOT(I))+DP*DP/(4.*
     1PDYN*PDYN)+DT*DT/((TO(I)-TINF)*(TO(I)-TINF)))
  220 CONTINUE
```

```
CC      CALCULATES  DEL2 AND RE-DEL2 BASED ON THE  ACTUAL ST-DATA.
        CALL  ENTHAL (FACT,TH,F,ST,END2,DEND2,D2,REEN,DD2,DREEN,DTH,DST,
       1DF,KM)
        CC=0.0
        DO 116 I=1,12
        IF (CI(I) .NE. 0.0) CC=CI(I)
    116 CONTINUE
        IF (CC .EQ. 0.) WRITE(6,333) DREX
        IF (CC .NE. 0.) WRITE (6,334) DREX,DF
    333 FORMAT  ( 12X,'UNCERTAINTY IN REX=',F6.0,/)
    334 FORMAT ( 12X,'UNCERTAINTY IN REX=',F6.0,9X'UNCERTAINTY IN F=',F7.5
       1,' IN RATIO'/)
        WRITE (6,600) (KOMMNT(I), I=1,40)
    600 FORMAT   (10X,40A2/)
        WRITE (6,310)
    310 FORMAT(10X'PLATE',3X'X',5X'REX',9X'TO',6X'REENTH',7X'STANTON NO',
       1 6X'DST',6X'DREEN',4X'M',4X'F',6X'T2',2X'THETA',3X'DTH')
        WRITE (6,320) NP1,X(1),REX(1),TO(1),REEN(1),ST(1),DST(1),DREEN(1)
    320 FORMAT(10XI3,2XF5.2,1XE12.5,1XF6.1,2(2XE12.5),2XE9.3,2XF5.0)
        DO 340 I=2,12
        WRITE (6,330)  I,X(I),REX(I),TO(I),REEN(I),ST(I),DST(I),DREEN(I),
       1SM(I),F(I),T2(I),TH(I),DTH(I)
    330 FORMAT(10XI3,2XF5.2,1XE12.5,1XF6.1,2(2XE12.5),2XE9.3,2XF5.0,2XF5.2
       1,F7.4,F6.1,F6.3,2XF5.3)
    340 CONTINUE
        DO 341 I=13,36
        WRITE (6,331) I,X(I),REX(I),TO(I),REEN(I),ST(I),DST(I),DREEN(I)
    331 FORMAT(10XI3,2XF5.2,1XE12.5,1XF6.1,2(2XE12.5),2XE9.3,2XF5.0)
    341 CONTINUE
CC      IF 2ND PLATE HAS NO SECONDARY INJECTION , THIS PROGRAM ASSUMES THAT
CC      IT IS A NO-BLOWING CASE.
        IF (CC .EQ. 0.0) GO TO 400
        IF(KT.EQ.0)  GO TO 350
        IF (KT.EQ.1)  GO TO 360
CC      STORE THE OLD VALUES OF STANTON NUMBERS ALONG WITH OTHER INTEGRAL
CC      PARAMETERS FOR THE COLD RUN.
    350 DO 351 I=1,12
        SMO(I)=SM(I)
        FO(I)=F(I)
        THO(I)=TH(I)
        DTHO(I)=DTH(I)
        STO(I)=ST(I)
        DSTO(I)=DST(I)
        REXO(I)=REX(I)
    351 CONTINUE
        DO 352 I=13,36
        STO(I)=ST(I)
        DSTO(I)=DST(I)
        REXO(I)=REX(I)
    352 CONTINUE
        FACTO=FACT
        DFO=DF
        DO 353 I=1,4
        NRNO(I)=NRN(I)
    353 CONTINUE
        GO TO 1000
CC      CALCULATES THE STANTON NUMBERS AT  THETA .EQ.  0  AND 1  BASED ON LINEAR
CC      SUPERPOSITION THEORY.
    360 FAVO=0.
        FAV=0.
```

```
      THAVO=0.
      THAV=0.
      DO 361 I=2,12
      THAVO=THAVO+THO(I)
      THAV=THAV+TH(I)
      FAVO=FAVO+FO(I)
      FAV=FAV+F(I)
  361 CONTINUE
      THAVO=THAVO/11.
      THAV=THAV/11.
      FAVO=FAVO/11.
      FAV=FAV/11.
      FBAV=.5*(FAVO+FAV)
      DO 362 I=2,12
      STS(I)=(STO(I)-ST(I))/(TH(I)-THO(I))
      STCOL(I)=STO(I)+THO(I)*STS(I)
      STHOT(I)=ST(I)+(TH(I)-1.0)*STS(I)
      FB(I)=0.5*(FO(I)+F(I))
      ETA(I)=STS(I)/STCOL(I)
      IF (L.EQ.2) GO TO 374
      STNOB(I)=.0295*PR**(-.4)*(REX(I))**(-.2)
      IF (L.EQ.1)STNOB(I)=STNOB(I)*(1.-(XVI/(X(I)-XVO))**(0.9))**
     1(-1./9.)
  374 STHR(I)=STHOT(I)/STNOB(I)
      IF (L.EQ.2) GO TO 375
      STNOB(I)=STNOB(I)*(REX(I)/REXO(I))**(0.2)
      IF (L.EQ.1)STNOB(I)=STNOB(I)*(1.-(XVI*FACTO/REXO(I))**(0.9))**
     1(-1./9.)
  375 STCR(I)=STCOL(I)/STNOB(I)
      STSR(I)=STHOT(I)/STCOL(I)
      BHCOL(I)=FO(I)/STCOL(I)
      BHOT(I)=F(I)/STHOT(I)
      STSF(I)=ALOG(1.+BHOT(I))/BHOT(I)
      BHOT(I)=STHR(I)/STSF(I)
      STSR(I)=STSR(I)/STSF(I)
      SF(I)=F(I)*STHOT(I)
      SFO(I)=FO(I)*STCOL(I)
  362 CONTINUE
      DO 363 I=13,36
      STS(I)=(STO(I)-ST(I))/(THAV-THAVO)
      STCOL(I)=STO(I)+THAVO*STS(I)
      STHOT(I)=ST(I)+(THAV-1.0)*STS(I)
      ETA(I)=STS(I)/STCOL(I)
      IF (L.EQ.2) GO TO 372
      STNOB(I)=.0295*PR**(-.4)*(REX(I))**(-.2)
      IF (L.EQ.1)STNOB(I)=STNOB(I)*(1.-(XVI/(X(I)-XVO))**(0.9))**
     1(-1./9.)
  372 STHR(I)=STHOT(I)/STNOB(I)
      IF (L.EQ.2) GO TO 373
      STNOB(I)=STNOB(I)*(REX(I)/REXO(I))**(0.2)
      IF (L.EQ.1)STNOB(I)=STNOB(I)*(1.-(XVI*FACTO/REXO(I))**(0.9))**
     1(-1./9.)
  373 STCR(I)=STCOL(I)/STNOB(I)
      STSR(I)=STHOT(I)/STCOL(I)
  363 CONTINUE
CC    CALCULATES THE  DEL2 AND RE-DEL2  BASED ON THE NEW VALUES OF STANTON
CC    NUMBER AT THETA .EQ. 0  AND  1 .
      STCOL(1)=STO(1)
      STHOT(1)=ST(1)
      STS(1)=STO(1)-ST(1)
```

```
      DO 370 I=1,12
      THO(I)=0.0
  370 TH(I)=1.0
      CALL ENTHAL(FACT,TH,F,STHOT,END2,DEND2,D2HOT,RENHOT,DD2,DREFN,DTH
     1,DST,DF,KM)
      CALL ENTHAL(FACTO,THO,FO,STCOL,END2,DEND2,D2COL,RENCOL,DD2,DREFN
     1,DTHO,DSTO,DFO,KM)
CC    OUTPUTS FOR THE NEW PARAMETERS.
      WRITE (6,371) (NRNO(I),I=1,4),(NRN(I),I=1,4)
  371 FORMAT (1H1,9X,'FOLLOWING IS THE DATA FOR THETA=0 AND THETA=1, WHI
     *CH WAS OBTAINED BY LINEAR SUPERPOSITION THEORY.'/,10X'THIS DATA WA
     *S PRODUCED FROM RUN ',4A2,' AND  RUN ',4A2,/;10X'FOR THE DETAIL CH
     *ANGES OF PROPERTIES AND BOUNDARY CONDITIONS, PLEASE SEE THE ABOVE
     *TWO RUNS')
      WRITE(6,364)
  364 FORMAT    (/,7X,'PLATE',3X,'REXCOL',4X,'RE DEL2',3X,'ST(TH=0)',4X,
     1'REXHOT',4X,'RE DEL2',3X,'ST(TH=1)',4X,'ETA',4X,'STCR',4X'F-COL',
     25X'STHR',4X'F-HOT',2X'PHI-1'/)
      WRITE(6,365)   (I,REXO(I),RENCOL(I),STCOL(I),REX(I),RENHOT(I),
     1STHOT(I),ETA(I),STCR(I),FO(I),STHR(I),F(I),BHOT(I),I=1,12)
  365 FORMAT((10X,I2,2(2XF9.1),1XF9.6,2(2XF9.1),1XF9.6,2(2XF5.3),2XF7.4,
     12XF7.3,2XF7.4,2XF5.3))
      WRITE(6,366)   (I,REXO(I),RENCOL(I),STCOL(I),REX(I),RENHOT(I),
     1STHOT(I),ETA(I),STCR(I),STHR(I),I=13,36)
  366 FORMAT((10X,I2,2(2XF9.1),1XF9.6,2(2XF9.1),1XF9.6,2(2XF5.3),11XF7.3
     1))
      GO TO 1000
CC    FLAT PLATE VALUES ARE STORED.
  400 DO 401 I=1,36
      STNOB(I)=ST(I)
  401 CONTINUE
      GO TO 1000
  402 DO 403 I=2,12
      XD(I)=(X(I)+1.-X(2))/0.406
  403 ETA(I)=(TO(I)-TINF)/(T2(I)-TINF)
      TS=0.
      DO 404 I=2,12
  404 TS=TS+T2(I)
      TS=TS/11.
      DO 405 I=13,36
      XD(I)=(X(I)+1.-X(2))/0.406
  405 ETA(I)=(TO(I)-TINF)/(TS-TINF)
      CC=0.0
      DO 117 I=1,12
      IF (CI(I) .NE. 0.0) CC=CI(I)
  117 CONTINUE
      IF (CC .EQ. 0.) WRITE(6,333) DREX
      IF (CC .NE. 0.) WRITE (6,334) DREX,DF
      WRITE (6,600) (KOMMNT(I), I=1,40)
      WRITE (6,406)
  406 FORMAT (10X'PLATE',3X'X',6X'REX',9X'TO',5X'X/D',5X'ETA',6X'M',
     18X'F',5X'T2')
      DO 407 I=2,12
      WRITE (6,408) I,X(I),REX(I),XD(I),ETA(I),SM(I),F(I)
  408 FORMAT (10X,I3,2X,F5.2,1XE12.5,1XF6.1,2XF6.2,2XF6.4,2XF5.2,2XF7.4,
     12XF5.1)
  407 CONTINUE
      DO 409 I=13,36
      WRITE (6,410) I,X(I),REX(I),XD(I),ETA(I)
  410 FORMAT (10X,I3,2X,F5.2,1XE12.5,1XF6.1,2XF6.2,2XF6.4)
```

```
  409 CONTINUE
 1000 GO TO 5
 2000 WRITE (6,900)
  900 FORMAT (1H1)
      RETURN
      END
      FUNCTION TC(T)
C    FUNCTION CONVERTS TEMP FROM IRON-CONSTANTAN MV TO DEG F
      TM=-2220.703+781.25*SQRT(7.950782+0.256*T)
      TC=TM+49.97-1.26E-03*TM-.32E-04*TM*TM
      RETURN
      END
      SUBROUTINE HUMID (PBAR,TAMB,RHUM,P,CP,RM,W)
C
C     THIS SUBROUTINE CALCULATES THE MASS FRACTION OF AIR AND WATER
C     VAPOR FROM THE RELATIVE HUMIDITY AND AMBIENT TEMPERATURE
C     THE MIXTURE GAS CONSTANT IS ALSO DETERMINED
C     SATURATION DATA FROM K AND K 1969 STEAM TABLES
C
C     DATA BLOCK FROM THE STEAM TABLES
C
      DIMENSION TEMP(10),PSAT(10),RHOSAT(10)
      DATA TEMP/      40.,       50.0,       60.0,       70.0,       80.0,
     1      90.0,      100.0,     110.0,      120.0,      130.0/
      DATA PSAT/      17.519,    25.636,     36.907,     52.301,     73.051,
     1      100.627,   136.843,   183.787,    244.008,    320.400/
      DATA RHOSAT/   .0004090, .0005868, .0008296, .0011525, .0015803,
     1      .0021381, .0028571, .0037722, .0049261, .0063625/
      REAL NU,MFA,MFV,MWA,MWV
C     CONVERT IN HG TO PSF
C     AT 59. DEG F P=2116.217 PSF = 29.92126 IN HG
C     SEE HESSE AND MUMFORD, JET PROPULSION, P554
      P=PBAR*2116.217/29.92126
      DO 10 N=1,9
      IF(TEMP(N).GT.TAMB) GO TO 20
   10 CONTINUE
   20 T = TEMP(N)
      EPS = T - TAMB
      VAPH = PSAT(N)
      VAPL = PSAT(N-1)
      VEPS = VAPH - VAPL
      RHOH = RHOSAT(N)
      RHOL = RHOSAT(N-1)
      REPS = RHOH - RHOL
      RHOG = RHOL + (10.0 - EPS)*REPS/10.
      RA=1545.32/28.970
      PG = VAPL + (10.0 - EPS)*VEPS/10.0
      PVAP = RHUM*PG
      PA = P - PVAP
      RHOA = PA/(RA*(TAMB + 459.67))
      RHOV = RHUM*RHOG
      W=RHOV/RHOA
      RHOM = RHOA + RHOV
      MWA = 28.970
      MWV = 18.016
      MFV = RHOV/RHOM
      MFA = 1.0 - MFV
      RM = 1545.32*(MFA/MWA + MFV/MWV)
      CP = MFA*0.240 + MFV*0.445
      RETURN
      END
```

```
      SUBROUTINE VEL (RM,P,W,PDYN,TRECOV,TINF,RHOG,UINF,VISC,CP,PR)
C     TUNNEL PRESSURE,PSF
C     CONVERT TO PSF USING VALUES FROM K&K GAS TABLES, P195,FOR H2O AT
C     60 DEG F
      PUNITS=144./27.7068
      GC=32.1739
      JF=777.66
      RCF=0.7**0.33333
      RHOG=(P/RM+PDYN*PUNITS*RCF/(CP*JF))/(TRECOV+459.67)
      UINF=SQRT(2.*GC*PDYN*PUNITS/RHOG)
      TINF=TRECOV-RCF*UINF*UINF/(2.*GC*JF*CP)
C     KINEMATIC VISCOSITY, FT*FT/SEC
      VISC=(11.+0.0175*TINF)/(1.E06*RHOG)*(1.-.7*W)
CC    PRANDTL NUMBER OF FREESTREAM AIR
      PR=.710*(530./(TINF+459.67))**(.1)*(1.+.9*W)
      RETURN
      END
      SUBROUTINE FLOW (KERROR,UINF,AH,W,TG,THEAT,CI,RHOG,SAFR,SM,F,KM)
      DIMENSION SAFR(1),SM(1),F(1),TG(1),X(5),Y(5),B(4),CI(1),FMC(12)
      DIMENSION  TM(12)
      DATA FMC/  1.0,  1.22,  .92,  .988,  .928,  .906,  .907,  1.01,
     1              .918,  .901,  .920,  .929/
      KERROR=0
C
C
C     THIS ROUTINE CONVERTS FLOWMETER READING TO SECONDARY
C        AIR FLOWRATE, AND COMPUTES M AND F PARAMETERS
C
C     TG, GAS STATIC TEMPERATURE, DEG F
C     W, HUMIDITY RATIO, LB VAPOR/LB DRY AIR
C     SAFR, SECONDARY AIR FLOWRATE, CFM, CORRECTED FOR TEMP AND HUMIDITY
C     SM, VELOCITY RATIO, SECONDARY AIR GAS TO MAINSTREAM GAS
C     F, MASS FLUX RATIO, SA TO MS, CONSIDERING 2*2 SQIN AREA
C          CONTAINING 2 BLOWING HOLES TOTAL, F=  AH*M/(4/144)
C
C     CALIBRATION CURVE DATA
      X(1)=0.35
      Y(1)=53.0
      X(2)=0.90
      Y(2)=4.05
      X(3)=1.12
      Y(3)=2.00
      X(4)=1.35
      Y(4)=1.00
      X(5)=1.5
      Y(5)=0.69
      DO 10 I=1,4
   10 B(I)=ALOG(Y(I)/Y(I+1))/ALOG(X(I)/X(I+1))
      FACT=1.0+0.22*W
      THEAT=TC(THEAT)
      DO 20 I=2,12
      IF (CI(I).EQ.0.) SAFR(I)=0.
      IF (CI(I).EQ.0.)  GO TO 20
      TM(I)=.5*(TG(I)+THEAT)
      SAFR(I)=SAFR(I)*(((TM(I)+459.67)/530.)**0.7)*FACT*(30.00/CI(I))**2
     1        *FMC(I)
   20 CONTINUE
      FACT=1.0+0.7*W
      DO 40 I=2,12
      IF (CI(I).EQ.0.) GO TO 40
```

```
      IF (SAFR(I).LT.X(1).OR.SAFR(I).GT.X(5)) GO TO 100
      DO 30 K=1,5
      IF (X(K).GT.SAFR(I)) GO TO 35
   30 CONTINUE
   35 Z=Y(K-1)*(SAFR(I)/X(K-1))**B(K-1)
      SAFR(I)=Z/((530./(TM(I)+459.67))**0.76)/FACT
   40 CONTINUE
      RHOS=.074843
      IF(KM.EQ.1) GO TO 300
      F8=AH*60.*UINF*8.*RHOG
      F9=AH*60.*UINF*9.*RHOG
      DO 50 I=2,12,2
      SM(I)=SAFR(I)*RHOS/F9
   50 F(I)=36.*AH*SM(I)
      DO 60 I=3,11,2
      SM(I)=SAFR(I)*RHOS/F8
   60 F(I)=36.*AH*SM(I)
      RETURN
  300 F5=AH*60.*UINF*5.*RHOG
      F4=F5*4./5.
      DO 310 I=3,11,2
      SM(I)=0.
  310 F(I)=0.
      DO 311 I=2,10,4
      SM(I)=SAFR(I)*RHOS/F5
  311 F(I)=  9.*AH*SM(I)
      DO 312 I=4,12,4
      SM(I)=SAFR(I)*RHOS/F4
  312 F(I)=  9.*AH*SM(I)
      RETURN
  100 CONTINUE
      WRITE (6,200) SAFR(I)
  200 FORMAT (10X,'FLOWMETER READING OUT OF RANGE, EMF='E12.5,//10X,
     1 'DATA SET REDUCTION TERMINATED')
      KERROR=2
      RETURN
      END
      SUBROUTINE WATT (Q,VAR)
      DIMENSION Q(1),VAR(1)
      DIMENSION RR(12),XP(12),RBO(12),RO(12),RSL(12),RL(12)
      DATA RL/8.022, 8.024, 8.067, 8.066, 8.064, 8.063,
     1         8.096, 8.073, 8.093, 8.099, 8.079, 8.060/
      DATA RSL/8.187, 8.186, 8.233, 8.227, 8.217, 8.220,
     1         8.259, 8.229, 8.256, 8.263, 8.241, 8.226/
      DATA RO/8.419, 8.456, 8.506, 8.488, 8.470, 8.504,
     1         8.566, 8.522, 8.503, 8.619, 8.498, 8.487/
      DATA RBO/8.320, 8.368, 8.400, 8.394, 8.375, 8.398,
     1         8.468, 8.451, 8.403, 8.523, 8.402, 8.384/
      DATA RR/0.04083, 0.05413, 0.04059, 0.04108, 0.04130, 0.04115,
     1         0.04096, 0.04147, 0.04090, 0.04086, 0.04058, 0.04064/
CC    THIS PROGRAM NEGLECTS THE EFFECT FROM THE REACTANCE OF POWERSTAT COIL.
      DATA XP/12*0.0/
      DATA RA,XA,RV/0.064, 0.063, 7500./
      DO 2000 I=1,12
C     THE FOLLOWING CORRECTS THE INDICATED POWER TO THE ACTUAL
C        POWER
      QP=Q(I)/75.
      CORQ=QP*(0.0728*QP-0.0427*QP*QP-0.0292)
      QCOR=0.99*Q(I)+CORQ*75.
C     THIS BLOCK CORRECTS THE WATTMETER FOR INSERTION LOSSES
      T=VAR(I)*RR(I)
      S=VAR(I)*XP(I)
      SA=S+XA
      ROT=RO(I)+T
```

```
      RBOT=RBO(I)+T
      ROI=ROT*ROT+SA*SA
      RBOI=RBOT*RBOT+S*S
      RLVI=1.+(RSL(I)+RA)/RV
      RXA=XA/RV
      RSLI=RLVI*RLVI+RXA*RXA
      RSLL=(RSL(I)+RA)/RL(I)
      Q(I)=QCOR*ROI*RSLI/(RBOI*RSLL)
 2000 CONTINUE
      RETURN
      END
      SUBROUTINE TEFFS (SAFR,TCAST,TO,TG,K,HM,T2,QFLOW,TCAV,KM)
      REAL KCONV(2),KFL(12),K(1)
      DIMENSION SAFR(1),TG(1),TO(1),T2(1),TCAST(1),QFLOW(1),TCAV(1)
      DIMENSION HM(1)
CC    THIS SUBROUTINE CALCULATES THE EFFECTIVE TEMPERATURE OF SECONDARY
CC    GAS AND CASTING FOR EACH PLATE. THEN  IT CALCULATES THE  PORTIN OF HEAT LO
CC    LOSSES DUE TO SECONDARY GAS.
CC     EFFECTIVE  TEMP FOR THE 4 FT PLATES.
      TW1=TO(45)+K(39)*HM(45)/20.5
      TW2=TO(13)+K(13)*HM(13)/20.5
CC      EFFECTIVE CASTING TEMP.
      TCAV(1)=0.375*TCAST(1) + 0.66667*TCAST(2) + 0.25*TW1 -
     1  0.125*TCAST(3) - 0.16667*TCAST(4)
      TCAV(2)=0.5*TCAST(1) + 0.66667*TCAST(2) - 0.16667*TCAST(4)
      TCAV(3)=0.5*(TCAST(1) + TCAST(2))
      TCAV(4)=0.25*TCAST(1) + 0.5*TCAST(2) + 0.25*TCAST(3)
      TCAV(5)=0.25*TCAST(1) + 0.3333*TCAST(2) + 0.25*TCAST(3)
     1  +0.16667*TCAST(4)
      TCAV(6)=0.3333*TCAST(2) + 0.5*TCAST(3) + 0.16657*TCAST(4)
      TCAV(7)=0.16667*TCAST(2) + 0.5*TCAST(3) + 0.3333*TCAST(4)
      TCAV(8)=0.16667*TCAST(2) + 0.25*TCAST(3) + 0.3333*TCAST(4)
     1  + 0.25*TCAST(5)
      TCAV(9)=0.25*TCAST(3) + 0.5*TCAST(4) + 0.25*TCAST(5)
      TCAV(10)=0.5*(TCAST(4) + TCAST(5))
      TCAV(11)=0.5*TCAST(5) + 0.66667*TCAST(4) - 0.16667*TCAST(2)
      TCAV(12)=0.375*TCAST(5) + 0.66667*TCAST(4) - 0.125*TCAST(3)
     1 -0.16667*TCAST(2) + 0.25*TW2
CC     PORTION OF ENERGY  WHICH IS LOST.
      FACT=.074843*.24*60.
      QFLOW(1)=0.0
      IF (KM.EQ.1) GO TO 100
      DO 10 I=2,12,2
      IF (SAFR(I).EQ.0.) GO TO 12
      IF (SAFR(I).GE.5.)  GO TO 11
      KFL(I)=.21+.0344*ALOG10(SAFR(I))
      GO TO 10
   12 KFL(I)=0.
      GO TO 10
   11 KFL(I)=.0762+.226*ALOG10(SAFR(I))
   10 CONTINUE
      DO 20 I=3,12,2
      IF (SAFR(I).EQ.0.) GO TO 22
      SAFR(I)=1.125*SAFR(I)
      IF (SAFR(I).GE.5.)  GO TO 21
      KFL(I)=.21+.0344*ALOG10(SAFR(I))
      GO TO 20
   22 KFL(I)=0.
      GO TO 20
   21 KFL(I)=.0762+.226*ALOG10(SAFR(I))
```

```
   20 CONTINUE
CC      EFFECTIVE  'T2',AND 'QFLOW'.
      DO 30 I=2,12,2
      IF (SAFR(I).EQ.0.) GO TO 31
      KCONV(2)=0.24*SAFR(I)**0.35
      E=EXP(-KCONV(2)/SAFR(I))
      T2(I)=TG(I)+(1.-E)*(KFL(I)*(TO(I)-TG(I))+(TCAV(I)-TG(I)))
      QFLOW(I)=FACT*KFL(I)*KCONV(2)*(TO(I)-T2(I))
      GO TO 30
   31 T2(I)=TO(I)
      QFLOW(I)=0.
   30 CONTINUE
      DO 40 I=3,12,2
      IF (SAFR(I).EQ.0.) GO TO 41
      KCONV(1)=0.2133*SAFR(I)**0.35
      SAFR(I)=SAFR(I)*8./9.
      E=EXP(-KCONV(1)/SAFR(I))
      T2(I)=TG(I)+(1.-E)*(KFL(I)*(TO(I)-TG(I))+(TCAV(I)-TG(I)))
      QFLOW(I)=FACT*KFL(I)*KCONV(1)*(TO(I)-T2(I))
      GO TO 40
   41 T2(I)=TO(I)
      QFLOW(I)=0.
   40 CONTINUE
      RETURN
  100 DO 101 I=1,11,2
      T2(I)=TO(I)
      QFLOW(I)=0.
  101 KFL(I)=0.
      DO 102 I=2,10,4
      IF (SAFR(I).EQ.0.) GO TO 51
      SAFR(I)=(9./5.)*SAFR(I)
      IF (SAFR(I).GE.5.) GO TO 103
      KFL(I)=0.21+.0344*ALOG10(SAFR(I))
      GO TO 102
   51 KFL(I)=0.
      GO TO 102
  103 KFL(I)=0.0762+.226*ALOG10(SAFR(I))
  102 CONTINUE
      DO 104 I=4,12,4
      IF (SAFR(I).EQ.0.) GO TO 52
      SAFR(I)=(9./4.)*SAFR(I)
      IF (SAFR(I).GE.5.) GO TO 105
      KFL(I)=0.21+.0344*ALOG10(SAFR(I))
      GO TO 104
   52 KFL(I)=0.
      GO TO 104
  105 KFL(I)=0.0762+.226*ALOG10(SAFR(I))
  104 CONTINUE
      DO 106 I=2,10,4
      IF (SAFR(I).EQ.0.) GO TO 53
      KCONV(2)=0.1333*SAFR(I)**0.35
      SAFR(I)=SAFR(I)*(5./9.)
      E=EXP(-KCONV(2)/SAFR(I))
      T2(I)=TG(I)+(1.-E)*(KFL(I)*(TO(I)-TG(I))+(TCAV(I)-TG(I)))
      QFLOW(I)=FACT*KFL(I)*KCONV(2)*(TO(I)-T2(I))
      GO TO 106
   53 T2(I)=TO(I)
      QFLOW(I)=0.
  106 CONTINUE
      DO 107 I=4,12,4
```

```
      IF (SAFR(I).EQ.0.) GO TO 54
      KCONV(1)=0.1067*SAFR(I)**0.35
      SAFR(I)=SAFR(I)*(4./9.)
      E=EXP(-KCONV(1)/SAFR(I))
      T2(I)=TG(I)+(1.-E)*(KFL(I)*(TO(I)-TG(I))+(TCAV(I)-TG(I)))
      QFLOW(I)=FACT*KFL(I)*KCONV(1)*(TO(I)-T2(I))
      GO TO 107
   54 T2(I)=TO(I)
      QFLOW(I)=0.
  107 CONTINUE
      RETURN
      END
      SUBROUTINE PLOSS (Q,TO,TCAV,TINF,A,K,S,QFLOW,QDOT)
      REAL  K(1)
      DIMENSION Q(1),TO(1),S(1),QFLOW(1),QDOT(1),TCAV(1)
CCCCCC***  THIS BLOCK CORRECTS FOR THE HEAT LOSS
      SF=1.
      EMIS=0.15
      TAR=(TINF+460.)/100.
      DO 109 I=1,12
      TOR=(TO(I)+460.)/100.
      IF(I.EQ.1)  GO TO  98
      QCOND=K(I)*(TO(I)-TCAV(I))+S(I)*(TO(I)-TO(I-1))+S(I+1)*(TO(I)-
     1   TO(I+1))
      GO TO 100
   98 QCOND=K(I)*(TO(I)-TCAV(I))+S(I)*(TO(I)-TO(45))
     1  +S(I+1)*(TO(I)-TO(I+1))
  100 QRAD=A*SF*EMIS*.1714*(TOR*TOR*TOR*TOR-TAR*TAR*TAR*TAR)
      QLOSS=QCOND+QRAD+QFLOW(I)
      Q(I)=Q(I)-QLOSS/3.4129
      QDOT(I)=Q(I)*3.4129/A
  109 CONTINUE
      RETURN
       END
      SUBROUTINE HFM (TO,TINF,HM,K,S,QDOT)
      REAL  K(1)
      DIMENSION  TO(1),HM(1),S(1),QDOT(1)
      SF=1.0
      EMIS=0.12
      TO(37)=TO(36)-.333*(TO(36)-TO(37))
      S(13)=7.0*S(13)
      TAR=(TINF+460.)/100.
      DO 100 I=13,36
      TOR=(TO(I)+460.)/100.
  100 QDOT(I)=K(I)*HM(I)*(1.+(80.-TO(I))/700.)
     1-S(I)*(TO(I)-TO(I-1))-S(I+1)*(TO(I)-TO(I+1))
     2  -SF*EMIS*.1714*(TOR*TOR*TOR*TOR-TAR*TAR*TAR*TAR)
      S(13)=S(13)/7.0
       RETURN
      END
      SUBROUTINE ENTHAL(FACT,TH,F,ST,END2,DEND2,D2,REEN,DD2,DREEN,DTM,
     1DST,DF,KM)
      DIMENSION TH(1),F(1),ST(1),D2(1),REEN(1),DD2(1),DREEN(1),DTH(1)
     1,DST(1)
C     COMPUTE ENTHALPY THICKNESS AND REYNOLDS NUMBER. ASSUME
C        THERMAL BOUNDARY LAYER BEGINS AT LEADING EDGE PLATE 1
C     COMPUTE ENTHALPY THICKNESS, ASSUMING THERMAL BL BEGINS AT
C        LEADING EDGE OF PLATE 1. COMPUTATION BASED ON CONTROL
C        VOLUME FOR ENERGY ADDITION WITH BOUNDRIES PLATE CENTER
C        TO PLATE CENTER(EXCEPT PLATE 1)
```

```
      TH(1)=0.0
      DTH(1)=0.
      F(1)=0.0
      DX=1.
      DWX=.515625
C    DDX: UNCERTAINTY IN DX, IN
      DDX=0.005
      D2(1)=END2
      DD2(1)=DEND2
      IF (END2.EQ.0.) D2(1)=ST(1)*DX
      IF(.NOT.END2.EQ.0.)  GO TO 229
C    DD2(I):  UNCERTAINTY IN ENTHALPY THICKNESS, D2, IN
      DD2(1)=SQRT(DX*DX*DST(1)*DST(1)+ST(1)*ST(1)*DDX*DDX)
  229 DO 230 I=2,12
      IF (KM.EQ.1) GO TO 399
      D2(I)=D2(I-1)+(ST(I-1)+ST(I)+F(I-1)*TH(I-1)+F(I)*TH(I))*DX
      GO TO 400
  399 D2(I)=D2(I-1)+(ST(I-1)+ST(I)+2.*F(I)*TH(I))*DX
  400 CONTINUE
      AL=ST(I)*ST(I)+ST(I-1)*ST(I-1)+F(I)*F(I)*TH(I)*TH(I)+F(I-1)*
     1F(I-1)*TH(I-1)*TH(I-1)
      BE=DST(I)*DST(I)+DST(I-1)*DST(I-1)+F(I)*F(I)*DTH(I)*DTH(I)+
     1F(I-1)*F(I-1)*DTH(I-1)*DTH(I-1)+DF*DF*(F(I)*F(I)*TH(I)*TH(I)+
     2F(I-1)*F(I-1)*TH(I-1)*TH(I-1))
  230 DD2(I)=SQRT(DD2(I-1)*DD2(I-1)+DDX*DDX*AL+DX*DX*BE )
      D2(13)=D2(12)+(ST(12)+F(12)*TH(12))*DX+ST(13)*DWX
      DD2(13)=SQRT(DD2(12)*DD2(12)+DDX*DDX*(ST(12)*ST(12)+ST(13)*ST(13)
     1+F(12)*F(12)*TH(12)*TH(12)) +DWX*DWX*DST(13)*DST(13)+   DX*DX*(
     2DST(12)*DST(12)+F(12)*F(12)*DTH(12)*DTH(12)+DF*DF*F(12)*F(12)*
     3TH(12)*TH(12)))
      DO 231 I=14,36
      D2(I)=D2(I-1)+(ST(I-1)+ST(I))*DWX
  231 DD2(I)= SQRT(DD2(I-1)*DD2(I-1)+DDX*DDX*(ST(I)*ST(I)+ST(I-1)*
     1ST(I-1))+ DWX*DWX*(DST(I)*DST(I)+DST(I-1)*DST(I-1)))
      IF (KM.EQ.1) D2(13)=D2(13)+F(12)*TH(12)*DWX
      IF (KM.EQ.1) D2(14)=D2(14)+F(12)*TH(12)*DWX
C     COMPUTE ENTHALPY THICKNESS REYNOLDS NUMBER FOR CENTER
C        OF PLATE BASED ON D2(I) FOR ENERGY ADDED TO THAT POINT
      DO 240 I=1,36
      REEN(I)=FACT*D2(I)
  240 DREEN(I)=FACT*DD2(I)
      RETURN
      END
```

SHEAR Program

```
$WATFIV        NOLIST
      DIMENSION UB(42),Y(42)
      DATA Y/.01, .011, .012, .013, .014, .015, .017, .019, .022, .025,
     1 .029, .033, .039, .046, .054, .062, .072, .087, .102, .122, .147,
     2 .177, .217, .267, .322, .397, .472, .547, .622, .697, .772, .847,
     3 .922, .997, 1.072, 1.147, 1.222, 1.297, 1.372, 1.472, 1.572,
     4 1.672/
C     FOLLOWING SIX LINES OF DATA IS FOR X=63.3 INCHES
      DATA UB/ .2977, .3069, .3169, .3285, .3373, .3467, .3617, .3736,
     1 .3887, .4018, .4158, .4254, .4374, .4469, .4562, .4630, .4686,
     2 .4761, .4816, .4874, .4942, .5033, .5171, .5413, .5713, .6097,
     3 .6435, .6760, .7085, .7415, .7748, .8057, .8366, .8663, .8932,
     4 .9185, .9404, .9598, .9745, .9882, .9957, .9987/
      DATA CF2,F,DEL,DEL2,RED2,N/.001352, .0069, 1.496, .2363, 6400.,42/
C     FOLLOWING SIX LINES OF DATA IS FOR X=69.3 INCHES
      DATA UB/.3255, .3345, .3487, .3604, .3709, .3794, .3936, .4063,
     1 .4206, .4324, .4456, .4565, .4684, .4783, .4872, .4947, .5006,
     2 .5094, .5150, .5221, .5310, .5423, .5621, .5898, .6218, .6638,
     3 .7016, .7387, .7752, .8112, .8448, .8756, .9047, .9302, .9519,
     4 .9691, .9824, .9906, .9963, .9989, .9999/
      DATA CF2,F,DEL, DEL2,RED2,N/.001492, .0069,1.291, .1955, 5320.,41/
      SUM1=.25*(UB(1)*UB(1)*Y(1)+(UB(2)+UB(1))*(UB(2)+UB(1))*(Y(2)-
     1Y(1)))
      SUM2=.5*(UB(1)*Y(1)+(UB(2)+UB(1))*(Y(2)-Y(1)))
      WRITE (6,3)
    3 FORMAT(12X'TAU+',5X'TAULAM+',6X'Y/DEL',7X'L/DEL',9X'Y+',13X'L+',
     1 5X'D1',6X'D2',/)
      YPUT=RED2*SQRT(CF2)/DEL2
      B=F/CF2
      UYP=DEL2/(RED2*CF2)
      N=N-1
      DO 10 I=2,N
      DY=Y(I)-Y(I-1)
      DUDY=.5*((UB(I+1)-UB(I))/(Y(I+1)-Y(I))+(UB(I)-UB(I-1))/DY)
      UA=.5*(UB(I)+UB(I-1))
      SUM1=SUM1+UA*UA*DY
      SUM2=SUM2+UA*DY
      TAU=1.+B*UB(I)+(1.+B)*(SUM1-UB(I)*SUM2)/DEL2
      TAUL=DUDY*UYP
      TAUT=TAU-TAUL
      XLP=SQRT(TAUT)/TAUL
      XL=SQRT(TAUT*CF2)/(DUDY*DEL)
      YPL=Y(I)*YPUT
      YL=Y(I)/DEL
      XL1=0.078*TANH(5.25*YL)+3.32*YL*EXP(-YL/0.1)
      XL2=0.078*TANH(5.25*YL)+33.2*YL*YL*EXP(-100.*YL*YL)
      D1=XL/XL1
      D2=XL/XL2
      WRITE (6,5) TAU, TAUL,YL,XL,YPL,XLP,D1,D2
    5 FORMAT (10X,2(F6.3,5X),2(F7.5,5X),F8.3,5X,F8.3,2(3XF5.3))
   10 CONTINUE
      STOP
      END
```

APPENDIX D

HOT WIRE FLOWMETER

For reasons mentioned in Chapter II, a hot wire type flowmeter was developed to be used in the program to measure the secondary air flowrate. Much data concerning a round wire in an infinite stream appears in the literature. If, however, a small rod is inserted into a pipe, then the exact heat transfer behavior will depend on the detailed geometry. Thus, although the behavior can be approximately predicted, the details require experimental study.

Initially, two types of flowmeters were conceived: one using a wire whose temperature was fixed, correlating the flowrate with the heating current supplied to the wire; the other with a fixed heating current, correlating the flowrate with the differential temperature between the hot wire and the oncoming stream. The initial investigation into this problem showed that the constant current mode is preferred because of its smooth variation over the entire flow range. The constant temperature mode showed that the correlation changed very sharply in the low flowrate range.

In final form, each flowmeter unit has two separate circuits: a heater circuit and a thermocouple circuit. All the heater circuits were connected in series to one controlled DC power supply. For each flowmeter element, power can be turned on or off independently, so that any number of flowmeters can be used selectively at one time. This arrangement saved considerable time in the measurement of the secondary air flowrate.

The thermocouple loop for measuring the temperature difference between the heater element and the coming air stream was made with iron-constantan, with one junction at the middle of the heater element inside the brass tubing and the other junction in the air stream 1/2 in. (1.27 cm) upstream with 90° rotation. Care was taken that the wake of this junction did not interfere with the heater and vice versa. Iron wires which come out of the two junctions were connected to the copper lead wires in a small space insulated with the double shrink tubing. These copper lead wires were connected to the selector switch.

To control the current supplied in the circuit, a shunt of 0.1Ω was inserted into the circuit, and the potential across the shunt was read by an H-P digital voltmeter. This potential was monitored to assure the desired current by controlling the current setting dial in the power supply.

A seven foot long, 3 in. (7.62 cm) PVC pipe was used to install the flowmeters. The upstream end had copper screens to make the flow uniform. The flowmeter was located six feet downstream of the copper screen. The current setting was such that the power dissipated by the heater was less than 1 watt, in most cases. Even at a very small flowrate, the temperature rise due to the flowmeter heater was very small (about 1°F at 3 cfm). The detail drawing appears in Figure D.1.

The flowmeters were calibrated in place against Meriam laminar flowmeters. The laminar flowmeters had been checked against standard ASME orifice meters. The initial calibration showed that all the calibration curves collapse by the horizontal shift of some distance in log-log coordinates. Corrections for the mean stream temperature level and humidity were incorporated to deduce the flowrate at standard conditions. After proper corrections were made, the flowmeter constants which are the multiplication factors to make them collapse were left as a functional of each flowmeter element. All flowmeters used the same calibration curves except for one constant, called the flowmeter constant.

In the following section, the correction formula, including the flowmeter constant, K_i , will be given. From the basic energy balance equation on the wire, we have

$$\dot{q} = I^2 R = \bar{h} A_s \Delta T \qquad \text{(D.1)}$$

where $\bar{h}$ is the average heat transfer coefficient around the wire across the span, A_s the total surface area of the wire, and ΔT the temperature difference between the wire and the coming air stream.

For the evaluation of heat transfer coefficient, $\bar{h}$, the following equation from Kreith [D.1] was used,

$$\overline{Nu}\, Pr^{-0.31} = f_1(Re_d) \qquad \text{(D.2)}$$

For the temperature dependence of properties, $T_{st} = 530°R$ was used as a reference temperature, and the following expressions were used;

$$\frac{k}{k_{st}} = \left(\frac{T}{T_{st}}\right)^{0.735}$$

$$\frac{\mu}{\mu_{st}} = \left(\frac{T}{T_{st}}\right)^{0.76} \qquad \text{(D.3)}$$

$$\frac{Pr}{Pr,_{st}} = \left(\frac{T}{T_{st}}\right)^{-0.1}$$

These correlations are the results of curve fitting in the temperature range of 70°F to 180°F by using data appearing in [D.1, D.2, and D.3]

For humidity dependence, the following expressions were used;

$$\frac{Pr}{Pr,_{d.a.}} = (1 + 0.9\ m)$$

$$\frac{\mu}{\mu_{d.a.}} = 1 - 0.055\ m \qquad \text{(D.4)}$$

$$\frac{k}{k_{d.a.}} = 1 - 0.7\ m$$

where m is the absolute humidity, lbm/lb of air. The relationship for Pr was taken from Kays [D.4], and the relationships for μ and k were obtained by using the recommendation appearing in Eckert and Drake [D.5], using the air properties and the vapor properties formed in Keenan and Keyes [D.6], and using the binomial expansion to simplify the expression.

Then all these were combined into Equation (D.2), then into Equation (D.1) and the binomial expansion used again to simplify the expression for humidity correction, and the following expressions were obtained,

$$E = f(X) \tag{D.5}$$

where

$$E = K_1 \cdot \text{emf} \cdot \left(\frac{I_o}{I}\right)^2 \left(\frac{T}{T_{st}}\right)^{0.70} (1 + 0.22\ m)$$

$$X = \text{SCFM}\left(\frac{T}{T_{st}}\right)^{-0.76} (1 + 0.70\ m)$$

and

emf = the emf of the thermocouple signal .

By the calibration procedure, the flowmeter calibration constant, K_1 , for each flowmeter unit and the function f were determined.

With the hot gas stream, some zero shift was noted. To reduce this, insulation was installed around the heater terminal on both sides of the 3 in. (7.62 cm) PVC pipe. After the insulation was installed, satisfactory performance was acquired by taking the zero point at the no-power signal to account for the zero drift.

The variable property correction and zero drift correction gave the quite satisfactory performance of the flowmeters. The calibration curve which displays the function f shows the scatter in X (or SCFM) about 3%. This is less than 1.5% in E coordinate. The high uncertainty in X coordinate is the penalty for getting a wider range of flowrate, because X varies as E^{-25} approximately.

The heater design and the current rating used are such that the heater would not be damaged even if there were no flow with the heater on. The highest temperature the heater can attain is about 160°F to 180°F, which is the safe temperature limit for the epoxy glue used to bond the heater wire onto the brass tubing. The use of a low temperature in the heater guaranteed against the accidental burning which might happen by inadvertently activating the flowmeter while no flow existed in the secondary system and against its aging with use. Also, the design is such that each flowmeter unit can be taken out and interchanged easily, because there is no permanent bond between the flowmeter and the 3 in. (7.62 cm) PVC tube.

References

D-1. Krieth, F., Principles of Heat Transfer, International Textbook Company, 1969, p. 412.

D-2. Rohsenow, W. M., and Choi, H. Y., Heat, Mass, and Momentum Transfer, Prentice-Hall, Inc., 1963, p. 522.

D-3. Eckert, E. R. G., and Drake, Jr., R. M., Heat and Mass Transfer, McGraw-Hill Book Co., 1959, p. 504.

D-4. Kays, W. M., Convective Heat and Mass Transfer, McGraw-Hill Book Co., 1966, p. 369.

D-5. Eckert, E. R. G., and Drake, Jr., R. M., Heat and Mass Transfer, McGraw-Hill Book Co., 1959, pp. 493-494.

D-6. Keenan, J. H., and Keyes, F. G., Thermodynamic Properties of Steam, John Wiley & Sons, Inc., 1936.

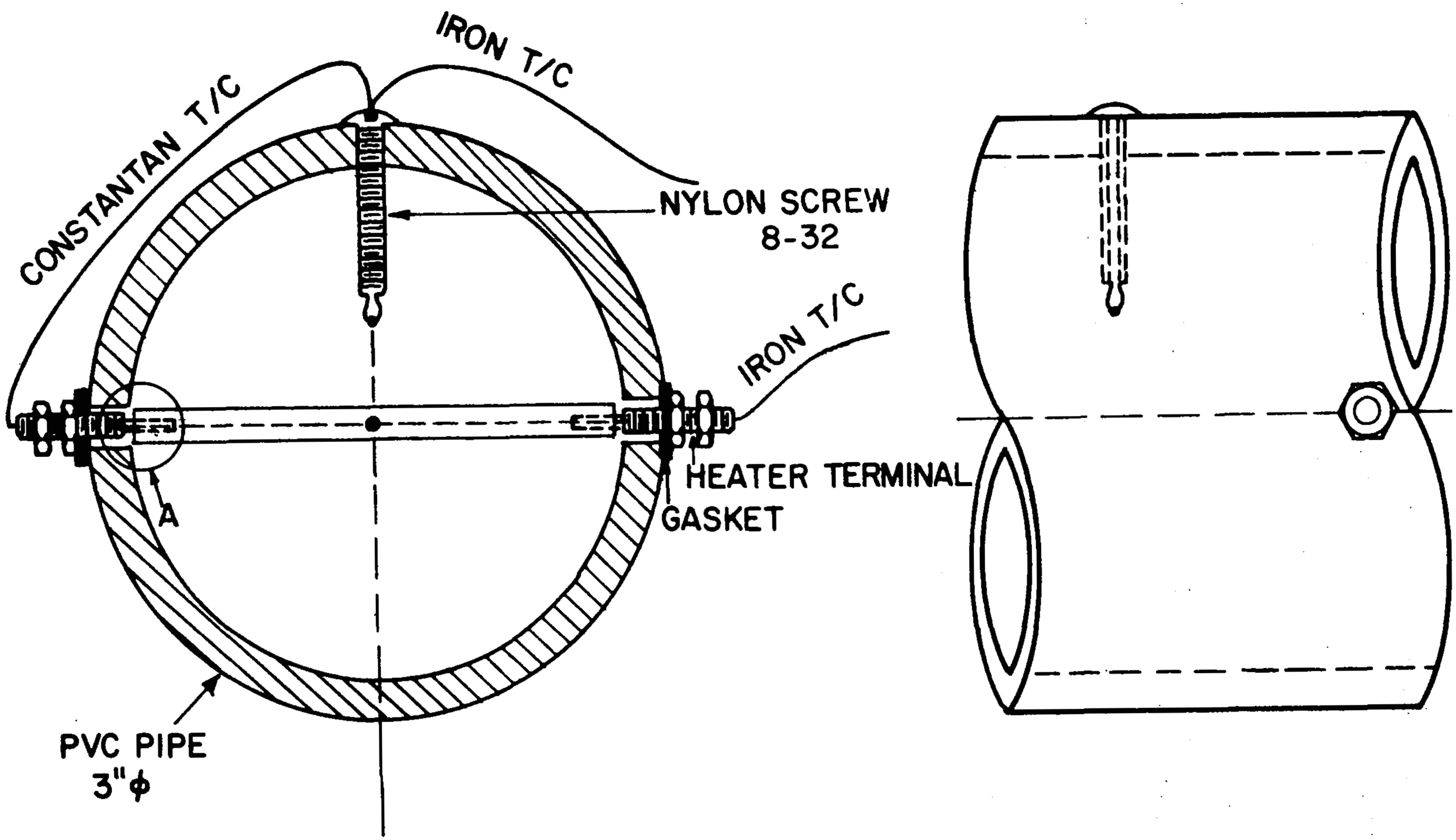

Figure D.1 Detail of hot wire flowmeter.

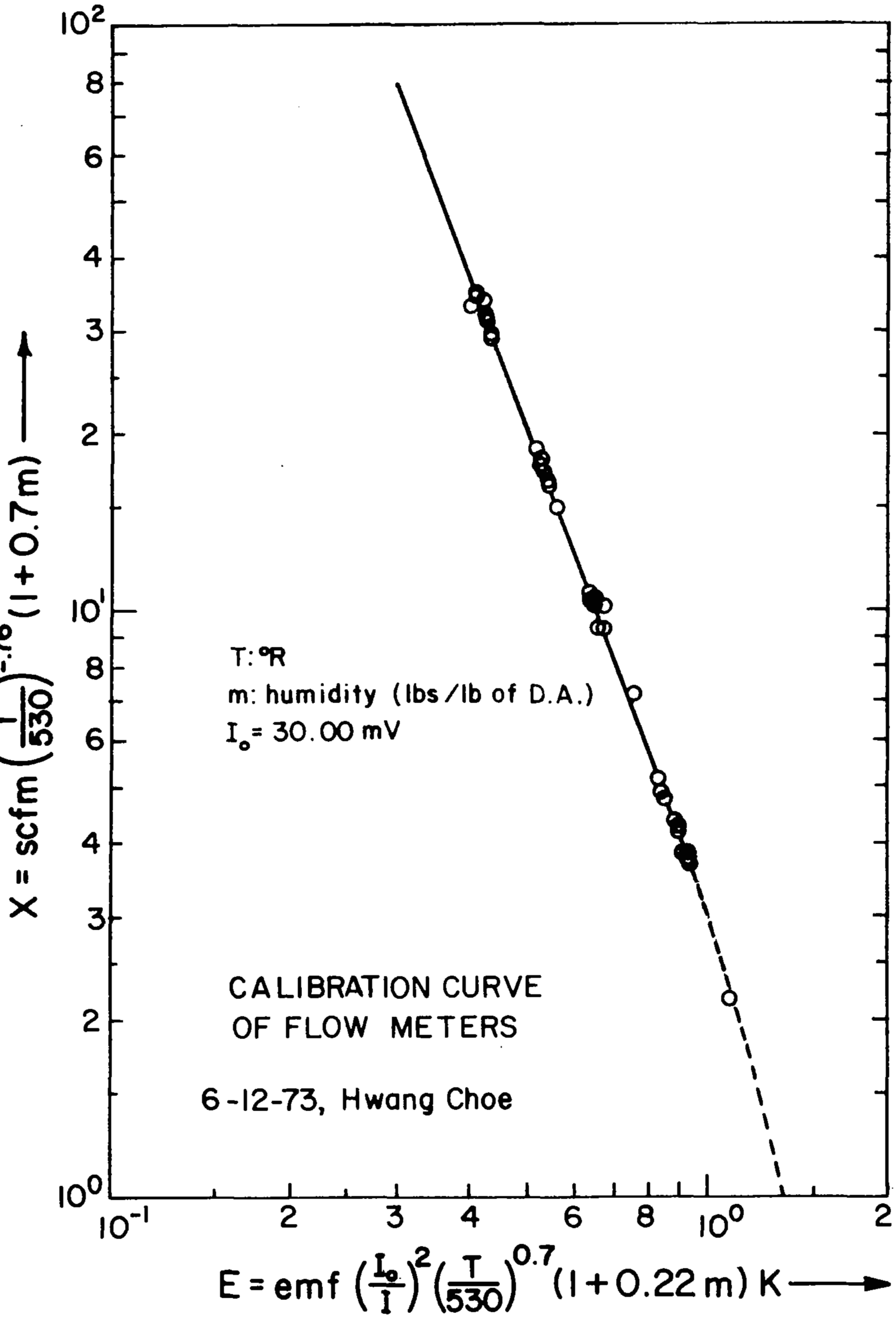

Figure D.2 Calibration curve for hot wire flowmeters.

APPENDIX E

THE MANIFOLD VALVE ADJUSTMENT

The difficulty with assuring the uniformity of flow rate through each hole in one manifold is that the laminar flowmeter used introduces too much resistance to the flow: the measuring device introduces too many disturbances. Even the flow resistance of a venturi meter would be comparable to the flow resistance through each hole. Also the integration of velocity profile at the outlet of each hole turned out not to be a very reliable method for flow rate measurement. This lead to the sensitivity study of the overall system to the flowmeter disturbance. To have a good readability, a 2 cfm (0.944 ℓ/sec) capacity laminar flowmeter was used in conjunction with a 2 in. (5.08 cm) inclined manometer whose smallest division is 0.005 in. (0.127 mm) on the scale.

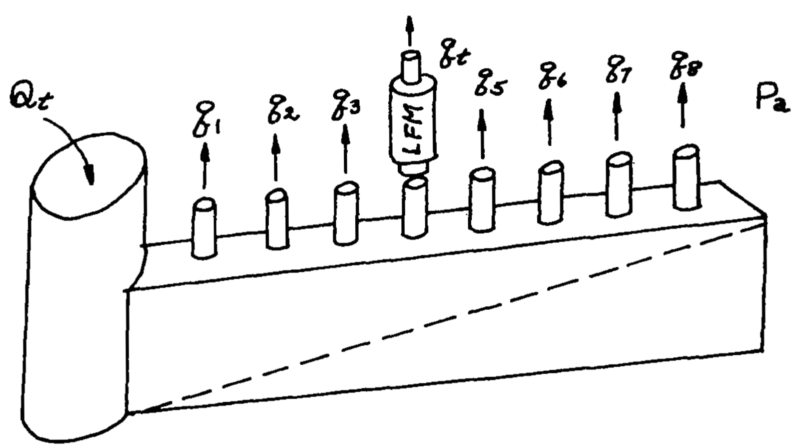

Figure E.1 Sketch of manifold.

First, all the valves were adjusted to give a uniform flowrate within 1% accuracy at the total flowrate of 92 cfm (43.4 ℓ/sec). Then 52 cfm (24.5 ℓ/sec) and 27 cfm (12.74 ℓ/sec) of total flowrate were tried with the same valve setting, and the same accuracy was maintained. This allowed the valve adjustment at one total flowrate. Then a simple flow circuit analysis was performed, assuming there are resistances to flow in the following form.

$$q_i = \frac{P_o - P_a}{r_i} = \frac{\Delta P}{r_i} \qquad (E.1)$$

Since the pressure drop ΔP is uniform for all the holes, the flowrate q_i is a function of the flow resistance, r_i, only. Then the individual resistance of each hole was determined by measuring the flowrate as the electrical resistances in the circuit across constant potential can be determined by measuring the current in each circuit.

In case ΔP is assumed to be proportional to v^2, we may put ΔP in the form

$$\Delta P = K_i q_i^2$$

Rearranging, we obtain

$$q_i = \frac{\Delta P}{\sqrt{K_i}} \qquad (E.2)$$

Since ΔP is constant, this will lead to the same conclusion as before if $\sqrt{K_i}$ is set to r_i. For the sake of simplicity, the first linear expression, Equation (E.1), was used to analyze the calibration accuracy. The conclusion of this analysis is that the flow resistance of PVC tubes which are used for the delivery of the gas from the manifold to the test plate was about 3.5 times the resistance of the manifold hole itself, and the laminar flowmeter used has about 10 times more resistance than the manifold hole resistance, and the measurement with single flowmeter on each hole in turn showed the accuracy of 0.3% to insure the 1% accuracy in the uniformity of flowrate in each hole at the test plate elevation. Also tested is the possible flowrate change due to thermocouple installation in some of the PVC tubing. The analysis showed that 1/2% decrease is possible. The secondary air flow rate in each hole in one manifold is uniform within ± 1 1/2% accuracy.

APPENDIX F

WATTMETER INSERTION LOSS

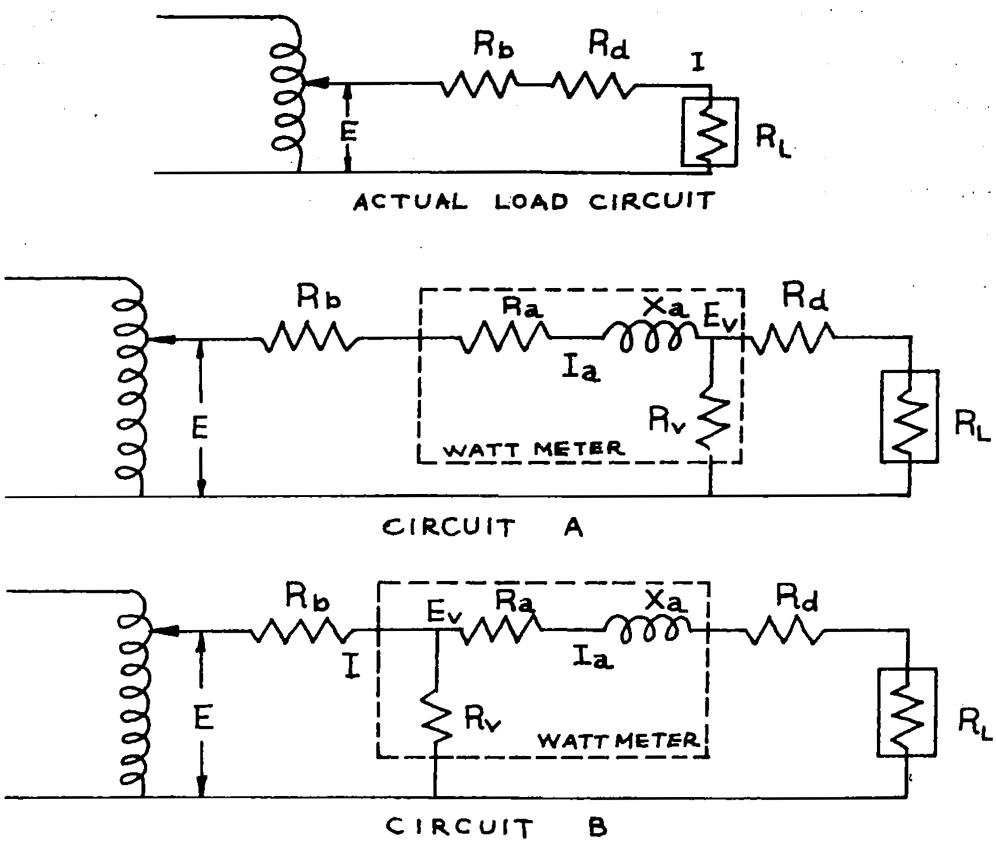

Figure F.1 Circuits for wattmeter circuit analysis.

The preliminary analysis on the circuits A and B showed that Circuit B is preferable, because Circuit B is less sensitive to the ammeter resistance change. In this part, the analysis will be done, including the ammeter reactance on the power factor applied to get the true power from the measured power in Circuit B. The potential supplied at the variac is assumed to be the same.

A. Actual Load Power with Switch On

In this circuit, there is no reactance component, and the power delivered to the load, R_L , is simply E x I product across R_L .

To calculate I , we have

$$I = \frac{E}{R_b + R_d + R_L}$$

The potential across the R_L is

$$E_v = I \cdot R_L$$

Thus, the ideal power can be expressed as

$$P_a = E_v \cdot I = \frac{E^2}{(R_b + R_d + R_L)^2} R_L$$

where $R_b + R_d = R_L = \Sigma\overline{R}$, total resistance without wattmeter inserted. Then

$$\therefore \quad P_a = \frac{E^2}{R_L}\left(\frac{R_L}{\Sigma\overline{R}}\right)^2 \tag{F.1}$$

B. <u>Indicated Power in Wattmeter (Circuit B)</u>

In this case, there is a reactance component in the wattmeter circuit. Considering the potential supplied at the variac with phase angle at 0 , we can calculate the I_a and E_v , and then power can be calculated as $|E_v| \cdot |I_a| \cos\theta$. θ is the angle between E_v and I_a .

The total impedance in the circuit is

$$\Sigma Z = R_b + \frac{R_v(R_a + R_d + R_L + j\, X_a)}{R_v + R_a + R_d + R_L + j\, X_a} \tag{F.2}$$

where $j \equiv \sqrt{-1}$. Now, E_v can be calculated as

$$E_v = E\,\frac{\Sigma Z - R_b}{\Sigma Z} \tag{F.3}$$

Since E_v is known I_a can be calculated in the load circuit as

$$I_a = \frac{E_v}{R_a + R_d + R_L + j\,X_a} \tag{F.4}$$

Thus, the measured power will be

$$P_i = |E_v|^2 \cdot \cos\theta \,/\, |R_a + R_d + R_L + j\,X_a|$$

Since the phase difference between E_v and I_a is due to the impedance $(R_a + R_d + R_L + jX_a)$, we can express $\cos\theta$ as

$$\cos\theta = \frac{R_a + R_d + R_L}{\left|R_a + R_d + R_L + j\,X_a\right|} \tag{F.5}$$

Combining Equations (F.3), (F.4) and (F.5), P_i is obtained as

$$P_i = \frac{E^2}{R_L} \frac{|\Sigma Z - R_b|^2}{|\Sigma Z|^2} \cdot \frac{}{|R_a + R_d + R_L + j\,X_a|^2}$$

Now

$$|\Sigma Z - R_b|^2 = R_v^2 \frac{|R_a + R_d + R_L + j\,X_a|^2}{|R_v + R_a + R_d + R_L + j\,X_a|^2}$$

$$P_i = \frac{E^2}{R_L} \frac{R_v^2\, R_L (R_a + R_d + R_L)}{|\Sigma Z|^2 |R_v + R_a + R_d + R_L + j\,X_a|^2} \tag{F.6}$$

C. Power Correction Factor

$$P_a = K\,P_i = \frac{P_a}{P_i}\,P_i \tag{F.7}$$

$$K = \frac{P_a}{P_i} = \frac{R_L^2}{(\Sigma\bar{R})^2} \frac{|\Sigma Z|^2 |R_v + R_a + R_d + R_L + j\,X_a|^2}{R_v^2\, R_L (R_a + R_d + R_L)}$$

By working out this algebra, we obtain

$$K = \frac{(\Sigma R)^2 + X_a^2}{(\Sigma\bar{R})^2} \frac{\left(1 + \dfrac{R_a + R_d + R_L}{R_v}\right)^2 + \left(\dfrac{X_a}{R_v}\right)^2}{1 + \dfrac{R_a + R_d}{R_L}}$$

with

$$\Sigma R = R_b + \frac{R_v (R_a + R_d + R_L)}{R_v + R_a + R_d + R_L}$$

This was incorporated into the data reduction program.

APPENDIX G

CALIBRATION OF HEAT FLUX METERS

The following procedure was used for calibrating the heat flux meters. This is to account for the small temperature difference between the adjacent plates and also to calculate the flow direction conductance between the two adjacent plates.

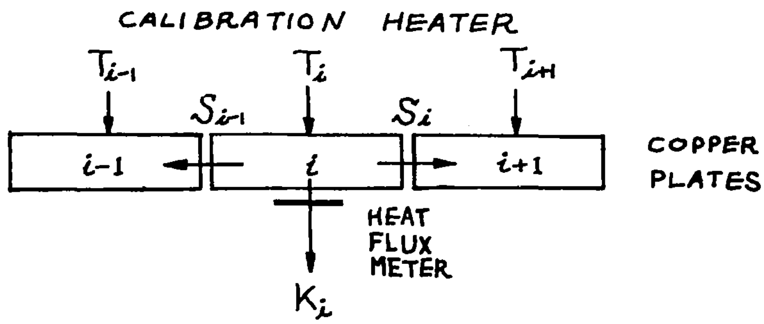

Figure G.1 Copper plate with heat flux meter in calibration mode.

We can write down the energy balance equation for the i^{th} plate. Power supplied = (heat conducted down through the heat flux meter) + (heat conducted to the two adjacent plates). By dividing this equation by the heat transfer area on the test surface, we can directly form the equation on the heat flux basis.

$$\dot{q}_i'' = K_i\ HF_i + S_{i-1}(T_i - T_{i-1}) + S_i(T_i - T_{i+1}) \tag{G.1}$$

where $\dot{q}_i''$ is the heat flux on the i^{th} plate. K_i is corrected for temperature dependence, as suggested by the manufacturer,

$$K_i = K_{o,i}\ (1 + (T_i - 80)/700) \tag{G.2}$$

T_i is the i^{th} plate temperature, HF_i the heat flux signal in MV, and S_i the conductance between the i^{th} and i+1 the plate. Then our purpose is to calculate $K_{o,i}$ and S_i from this calibration.

The calibration heater has three heaters; the center heater which supplies the heat to i^{th} plate is instrumented to measure the power supplied within the accuracy of ±1% ; the other two heaters act as guard heaters and can be turned off independently for calibration purpose. Then we can operate in three different modes: the first mode has all the heaters on with approximately the same power; the second mode has one of the guard heaters off; and in the third mode both of the guard heaters are off. Then we can write the energy balance equation on the i^{th} plate for three different modes considering the temperature compensation on the K_i .

$$\dot{q}_i''^F = K_{o,i}(1 + (T_i^F - 80)/700)\ HF_i^F + S_{i-1}(T_i^F - T_{i-1}^F) + S_i(T_i^F - T_{i+1}^F) \tag{G.3a}$$

$$\dot{q}_i''^S = K_{o,i}(1 + (T_i^S - 80)/700)\ HF_i^S + S_{i-1}(T_i^S - T_{i-1}^S) + S_i(T_i^S - T_{i+1}^S) \tag{G.3b}$$

$$\dot{q}_i''^T = K_{o,i}(1 + (T_i^T - 80)/700)\ HF_i^T + S_{i-1}(T_i^T - T_{i-1}^T) + S_i(T_i^T - T_{i+1}^T) \tag{G.3c}$$

where superscripts, F , S and T , denote the different modes of measurement. If for each mode, Q_i , T_i , T_{i+1} , T_{i-1} , and HF_i are measured, the above three equations can be solved for three unknowns: $K_{o,i}$, S_{i-1} , and S_i . A small computer program was written to solve these equations for $K_{o,i}$, S_{i-1} , and S_i . The above mentioned three modes make the determinant of the above equations diagonally dominant, which prevents the singular behavior in the solution process. This program directly uses Kramer's rule.

The power to the two guard heaters is from AC variac, and the central heater is powered by the controlled DC power. The Weston precision voltmeter and ammeter are used to measure the DC power. Both the ammeter and voltmeter are accurate to 1/2% of the full scale. The DC ammeter and voltmeter remained in the circuit and the extra resistance beside the heater is considered to calculate the true power delivered to the plate. All these are incorporated into the above computer program. The flow direction conductances of the two end plates on the blowing section were determined as part of this procedure.

APPENDIX H

AN EXACT SOLUTION OF LAMINAR SUBLAYER EQUATION

In evaluating the wall shear stress and the wall heat flux from the numerical solution of the boundary layer equations, one accurate and convenient way is to use the laminar sublayer equations in non-dimensional form and to compare this solution with the numerically obtained solution (see Reference 10).

The values of y and u, along with the viscosity, are given from the numerical solution at a point nearest to the wall (inside the laminar sublayer). Then, using the fact that

$$Re_w \triangleq \frac{uy}{\nu} = u^+ y^+$$

the wall shear stress (or y^+) can be calculated.

In the case of the flat plate, $u^+ = y^+$, and

$$y^+ = \sqrt{Re_w}$$

From the definition of y^+, the wall shear stress can be calculated. However, if we have the pressure gradient or wall mass transfer, the problem is not that simple, because

$$u^+ = y^+ + (G^+ + P^+) \frac{e^{G^+ y^+} - 1 - G^+ y^+}{(G^+)^2}$$

and we have to solve the transcendental equation.

The STAN program [61] obtains the approximate solution with the successive substitution:

$$y_1^+ = \sqrt{Re_w}$$

$$y_2^+ = \frac{y_1^+}{\sqrt{1 + G^+ y_1^+ + P^+ y_1^+}}$$

$$y_3^+ = \frac{y_2^+}{\sqrt{1 + G^+y_2^+ + P^+y_2^+}}$$

From the initial guess, it does two iterations. This turned out to be satisfactory for most of the transpiration cooling problem, because G^+ is normally less than $0.1 \sim 0.2$ and P^+ is much less than G^+. In the case of discrete hole blowing, G^+ is much higher than in the transpiration cooling. And at $G^+ \simeq 1.0$, the above scheme introduces considerable error. Thus the exact solution of the following equation is required.

$$u^+y^+ = Re_w = y^{+2} + y^+(G^+ + P^+) \frac{e^{G^+y^+} - 1 - G^+y^+}{G^+}$$

Let $f(y^+) = u^+y^+ - Re_w$, then the problem becomes how to find the zero in $f(y^+)$.

Using the Newton-Raphson method, we can have the following algorithm to get the exact solution numerically.

$$y^+_{(n)} = y^+_{(n-1)} - \frac{f(y^+_{(n-1)})}{f'(y^+_{(n-1)})}$$

About $4 \sim 5$ iteration, y^+ comes to the exact solution within 10^{-3} in most cases. The addition of this procedure does not change the total computation time appreciably. If we obtain y^+, we can also solve for h^+, because we know the laminar sublayer solution for h^+ in terms of y^+.

$$\frac{dh^+}{dy^+} = Pr(1 + G^+h^+ + S^+y^+ + C_4X^+\int_o^{y^+} u^+dy^+) + C_3u^+ \frac{du^+}{dy^+}$$

where

$$C_4 = \frac{g_c \tau_o^2}{J \dot{q}_o'' \rho_o}, \quad C_3 = (Pr - 1) \frac{u_\tau \tau_o}{J \dot{q}_o''}$$

The C_3 and C_4 terms represent the energy source due to viscous dissipation and body force work. S^+ represents the other source terms for the energy equation. The exact solution for h^+ becomes rather involved, with all the source terms present. In case all the source terms are absent, h^+ becomes

$$h^+ = \frac{e^{PrG^+y^+} - 1.0}{G^+}$$

Once h^+ is obtained, $\dot{q}_o''$ can be obtained from the definition of h^+.

APPENDIX I

LINEARIZED SOLUTION FOR DISCRETE HOLE BLOWING UNDER AN IDEALIZED CONDITION

This analysis is done to give some insight into the terms $-\overline{\tilde{u}\tilde{v}}$, which appear in Chapter IV. This was not intended to give a quantitative estimation of the $-\overline{\tilde{u}\tilde{v}}$. It follows the analysis done by Saeger and Reynolds [I-1], specialized for the standing wave. The following assumptions are made:

1. Low speed, $M_a << 1.0$
2. Constant property, constant density
3. Small perturbation, which allows the linearization of the governing equation
4. The discrete hole pattern is periodic in the z-direction and in the x-direction. This assumption, combined with the linearization, makes Fourier expansion of the discrete hole blowing in the x- and z-direction as a standing wave.
5. Also, for the purpose of this analysis, the y- and z-component mean velocities were assumed zero and constant, and the x-component mean velocity was assumed to be a function of only the y-coordinate.
6. Quasi-laminar assumption was used to account for the turbulent correlation terms.

For the perturbation properties, the following expansion is used.

$$\tilde{u} = \sum_{m=-\infty}^{\infty} \sum_{n=-\infty}^{\infty} U_{mn} \, e^{i(m\alpha x + n\beta z)} \qquad (I.1)$$

where $\alpha = \pi/L$, and $\beta = 2\pi/P$.

Similar expansions for $\tilde{v}$, $\tilde{t}$, $\tilde{p}$ can be used, and using the linearized perturbation equations, the following equations were obtained from continuity, momentum, and energy equations.

$$im\alpha u_{m,n} + Dv_{m,n} + in\beta w_{m,n} = 0 \tag{I.2}$$

$$im\alpha U u_{m,n} + V_o Du_{m,n} + v_{m,n} DU = -im\alpha p_{m,n} + \nu_T (D^2 - m^2\alpha^2 - n^2\beta^2) u_{m,n} \tag{I.3}$$

$$im\alpha U v_{m,n} + V_o Dv_{m,n} = -Dp_{m,n} + \nu_T (D^2 - m^2\alpha^2 - n^2\beta^2) v_{m,n} \tag{I.4}$$

$$im\alpha U w_{m,n} + V_o Dw_{m,n} = in\beta p_{m,n} + \nu_T (D^2 - m^2\alpha^2 - n^2\beta^2) w_{m,n} \tag{I.5}$$

$$im\alpha U t_{m,n} + V_o Dt_{m,n} = k_T (D^2 - m^2\alpha^2 - n^2\beta^2) t_{m,n} \tag{I.6}$$

where D denotes (d/dy) .

If the solutions for $u_{m,n}$, $v_{m,n}$, and $t_{m,n}$ are obtained, $-\overline{\tilde{t}\tilde{v}}$ and $-\overline{\tilde{u}\tilde{v}}$ can be expressed as

$$-\overline{\tilde{u}\tilde{v}} = -\sum_{m=-\infty}^{\infty} \sum_{n=-\infty}^{\infty} u_{m,n} \cdot v_{-m,-n}$$

$$-\overline{\tilde{t}\tilde{v}} = -\sum_{m=-\infty}^{\infty} \sum_{n=-\infty}^{\infty} t_{m,n} \cdot v_{-m,-n}$$

A. Near the Wall

Now, to simplify the algebra near the wall, the following additional assumptions are made.

7. $V_o \simeq 0$

8. The conduction or diffusion in the y-direction is negligible because the jets are directed in the y-direction.

To simplify the notation, all the subscripts will be deleted for the perturbation equations, and $m\alpha$ and $n\beta$ will be replaced by simply α and β . This will give the following simpler equations.

$$i\alpha u + Dv + i\beta w = 0 \tag{I.7}$$

$$i\alpha Uu + vDU = -i\alpha p - \nu_T(\alpha^2 + \beta^2)u \tag{I.8}$$

$$i\alpha Uv = -Dp - \nu_T(\alpha^2 + \beta^2)v \tag{I.9}$$

$$i\alpha Uw = -i\beta p - \nu_T(\alpha^2 + \beta^2)w \tag{I.10}$$

$$i\alpha Ut + vDT = -k_T(\alpha^2 + \beta^2)t \tag{I.11}$$

First t can be solved in terms of v . From (I.11),

$$t = -\frac{v}{k_T(\alpha^2 + \beta^2) + i\alpha U} DT \tag{I.12}$$

Equations (I.7) to (I.10) were combined to eliminate p and w and then u can be solved as a function of v

$$u = -\frac{\beta^2/(\alpha^2 + \beta^2)\ v}{\nu_T(\alpha^2 + \beta^2) + i\alpha U} DU + \frac{i\alpha}{\alpha^2 + \beta^2} Dv \tag{I.13}$$

and also the equation for v can be derived as

$$D^2v - \left\{(\alpha^2 + \beta^2) + \frac{i\alpha U''}{\nu_T(\alpha^2 + \beta^2) + i\alpha U}\right\} v = 0 \tag{I.14}$$

where $(\ )' \equiv D$.

From (I.12) and (I.13), the following expressions are obtained:

$$-\overline{\tilde{t}\tilde{v}} = T' \sum_{m=-\infty}^{\infty} \sum_{n=-\infty}^{\infty} \frac{v_{m,n}\, v_{-m,-n}}{k_T(m^2\alpha^2 + n^2\beta^2) + im\alpha U}$$

$$-\overline{\tilde{u}\tilde{v}} = U' \sum_{m=-\infty}^{\infty} \sum_{n=-\infty}^{\infty} \frac{v_{m,n}\, v_{-m,-n}}{\nu_T(m^2\alpha^2 + n^2\beta^2) + im\alpha U} \frac{n^2\beta^2}{m^2\alpha^2 + n^2\beta^2}$$

$$+ \sum_{m=-\infty}^{\infty} \sum_{n=-\infty}^{\infty} \frac{im\alpha(Dv_{m,n})v_{-m,-n}}{m^2\alpha^2 + n^2\alpha^2}$$

By solving Equation (I.14), we can evaluate $(-\overline{\tilde{t}\tilde{v}})$ and $(-\overline{\tilde{u}\tilde{v}})$ terms ideally. The expression for the $-\overline{\tilde{t}\tilde{v}}$ term shows that it has a multiplification factor T' , and the summation term which is independent of the mean temperature field. $v_{m,n} \cdot v_{-m,-n}$ will be positive because v is an even function in the z- and x-directions. This indiciates that the summation term will be positive. The same argument can be applied to the first term in $(-\overline{\tilde{u}\tilde{v}})$.

To simplify the expression for $-\overline{\tilde{u}\tilde{v}}$, the following algebraic manipulation was done by using Equation (I.14):

$$\frac{d}{dy} \sum_{m=-\infty}^{\infty} \sum_{n=-\infty}^{\infty} \frac{im\alpha(Dv_{m,n})v_{-m,-n}}{m^2\alpha^2 + n^2\beta^2}$$

$$= U'' \sum_{m=-\infty}^{\infty} \sum_{n=-\infty}^{\infty} \frac{v_{m,n}v_{-m,-n}}{\nu_T(m^2\alpha^2 + n^2\beta^2) + im\alpha U} \frac{m^2\alpha^2}{m^2\alpha^2 + n^2\beta^2}$$

Using these results, we obtain

$$\frac{d}{dy}(-\overline{\tilde{t}\tilde{v}}) = \frac{d}{dy}(e_H \frac{dT}{dy}) \tag{I.15}$$

$$\frac{d}{dy}(-\overline{\tilde{u}\tilde{v}}) = \frac{d}{dy}(e_M \frac{dU}{dy}) - \frac{de_1}{dy}\frac{dU}{dy} \tag{I.16}$$

where

$$e_H = \Sigma\Sigma \frac{v_{m,n}\, v_{-m,-n}}{k_T(m^2\alpha^2 + n^2\beta^2) + im\alpha U}$$

$$e_M = \Sigma\Sigma \frac{v_{m,n}\, v_{-m,-n}}{\nu_T(m^2\alpha^2 + n^2\beta^2) + im\alpha U}$$

$$e_1 = \sum\sum \frac{m^2\alpha^2}{m^2\alpha^2 + n^2\beta^2}\ \frac{v_{m,n}\, v_{-m,-n}}{\nu_T(m^2\alpha^2 + n^2\beta^2) + im\alpha U}$$

The reason that e_H , e_M , and e_1 are taken as real is because $-\overline{\tilde{t}\tilde{v}}$ and $-\overline{\tilde{u}\tilde{v}}$ must be real. Also, as we have discussed earlier, e_H , e_M , and e_1 must be positive numbers. The forms given in Equations (I.15) and (I.16) merely confirm that $-\overline{\tilde{t}\tilde{v}}$ and $-\overline{\tilde{u}\tilde{v}}$ can be treated as shear stress or heat flux and that mixing length type formulations can be used for their modeling near the wall.

B. <u>Near the Free Stream</u>

Near the free stream, U can be approximated as U_∞ , and the diffusion or conduction terms can be neglected. These assumptions lead Equations (I.7) to (I.11) to

$$i\alpha u + Dv + i\beta w = 0 \tag{I.17}$$

$$i\alpha U_\infty u = -i\alpha p \tag{I.18}$$

$$i\alpha U_\infty v = -Dp \tag{I.19}$$

$$i\alpha U_\infty w = -i\beta p \tag{I.20}$$

Eliminating w and p, we obtain for u and v,

$$D^2 v - (\alpha^2 + \beta^2) v = 0 \tag{I.21}$$

and

$$D^2 u - (\alpha^2 + \beta^2) u = 0 \tag{I.22}$$

Thus, u and v must have solutions of the type $e^{-\{\alpha^2 + \beta^2\} y}$

$$-\overline{\tilde{u}\tilde{v}} = \sum\sum u_{m,n}(o) v_{-m,-n}(o)\ e^{-2\{m^2\alpha^2 + n^2\beta^2\} y}$$

This suggests that $-\overline{\tilde{u}\tilde{v}}$ (and $-\overline{\tilde{t}\tilde{v}}$) will damp out toward the free stream, and that for this particular solution the value of $-\overline{\tilde{u}\tilde{v}}$ should not be zero at the wall.

Reference

S-1 Saeger, J. C., and Reynolds, W. C., "Perturbation Pressure Over Travelling Sinusoidal Waves with Fully Developed Turbulent Shear Flow," Technical Report Number FM-9, Thermosciences Division, Dept. of Mech. Engrg., Stanford Univ., May 1971.

*U.S. GOVERNMENT PRINTING OFFICE: 1976 - 635-275/64